



EUROPEAN FORUM
for RECIPROCATING
COMPRESSORS

**7th Conference of the EFRC
October 21th / 22th, 2010, Florence**

Contents

OPERATIONS

- Reliability Check for a 70 Year old Compressor** - 21 -
Qing Yang, Harry Lanckenau; BASF, NEAC COMPRESSOR SERVICE
- Modernization of reciprocating compressors for actual and future requirements** - 31 -
Thomas Knebel, Andreas Raschke, Samuel Burkhalter, Manfred Straessler; VNG, BURCKHARDT COMPRESSION
- Best practices in Compressor Mounting** - 40 -
James A. Kuly, ITW Polymer Technologies

CONDITION MONITORING

- Automatic Early Failure Detection and Shutdown of a Critical Compressor due to a Crosshead Fracture** - 51 -
Tobias Ahlert; PROGNOST SYSTEMS
- Experiences of a new generation of machinery monitoring for reciprocating compressors** - 58 -
Martin Schubert, Christian Prinz; HOERBIGER VENTILWERKE
- Integration of a Advanced Diagnostic Tool in an Optimization Platform** - 65 -
Riccardo Fani, Ms Gaia Rossi; GE OIL AND GAS, GE ENERGY

OPERATIONS

- Piston rod vibrations of excessive amplitudes on a CO2 compressor-simulation, measurements and reengineering to solve the effect** - 75 -
Thomas Heumesser, Roman Gabriel; LEOBERSDORFER MASCHINENFABRIK
- Lessons Learned from a Reciprocating Compressor for CO2 Injection** - 83 -
Marlies van Osch, Bas van den Beemt, Jeroen van Meel, Michel Bezemer; TNO SCIENCE AND INDUSTRY, CONPACKSYS
- Straight or Twisted? – ‘Laser Talks’** - 90 -
Stefan Damberg, Harry Lanckenau; NEAC COMPRESSOR SERVICE

INNOVATION & TECHNOLOGY

- Development of innovative sensor and method for direct measurement of rider ring wear** - 105 -
Lau Koop, Peter Duineveld; THOMASSEN COMPRESSION SYSTEMS
- The BCD Paking Ring - a New High Performance Design** - 112 -
Tino Lindner-Silwester, Christian Hold; HOERBIGER VENTILWERKE
- Development of a Stepless Flow Control System** - 120 -
Roland Aigner, Alexandre Voser, Andreas Allenspach; BURCKHARDT COMPRESSION

PULSATION & VIBRATIONS

- The Impact of an API 618 4th of 5th Edition Analysis on the Design of a Very Large Hydrogen Compressor** - 133 -
Leonard van Lier, Bert Egas, Cesar Luis, Fernandez Valdes; TNO SCIENCE AND INDUSTRY, REPSOL
- Dynamic Pressure Losses in Piping Systems** - 142 -
Klaus Brun, Marybeth Nored, Dennis Tweten, Rainer Kurz; SOUTHWEST RESEARCH INSTITUTE, SOLAR TURBINES
- Cylinder Manifold Forced Response** - 151 -
Marco Passeri, Stefano Generosi; GE OIL AND GAS

DESIGN & ENGINEERING

- A Review on the Methods of Load and Strength Evaluation of Connecting Rods** - 165 -
Gerhard Knop, Marcel Naumann; NEUMANN & ESSER
- A Comparison of High-Speed Upstream to Moderate-Speed Downstream Short Stroke Reciprocating Compressors** - 174 -
Greg Phillipi, Joe Spiller; ARIEL, SHELL
- Supplementary Challenges for UGS Applications of Reciprocating Compressors with Centrifugal Machinery** - 181 -
Burkhard Lenth, Joachim Wermeling; RWE GASSPECHER

EFRC

Comparison of Field Vibration Data with ‘EFRC Guidelines for Vibrations in Reciprocating Compressor Systems’ - 191 -

Roland Schumann, Andre Eijk; BASF, TNO SCIENCE AND INDUSTRY

Educating Reciprocating Compressor Engineers at the EFRC - 202 -

Siegmund Cierniak; RWE

OPERATIONS

Compressor Reliability Survey - 211 -

Andre Eijk, Leonard van Lier; TNO SCIENCE AND INDUSTRY

Stabilization of compressor foundations - 223 -

Thorsten Reisser, Wolfgang Blankart, Stefan Irrgang, BASF, SHELL

Fracture Mechanics Life Assessment for Hypercompressor Lubrication Quills - 228 -

Marco Manetti, Carmelo Maggi, Nicola Campo, Guido Volterrani, Marco Innocenti; UNIVERSITY OF FLORENCE, GE OIL & GAS

DESIGN & ENGINEERING

Decreasing Time and Cost Effort by Virtual Prototyping in the Compressor Development - 239 -

Tobias Spilker, Matthias Budde, Martin Rebbert, Christoph Steffens; FEV MOTORENTECHNIK

New Crosshead Lubrication Design to Uprate the Power Density of LDPE Reciprocating Compressors - 248 -

Carmelo Maggi, Nicola Campo, Filippo Gerbi; UNIVERSITY OF FLORENCE, GE OIL & GAS

Design Challenges for Reciprocating Compressors in Specialty Gas Services - 259 -

Mike Cyca, Kelly Eberle, BETA MACHINERY ANALYSIS

FUNDAMENTALS

- Challenges in use of analog of the four pole transfer matrix in the 1D time domain pulsation simulations** - 271 -
Grzegorz Zelek, Piotr Cyklis; CRACOW UNIVERSITY OF TECHNOLOGY
- Material Development – Transferability Counts** - 280 -
Marc Langela; STASSKOL
- Thermo-fluid-dynamic design of Reciprocating Compressor Cylinders by Fluid Structure Interaction Software simulation** - 286 -
Riccardo Traversari, Marco Faretra; CST COMPRESSION SERVICE TECHNOLOGY

PULSATION & VIBRATIONS

- Gas Passage System Pulsation Analysis for Modern Reciprocating Compressors** - 299 -
Marybeth Nored; SOUTHWEST RESEARCH INSTITUTE
- Development and application of vibration improvements** - 309 -
Johann Lenz; KOTTER CONSULTING ENGINEERS
- Noise Reduction at a Hydrogen Compressor Plant** - 318 -
Andreas Allenspach, Samuel Burkhalter; BURCKHARDT COMPRESSION

RINGS, VALVES & PACKINGS

- Next Generation Valve Technology for High Speed Compressors** - 327 -
*Bernhard Spiegl, Markus Testori, Gunther Machu;
HOERBIGER KOMPRESSORTECHNIK HOLDING*
- Heavy & unusual wear of Peek1 piston rings in a lubricated air-cooled high-speed and high-pressure compressor** - 335 -
Georg Holtl, Thomas Heumesser; LEOBERSDORFER MASCHININFABRIK
- Operating Experience of CC Valves Installed in Refinery Plant** - 341 -
Andrea Raggi, Fabio Manfrone; DOTT. ING. MARIO COZZANI



EUROPEAN FORUM
for RECIPROCATING
COMPRESSORS



Dynamic Pressure Losses in Piping Systems

by:

Klaus Brun, Ph.D.
Marybeth Nored – Dennis Tweten
Fluids & Machinery Engineering
Department
Southwest Research Institute
San Antonio, Texas, USA
klaus.brun@swri.org

Rainer Kurz, Ph.D.
Solar Turbines, Inc.
Systems Analysis & Field Testing
San Diego, California, USA
kurz_rainer_x@solarturbines.com

7th Conference of the EFRC
October 21th / 22th, 2010, Florence

Abstract

The term “dynamic pressure loss” is used to describe pressure drops that are associated with the dynamic component of the flow through the piping system in a compressor station. Conventionally, dynamic pressure losses are determined by assuming a periodically pulsating 1-D flow profile and calculating the transient pipe friction losses by multiplying a friction factor with the flow dynamic pressure component. In reality, the dynamic pressure loss is more complex and is not a single component but rather consists of different physical effects. One physical effect, the pressure losses due to fluid-structure interactions, is not well understood and has not been previously quantified.

A number of experiments were performed by SwRI in a reciprocating compressor closed loop facility to determine this loss component using dynamic pressure and vibration measurements for resonant, non-resonant and resonant-clamped pipe operating conditions. Results show that pressure losses associated with the piping fluid-structure interaction loss component can be significant and cannot be ignored when predicting dynamic pressure losses. This paper describes findings from these experiments and aims to quantitatively assess the above described components individually for a typically reciprocating compression system. The analytical method, computational fluid dynamic solution and comparable experimental data are presented.

1 Introduction

The process gas flow through reciprocating compressor station piping systems is usually highly unsteady. Compressor excited resonance peak-to-peak pulsations in excess of 10% of the mean flow are not uncommon [Brun et al. 2007]. To avoid flow induced vibrations and structural damage to the piping system, pulsation attenuation devices, such as bottles, choke tubes, orifice plates, and Helmholtz resonators are often utilized in compression stations. However, any flow pulsation attenuation through choking, absorption (dampening), or acoustic cancellation has an inherent pressure drop associated with it [Brun et al. 2008]. These intrinsic inefficiencies can result in a significant piping system energy loss, often exceeding 5% of the total compression power. Clearly, to properly design reciprocating compressor stations, an accurate prediction of these pressure losses is imperative.

Pipe flow pressure losses can be divided into steady state pipe friction and time-transient losses. In the reciprocating compression industry, the term “dynamic pressure loss” is used (somewhat freely as it has a completely different meaning in the field of conventional fluid-dynamics) to describe the sum of the time-transient pressure losses. These losses include periodic flow fluctuations (pulsations), process system transients, and random flow (usually turbulence) unsteadiness.

Thus, the dynamic pressure drop in reciprocating compression are flow energy losses that are associated with the unsteady component (rather than steady-state) of the highly transient flow through the piping system in a compressor station. Conventionally, dynamic pressure losses are determined by assuming a periodically pulsating 1-D flow profile and calculating the transient pipe friction losses by multiplying a friction factor from the Moody diagram with the flow dynamic pressure component ($\frac{1}{2}\rho v^2$) for each time step for a single time-discretized pulsation period. Unfortunately, this simplification does not capture all physical mechanisms that contribute to the actual dynamic pressure loss. Namely, the dynamic pressure loss is more complex and is not a single component but rather consists of four different physical mechanisms.

2 Physical Basis: Formulation of Fluid Equations

The dynamic pressure drop in reciprocating compressors are flow energy losses that are associated with the unsteady component (rather than steady-state) of the highly transient flow through the piping system in a compressor station. Conventionally, dynamic pressure losses are

determined by assuming a periodically pulsating 1-D flow profile and calculating the transient pipe friction losses by multiplying a friction factor from the Moody diagram with the flow dynamic pressure component ($\frac{1}{2}\rho v^2$) for each time step for a single time-discretized pulsation period. Unfortunately, this simplification does not capture all physical mechanisms that contribute to the actual dynamic pressure loss. Namely, the dynamic pressure loss is more complex and is not a single component but rather consists of four different physical mechanisms. The origin of three of these individual mechanisms can be identified in the governing equations of transient 1-D fluid dynamics, the Navier-Stokes equations. The Navier-Stokes equations consist of (1) the conservation of mass (continuity), (2) the conservation of momentum, and (3) the conservation of energy equations. These are:

$$\frac{\partial \rho}{\partial t} + \frac{\partial(\rho u)}{\partial x} = 0$$

- Conservation of Mass

$$\rho \frac{\partial u}{\partial t} + \rho u \frac{\partial u}{\partial x} + \frac{\partial p}{\partial x} = \mu \nabla^2 u$$

- Conservation of Momentum

$$\rho c_v \frac{\partial T}{\partial t} + \rho c_v u \frac{\partial T}{\partial x} = \mu \nabla^2 T + \Phi$$

- Conservation of Energy

where temperature is related to pressure and density through an equation of state and Φ is the viscous dissipation function. The individual terms of these equations and their physical meaning in transient pipe flow have been previously described [Brun et al. 2007] and are, thus, not further discussed herein.

The aforementioned four individual dynamic pressure loss mechanisms, which will be described in more detail below, are mathematically coupled by the governing equations and are functions of the dependent variables of the equations (velocity, pressure, density) and the physical properties of the fluid (determined from the real equations of state). However, the dynamic loss mechanisms are only weakly physically inter-related and can be individually assessed to determine an additive combined pressure drop of unsteady and periodically pulsating flow in reciprocating compressor piping networks. These four pressure loss components are:

- 1 Transient boundary layer viscous losses
- 2 Non-uniform flow internal profile shear stresses, secondary flows and turbulence

- 3 Inertial momentum change losses
- 4 Fluid to piping driven dynamic structural losses

The first mechanism (transient boundary layer viscous loss) is well understood and derives from the normal and bi-normal viscous terms of the momentum equation:

$$\mu_T \nabla^2 u = \mu_T \left(\frac{\partial^2 u}{\partial x^2} + \frac{\partial^2 u}{\partial y^2} + \frac{\partial^2 u}{\partial z^2} \right) = \mu_T \frac{\partial^2 u}{\partial x^2} + \frac{1}{2} \rho V^2 \frac{l}{d} c_f$$

where μ_T is the combined viscosity and turbulent eddy viscosity, V is the streamwise bulk flow velocity, and c_f is a viscous loss coefficient for pipe flow. This is, as described above, determined from pipe friction loss coefficients using Moody diagrams or other empirical tabulations. Specifically, the dynamic pressure loss is:

$$\Delta P = \iint \mu_T(x,t) \nabla^2 u(x,t) \cdot dxdt$$

For this calculation it is important to consider the effects of the local Reynolds number, and for high flow velocities also the Mach number, of the profile-averaged pipe flow (for every time step and at every calculation node) on the empirical loss coefficient, c_f . Transient boundary layer losses are usually the largest contributor to the total pipe flow dynamic pressure drop.

The second dynamic loss mechanism, the non-uniform flow profile shear stresses, secondary flows, and turbulence losses, are usually very low in pipe flow and do not contribute significantly to the associated dynamic pressure drop. However, they can be a primary cause for acoustic noise generated in pipe flow, especially for highly turbulent or three-dimensional flow profiles. This energy loss is caused by internal (non-boundary layer) transient shear stresses of the non-uniform unsteady flow profile and secondary flows. To properly calculate this, the viscous loss terms from the energy equation (also called the viscous dissipation function) must be integrated over space and time in all three dimensions as shown in this equation:

$$\begin{aligned} \Delta P &= \iiint \Phi(x,t) \cdot dxdt \\ &= \iiint \mu \cdot \left(2 \cdot \left(\frac{\partial u}{\partial x} \right)^2 + \left(\frac{\partial u}{\partial y} \right)^2 + \left(\frac{\partial u}{\partial z} \right)^2 \right) \cdot dxdt \end{aligned}$$

This calculation can also capture the above described boundary layer losses if the integration is carried all the way into the flow's boundary layer region. However, this is mathematically inconvenient, and it is more practical to utilize the previously described approach. Since for most piping transient flow analysis, the flow is assumed

to be one-dimensional, it is often difficult to properly perform this 3-D calculation. Sometimes the relative contribution of the secondary flow losses to the overall pressure drop can be estimated from empirical co-relations, but for complex three-dimensional piping configurations, these approximations tend to be poor.

The third contributor to the dynamic pressure loss, the inertial momentum change of the fluid, is caused by the continuous acceleration and deceleration of the fluid molecules in unsteady pipe flow. This is identical to the mass times acceleration terms in Newton's law of force balance ($F=ma$). The energy expended for this momentum change can be determined from an integration of the time and space inertial terms of the momentum equation:

$$\Delta P = \iint \rho(x,t) \left(\frac{\partial u}{\partial t} + u \frac{\partial u}{\partial x} \right) dxdt$$

This dynamic loss is often overlooked, but can significantly contribute to the dynamic pressure loss in highly pulsating flows. However, if a transient flow solver of piping flow is properly implemented and computes the discretized inertial terms of the momentum equation accurately, this pressure loss becomes implicit to the solution and does not have to be separately calculated or added.

The fourth mechanism to contribute to dynamic pressure losses in transient pipe flow, the fluid to piping driven dynamic structural losses, requires an improved physical understanding of the piping system as it involves fluid and structural interaction. This is the only mechanisms that cannot be directly identified in the governing fluid flow equations as it interacts with the fluid in the form of an externally applied body force. Specifically when pressure pulsations from the unsteady pipe flow become excessive, they cause pipe vibrations. These structural vibrations require excitation energy to overcome structural damping of the piping which must be absorbed from the transient flow energy. To generate piping vibrations, the flow must transfer some energy to the pipe structure which necessarily results in a pressure loss. This loss calculation is often neglected as it requires complex dynamic modeling of the energy transfer from wall pressure fluctuations onto the piping structure. Unfortunately, these losses can be rather significant contributions to the dynamic pressure loss in pulsating pipe flow. Furthermore, the dynamic pressure losses due to flow pulsation driven piping vibrations are not well understood and have not been previously quantified in the public domain and literature, particularly for highly pulsating piping flow.

A number of experiments were performed by SwRI in a reciprocating compressor closed loop facility to determine these loss components using dynamic pressure and vibration measurements for a number of resonant, non-resonant, and resonant-clamped pipe operating conditions. Results show that the dynamic structural loss component can be significant and cannot be ignored when predicting dynamic pressure behavior. This paper describes findings from these experiments and aims to quantitatively assess the above described components individually for a typically reciprocating compression system. Analytical, CFD and experimental data are presented.

3 Background: Literature Review

Fluid Structure Interaction (FSI) is a phenomenon which has been studied for various fluid types (water and other liquid flow, gaseous flows, multi-phase regimes) and for a range of structural systems (bearings, tubing lines, reactor vessels, “stiff” piping). Research in the energy industry has investigated FSI for applications such as flow induced vibration in power plants, pressure pulses generated by valve opening/ closing (water hammer events), and dynamic pressure loads on pressure vessels. Though physically relevant, the majority of previous modeling and experimental work has focused on incompressible flows or transient fluid loads on a structure. The majority of significant developments over the last thirty years in modeling and experimentally documenting FSI for the energy industry are contained in the ASME Journals, Pressure Vessels and Piping (PVP) Division. Sloshing effects caused by fluid dynamic loads were also studied by NASA in the context of spacecraft design throughout the period of 1960-1980.

Fluid slosh in liquid propellant tanks was found to influence the spacecraft attitude and position if left uncontrolled [Abramson, 1966]. The resulting propellant tank design was governed by control and stabilization of the interacting fluid and structure systems. Kana (1966) extended the work further to analyze compressible fluids with inertial forces. Kana discusses solution of the wave equation with boundary conditions for the unsteady fluid pressure at the cylinder wall in a tank. Similar studies were also performed by Moody in 1990 and 2007 in relating gas effects to acoustic amplifications in liquids.

Previously, the use of the acoustic wave equation was more relevant because fluid flow in a tank was negligible and higher order effects of the pressure perturbation were not a considerable percentage of the pressure forces. This is no longer the case in high pressure pulsating gas flows.

The FSI equations and methodology is discussed in the context of hydrodynamic sloshing loads, bending of pipes due to temperature differentials and establishment of design guidelines for pipe line size and velocity based on allowable vibrations induced by fluid flow [Diwakar and Lin, 2007]. In the 2007 modeling by the two authors, a combination of CFD and FEA is utilized to predict pipe vibration in compressor discharge piping. The unsteady flow rate from two compressors is simulated in CFD and used to predict vibration in a 12-inch diameter header connected by 10-inch diameter lateral lines using FEA. The erosion velocity limit was assumed to be 100 m/s, and this limit was also validated in the work. Both single phase and multiphase fluid domains were utilized in CFD. Fluid pressures on the piping system due to the unsteady flow are superimposed in the FEA to obtain stress on the pipe network. This work extended the use of the FSI approach by combining a fluid domain model with structural model – but no experimental data was available to correlate the results to verify the approach.

Tweten et al. (2008) studied the physics of pulsations in piping systems. This paper focused primarily on the pressure pulse behavior in different attenuating circumstances, typically used or seen in reciprocating compressors. These included the influence of friction, orifice plate restrictions (choking effect) or branch lines/ choke-volume systems (shifting of phase.) The paper also highlighted the improvements to pulsation analysis methods realized by a new formulation of the Navier Stokes equations, which includes the critical terms typically left out by the acoustic wave equation or method of characteristic solutions. These terms include the mean through-flow, second order pressure/ velocity terms, and viscosity terms. As pulsations in real piping systems are non-negligible portion of the flow stream, and the mean flow component is significant, the inertial transport terms and the viscous terms of the governing equations must be included in the analysis to prediction transient dynamic pressures.

4 Fluid Structure Interaction

The fundamental FSI equations may be presented in terms of energy conservation, where the overall energy of the system is conserved and essentially consists of trading energy back and forth, from the structure to the fluid and vice versa. One of the expressions of the energy conservation approach is provided by the variation formulation [Shaaban, 1979]. The structural force equation includes a coupling matrix multiplied by the incident pressure:

$$\{F_S\} = [K]\{\delta_U\} + [M + ADM]\{\ddot{\delta}_U\} + [S]^T\{\delta_{Pi}\}$$

The added mass matrix [ADM] is defined as a product of the coupling matrix transposed, a stiffness matrix, and the coupling matrix itself:

$$[ADM] = [S]^T [K_{UU}]^{-1} [S]$$

The ADM term represents the inertial fluid mass exerted on the structure as force, based on the acceleration term.

The entire pressure in the system (Pu) is represented by:

$$\{\delta_{Pu}\} = \{\delta_{Pr}\} + \{\delta_{Pi}\}$$

This is a combination of the incident pressure (Pi) attributed to the known pressure prescribed in the fluid flow and the fluid-structure interaction pressure (Pr) determined by the hydro-elastic fluid coupling:

$$\frac{\partial^2 \mathbf{w}}{\partial t^2} = \frac{-1}{\rho_f} \frac{\partial P}{\partial \mathbf{n}}$$

Based on these equations, it becomes apparent that a balance exists between the stiffness (affected by clamping the pipe in place), movement of the pipe wall (measured by strain gage measurements as vibrations) and the incident pressure force (measured in terms of dynamic pressure) exerted on the structure by the fluid, through a coupling coefficient. Although this formulation may be over simplified, it can be shown that the higher order acceleration term of a pipe at resonance will act as a method of dissipating (or removing) energy from the fluid forces within the pipe. If the pipe is held rigid, and the displacement and acceleration terms are restrained, the total system energy resides in the fluid itself or in the damping produced by the clamps on the structure. The acceleration term is believed to play a significant part in dissipating energy at resonance. In the non-resonant condition, the acceleration term is much smaller and not able to influence the incident pressure significantly.

The net effect is that at resonance: the structural vibrations remove energy from the fluid flow and result in quantifiable power loss which can be considered dynamic pressure losses.

The present research is concerned with large pressure pulses (relative to the mean fluid pressure)

in compressible flows during a resonant condition, where the structure itself is coupled strongly to the fluid forces exerted on the structure at a single resonant frequency, determined by the compressor generated pressure pulse. Because of the complexity of the pressure pulse behavior outside the compressor cylinder, the piping system response, and the fluid/ structure coupling, the classic FSI equations may not be directly applicable in all instances. Furthermore, the present findings suggest further study of the coupling between fluid and structure at resonance is warranted.

5 Experimental Setup

In order to obtain a practical basis for the interaction of the fluid flow pulsations with the piping vibrations on and off resonance, a simple set-up was constructed using the SwRI reciprocating air compressor laboratory. This testing also provided experimental dynamic pressure and pulsation data to compare against the computational fluid dynamics model. The purpose of the test was to accurately determine the flow pulsations/ dynamic pressure losses and pipe displacement/ acceleration in three directions, in a normal operating mode without an acoustic resonance and in a resonant condition when the half-mode wavelength frequency coincided with the compressor excitation frequency. The compressor discharge piping was installed with a long, straight length of 4-inch diameter pipe exiting the compressor discharge. The length of piping was approximately 18 feet from the exit of the discharge valve to the entrance of the first volume bottle. The half-wave mode of the resonant length (which included all loop piping back to the volume control bottles) coincided with a 14.5 Hz response. This pipe acoustic response coincided (purposefully) with the second order response of the compressor at 435 RPM. A speed sweep used to determine the primary system resonance is shown in Figure 1.

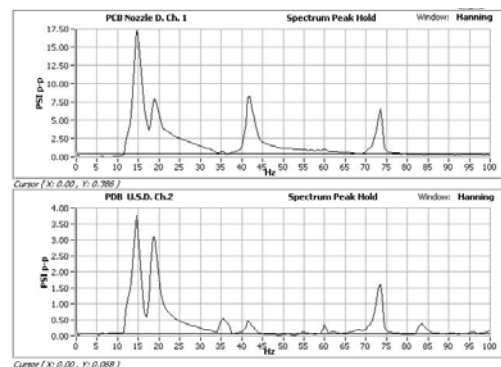


Figure 1: Speed Sweep Data to Determine System Resonance at 435 RPM for 2x Order (Both Dynamic Pressure Transducers on Upstream and Downstream End of Pipe Shown)

The discharge piping was instrumented with fast response dynamic pressure transducers as well as strain gages oriented in the horizontal, vertical and pipe axial directions on the primary discharge pipe as indicated in Figure 2 below. The test set-up allowed the pulsations in the discharge flow to be measured at the true compressor nozzle, immediately downstream of the discharge valve, and at the inlet to the first volume bottle.

The differential pressure drop between these two test points was also measured with a fast response dynamic pressure transducer. A diagram of the test points and piping lengths is shown in Figure 2. The pre-test photograph of the loop piping is shown in Figure 3.



Figure 2: Schematic of Experimental Test Setup and Measurement Points

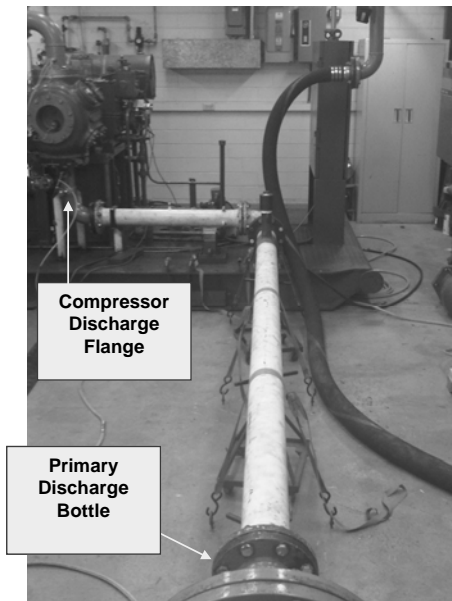


Figure 3: SwRI Air Compressor Discharge Piping

A calibrated Validyne dynamic differential pressure transducer was used to determine dynamic pressure loss across the discharge pipe.

The average dynamic pressure was recorded for each 2-minute “steady state” test run. The three directional strain gages were used to record vibrations for total pipe movement.

The air compressor was operated at a pressure ratio of 2.5 (with a fixed suction pressure at 25 psia) over its speed range of 300-1000 RPM. The test matrix consisted of measuring the pulsations, differential pressure, and vibrations at fixed operating speeds - on and off resonance - including 435, 600, 870, and 1000 RPM. The test matrix was repeated for the clamped case where the pipe was firmly held clamped to piping supports. Knowing the precise resonant and non-resonant conditions, each test run was recorded for a 2-minute time period once steady state upstream/ downstream pressures had been established.

(Note: the first order (1x) excitation at 870 RPM coincided with the acoustic mode of the straight discharge pipe as well. However, the compressor was double-acting and did not have a strong 1x response, as reflected in the data).

6 Test Results

The differential pressure loss is plotted in Figure 4 for each test run. At the non-resonant speeds of 20, 28, and 34 Hz, the dynamic pressure loss is less than 0.1 psi for both the clamped and unclamped condition. Due to the uncertainty of the measurement, the free pipe and clamped pipe exhibited statistically equivalent pressure losses. However, at the resonant condition of 14.5 Hz, the free pipe showed a significantly greater dynamic pressure loss 0.51 psi, compared to 0.14 psi for the clamped pipe. This dynamic pressure loss is separate from the steady state fluid loss component.

The results show a clear difference between resonance and off-resonance conditions for dynamic pressure loss. The benefit of restraining the pipe movement is demonstrated in the reduced dynamic pressure loss in the case of the clamped pipe. These results show the importance of considering structural movement as a loss mechanism at resonance. By considering only flow-induced pulsations, the dynamic pressure loss would be under-estimated, especially in the case of unrestrained pipe.

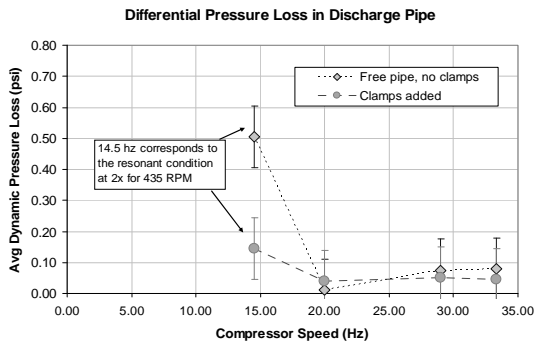


Figure 4: Experimental Dynamic Pressure Losses for Free (Unrestrained) and Clamped Pipe

7 Computational Fluid Dynamic Model Comparison

Models of the system were created in the CFDesign V.10 Computation Fluid Dynamics (CFD) package. The purpose of the models is to predict the pressure loss in the discharge pipe due solely to fluid effects. This modeling effort allowed the energy dissipation to the structure – which was measured experimentally – to be characterized apart from the fluid dynamic losses, which were predicted by the CFD program. Two models were considered: a steady state flow model and a transient flow condition imposed at the discharge flange boundary. The transient model is more representative of the actual reciprocating compressor flow and highlights the additional dynamic pressure loss due to a pulsation flow. The two models begin at the discharge nozzle, include the bottle, and end at the output to the flexible hose (See Figure 5 below). CFD analysis included three-dimensional effects and highly sophisticated fluid models which provided good accuracy especially compared to one-dimensional models.

The first CFD model is the time domain transient model that includes a harmonic flow at the discharge nozzle. The peak flow and frequency of this boundary condition were modeled after the actual experimental conditions. The output of this transient model include the flow and pressure in the model at sampled times. The average pressure at the nozzle and at the bottle can then be calculated over a cycle. The second CFD model is a steady state model that has a single constant flow applied at the discharge nozzle. This steady flow is equivalent to the average flow through the experimental setup. The dynamic model provides pressure loss due to both steady flow and pulsations while the steady model only includes losses due to steady flow. A comparison of the calculated pressure loss in the discharge pipe by both models is shown below in Figure 5.

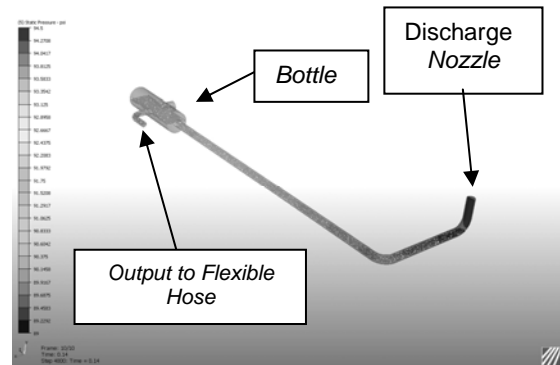


Figure 5: CFD Model of Experimental System

Apart from the CFD models, a one-dimensional (1D) model was also created to compare to the experimental test data and CFD results. The 1D model uses the TAPS time domain solver that includes all of the Navier-Stokes terms. This type of solver provides an accurate model of pulsation systems. However, since the model is one-dimensional, the 1D model will not be as accurate as the CFD model, especially for pressure loss calculations. Two 1D models were created to match the dynamic and steady CFD models. The 1D models include the cylinder gas passages, discharge pipe, bottle, flexible hose, and a second bottle at the end of the hose. Pressure losses of the discharge pipe were calculated for both models and compared with the CFD results and experimental data in Figure 6 below.

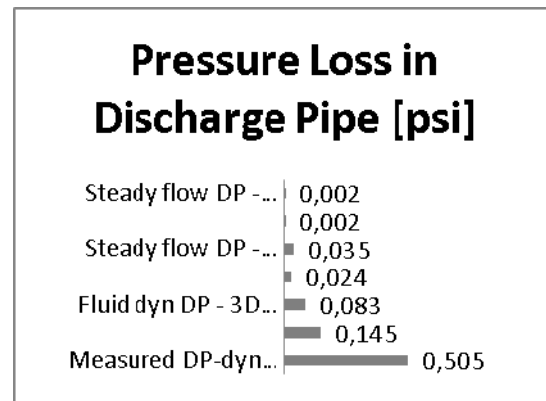


Figure 6: Comparison of Measured and Calculated Pressure Losses in the Discharge Pipe

The above results for dynamic pressure loss predictions and measured data provide insight into the many sources of dynamic pressure loss and the actual losses departure from steady flow in one-dimension. Figure 6 above shows the pressure losses measured and calculated across the 18-foot length of discharge pipe. All calculations assume the exact same geometry, length, friction factor, and gas conditions. The two largest losses were both measured on the experimental setup. The largest loss (0.505 psi) was measured in the experimental case when the discharge pipe was free to vibrate.

The loss for the free vibrating pipe was approximately three times the energy loss of the clamped pipe. The most sophisticated model, with a transient flow condition imposed in the three-dimensional CFD code, under-predicts the dynamic pressure loss by a factor of 6.

The second experimental data point was collected while the discharge pipe was constrained and has a measured loss of 0.145 psi. The clamped test condition also exposed higher losses than any of the models predicted which highlights the structural energy dissipation at resonance even in the case of clamped pipe. In the case of the clamped pipe, the 3-D transient fluid model still under-predicts dynamic pressure loss by a factor of approximately 2.

8 Conclusions

In many compressor stations and fluid piping systems, acoustic and mechanical resonance occurs when the piping natural modes correspond to the excitation source energies. The present work demonstrates that the dynamic pressure at resonance behaves differently than at off resonant conditions.

The experimental test results show a clear difference between resonance and off-resonance conditions for dynamic pressure loss. Furthermore, dynamic pressure losses in the case of unclamped pipe exceed the steady state pressure loss. This can be explained by both the high pulsation flow induced losses and the transferred energy to the structural vibrations. Restraining the pipe movement considerably reduces dynamic pressure loss. These results show the importance of considering structural movement as a loss mechanism at resonance.

Neither the CFD nor the 1D transient model can predict losses due to mechanical phenomenon, and as expected, neither model is close to the experimentally measured dynamic pressure loss. Differences between the calculated and measured dynamic pressure losses are likely due to:

1 *Structural/ mechanical losses in the actual experimental setup:* Fluid structure interactions are not considered in models of reciprocating compressor systems, and these structural energy dissipations will add or remove energies at resonance. Based on data shown here, (depending on clamped or unclamped pipe) **the structural energy dissipation at resonance is 2 to 6 times the predicted dynamic pressure loss due to fluid effects alone.**

- 2 *Three-dimensional fluid dynamic effects:* The calculated pressure loss from the 1D model is much lower than the measured pressure drop. This is expected since 1D models tend to be less accurate than CFD models when calculating pressure drop even if the pulsation levels are predicted accurately.
- 3 *The effect of pulsating flow:* All of the steady flow calculated pressure drops are much lower than the measured pressure drops. Steady pressure losses are expected to be lower than dynamic pressure losses since pulsations have peak velocities that are larger than the steady velocity (due to $\rho \cdot V^2$), and these are not considered a steady flow calculation. The peak velocities in dynamic flow increase the overall pressure loss in a section of pipe.

By considering only flow-induced pulsations, the dynamic pressure loss is underestimated, especially in the case of unrestrained pipe. Accurate depiction of dynamic pressure loss must consider the energy losses due to structural vibrations as well as the fluid forces.

Since the resonance condition introduces a strong coupling between the fluid and structure, the fluid dynamic pressure can become very large, and the system will attempt to dissipate energy in the form of $F=ma$ (the structural mass multiplied by the pipe wall acceleration). The experimental data shows a clear amplification of dynamic pressure loss at resonance when the pipe is not clamped down. In this case, the fluid-structure interaction becomes more pronounced, and the fluid loses energy to the structure itself.

The application of these results shows the necessity of avoiding resonance through careful design of the piping system. In the case of strong fluid-structure interaction, the data also suggest that the full value of dynamic pressure losses must consider two terms - the losses due to structural movement as well as the pulsating flow. Through both analytical and experimental results, the dynamic structural loss component is shown to be significant when at a resonant condition with close fluid/ structure coupling. This structural loss should not be ignored when predicting dynamic pressure behavior. However, without detailed field test measurements, it is difficult to characterize or estimate the dynamic pressure losses based on fluid models alone.

References

Abramson, H. Norman, "The Dynamic Behavior of Liquids in Moving Containers," NASA SP-106, Published by NASA, Washington, D.C., 1966

Divakar, Phillip and Lin, Lorraine, "Study of Dynamic Stress in Piping Networks and Pressure Vessels using Fluid-Solid Interaction Models," 2007 Proceedings of ASME Pressure Vessel and Piping Division Conference, ASME Paper No. PVP 2007-26009

Moody, F. J., "Acoustic Amplification of a Vertical Liquid Column Bouncing on a Gas Volume, 2007 Proceedings of ASME Pressure Vessel and Piping Division Conference, ASME Paper No. PVP 2007-26031

Tweten, D., Nored, M., and Brun, K., "The Physics of Pulsations," Gas Machinery Conference 2008 Proceedings, Albuquerque, New Mexico, October 6, 2008



Gas Passage System Pulsation Analysis for Modern Reciprocating Compressors

by:

Marybeth Nored

Eugene “Buddy” Broerman

Klaus Brun, Ph.D.

Fluids & Machinery Engineering Department

Southwest Research Institute

San Antonio

USA

marybeth.nored@swri.org

eugene.broerman@swri.org

klaus.brun@swri.org

**7th Conference of the EFRC
October 21th / 22th, 2010, Florence**

Abstract

Pulsation models of reciprocating compressor systems commonly utilize a one-dimensional (1-D) representation with acoustic length modifications to represent the three-dimensional system. Given the simplicity and cost-effectiveness of this approach, one-dimensional models are the preferred means of analyzing dynamic pressures in the compressor system and generally accurate for piping systems where the dominant physical length is in the flow direction. In the areas near the compressor cylinder, very close to the fluid force excitation from the piston, the 1-D assumptions break down since many of the high-frequency energy components have not diminished. The following paper describes a new methodology and its benefits for pulsation analysis of the gas passage system (which includes the cylinder nozzle and primary volume bottle). The intent of the investigation by Southwest Research Institute was to determine the most effective method of predicting natural acoustic responses and expected pulsation levels within the gas passage system. The study resulted in an improved means of developing a 1-D representation using a 3-D acoustic modal analysis, which provides much improved predictions of nozzle and gas passage resonances. This work validated the new approach and refined the SwRI 1-D Navier Stokes fluid modeling method. SwRI also determined the potential benefit of a small Helmholtz resonator designed to attenuate problematic gas passage responses in the range of 100-300 Hz.

1 Introduction

Pulsation models of reciprocating compressor systems commonly utilize a one-dimensional (1-D) representation with acoustic length modifications to represent the three-dimensional system, given the simplicity and cost-effectiveness of this approach. One-dimensional models are generally accurate for piping systems where the dominant physical length is in the flow direction. In the areas near the compressor cylinder, very close to the fluid force excitation from the piston, the 1-D assumptions break down since many of the high-frequency energy components have not diminished. A new methodology and its benefits for advanced pulsation analysis of the cylinder gas passage system (which includes the cylinder nozzle and primary volume bottle) is studied in this work. The intent of the investigation by Southwest Research Institute was to determine the an improved method of predicting natural acoustic responses within the gas passage system and the potential value to operating companies in applying the new methodology.

Without accuracy in both frequency and amplitude predictions of the related gas passage resonances, it is unclear whether a significant acoustic resonance exists. For new compressor cylinder designs, certain 1-D representations of the gas passage may not be valid and could lead to incorrect predictions. Uncontrolled responses associated with the cylinder gas passage system are primarily evident as higher frequency pulsations and vibrations at the compressor valves, cylinder body and in the cylinder nozzles. Incorrect designs will lead to use of cylinder nozzle orifice plates, poor valve life and low compressor efficiency due to high dynamic pressure drop.

SwRI conducted an investigation of the acoustic responses related to typical high speed reciprocating compressor cylinder gas passageways. Many times, a 3-D transient CFD model is too time and cost intensive and cannot be justified for standard design studies (i.e., API 618 acoustic analyses). However, the combination of a 3-D acoustic response model and a 1-D fluid representation model can provide accurate predictions of all gas passage system responses in a cost effective manner. This work validated the new approach and refined the SwRI 1-D fluid modeling method.

2 Background

Three-dimensional (3-D) acoustic responses in the compressor cylinder gas passageways due to the dynamic flow through the compressor valves can have a significant influence on the performance of the compressor. In some cases, the high-frequency

uncontrolled acoustic resonances could lead to valve failures, cylinder pulsations and vibrations, and compressor manifold system vibrations. Since the acoustic frequency content tends to be much higher in the gas passageways than in other areas of the manifold system, the cycles to metal fatigue failure are considerably reduced. Additionally, cylinder nozzle pulsations near the gas passage / nozzle resonant frequency can produce major nozzle vibrations and require the addition of power consuming orifice plates in the flow stream to adequately control pulsations.

Standard fluid models of reciprocating compressor systems use a one-dimensional representation with acoustic length modifications to represent the three-dimensional system. This is adequate except in two cases: (1) when the overall geometry is highly three-dimensional, such that one particular length does not dominate and it is difficult to collapse to a one-dimensional representation (this is the case in the internal gas passages (IGP's)); and (2) when dynamic pressure frequency content is high enough that the wavelength of the response frequency is not influenced by the corrections for one dimension.

There are several significant acoustic responses related to the gas passage and its connection to the pulsation filter bottles:

- 1 Valve-to-valve (VTV) acoustic responses are more analogous to an acoustic length response than a classic Helmholtz response. These types of responses are typically half-wave modes or higher orders of a length response – as indicated by responses 1 and 2 shown in Figure 1. These occur at higher frequencies in the range of 100-300Hz for most high speed compressors. This response depends on the length between valves and can be calculated by hand as a general approximation (as a closed-closed half wave response). Depending on the amount of high frequency excitation and the passage design, these can be strong sources of high frequency pulsation and vibration. These are internal to the gas passage and do not typically propagate beyond the compressor cylinder flange. If the reciprocating compressor valves have a mechanical natural response near the VTV pulsation wave frequency, this acoustic response can complicate the valve behavior and will adversely impact valve life.
- 2 The so-called “cylinder nozzle resonance” (CNR) is actually a combined effect of the gas passage, cylinder nozzle, and primary volume bottle. As such, it should be termed the passage-nozzle-bottle response – see response 3 in Figure 1.

- 3 These three component geometries in combination produce a small choke tube and open volume which produces a quasi Helmholtz acoustic response. Since the gas passage and nozzle dimensions often have similar diameters and lengths, the response is difficult to calculate by hand and must be simulated in a one-dimensional (or 3-D) fluid model. The nozzle resonance is often misrepresented as a quarter wave acoustic response (with open-end, closed-end boundaries) but it is in typically much closer in its behaviour to a Helmholtz type acoustic response.
- 4 Other acoustic responses at even higher frequencies (above 250 Hz) are possible due to radial modes, side-to-side length responses, and higher order components of the above responses. These are less likely to be problematic for modern high speed reciprocating compressors but coincidence with cylinder stretch excitation frequencies or mechanical resonances in the manifold system can still cause significant vibrations at times.

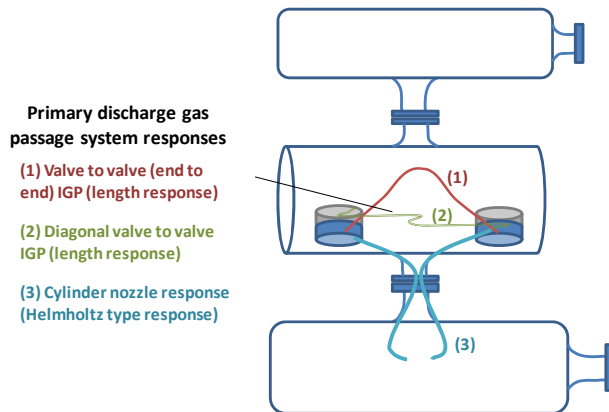


Figure 1: Conceptual View of Primary Gas Passage System Responses for a Typical Discharge Gas System on a Reciprocating Compressor

The various fluid dynamic models, which were used in this investigation, required either a fluid dynamics based approach or a finite element approach. The finite element solution was effectively an inverted solid model which allowed the fluid space to be created. The fluid space could then be analyzed for its natural resonances similar to how a solid body finite element model would predict mechanical natural frequencies. The 3-D response analysis using an acoustic modal tool provides only the resonant frequencies in the fluid domain (not their relative strengths or amplifications).

Both the 1-D and 3-D fluid dynamic models utilize the kinematics of the piston in the compressor

cylinder to determine a transient boundary condition based on the generated pressure pulse.

The models can determine acoustic responses of the fluid based on the natural acoustics and the excitation forces. However, the fluid models are more versatile than the finite element response modeling because the excitation forces modeled through the piston's compression process provide a "forcing function" to the fluid resonances, which allows the fluid models to predict the frequency and amplitude of the dynamic pressures. Frequency and amplitude determination are critical to an effective design process since many responses will arise in a given piping system and the design must focus on attenuating the high amplitude pulsations which can lead to component failures and poor performance.

After characterizing the forcing function in the fluid model, the boundary condition is then applied to the mass, momentum, and energy equations. The finite element approach utilizes the geometry of the gas passage to determine the natural acoustic resonances. The state of the gas in the compressor and manifold is determined by two factors: (1) the kinematics of the drive, which determines the volume inside the cylinder and the isentropic change of state in the gas, and (2) the inflow and outflow through the suction and discharge valves at the boundaries. The piston position, $z(\varphi)$, with respect to crank angle is given by:

$$z(\varphi) = \frac{V_s}{A_p} + r \times (1 - \cos \varphi) + \frac{r}{\lambda} \times \left(1 - \sqrt{1 - \lambda^2 \sin^2 \varphi}\right) \quad (1)$$

- where:
- r = crank radius
 - λ = rod ratio
 - V_s = clearance volume
 - A_p = piston area

The piston position translates to the transient gas pressures during the compression process. With the pressure-volume card which is generated by the piston position versus time trace, the boundary condition for a 1-D or 3-D fluid model is provided. This is effectively the velocity or pressure of the gas as it enters the suction valve (for a suction side model) or exits the cylinder through the discharge valve (for the discharge side model).

In order to calculate the velocity and the pressure at every time-step, the transient one-dimensional Navier-Stokes equations of fluid dynamics must be solved (Brun, 2007):

$$\frac{\partial \rho}{\partial t} + \frac{\partial(\rho v_x)}{\partial x} = 0 \quad (2)$$

$$\rho \left(\frac{\partial u}{\partial t} + u \frac{\partial u}{\partial x} \right) = -\frac{\partial P}{\partial x} + \mu_s \frac{\partial^2 u}{\partial x^2} \quad (3)$$

$$\Delta h_i + e = 0 \quad (4)$$

This equation can also be solved for all three directions with more terms as in a CFD code. However, the discretization method is important to the solution of this type of highly dynamic flow from a reciprocating compressor. The third equation of the Navier-Stokes equations (4) will provide for heat transfer effects, important to the performance calculations. However, the mass and momentum equations are the governing solution for the prediction of pulsation levels from the reciprocating compressor cylinder.

In the past with a linearized wave equation solution to the one-dimensional fluid problem, all physical lengths were adjusted to "acoustic dimensions" which also compensated for 3-D effects. One of the classic end effect equations for a choke tube within a larger pulsation bottle is provided below:

$$L_e = L + D_c \left(0.85 - 1.06 \left(\frac{D_c}{D_b} \right) \right) \quad (5)$$

where:

L_e = new length with the end-effect included

L = length without the end-effect

D_c = smaller diameter (typically the choke tube)

D_b = larger diameter (typically the bottle diameter)

Another effect that becomes more important in smaller dimensioned bodies is the effect of compressibility on a small gas passageway. Typically, to adjust for a smaller cavity volume and the compressibility effect, a damping coefficient and modified frequency may be calculated that includes the density and viscosity terms of the fluid (Persico, et al., 2005):

$$\omega_n = \frac{c}{L \sqrt{\frac{1}{2} + \frac{v}{v_t}}} \quad \text{and} \quad \zeta = \frac{16\mu L \sqrt{\frac{1}{2} + \frac{v}{v_t}}}{d_t^2 c \rho} \quad (6)$$

However, these correction terms are only general methods of adjusting the classic linear wave equation models. It is now possible using advanced models with viscous effects, fluid compressibility and non-linear dynamic velocity terms to accurately predict these effects.

3 Approach

The SwRI study compared the fluid and finite element model results to data obtained on two high speed compressors. To focus the investigation, only the discharge system was studied from the discharge valves through the gas passage in the cylinder, through the cylinder nozzle to the first volume bottle. The discharge system is typically where higher pulsation amplitudes are observed, which makes this system easier to characterize through field measurements. Two data sets were available to verify the models:

- Case A: A fixed speed machine operating at 890 RPM. Data was recorded at the discharge valve at various load steps including fully double acting and other unloading steps using volume pockets. The discharge nozzle response was measured after the addition of orifice plates at the cylinder nozzle flange, which dampened the nozzle response.
- Case B: A variable speed machine operating from 825-1,000 RPM. Data was recorded on both the head and crank end in the discharge valves for the double acting (fully loaded) cylinder. Data was recorded prior to installing orifice plates at the nozzle flange.

The discharge valve cap on each of the machine cylinders was used as the dynamic pressure measurement point for the field pulsation data. The following advanced models were developed to compare to the gas passage and cylinder nozzle responses seen in the field data:

- 1) A 1-D representation model in the advanced SwRI pulsation modeling tool (TAPS). This model includes all terms of the Navier-Stokes equations in one-dimension.
- 2) A 3-D finite element type model using acoustic modal analysis tools, used to predict frequency responses and modes (using ANSYS FEA).
- 3) A full 3-D computational fluid dynamics (CFD) model solved with a transient boundary condition at the discharge valves, used to predict magnitude of pressure variation (%) and primary frequency responses.

The goal of the study was to determine if a combination of these advanced models could be used to better identify and predict both the cylinder nozzle response and the higher frequency gas passage responses for modern low and high speed compressors.

PULSATION & VIBRATIONS

Dynamic Pressure Losses in Piping Systems, *Marybeth Nored, Eugene Broerman, Klaus Brun;*
SOUTHWEST RESEARCH INSTITUTE

As part of the investigation, SwRI also examined possible design solutions for the higher frequency gas passage resonances using advanced pulsation control concepts from the Gas Machinery Research Council compressor research program. The use of a miniature virtual orifice (modified Helmholtz resonator) to absorb the valve-to-valve response showed particular benefit in mitigating high frequency pulsations.

3.1 Data Review of Primary Responses

In Case A, SwRI recorded field data at the fixed speed of 890 RPM for one cylinder of a six cylinder unit. The field data was taken at the discharge valve cap at various load steps. The field data showed somewhat high frequencies in the nozzle resonance region at 60 and 90 Hz – see Figure 2. However it was difficult to pinpoint the location of the true cylinder nozzle resonance due to the fixed speed operation. In comparing the double acting case when the unit was fully loaded to a more unloaded cylinder condition, SwRI found that the 5x excitation at near 75 Hz increased to 36 psi pk-pk (see unloaded case – Figure 3). This excitation is likely due to the primary nozzle resonance peak lying close to this frequency. Pulsation data for the two load steps is shown below:

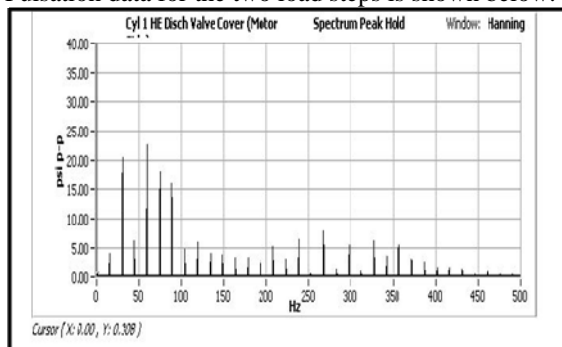


Figure 2: Case A Pulsation Levels at the Discharge Valve for the Fully Loaded Case

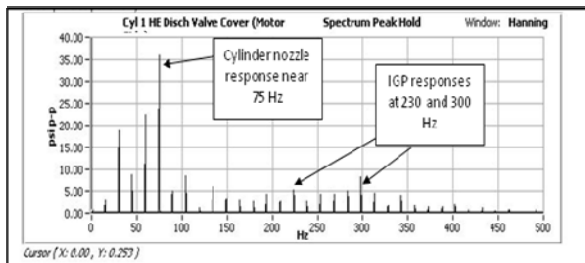


Figure 3: Pulsation Levels Measured at Discharge Valve in Unloaded Cylinder Operation, for Case A field site

As shown in Figure 1-2, the high frequency content of the dynamic pressure also showed significant responses in the gas passage at 200-250 and 300-350

Hz range, although it was difficult to determine the exact response due to the fixed speed test. These higher frequency responses were significant because the pulsation amplitudes were all measured to be between 5-10 psi pk-pk and had corresponding vibrations at the same frequencies. The gas passage responses were due to excitation of the various acoustic lengths across the cylinder chamber.

For Case B, field data was recorded during a speed sweep of the unit such that the responses coinciding with excitation from 825-1000 RPM (primary first order = 13.75-16.6 Hz). This case was added to the SwRI investigation of gas passage responses in order to further verify the 3-D response model and the fluid models. The speed sweep in the field allowed the responses in the gas passage system to be fully traced out, showing the exact location of pulsation maximums. The field data showed a fairly broad cylinder nozzle resonance at 65-75 Hz. The pulsation levels at the discharge valve cap due to the nozzle resonance were as high as 85psi pk-pk. Crank end pulsation levels recorded at the discharge valve cap are shown in Figure 3 for Case B. Lower amplitude responses were evident at 250 Hz and around 270 Hz on both ends of the cylinder. These responses were attributed to valve-to-valve length responses across the cylinder in the piston direction. (The nozzle resonant pulsations were causing high vibrations and were the primary cause of concern. The vibration issue was later rectified with orifice plate installation at the nozzle cylinder flange).

Both Case A and Case B were relatively high horsepower units which tended to cause higher frequency excitation in the gas passage area due to the added energy at higher orders in the system. Both cases exhibited acoustic valve-to-valve type responses in this higher frequency range.

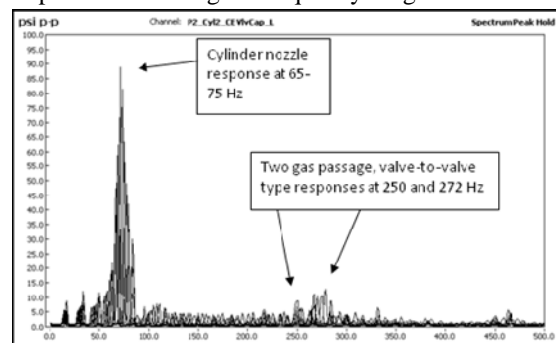


Figure 4: Pulsation Levels at the Discharge Valve Measured for Case B Field Site

3.2 3-D Response Model

The 3-D response analysis was performed using a combination of Solidworks and ANSYS finite element models to analyze the fluid space of the cylinder gas passage, nozzle, and filter bottle system. Acoustic modal analysis aims at determining the acoustic natural frequencies of a volumetric model. While all responses in a desired frequency range are determined using this type of analysis, not all responses are necessarily excited and are dependent on operating conditions. The outputs from the acoustic modal analysis are the natural frequencies and their corresponding mode shapes.

The acoustic modal analysis tool is an effective means of determining the natural responses of a solid or fluid domain but when used by itself, this type of analysis will not determine the amplification of the various responses. It is a true three-dimensional model and provides a means of visualizing the acoustic response, which can be beneficial in determining means of attenuating, altering or shifting the acoustic response.

In determining the significance of the various responses, the designer must review the dimensions and acoustic node and anti-node points in the response plots.

For Case A, the 3-D acoustic response model predicted four responses in the gas passage system – see Figure 5. The primary responses of significance to the manifold system were the cylinder nozzle response predicted at 80.5 Hz and the valve-to-valve response at 302 Hz, in the piston direction. Other internal gas passage responses predicted for Case A included a side-to-side response opposite the piston direction at 236 Hz and a diagonal valve-to-valve response at 333 Hz.

Although the field data for Case A was only available at the fixed speed of 890 RPM, the cylinder nozzle response at 80 Hz was close to the field data high pulsations at 35 psi pk-pk observed at 75 Hz during the unloaded operation (when off order excitation for 1x, 3x, 5x etc. would have been higher). The primary length response within the gas passage was predicted at 302 Hz. This response had good correspondence in the field data at the same frequency because it was the dominant acoustic response to the gas passage.

For Case B, the 3-D acoustic response model predicted four responses in the gas passage system which matched very closely to the field data – see Figure 6. The primary responses of significance to the manifold system were the cylinder nozzle response predicted at 67 Hz and the valve-to-valve response at 258 Hz and 277 Hz.

The cylinder nozzle resonance predicted to be at 67 Hz in the 3-D response model, actually peaked at approximately 70 Hz in the field data. The small

frequency shift from the field data was likely due to damping effects and the magnitude of excitation frequencies in the actual field system. This was also a fairly broad cylinder nozzle response which could be excited by multiple compressor orders, as shown by the field data speed sweep.

The gas passage responses at 258 and 277 Hz also matched the field data closely (shown in Figure 3). Both of these responses were aligned with the piston direction, which served as the forcing excitation for the fluid system. The side-to-side gas passage response at 180 Hz was not as amplified in the actual system. One reason for the diminished amplification of this response is due to its direction conflicting with the piston direction. As such, this response was not as evident in the field data.

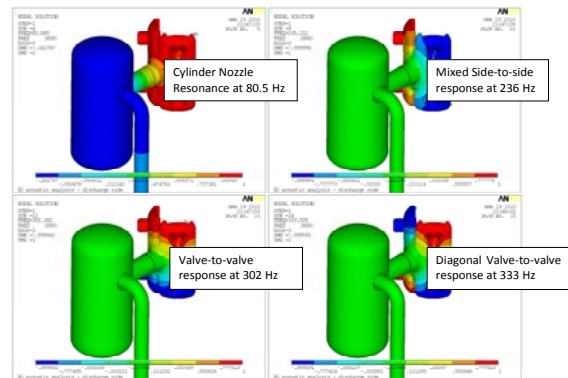


Figure 5: 3-D Response Analysis for Case A – Primary Responses Shown at 80.5 Hz, 236 Hz, 302 Hz and 333 Hz

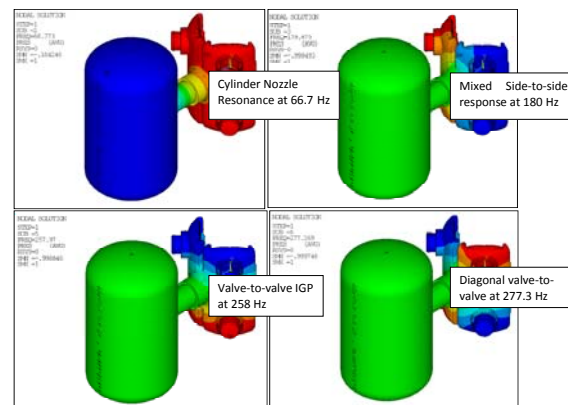


Figure 6: 3-D Response Analysis for Case B – Primary Responses Shown at 66.7 Hz, 180 Hz, 258 Hz and 277.3 Hz

3.3 3-D Transient Fluid Model

The next option considered in the gas passage pulsation analysis was to utilize a full 3-D fluid dynamic model run for a transient condition.

PULSATION & VIBRATIONS

Dynamic Pressure Losses in Piping Systems, *Marybeth Nored, Eugene Broerman, Klaus Brun;*
SOUTHWEST RESEARCH INSTITUTE

Any CFD analysis depends on the solution of the Navier-Stokes equations, which define any single-phase fluid flow. In this case, the fluid equations were solved using the ANSYS CFX tool after the computational mesh of the fluid space was generated. Then the boundary conditions were applied and the simulation was started, where the equations were solved iteratively as a transient problem. The simulation was appropriate because the pulsations associated with a reciprocating compressor are highly transient and the acoustic mode excitations must be studied using a transient model.

To limit the computational time, only the Case A system was studied. The computational domain used for the analysis discharge side of the compressor is shown in Figure 7. In order to monitor the pressure pulsations inside the domain, twelve (12) monitoring points were setup and the time history of the pressure at each point was recorded. A square wave type flow pulse was used at the inlet to simulate the alternate crank-end and head-end valve openings, with a volumetric efficiency matched to a typical high speed compressor. Boundary conditions used for the simulation were based on the compressor operating conditions from the field data for Case A.

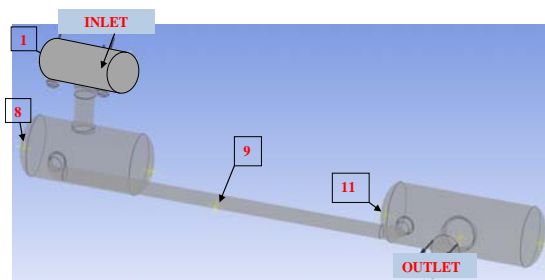


Figure 7: Overall Computational Domain for the 3-D Transient Model (Cross marks represent the monitoring / sample points inside the domain)

In order to obtain the frequency content of the dynamic pressure at each test point, a fast Fourier transformation (FFT) was performed on the time history of the pressure at the various monitoring points. An appropriate transient simulation time step was used such that frequency content up to 400 Hz was captured. The FFT program determined the spectral content in terms of maximum pulsation amplitudes obtained during the sampling time period. Figure 8 and Figure 9 show the FFT results for the pressure at test points 1 and 8, in the gas passage and at the end of the first volume bottle, respectively.

The transient fluid model predicted a dominant 5x response at 75 Hz, which corresponds well with the cylinder nozzle resonance seen in the field data (also at approximately 75 Hz) and the 3-D acoustic response model and 1-D representation model

(predicted to be at 80Hz). Also evident was the Helmholtz response of the two-bottle system which fell below the 1x excitation at approximately 10-11 Hz. The amplitude predicted was less than the field data showed for the nozzle resonance (35 psi pk-pk compared to 25 psi pk-pk in the transient model). However, if the damping factors can be adjusted, the transient 3-D fluid model may be able to determine accurately the amplitude and frequency of cylinder nozzle resonances. Higher frequency gas passage responses are not predicted as well with the current transient fluid model and need to be further investigated in the representative one-dimensional fluid model. Since the transient fluid model was not able to delineate the higher frequency internal gas passage responses, this task was discontinued until the method could be better refined.

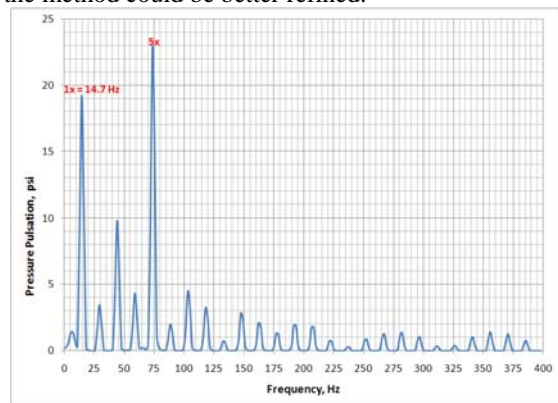


Figure 8: 3-D Transient Fluid Model Results for Dynamic Pressure Predicted Internal to Cylinder (Test Point 1)

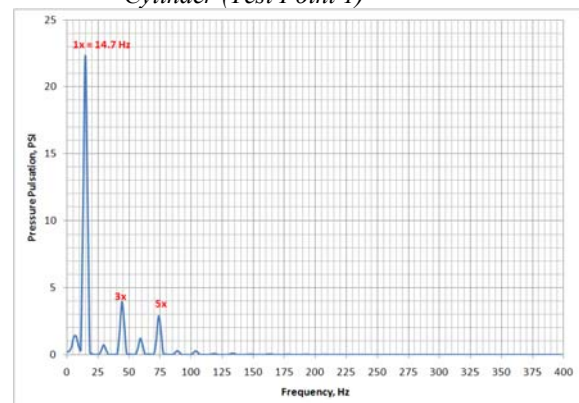


Figure 9: 3-D Transient Fluid Model Prediction of Pulsations within the Primary Volume (Test Point 8)

3.4 1-D representation fluid model

Construction of the one-dimension (1-D) acoustic model required conversion of the 3-D system into a 1-D representation.

PULSATION & VIBRATIONS

Dynamic Pressure Losses in Piping Systems, *Marybeth Nored, Eugene Broerman, Klaus Brun;*
SOUTHWEST RESEARCH INSTITUTE

The 1-D representation was comprised of specific lengths and diameters of circular pipe.

The boundary conditions for the Case A suction and discharge models included an infinite line upstream (suction) or downstream (discharge) of the compressor bottle filter (secondary) volume, the filter volume, the choke tube, the primary volume, the cylinder nozzle, and the internal gas passage to the compressor cylinder valves. Two different variations of the 1-D representation were analyzed for Case A, including a branched style H-pattern and central volume / distributed X-pattern for the gas passage area – see Figure 10 for conceptual depictions.

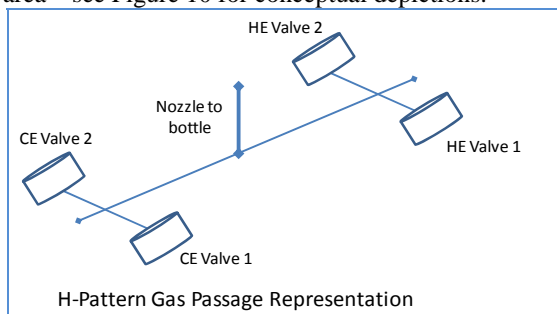


Figure 10A: Gas Passage H-Pattern 1-D Representation Style

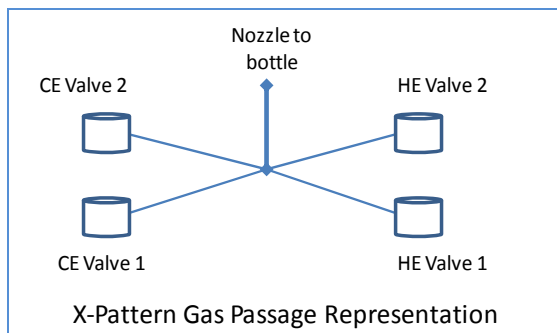


Figure 11B: Gas Passage X-Pattern 1-D Representation Style

The boundary conditions for the Case B discharge model included an infinite line downstream of the compressor bottle filter (secondary) volume, the entire filter bottle (the two choke tubes, the two primary volumes, and the filter chamber), the two cylinder nozzles, and the two internal gas passages to the compressor cylinder valves. Four variations of the 1-D representation were developed for Case B, including both the branching type and central-volume / distributed type system.

Once the 1-D representation was developed and the operating conditions matched to the field data, the fluid system was modeled using the SwRI full Navier-Stokes solution in one-dimension (termed the Transient Analysis Pulsation Solver or TAPS). This solver is applicable to any complex manifold and

piping system and was developed internally by Southwest Research Institute (Brun, 2008). This is a more physically realistic model than the acoustic wave equation and includes effects of compressibility and non-linear pressure and velocity effects in time and space. Boundary conditions were modeled as pressure varying boundary conditions at the discharge valves at the speeds and operating conditions specific to the system being analyzed. Output data from the 1-D pulsation analysis can be directly compared with the field data plots. For the first case, SwRI developed two internal gas passage (IGP) representations of the 3-D system, termed IGP1 and IGP2. IGP1 was an X-pattern type model while IGP2 was a distributed H-pattern gas passage. After comparing to the field data and 3-D response analysis, SwRI determined the H-pattern provided much improved frequency matches and better correlation with the other two data sets for this particular gas passage design.

Case a results using IGP2 for the discharge valve test point is shown in Figure 12. The model matched the predictions of the response model for responses at 75-77 Hz and the broad gas passage valve-to-valve response shown at 235-240 Hz. Other system responses predicted at 160 and 320 Hz. Damping factors are needed to reduce these responses which are believed to be less Figure 12 significant as they are not primary length responses or valve-to-valve type responses. This additional refinement to the 1-D fluid model was completed using Case B.

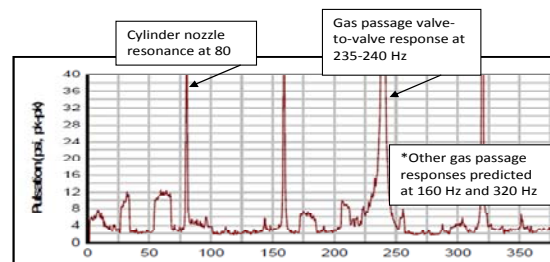


Figure 12: Case A Results using IGP2 – Discharge Valve Cap Pulsations Predicted at 76 Hz, 160 Hz, 230 Hz and 320 Hz

After determining the one-dimensional representation to use, SwRI further developed the 1-D representation model using Case B data by investigating the use of physical lengths versus acoustic lengths. Damping factors were also adjusted, which affected the amplitude of some responses and the frequency prediction of the cylinder nozzle resonance.

PULSATION & VIBRATIONS

Dynamic Pressure Losses in Piping Systems, *Marybeth Nored, Eugene Broerman, Klaus Brun;*
SOUTHWEST RESEARCH INSTITUTE

This investigation was completed for the Case B system where more useful field data was available because of the variable speed operation. Damping was added to the small passageways near the valves. A preferred 1-D representation was also utilized. In addition, two models were run, where the first model used an acoustically modified length for the nozzle and the second model used the actual physical length of the nozzle.

Using the physical length of the nozzle resulted in a frequency shift closer to the actual nozzle resonance at 72 Hz (see blue line in Figure 12.) The physical length model also showed a better match with the 180-185 Hz mixed passage response and the 255-258 Hz valve-to-valve response. **Both gas passage responses matched very closely to the field data and the predictions of the 3-D response model. These results were to be expected since the new SwRI pulsation tool is a physical model without the acoustic wave equation simplifications.**

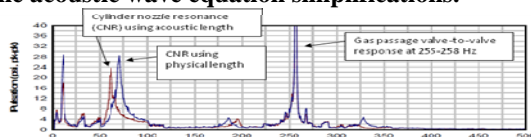


Figure 13: Case B Pulsation Predicted at Discharge Valve Cap. Blue Line Shows Shift in Nozzle Response to 70-72 Hz, using Cylinder Nozzle Physical Length Compared to Acoustic Length Model (Red Line)

The final investigative task was to determine if a small Helmholtz resonator could be effective at attenuating high frequency internal gas passage valve-to-valve type responses in the cylinder. The design of the Helmholtz resonator is based on the GMRC Virtual Orifice device developed for nozzle resonance control (Broerman, 2008). A small volume with an internal orifice and tube projection was sized for an absorption of the pressure pulsation at 258 Hz. This volume and choke tube was added to the 1-D representation model to represent installation near a valve cap or mounted on the compressor cylinder and connected to the gas passage internals (either head end or crank end can be used, but only one volume is required per side of the cylinder.) The results shown in Figure 14 suggest a reduction of about 20:1 in the pulsation amplitudes within the gas passage. This amount of attenuation would be effective in reducing cylinder vibrations and extending valve life.

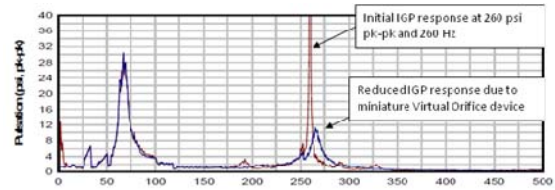


Figure 14. Reduction in Gas Passage Valve-to-valve Response at 260-270 Hz using the Miniature Virtual Orifice in the Gas Passage System

4 Conclusions

The SwRI investigation resulted in an improved methodology for accurate pulsation modeling of new compressor cylinders. This advanced multi-faceted design approach can be used in combination with OEM / bottle design options to place the gas passage and cylinder nozzle responses at optimal frequencies for lower pressure drop compressor manifold systems. Other specific conclusions are as follows:

- 1 One dimensional representations of the gas passage can influence the nozzle and gas passage responses. The current SwRI investigation showed that the representation affects the model predictions for the gas passage system responses. The methodology developed is a reliable means of validating the 1-D fluid representation model, which can then be used to run the more extensive compressor manifold and piping system. It is important to utilize a rigorous full Navier-Stokes fluid solution for high horsepower systems with larger pulsation amplitudes.
- 2 The 3-D finite element response model of the fluid system can be used to calibrate the one-dimensional fluid model for correct nozzle frequency response and gas passage response frequencies. The response model will predict less important responses as well and must be reviewed by an experienced engineer. Verification of the one-dimensional model must still be performed to verify gas passage volume similarity in the 1-D representation and correct damping due to the gas passage diameters and valve boundaries.

- 3 The miniature “virtual orifice” developed in the GMRC research program warrants further development. The model predictions showed a reduction in pulsation amplitudes of approximately 20:1 for the high frequency valve-to-valve response at 270 Hz, evident in Case B. The mini VO would likely be designed to fit on the head or crank end of the cylinder and resemble a small pocket unloader in its overall dimensions. The mini-VO would be much smaller than the previously developed Virtual Orifice. It would be designed to tune out problematic higher frequencies in the gas passage to potentially reduce cylinder vibrations and increase valve performance.

References

1. “Development of a Transient Fluid Dynamic Solver for Compression System Pulsation Analysis,” by K. Brun, E. Bowles and D. Deffenbaugh, 6th European Forum for Reciprocating Compressors, Dusseldorf, Germany, 2008
2. “Benefits of the Virtual Orifice: Pulsations and Vibrations Reduced, Performance Improved,” by E. Broerman, R. McKee and M. Nored, 2008 Gas Machinery Conference, Albuquerque, New Mexico, October 1-4, 2008
3. “Design and analysis of new concept fast-response pressure probes,” by G.Persico, P. Gaetani and A. Guardone, Institute of Physics Publishing, Measurement Science and Technology, Volume 16, 2005

A Review on the Methods of Load and Strength Evaluation of Connecting Rods

by:

Gerhard Knop

Marcel Naumann

Central Division of Technology

Neuman & Esser GmbH & Co. KG

Übach-Palenberg

Germany

gerhard.knop@neuman-esser.de

marcel.naumann@neuman-esser.de

**7th Conference of the EFRC
October 21th / 22th, 2010, Florence**

Abstract

Reciprocating compressors, equipped with large diameter pistons and / or driven at high speed, often produce high tensile rod loads which can cause the con-rod to be the bottle neck of the crank mechanism. For these cases, the con-rod design becomes a focus of attention.

This paper gives an overview on the strength calculation methods which had been applied during the recent history of con-rods for recips. Starting from plain analytical approaches in the early days, followed by simple Finite Element models of the bare con-rod utilizing classical fatigue strength diagrams, up to complete simulation models of the whole con-rod assembly making use of comprehensive fretting fatigue approaches to evaluate its strength. This report focuses on the small and big end bore as these normally offer the lowest loading capacities of the connecting rod.

Contents

- 1 Introduction
- 2 Calculation Models
 - 2.1 Simple analytical Calculation Model
 - 2.2 More comprehensive analytical Calculation Model
 - 2.3 FEA of the bare Con-Rod
 - 2.4 FEA of the Con-Rod Assembly
 - 2.5 Overview and Comparison of Calculation Models
- 3 Load Plots
- 4 Relevant Rod Load (Tension or Compression)
- 5 Calculation Error caused by Rod Load Application
- 6 Design Aspects
 - 5.1 Bearing Crush
 - 5.2 Bearing Fit Friction
 - 5.3 Con-Rod End Stiffness
- 7 Failure Modes
 - 7.1 Fatigue Fracture
 - 7.2 Crack Initiation without Propagation
 - 7.3 Wear
- 8 Conclusions

1 Introduction

The methods used to evaluate the loading capacities of connecting rods have changed a lot during the recent decades. As the con-rod end bores typically offer the lowest loading capacities, this report focuses on these areas. There are generally two aspects which need to be considered: The evaluation of load and strength. Compared to previous days the methods for both aspects have been much enhanced and the latest approaches allow a pretty complete and accurate quantification of all relevant influencing effects and parameters.

The historical development of the calculation methods and a detailed description of the current state of the art are summarized in this paper.

2 Calculation Models

2.1 Simple analytical Calculation Model

A simple calculation model¹ is shown in Fig. 1. It consists of a uniform straight bar supported at both ends and loaded by one or two forces.

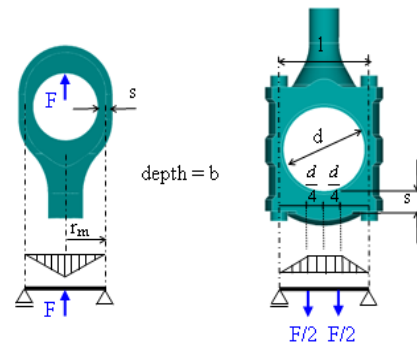


Figure 1: Straight bar model

For the small end bore applies:

$$\sigma_b = \frac{3 \cdot F \cdot r_m}{b \cdot s^2}$$

For the big end bore applies:

$$\sigma_b = \frac{3 \cdot F \cdot (l - 0,5 \cdot d)}{2 \cdot b \cdot s^2}$$

The resulting bending stress σ_b is utilized to evaluate the load limit. It is clear that this stress has the character of a nominal stress (meaning: stress value differs from real stress) the limits of which were settled by experience or educated guessing. This used to be a common method to dimension connecting rods of a compressor frame line by comparing the nominal stress values of the different sizes and keep them on the same level.

2.2 More comprehensive analytical Calculation Model

More accurate results can be obtained by applying curved beam models^{2,3} as shown in Fig. 2. The rod load causes a combination of uni-axial tensile stress and bending stress.

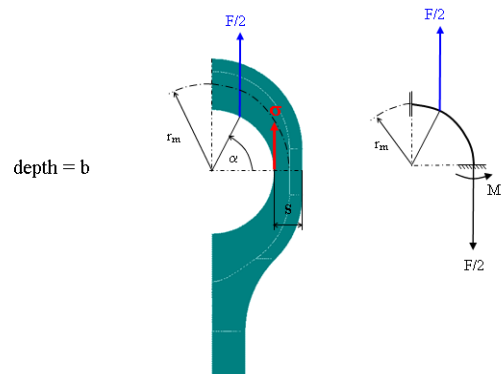


Figure 2: Curved beam model

$$\sigma = \frac{1}{s \cdot b} \left[\frac{F}{2} - \frac{M_1}{r_m} \left(1 \pm \frac{1}{k} \cdot \frac{s}{r_m \pm \frac{s}{2}} \right) \right]$$

$$k = -1 + \frac{r_m}{s} \cdot \ln \frac{2r_m + s}{2r_m - s}$$

$$M_1 = F \cdot r_m \left[1 - \frac{2}{\pi} \sin \alpha - \cos \alpha \cdot \left(1 - \frac{\alpha}{\pi/2} \right) \right]$$

The angle α is a function of the clearance between pin and bushing.

The resulting stress values approach the reality much better than the ones of the straight bar model. They can be considered as ‘real’ stress values rather than ‘nominal’ stress values. The strength was assessed by standards like FKM⁴ or by other common evaluation methods utilizing fatigue diagrams (e.g. Smith, Haigh, Goodman). Those however did not include strength loss caused by fretting effects, so the strength evaluation was still rather nebulous.

2.3 FEA of the bare Con-Rod

Other than the analytical approaches, FEA is not restricted to simple geometry. Fig. 3 shows an example of such a model.

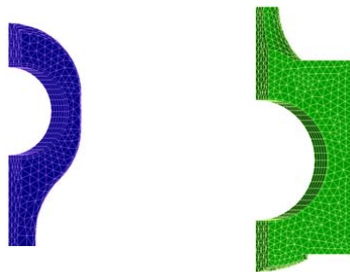


Figure 3: FEA of bare con-rod

Often, the modeling of only one single component, leaving out the adjacent components, ends up in inaccurate results caused by insufficient boundary conditions. Here it is especially the missing bearing which may lead to faulty results.

Same as with the previous analytical approach, the strength was typically evaluated utilizing ‘classical’ standards like FKM⁴ or similar methods. FEA allows a better assessment of the K_t - K_f ratio (stress concentration factor - fatigue notch factor ratio) which is determined by the height of the stress gradient. Still, because of not considering fretting effects, the strength quantification was again rather bad.

2.4 FEA of the Con-Rod Assembly

The most complete simulation model is shown in Fig. 4. It includes all relevant parts which are connected by contact conditions, modeled with the respective clearance or shrink fit.

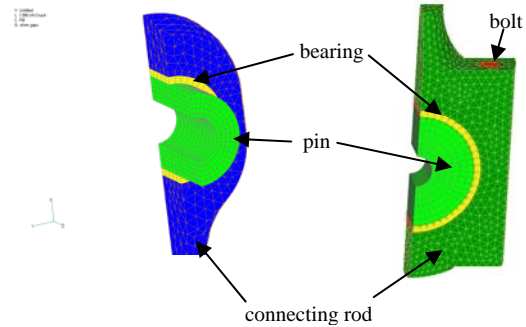


Figure 4: FEA of con-rod assembly

These models allow the quantification of not only stress and stress gradient, but also slip between bushing and con-rod bore as well as contact pressure. This permits the assessment of fatigue strength influenced by fretting. The methods are described in more detail below (Paragraph 7).

2.5 Overview and Comparison of Calculation Models

	Load Evaluation	Strength Evaluation
2.1	Simple analytical calculation model Result: Nominal stress value	Nominal stress limit, settled by experience or educated guessing
2.2	More comprehensive analytical calculation model Result: Stress value	Classical fatigue strength diagram (like FKM, Goodman etc.)
2.3	FEA of the bare con-rod Result: Stress and stress gradient	dito
2.4	FEA of the con-rod assembly Result: Stress, stress gradient, relative slip, contact pressure	Comprehensive fretting fatigue evaluation

3 Load Plots

Fig. 5 and 6 show the distribution of the tangential stress in the con-rod bore and the tangential slip between con-rod bore and bearing (or bushing).

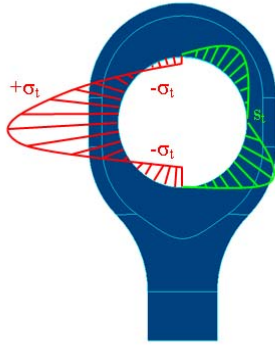


Figure 5: Load plot: Small end bore (left: tangential stress, right: tangential slip)

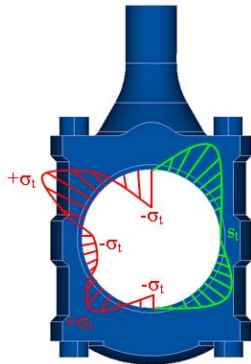


Figure 6: Load plot: Big end bore (left: tangential stress, right: tangential slip)

The highest tensile stress can be found at around 90° at the con-rod small end. This is the critical area in terms of fatigue failures. The con-rod big end normally shows compressive stress at this location because of the pre-load of the bolts.

The slip is zero at 0°, 90°, 180° and 270° and has its maxima at approximately 45°, 135°, 225° and 315°.

The con-rods of compressor lines are usually dimensioned in a way that the stress at the respective design rod load is in the same range for all frame sizes.

As stress is proportional to strain ($\sigma \sim \Delta l / l$), the absolute deformation Δl and therefore the slip between bearing and con-rod bore is increasing with the con-rod size. At large machines, the slip can be in a range of 20 to 60 μm .

4 Relevant Rod Load (Tension or Compression)

Fig. 7 and 8 compare the two load cases “tension” and “compression”. It is obvious that only tension load deforms the con-rod bore to a non-circular shape whereas compression load mainly acts on the con-rod shank without significantly deforming the bore. Consequently the critical location of the con-rod eye (illustrated by the balloon in Fig. 7+8) is only loaded during the tension part of the rod load. This means that for the small and big end bore, mainly the tension part of the rod load curve is of primary importance.

Fig. 9+10 show two examples of load curves (rod load vs. crank angle). Although both give a maximum rod load of around 400 kN, Fig. 9 has a max. tension load of 350 kN whereas Fig. 10 has only 120 kN and is therefore much less critical.

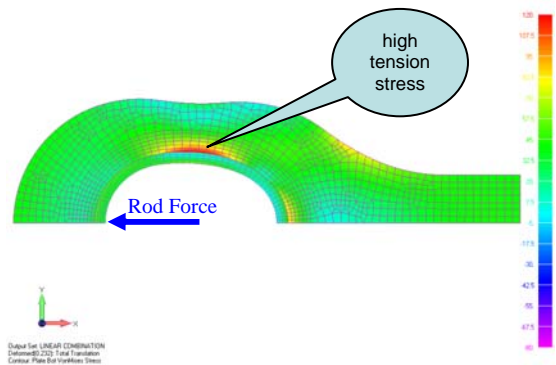


Figure 7: Stress plot, tension load

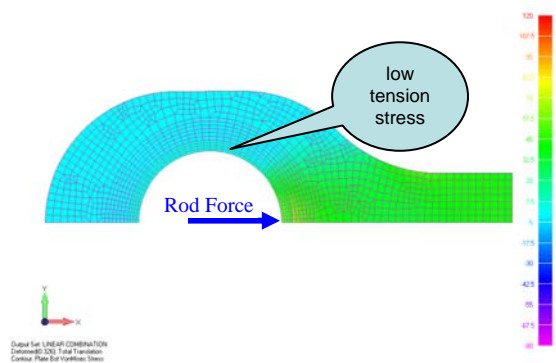


Figure 8: Stress plot, compression load

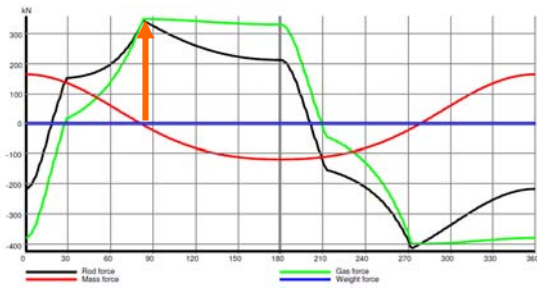


Figure 9: High tensile rod load

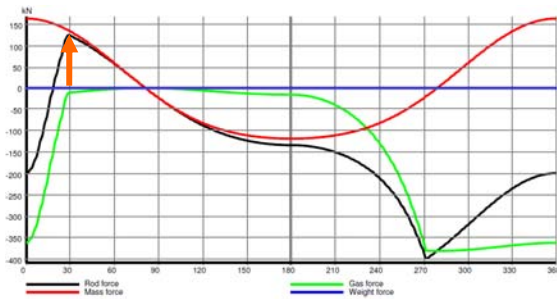


Figure 10: Low tensile rod load

5 Calculation Error caused by Rod Load Application

In paragraph 2.3 it was already pointed out that insufficient boundary conditions may lead to faulty calculation results. The consequent question is: Where are adequate boundaries for the simulation model or how should the rod load be applied?

There is a rule of Saint Venant (France, *1797, †1886) which says that if the location of the load introduction is sufficiently away from the analyzed location, then the stress at this location is independent of the kind of load introduction. In this chapter it is analyzed, how this rule applies for an FE model consisting of small con-rod end and its bushing. The load is applied in different ways at the bushing and the locations of interest are the areas of highest tensile stress inside the bore and largest slip between bore and bushing (see Fig. 5).

Common methods of load application are shown in Fig. 11 to 13.

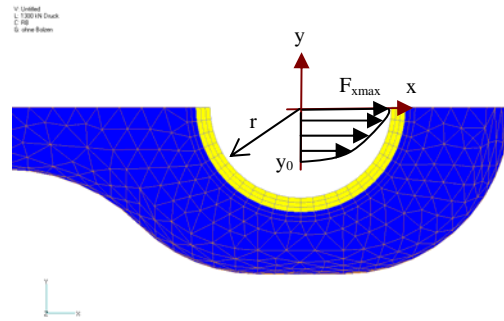


Figure 11: Load application: Parabolic

$$F_x(y) = F_{xmax} \left[1 - \left(\frac{y}{y_0} \right)^2 \right]$$

$$F_{rod} = \int_{-y_0}^{+y_0} F_x(y) dy$$

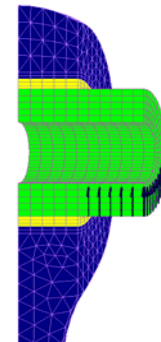


Figure 12: Load application: Via crosshead pin structure

In Fig. 12 the rod load is applied on the crosshead pin (where it is fixed inside the cross head) which distributes the load on the crosshead pin bushing according to the respective stiffness and deformation of all parts included. This method reflects the reality quite well, however it neglects the influence of the oil film (oil pressure distribution) between pin and bushing. This again can be included in an EHD model (Fig. 13).

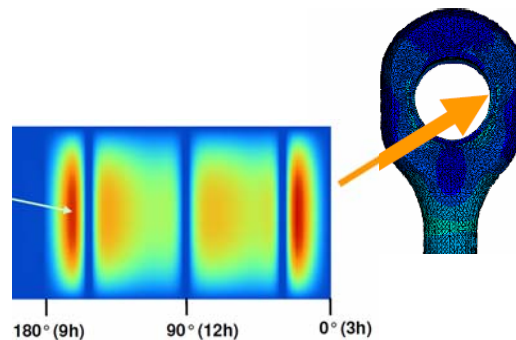


Figure 13: Load application: EHD⁷

EHD (Elasto-Hydrodynamic analysis) simulates the interaction between the hydrodynamics of the lubrication oil and the elastic deformation of the structure (con-rod, pin and bushing). The stiffness matrix of the structure is derived from FEA and included in the EHD. The resulting pressure map of the EHD analysis is then used as the load of a subsequent FEA.

The following chart shows the different slip and tension results for the different load application approaches according to Fig. 11-13.

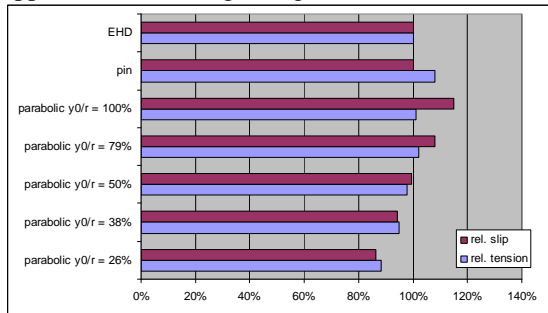


Figure 14: Tensile stress and slip depending on the kind of rod load application.

All values are relative values which relate to the results of the EHD case.

- Rel. slip means the maximum tangential movement between the outer diameter of the bearing and the bore diameter of the con-rod
- Rel. tension means the maximum tangential stress at the bore diameter of the con-rod

It turns out that max. slip and max. tension are more or less independent of the chosen method of load application! Obviously the rule of Saint Venant applies for this purpose.

6 Design Aspects

In this paragraph some design aspects are investigated which may influence the 2 important load parameters tangential stress and slip.

6.1 Bearing Crush

The diagram below shows the effect of shrink between bearing and con-rod bore. Although this parameter study was carried out over a wide range from zero shrink up to heavy shrink corresponding to around H6/s5, no significant change in stress and slip can be noticed!

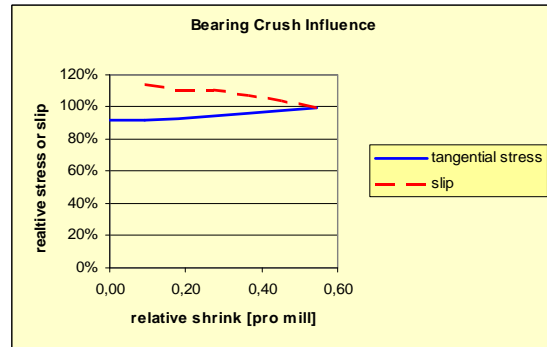


Figure 15: Bearing crush influence on stress and slip

At low shrink, the contact between bearing and con-rod bore may get lost at the circumferential location near the shank during the tensile rod loading (Fig. 16). This would allow some oil to enter this gap which would crack after a while leaving ugly black spots on the back of the bearing (Fig. 17). This however has only a visual aspect without technical disadvantages.

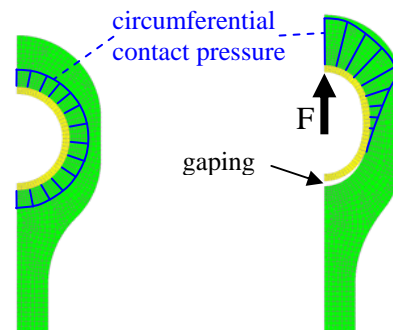


Figure 16: Lost contact pressure (left: unloaded; right: tensile rod load)



Figure 17: Oil cracking

Another aspect of little shrink is the fact that a bearing which is not exposed to helpful compressive pre-stress due to the shrink would be more critically loaded by the rod force. In this case, tensile stress caused by the rod load is not partly compensated by the compressive pre-stress.

This is an issue that must be checked during the bearing design. It is principally feasible to do without pre-load. There are many bearings without any shrink which are running successfully.

6.2 Bearing Fit Friction

Fig. 18 shows the influence of the friction coefficient on tangential stress and slip. In this diagram 'slip 1' refers to the slip maximum closer to the con-rod shank, whereas 'slip 2' refers to the second slip maximum further away from the shank.

It can be noticed that for typical friction coefficients ranging from 0 to 0.3, 'slip 1' is little influenced by friction. However, friction measurements showed the frictional coefficient to go up to around 0.9 after some time, caused by tribological mechanisms⁶. This would reduce 'slip 1' to around 60% compared to the theoretical zero-friction case. 'Slip 2' on the other hand would go down much more with increasing friction. The difference between 'slip 1' and 'slip 2' can be explained by the little contact pressure in the area of 'slip 1' (see Fig. 16) as slip is generally determined by shear forces which are related not only to friction but also to contact pressure. The local contact pressure again is much more determined by the rod load (Fig. 16) than by the bearing crush (paragraph 6.1).

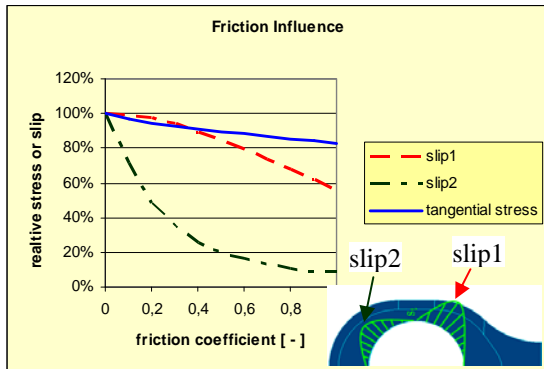


Figure 18: Friction influence on stress and slip

Anyhow, because of its strong tribological influences, friction can hardly be controlled in a reproducible manner by any method.

6.3 Con-Rod End Stiffness

Of all possible ways to significantly reduce tangential stress and slip (in a reproducible way), only an increased stiffness of the con-rod end is successful. The chart below shows that an increased radius R of only 20% reduces stress and slip down to around 70%.

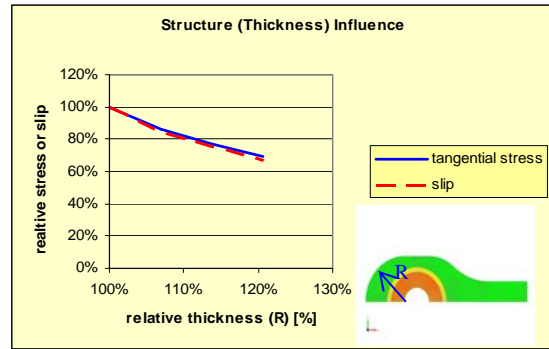


Figure 19: Thickness influence on stress and slip

7 Failure Modes

There are basically three failure modes which are:

- Fatigue Fractures
- Crack Initiation without Propagation
- Wear

All three of them are related to fretting, however, only the first two modes have been reported in the context of connecting rods.

7.1 Fatigue Fracture

Fig. 20 shows a fractured connecting rod (small end).



Figure 20: Fractured con-rod small end

The crack was initiated near the area of the highest tangential stress (see Fig. 5) and went through the whole con-rod eye side wall. The opposite side was then ruptured due to excessive bending load.

The evaluation of fretting fatigue is complex as there are plenty of parameters like oscillatory slip, material, surface treatments, friction, stress situation and load frequency with more or less influence.

The following descriptions give the most interesting aspects in a qualitative manner.

Fig. 21 shows an influence of the slip between bearing and con-rod bore on the fatigue strength.

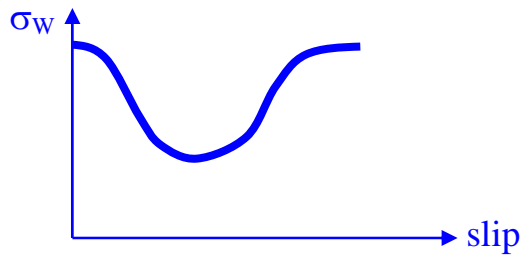


Figure 21: Fatigue strength vs. slip⁸

It turns out that above a certain quantity of slip the fatigue strength is significantly reduced. At very large slip values, strength goes up again which is explained by the assumption that any crack which has just been initiated is worn off right away by the slipping surfaces and that way prevented from propagation. This effect however would cause wear (= material loss, see paragraph 7.3) which is not observed at con-rods.

Fatigue strength loss is very much related to material. A high-strength quenched and tempered steel loses much more fatigue strength than a low-strength carbon steel (see Fig. 22). This means that a change in material from low-strength to high-strength will improve the fretting fatigue limit much less than expected by the pure material strength values.

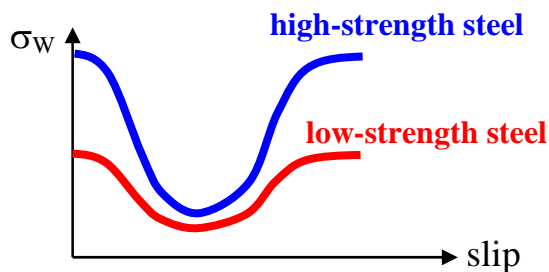


Figure 22: Material dependence

Probably the most famous approach to evaluate fretting fatigue is the FFDP parameter (fretting fatigue damage parameter) or Ruiz criterion⁵.

$$FFDP = \sigma_t \cdot \tau \cdot s$$

σ_t = tangential stress

τ = shear stress

s = slip

For a certain shear stress and FFDP, the Ruiz equation above yields the qualitative relation

$$\sigma_{t-admissible} = \sigma_w \sim \frac{1}{s}$$

which is reflecting the decreasing branch of the curve in Fig. 21.

The Ruiz criterion predicts pretty well the location of a prospective crack. This would be the location of the highest FFDP, *not* the one of the highest stress⁵.

The Ruiz criterion approaches fretting fatigue to be proportional to shear stress τ which again is proportional to contact pressure. This means that stronger shrink increases the danger of fretting fatigue! (Note that slip s , which is also part of the Ruiz criterion, is not much affected by shrink → Fig. 15).

It must be noted, that there is still no generally approved fretting fatigue evaluation method that can be used for all kind of applications in the same way with sufficient accuracy. Research has only been carried out for special applications with their individual load parameters. Most quantifications can be found for shaft-hub connections but only few^{5,6} is published suitable to connecting rods.

Therefore, there was no other way than running tests of one's own. With the test results it is possible to evaluate the fatigue strength of con-rod bores under the influence of fretting sufficiently well.

7.2 Crack Initiation without Propagation

The second failure mode is the creation of cracks which stop propagating after typically below 1 mm depth and which are located at areas with high relative slip but low tensile stress (Fig. 23). The high relative slip creates the cracks but the tangential bulk stress is not high enough to drive crack growth. It is noticed that these cracks mainly turn up a large con-rods because of the large slip values there (see paragraph 3 above).

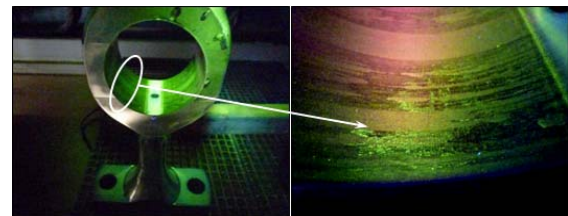


Figure 23: Cracks inside the con-rod bore, made visible by magnetic particle test

The integrity of such cracks can be verified by applying crack mechanics. For crack depth above around 0.5mm applies:

$$\Delta K = F \cdot \Delta \sigma \cdot \sqrt{\pi \cdot a}$$

ΔK = ptp stress intensity factor
 F = factor accounting for structure and crack geometry
 $\Delta \sigma$ = ptp nominal stress
 π = 3.14159
 a = crack depth

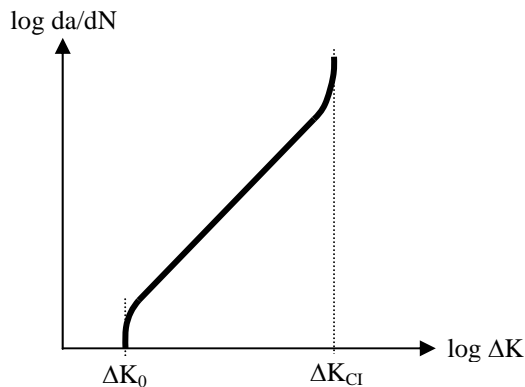


Figure 24: Crack growth vs. cyclic stress intensity factor

Fig. 24 shows the well known crack growth diagram valid for linear-elastic behavior (crack tip plastification area is small compared to the crack length). The value ΔK_0 is the threshold below which a crack would not propagate. It depends mainly on material and stress ratio. Together with the equation above, an admissible nominal cyclic stress can be defined at areas, where crack initiation of a certain crack depth caused by large tangential slip cannot be avoided. Taking this maximum crack depth plus some sufficient safety, the maximum admissible stress is

$$\Delta \sigma_{adm} = \frac{\Delta K_0}{F \cdot \sqrt{\pi \cdot a_{max}}}$$

ΔK_0 = stress intensity factor - threshold of crack growth
 $\Delta \sigma_{adm}$ = admissible ptp nominal stress
 a_{max} = maximum expected crack depth

This nominal ptp stress limit is compared to the calculated FEA values.

7.3 Wear

Mating surfaces which are subject to very excessive oscillatory slip may cause wear (= loss of material).

However, at connecting rods, this kind of failure mode has not been reported.

8 Conclusions

All compressors having high tensile rod load must be properly examined in terms of con-rod loading capacity.

Special attention must be given to the small and big end bores as their fatigue strength is much affected (reduced) by the relative tangential slip between bearing and bore.

The quantification of the loading capacity firstly requires an accurate assessment of the load parameters like stress, stress gradient, contact pressure and slip. Today it is state of the art to create a FE model of the complete assembly including con-rod, bearing or bushing, pin and bolts for this purpose. Because of the distributing effect of the bearing or bushing on the load flow, the method of load application is of minor importance.

As a second step the fatigue limits need to be evaluated under the enormous influence of fretting. There is no approved method that is valid in the same way for all kind of applications. It is therefore necessary to find load limits (using appropriate approaches) by individual tests for the special load situation of connecting rod bores. With these test results it is possible to evaluate con-rod fretting fatigue sufficiently well.

References

- ¹ Küttner, Kolbenverdichter, Springer-Verlag 1992
- ² Kleinert, Taschenbuch Maschinenbau, Band 5, VEB Verlag 1989
- ³ Roark's Formulas for Stress and Strain, McGraw-Hill, 2002
- ⁴ FKM, Forschungskuratorium Maschinenbau, Analytical Strength Assessment of Components in Mechanical Engineering, 5th Edition 2003
- ⁵ Merritt, Zhu, The Prediction of Connecting Rod Fretting and Fretting Initiated Fatigue Fracture, 2004, SAE International
- ⁶ Rabb, Hautala, Lehtovaara, Fretting Fatigue in Diesel Engineering, CIMAC Congress 2007, Vienna
- ⁷ A. Voncken, FEV, Conrod Analysis M19092
- ⁸ Vinsbo, O.; Söderberg, S.: On fretting maps, Wear, 1988, 126(2), 131 - 147



Compressor Reliability Survey

André Eijk and Leonard van Lier
Flow and Structural Dynamics Department
TNO Science and Industry
Delft, The Netherlands
andre.eijk@tno.nl
leonard.vanlier@tno.nl

**7th Conference of the EFRC
October 21th / 22th, 2010, Florence**

Abstract

In parts of the industry, in the past a poor image of the reciprocating compressors has often been encountered, compared to other types of fluid machinery e.g. turbo machinery and screw compressors. The first question is which of the following reasons caused the poor image: efficiency, costs of ownership, noise, vibration, reliability, maintenance and repair costs or other? Secondly, whether the image has been improved over the last decades. Part of this image may be a dated, prejudicial conception. A reliable, representative analysis of this phenomenon has not been made to now. Therefore, this has been investigated via a robust research approach, in order to quantify this phenomenon, and to formulate marketing and research strategies to improve the image of reciprocating compressors. The compressor reliability survey project was carried out by TNO Science and Industry on behalf of the R&D group of the EFRC. The survey has shown that the general view on the reliability of reciprocating compressors has been improved because of recent developments. However, a further improvement of the reliability of reciprocating compressor systems can only be obtained in close cooperation between the end users, engineering contractors and OEMs, since they are impacted by both design and operation of the compressor.

1 Introduction

The increasing demand for economic plant operation has led to a critical discussion of the equipment as to selection, design, maintenance and automation. The well-known advantages of the reciprocating compressor – such as high efficiency under many different operating conditions, comparatively easy regulation possibilities, suitability for light gasses, high compression ratios, and many more - have led to a renaissance of this type of machinery. Nevertheless manufacturers of reciprocating compressors are still faced with prejudices with regard to the relatively complex mechanical design, resulting in high maintenance costs and lower perceived reliability. It is a firm belief by the EFRC that with the recent developments, reciprocating compressors can now meet all the requirements of modern machines and even create new possibilities.

Despite the fact that the reciprocating compressor has many advantages and has significantly improved the last years, for example in the area of flow control, improved valve design, new materials, improved efficiency etc., it is believed that, in parts, the industry still has a perception on poor reliability of reciprocating compressors compared to other types of rotating equipment such as turbo machinery and screw compressors. The question is what the reasons are of the poor image: efficiency, costs of ownership, noise, vibration, reliability, maintenance/repair costs or other? Part of this image may be a dated, prejudicial conception and a reliable, representative research to this phenomenon is not yet available.

A need is expressed to investigate this via a robust research approach, to quantify this perception, and formulate strategies to improve the image of reciprocating compressors. For that purpose an R&D project¹ is initiated by the EFRC to investigate the user's experience with different types of compression equipment in regard to robustness and reliability.

The reciprocating compressor has been evaluated on various technical, operational and economic aspects and has been compared with the other main types of fluid machinery which include the turbo and screw compressor. The purpose of the survey is to evaluate the most recent perception on reciprocating compressor reliability. If this is based on dated prejudices and/or misconceptions, the results of the study can be used to change the industry's perception on poor reliability of reciprocating compressors and to define focal points for future research activities and strategies

marketing to improve on the critical drawbacks of reciprocating machinery.

The approach has been as follows: first a literature survey has been undertaken to analyse the existing literature and review the recent development in the design and operation of the reciprocating compressor. Then an internet survey has been sent to some 350 rotating equipment engineers around the world, both from operators as well as engineering contractors and manufacturers. Finally some key persons with an extensive experience in rotating equipment, in particular reciprocating compressors, have been interviewed.

This paper presents the results of the analysis and discusses options for further improvement.

2 Literature survey

2.1 Introduction

The first activity was a literature survey to investigate the perception and the possibly 'ghost' stories of the reciprocating compressors reliability that may exist in the industry. This is done by using the available information on the internet, conference proceedings and other literature. About 60 papers have been analysed, most of them from technical conferences such as EFRC conference, GMRC and Turbo machinery conferences, web pages etc. The list of references is too long to summarise in this paper and the EFRC may be contacted to retrieve this list from the EFRC final report¹. The results have been used to provide the necessary background and input for the following subsequent tasks. Keywords that have been searched for were: efficiency, reliability, maintenance, safety, operation costs, installation costs, etc..

2.2 Definitions²

In judging a reciprocating compressor several applied definitions which are frequently used are defined as follows:

Reliability, Availability and Maintainability:

Generally speaking the first two criteria (R & A) are considered together and the third, maintainability (M), although equally important, is usually separated from the other two.

The reason for this is that with the R and A the definitions can be clearly specified and in many cases now can be included in guarantee clauses within a contract whereas the M only the principles and guidelines can be specified, as there can be many variables and constraints affecting the designer's ability to meet the ideal solution in many cases.

Although there are some variations of the definitions of R and A, the most commonly accepted definitions are as follows:

$$\text{Reliability (\%)} = \frac{8760 - SD - UD}{8760 - SD} \cdot 100$$

$$\text{Availability (\%)} = \frac{8760 - SD - UD}{8760} \cdot 100$$

Explanation of terms:

- 8760 is the amount of hours in 1 year
- SD: scheduled downtime in hours in 1 year
- UD: unscheduled downtime in hours in 1 year

Maintainability, the ability to maintain a machine is really self-explanatory; however, it does have a direct effect on the availability. Quite simple, if the scheduled downtime (SD) is extended because the machine is difficult to maintain, the availability is compromised. Unscheduled failures have the greatest impact on the reliability. The goal of a reciprocating compressor system is continuous operation without shutdown of 3 years, which is also stated in the API Standard 618³

Integrity

This parameter is defined as how many failures would occur. The integrity is focusing upon the economical damage and loss of production due to unscheduled failures.

Safety

Safety is often seen as one of a group of related disciplines: quality, reliability, availability and maintainability. It is extremely important that all compressors are monitored to avoid failures and disasters. The parameter safety will focus therefore on injuries of human and environmental damage. Gas leakage can for example occur in a compressor which is a serious issue since gas leakage can create a major disaster. Nowadays, safety is one of the most important factors and the end user is willing to pay for guaranteeing the safety of a compressor system.

2.3 History lessons

The paper of Jerry Jones⁴ about operation and maintenance of reciprocating compressors in the

new millennium gives a very good summary of the past, present and future. For that reason a short summary is given in this paper as follows:

Past

“Recips are a pain in the neck, recips are nothing but a maintenance workout, recips are out of date and should be considered to a museum where they belong, along with the other Dinosaurs”. These are some of the sentiments of engineers from the past. One of the hurdles to installing reciprocating compressors in the past was the perception of un-liability. This was often the result of a lack of understanding coupled with a legacy of the 1970's when a lot of poor installations were completed.

Then the ‘Dark Ages (1970-1990)’ began! Changes have occurred like trimming down the manning levels, reducing the trainee schemes and loading up people left with the workload of the personnel who had already left. The period also saw a computerized maintenance management system. In that period this computerized maintenance was generally accepted. This causes in general a significant loss of experienced personnel. We slipped from scheduled maintenance into reactive maintenance – ‘fire fighting’ ruled the day.

Before the dark ages the reciprocating compressor was more reliable. Many maintenance resources were available and maintenance was solely time based due to the lack of modern monitoring systems. In the dark ages the OEM was losing out on the feedback of the end-user, which is vital. The end-user was losing out on the injection of experience and technical knowledge of the OEM. Manufacturers of valves and wearing parts were aiming its work on the occurring symptoms rather than the root causes of the problems, however in absence of respective service offerings of OEM's, at that time, this was the best way curing the problems.

Present

Many improvements over the last decades in all aspects of the reciprocating compressor have been made. From a paper³ of Jerry Jones from BP Grangemouth, Scotland it is concluded that they have arrived at a point where the reciprocating compressor is being recognized as a critical component in many of the processes. This has been brought home recently with a series of incidents where reciprocating compressor unreliability has been the root cause of significant lost production. A lot of this has been the result of historical unreliability that had not been solved.

Concerns:

- Correct lubrication is an absolute must on all types of duties
- Debris or liquids in the system causes mechanical damage

- Bad alignment and foundation design is inadequate (often the way the reciprocating compressor is attached to the foundation block)
- Off-design operations
- Valve failures, which are often also a symptom of more fundamental problems in operation, such as excessive lubrication

Progress:

- Big wear parts improvements since approximately 1980
- Major improvements in compressor valves
- Condition monitoring systems

Future

The future is green. Reciprocating compressors have the historical mantle of unreliability, which is more by perception than reality. At the end of the day, the reciprocating compressor is a reliable, low total cycle cost machine; we have just got to ensure that this happens. Identification of the vital parts/aspects is therefore needed, so improvements can be made in order to reach this goal.

2.4 Reliability survey on Hydrogen reciprocating compressors

A compressor reliability survey has already been carried out by Dresser-Rand⁵ approximately 15 years ago, specifically on Hydrogen compressing machines. The results of this survey are summarized in figure 1 which illustrates the majority of the reciprocating compressor systems and components identified to result in unscheduled shutdowns. According to the results, eight systems and component areas are responsible for nearly 94% of all unscheduled shutdowns of reciprocating compressors. One interesting result was the ranking of the cylinder lubrication system as one of the top eight problem areas. This was determined to be significant as the reliability of the systems can directly affect the reliability of three other components also ranked among the top eighth problem areas: pressure packings (#2), piston rings (#4) and rider bands (#5).

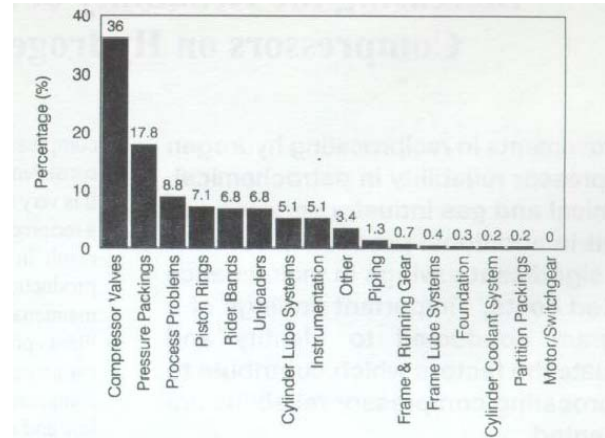


Figure 1: Components which cause the unscheduled shut-down of reciprocating compressor compressing Hydrogen in 1995

The survey discussed the following issues:

Based on the compressors surveys conducted, it became very evident that the old phrase “it is better to have too much cylinder lubrication rather than too little” is a serious and widely applied misconception. Excessive amounts of cylinder lubrication can be just as detrimental to the reliability of the reciprocating compressor cylinder components as having insufficient cylinder lubrication. Too much of the wrong type of lubrication can increase the effects of compressor valve stiction (viscous adhesion) causing compressor valves to open and close late. This results in the valve elements "slamming" open and closed resulting in a significant reduction in compressor valve reliability. By cutting back to the proper cylinder lubrication rates, the ring breakage and erosion problems in those cases were significantly reduced. Insufficient lubrication can result in premature wear of the wearing components of a reciprocating compressor cylinder. The survey helped to confirm that when the correct amount of the proper type of lubrication is used, the life of PTFE based piston rings, rider bands and pressure packings can commonly meet, and in many cases exceed, 3 years (25,000 hours) of operation in hydrogen service.

Currently there is no such thing as an indestructible compressor valve. However, some designs and types are more tolerant than others to the actual service conditions.

The survey identified that piston rod and packing life on higher pressure applications (approaching 150 bar) could be improved two to three times by adding the proper tungsten carbide piston rod coating.

The survey clearly illustrated that users with well followed and structured maintenance procedures carried out by knowledgeable, well trained maintenance personnel, tended to have more reliable compressors than those who used lesser trained and experienced personnel. The survey also identified that users who faithfully used a well-organized maintenance documentation system tended to have more reliable compressors.

The use of original equipment manufacturer (OEM) parts can play a major role in reciprocating compressor reliability. While this may seem like a sales ploy, it is not intended to be. Many compressor surveys were conducted on reciprocating compressors which used non-OEM parts. End users who had good working relationships between the maintenance group and the operations group tended to have more reliable reciprocating compressors.

The paper concludes that significant improvement in the operation of reciprocating compressors can and should be made by improving the following: process conditions (clean and dry gas and know off-design conditions), design, material, compressor valves, cylinder lubrication and instrumentation.

2.5 Conclusions

Based on the results of the literature survey it can be concluded that according to the found literature, it seems that in the past the negative reputation on the overall reliability of reciprocating compressors was justified by several field cases. This was especially true for the compressors which were installed between 1970-1990. Many improvements have however been made since 1990. . Nowadays, the bad reputation from the past has grown to be more a perception than reality and the future of the reciprocating compressor is green, we have just got to ensure that this happens.

3 Electronic inquiry

3.1 Introduction

To get real facts and figures an electronic inquiry has been carried out. For that purpose a comprehensive list of questions was made which have been formulated with the results of the literature survey. The questions were mainly focused on valves, spare parts, off-shore applications, safety, maintenance, monitoring systems, pulsations and vibration control, flow control and improving reliability. The questionnaire has been sent out mainly to rotating equipment, reliability and maintenance engineers of operators (on-shore, off-shore),

engineering companies and maintenance companies. Special care has been taken to ensure that the questions are formulated in an ‘unbiased’ way, so that the user’s experience with compressors is interpreted from an independent point of view; buyers (costs of ownership and total life cycle costs), maintenance managers (maintenance costs) and operation managers (reliability and safety robustness and versatility). This will give a detailed view on how the different perceptions are within the industry.

3.2 Discussion of results

To achieve optimum results the questions have been grouped to items which have a direct or indirect effect on reliability. Detailed results of most of the grouped items have been summarised in the next chapters.

3.2.1 General

The inquiry was sent out to 348 participants of whom 19% sent back a complete response. The participants had all different type of positions within all type of different companies which are active in the oil and gas industry. Most of the participants are working in Europe (77 %). Most of the installed compressors on-shore of the participants are reciprocating compressors (46 %) and most of the installed compressors off-shore are turbo compressors (43 %). The compressed gas of all type of compressors is mainly natural gas and hydrocarbons. Hydrogen and CO2 are mainly compressed with reciprocating compressors, see also figure 2.

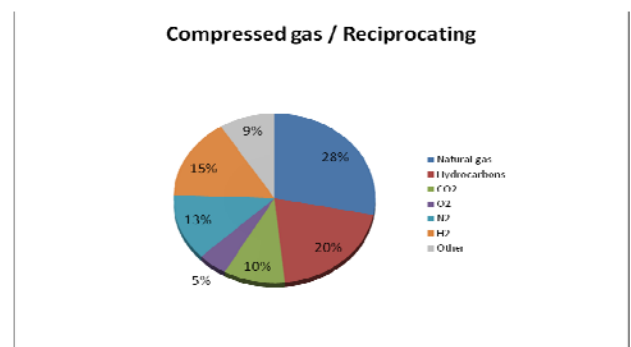


Figure 2: Gases compressed by reciprocating compressors

3.2.2. Overall reliability of the reciprocating compressor now compared to the past

One of the most important questions was focussed on the general perception of the overall reliability of the reciprocating, screw and turbo compressor in the past and nowadays.

From figure 3 it can be concluded that the perception of the participants was that the reliability of reciprocating compressors in the past and nowadays is less than that of the screw and turbo compressor. Further on it can be concluded from figure 3 that the perception of the reliability nowadays has been improved considerably. The perception of reliability of reciprocating compressors in the past and nowadays is not yet as high as turbo compressors or screw compressors.

The increase in reliability of the reciprocating compressor was even higher than that of the turbo and screw compressor which is to the opinion of the authors of this paper caused by many improvements of compressor valves, wearing parts (rider bands, piston rings, pressure packings), pulsation and vibration control, and improved compressor design.

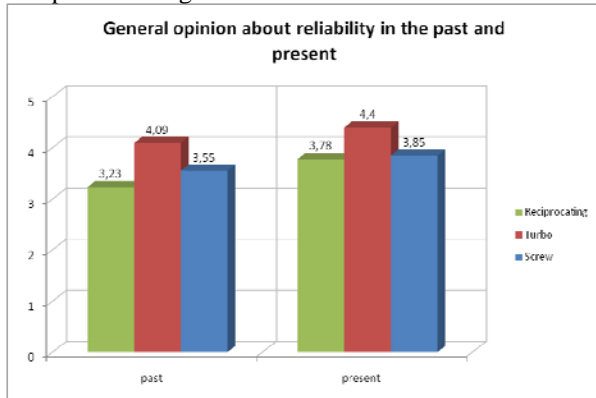


Figure 3: General opinions about the reliability

3.2.3 High speed versus low speed reciprocating compressors

The general opinion (52%) is that the reliability of high speed compressors is less than that of low speed compressors. 32% had the opinion that this is not true and 16% had no opinion.

It is also mentioned several times that besides the rotation speed also the piston speed plays an important role in the reliability. Due to the higher speed of the compressor, high(er) pulsation and vibration frequencies, especially at the compressor valves, can lead to more unscheduled shut downs. However, this should not be a problem if an adequate pulsation and vibration analysis will be carried out. The selected materials for rider bands, piston rings and stuffing box sealing rings and sealing ring arrangements play also a very important role in the unscheduled shut downs.

It has been indicated that there is also a lack in experience & knowledge of how to operate a high speed compressor. This is probably not the case for operators in the USA because much more high speed compressors are installed.

Remarkable is the reverse evaluation of reliability by users of high and medium speed machines compared to users of low speed machines: end users with high speed compressors do not have the opinion that high speed compressors are less reliable than low speed compressors and end users with low speed compressors have indicated that high speed compressors are less reliable, see also figure 4.

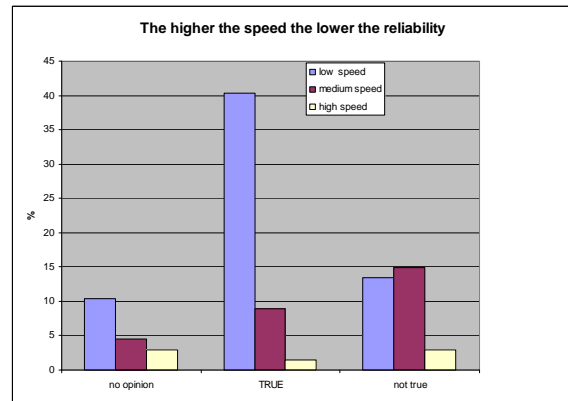


Figure 4: Perception of reliability of users with different speed of compressors installed

In the USA much more high speed compressors are installed than in other countries. The reply from participants from the USA was very limited (only 8%). The conclusion that high speed compressors are less reliable than low speed compressors is for that reason probably more perception than reality.

To get a more reliable conclusion, additional information should be retrieved from more operators of high speed compressors, in particular from the USA.

3.2.4 Off-shore applications

From the inquiry it is concluded that one of the most important reasons why reciprocating compressors are not preferred off-shore, are the pulsation and vibration problems, see figure 5. Also the maintainability is more difficult (and consequently the costs involved) and the weight and footprint are higher than that of a turbo compressor.

On the other hand the reciprocating compressor is the best solution to handle variable process conditions, especially for high pressure applications.

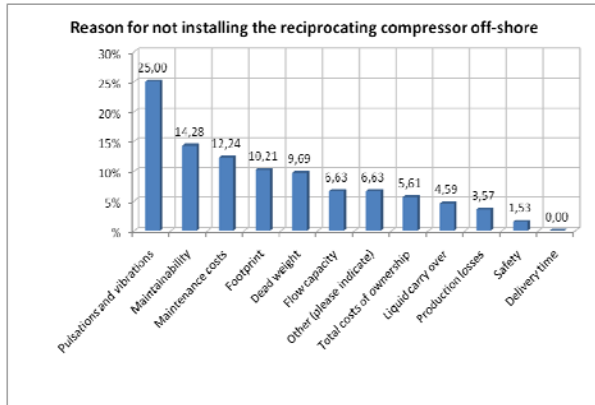


Figure 5: Reasons for not installing a reciprocating compressor off-shore

3.2.5 Compressor valves

A reciprocating valve is one of the most critical components and has a large effect on the reliability. Valve failures were the main cause of the rather short uninterrupted service life from several weeks up to several months in the past. Valves have been improved considerably last years by developing other materials (PEEK and other high performance materials) and other type of valves, which have lead to much longer uninterrupted service times. Nowadays it is possible to achieve an uninterrupted service life of 3 years. The compressor valve is and will remain probably one of the most critical parts of a reciprocating compressor. Dust (fouling), liquids, polymerisation, (unknown) variable operation conditions, pulsations and vibrations, incorrect choice of the material and spring elements, incorrect cylinder lubrication (too much will cause a too late opening and closing, too little will give more wear) will cause unscheduled shut downs and will have a negative effect on the reliability of the compressor.

The opinion of the authors is that continued R&D programs are necessary to further improve the quality of the valves. Adequate filters and separators⁶ must be installed to avoid fouling and liquids entering the compressor cylinder. The process conditions must be known and if necessary the valves must be designed for the known off-design conditions. The effect on the valve life can be further investigated and improved by applying a valve dynamic analysis, including pulsation effects.

3.2.6 Safety

The general opinion (68% of the participants) is that the reciprocating compressor is not less safe than the turbo or screw compressor. However, the general opinion is that if an internal part of a reciprocating compressor is broken, the consequence can be much more severe: parts can come out of the reciprocating compressor while it will generally stay within the turbo and screw

compressor, which will lead to a loss of containment. The opinion of 21% of the participants was that the reciprocating compressor is less safe than a turbo compressor. In figure 6 the perception of the most important reasons are indicated in case the participants had indicated that the reciprocating compressor was less safe than the other investigated compressors. It is well known that liquid carry over can be very dangerous which has been indicated in 14% as one of the reasons. Especially if liquid is entrapped into the cylinder of a reciprocating compressor, a catastrophic failure can occur. This means that good designed separators are essential in reciprocating compressor systems.

In general turbo and screw compressors are less sensitive to liquid carry over.

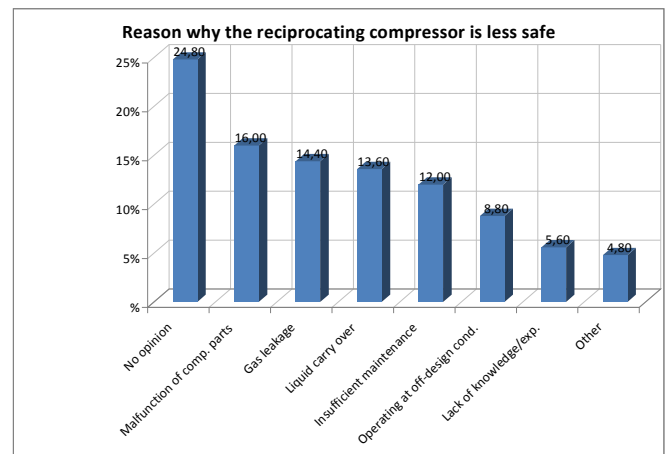


Figure 6: Perception of reasons why the reciprocating compressor is less safe than a turbo compressor

From figure 6 it can also be concluded that too little and inadequate maintenance can also lead to unsafe situations and for that reason trained & experienced engineers and good maintenance procedures are essential. Fatigue failures, caused by too high vibrations, can cause unsafe situations. For that reason adequate pulsation and vibration control analyses and measures should be taken.

Good monitoring equipment is therefore necessary to detect potential failures and in this case a reciprocating compressor can be as safe as a turbo and screw compressor.

3.2.7 Maintenance

It is well known that reciprocating compressors need more maintenance than a turbo or screw compressor. This is mainly caused by the fact that the reciprocating compressor has more wearing parts than other compressors.

The maintenance time and costs involved can be decreased by the installation of monitoring systems, the application of correct valves and wearing parts, clean and dry gas and by the application of compressors with less wearing parts (solutions are available where e.g. the piston weight is carried by the process gas thus reducing the load on the rider bands or a special piston design allows an oil free and contact free compression). The design of the compressor can also have an influence on the maintenance: less maintenance time (and costs involved) is necessary if compressor systems are designed in such a way that easy access is possible to change out parts easily, especially for off-shore platforms with limited space.

3.2.8 Monitoring systems

From figure 7 it can be concluded that the general perception (87%) is that the installation of monitoring systems will increase reliability.

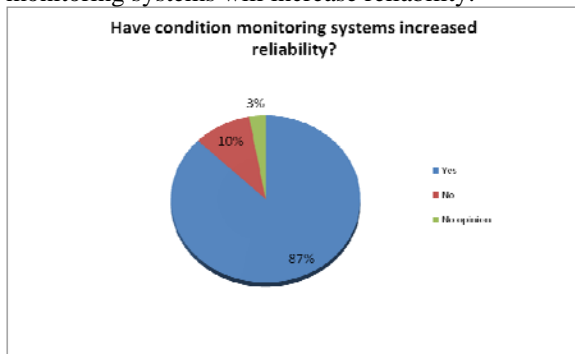


Figure 7: Perception of reliability with condition monitoring systems

From figure 8 it can be concluded that there is not enough knowledge for a correct interpretation of data amongst the end-users. Further improved of reliability can be achieved with good manuals, training etc..

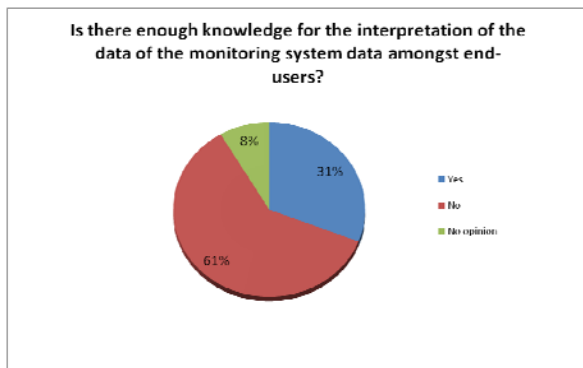


Figure 8: Perception of knowledge of monitoring systems

Further on the general opinion is that monitoring systems are able to give enough and correct data (61% has a positive reply) for a correct preventive maintenance program (75% had a positive reply).

In figure 9 several items are shown which should be improved to achieve a higher reliability to the opinion of the participants.

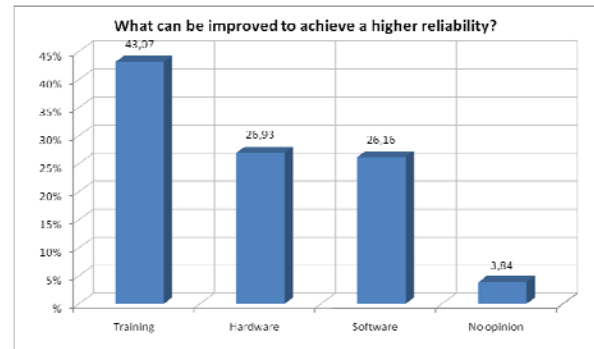


Figure 9: Items which can improve monitoring systems

3.2.9 Pulsation and vibration control

Many fatigue failures have led in the past to unscheduled shut-downs and to unsafe situations, especially for off-shore platforms which had a direct negative effect on reliability and safety.

The general perception of 56% of the participants is that the applicable standards cover enough items to understand this rather complex area, 21% had the perception that this not the case and 23% had no opinion, see figure 10.

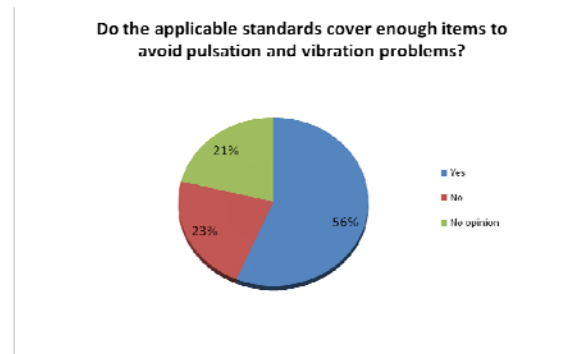


Figure 10: Perception of pulsation standards

Figure 11 shows a summary of items which should be improved to the opinion of the participants. It can be concluded from this figure that knowledge transfer is essential which can be achieved by means of courses, seminars, workshops etc..

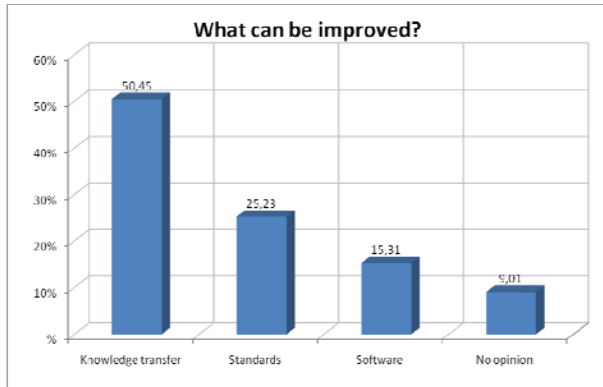


Figure 11: Items which can be improved on pulsation and vibration analysis

3.2.10 Flow control

The flow of most of the compressors is controlled as indicated in figure 12.

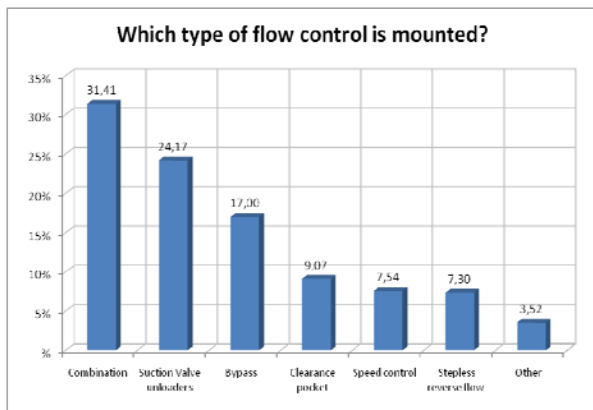


Figure 12: Overview of applied flow control systems

Although not investigated throughout this study it is well known from experience that reliability problems have been encountered with different type of flow control system which are summarised as follows:

- Variable speed drive (VSD): pulsation and vibration related problems, mechanical integrity problems due to resonance
- Variable clearance pocket (VCP): mechanical integrity problems and wear problems inside the control system
- Valve Unloading: overheating of cylinders and consequential damage to valves and wear parts, accumulation of lubricant and subsequent liquid slug problems and oil stiction problems
- Clearance pockets: problems with actuation devices
- Bypass control: problems associated with poor dynamic of control components

One of the most economic and efficient ways to control the flow of the reciprocating compressor is to apply the step-less reverse flow control.

The opinion of 13% of the participants is that the reliability will increase, 21% had the opinion that there is a decrease and 66% had no opinion which can mean a decrease or increase.

Only 7% of the participants have installed step less flow reverse control systems on their compressors, so the provided information is therefore very limited and can give incorrect conclusions.

Another crucial point is that Reverse Flow Control Systems have been on the market for a long period. Since 1996 the pneumatic control systems have been replaced by hydraulic control systems.

As the survey does not differentiate between the old and new system, there can be a misleading perception of the step less flow control system.

Maintainability (25%), pulsations and vibrations (24%), control systems (21%) and other reasons (26%), were indicated as the most important factors which can decrease reliability.

The opinion of the authors is that pulsations and vibration problems, generally with high frequencies for this type of flow control, can be avoided if an adequate pulsation and vibration control analysis is carried out with tools which are able to simulate this type of flow control.

To achieve better results and more reliable conclusions about the reverse flow control system more detailed information should be collected.

3.2.11 Improving reliability

Dresser Rand has carried out the same type of reliability survey for Hydrogen reciprocating compressors 15 years ago. From the results of this survey it was concluded that eight systems and components were responsible for nearly 94% of all unscheduled shut downs of reciprocating compressors, see also figure 1. From the survey it was also concluded that incorrect cylinder lubrication has the largest negative effect on the piston rings followed by the compressor valves.

In this EFRC project it was not easy to achieve the percentage of each parameter which is responsible for the unscheduled shut downs. Instead of that, the criticality of components with respect to unscheduled shut down (1-not critical, 5 very critical) were requested to get an idea which components play an important role in the reliability. The results are shown in figure 13 and it can be concluded that the same eight parameters are most critical and also the ranking is almost the same as the ranking of the survey as carried out by Dresser Rand.

However, it should be kept in mind that the survey as carried by DR was focussed on Hydrogen compressor, whereas the results of the EFRC survey are applicable to all type of gas applications, see chapter 3.2.1.

On the other hand it can be concluded that compressor valves had the most significant improvements which have led to a higher reliability followed by pressure packings and piston rings. Also remarkable to mention is that pulsation and vibration control had also major improvements with a positive effect on the reliability.

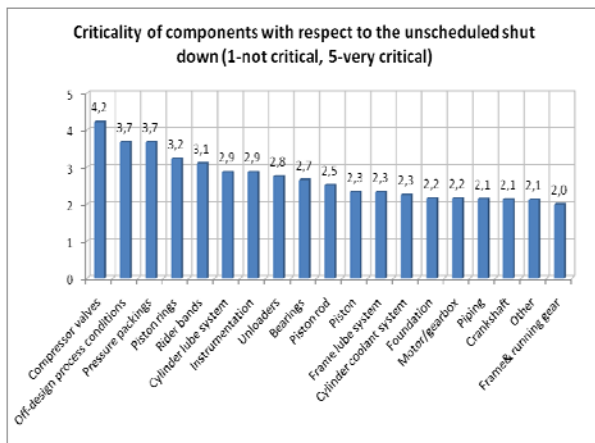


Figure 13: Criticality of components with respect to unscheduled downs

In figure 14 a summary is given of parameters which have increased the reliability of reciprocating compressors last decades to the opinion of the participants.

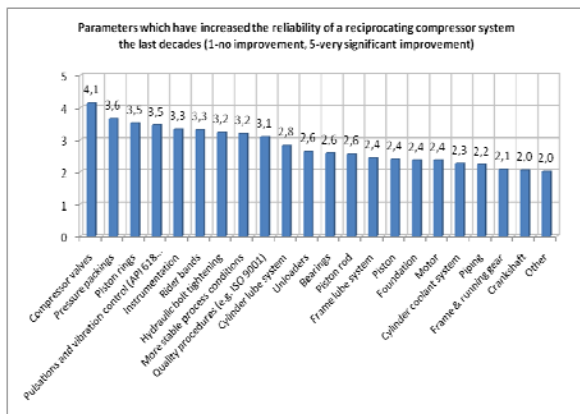


Figure 14: Summary of parameters which have increased reliability of reciprocating compressors last decades

To further increase the reliability, continued effort should be undertaken to improve the compressor valves, pressure packings, piston rings, pulsation and vibration control, instrumentation, rider bands, hydraulic bolt tightening and stable process conditions.

3.2.12 Cooperation between OEM, end user and engineering companies

The reliability of a compressor system does not only depend on the reliability of the reciprocating compressor alone. It also strongly depends on how a compressor will be operated and maintained. A further increase of reliability is therefore a task of both OEM's (Original equipment manufacturers) and End users (operators) to achieve an uninterrupted service time of minimum three years.

The experience of the end user is very valuable for the OEM because the end users have experience with the problems of their compressors and know in many cases the solutions to improve the compressor. Feed back to OEM's is therefore essential to improve the compressor for that application. For that reason a question was formulated for the participant who should take the lead in achieving a significant improvement. Figure 15 indicates the perception of the participants and the encircled parts indicate the items for which all parties involved should take the lead. The overall perception is that for 48% of all items all parties should be involved.

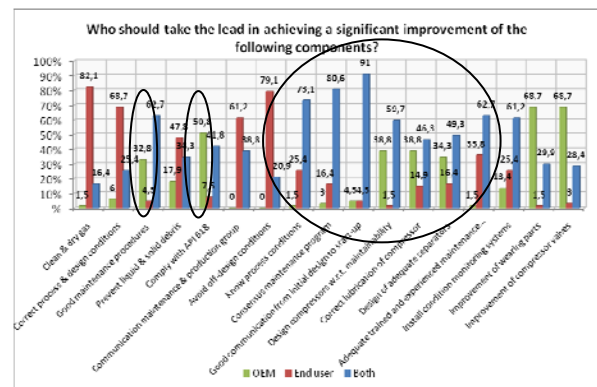


Figure 15: Overview of who should take the lead on improving reliability

3.3 Conclusions and recommendations of the electronic inquiry

It can be concluded from figure 3 that the perception of the reliability nowadays has been improved considerably. The perception of reliability of reciprocating compressors in the past and nowadays is not yet as high as turbo compressors or screw compressors

From the results it can be concluded that the general opinion about the reliability in the past of the reciprocating compressor was less than that of the screw and turbo compressor. The reliability nowadays has been improved and is higher for all investigated type of compressors.

There was a considerably increase in reliability of the reciprocating compressor and was even higher than that of the other investigated compressors.

To the opinion of the authors of this paper this is probably caused by many improvements of compressor valves (material and type), wearing parts (rider bands, piston rings, pressure packings), new compressor designs (solutions are available where e.g. the piston weight is carried by the process gas thus reducing the load on the rider bands or a special piston design allows an oil free and contact free compression) and pulsation and vibration control.

Despite the fact that the reciprocating compressor is nowadays a reliable compressor, it is believed that a further improvement of the reliability can be achieved. Together with the results of the survey and the opinion of the authors of this paper the reliability can be further improved as follows:

- Continues improvements of valves and wearing parts
- Better transfer of knowledge and standards on pulsation and vibration control
- Better transfer of knowledge of condition monitoring systems
- Apply/design adequate designed filters and separators
- Achieve better cylinder lubrication
- Avoid off-design conditions and take into account possible off-design conditions in the design
- Take care of good and enough maintenance according adequate maintenance procedures with experienced and trained employees
- Apply pulsation and vibration control analysis according to the highest level (Design Approach 3) of the API Standard 618, a valve dynamic analysis can be important
- Extensive dynamic design analysis for off-shore applications
- Better and more cooperation between OEM, end user and engineering companies in the design of a system and use feed back from experience from end user in the design process
- Design compressors with respect to easy access and less maintenance

4 Interviews

Detailed interviews by means of teleconferences and visits have been carried out to obtain more detailed information. Open questions have been formulated encouraging the enthusiasm of the interviewed operators and triggering them to give information which will normally not be disclosed. The questions were also focussed on the advantages of the reciprocating compressor in

comparison with turbo compressors and screw compressors.

The interviews have been held with employees with different disciplines e.g. buyers, operation managers and maintenance managers to get detailed information from different angles.

Despite the fact that much of the achieved information was already known from the electronic inquiry, some additional important information is retrieved which can be applied to further increase the reliability of the reciprocating compressor and has been summarized as follows:

- Better start-up procedures
- Better cooperation between OEM and end users; feed back from field experience is important for OEM's
- Define the uninterrupted service life of parts and introduce a penalty/bonus system
- Define start-up conditions which can have an effect on e.g. material choice
- Better training and education of local employees for maintenance of the reciprocating compressor
- Develop guidelines for selection, design, maintenance, mounting (especially for off-shore systems) of reciprocating compressors
- Develop repair guideline for reciprocating compressors (identical to e.g. the API rotor repair standard)
- Apply a comprehensive, integral specification in the basic design phase, with input from end user and OEM, taking into account the full cost of ownership of the installation
- More knowledge transfer on how to operate high speed compressors, especially in Europe
- Possibility to detect early failures and valve wear: develop pre-active or predictive monitoring systems
- Apply secondary field measurements to validate the monitoring system and to increase confidence for predictive maintenance
- Apply enhanced QA procedures especially for high loaded connections (double check)

5 Summary

The industry has expressed an interest to investigate the perception of the reliability of a reciprocating compressor in comparison with a turbo and screw compressor. For that reason a robust EFRC project has been carried out to quantify this phenomenon, and to formulate possible marketing and research strategies to improve the image of reciprocating compressors. A literature study followed by an electronic inquiry and several interviews with industry leaders in the field of reciprocating compressors have been carried out to get enough and accurate data for the survey. The survey resulted in extensive database from over 70 industry experts, both from end users, engineering contractors and manufacturers and component suppliers.

Identification of the vital components and operational aspects has been encountered by this survey. From the project it can be concluded that the reciprocating compressor had built up a bad image between 1970- 1990 caused by several reasons. After that period major improvements have been made by the industry to increase the reliability, availability, integrity and safety by improving components such as compressor valves, wearing parts and pulsation and vibration control. This has clearly resulted into a significant improvement of the perception of reliability by the industry, although not yet as high as turbo compressors or screw compressors.

Further improvement of the reliability should come from a close cooperation between operators and manufacturers, since the main contributing factors to the current perception of reliability of the machine depends on aspects which are affected by operations, such as optimal lubrication of the machine, off-design operating conditions, liquid carry-over in separators and pulsation and vibrations in the system. These challenges should be faced in joint effort between all parties involved, for example by improved training and knowledge transfer and joint R&D.

The future however is green. Reciprocating compressors sometimes still have the historical mantle of unreliability, which however now appears to be more perception than reality. At the end of the day, the state of the art reciprocating compressor is a reliable, low total cycle cost machine which should be able to run for minimum 3 years without uninterrupted operation.; We now have just got to ensure that this happens.

Recommendations given in the full report, available to the members of the EFRC R&D group, support

further improvement of the reliability and can be used by OEMs and operators in the formulation of technical roadmaps and marketing strategies.

6 Acknowledgements

The authors would like to thank the R&D sponsors of the EFRC for their permission to publish the results of this project and all participants of the electronic inquiry and interviews for their active contribution and openness.

References

- ¹ EFRC R&D report: "Compressor Reliability Survey, 2010
- ² Ian. D. MacKenzie Peter Brotherhood, "Availability, Reliability and Maintainability (A.R.M.)", 1st EFRC Conference 1999, Dresden, Germany
- ³ API Standard 618, 4th edition June 1995 & API Standard 618, 5th edition December 2009
- ⁴ Jerry Jones, BP Grangemouth, Scotland, "Operation and Maintenance of reciprocating compressors in the new millennium, 2nd EFRC conference 2001, The Hague, The Netherlands
- ⁵ Stephen M. Leonard, Dresser Rand, Painted Post, NY, USA, "Increasing the Reliability of Reciprocating Compressors on Hydrogen Services,
- ⁶ EFRC R&D report: "Optimization of separators in respect to effects of pulsating flow", 2004

A Comparison of High-Speed Upstream to Moderate-Speed Downstream Short Stroke Reciprocating Compressors

by:

Greg Phillippi

Director, Process Compressor Marketing and Sales

Ariel Corporation

Mount Vernon, Ohio

USA

gphillippi@arielcorp.com

**7th Conference of the EFRC
October 21th / 22th, 2010, Florence**

Abstract

This paper compares short stroke reciprocating compressors designed for and applied in upstream (primarily natural gas) applications to those designed for and applied in downstream (primarily refinery) applications. All short stroke reciprocating compressors tend to get grouped into the “high-speed” category no matter the driven speed or how they are configured and applied. This paper explores the potential diversity of application of short stroke reciprocating compressors. The following topics are reviewed and discussed:

1. Rotating speed – What is “slow-speed”? What is “high-speed”? What is “moderate-speed”?
2. Average piston speed – Average piston speed is a key parameter - why?
3. Compressor valve configuration – How do the compressor valves differ between a “high-speed” and “moderate-speed”?
4. Distance piece configuration – How are the distance piece configurations different? Why?
5. Piston rod packing configuration – How and why are the rod packing cases configured differently?
6. Drivers – What are the typical upstream and downstream compressor drivers? Why are they different?
7. Maintenance and reliability goals and experience – Do the upstream and downstream compressor users have the same maintenance and reliability goals? Why or why not? What is the real experience?
8. Capacity control – How do high-speed upstream and moderate speed downstream compressors control capacity and/or power? How are unloaders utilized?

A discussion of these topics will help to understand the different short-stroke compressors that are available today and the philosophy behind their design and use.

1 Introduction

Many people in downstream related industries (“process”, refineries and petrochemical plants) categorize reciprocating compressors as being “slow speed” (long stroke) or “high speed” (short stroke). A third category exists, and that is “moderate speed” short stroke. The purpose of this paper is to explore that concept and review and discuss the differences between moderate speed and high speed short stroke design, reliability and appropriateness for process applications.

Short stroke reciprocating compressors (those with a stroke in the range of 76 to 203 mm, 3 to 8 inches) oftentimes get grouped into the “high-speed” category no matter the rotating speed at which they are being driven. In other words the categories seem to be as follows:

	”Low Speed“ (Long Stroke)	”High Speed“ (Short Stroke)
Stroke, mm (inch)	203 to 508 (8 to 20)	76 to 203 (3 to 8)
Driver Speed, rpm	250 to 600	600 to 1,800

Figure 1: Table comparing “Low Speed” to “High Speed” reciprocating compressors

A third category should be added to this chart:

	”Moderate Speed“ (Short Stroke)
Stroke, mm (inch)	76 to 203 (3 to 8)
Driver Speed, rpm	450 to 1,200

Figure 2: Table showing “Moderate Speed” to reciprocating compressor

2 Main Text

2.1 Background

Since the first crude oil refinery began making kerosene around 1860 in Pennsylvania, USA, the slow speed long stroke reciprocating compressor has been the preferred choice for the majority of high differential pressure refinery gas compression applications. And for good reason - in those early years that was the only machine available. Since then the downstream industry has not strayed far from that path. And again for good reason - it is believed that the slow speed long stroke machine offered the best possible reliability at a reasonable capital cost. The upstream (natural gas gathering and production) industry has followed a slightly different path. In that industry’s early years, say

prior to the 1960’s, the slow speed long stroke reciprocating compressor was also the compressor of choice - again primarily because that was the only machine available. However, the 1960’s and 1970’s saw the introduction of the short stroke “high speed” compressor by several manufacturers. Today, the short stroke high speed compressor dominates the upstream market. This configuration has proven to meet that industry’s requirements for reliability and efficiency at substantially lower capital cost. It is a common misconception that the upstream and downstream industries have differing reliability and efficiency expectations and requirements. However, many upstream users are expecting availability in excess of 98% with reciprocating compressors being driven by natural gas fueled engines. It should be noted that in these applications the engine is the weak link by a wide margin.

Today’s typical upstream reciprocating compressor is driven by a natural gas fueled reciprocating engine and is skid mounted (“packaged”). This makes for a self-contained module, meaning that no utilities, such as electricity, have to be brought to the package to allow it to operate. The engine burns field natural gas (the compressed gas) with no or minimal pre-treatment. Being packaged makes the unit portable which is quite often very attractive to the upstream end-user. A package also significantly lowers installation cost. The packages of today are very robust and are designed to be installed with or without a foundation, depending on size. The skids are typically filled with concrete under all vessels, as well as in the entire engine and compressor mounting structure. Additionally, the majority of larger skids (say greater than 1,000 horsepower) are installed on an engineered foundation with an epoxy grout interface.

Today’s typical refinery (“process”) reciprocating compressor is driven by an electric motor and is mounted directly onto a concrete block foundation (block mounted). The electric motor is utilized as a driver because it is essentially maintenance-free and has very high availability. Reliability then becomes an issue of the compressor itself, the controls and instrumentation, auxiliary systems, and the installation. Today, a second option exists for the process market and that is the short stroke moderate speed reciprocating compressor as described in Figure 2.

This is a “high speed” short stroke compressor that is driven by an electric motor at a speed that is typically 50 to 65 percent of it’s full rated (upstream, natural gas engine driven) speed. This reduced speed allows the compressor to meet the reliability requirements demanded by the process end-user.

2.2 Reliability

The previous paragraphs refer to a difference between upstream and downstream end-user’s reliability requirements. This difference requires some further explanation and clarification. In this paper the terms reliability and availability tend to be used interchangeably. It is best to consider availability a measure of reliability and therefore speak only in terms of availability. A true availability number should include *all* maintenance events either scheduled or unscheduled that result in the machine being unavailable to operations. The only exception to this is scheduled major overhauls which is consistent with the approach used on downstream equipment which is overhauled during process unit major turnarounds. If reliability is defined and measured by the frequency of scheduled and unscheduled shutdowns, the upstream and downstream users have very similar reliability goals. The difference is that the upstream users achieve very high reliability with rather frequent scheduled shutdowns for preventive maintenance (PM). The downstream user desires high reliability with essentially zero PM - at least PM that requires a shutdown - for an extended period of time, typically three years (26,280 operating hours). The upstream compressor’s mean time between repairs (MTBR) is typically defined by that which can be achieved by the engine driver. MTBR is at a minimum limited by the requirement to regularly change the engine’s lube oil, filters, and spark plugs. This is roughly every 1,000 to 1,500 hours, or every 45 to 60 days. This necessary shutdown is typically performed in one maintenance shift and provides an opportunity to perform some minor compressor maintenance such as, change a hot compressor valve, or a leaking piston rod packing, or a failed instrument. This regular PM accounts for about 0.6% (~48 hours per year) of lost availability. Therefore, for the typical gas engine driven upstream reciprocating compressor MTBR is not determined by the compressor, but rather by the natural gas engine driver. The typical upstream natural gas engine driven compression system can then be characterized as having high reliability with relatively short MTBR.

Some upstream users have demonstrated availability of 98% and higher with this configuration. This availability includes the previously mentioned 0.6% for PM.

Furthermore, 60% to 80% of the unscheduled (non PM) maintenance is associated with the engine, leaving 20% to 40% of the unscheduled to be associated with the compressor. So typical high speed short stroke natural gas engine driven upstream compressor availability works out as follows:

High-Speed, Short Stroke Engine Drive Availability	
Task	Availability
Total availability (8,760 hours)	100%
Engine PM (80% of 6 x 8 hours)	-0.44%
Compressor PM (20% of 6 x 8 hours)	-0.11%
Availability with PM	99.45%
Unscheduled maintenance (123 hours) <ul style="list-style-type: none"> • Unscheduled for the engine (60% of 123 hours) • Unscheduled for the compressor (40% of 123 hours) 	-0.84% -0.56%
Achieved Availability	98.05%

Figure 3: Table showing the calculation of availability for a High Speed Short Stroke natural gas engine driven reciprocating compressor package

Figure Nr. 3 Notes:

1. The typical application being 1150 to 1400 rpm, suction pressure of 2.8 to 20.7 bar (40 to 300 psig), discharge pressure of 75.8 bar (1100 psig), in one, two or three stages with possible side streams, compressing untreated sweet natural gas (SG = 0.65), using a four throw short stroke compressor with a 133 to 165 kN (30,000 to 37,000 lb_F) rated tension rod load.
2. It is important that the compressor be reviewed for the application consistent with good practice for any piece of rotating machinery.
3. A major overhaul takes three or four ten to twelve hour days for the upstream high speed compressor package. This is performed in the field with two or three people. This overhaul typically consists of all frame (all bearings) and cylinder wear parts (valves, packing, piston rings, wearbands), and crosshead inspection.

Obviously, not all upstream reciprocating compressors are driven by natural gas fueled engines as some are driven by electric motors and therefore, don’t require regular preventive maintenance shutdowns for the driver. In this situation the compressor, the rest of the package (instrumentation and controls) and the specifics of the application - cleanliness of the gas, compressed gas discharge temperature, range of conditions, etc., determine MTBR.

The importance of the previous sentence cannot be overemphasized and should be properly accounted for regardless of the compressor design applied. The following table summarizes the achievable availability for a short stroke high speed electric motor driven upstream compressor:

High-Speed, Short Stroke Electric Motor Drive Availability	
Task	Availability
Total availability (8,760 hours)	100%
Electric Motor PM (zero hours)	-0.0%
Compressor PM (20% of 6 x 8 hours)	-0.11%
Availability with PM	99.89%
Unscheduled maintenance • Unscheduled for the electric motor (zero hours) • Unscheduled for the compressor (40% of 123 hours)	-0.0%
	-0.56%
Achieved Availability	99.33%

Figure 4: Table showing the calculation of availability for a High Speed Short Stroke electric motor driven reciprocating compressor package

By taking steps to apply the compressor more conservatively this availability can be increased to 99.5% and even higher. The steps might include slowing it down (making it a “moderate-speed” compressor rather than “high speed”) and being more conservative with the valve selection and discharge temperature. The compressor PM can also be driven to zero through the utilization of a frame lube oil system that allows for online filter changes and oil sampling. This alone might increase availability to 99.45%.

2.3 Average Piston Speed

A discussion of reciprocating compressor reliability or MTBR would be flawed without discussing a key parameter, average compressor piston speed.

Average piston speed is the average linear speed at which the piston travels in one revolution of the crankshaft, or through two stroke lengths. It is expressed in units of meters per second (m/s) or feet per minute (fpm).

Average piston speed directly impacts the wear, and therefore the MTBR, of the rubbing seal elements: the piston rings, wear bands (rider bands), and piston rod packing.

The equation used to calculate average piston speed is:

$$\text{Average Piston Speed} = \frac{2 \times \text{Stroke} \times \text{Speed}}{C}$$

Where:

Average piston speed = m/s (feet per minute)

Stroke = mm (inches)

Speed = compressor rotating speed, rpm

C = 60,000 (12)

Seal elements that wear primarily due to rubbing will last longer at lower piston speeds. So, MTBR can be increased by lowering the average piston speed.

The obvious next question is - why don't end-users always buy compressors having a “low” piston speed for each and every application? Obviously everyone wants MTBR to be as long as possible! The answer is capital cost (first cost). There is some relationship between piston speed and capital cost - the higher the piston speed, the smaller the physical size of the machine, the lower the manufacturing cost, the lower the capital cost. Upstream end-users have actually driven compressor manufacturers towards higher and higher compressor piston speeds while accepting the trade-offs with MTBR and efficiency that go with the higher piston speeds. Again, they are very comfortable with the reduced MTBR that might arise with the higher piston speed because their MTBR is primarily driven by the driver and not the compressor.

Upstream end-users that drive their compressors with electric motors oftentimes do consider lower piston speed machines, but always consider the capital cost. For example if the lower piston speed moves the compressor selection to the next larger frame (physically larger and higher price) then the savings from greater MTBR and efficiency must be significant enough to drive the machine's net present value down to the point where that purchase can be justified. These can be very difficult decisions to make because of the guesswork involved in deciding the differences in efficiency and MTBR, when the difference in first cost is a known fact.

Another maybe obvious question might be asked - what is an acceptable average piston speed that would lead to longer MTBR numbers? Most refinery rotating equipment and reliability engineers would offer guidance that something around 3.8 to 4.1 m/s (about 750 to 800 fpm) would be a comfortable maximum for a typical critical refinery application. Figure 5 is a plot of average piston speed versus rotating speed using published stroke and speed data from many reciprocating compressor manufacturers.

The piston speed for “slow speed” machines ranges from about 3.8 to 5.1 m/s (750 to 1,000 fpm) with a concentration from 4.1 to 4.8 m/s (800 to 950 fpm).

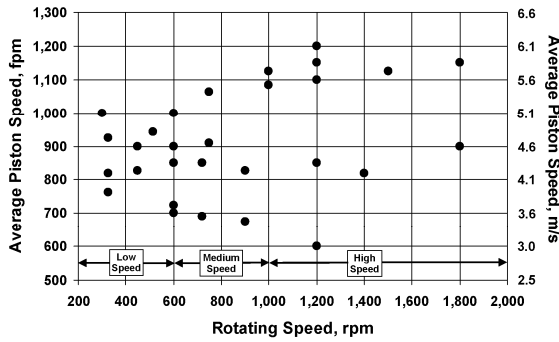


Figure 5: Chart showing the range of piston speed for available reciprocating compressors

Looking at the “high speed” range reflects today’s trend in the upstream market. These piston speeds range from 4.1 to 6.1 m/s (800 to 1,200 fpm) with the concentration being 5.6 to 6.1 m/s (1,100 to 1,200 fpm), or 30% to 50% higher than the concentration of slow speed.

The “moderate speed” range reflects the fact that these are typically short stroke high speed compressors operated at 50% to 65% of their rated operating speed yielding piston speeds reduced by the same amount. So, the cluster is in the 3.6 to 4.6 m/s (700 to 900 fpm) range.

The following table summarizes the discussion of piston speed:

	Piston Speed, m/s (fpm)	
	Range	Concentration
Slow Speed	3.8 – 5.1 (750 - 1,000)	4.1 – 4.8 (800 – 950)
Moderate Speed	3.6 – 5.6 (700 - 1,100)	700 – 900 (3.6 – 4.6)
High Speed	4.1 – 6.1 (800 - 1,200)	5.6 – 6.1 (1,100 - 1,200)

Figure 6: Table summarizing the range of piston speed for available reciprocating compressors

3 Specific Design Differences

3.1 Compressor Valves

The typical upstream high rotating speed high piston speed short stroke compressor uses a high-lift high efficiency (high flow area) compressor valve to minimize the reduction in efficiency resulting from the high piston speed. The valve plate material, lift and springs are specifically selected to fit the application.

To further explain the importance of using high lift high efficiency compressor valves in a high piston speed reciprocating compressor (be it long or short stroke), Figure 7 has been prepared to compare “high” lift to “low” lift valves. Specifically, the

figure shows curves of compression efficiency versus compression ratio at 5.6 m/s (1,100 fpm) average piston speed for the same cylinder utilizing two different valve lifts, “high” and “low”.

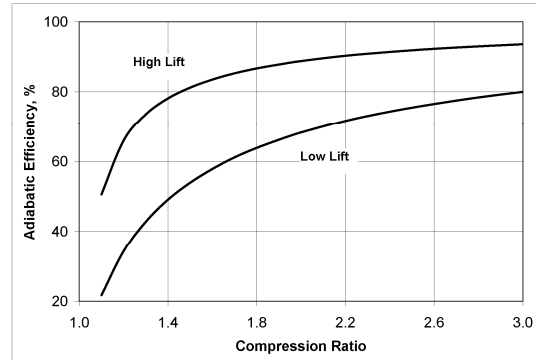


Figure 7: Chart compares the compression efficiency of a compressor cylinder using “high lift” versus “low lift” compressor valves

This shows the penalty of using a low lift low efficiency high reliability compressor valve at a high piston speed.

Figure 8 shows the same plot but changes the compressed gas from natural gas to hydrogen (a very common refinery or process gas) and reduces the rotating speed (and therefore, the average piston speed) by 50%.

Notice in Figure 8 how the two efficiency curves are almost on top of each other, begging the question - why use the higher lift valve when it offers no significant improvement in efficiency and will most likely be less reliable? It should now be obvious why downstream hydrogen compressors use low lift compressor valves - the very favorable trade-off between efficiency and reliability.

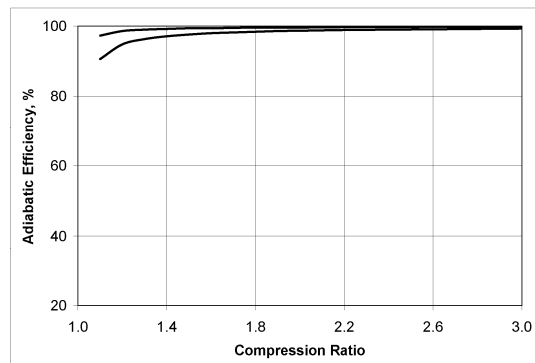


Figure 8: Chart comparing efficiency when compressing hydrogen with high-lift to low lift compressor valves

3.2 Distance Pieces

The typical upstream high speed compressor is equipped with a very short distance piece, if any at all. This allows the compressor to be as narrow as possible benefiting portability. The short distance piece also keeps the mass of the reciprocating components to a minimum by minimizing the length of the piston rod. Lower mass means lower inertia loads which is a critical design factor for short stroke high speed machines.

A moderate speed downstream compressor is often equipped with a long two compartment distance piece (API-618 Type C design). The process industry's practice is to use a Type B, C or D depending upon the user's preference. Portability and inertia loads are typically not important issues with these compressors.

3.3 Piston Rod Packing

Water cooled piston rod packing cases are not common in upstream applications, probably mostly due to a lack of relatively cool cooling media to make packing cooling beneficial. On the other hand, cooled packing is quite often utilized in downstream short stroke moderate speed compressors. Cold cooling media is readily available and the cooling benefits the rod packing reliability.

3.4 Wearbands (Rider Rings or Rider Bands)

While the maximum average piston speeds remained in the 4.1 to 4.3 m/s (800 to 850 fpm) range, the use of wearbands by high speed short stroke manufacturers was not common. Pushing the maximum piston speed into the 5.6 to 6.1 m/s (1,100 to 1,200 fpm) range made the use of a wearband a requirement to avoid rapid wear of the compressor cylinder or liner main bore.

Wearband bearing pressure loads in the 0.7 to 0.8 bar (10 to 12 psi) range have proven to provide more than adequate wearband life in the typical upstream application. However, many end-users and manufacturers have found this to be inadequate for many downstream applications where very long MTBR is desired. Wearband bearing pressure loads in the 0.35 to 0.4 bar (5 to 6 psi) range are desired. This certainly presents a challenge to the high-speed manufacturer with the desire to create a suitable moderate speed short stroke downstream design.

Reducing the bearing pressure loads 50% in existing piston and rod assembly designs requires

reducing the piston and rod assembly weight by 50% or doubling the installed wearband width. A very difficult design challenge.

$$\text{Wearband Bearing Pressure} = \frac{\text{Weight}}{(C)(D)(W)}$$

Where:

Wearband Bearing Pressure = bar (psi)

Weight = Weight of the complete piston assembly plus one-half the weight of the piston rod, kg (lb_M)

C = 0.00883 (0.866)

D = diameter of the piston mm (inches)

W = total width of all the wearbands on the piston, mm (inches)

3.5 Capacity Control (Unloaders)

This is a topic that is considered quite differently between upstream and downstream compressor users. The typical upstream compressor must be capable of handling varying conditions (gas inlet and outlet pressure, and flow) and therefore requires the use of "unloaders". The term unloader is very generic and encompasses many different types of hardware, i.e. finger-type suction valve unloaders, plug-type suction valve unloaders, head end pneumatic fixed volume clearance pockets, head end manual variable volume clearance pockets, etc..

Describing all the different kinds of available unloader hardware is beyond the scope of this paper. However, it can be stated that all of these devices either change the piston displacement or change the fixed clearance – they all change the gas throughput and therefore the horsepower consumed.

The upstream user utilizing a natural gas fueled engine also has the possibility to vary the rotating speed. Speed variation does not reconfigure the compressor to adapt to new operating conditions, but does provide for easy variation of throughput.

The typical downstream user tends to see all these devices as adding to the unreliability (decreasing availability) but understands their necessity. This user's first choice for throughput control is a process gas recycle around the compressor. Given that the process conditions are typically very stable this method works very well and is very reliable. It is not an efficient method as the compressor is always running at 100% capacity and 100% power. For example, maybe only 95% of the gas is actually going to the process (5% is going around the recycle loop), so 5% of the power is completely wasted.

The upstream user sees unloaders as being necessary and therefore accepts their negative impact on availability.

With the conditions continually changing this is the only way to make the compressor fit the application and allow it to operate safely and continually.

4 Conclusion

It was the purpose of this paper to compare two different short stroke reciprocating compressors; “high-speed” designed for upstream applications and “moderate-speed” designed for downstream applications. The configuration and reliability differences were discussed and reviewed. Specifically, the differences in configuration and design required to achieve the very high availability required by process end-users was explained. A properly configured moderate-speed short stroke reciprocating compressor offers a mechanically viable and economically attractive alternative to the traditional slow-speed long stroke machine which has been used in process applications for the last one hundred plus years.

5 Acknowledgement

Joe Spiller, Principal Engineer - Rotating Equipment Team Leader - North America, for Shell Exploration & Production Company in Houston, Texas, USA was a major contributor to this paper.



Material development transferability counts

Dr Marc Langela
Research and Development
STASSKOL GmbH
39418 Staßfurt
Germany
marc.langela@stasskol.com

7th Conference of the EFRC
October 21th / 22th, 2010, Florence

Abstract

In compressor applications sealing elements out of PTFE and PEEK compounds, with additives for reinforcement and self-lubrication are frequently used. The life-time of the sealing elements is sometimes the bottleneck towards a sufficient service time between two routine maintenances. Especially in industrial applications the wear behaviour can be negatively influenced by reducing atmospheres and/or low dew points. In order to improve the performance of the materials, several tribological investigations were conducted on compounds with different filler and lubricant concentrations, but the transferability of the results into the real application was seldom in the scope of these investigations.

To fill this gap, a special reciprocating tribometer was developed for testing samples under close-to-service conditions. Additionally, the real wear behaviour was determined using an on-site test compressor to evaluate the transferability of the results.

It can be shown by the results of the investigations, that the tribological behaviour of the sealing materials is only one side of the medallion. Also other aspects like for example mechanical properties have to be taken into account and the most important task is to combine all material properties to predict the life-time of the sealing elements at the real application. Only by this approach it is possible to speed up the material development process significantly, which will leads to shorter development times for customized materials.

1 Introduction

Reciprocating compressors are widely used to compress gaseous media for industrial applications, for example at chemical plants for hydrogenation reactions, polymerizations or Polysilicon production. These are full-integrated and automated industrial processes, which are running continuously and therefore, a failure in compressor operation, can cause unexpected and expensive down-time.

In consequence, the reliability is one of the most important properties of a reciprocating compressor system. The crucial items in respect to reliability are often the sealing elements such as piston rings and piston rod sealings which are mostly produced out of Polytetrafluorethylene (PTFE) and Polyetheretherketone (PEEK) compounds with increased wear resistances. These materials are optimized for compressor applications and the development is achieved by tribological characterizations of material compositions with different contents of fillers and/or lubricants.

To achieve material development effectively, it is highly important that the results from tribological testing can be compared to the material performance at the real compressor applications. In general, the transferability of polymer testing into the target application is the pre-dominant factor for optimizing material compositions.

At tribological characterizations, three main factors (*Test Rig Design, Materials and Test Conditions*) of the so-called “tribological system” have to be reproduced and designed according to the target application. Therefore, a test rig was designed that enables the determination of the wear resistances under reciprocating sliding conditions with parameters that are as close as possible to compressor applications.

However, even the most sophisticated experimental setup can never provide 100 % comparability to the “reality of the field”. In order to overcome this weakness we also have to concentrate on other material properties than only on pure wear resistances and we have to determine how these properties are interconnected to result in the observed material performances at the compressor applications.

In this paper we will explain how the experimental setup was designed to perform close-to-service measurements and in which way we defined the important parameters of the tribological system in comparison to reciprocating compressors.

We will describe how experimental results at the test rig are correlating with wear resistances at service conditions and we will propose how this correlation should be improved.

2 Tribological testing

Tribology origins from the Greek word for friction (\Rightarrow tribos) and it is an interdisciplinary part of mechanical engineering. It combines engineering, material science, physics and chemistry to a scientific description of friction, wear and lubrication. Tribology is of high general economic importance as on average about 5 % of the gross products of the industrial nations are destroyed by friction and wear¹.

To determine the wear resistance and the friction coefficient of certain materials, tribological experiments have to be conducted according to the general setup at Figure 1:

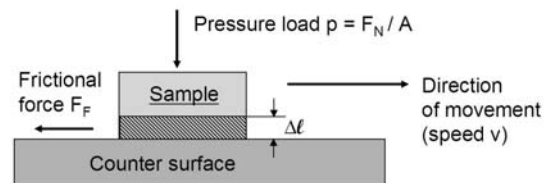


Figure 1: General setup of tribological testing

A sample is sliding under a pressure load p against a counter surface with a relative velocity v . The movement causes a frictional force F_F which is oriented against the sliding direction and it results in wear which is observed by a reduction Δl of the sample height. From these observations together with the duration t of the tribological experiment the wear rate (Equation 1) and the friction coefficient (Equation 2) can be calculated as two important results.

$$\text{Wear rate } k = \Delta l / (p \cdot v \cdot t)$$

Equation 1: Calculation of the wear rate

$$\text{Friction coefficient } \mu = F_F / F_N$$

Equation 2: Calculation of the friction coefficient

The lower the wear rate the higher is the wear resistance of the material in the certain tribological environment and the higher should be in theory the service-life-time of the material at the application. The friction coefficient should correlate with the frictional energies that are caused during the application and therefore determines the level of thermal energy that will be produced.

The principle of tribological measurements is straight forward and easy to understand, but tribological characterizations are very sophisticated because of the complexity of the tribological system. We will describe the tribological system at the next section.

3 The tribological system

The *test rig design*, the *materials* and the *testing conditions* are the three major components of a tribological system. Maximum transferability of material testing can only be achieved if all three factors are as close as possible to the corresponding factors of the target application.

In case of the reciprocating piston compressor, the three tribological factors are described below.

3.1 Test rig design

A huge variety of different tribological *test rig designs* to characterize the tribological properties of polymers are reported at the literature². One of the most popular designs is represented by the pin-on-disc layout, where a test pin is sliding on a disc that rotates with a constant velocity v (see Figure 2).

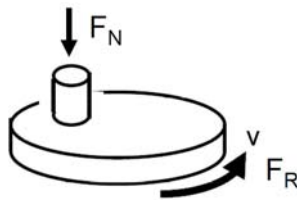


Figure 2: Illustration of the pin-on-disc layout

This test design is often used to develop wear resistant materials; however, the principle of movement is totally different from those of reciprocating compressors.

To proof the transferability between this characterization method and the compressor application we conducted several experiments with a pin-on-disc tribometer and a setup, where a sample pin was mounted on a reciprocating piston (see Figure 3).

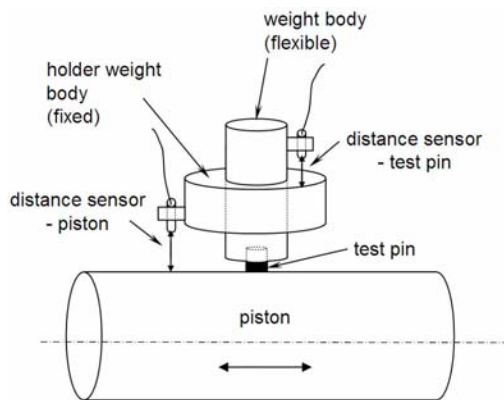


Figure 3: Illustration of the pin-on-piston layout

A set of different materials were characterized by using both test rig designs and the results are shown at Table 1.

Material composition	Rotation		Reciprocation	
	wear	T	wear	T

	rate*	[°C]	rate*	[°C]
PTFE + Bz + carbon + MoS ₂	0,1	80	13,3	79
PTFE + glass fibers	18,6	95	37,9	90
PTFE + carbon fiber	1,2	40	15,2	50
PTFE + PEEK	0,1	80	4,6	87

* wear rate in [10⁻⁷ mm³/Nm]

Table 1: Comparison of results between rotating and reciprocating characterization

The results at Table 1 are obtained by using the same parameters at the pin-on-disc and at the pin-on-piston system. For example the counter surfaces were made out of stainless steel with tungsten carbide, average velocities were 2.7 m/s and test durations were 24 hours to 48 hours.

By assessing the wear rates at Table 1 one can easily see, that the results at the different test layouts are not corresponding to each other. Furthermore, the relation between the wear rates at the rotating equipment and the wear rates at the reciprocating equipment seem to be dependent on the material compositions itself. Therefore, it's not possible to perform measurements with rotating equipment in order to predict wear resistances at an application which is carried out under reciprocating movement.

In section 4 we will explain how we achieved a better correlation between testing and application performance by designing a novel tribological testing device.

3.2 Materials

The *Materials* comprise of the sealing material in use, the material of the counter surface, the surrounding medium, the lubricant (if used) and also the impurities that are influencing the performance of the materials.

At a reciprocating compressor application for example the counter surface at the tribological testing has to be the same as the surface of the piston rod or the cylinder (including the surface roughness). The surrounding media are the gases that have to be compressed and lubricants are not present if we want to optimize materials for dry-running applications. However, tribological material optimization always takes place under laboratory conditions and it would be very difficult to reproduce the impurities that are influencing the sealing materials at the industrial processes.

Another important factor is the humidity of the gaseous media, because the dew point directly affects the wear resistance due to its influence on the formation of transfer films³.

3.2 Test conditions

The test conditions are the last factor that has to be transferred from field to material testing. At reciprocation compressor applications the relevant parameters are that affect the performance of the sealing material are temperature, sliding speed and the contact pressure of the sample against the counter surface.

4 Experimental setup

In the last section we described, that the design of the test equipment, the materials in use and the test parameters are all influencing the material performance under tribological testing. We also mentioned that all these factors have to be very close to the real application in order to ensure transferability and to enable efficient material development for sealing applications.

In this section we describe how the experiments were set up in order to provide this transferability.

4.1 Tribological characterization

A novel test rig was build which allows tribological measurements under close-to-service conditions (see Figure 4). A reciprocating rod is equipped with a sample holder and the moving samples are surrounded by counter surfaces. The contact pressures p , the average sliding velocities v and the temperatures T of the counter surfaces can be varied according to the parameters of the application. Sensors constantly detect the distance between the counter surfaces and the sample holder in order to ensure on-line wear measurements. Furthermore, the temperatures of the counter surfaces and the friction coefficients can be constantly monitored.

Additionally, the tribometer has a housing that allows the application of different gaseous media like Air, Hydrogen, Nitrogen and Methane and the gas supply system is capable of adjusting the dew point of the gas by a controlled drying and moistening procedure.

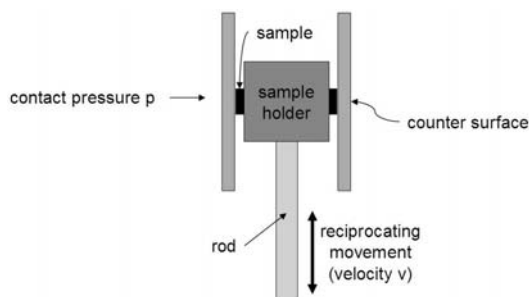


Figure 4: Design of the reciprocating tribometer

4.2 Compressor testing

In order to compare the results of tribological characterization with the performance of the materials at the compressor application we used an on-site test compressor with a vertical and a horizontal axis. (see Figure 5) The piston rod diameter of the compressor is 70 mm and the average piston speed is 2.7 m/s at a stroke of 130 mm, which is the same stroke that is realized at the reciprocating tribometer.

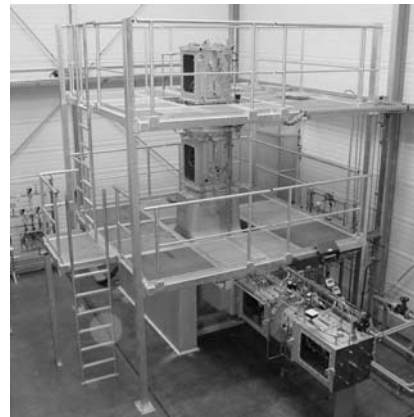


Figure 4: On-site test compressor

The materials were tested by using them as piston rod sealing elements. However, an on-line monitoring of the wear behaviour of the sealing materials like at the reciprocating tribometer is not possible. To distinguish between run-in wear and constant wear the piston rod sealing was dismounted after a “run-in phase” of 250 hrs and the dimensions of all sealing elements were measured. After assembling and re-installing the piston rod, the compressor testing was continued for additional 250 hrs at the “test phase”.

After the total test duration of 500 hrs the piston rod was disassembled in order to measure the sealing elements a second time. The incremental wear of the sealing elements between the “run in phase” and the “test phase” was used to calculate the wear rates in combination with the pressure differences throughout the packing that were measured on-line during the testing procedure.

5 Results & Discussion

A set of materials with different compositions was tested at the reciprocating tribometer and at the on-site test compressor in order to compare tribological characterization with the performance of the materials under service conditions.

The materials are PTFE compounds with different carbon black (filler) and graphite (lubricant) concentrations. The combined fraction of the two additives is always 35 weight percent, but the relation between carbon black and graphite varies from 25:1 to 2.5:1 (see Table 2).

	Carbon black	Graphite
Material A	24 w-%	1 w-%
Material B	23 w-%	2 w-%
Material C	20 w-%	5 w-%
Material D	15 w-%	10 w-%

Table 2: Composition of the PTFE compounds

Semi-finished products were obtained by mixing the raw powders at a PTFE mixing device followed by cold compression molding. All processing steps were well controlled in order to guarantee comparable conditions. After machining the sample pins, characterization was performed at the reciprocating tribometer by using the following parameters:

average velocity = 2.7 m/s
 contact pressure = 30 barg
 stroke = 130 mm
 temperature = 120 °C
 surrounding medium = Hydrogen
 dew point = - 80 °C
 counter surface = stainless steel with tungsten carbide coating
 counter surface roughness = 0.12 my (R_a)

The materials were allowed to run in at the reciprocating tribometer for a time period of 24 h in order to achieve a regime of constant wear development. The test was continued for another 24 h after reaching the steady state in order to collect the data to calculate the wear rates listed at Table 3.

	Wear rate (tribometer)
Material A	$3.5 \cdot 10^{-7} \text{ mm}^3/\text{Nm}$
Material B	$2.1 \cdot 10^{-7} \text{ mm}^3/\text{Nm}$
Material C	$4.8 \cdot 10^{-7} \text{ mm}^3/\text{Nm}$
Material D	$8.1 \cdot 10^{-7} \text{ mm}^3/\text{Nm}$

Table 3: Wear rates of the materials measured at the tribometer

Table 3 reveals that the wear resistance depends on the composition of the PTFE compound. Material B has the lowest wear rate and thus shows the best

performance under the conditions of the tribological characterization.

The same materials were processed into piston rod sealings for additional testing at the on-site compressor. The conditions at the on-site compressor were chosen to ensure maximum comparability to the tribological characterization:

average velocity = 2.7 m/s
 suction pressure = 30 barg
 discharge pressure = 30 barg
 stroke = 130 mm
 temperature = 120 °C (adjusted by cooling)
 compression gas = Hydrogen
 dew point = - 80 °C
 piston rod surface = stainless steel with tungsten carbide coating
 roughness of piston rod surface = 0.12 my (R_a)

The on-site compressor is capable of testing four different materials at four piston rod sealings at one test sequence. The internals of each piston rod sealing are four ring pairs with tangential cutted cover and sealing rings.

After the “test phase” all ring segments at each piston rod packing were measured to determine the performance of the materials as explained at section 3. The wear rates were calculated by dividing the volume loss of the sealing elements by the pressure difference, the average velocity and the test duration (see Equation 1). This was done separately for every ring pair and the results were averaged for every material to achieve the wear rates listed in Table 4:

	Wear rate (compressor)
Material A	$5.7 \cdot 10^{-7} \text{ mm}^3/\text{Nm}$
Material B	$3.8 \cdot 10^{-7} \text{ mm}^3/\text{Nm}$
Material C	$7.5 \cdot 10^{-7} \text{ mm}^3/\text{Nm}$
Material D	$9.3 \cdot 10^{-7} \text{ mm}^3/\text{Nm}$

Table 4: Wear rates of the materials measured at the on-site compressor

A comparison between Table 3 and Table 4 shows, that at both, tribological characterization and compressor testing material B shows the highest wear resistance by having the lowest wear rate. Furthermore, also the other materials are at the same order in respect to their wear resistances.

However, the values are not identical between these two alternative characterization methods and they do not show a constant correlation.

The wear rate of material B is nearly doubled at the compressor whereas the wear rate of material D is only slightly higher compared to the tribological characterization.

6 Conclusion & Outlook

We investigated the wear resistance of four different PTFE compounds at a new reciprocating tribometer as well as at an on-site compressor under service conditions. The task was to achieve maximum comparability between these two characterization methods in order to enable an effective approach to the development of sealing materials.

The sequences of the wear resistances are the same at each characterization method, indicating a high degree of transferability of the results. However, the measured wear rates determined at the tribometer and the on-site compressor are not identical.

Although we tried to adapt the reciprocating tribometer to the real application; 100 % comparability will never be possible between these 2 systems. As a very important difference, dynamic mechanical loads are stressing the materials at the reciprocating compressor application, while a constant counter surface pressure is applied at the tribological characterization.

As already described in the latest literature^{4,5,6}, the wear resistance can significantly be influenced by the mechanical properties of the investigated materials. The task for future research is to clearly identify the relationships between the mechanical and tribological properties at compressor applications in order to enable increased efficiency at material development processes and to provide predictability of service life-times for customer applications with a higher accuracy.

This will lead to new performance levels of spare-parts such as piston rod sealings and piston rings, which are sometimes the crucial elements for driving sophisticated industrial processes towards higher reliability.

References

- ¹ Society of tribology; 2007
- ² Sinha, S.K.; Briscoe, B. J. *Polymer Tribology* 2009, Imperial College Press, Singapore
- ³ Radcliffe, C. , *Sealing Technology*, 2005 (11), p.7-11, Nov 2005
- ⁴ Tariq, N.H.; Hasan, B.A.; Akhter, J.I.; Ali, F. *Journal of Alloys and Compounds*, 469 (1), p.179-185, Feb 2009
- ⁵ Musil, J. / Louda, M. / Soukup, Z. / Kubasek, M. , *Diamond & Related Materials*, 17 (11), p.1905-1911, Nov 2008
- ⁶ Sharma, M. / Rao, I.M. / Bijwe, J. , *Wear*, 267 (5), p.839-845, Jun 2009

Decreasing time and cost effort by Virtual Prototyping in the Compressor Development

by:

**Tobias Spilker, Antonius P. J. Voncken, Matthias Budde,
Christoph Steffens, Martin Rebbert
FEV Motorentchnik GmbH
Germany
ecca@FEV.de**

**7th Conference of the EFRC
October 21th / 22th, 2010, Florence**

Abstract

The layout of compressor components strongly focuses on the reliability of the design and is often based on long time experience. The modern market demands more and more energy efficient machines. This demand imposes new challenges on the design as a compromise between high reliability and a reduction of the energy demand seems difficult to achieve. Here modern Computer Aided Engineering (CAE) simulation programs come into play. They allow the prediction of relevant system parameters with respect to design changes at the virtual design phase. Together with the wealth of information on proven reliable machines in the field, a benchmark via CAE modelling is possible. With this benchmark database a new generation machine can be benchmarked regarding its performance, reliability, etc via the appropriate CAE-simulations. This procedure seems at first expensive, but it allows a solid procedure to minimize the risk of failures in newly designed components. In the long run, the company image damage is often more expensive than the costs involved to solve a machine failure. Especially with the quality of today's CAE-tools, reliable predictions of relevant system parameters of newly designed components are possible.

Typical analysis results that CAE tools make available are:

- Dynamic simulation of parts or the complete system via Multi Body System (MBS) tools. Typical results will be the forces and motion of all modelled components. These data can be used for further analysis
- Stress analysis of components. Once the dynamic loading of a component is calculated from an MBS analysis, the corresponding dynamic deformation and stress distribution can be analyzed via Finite Element Method (FEM)
- The outcome of a FEM analysis can serve as input for Fatigue Analysis and/or
- Acoustic analysis. Whereas MBS and Computational Fluid Dynamics (CFD) calculations can also provide necessary data for such analysis
- Gas exchange analysis via 1D- (for a whole system) or 3D-CFD analysis (for a detailed valve flow calculation)
- From the results of a MBS analysis the dynamic forces acting on bearings can be used to perform an Elasto-Hydrodynamic (EHD) analysis of a journal bearing. This EHD analysis allows a detailed simulation of the behaviour of the lubricating oil film in a dynamically loaded bearing. The major outcome of such an analysis is a prediction of the wear tendency, the wear region, maximal oil-film pressures, minimal oil film thickness and oil feed through

In short, modern CAE-tools allow a reliable prediction of the system behaviour under realistic operation boundary conditions at the design stage.

In the following four examples are presented in which CAE tools, introduced in engine development processes, are applied in compressors analysis:

1. Acoustic analysis
2. Gas exchange analysis
3. EHD bearing analysis
4. Cylinder lubrication

1 Introduction

The importance of the acoustics and vibration behaviour of large compressors is still increasing due to marketing aspects and customer demands. Typical noise issues of e.g. piston compressors are orifice noise, noise due to valve dynamics and effects due to the large noise radiating surfaces. Low frequent noise appears in the area of the air intake. This orifice noise can be eliminated by suitable silencers or damper. Another important noise issue occurs due to opening and closing events of the valves. On the one hand the corresponding impacts lead to a broad band excitation of the housing structure, on the other hand an excitation occurs due to sudden pressure drops and/or air pulsations. Hydraulically actuated pressure valves can be classified, in this case, as especially critical. This leads to the fact, that all the above mentioned components have to be designed and optimized carefully regarding noise and vibration. In addition, large radiating surfaces of the compressor system lead to high noise level – even in combination with relative low excitation forces. The large surfaces arise due to the “disintegrated” design of the piston compressor type (generator, long cylinder, long piping) and big smoothing tons for the pulsating air flow. Additionally, today’s design of the compressors with completely more or less rigid coupling or screwing of the different components leads to a critical structure borne noise transfer. Accordingly a high degree of attention has to be paid to the design of the housing structures.

Against this background CAE-based methodologies and tools, which improve the noise and vibration quality, can help to minimize time and costs during the development process. In this context commercial programs are typically used, which are based on MBS, FEM and CFD. These tools allow the simulation of the noise generation chain. A deeper understanding of the noise mechanisms and the elaboration of measures for an improved noise and vibration behaviour of single components or the entire compressor system are the results.

As already mentioned, piston compressors often have large radiating surfaces which can be critical for the noise and vibration behaviour. The demand for a stiff structure with low radiation efficiency is the consequence. The design process of such a stiff housing structure should be supported by FEM-based simulations. Therefore FE-models of the housing structures are excited with realistic excitation spectra and the response at the radiating surfaces is calculated. In this context FEV

Motorentechnik tools as FEV DIRA (Dynamic Impact Response Analysis) and FEV FERS (Fast Estimation or Radiated Sound Power) are used, which are based on commercial software products. Output of FEV DIRA is the surface velocity at the

radiating surface; output of FEV FERS is the radiated sound power in the far-field of the component. The determination of the excitation forces can be based on measurements. However, it is also possible to ascertain the excitation with the help of MBS calculations. For this, the simulation model will be set up in FEV Virtual Engine. Based on this model, dynamic effects as well as bearing reaction forces at the intersections of the cranktrain and the compressor body are calculated. Hydrodynamic bearings are represented by special subroutines which calculate the bearing reaction forces as well as the interaction between hydrodynamic oil film, crankshaft and housing structure based on the solution of the Reynolds differential equation. A more detailed investigation method of journal bearings is presented later.

The dynamic characteristics of the components are considered by integrating flexible structures into the MBS model. The calculated force spectra are used to excite the housing structure of the compressor and to determine the surface velocities at the radiating surfaces and the sound power in the far field. This allows the identification of weak areas of the structure and the development of structural improvement measures.

Other noise issues were mentioned previously: orifice noise and valve dynamics. In this context, in the acoustic and gas dynamic development process one-dimensional CFD calculations are used. Component analysis and complete system simulations can detect the weak points of the system in the concept phase (see figure 1). The simulation provides all thermodynamic values and the valve kinematics in the time domain. Solutions for pulsation noise reduction can be worked out by the use of (virtual) test methods within a short time.

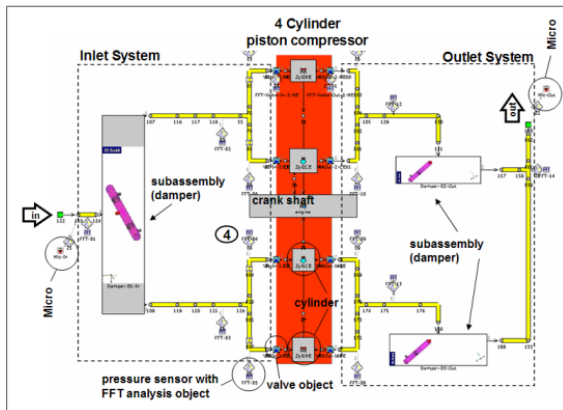


Figure 1: Map of the complete simulation system in GT-Power

The gas dynamics in the system determine for instance the radiated orifice noise. Aim of an acoustic engineering is the noise reduction or pulsation reduction.

If the orifice noise is the relevant development parameter, typically a rotational speed sweep (which is sometimes only possible in simulation) is performed to analyze resonances of the inlet or outlet system. In the Campbell diagram the resonances (see arrows in figure 2) of the inlet or outlet system can be seen as a constant band over the complete speed range. These resonances are the weak points of the system regarding acoustics. With the knowledge of this information, silencer and damper systems can be designed to reduce the orifice noise.

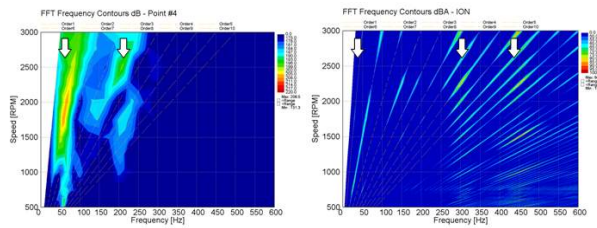


Figure 2 Campbell diagrams, left: point #4; right: radiated intake orifice noise

2 Gas exchange analysis

Although different in their purpose of use (engines are used to transform energy into crankshaft work whereas compressors transform crankshaft work into pressure energy), both engines and compressors face the same problems in terms of gas exchange, volumetric efficiency or pumping losses. For the development process of combustion engines several simulation methods have been established. Especially the early design phase of all parts related with the intake and exhaust air duct is accompanied very thoroughly by 1D or 3D simulations as changes of design during that phase

are cheap compared to a later phase when hardware is ready for test bench testing. Therefore, 1D gas exchange simulations are used to analyze the behaviour of the complete system “engine” and the effects of changes in tube lengths or diameters, changes of restriction coefficients and changes in valve timings. 3D simulations are used to optimize the design of one specific part such as intake ports, intake or exhaust manifolds. Figure 3 shows the 3D CFD simulation of the flow through an intake valve of an SI engine using a moving mesh for the piston and valve motion.

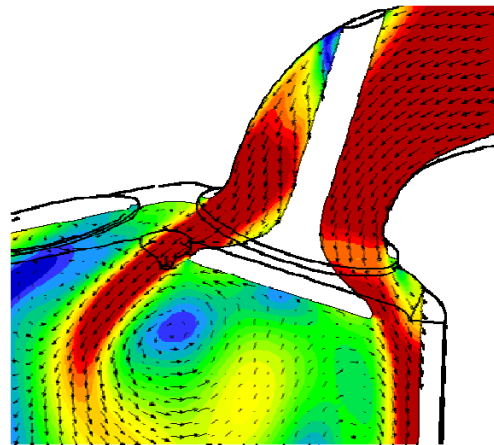


Figure 3: CFD simulation of the intake flow in an SI engine using a moving mesh

Gas exchange analysis: 1D simulation for piston compressors

1D gas exchange simulations can also be applied to design process of piston compressors. Especially the behaviour of multi-stage compressors can be analyzed in modeling the air ducts between the cylinders, the heat exchangers and the cylinders itself. The well introduced software tool GT Power uses standard elements like tubes, bends, flow restrictions and cylinders. One can model the pressure losses due to friction or shape resistances, pressure gain due to compression and pressure waves due to the transient behaviour of a pressure system with moving parts. Also the thermo dynamical behaviour of the system is calculated when gas is compressed or expanded and heat is transferred from walls to the gas or vice versa. Figure shows the layout of a GT Power model for the gas exchange simulation of a 3-stage compressor. Cylinders #1, #3 - #5 work in the first stage, cylinder #2 works in the second stage and cylinder #6 works in the third stage. The intercoolers and the aftercooler are modeled using heat transfer models in the tubes that connect the stages.

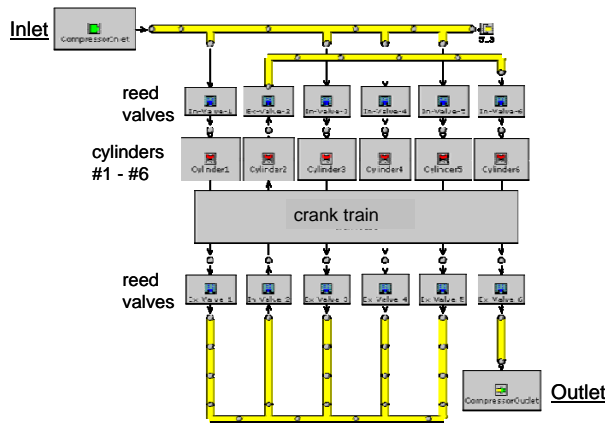


Figure 4: GT Power model of a 3-stage compressor

Using such a model one can simulate the effects of different control strategies on the effective power consumption of the compressor, or the pressure ratios and efficiencies in single stages. Figure shows the effects of different control strategies on the pressure ration in all three stages. Whereas the speed control works on all three stages the intake pipe throttling and the change of dead volume for a change of the effective compression ratio is applied only to the first stage. However, it becomes obvious that the biggest effect occurs in the second stage which could be subject to overheating due to the increase in pressure ratio Π .

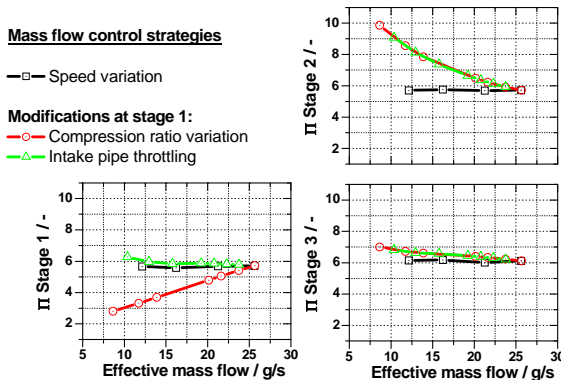


Figure 5: Results for different control strategies in a 3-stage compressor

Gas exchange analysis: 3D CFD analysis of the valve flow in a reed valve

As with combustion engines 3D simulations can be used to optimize special parts of the air duct such as valves or manifolds in order to minimize pressure losses or to optimize the distribution of secondary gases to several cylinders. 3D simulations allow for the modeling of complex geometries and the resolution of the flow field in three dimensions; on the negative side there are higher computational times as with 1D simulations. Figure 6 shows the model of a reed valve where the valve gap is modeled as a moving mesh in order to

simulate the opening and closing of the valve. On the right side the results for the flow field are shown in a section view. It can be seen how the flow uses only three out of four outlet slots which results in higher pressure losses in that valve. An optimization for such a valve could lead to a better volumetric efficiency for the compressor.

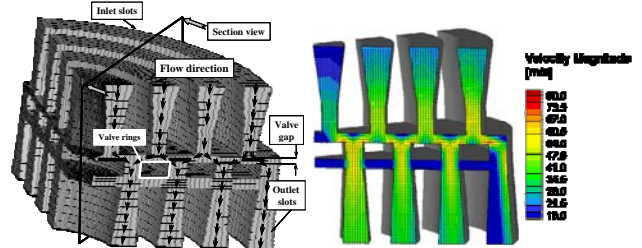


Figure 6: 3D model and results for the CFD simulation of a reed valve

3 EHD journal bearing analysis

The most obvious parameters that are used in a journal bearing design are its length, diameter, clearance, and loading conditions. The choice of the oil-type is usually defined by the temperature range of the bearing at operation and the gas-environment the oil is exposed to. Based on these primary parameters and an ‘in-house’ applied rule for scaling bearing dimensions, conservative bearing layouts can be made. However, a question like: ‘How much reduction of the bearing length is then still possible given the fact that the bearing is still safe’ can not be answered with this procedure. If similar kind of questions need attention, for instance if friction reduction issues and/or energy efficiency constraints must be met in the new design, then an EHD analysis is the adequate tool to address these topics.

An EHD analysis will perform a result set in the time domain of:

- Relative motion of the pin in the bearing housing (although only in the range of the clearance)
- Simultaneously the oil film pressure distribution in the lubricating oil film
- Local deformation of the bearing shape due to this oil film pressure

The basic equation that stems this calculation is the mass conservation of the oil in the bearing. When applied to bearings, this equation can be simplified to the so called Reynolds-equation. The Reynolds-equation is a partial differential equation that allows the calculation of a pressure profile as a result of an oil film profile.

Due to the load on the bearing the bearing pin is forced to move to that particular new position and with that particular speed (thus creating an oil film height change), that will result in reactive oil film pressure distribution that will counter balance the applied force. The major part of the oil film pressure distribution results from the rotation of the bearing pin with respect to the housing. Its pressure peak position and shape depends, apart from the bearing primary design parameters (length, diameter, clearance, oil viscosity), on the pin's eccentricity position and rotational speed. The other part of the oil film pressure distribution results from the squeezing speed of the oil film i.e. the pins eccentricity velocity. If the elastic coupling is included, the shape of the oil film (that governs the pressure profile shape) itself depends on the pressure profile due to induced deformations. The inclusion of the elastic coupling requires an iterative solution scheme at every time step. In almost all bearings the influence of the elasticity is significant.

The impact of the elasticity is that it has the tendency to 'broaden' the oil film pressure peak as shown in the examples below.

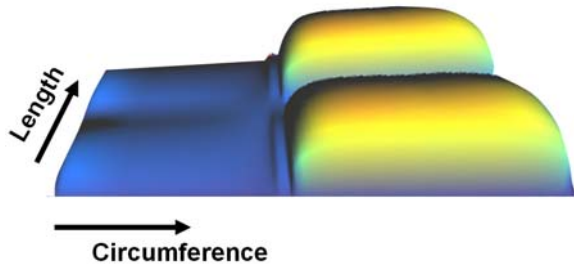


Figure 7: Example of a pressure profile of an EHD analysis with 360 degree ring groove and two grooves over the full bearing length

Depending on the bearing's stiffness two or more local pressure peaks can occur. Once the EHD simulation is done an analysis of the minimal oil film thickness (MOFT) and maximal oil film pressure (MOFP) over time is conducted.

EHD analysis: Mixed Friction

In most cases, the bearings are loaded to such extend that the minimal oil film height will be below the value of the surface roughness of shell and pin. In this case, the bearing is said to enter the mixed-friction regime. Now an extra pressure contribution will show up that represents the metal-metal contact pressure the bearing shell and pin exhibit at that particular time step. This mixed friction contact pressure depends on the amount of overlap that the two rough surfaces exhibit. Note that the contact zone is still filled with oil. The mixed friction model uses an effective local oil film height that is surface roughness averaged. As a

consequence, an EHD analysis that shows regions with significant metal-metal contact pressure values in comparison to the hydrodynamic pressure, predict a high wear tendency at that particular moment in time and at that particular region.

A typical example of a wear tendency distribution is shown in the figure 8. On the x-axes the circumferential angle in degrees is plotted; on the y-axes the Minimal Oil Film Thickness (MOFT). Distribution is plotted in percent. MOFT-Distribution represents the one cycle averaged value of the local oil film height measured in height-units sigma, where sigma represents the root mean square surface roughness of the bearing. Typically sigma is in the 1.4 micron range for well treated bearings. Figure 8 depicts that if one were an observer sitting at for instance the 67° circumference position on the bearing housing (the magenta vertical line in the figure), you would see per cycle: 22% of the time local oil film heights values above 20*sigma (dark blue), 5% of the time oil film heights between ten and twenty sigma (blue), 15% of the time oil film heights between five and ten times sigma (light blue), ... and 5% of the time oil film heights between 0.75 and 0.5 times sigma (red). The red and orange areas indicate wear. In this example the predicted wear region would be from 40° to 110° circumference and this wear is valued as critical as a noticeable red area is visible.

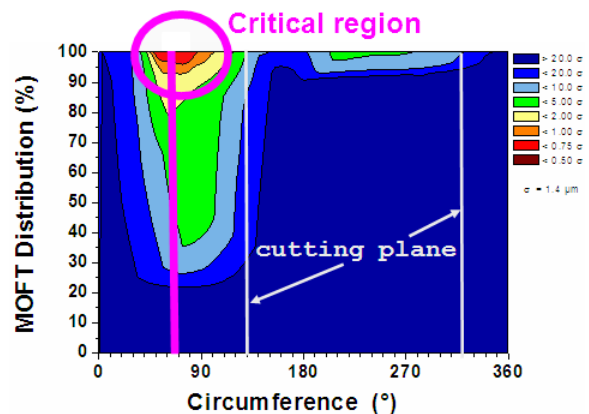


Figure 8: Example of a wear tendency distribution of a con rod big eye bearing

EHD analysis: Inlet Boundary Conditions

Special care must be taken on the oil inlet boundary conditions. In most EHD-tools the oil inlet boundary conditions are incorporated as predefined pressure boundary values over time. These usually suffice to investigate the bearings dynamic behaviour.

However, especially if oil starvation on bearings seems to be a problem, these ‘simplified’ oil inlet boundary conditions are too poor to adequately determine a bearing’s behaviour under these critical conditions.

Apart from most trivial inlet geometries like grooves or oil inlet bores, more complex oil inlet layouts can be analysed. A typical example is shown below for a connecting rod small eye bearing with six oil inlet grooves over the complete length of the bearing.

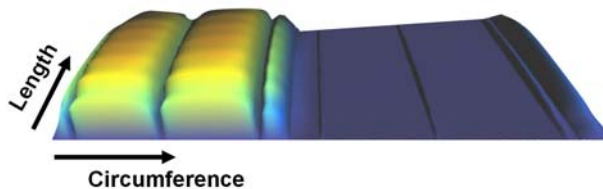


Figure 9: Example of a pressure profile of an EHD analysis of a con rod small eye bearing with various grooves over the full bearing length

EHD analysis: Summary

EHD-analysis is a strong tool to investigate the quality of a bearing layout. These analysis are most often used when bearing problems occurred (root cause analysis) or when a new bearing layout must be evaluated. An absolute classification of a bearing (fail / safe) however is not trivial, as the whole range of parameter variants that such a bearing will exhibit in the field (different bearing tolerances, different temperature ranges, different loading conditions, different oil types, oil contamination, influence of wear over time, etc.) can not be covered by such analysis. A practical compromise is to cover that range of parameter variations that are most likely to occur for that particular bearing and are known to have most significant change in the bearings behaviour. Together with a similar EHD analysis of a “nearly similar” bearing layout that has proven to run safely over the years with comparable boundary conditions (oil, temperature, loading, material types) an EHD analysis is a reliable predictor for the bearing layout.

4 Cylinder Lubrication

There are two types of reciprocating compressor systems. Lubricated and non-lubricated. The choice of concept depends primarily on the compressed gas, because of its interaction behaviour with the surrounding materials and if so lubricants.

While the non lubricated compressors are guided by a PTFE transfer layer after the run-in procedure, the lubricated compressors provide permanently an oil film which avoids the build up of transfer layers and finally a significant reduction of rider and piston ring wear. Moreover, there is an interest of having as less oil as possible in the compressor due to gas pollution by the lubricant. A proper lubrication rate is required. This rate is usually calculated by formulas based on literature sources as well as on experience to adapt the given formulas.

In case of changes regarding rider ring materials and compressor design these formulas can become obsolete. The mechanisms of oil consumption, oil viscosity reduction due to the gas influence, etc. are not taken into account as separate factors but usually as one accumulated correction factor.

To figure out the weighting of the influences in more detail a dynamic calculation model will be set up to solve this problem.

General Model

To determine the optimum oil feed rate with respect to the demands of lubrication and gas purity the concept of the calculation model must deliver many results in a short time due to the high number of possible variations regarding gases and lubricants. To satisfy this point the approach of multi body systems (MBS) promises to be the best choice. On the one hand it is possible to generate many time depending influences and on the other hand the small amount of degrees of freedom of the general system leads to short calculation times. Although mechanical systems can be highly simplified it is possible to create complex and detailed submodels e.g. via subroutines.

MBS Compressor Model in Virtual Engine

The model consists of rigid bodies and contains the full three dimensional assembly of a one stage compressor. Further stages can be calculated with the same model and adapted boundary conditions. The model includes the gas pressure curves, measured or calculated, all necessary cranktrain components and the piston group with rider and piston rings. Because the piston rings play a major role in the model their flexibility has to be implemented. To do so, they are divided in segments; each segment is connected to the adjacent one by so called field elements.

These force elements contain a 6x6 stiffness matrix which input is delivered by a corresponding NASTRAN calculation.

Finally, the model contains the stiffness, material damping, mass, inertia and geometry of rider and piston rings.

To determine the minimum oil need subroutines are linked to describe the lubrication film build up, gas dynamics between the piston rings, friction generation, wear tendency and the oil consumption.

MBS Linked Subroutines

To describe the ring and rider dynamics as good as possible the following variables has to be considered:

- Radial hydrodynamic oil film pressure (p_{HD}) at the running surfaces of the rings
- Axial friction force (F_K) of the lubrication film at the ring running surface
- Gas pressure above (p_1), behind (p_{12}) and below (p_2) the rings
- Friction force (F_R) at the contact surface in the ring groove
- Contact force at the contact surface in the ring groove
- Mass forces (F_M) of the rings
- If need: preloads due to residual stresses (F_V) of the assembled ring

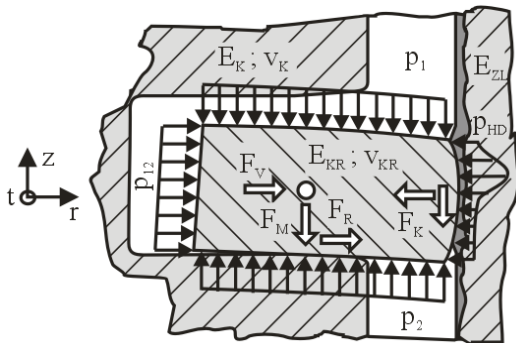


Figure 10: Acting forces on a ring

In the following the subroutine main features and approaches are presented.

The lubrication subroutine provides the build up of a lubrication film between two contacting bodies. It considers two different contact conditions. Hydrodynamic lubrication and mixed lubrication which are based on the modified Reynolds equation /3/. The prevailing lubrication condition depend on several factors like the contact body dynamics, the resulting gap between the contact bodies, the surface and oil properties and more.

To describe the gas influence on the ring dynamics the gas subroutine is able to calculate the interring pressures with given pressures and temperatures in the compression chambers (for double-acting

compressors), respectively compression chamber and crankcase. The subroutine is based on the Labyrinth Theory, described in /4/.

The resulting friction forces at the running surfaces of the rings, which are an output of the lubrication subroutine, lead to wear tendency if the surface hardness and wear coefficients are given by the user. The wear model provides the two mechanisms of wear: abrasion and adhesion.

The oil consumption subroutine determines the evaporation of the lubricant in due consideration of the prevailing pressure and temperature.

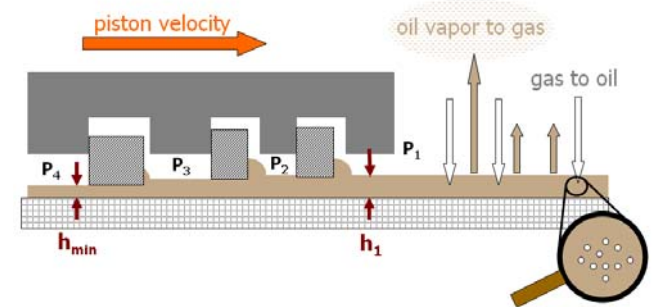


Figure 11: Influences on lubrication

Outcome of Model

Generally the outcome of MBS models depends on two main influences. On the one hand a proper mechanical model due to assumptions and simplifications which had to be made and on the other hand the quality of data input, respectively boundary conditions.

This leads to the complex field of gases and lubricants which are applied to several designs of reciprocating compressors. The severity of viscosity influence of the gas depends on several properties. These have to be provided by the oil supplier or figured out of literature sources. One of the main challenges is the various behaviour of one lubricant in combination with different gases.

Finally the MBS-Compressor-Model will deliver the following output:

- Motion, forces and torques of all included bodies and connector elements
- Oil film height over circumference and height
- Gas blow by
- Wear tendency of rider rings and piston rings
- Oil consumption and oil feed rate

5 Conclusion

Most of the above presented CAE-tools are well established in the automotive engineering world. The large synergy suggests a swift and beneficial transfer of these tools into the field of reciprocating compressor development. These tools can bring, besides a solid virtual prototyping based on CAD plus CAE, cost reduction and a minimization of the risk of technical failure if this failure mode is covered by an “up to date” CAE-modeling tool.

References

- 1 *GT-Suite Flow theory manual, Version 7.0*; Gamma Technologies, September 2009
- 2 S. Pischinger, M. Hopp; *Pumps and Compressors*, Lecture notes; Institute for combustion engines VKA; RWTH Aachen University; 2008
- 3 N. Patir, H.S. Cheng; *An average flow model to lubrication between rough sliding surfaces*, ASME Vol. 100 p.12 et seq.; 1978
- 4 Tang-Wei Kuo, Mark C. Selinau, Mark A. Theobald, John D. Jones; *Calculation of flow in the piston cylinder ring crevis of a homogeneous charge engine*, SAE-Paper 890838; 1989



Development and application of vibration improvements

by:

Dr Johann Lenz

Technical Director

KÖTTER Consulting Engineers KG

Bonifatiusstrasse 400, 48432 Rheine, Germany

lenz@koetter-consulting.com

**7th Conference of the EFRC
October 21th / 22th, 2010, Florence**

Abstract

Piston compressors are used in very different industrial sectors. Big advantages of these compressors are the variable operating conditions, the good efficiency and the manifold possibilities of flow regulation. The dynamic behaviour of the piston compressors and the connected piping depends strongly on these basic conditions. Therefore, this influence must not be neglected in vibrational investigations. Compared to other compressor systems, at piston compressors the influence of acoustic induced vibration has to be considered together with the connected pipe work. Increased structural vibrations can be caused by mechanical and often by acoustic resonances, too. Accordingly, measures for an effective vibration reduction have to be adjusted. In this article an approach for a vibration investigation is described on the basis of two case-studies with adjusted measures applicable at acoustic and mechanical resonances.

1 Case study A: Mechanical resonance problem

In a cavern storage system natural gas is fed into underground storage using reciprocating compressors at pressures of up to 160 bar to cover consumption peaks. The examined reciprocating compressor is equipped with 4 cylinders in Boxer design and is operated at speeds varying between 270 and 350 rpm in 2 pressure stages. High pipeline vibrations were observed at the pipeline between the two pulsation vessels on the suction side (figure 1).

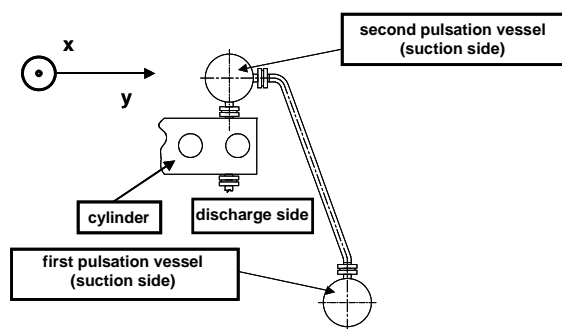


Figure 1: Pipeline between the first stage pulsation vessel on the suction side

At first, the current situation was analyzed by taking measurements. The speeds of oscillation were recorded at different operating speeds at three positions with the compressor at a constant load (figure 2). Figure 3 shows an excerpt of the effective vibration velocity in one direction.

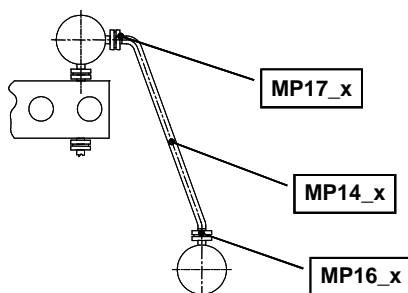


Figure 2: Measuring positions to record the pipeline vibrations

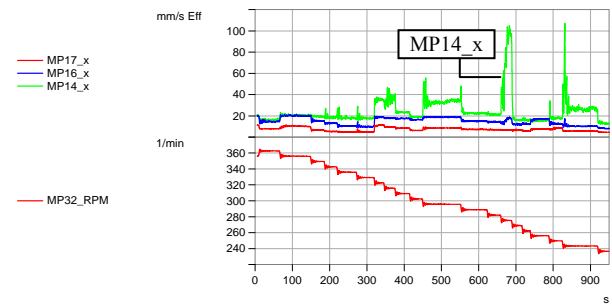


Figure 3: Current pipeline vibration situation correlated with the compressor speed

It can be seen that the vibrations in the middle of the pipeline increase strongly. To analyze this in more detail, figure 4 shows the amplitude spectra for measuring point MP14_x (middle of the pipe) generated over time as a color chart.

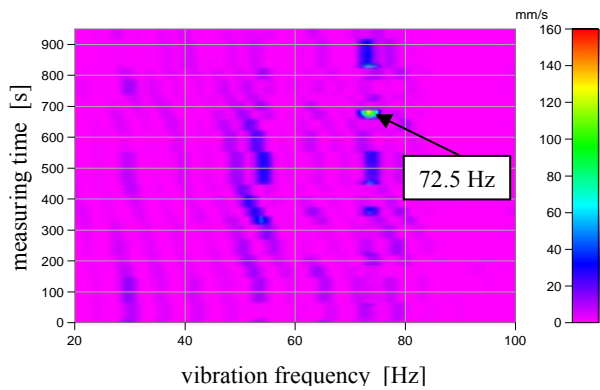


Figure 4: Amplitude spectra of the measured operational vibration from figure 3 at measuring point MP14_x as a color chart

The maximum vibration level arising during operation (figure 4, time T = 680 s) occurred at a frequency of 72.5 Hz (16 x operation speed). To examine this further, bump tests were performed on the pipeline section when the compressor was shut down (figure 5).

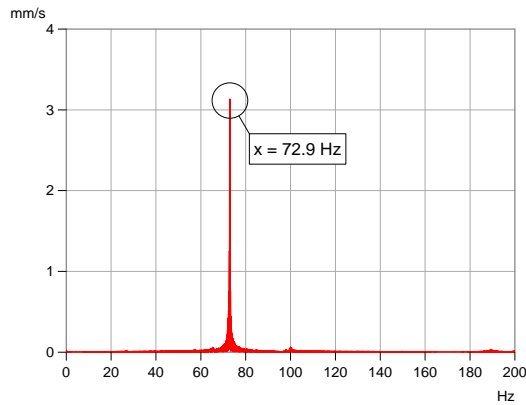
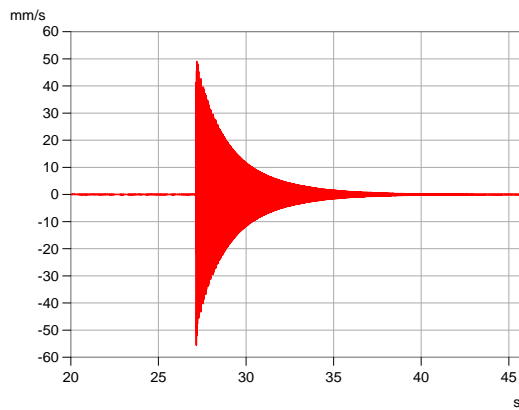


Figure 5: time signal (above) and spectrum (below) of the bump tests at measuring point MP14_x (response)

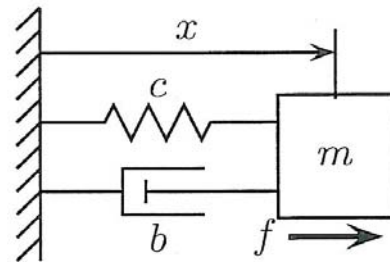
From the bump test it can be seen that the pipeline has a weakly damped resonant mechanical frequency of approx. 73 Hz. Additional pressure pulsation measurements during operation of the plant indicated that the excitation level of the pulsations was of a negligible magnitude. It was deduced that the mechanical excitation of the 16th order frequency of rotation was the actual cause of the high vibrations. Reduction measures such as detuning the system (by stiffening, additional mass) were not promising because the speed of the compressor was variable. Additional damping using a pipeline damper was also not recommended because of the low efficiency of such dampers at high frequencies. Therefore, a damped vibration absorber tuned to the frequency of the pipeline vibrations was suggested as an alternative. Furthermore, the absorber has the advantage that the damping forces for example do not have to be transmitted to a supporting device.

1.1 Theory of the vibration absorber

Vibration absorbers compensate the excitation forces using mass forces so that at certain frequencies individual points in the structure remain at rest or at least vibrate much less. There are two main types of vibration absorbers:

- Standard vibration absorbers with a relative small damping effect only work at a fixed or only slightly varying excitation frequency
- Dampened vibration absorbers with a relative large damping effect work in a wide range of excitation frequencies

In the following, the theory of the vibration absorber will be explained by using a simple model and without a detailed explanation of the corresponding mathematics. An oscillator with one degree of freedom describes the basic vibration system.



— one degree of freedom model

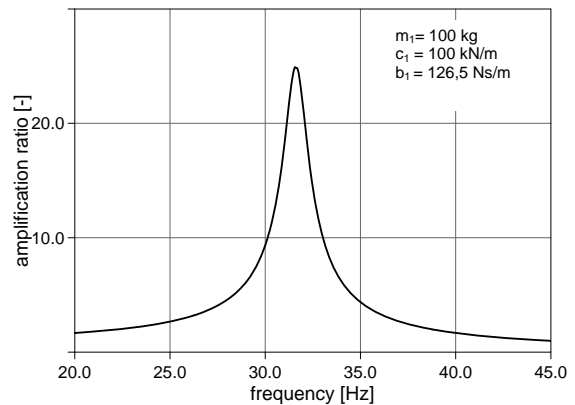


Figure 6: Frequency response function (FRF) of the one degree of freedom oscillator with the corresponding amplitude response

The model consists of mass m , spring with stiffness c and damper with damping constant b . When the excitation frequency Ω matches the natural frequency of the system $\omega = \sqrt{\frac{c}{m}}$, the result is a high amplitude (resonance case).

To describe the dynamic behavior of the system, figure 6 shows the frequency response (FRF) for the specified parameter values (m , c , b). With the help of this simple model a lot of vibration problems can be described. In the following the absorber will be explained based on this model.

The one degree of freedom system (figure 7) is expanded by a second oscillator which represents the absorber.

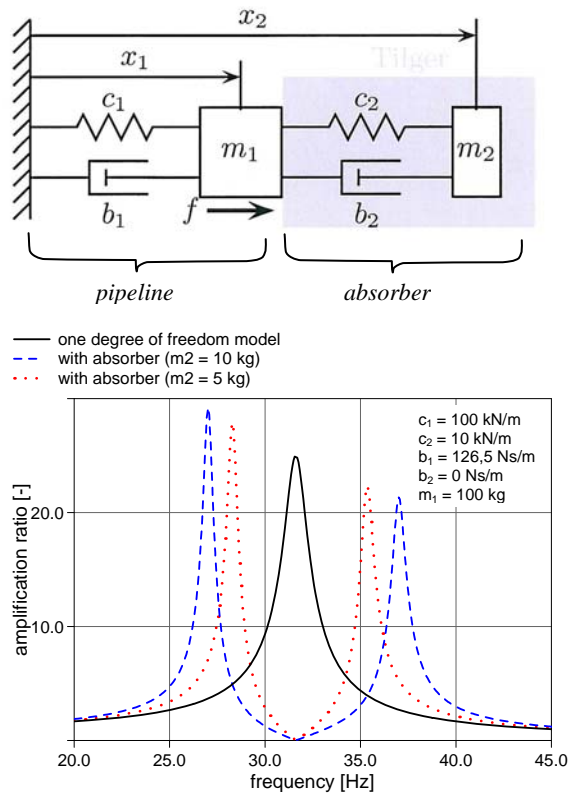


Figure 7: Extended vibration model with an absorber (above) and the correlated frequency response functions (below)

This absorber model consists of the mass m_2 , the spring stiffness c_2 and the additional damping described using the damping constant b_2 . To absorb the vibrations, the natural frequency $\omega_2 = \sqrt{\frac{c_2}{m_2}}$

to be adjusted so that it matches the resonant frequency of the original system. Figure 7 shows the frequency response for a system without damping ($b_2 = 0$) and different mass ratios $\frac{m_1}{m_2}$.

The amplitude response in case the absorber mass m_2 is 10 % ($m_2 = m_1 \cdot 0.1$) of the oscillating mass m_1 is compared to the response of the one degree of freedom oscillator (thick line) in figure 7.

It can be seen that two new resonance peaks were generated to the left and right of the original peak in the amplitude response. The actual absorption occurs at the original resonance point $\Omega = \omega$, where the amplitude of the vibration has been reduced to 0.

This also has the disadvantage of an undamped absorber. The absorber system detunes the initial system so that two new resonance peaks arise directly next to the old resonance peak. If the excitation frequency is not constant vibration problems can arise in the neighboring frequency ranges.

To avoid this, the extra damper b_2 (see figure 8) is adjusted. This damper reduces the amplitudes at both resonant frequencies.

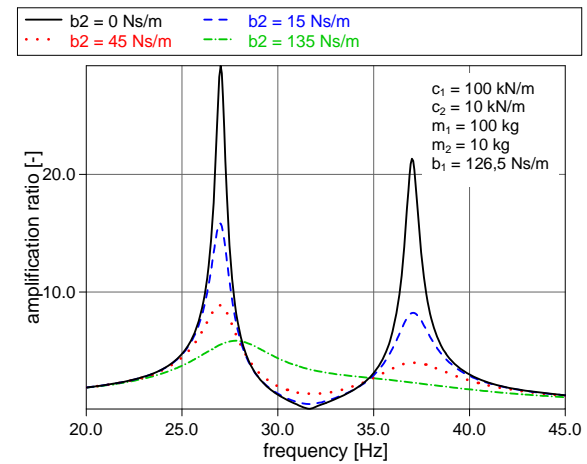


Figure 8: Frequency response and the effect of different absorber damping values on the vibration response

The higher the damping is selected, the lower are the neighboring resonance amplitude peaks, which means equally poorer vibration absorption at the old location resonance. The damping has to be adjusted for optimization purposes depending on the situation.

1.2 Realization and implementation

For the absorption of the pipeline vibrations at the often existing neighboring resonant frequencies on rotation-symmetric cross-sections, a three-dimensional vibration absorber (figure 9) has been developed.

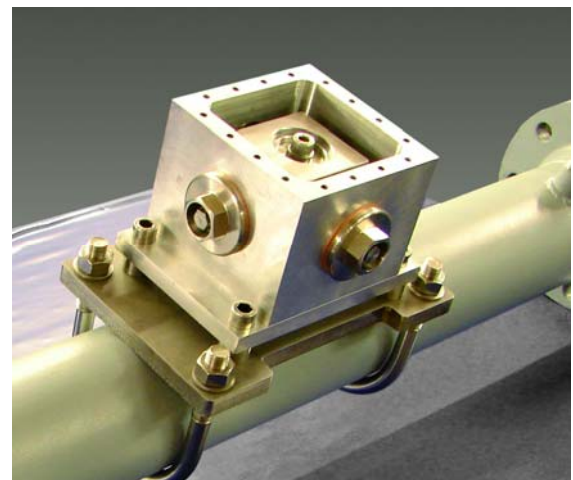


Figure 9: Three-dimensional dampened vibration absorber mounted on pipeline section DN = 100 mm (without housing cover)

The vibration absorber consists of an aluminium housing with a tuned absorber mass and a total of 6 tuned springs. Damping is achieved by filling with a silicone oil with a constant viscosity at temperatures between -40 °C and +150 °C. Figure 10 shows the tuned vibration absorber mounted on the critical section of the pipeline. The absorber was designed in that way that vibrations in both horizontal planes are absorbed.

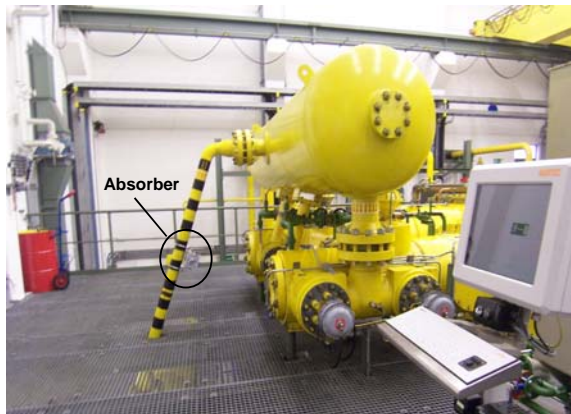


Figure 10: Photograph of the installed three-dimensional vibration absorber

For the purpose of comparison, figures 11 and 12 show the pipeline vibrations in both horizontal planes with and without the absorber at different compressor speeds.

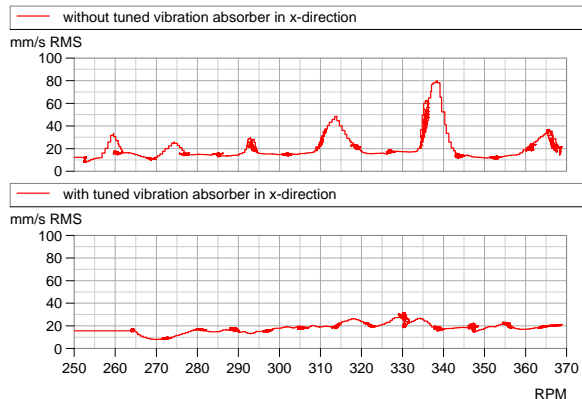


Figure 11: Measured pipeline vibrations with and without the tuned absorber in x-direction

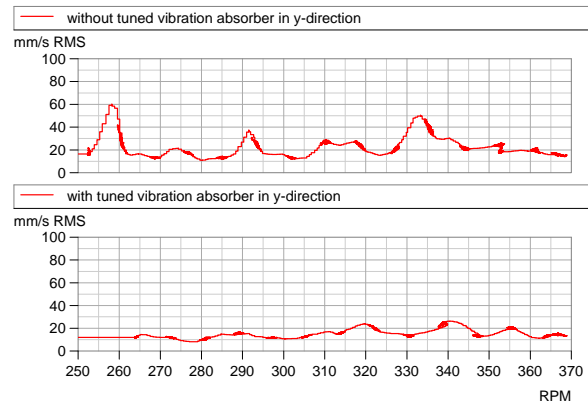


Figure 12: Measured pipeline vibrations with and without the tuned absorber in y-direction

It can be seen clearly that the individual resonant oscillation peaks are significantly reduced independently from the compressor speed or the direction. The absorber has therefore proven to be an effective measure for reducing pipeline vibrations without any external support when specifically designed for the problem.

2 Case study B: Combination of acoustic and mechanical resonance

As extension of a natural gas compressor plant two VFD driven 6-cylinder reciprocating compressors in Boxer design have been installed. The 2-stage compressors (figure 13) operate between 500 1/min and 1,000 1/min, the e-motor has a maximum power of 4.5 MW.



Figure 13: 1st stage of the 6-cylinder reciprocating compressor plant with VFD-driven e-motor drive

In order to meet the higher demand with respect to remaining pulsation level within the pipeline system, the pulsation dampers have been designed as 4-chamber-damper. Three of these chambers are directly assigned to the 3 cylinders.

The 4th chamber is implemented as acoustic filter. In turn, this allows a quite compact design of the pulsation damper and simultaneously a good reduction of pulsations towards the connected piping system.

During the commissioning of the compressor plant increased pipeline vibrations were observed. To conduct the root cause analysis and to develop adequate measures, KÖTTER Consulting Engineers have been assigned.

2.1 Measurement based investigation

The conducted measurement based investigation of the pipeline system showed higher vertical vibrations, particularly in the area of the 2nd stage at the compressor cylinder. This phenomenon was detected at both compressors which are designed identically. For a detailed investigation the vibrations (z-direction) in that area were recorded at the cylinders and at the pulsation damper for different speeds of the compressor. The measuring positions are shown in figure 14.

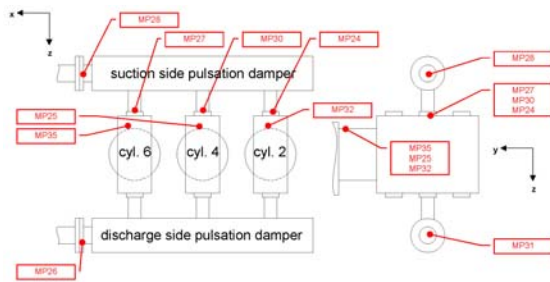


Figure 14: Vibration measuring positions at the 2nd stage of the compressor in z-direction

The following diagram (figure 15) shows the progression of the measured vibration velocities at the compressor as well as the RPM during the start-up from 500 1/min to 1,000 1/min.

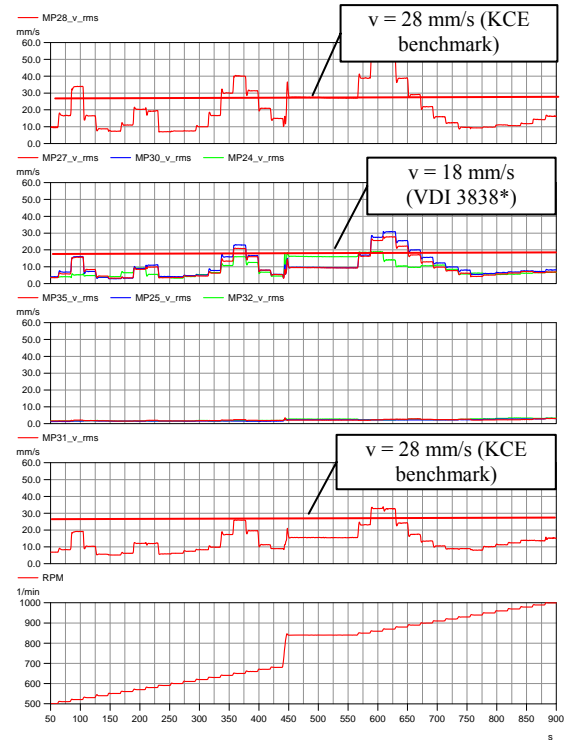


Figure 15: RMS-vibration velocities (z-direction) and guideline at the 2nd stage of the compressor as well as the RPM (*VDI: Verein Deutscher Ingenieur: Association of German Engineers)

Beside the increased vibrations of the pulsation dampers at the suction and discharge side considerably higher vibration velocities of up to 31 mm/s appeared at the cylinders (measuring points MP24, MP27, MP30). The cylinder vibrations increased during the run-up, particularly in the RPM-range 520 1/min, 640 1/min and 860 1/min.

The vibrations at the cylinders exceeded the guideline value of 18 mm/s rms clearly. Simultaneously to the increased vibrations at the cylinders, the vibrations at the pulsation dampeners (MP28 and MP31) increased as well. For a detailed frequency analysis figure 16 shows the determined amplitude spectrum of measuring point MP28 as color chart generated over the measurement time (T > 800 s).

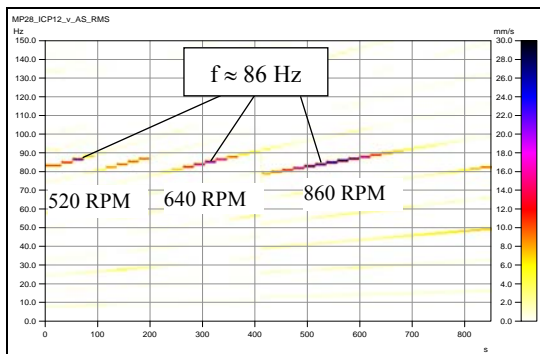


Figure 16: Color chart of the amplitude spectrum during run-up at MP28, RPM-range 500 1/min – 1,000 1/min

A comparison of figure 15 and figure 16 shows the appearance of increased vibrations at different points of time (T1 = 70 s, T2 = 310 s, T3 = 600 s) always at a frequency range of about 86 Hz at MP28. This was ascertained for all three measuring points.

To identify the responsible cause and effect mechanism, the synchronously recorded pressure pulsations upstream to the suction side - and downstream to the discharge side pulsation dampers were analyzed. It resulted that the pressure pulsations do not correlate to the recorded vibrations.

Subsequently conducted impact hammer investigations during standstill of the compressor could not detect any prominent mechanical resonance frequency at 86 Hz. It has to be considered that impact hammer tests during standstill in the area of the cylinders do not show definite results due to mass oscillation (piston etc.) of the running compressor.

Out of the operation vibration analysis it showed that the phase of the vibration signal turned during the increasing of the amplitude changed. The phase turned to 90° in the maximum and to 180° after reaching the next vibration minimum. This indication defines the position of an additional mechanical resonance frequency at 86 Hz.

Figure 17 shows the measured vibration mode in the following three points of displacement.

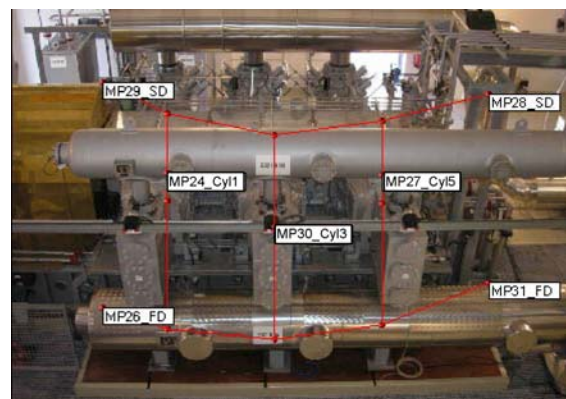
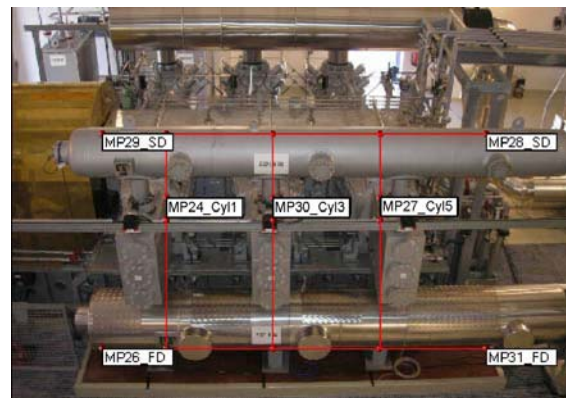
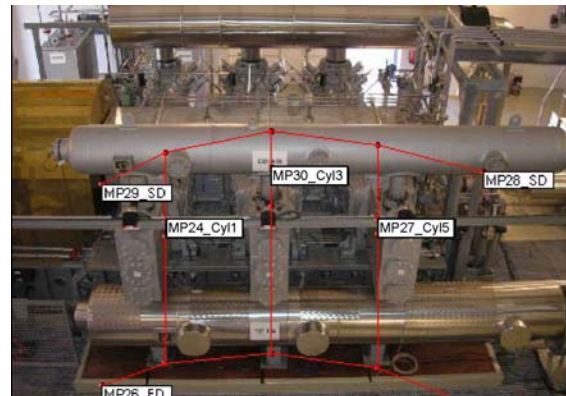


Figure 17: Description of the vibration mode of the 2nd stage of the compressor at 86 Hz

This vibration mode always turned up at the compressor speeds of 520, 640 and 860 1/min. For a deeper investigation of the cause and effect mechanism, one cylinder-internal pressure (head end) was recorded synchronously.

The analysis of the cylinder pressure trend showed that at the moment of increased vibrations - during the exhaust stroke of the gas - pressure pulsation of approx. 86 Hz occurred (see figure 18).

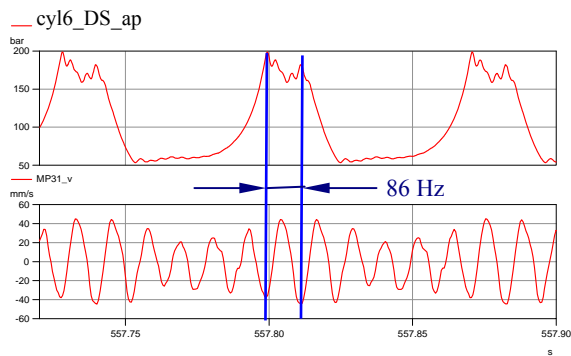


Figure 18: Trend of internal cylinder pressure (head end) and vibration velocity at measuring point MP31

Based on the typical operating conditions, an additional acoustical calculation of the 2nd stage was conducted to verify the pressure pulsation situation. The check confirmed that an acoustic resonance appears between the cylinders and the pulsation damper of the discharge side at around 85 Hz.

With this result the cause and effect mechanism, which led to the higher pipeline and cylinder vibrations, was clearly worked out. Due to the acoustic resonance at the cylinder outlet of the 2nd stage combined with a mechanical resonance highly increased vibrations occurred.

2.2 Realisation of measures

For an effective reduction of the vibrations different possibilities were checked with calculations. Figure 19 shows the design and the used acoustic model of the discharge pulsation damper (2nd stage).

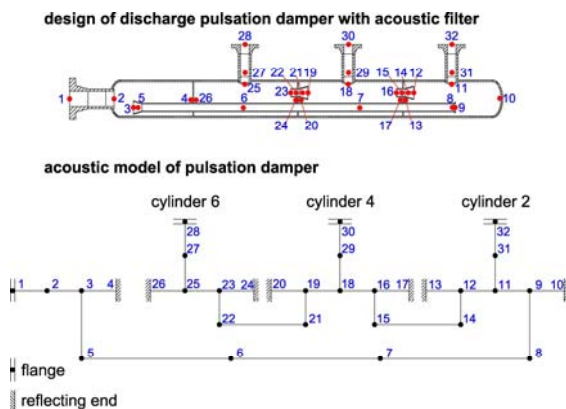


Figure 19: Design and acoustic model of the discharge pulsation damper

Finally, modified taper-lok-plates in KÖTTER design (see figure 20) were installed between the cylinders of the 2nd stage and the pulsation damper of the pressure side. The advantage of this patented

design is a good ratio between pressure drop and pulsation reduction at higher frequencies.

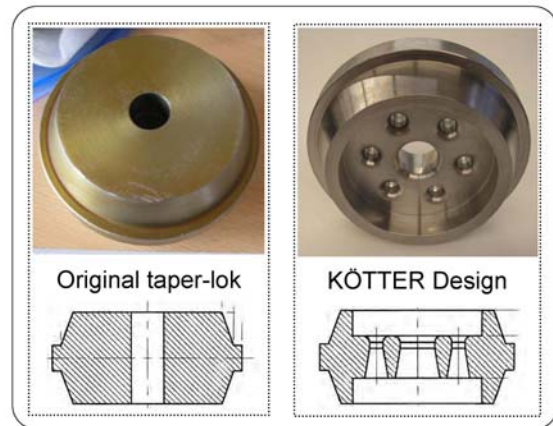


Figure 20: Original and modified taper-lok-plates

After installation of the modified taper-lok-plates the measurements were repeated under comparable operating conditions (figure 21).

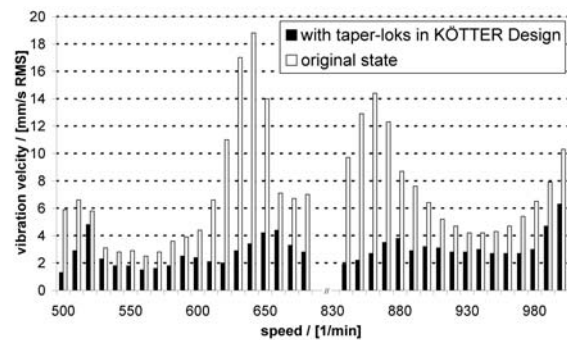


Figure 21: Cylinder vibrations before and after installation of modified taper-loks.

The measurement results confirmed a considerable reduction of the cylinder vibrations below the guideline values. It has been shown that by combining a theoretical and a measurement based investigation at a reciprocating compressor effective measures have been worked out.

3 Summary

This paper shows typical procedures for investigations of vibration problems at reciprocating compressors. The ascertained vibration phenomena have been analyzed in detail, the cause and effect mechanism has been revealed.

In the first example, the higher pipeline vibrations could be traced back onto a weakly dampened mechanical natural frequency. As a measure a three-dimensional vibration absorber has been introduced and explained.

Following to the installation of the absorber a measurement confirmed the broad-band vibration reduction at the pipeline of variable speed driven reciprocating compressor.

In the second example, an acoustic resonance between cylinder and succeeding pulsation damper was detected as critical cause and main effect mechanism. As a measure the available taper-lok-plates were modified in KÖTTER design. Again, the subsequently conducted measurement confirmed the effectiveness of the measure.



Thermo-fluid-dynamic design of Reciprocating Compressor Cylinders by Fluid Structure Interaction Software simulation

by:

**Riccardo Traversari, Rotating Machinery Design Manager
Compression Service Technology, Florence, Italy
riccardo.traversari@cstfirenze.com**

**Marco Faretra, Mechanical Engineering Consultant
Barbalab S.r.l., Casalecchio di Reno (Bologna), Italy
marco.faretra@barbalab.it**

**Daniele Bucci, Technical Director
Lapcos S.c.r.l., Vignola (Modena), Italy
daniele.bucci@lapcos.it**

**Sanzio Bassini, Director System & Technology
CINECA – Supercomputing Center,
Casalecchio di Reno (Bologna), Italy
s.bassini@cineca.it**

**7th Conference of the EFRC
October 21th/ 22th, 2010, Florence**

Abstract

The classical methods to calculate pressure losses at cylinder valves showed limits especially with high speed compressors. An advanced approach, based on Fluid Structure Interaction (FSI) analysis, was utilized for an improved calculation. FSI allows dealing simultaneously with thermodynamic, motion and deformation phenomena. By this method a 3D CFD Model, simulating the cylinder with mobile piston and valves, was developed and experimentally validated. The analysis was performed in transient and turbulent conditions, utilizing a deformable mesh. The 3D domain simulating the compression chamber changes with the piston motion law while valve rings move according to the fluid dynamic forces.

1 Introduction

It is not rare that reciprocating compressors experience in the field diminished cylinder performance, both in terms of smaller throughput and higher specific energy consumption than expected. This is more frequent when high speed units are used, as it happens more and more for natural gas transmission, field extraction and process plants applications [1], [4]. Many investigations have been conducted and papers published on the modeling of the reciprocating compressor cylinders. The first one was M. Costagliola [2] who wrote in 1950 the two very famous equations describing the valve motion under the gas, spring and inertia forces which led, when at the beginning of the seventies the computers started to be widely available, to a proliferation of models, [3], 0 and others, applied both in the academic and industrial worlds for evaluating the valve behavior. Then, from models confined to the valve behavior prediction, more recently the researchers have started to extend the simulation from the valve to the whole cylinder [4], [5], [6]. Many of the researchers have dedicated their efforts to the improvement of the simulation of the thermodynamic phenomena within the compression chamber and of the valve behavior, including pressure wave propagation, valve motion and impact velocity and so on. As far as the authors know, not much has been published on the influence of the various cylinder design parameters on the performance of the compressors, which is the practical problem that the compressor design engineer has to face every day. The purpose of this paper is to report on the work done by the authors to find a robust design method to be given to the design engineer to let him have a very practical set of tools, for every day use, to avoid the experienced performance problems and optimize cylinder design. This new design method is based on a first numerical design tool able to identify easily a set of main cylinder geometric parameters for a solid viable solution and a second tool to verify and fine tune the selected parameters by means of a very accurate and tested 3D Fluid Structure Interaction (FSI) simulation, brought to reasonable computation times by means of a combination of advanced commercial software and HPC (High Performance Computing) availability.

2 The standard way to evaluate cylinder valve influence

The evaluation of the cylinder performance is normally done by the manufacturers by means of more or less sophisticated computer programs that consider the compressor as a whole and determine the main performance parameters (throughput, adsorbed power, gas temperature, interstage pressures, gas and combined loads, etc.).

One very important factor influencing the behavior of compressors is the pressure drop at cylinder valves which is generally calculated by the following formula:

$$\Delta P_v = \xi \cdot \rho \cdot W^2 / 2 \quad (1)$$

where:

ΔP_v = Differential pressure across the valve

ξ = Coefficient of valve flow resistance

ρ = Gas density

W = Gas speed through valve lift area

The coefficient of valve flow resistance ξ is normally determined by the manufacturers with the valve mounted in a straight line pipe without any flow distortion. The gas flow across the discharge valve, uniformly fed in a straight pipe, is conventionally calculated as flow passing through a convergent nozzle and assuming constant ratio of heat capacities. Under this condition gas flow G , with the hypothesis that the valve is the only obstacle to the gas, can be estimated as follows :

$$G_v = \sqrt{\Omega K_s \left[\frac{P_d}{P_u} \right]^{\frac{1}{k}} \left[\frac{2k}{k-1} \left(\frac{P_u}{\rho_u} \right) \left(1 - \frac{P_d}{P_u} \right)^{\frac{k-1}{k}} \right]} \quad (2)$$

Where:

G_v = Gas flow by weight

Ω = Geometric area below ring valve lift

k = Ratio of heat capacities

$K_s = [1/\xi]^{1/2}$ = Flow coefficient for discharge valve

P_d = Pressure downstream discharge valve

P_u = Pressure upstream discharge valve

ρ_u = Gas density up stream the discharge valve

However compressor manufacturers have to consider that the valve performance, when it is installed in a cylinder, changes and can be highly affected by its positioning in the cylinder, as between the valve and the compression chamber there is the valve port narrow area through which the gas passes with an additional pressure drop. So, the total pressure drop generated by the gas entering and leaving the cylinder is distributed in two main areas: the valves (suction and discharge) and the relevant valve port areas defined also as "valve pockets". As an example, *Figure 1* shows the discharge valve with the narrow area of the cylinder considered in this paper.

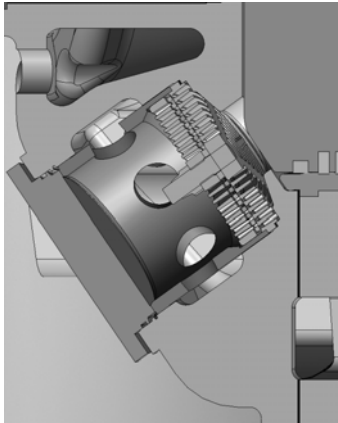


Figure 1: Discharge valve 3D Model

To take into account this additional loss, compressor manufacturers generally modify equations (1) and (2) introducing a factor P_f , called “Pocket Factor” [7], so that the two equations become:

$$\text{Total pressure drop: } \Delta P = \xi \cdot P_f \cdot \rho \cdot W^2 / 2 \quad (3)$$

$$\text{Gas throughput: } G = G_v / [P_f]^{1/2} \quad (4)$$

Conditions being equal and assuming that there are no major perturbations from abnormal cylinder operating conditions such as valve fluttering or important pressure waves in the cylinder, the higher is the Pocket Factor the greater is the difficulty to expel the gas during discharge stroke, with a consequent reduction of the gas throughput, increase of compressor brake power and load on crank mechanism. Figure 2 shows, for instance, how a higher discharge pressure at the end of the delivery causes a delay of the beginning of the suction with the consequent reduction in throughput.

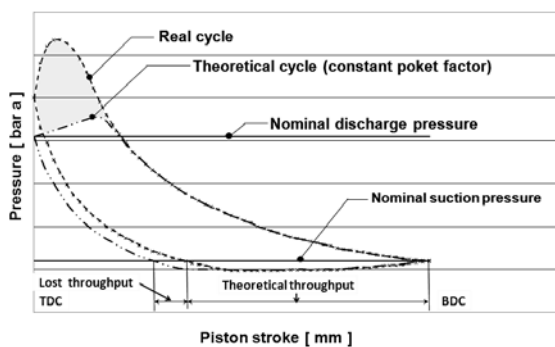


Figure 2: Example of throughput reduction due to higher discharge pressure

Common practice is to consider the Pocket Factor, both for suction and discharge phases as being constant along the piston stroke. This would be acceptable assuming that the narrow area of valve port between compression chamber and valves remains unchanged during the complete stroke of the piston. This hypothesis is fairly valid for the suction stroke, because during the expansion of the gas trapped in the cylinder at the end of the delivery phase,

the piston clears the valve area facing the cylinder below the suction valve port or masks it only very marginally. On the contrary, the use of constant Pocket Factors may result inadequate for discharge valves, as it can lead to big errors in calculating cylinder performance, because the discharge valve masking by the piston starts as soon as the piston reaches the opening below the discharge valve port and becomes more and more important when the piston approaches the dead centers. In fact, in the proximity of dead centers, the gas port area decreases more rapidly than the piston speed, and consequently the relevant gas velocity stays high, keeping pressure drop at high level.

This phenomenon occurs especially at the top dead centre where the first and second order piston speed components add up. Besides, the discharge valves at dead centers, due to the piston masking effect, are no more fed symmetrically, because the masked valve port area is displaced in respect of valve axis, and the distance between piston and valve is drastically reduced. Therefore the pressure drop across the discharge valves becomes bigger than that measured in a straight line pipe with a valve port aligned. This situation is particularly evident when high density gases are handled in cylinders designed for high speed - short stroke compressors, for two main reasons:

- High speed compressors allow short time to discharge the gas from the compression chamber to the delivery plenum
- Short stroke compressors deliver the gas mostly with the discharge valve masked by the piston (see Figure 3)

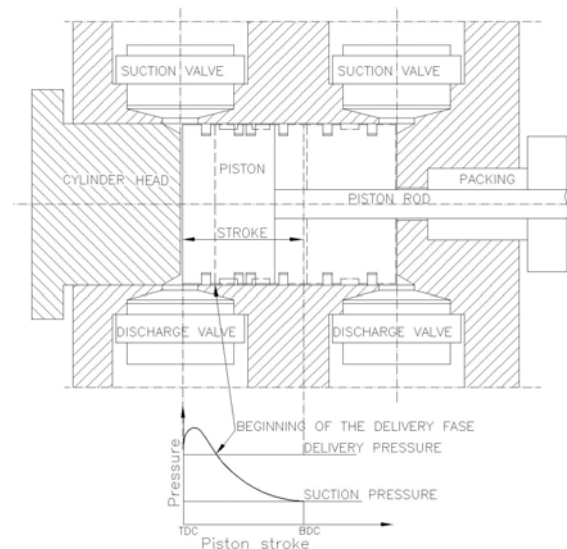


Figure 3: Example of piston masking in a short stroke compressor cylinder

What above tells us that, in certain cases, one cannot utilize a constant Pocket Factor but also the piston masking effect has to be taken into account.

In other words one must consider the Pocket Factor as a function of the piston position whose value is rapidly growing when the piston moves towards the dead center. Some compressor manufacturers, trying to better estimate compressors brake power and loads, use, for the complete piston stroke, a constant Pocket Factor, greater than the one valid when valve masking is not started yet. This approach may involve other errors if the brake power is calculated with the assumption that gas throughput is correct.

On the contrary also the gas throughput has to be calculated, considering the dynamic pressure drop generated by cylinder valves and cylinder valve ports, in several positions during the piston stroke. Particularly important is the residual pressure drop at dead centers, because it is capable to strongly affect gas throughput by modifying the effective pressure ratio. In fact higher discharge pressure involves longer expansion of the gas trapped into the clearance volume with delay in the beginning of the suction stroke, as previously explained.

3 A 3D FSI Model to simulate compression chamber/valve ducts performance

The above described situation and the availability of newly developed computer programs have led the authors to deepen the matter [8]. A new approach, based on the *Fluid Structure Interaction* (FSI) analysis, has been utilized for the purpose to better evaluate compressor cylinder thermo-fluid-dynamic performance. This analysis allows in fact dealing simultaneously with thermodynamic, motion and deformation phenomena and allows simulating the complex phenomena that occur in a cycle of a reciprocating compressor cylinder during the motion of the piston and in particular the pressure loss through automatic valves, ducts and manifolds. This analysis is very demanding in terms of operator's competence and computing facilities; this is the reason why industrial applications were rather limited up to now and restricted to very advanced worlds. A more extended application requires a different approach capable to reduce its heaviness.

For the specific case three different types of competence needed to be merged: machine design, CAE and HPC. The integration of these three competences allowed creating an original method for the set up of very accurate models that, coupled with the availability of a high level Hardware infrastructure (CINECA HPC) provided with an extended program library, made the utilization of this type of advanced analysis utilizable in the normal industrial design process. The cylinder considered in this study was selected in manner to test the new method in a difficult environment both in terms of accuracy of the simulation and computing time. In fact, looking at the characteristics listed below, one realizes that it is a rather large cylinder, running at

high speed, with many valves which complicate its shape and it handles a heavy gas.

The cylinder object of this study has the following main characteristics:

- Cylinder type: double acting;
- Bore: 630 mm
- Stroke: 150 mm
- Clearance volume: 13,5%
- Number of suction/discharge valves: 3+3 per cylinder end
- Compressor speed: 740 RPM
- Nominal suction pressure: 1,2 bar a
- Nominal discharge pressure: 4,1 bar a
- Gas Molecular Weight: 50,7
- Shape of cylinder: see *Figure 4*

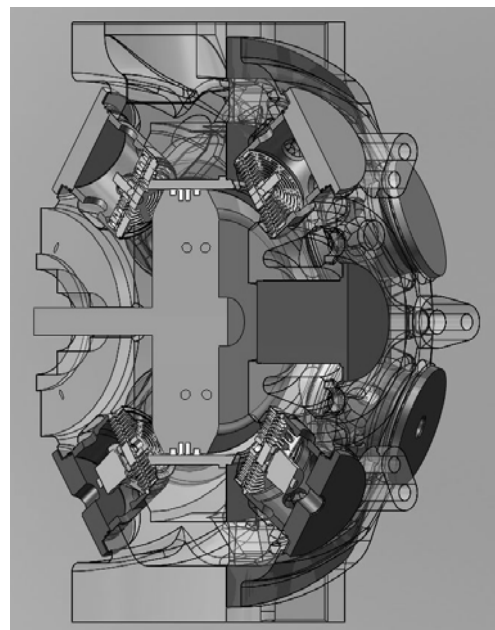


Figure 4: 3D Model of the cylinder studied

The purpose of the study reported in this paper was to determine all the thermo-fluid-dynamic parameters in the domain of the complete compression chamber of the outboard end starting from the suction valves and arriving to the discharge plenum chamber in the time period starting from the discharge valve opening up to 25,7 crank angle degrees after the top dead center. The relevant model (see *Figure 5*), taking advantage of the cylinder symmetry with regard to a plane passing through the cylinder axis and the suction/discharge flanges, includes one half of the outboard end, the discharge valves with all their geometric/mechanical/mass characteristics, the mobile outboard piston face and the discharge plenum; the suction valves, considered as closed, are simulated as blind flanges.

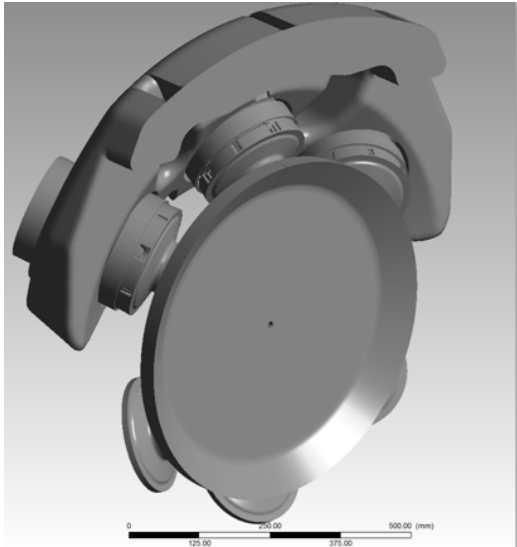


Figure 5: 3D CFD Model

3.1 The 3D simulation Model

The fluid analysis was performed in transient and turbulent condition, under the assumption of compressible flow, and using deformable mesh calculation. The deformation of the 3D domain changes the configuration of the cylinder, whose volume varies with the time law imposed by the law of motion of the piston, and changes the configuration of the valve also, whose rings are moving according to fluid-dynamic forces acting on them.

The mobile surfaces are those of the piston and valve rings within the valve. The simulation of opening and closure of the valve rings is obtained by the CFD software by solving the equations of the motion of the rings, treated as non deformable and with only one degree of freedom (translational). In the valve motion calculation, the dynamic forces acting on the rings, the characteristics of inertia and the forces due to springs have been taken into account. At this stage, notwithstanding that the FSI analysis is capable to evaluate ring elastic deformation, it has been deemed acceptable to consider the rings as infinitely rigid and to calculate the movement of pure translation, since the elastic deformation of the rings does not alter appreciably the gas flow through the valves.

At the end of a functional construction of the calculation mesh and the definition of 3D regions with mobile walls, four different fluid domains were defined. In the various regions of fluid, meshes with hexahedral elements were realized, which allow better quality control of the mesh during the motion of the piston and piston rings, while tetrahedral prism mesh were used in those regions where deformations of the geometry do not occur: in fact a tetrahedral mesh is able to better describe in detail the geometric complexity of the areas close to the valve. The flow was considered transitional and turbulent ($k-\epsilon$ turbulence model standard).

The resolution of the equation of total energy allowed taking into account the conditions of compressible flow. Other conditions taken for the analysis are listed below:

- As said above for valve rings, all mechanical parts are considered as non deformable (f.i. the law of motion of the piston is known and its deformation does not influence significantly the fluid dynamic field)
- The initial conditions for the 3D analysis are derived from a 1-dimensional method
- No impulse coming back from the delivery side due to pressure pulsations in the system downstream the cylinder

3.2 The results of the simulation

The results of the analysis are expressed in terms of pressure, temperature and velocity in the whole field. So, by postprocessing these values, it is possible to determine their development both in the time and space domains. *Figure 6 to Figure 15* are reported to show some of the most significant results.

Figure 6 and *Figure 7* show the uneven velocity vectors in the space between cylinder head and piston surface in two piston positions, respectively 12mm before TDC and at TDC. The maximum gas velocity is reached at the inlet of the discharge valve port area. It must be emphasized that at TDC, notwithstanding that the piston speed is zero, the gas velocity is much higher than the one when the piston is at 12 mm before TDC. This is due to the fact that the gas moves with a delay from the clearance volumes, f.i. those under the suction valves, where it was confined by the piston movement, towards the lower pressure zones, f.i. the discharge valve pockets. For a better understanding of this situation *Figure 8* reports the maximum gas velocity vs. the piston position. From this figure one can see that the largest maximum gas velocity is reached at 5 mm before TDC.

Figure 11, 12, 13 and *14* show the pressure distribution in the compression chamber under different piston position.

Figure 15 shows the temperature distribution in the compression chamber at the TDC.

Figure 9 shows the gas velocity vector trajectories which indicate that the gas, for penetrating the discharge valve channels, has to make important direction changes to feed the valve.

From *Figure 10* one can see also the flow asymmetry of the gas entering the valve port. Preferential paths of the gas towards one portion of discharge valves are present during all the discharge stroke but they become particularly high when the piston is approaching TDC.

FUNDAMENTALS

Thermo-Fluid-Dynamic Design of Reciprocating Compressor Cylinders, *Riccardo Traversari, Marco Faretra, Daniele Bucci, Sanzio Bassini; CST COMPRESSION SERVICE TECHNOLOGY*

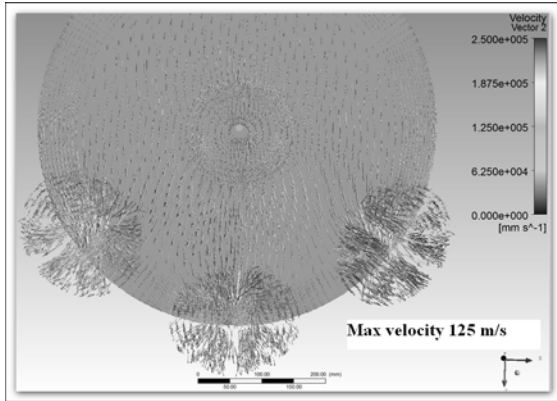


Figure 6: Gas velocity vectors in the space between cylinder head and piston surface at 12 mm before TDC

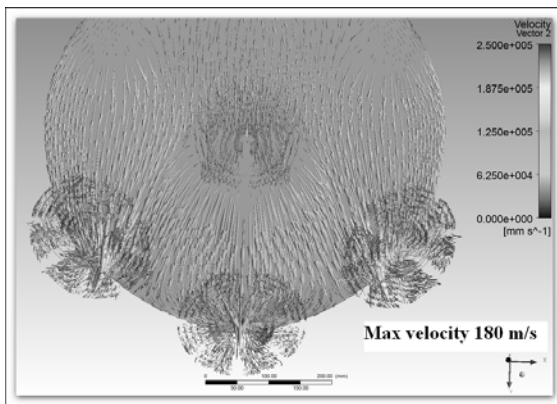


Figure 7: Gas velocity vectors in the space between cylinder head and piston surface at TDC

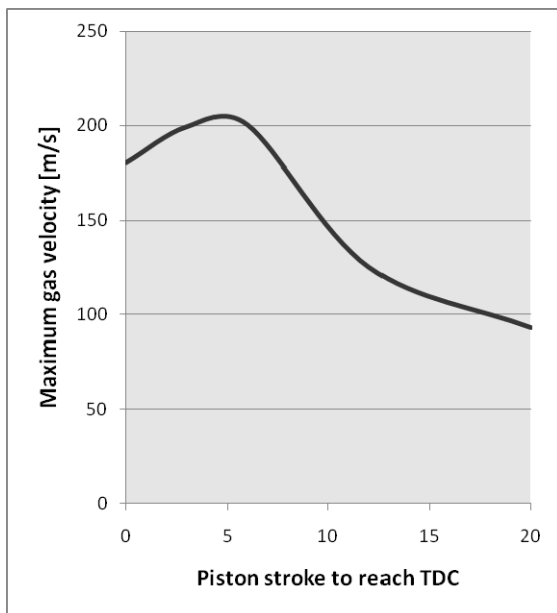


Figure 8: Maximum gas velocity in the space between cylinder head and piston surface

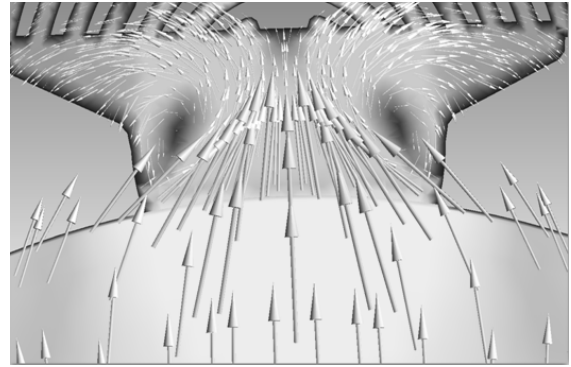


Figure 9: Gas velocity vectors in the discharge valve pocket at TDC

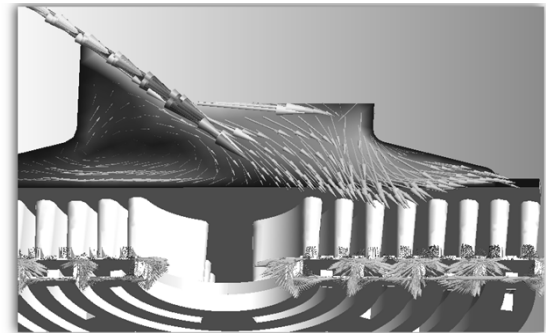


Figure 10: Flow asymmetry of gas feeding the discharge valve at TDC

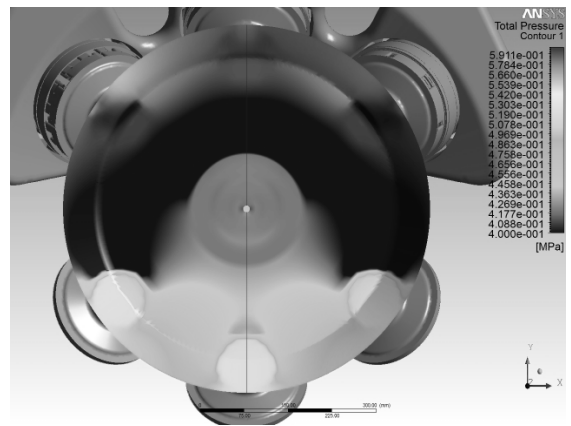


Figure 11: Pressure distribution in the compression chamber 23 mm before the TDC

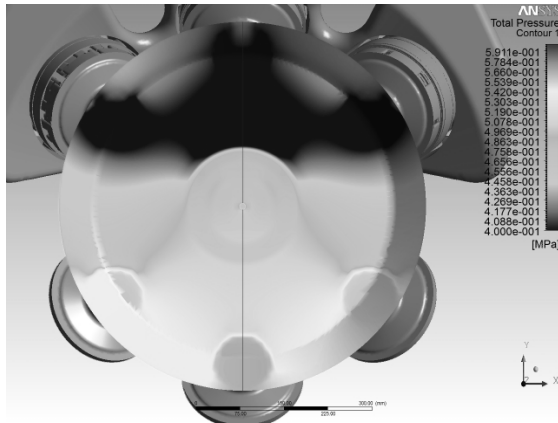


Figure 12: Pressure distribution in the compression chamber 17 mm before the TDC

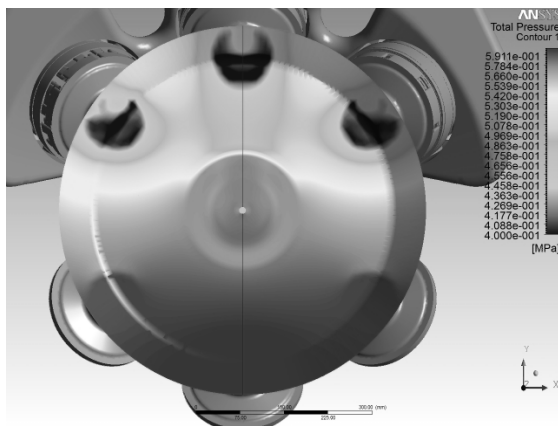


Figure 13: Pressure distribution in the compression chamber 5 mm before the TDC

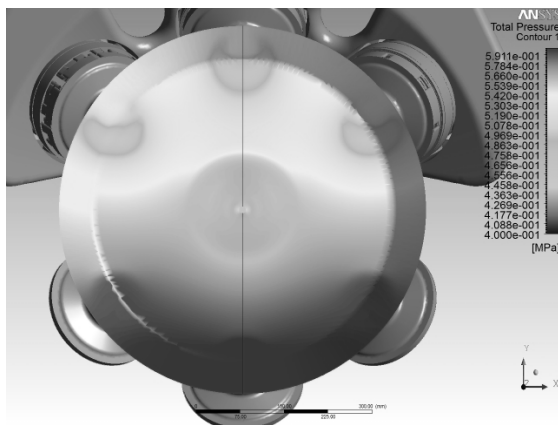


Figure 14: Pressure distribution in the compression chamber at TDC

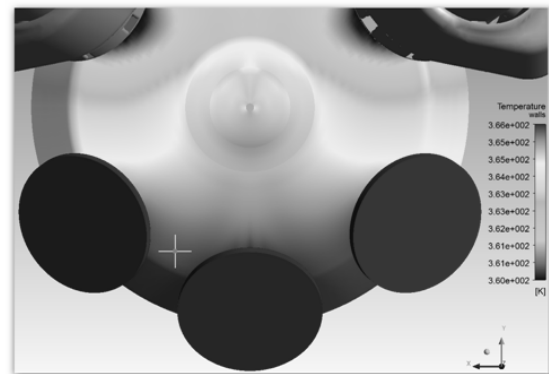


Figure 15: Temperature distribution in the compression chamber (suction side) at TDC

4 Validation of the Model by field measurements

A compressor equipped with one cylinder of the type investigated has been instrumented in the field to measure the indicated pressure in the outboard end and the relevant measurements have been compared with the results of the FSI analysis.

The comparison between the measured and calculated values has been done taking the pressure as reference parameter. In order to make this comparison in the most correct terms, one has taken the pressure on the FSI model by means of a probe positioned in the same position on the cylinder head where the pressure transducer was positioned on the real cylinder. The two readings, FSI calculated of curve a) and measured of curve c), have been superimposed in *Figure 16*. As further comparison in *Figure 16* also the theoretical indicated cycle of curve b) calculated with a constant Pocket Factor P_f not accounting for the modification of the gas passage due to the piston masking, is reported. Curve d) shows the FSI average pressure on piston surface which has been utilized for the calculation of power lost due to the masking effect.

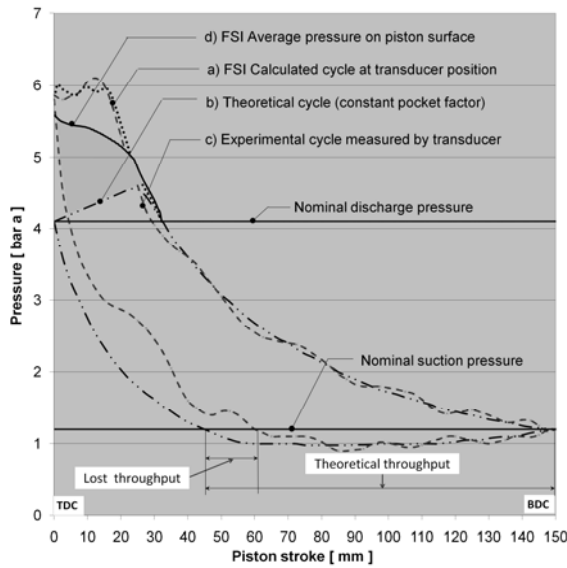


Figure 16 : Pressure diagrams: a) FSI at the probe position, b) Theoretical, c) Experimental at the probe position, d) FSI average pressure on piston surface

This comparison shows that there is an almost perfect coincidence of the values of the FSI calculated and measured pressure at the TDC. Also the a) and c) pressure profiles during the delivery phase show a good correspondence. The slight difference in the waves of the two profiles may be explained by the assumption made for the FSI analysis that the pressure on the plenum chamber be not influenced by the system downstream, which is not correct. Besides, the wave reported by the experimental cycle might be distorted also by some resonance in the small duct feeding the measuring transducer [6]. However, the aim of this study is not the perfect coincidence between experimental and calculated cycles, which anyway appears satisfactory, but the extension of the shaded area in *Figure 16* which determines compressor adiabatic efficiency and the value of the pressure at the TDC which determines the throughput.

One can conclude that the FSI Model has a good degree of accuracy for the two main characteristics necessary for a correct cylinder design:

- The value of the energy lost at the valves
- The pressure at the end of the delivery phase

It is also interesting to calculate backwards the real value of the pocket factor from equation (3) assuming the value of ΔP coming out of the FSI analysis. The result of this calculation is reported in *Figure 17* from which one can see that this factor is anything but constant and, due to the masking effect, reaches values much higher than those known by the literature, which in this case results $P_f = 2,6$.

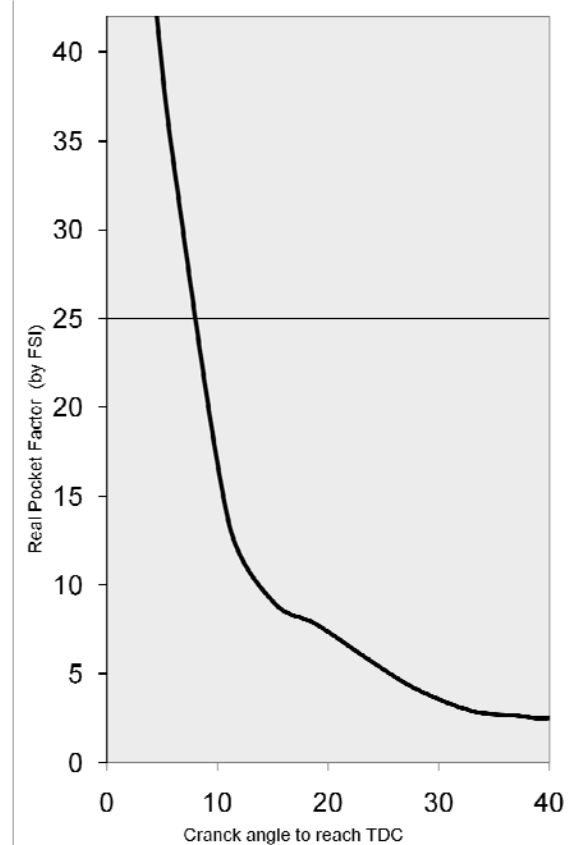


Figure 17: P_f real value calculated backwards from measurements

This cylinder is in fact a typical example where if one evaluates the performance with the classical equations (3) and (4) utilizing the normal constant ξ and P_f factors available from the literature, one would arrive to expected compressor performance much better than the real ones. In fact, if one compare diagram b) of *Figure 16* calculated with the conventional P_f factor with diagram a) of the FSI and c) measured, one can see that there are the following major discrepancies in terms of gas throughput and power.

Gas throughput

The residual pressure at the end of the delivery phase resulted much higher than that of diagram b), which causes that the real suction starts with a delay of 16 mm stroke thus reducing the cylinder throughput of about 16 %.

Increased specific power

The higher pressure drop generates an increased energy required for compression. This energy is measured by the shaded area of *Figure 16*. The combination of the increased energy requirement and the reduced gas throughput leads to an increase of the specific adsorbed power of about 9%.

5 Uneven pressure distribution on the piston face

The pressure distribution on the piston surface is fairly uniform at the beginning of compression and remains such during compression stroke. The gas moves along the cylinder axis until the discharge valves open. After this event the gas inside the cylinder continues the motion towards the cylinder head but it acquires also velocity components in the direction of discharge valves (see *Figure 6* and *Figure 7*). These components become bigger and bigger when the piston approaches the TDC while the axial velocity reduces. In the vicinity of the TDC the radial velocity towards the discharge valves is prevalent with respect to the one along the piston axis and becomes very high in the area feeding the discharge valves, causing an important pressure drop. Besides, the gas moving from suction to discharge area generates an uneven pressure distribution on piston surface, with higher pressure on suction side as shown by *Figure 11, 12, 13* and *14*. This pressure distribution generates a moment on piston which reaches the maximum value of 2338 [Nm]. This moment induces bending on the piston rod and consequently the modification of piston rod run out. A counter rotation occurs when the pressure on the piston surface is being equalized, during the expansion stroke, thus generating piston and piston rod oscillation. This instability can become particularly high in high speed compressors when large cylinder bores and small rod diameters are used.

6 The new correct sequence for an adequate cylinder design

The availability of the above described 3D FSI Model allows the design engineer to develop new cylinders that will show in the field the predicted optimized performance. The authors deem that at this point the most suitable way to get this aim is to follow the sequence described below.

6.1 Preliminary design by applying best practices

As for most of the machine design activity, when a design engineer starts to work on a new compressor cylinder he must do some preliminary work and particularly:

- Look at his previous experience, at the “best practices” and the “state of the art”
- Select the main cylinder accessories, such as valves (number and size), piston ring set, packing, cylinder flanges

- Decide the main cylinder structure and in particular the geometric relationship of a few critical dimensions such as: stroke, piston ring arrangement, valve diameter, clearance between piston and cylinder head at the top and bottom dead centers, valve position, valve pocket shape

6.2 Project review by a parametric analytical design tool

In order to limit the number of runs of the subsequent 3D FSI Model which has been simplified by the new method but is still demanding in terms of man-hours, it is advisable to have a simple numerical tool which allows the design engineer to “play” easily with the different geometric parameters to see the relevant influence and make a preliminary selection of them, in order to define a basically good design to be submitted to the following step of the FSI analysis. The authors developed a 1-dimensional model, which is not object of this paper, for the purpose. This model considers six most common valve pocket configurations; for each of them all significant geometric parameters are taken into account in order to evaluate the relevant influence. The resulting performance, in terms of “gas throughput” and “specific consumption”, of the various sets of parameters considered is tabulated and the best option chosen.

6.3 Final optimization by FSI Model

As we have seen, the FSI 3D Model is some kind of Virtual Prototype that simulates the reality with great accuracy. So it can be considered a test bench where the design elaborated through the steps 6.1 and 6.2 can be tested and the design validated. Of course, in case the preliminary design optimized through the 1-dimensional model results to be not completely effective at the FSI test, modifications shall be introduced and the “test” repeated in order to find a completely satisfactory design.

This sequence may seem to be heavy but if one considers that the introduction of a new cylinder normally implies several additional costs such as pattern construction, machining programs, testing tools and so on, and, last but not least, the possibility to compete on the market with a better product, the relevant expense is certainly justified.

Steps 6.2 and 6.3 may be valuable not only for the design of new compressor cylinders but also for the improvement of existing cylinders in order to introduce the necessary modifications to get a better performance.

7 Conclusions

This study has shown that the FSI software is a very powerful and promising tool that allows the creation of Virtual Prototypes simulating with great accuracy the fluid-dynamic behavior of reciprocating compressor cylinders. This new technique, preceded by a 1-dimensional model for the first screening of the various geometric parameters, enables the design engineer to evaluate and optimize the cylinder performance as a final step of a new advanced design sequence. The new design method avoids the expense of the construction of a physical prototype or the even more expensive exercise to put in production, with the relevant introduction costs (pattern, machining programs, manufacturing tools etc.), a poor product in terms of efficiency and unable to make the most of the compressor frame load capability. The utilization of the new tool will also allow avoiding to have reduced throughput and increased specific power than expected with the calculation of the compressor performance with constant flow coefficients along the piston stroke.

The integration of machine design and CAE resources, together with the utilization of a high level hardware infrastructure, allowed reaching extremely interesting results reducing drastically the computing time thus letting this very powerful set of tools become an every day means. The availability of even higher power hardware will reduce the computing time even further.

As it applies to all Virtual Prototypes, also the FSI model discussed in this paper, can be rerun for introducing any modifications at a later time with great advantage with respect to the physical prototypes.

References

- [1] Cristine M. Gehri, Ralph E. Harris (SRI): *High speed reciprocating compressors – The importance of interactive modelling*, Gas Machinery Conference, Houston (TX), October 1999
- [2] Costagliola M.: *The theory of spring loaded valves for reciprocating compressors*, Journal of Applied Mechanics, Dec 1950
- [3] Mac Laren J.F.T., Kerr S.V.: *Analysis of valve behaviour in reciprocating compressors*, Paper 3.39, Proc.XII Int. Congr. Refrig., Madrid, 1967
- Traversari A., Lacitignola P.: *Utilization and calculation of ring valves for reciprocating compressors*, Quaderni Pignone N. 16, September 1970
- [4] Machu E.H.: *Increased power requirement due to pocket losses, piston masking and gas inertia, eccentric load on the piston*, Gas Machinery Conference, Denver/Colorado, USA, October 1998
- [5] Aigner R., Meyer G., Steinruck H.: *Valve Dynamic and Internal Waves in a Reciprocating Compressor*, 4th Conference of the EFRC, Antwerp, June 2005
- [6] Aigner R.: *Internal Flow and Valve Dynamics in a Reciprocating Compressor*, Dissertation, Technischen Univeritat Wien, June 2007
- [7] Friedrich Bauer: *Valve losses in Reciprocating Compressors*, 1988 International Compressor Engineering Conference at Purdue University, July 1988, West Lafayette, Indiana, USA
- [8] Faretra M., Barbanti G., Traversari R., Galbiati M.: *Multi-phase CFD study of a reciprocating gas compressor with liquid slug injection*, EnginSoft International Conference 2009
- [9] Shiva Prasad B.G., Heidrich F.L.: *A study of indicator passage error correction schemes*, Journal of Engineering for Gas Turbines and Power, Volume 113, Issue 3, July 1991

Development of innovative sensor and method for direct measurement of rider ring wear

by:

L.G.M. Koop, P.N. Duineveld
Senior Engineer, Manager
Technology department
Thomassen Compression Systems B.V.
lk@thomassen.com, pd@thomassen.com

7th Conference of the EFRC
October 21th / 22th, 2010, Florence

Abstract

The paper describes the development, realization and testing of a sensor system for the highly accurate measurement of rider ring wear. The sensor is located inside the cylinder and is therefore subjected to extreme operating conditions. It measures the gap between the piston and liner, which is directly proportional to rider ring wear. This system eliminates all disadvantages and inaccuracies related to the standard rod-drop systems. The sensor has been developed in a joint effort between Thomassen Compression Systems and a sub-supplier specialized in innovative products with in-depth experience and expertise across the complete spectrum of sensors. The in-house testing and certification has been successfully completed. Field testing and patent procedures are in progress.

1 Introduction

In horizontal reciprocating compressors the lifetime of rider rings, also referred to as wear bands, is

strongly dependent on operating and process conditions, gas composition, lubrication and presence of particles and/or liquids, among other things. Not all of these parameters are always known in detail and therefore it is well-known that

the actual lifetime of rider rings can be unpredictable and, when not replaced in time, the piston can come into contact with the liner, damaging it (Figure 1). Alternatively, the actual lifetime can exceed scheduled maintenance intervals resulting in unnecessary replacement.



Figure 1: Damage to liner, rider ring wear not detected

In view of the above it is logical that users are interested in a method to measure the wear of the rider rings in order to ensure safe and reliable operation and to be able to plan maintenance stops. Over the years several methods have been developed for measuring rider ring wear. The most common method is to use a rod drop system which measures the drop of the piston rod just outside the stuffing box and calculates the gap between the liner and piston (equal to the thickness of the rider rings). This method usually produces unreliable readings.

The background of rod-drop measurements and the parameters that influence the measurement will be discussed in chapter 2. The new method and sensor that directly measures the gap between the liner and the piston will be presented in chapter 3. In this chapter also the development, testing and installation of the sensor is described. In the last chapter a summary will be given and conclusions will be drawn.

2 Existing Rod-Drop Monitoring Systems

2.1 Introduction

The most commonly used method to monitor the wear of rider rings is by measuring the vertical displacement of the piston rod using a Eddy-current probe. This probe is installed in the outboard compartment, immediately in front of the stuffing box flange (Figure 2). This means that the

measuring location is approximately between one-third and half way along the length of the piston rod. These so called rod-drop monitoring systems do not measure the rider ring wear directly but derive it from the rod-drop measurement.

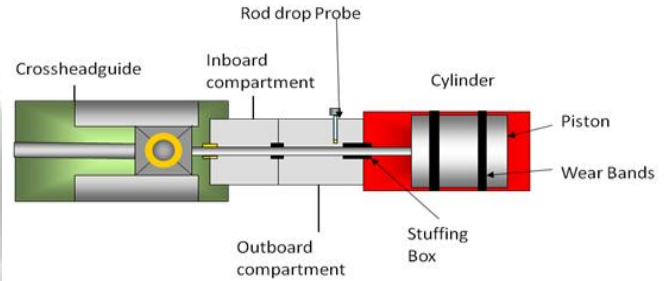


Figure 2: Schematic view of Rod drop Probe position

2.2 Piston rod-drop measurements

The vertical displacement of the piston rod as measured is composed of and influenced by the following factors:

<u>Thermal expansion</u>	With changing operating temperatures (operating conditions) the piston centre, and attached piston rod, will rise and drop relative to the bottom of the cylinder due to thermal expansion of the piston. The cylinder bottom location is more or less fixed by the supporting structure. This will change the sensor-reading.
<u>Clearance of the crosshead</u>	The loading on the crosshead varies over a stroke. Depending on the direction of rotation and the position of the crosshead guide, the crosshead is lifted from the bottom guiding shoe and rests on the top guiding shoe. It will also fall back because of its weight when the load reverses. This will induce vibrations and changes in the rod position reading.
<u>Bending of the rod</u>	The load on the front of the piston is not evenly distributed. Varying pressures on the surface at valve locations will lead to the piston tilting during the stroke. This tilting-effect bends the rod.
<u>Stuffing box forces</u>	The stuffing-box elements seal the gas pressures in the cylinder from the atmosphere. The sealing elements can move vertically in the cups to allow for vertical piston rod movements. However, axial forces resulting from the gas pressure on the sealing elements are considerable, therefore a large force is required to overcome the vertical frictional force in the cups. The rod will be

	“clamped” by the stuffing-box until the weight of the rod and piston overcomes the frictional force, or until the gas force decreases during the stroke. This leads to a sudden vertical displacement.
<u>Static rod run out</u>	Every compressor cylinder has its own run-out due to misalignment. The allowable values are prescribed in API 618.
<u>Piston rod wear</u>	After a certain amount of time the running section of the stuffing-box on the rod will wear down. Sometimes a small edge will occur on the ends. This edge runs under the probe and will influence the reading.
<u>Un-equal sensor calibration</u>	The sensor calibration may differ over the length of the stroke, particularly on coated rods. This is also called electrical run-out.
<u>Wear of rider rings</u>	The total decrease in rider ring thickness is approximately 2 to 2.5 mm, depending on piston size. However, the accuracy of the measurement must be relatively high.

In addition to the above, lateral vibrations of the rod have a major influence on the accuracy of the rod-drop measurement. As the measuring position relative to the distance to the piston varies with the stroke, the value measured is not constant over a revolution. In fact the probe will detect a run-out. This run-out reading disappears completely in the amplitude of the vibrational amplitude. The shape of the reading varies with changing cylinder load and pressure.

Figure 3 shows the horizontal and vertical amplitude measured by the probe. Figure 4 shows the orbit of the piston-rod vibrations. Several methods of data processing were used to abstract a rider ring wear from these measurements, without reliable results.

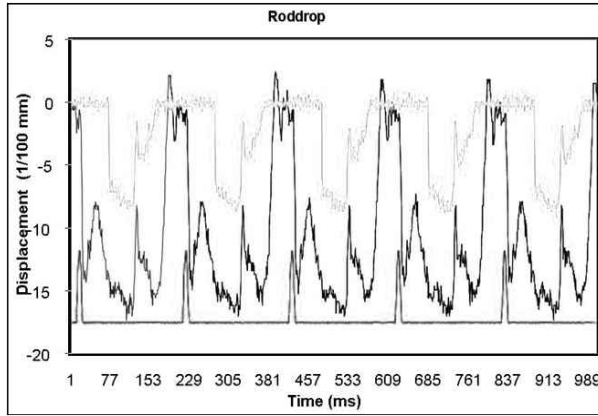


Figure 3: Piston rod vibrations

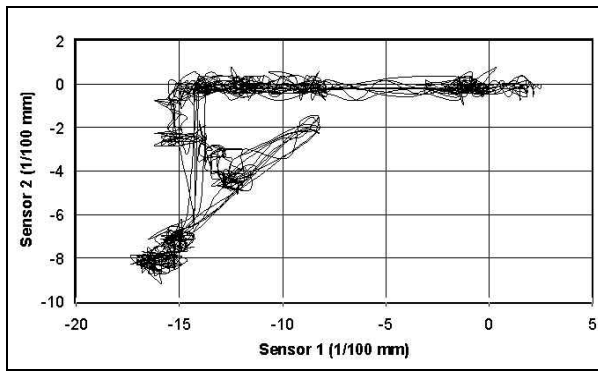


Figure 4: Piston rod vibrations orbit

2.3 Discussion

The rod-drop probe detects all vertical movements of the rod and wear of the rider rings is only one component in the measured signal of vertical displacement. Extracting/calculating rider ring wear from this signal is very difficult, resulting in unreliable results.

Measurements in the field and response from users clearly indicate that detection of rider ring wear by the rod-drop method is not reliable.

2.2 Innovative New Sensor and Method

3.1 Introduction

As early as the late 90's Thomassen concluded that the only way to achieve reliable, accurate measurements of rider ring wear is by measuring the gap between piston and liner. This means that, somewhere inside the cylinder, a sensor has to be installed where it must be able to withstand process gas conditions, high pressure, high temperature, corrosive attack, oil, and other contaminations. Such a sensor is not available on the commercial market. For this reason Thomassen developed a sensor that directly measures the position of the

piston relative to the liner wall. This sensor was presented on the Fluid Machinery Conference in The Hague in 1999 (Koop, 1999). Major drawbacks were that it was relatively large and holes had to be drilled in the cylinder wall to accommodate it. This leads to a complex and time consuming installation procedure, especially when fitting it in existing cylinders (TCS, 2000). Therefore, in cooperation with a specialized sensor company, we have developed a new sensor called Rsens™ (Figure 5). Our innovative new sensor and method for measuring rider ring wear is smaller, and easier to install.

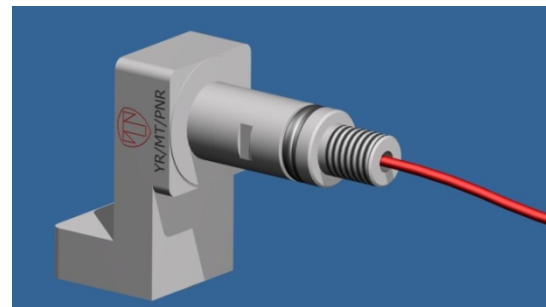


Figure 5: New sensor (Rsens™)

3.2 Method

The newly developed sensor measures the gap between the liner and piston, which is equal to the thickness of the rider rings. It is positioned inside the cylinder cover at head-end side, with the sensor head in the pocket above the discharge valve (Figure 6 and Figure 7). It automatically detects when the piston is above the sensor, and then performs a number of measurements. There is no key phasor required and all metallic materials can be detected.

The detection method is based on the de-tuning of a resonating circuit and can therefore operate at very low power, making it suitable for certified operation even in the most hazardous of environments. The sensor is calibrated automatically by the software when installed. The signal is a direct representation of the rider ring wear with an accuracy of 0.1mm. This system and method eliminates disadvantages and inaccuracies related to the standard rod-drop systems, as described in the previous chapter.

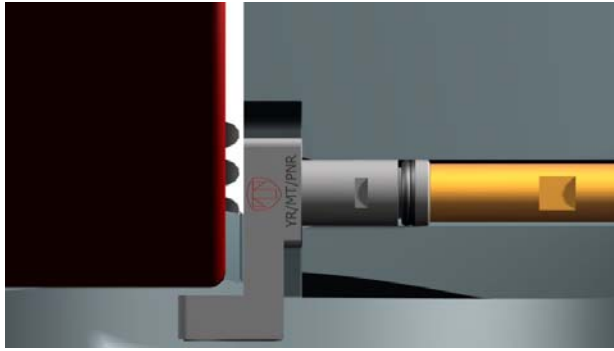


Figure 6: Piston above sensor

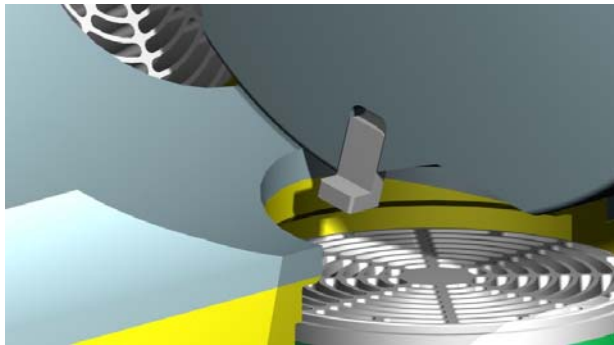


Figure 7: Sensor in cylinder head

The sensor system, which is Ex certified, supplies a 4-20mA output signal with a linear representation of the measured distance. This signal can be linked to a local reading or a PLC or DCS system.

3.2.1 Development

The sensor and electronics have been developed in a joint effort between Thomassen Compression Systems and a sub-supplier specialized in innovative products with in-depth experience and expertise across the complete spectrum of sensors.

The development consisted of three major subjects:

- Sensor housing, which is mechanical design
- Electronics, which must be small and resistant to the temperatures inside the cylinder
- Software development

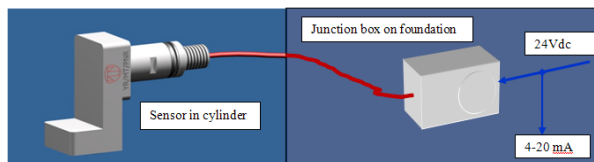


Figure 8: Schematic overview sensor system

These three development subjects will be described in more detail in the following paragraphs.

3.2.2 Sensor housing

The robust housing of the sensor is made of a stainless steel material which conforms to specifications according to NACE and has a design pressure of 250 bar. The separate components of the housing are welded through Laser Beam Welding (LBW) techniques (Figure 8 and **Error! Reference source not found.**), which guarantees deep weld penetration, minimum heat input and a high quality weld. Several design reviews have been conducted by a team of experts. This resulted in multiple design changes in order to assure safe operation and accuracy and reproducibility of the measurements.

The housing contains the sensor and a wire which is connected to the processing unit in the junction box outside the cylinder.



Figure 9: Laser beam weld in sensor housing

3.2.3 Electronics

The electronics (Figure 10) have been specially designed to obtain a high resolution for a large measuring distance.

The electronics and microprocessor are installed in a Exd junction box, which is mounted on the foundation or a structure not far from the compressor (Figure 11). The sensor system consists of two parts:

1. The sensor installed inside the cylinder and wired to the processing unit.
The wire is conducted through a SS tube and connected to a strip inside a IP65 junction box on the outside of the cylinder cover.
From this point the wire is conducted through a flexible metallic tube to the junction box on the structure. This is done for ease of dismantling the cylinder cover.
2. The electronics in the junction box require 24Vdc supply.
It supplies a 4-20mA output signal with a linear representation of the distance measured. This output signal is protected by zener barriers and can be used to drive a display unit or a read-out in the control room.

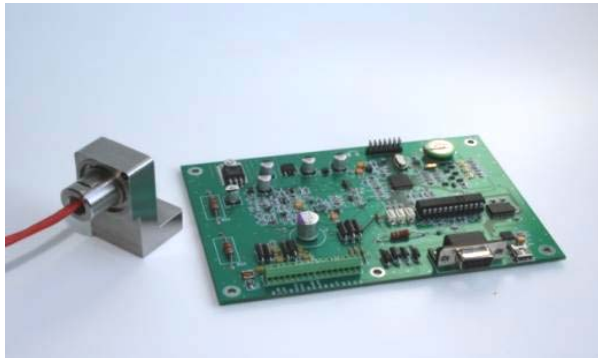


Figure 10 : Sensor and electronics

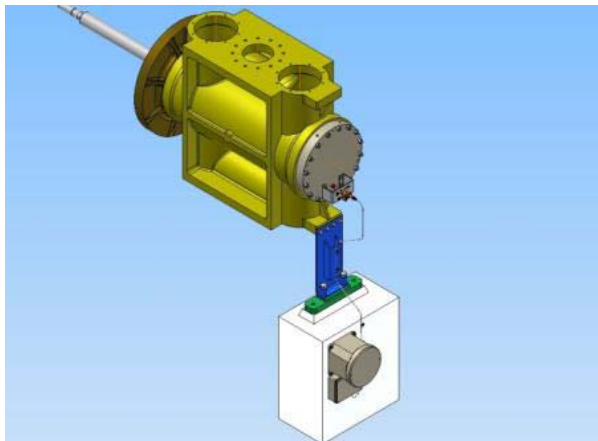


Figure 11 : Sensor and junction box arrangement

3.3.3 Software

The software detects when the piston is in the correct position to measure the gap between the piston surface and the sensor/liner (no additional key phasor sensor is required). In this position it first measures the temperature for correct

calibration, takes a high number of measurements, performs a statistical analysis and converts the measured signal into a mA signal for output.

3.3 Installation

The sensor is installed in the Head End cover (Figure 12). Machining the cover is relatively simple and no further modifications of cylinder or other parts is required. O-ring seals and back-up rings are located very close to the sensor, preventing the bore in the cover from being pressurized.

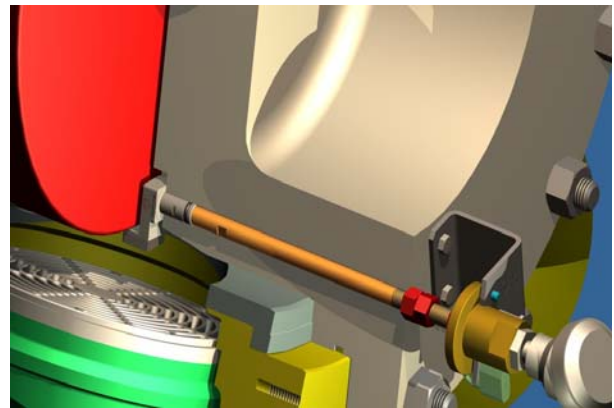


Figure 12: Sensor in Head End cover

When the sensor head is in measuring position it is below the surface of the liner. For this reason special provisions have been made for ease of dismantling the sensor, and to protect it when the cover has to be removed from the cylinder. Calibration for the piston material and geometry can be done in the field.

3.4 Testing and certification

After development and prototyping, a number of sensors were tested for environmental and operating conditions.

Static tests

- Pressure test up to 375 bar (1.5 times the design pressure)
- Leaktest
- Temperature range and shocks
- Linearity of output signal
- Sensitivity for counter material
- Sensitivity for geometric parameters (piston diameter, radius, clearances, roughness)
- Corrosion tests (H2S)

Dynamic tests

- Limited fatigue test
- Varying compressor operating conditions

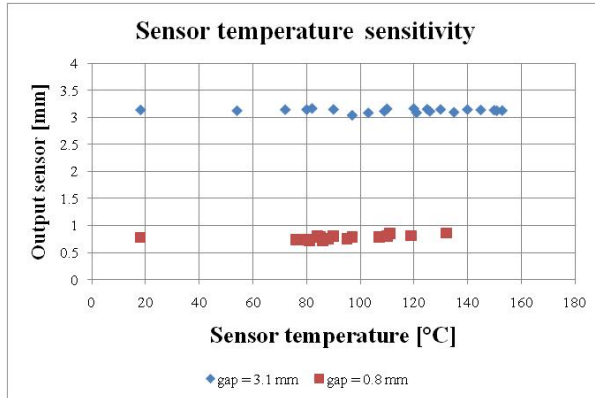


Figure 13: Dynamic test: sensor temperature sensitivity test

Figure 13 shows that there is almost no effect on the sensor output with changing sensor temperatures. This temperature test was performed in the Thomassen R&D test compressor by changing the operating conditions.

After successfully passing all above mentioned testing the sensors was ATEX certified (Ex II 1G Ex ia IIC T4) by KEMA Quality BV.



Figure 14: Certified sensor

Field tests to verify the long term stability of the system under actual process conditions started in December 2009. The first results in Hydrogen and natural gas compressors are very encouraging.

4 Summary and Conclusion

The lifetime and wear of rider rings can be unpredictable. Users want to be able to measure the wear of these rider rings to ensure safe and reliable operation, and to be able to plan a maintenance stop. The most common method is to use a rod-drop system.

This system often produces unreliable readings because the measured signal is composed of and influenced by many factors.

The only way to achieve a reliable and accurate measurement of the rider ring wear is by measuring the gap between piston and liner inside the cylinder. Thomassen started the development for such a system in the 90's and has now developed a innovative method and sensor for the direct measurement of the rider ring wear with no correction factors required.

The newly developed sensor, Rsens™, is able to withstand the aggressive gasses, extreme dynamic pressure and temperature behavior, and other harsh and difficult measuring circumstances inside the cylinder. It has a high accuracy (0.1mm), stability and repeatability, and since there are no moving parts. No additional key phasor is required. The sensor is installed in the Head End cover and, in most cases, can be retrofitted by machining the cover.

With the new Thomassen Rsens™ it is possible to get a real and reliable real time value for rider ring thickness in almost any cylinder, improving the reliability of the compressor.

References

Koop, L. (1999). A new approach for reciprocating compressor wearband thickness detection. *Fluid machinery for the oil, petrochemical and related industries (IMechE)* (pp. 235-240). The Hague: Professional Engineering Publishing.

Schrijver, J. (1999). *Report on testcompressor rod drop measurements*. TCS.

TCS. (2000). *Rod drop measurements on NAM natural gas compressors*.

Stabilization of compressor foundations

by

Mr Thorsten Reisser

Senior Engineer Rotating Equipment - Reciprocating Compressors

thorsten.reisser@basf.com

BASF SE

Ludwigshafen, Germany

and

Mr Wolfgang Blankart

Civil Engineer

wolfgang.blankart@basf.com

BASF SE

Ludwigshafen, Germany

and

Mr Stefan Irrgang

Reliability Engineering Manager

stefan.irrgang@shell.com

Shell

Wesseling, Germany

**7th Conference of the EFRC
October 21th / 22th, 2010, Florence**

Abstract

BASF SE - Ludwigshafen is situated in the Rhine valley where the river Neckar meets the Rhine. The Rhine valley is a result of continental movements leaving behind a mountain range to the east and to the west. The fault gave way to the river bed and together with regular flooding shaped the flat area consisting of sand and other debris. The ground gives sufficient support to static buildings and roads however an oscillating load has further influence on the rigidity. At BASF SE changes to the ground stiffness have been observed in conjunction with reciprocating compressors leading to sinking foundations and vibration after years of service. Several methods have been applied to compensate for this phenomenon such as changing the natural frequencies and stabilizing the ground. This presentation will show the effects of oscillating loads to the ground and action taken to overcome these effects. The lessons learned will be displayed.

1 Introduction

BASF SE is the world-wide largest chemical company with the head office in Ludwigshafen/Rhine.

Picture no. 1 - The BASF headquarter in Ludwigshafen consists of over 2.000 buildings and spreads over 10 km² being the largest interdependent chemistry area of the world. A wide network of pipeline enables efficient supplying of the plants with raw materials and energy. In the production group intermediate materials for the followers are manufactured just in time.



Picture no. 1: BASF SE in Ludwigshafen/ Rhine

BASF SE in Ludwigshafen is operating various reciprocating compressors of different age. Through that a wide knowledge about how to run and maintain compressors has been accumulated. Process requirements have changed over the decades and some of the compressors were modified. Safety aspects force BASF SE to ensure that all units are safely operated as per today's requirements.

Through years of operation not only the compressors but also the foundations on which they are supported experience a tremendous number of load cycles. Failures of foundations appear in different modes such as cracks, change in position, oil contamination.

This paper will show some examples of changes to foundations that appeared in the recent years and the engineering work carried out to overcome the obstacles both at BASF SE and Shell.

2 BASF – NEA- TEL 50

Problem description:

A single stage compressor of the Type NEA TEL 50 has been in service for more than 28 years. The piston is double acting and horizontally arranged. It provides a gas mixture of carbon monoxide and propylene from 0.1bar to 4.5bar at a rotational speed of 630 rpm. The volume flow rate is controlled by a bypass. The compressor is located open air on a concrete foundation reaching in the ground for 1.5 meters. The overall dimensions of the foundations are 3 x 1.5 x 1.5 meters.

In the year 2008 the operators reported vibrations of the pipe work of an uncommon mode. The vibrations where assumed to have been caused by the compressor. A subsequent measurement of the natural frequencies proved the rotational speed of the compressor.

Scope of investigation:

As a first action the supports of the pipe work where checked for a tight fit and new supports where installed. This led to less vibration of the pipe work however high amplitudes where measured on the compressor and the foundation. The Frequency complied with the rotational speed of the crank shaft.

Secondly the mechanics of the compressor were checked in particular the flywheel of the crankshaft, the counterweights and the connections between crosshead, piston rod and piston were checked. Furthermore the electric drive and the V-belts were investigated. However no deviations where discovered, the flywheels were precisely balanced, V- belts had been replaced, all connections were found to be tight. A test run however proved the vibrations still to be existing with the excitation to be equal to the rotational speed.

Now the foundation was inspected using a shaker for excitation in order to determine the natural frequencies of the foundation. It was assumed that cracks in the foundation had changed its mode shape and natural frequency to meet the rotational speed. The results however showed that the amplitudes gradually dropped with the exiting frequencies so there was no sign for cracks. It showed however that the Amplitudes at 2/3 of the rotational speed appeared in a reasonable range.

Gas pulsation as a cause for the vibration where also investigated simply by running the compressor without Pipe work. Yet vibrations of the foundation and the compressor were strong.

Finally the ground underneath the foundation was investigated. In order to achieve an insight two test specimen were taken and analysed. Furthermore a dynamic probing was conducted to find out the stiffness and rigidity of the ground. It showed that the rigidity had changed tremendously so the support of the foundation was not sufficient anymore. The reason for the change is yet unknown since the surface in the vicinity of the foundation is sealed by concrete and there had been no caverns observed.

Action taken:

Short term

As a first action it was decided to change the excitation of the foundation by reducing the rotational speed of the compressor. By using the shaker it was found out that 2/3 of the rotational speed gave reasonable values for vibration. Since this leads to different loads within the compressor and to a reduced flow rate an engineering study was conducted by NEAC. The results showed that the load safety factor was still sufficient. The lack of flow rate was overcome by the fact that the compressor had been run at reduced load in the past months since current demands were below maximum. So by reducing the bypass flow sufficient volume was yet to be processed. Changing the rotational speed was done by replacing the electric motor. No operation was possible with reduced flow rate.

Long term

Since the low flow rate was only temporarily acceptable further action was taken to bring the compressor back to normal operation. For this reason the foundation was enlarged in size and weight by adding a concrete block to its small end. The new enlargement reaches 2.5 meters below ground and provides enough mass to further change the natural frequency of the foundation and to provide a better hold in the ground. With this action the compressor was now ready to service under original conditions.

3 BASF – GHH- B2g30- Hyper

A two stage hyper compressor of the Type GHH B2g30 has been in service since 1982. It is a two crank double acting compressor with the plungers working horizontally. It provides ethylene at a pressure from 300 to 2500 bar at a rotational speed of 210 rpm. The compressor is located in house on a concrete foundation reaching from the ground floor through the basement into the ground for 2 meters. The overall dimensions of the foundations are 8 x 5 x 8 meters.

Over the years the position of the foundation was regularly measured in relation to the surroundings. It was observed that a lowering of the entire foundation took place. As a result the pipe work experienced stress. Moreover the isolation from the ground floor was no longer given since it had leant to the side as well. Finally the misalignment of the crank cases and the crank shaft resulting from this caused regular failure of the main bearing.

Scope of investigation:

Since the process of lowering continued for many years and did not seem to stop action had to be taken. To get a better understanding of the process an analysis of the ground underneath the foundation was carried out comprising the analysis of test specimen and a dynamic probing. The results did not show any significant change in the ground structure so the reason must be due to the high oscillating inertia of the compressor. Since this cannot be varied a method had to be applied giving more stability to the ground.

Action taken:

One method available on the market provides a resin to be injected underneath the foundation. This method not only increases the rigidity of the ground but also provides enough pressure to lift the foundation up if applied properly. In a first step the resin is injected 2 m below the foundation to lift it. In a second step the Injection takes place some 6m below the foundation to create the required rigidity.

In order to monitor the lifting process a measuring system based on laser was installed both to the foundation and the near surrounding in relation to the basement.

For Injection small holes (12mm) were drilled through the foundation to install the jets. After the resin together with a hardener was provided by an injector gun. The chemical reaction takes place as soon as both chemicals are mixed and injected. Together with the reaction the pressure rises and the lifting can be observed.

In this particular application the lifting process was stopped after 2 mm. It was observed that not only the foundation but also the surrounding floor started lifting. This is due to the inhomogeneous underground structure with the floor of the basement being only 0.3 m and the foundation reaching down 2 m.

Further work focused on the deep injection only. This process proved to be applicable. The entire process lasted 5 – 6 days.

The method of resin injection described here can be applied to homogeneous structure. However if there are structural steps underground it is virtually impossible to control the process of lifting. The evidence of the subsequent deep injection will be proven by regular measurements of the foundation after months and years of compressor service.

4 Shell – Einheitsverdichter Borsig Type

The Rheinland refinery

The Rheinland refinery is located directly at the river Rhine. The refinery consists of two production site's, one near to Cologne (North Part) and one next to the town Wesseling (South Part), both are in North Rhine-Westphalia, North-West part of Germany (see picture no.2)

The ground conditions are very similar to one at the BASF SE Ludwigshafen location.

The Rheinland refinery is part of the Shell Deutschland Oil GmbH and belongs to the Royal Dutch Shell plc. Refinery network.

The refinery is developed from a joint venture between Shell and DEA and it is the largest refinery in Germany and one of the largest refineries globally. Beside the classical refinery production units some petrochemical / chemical production units are located on the area.

The line-up of the refinery allows the import of a high number of various crude oils and gives a huge flexibility in operation.

The location directly at the river Rhine with two own harbors enable the import of feedstock and export of products via barge in a significant range, other transport ways are pipelines and road trucks. The location of several chemicals productions (BASELL, Evonik) between the both site's, makes refinery an integrated part of the area industrial infrastructure of the region.



Picture no. 2: Shell Rheinland Refinery

The Wesseling site of the Rheinland Refinery still operates 5 of formerly 12 installed heavy reciprocating compressors.

These machines are called "Einheitsverdichter" and were built before and during the 2nd World War according to one design from different manufactures.

None of the OEM's (original equipment manufacturers), i.e. Demag, Borsig, Schwarzkopf, E&S is dealing with reciprocating compressors any more. The compressors are part of the HCU (Hydro Cracker Unit) providing hydrogen rich gas to the reactors, which are operated at about 300 bars.

Problem description

The compressor is quite unique in design by realizing the compression ration in 4 stages being arranged inline. In comparison with the original design using the pressure stages 1 to 6 only the 3rd stage (low pressure stage) and the 4th to 6th stages (high pressure stages) are remaining after several modifications to meet the refinery production requirements.

This arrangement is valid on both sides of the machine. The 3rd stage suction pressure is 18bar and supplies hydrogen of 30bar to the header. The HP-Section (high pressure section) is fed from the 30 bars header and delivers hydrogen at a discharge pressure of about 320 bars by passing the 4th stage (plus additionally the optional 4th stage) -> intercooling -> 5th stage -> intercooling -> 6th stage to the 300 bars header.

The capacity of each LP-HP line is 12.000 Nm³/hr.

The compressor is located in a compressor hall on the 4m level above hall ground, standing on a U-shape foundation.

Various vibrations of the crankcase were detected of a certain period of time. In Spring 2008 a crack in the crankcase was reported.

Scope of investigation

After detecting the crack in the crankcase several inspections took place and findings were more significant in terms of conditions of the foundation as expected. A further finding was that the compressor crankcase was not longer properly connected to the foundation concrete and was "loose rattling" on the foundation during operation. This caused several damages at the bearings and other parts.

After shutting down of the compressor a detailed inspection of the foundation was performed and several cracks in the foundation running vertically and horizontally through the entire foundation were identified. The foundation was saturated with liquids, coming according first assumptions out of cracks from the tub of the crankcases and piping connections.

Action taken

Immediately after detecting the remarkable damages of the foundation and the fact that the crankcase was irreparably damaged it was obviously that a short-term mitigation of the issues identified was not feasible.

A lift up of damaged crankcases was unavoidable to substitute them against others. The lift up was one of the major basic prerequisite to realize the later chosen repair method.

For the foundation renovation or substitution, several concepts were examined in diverse challenge rounds. At the end a concept was chosen to rejuvenate the old foundation using anchor bolts and oil resistant epoxy resin.

Several holes and drills have been carried out into the foundation.

- 4 vertical holes of 6m lengths at both sides of each compressor cylinder head plinths. These perforations have crossed the main block of the foundation vertically until reaching - 1.25m from the ground level to ensure the connection with the sub slab
- The main block has been crossed with 18 vertical holes of meter length. Their distribution has been done to ensure the later homogeneous and horizontal distribution of the epoxy resin through the foundation. A special care was also taken to avoid tunnels and other voids existing inside the foundation. These perforations have crossed the main block also vertically until reaching - 1.25m from ground level to ensure connection with the sub slab

2 oblique holes to fasten the main block with each arm supporting the compressors cylinders

Inside each hole a corrugated high yield strength rods were inserted. Top ends were sealed and prepared to press in epoxy resin to release oil, water and air out of the cracks.

The external cracks were sealed with epoxy putty in order to keep as much as possible epoxy resin into the foundation, before releasing it just to displace as much oil as possible.

Finally oil resistant epoxy resin was injected controlling the cycles of pressure to push out the resident oil inside the cracks. Several holes were revealed and totally fixed by the expulsion of the resin outside the different faces of the main block.

The chosen concept, injection of oil resistant epoxy resin in conjunction with steel anchor bolts is an effective and efficient alternative to demolish the old one and build a new foundation. It is less time consuming and makes it possible to keep other essential parts like the electrical motor etc. in place, during executing the work. The evidence of the concept will be proven earliest after several months of operation, by measurements of vibrations and operational stability of the compressor.

5 Conclusion

Reciprocating compressors provide oscillating forces and moments by design. Especially for horizontally acting compressors particular focus must be given to the design of the foundation. As can be seen from the previous explanations it is not only down to heavy machinery but can also occur to small compressors. Even if the initial design was correct problems can occur after many years of service. The previous examples however show that there is a solution to virtually every problem. The solutions can be found if all people from different discipline work closely together and everybody is willing to provide their knowledge.



The impact of an API 618 4th or 5th edition analysis on the design of a very large Hydrogen compressor

by:

César Luis Fernández Valdés
C.D Engineering & Technology
Repsol, Madrid, Spain
cfernandezv@repsol.com

Leonard van Lier and Bert Egas
Bussiness Unit Oil and Gas, department of Flow and Structural Dynamics
TNO, Delft, The Netherlands
leonard.vanlier@tno.nl, bert.egas@tno.nl

7th Conference of the EFRC
October 21th / 22th, 2010, Florence

Abstract

For the two largest hydrogen compressors ever built (14 MW), Dresser Rand model BDC-OF18 with three stages and six cylinders, TNO has carried out an API 618 analysis according design approach 3. The new compressors provide make-up hydrogen to the new hydrocracker unit in the Repsol refinery in Cartagena, Spain. During the course of the analysis, Repsol asked TNO to investigate the impact on the mechanical design of the piping and the required pressure loss to reduce the pulsations, in case the applied allowable pulsation level is 2 times the level according the 4th edition of the API Standard 618. (Called the “Repsol approach”). This approach is comparable with the allowable levels of design approach 3 of the 5th edition of the API Standard 618. In case the higher allowable pulsation levels of the 5th edition will be applied, orifice plates or other pulsation damping devices with less additional pressure loss will be necessary to achieve the specified allowable pulsation levels. So operating costs will be reduced because of less consumed power. However, the remaining pulsation-induced forces on the pipe sections will be higher, although due to the low molecular weigh of the gas (pure hydrogen) the expected impact was low. So, in general, this approach requires more pipe supports to achieve acceptable vibration levels of the piping. In this paper the results and recommendations of the pulsation and mechanical response analysis of both approaches are given. For each part of the pipe system the difference in required additional pressure loss and installed number of required supports is given. Moreover a comparison has been made between the reduced operating costs due to lower power consumption and the supplemental costs for the installation of additional pipe supports and, eventually, larger installed pulsation dampers.

1 Introduction, description of the project

Due to the large rated power of these compressors REPSOL had in mind the pulsation analysis since the very beginning of the project, as decisions made at the engineering stage have a remarkable impact in the Total Cost of Ownership (TCO). Two cost issues were addressed:

- Sizing of the pulsation suppressors, and
- Allowable pressure pulsations

The cost of pulsation suppressor devices is a significant part in the overall cost of a reciprocating compressors order and therefore, unless otherwise requested by the purchaser, the compressors vendors tend to often the minimum possible size in order to be competitive. API 618 provides a formula to estimate the preliminary sizing of the surge volumes, in order to provide a fair comparison basis at bid stage; however, most vendors are reluctant to use this formula on the grounds that required volumes are not based on sound design criteria.

In order to make a fair comparison REPSOL requested all vendors for this project to make the preliminary sizing of the volume bottles based on TNO's Damper Check tool; also, this ensures that a large enough volume is used in order to minimize pressure pulsations and try to avoid the need for a large amount of pressure drop being introduced in the system when the pressure pulsation analysis is performed. It is estimated that the cost increase of the volume bottles due to this sizing method is approximately 15%, which is worth compared to the reduction in pressure drop.

With regards to allowable pressure pulsations, it was felt that the values specified by API 618 might be too low for a pure hydrogen service, due to its low molecular weight. It is well known that the higher the pressure pulsations the higher the pulsation-induced forces; also, it is a fact that the lower the molecular weight, the lower the pulsation-induced forces. As both effects work in opposite directions it was felt that a sensible approach would be to allow higher pulsation values than API 618 4th edition –the latest revision of this standard at the time the project was started up-, and two times the values allowed by API was deemed to be a good compromise between project CAPEX and OPERating EXpenditures (OPEX); the cost of the required additional supports would

be offset by the lower energy consumption, leading to a reduced TCO.

2 Description of the API 618 analysis

For this large system with large compressors and a very long pipe system (Totally a length of 1900 meters of piping has been investigated) a full analysis according the API Standard 618, design approach 3 has been ordered by Dresser Rand S.A . At the start of the project the analysis has been ordered according the 4th edition [1,2]. Referring to appendix M of this standard, the scope of the analysis consists of the following items:

- M2 and M3: Pulsation analysis of compressor, pulsation dampers and piping. The pulsation analysis will be discussed in detail in this paper
- M4 and M7: Mechanical response analysis of the pipe system. The mechanical response analysis will be discussed in detail in this paper
- M5 and M6: Compressor manifold analysis [3]. This is a mechanical response analysis of the complete compressor, the pulsation dampers, the piping around the compressor and the supporting steelwork. The vibration levels caused by the pulsation-induced forces have been calculated and in case vibration (and cyclic stress) levels have been calculated which exceed the acceptable levels, additional supports or increasing the stiffness of the supporting steelwork has been recommended
- M8: Mechanical analysis of the damper internals. For this project a simplified analysis has been carried out: By mismatching of mechanical natural frequencies of the installed baffle plates and the frequency of the pulsation-induced forces on the baffle plates, the resulting vibration levels of the baffle plates and the resulting cyclic stress level are within the allowable levels
- M9: Compressor valve dynamic analysis. In this analysis the effect of pulsations on the opening and closing impact velocities of the valves have been calculated. Moreover possible fluttering of the valves has been investigated. The result of the analysis has been sent to the compressor manufacturer for a further evaluation

Even though the scope of the project was based on the 4th edition of API 618, in the course of the project, the considerations as reflected in the 5th edition were also taken into account. One of the most important differences is the allowable pulsation level, which is significantly higher in the 5th edition in case of hydrogen systems.

This difference will have an impact on the important design choices, such as damper volume,

pressure drop over restriction orifices and the total number of support. These aspects will be considered in detail below.

The capacity of the compressors is controlled by a Hoerbiger HydroCom system. In general, a stepless capacity control system generates pulsations in the system of higher frequency. Therefore the frequency range of the pulsation analysis has been extended from the 16th harmonic up to the 64th harmonic. To reduce the higher frequency pulsations, the installation of multiple bore orifice plates has been recommended instead of the normally applied single bore orifice plates. In this way high frequency problems can be avoided [4].

3 Pulsation analysis

The pulsation analysis of the system consists of two steps:

- The check of the damper design
- The pulsation analysis of the pipe system

3.1 Check of the damper design

The first step in a pulsation analysis is the check of the damper design. At the start of the project an analysis according the 4th edition of the API Standard 618 has been ordered. Therefore the calculated pulsation levels have been compared with the allowable levels according to the 4th edition. During the damper check the piping has been replaced by a simplified boundary condition (an infinitely long line). Of each of the stages, the cylinder and dampers have been modeled. For these systems one duty has been simulated: the normal.

duty (this is H₂ duty). The pulsations in the cylinders and dampers have been calculated, taking into account the higher harmonics by filtering the results of the 64th harmonic and higher, instead of filtering of the 16th harmonic and higher. This is done because this is a system with a stepless capacity control system which causes in general pulsations of higher frequencies. Furthermore, the pulsation-induced forces on the dampers have been calculated. For all the duties simulations have been carried out for 100%, 75%, 50% and 30% load.

The calculated pulsation levels at the cylinder flanges and line connection of the dampers have been compared with the allowable level according the 4th edition of the API Standard 618, design approach 3. As an example the results of the 1st stage dampers will be discussed.

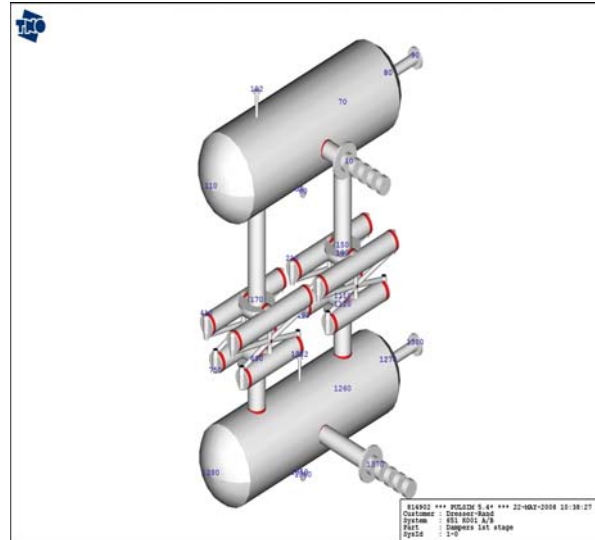


Figure 1: Plot of the original model of the 1st stage cylinder with pulsation dampers

The maximum calculated pulsation levels (comparison (ratio) with allowable API-levels) and forces for the original 1st stage dampers for the investigated range of the velocity of sound are given in **Table 1**. For each pulsation the dominant frequency component (harmonic of compressor speed) is given after ‘/’.

Damper	Pulsation levels		Forces on damper
	Cylinder flange	Inlet/Outlet	kN pp and dominant harmonic
Suction	0.46/14	0.54/2	19/34
Discharge	0.42/22	0.73/2	96.35

Table 1: Pulsation levels and forces for original layout

Clearly the pulsation levels at the line connections are lower than the recommended 0.8 times the specified API levels for systems with only one compressor in operation. Therefore we can conclude that the dampers are sufficiently large. Also the pulsations at the cylinder flanges are allowable. However, the axial forces on the dampers of the system are too high in amplitude and/or in frequency.

On the discharge damper, a pulsation-induced force of 96 kN is computed, dominated by the 35th harmonic of the compressor speed, which is unacceptable. In Figure 2, the force is illustrated as a function of the deviation of the speed of sound over a range of ±15%.

PULSATION & VIBRATIONS

The impact of an API 618 4th or 5th edition analysis on the design of a very large Hydrogen compressor,
Leonard van Lier, Bert Egas, Cesar Luis Fernandez Valdes; TNO SCIENCE AND INDUSTRY, REPSOL

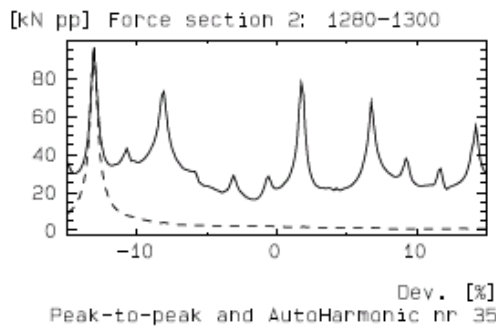


Figure 2: Plot of the force on the original discharge damper as function of the velocity of sound

To reduce the forces on the dampers the following modifications have been recommended in close cooperation with Dresser Rand:

- Install a curved baffle plate in the dampers exactly between the two cylinder connections
- Make the length of each damper compartment such that the cylinder connection is in the axial middle
- Install multiple bore orifice plates with a pressure loss of 0.2% in the cylinder connections of the suction and discharge damper
- Extend the line connection internally to both sides of the baffle to 1/8 length of the damper.
- Reduce the internal extended line connection is such a way that the pressure loss is maximum 0.2%

The layout of the final modification is shown in Figure 3. In the plot the baffles are represented by two caps.

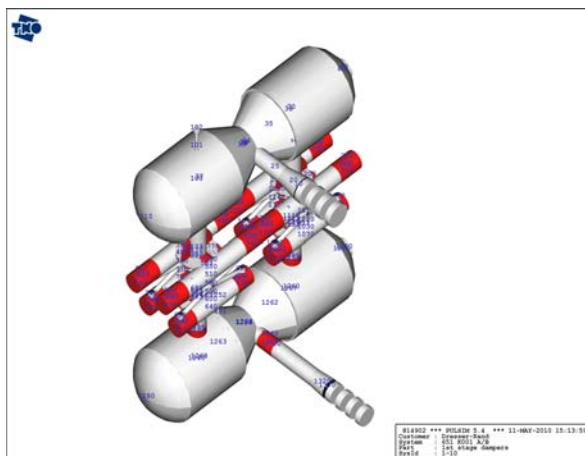


Figure 3: Plot of the recommended model of the 1st stage cylinder with pulsation dampers

The drawing of the suction and discharge damper is shown in Figure 4.

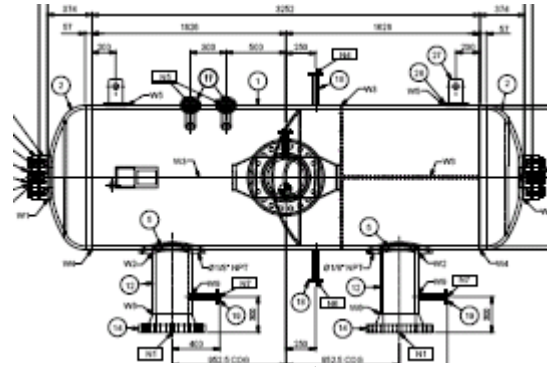


Figure 4: Drawing of the 1st stage suction/discharge damper

The maximum calculated pulsation levels (comparison (ratio) with allowable API-levels) and forces for the recommended 1st stage dampers for the investigated range of the velocity of sound are given in **Table 2**.

Dampers	Pulsation levels		Forces on damper kN pp and dominant harmonic
	Cylinder flange	Inlet/outlet	
Suction	0.44/2	0.76/2	2.0/4
Discharge	0.56/2	0.81/2	6.3/7

Table 2: Pulsation levels and forces for recommended layout

The forces and frequencies have been reduced significantly. Also the pulsation levels have been reduced. The reduction of the force over the discharge damper is illustrated in Figure 5.

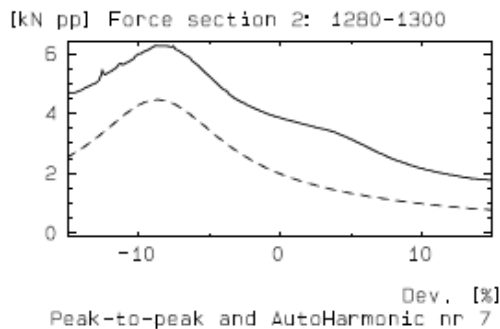


Figure 5: Plot of the force on the recommended discharge damper as function of the velocity of sound

The dynamic force over the baffle plate is considerable. However, it has been verified that acceptable stress levels are obtained and that the resonance frequency of the baffle is shifted sufficiently far from the excitation frequency, so that no resonant behaviour will occur. In addition to simplified analytical models, also a finite element analysis of the baffle has been made. Also, the effect of the damper wall flexibility on the resonance frequencies has been considered.

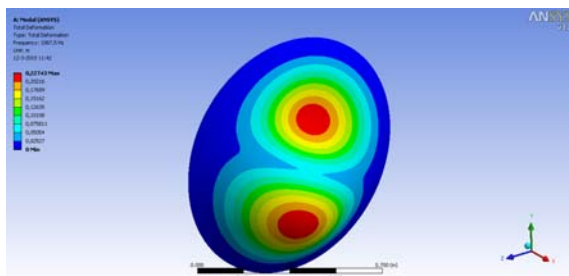


Figure 6: Example of mode shape of curved baffle plate

3.2 Pulsation analysis of the pipe system

The pipe system has been investigated with the pulsation dampers with all recommendations which resulted from the check of the damper design. During the pulsation analysis of this very large pipe system (1900 meters), the system has been divided in 4 subsystems:

- Suction 1st stage piping
- First inter-stage piping
- Second inter-stage piping
- Discharge 3rd stage piping

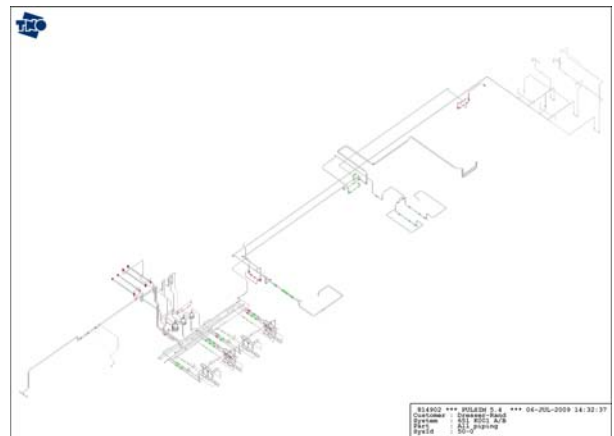


Figure 7: Plot of the complete pulsation analysis model

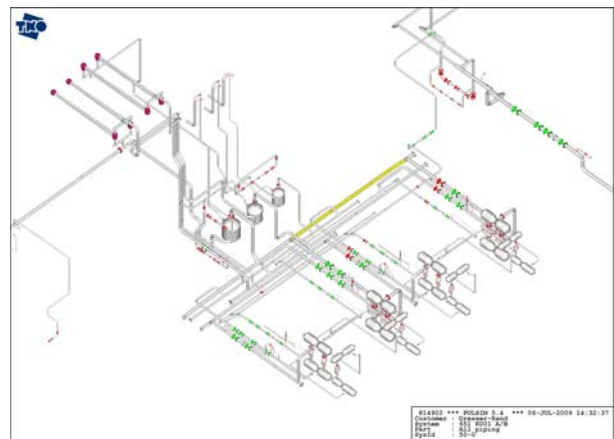


Figure 8: Plot of the model around the compressors

The pipe systems (see Figures 7 and 8) have been investigated for single operation of the compressors for 4 load cases (100%, 75%, 50% and 30% load). The compressors have been investigated for a hydrogen duty (with a molecular weight of 2.03). For this duty a range of +/-20% around the expected velocity of sound (VOS) has been investigated. This range is applied to account for deviations in gas conditions (density, temperature), and geometry deviations in the simulation models.

In the original pipe system, the pulsations exceeded the allowable level at various locations and at almost all load conditions. The exceeding is caused by acoustical resonances present in the pipe system. The pulsations can be reduced to acceptable levels (compared with the allowable level according the 4th edition of the API Standard 618) by installing orifice plates at several locations.

The locations of the recommended orifice plates, which cause additional pressure loss in the system, are shown in **Table 3**.

PULSATION & VIBRATIONS

The impact of an API 618 4th or 5th edition analysis on the design of a very large Hydrogen compressor,
Leonard van Lier, Bert Egas, Cesar Luis Fernandez Valdes; TNO SCIENCE AND INDUSTRY, REPSOL

Part of the system	Location	% pressure loss
Suction 1 st stage	Outlet separator	0.5
	Inlet suction damper	0.5
First interstage	Outlet discharge damper	0.6
	Outlet separator	0.5
	Inlet suction damper	0.5
Second interstage	Outlet discharge damper	0.6
	Outlet separator	0.5
	Inlet suction damper	0.5
Discharge 3 rd stage	Outlet of the damper	0.5

Table 3: Recommended orifice plates, according to API 618 approach

During the course of the pulsation analysis REPSOL asked TNO to investigate the effect of accepting a pulsation level of 2 times the allowable level according to the 4th edition of the API Standard 618. This level is comparable with the allowable level of the 5th edition of the API Standard 618. Of course the resulting pulsation-induced vibration forces will increase and probably more pipe supports have to be installed to achieve acceptable vibration levels.

Table 4 list the orifice plates required with this new approach and their corresponding pressure drop.

Part of the system	Location	% pressure loss
Suction 1 st stage	Outlet separator	0.2
	Inlet suction damper	0.3
First interstage	Outlet discharge damper	0.2
	Outlet separator	0.5
	Inlet suction damper	0.1
Second interstage	Outlet discharge damper	0.2
	Outlet separator	0.2
	Inlet suction damper	0.2
Discharge 3 rd stage	Outlet of the damper	0.1

Table 4: Recommended orifices plates, according to the "REPSOL" approach

The reduction in the required pressure losses is shown in **Table 5**.

Part of the system	Reduction in pressure loss (%)
Suction 1 st stage	0.5
First interstage	0.8
Second interstage	1.0
Discharge 3 rd stage	0.4

Table 5: Reduction in required pressure loss

The reduction in pressure loss results in a reduction of power consumption of 2.948 MWh per year. Due to the increased suction pressure (0.5%), also the capacity increases correspondingly.

This reduction in pressure loss is also possible by the fact that the pulsation dampers have been designed in order to match the pulsation criteria of API 618 4th edition. In case the dampers should have been designed according the 5th edition, smaller dampers should have been designed and the reduction in pressure loss should be less. Roughly the diameter of the dampers could have been reduced about 25%.

4 Mechanical response analysis

4.1 Introduction

From the results of the pulsation analysis the load case with the maximum pulsation-induced forces has been selected. For this load case, the deviations of the velocity of sound where maximum pulsation-induced forces occur have been selected (acoustical resonance conditions), see Figure 9. The pipe system has been excited with these maximum possible pulsation-induced forces.

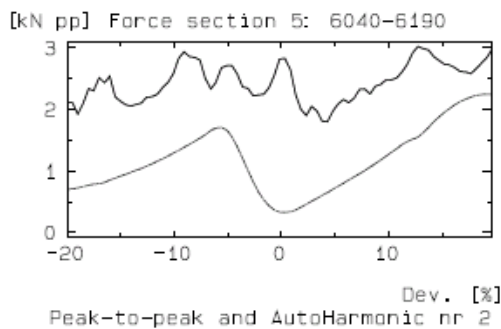


Figure 9: Example of a plot of the pulsation-induced forces on a piping section as function of the velocity of sound

During the mechanical response analysis the following approach has been applied:

- In the first step it has been assumed that all the present supports (totally 450 supports) fix the piping in 3 translational directions by means of friction. The piping is assumed to be free for the rotating directions. It has also been assumed that the supporting steelwork is much stiffer than the piping. In case unacceptable vibrations or cyclic stress levels are calculated, additional supports will be recommended
- Besides the calculated vibration and cyclic stress levels the calculations of step 1 also result in the maximum reaction forces acting on the supports. In step two the calculated reaction forces have been compared with the available friction force in the supports. This available friction force is a result of the static analysis. In case the available friction force is not sufficient, spring hold-down supports will be recommended to increase the friction
- In the last step it will be checked if the supporting steelwork is stiff enough

4.2 Results of the mechanical response analysis

The mechanical response analysis has been carried out with the maximum forces calculated according to the 4th edition of the API 618 and with the forces according to the "Repsol" approach.

For the original support layout (Figure 10), designed by the engineering contractor, it appeared that for this system during step 1 all calculated vibration and cyclic stress levels were within the recommended level for the forces of both approaches. So no additional supports are required.

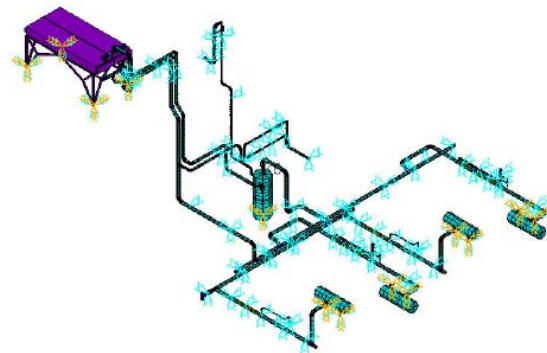


Figure 10: Plot of the mechanical model of the 1st interstage piping, with original supports

During step 2, the maximum calculated reaction forces of 260 supports have been compared with the available friction forces. This resulted in the count of required spring hold-down supports shown in Table 6.

Part of the system	According API 618 4 th edition	According the "Repsol" approach
Suction 1 st stage	5	8
First interstage	6	13
Second interstage	6	9
Discharge 3 rd stage	5	8

Table 6: Required number of spring hold-down support, for both approaches

So in case the allowable pulsation levels of the "Repsol" approach (comparable with the allowable level of the API 618 5th edition) will be applied, totally 38 supports have to be of the spring hold-down type instead of 22 supports according to the API 618 approach.

Normally, a spring hold-down support applies an increased friction force, due to the spring load. Due to the clearance around the bolts, thermal expansion is allowed in 1 direction. In case thermal expansion should be possible in 2 directions, a special construction can be applied, as illustrated in *Figure 11*.

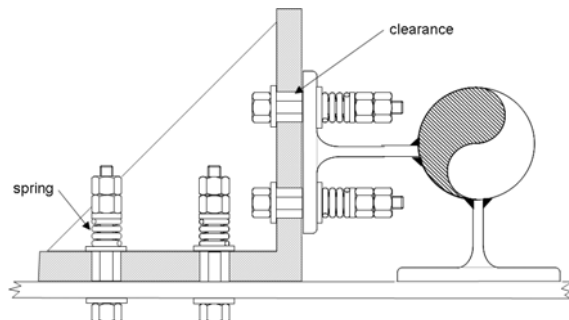


Figure 11: Example of a special spring hold-down support allowing thermal expansion in 2 directions

Based on the presented reaction forces, the engineering contractor stated that the supporting steelwork is stiff enough to withstand these forces. This statement has to be checked during start up of the system and in case of local exceeding of the allowable vibration level, the stiffness of the supporting steelwork has to be increased locally.

5 Comparison of costs for both approaches

For this system the dampers have been designed according to the allowable pulsation levels of the 4th edition of the API 618 Standard. Therefore the diameter of the dampers is about 25% larger than required according to the “Repsol” approach or according to the 5th edition. For this project the additional price was about 180k EUR, at the time of the order (2008) for a total of 2 compressors.

The additional price for the additional required spring hold-down supports is 30k EUR.

The reduction in power consumption of the “Repsol” approach results in a reduction in energy costs of 153k EUR per year¹.

So the simple pay-out period of the so-called REPSOL approach is 1.4 years².

¹ Based on electricity cost of 53 €/MW-h and 98% on-stream time per year.

² The payback period does not take into account the reduction in CO₂ emissions due to the reduced power consumption.

6 Conclusion

For hydrogen systems the allowable pulsation level in the piping according to the 5th edition is about 2 times higher than according to the 4th edition. So the pulsation-induced forces according to the 5th edition are approximately a factor 2 higher than according to the 4th edition. So normally for the design according to the 5th edition more supports are necessary than for the design according to the 4th edition.

By designing the pulsation dampers with the allowable levels according to the 4th edition of the API Standard 618 (which results in larger pulsation dampers) less pressure loss is required to achieve pulsation levels in the piping according to the 5th edition. Thus a ‘hybrid approach’ of a damper check with the 4th edition and the pulsation and mechanical response analysis according to the 5th edition leads to the most favourable economic and environmental system design.

In this system it appeared to be very cost effective to apply the larger pulsation dampers and modify a number of pipe supports and install less pressure loss. In about 1.4 years the break-even point of additional installation costs and energy costs have been reached. During the lifetime of the system of 30 years, more than 86 GWh will be saved.

Moreover a significant CO₂ reduction (the exact amount will depend on the energy supply used to drive the compressor) will be achieved during the lifetime of the plant.

Based on these results we expect it will probably very worthwhile to follow the same approach for medium to large hydrogen compressors.

References

- [1] API 4th edition, “Reciprocating Compressors for Petroleum, Chemical, and Gas Industry Services”, June 1995
- [2] API 618 5th edition, “Reciprocating Compressors for Petroleum, Chemical, and Gas Industry Services”, December 2007
- [3] André Eijk, Bert Egas en Jan Smeulers, “Cost-effective and detailed modelling of compressor manifold vibrations”, ASME Pressure vessels and piping conference, Montréal, Canada, 1996
- [4] Harry Korst and Leonard van Lier, “Mitigation of high-frequency pulsations using multi-bore restriction orifices”, 5th EFRC conference, Prague 2007



Experiences of a new generation of machinery monitoring for recipcs

by:

Smail Hadaddi
CERT-Technical Assistance
Division
TOTAL Raffinage Marketing
Harfleur
France
smail.haddadi@total.com

Markus Wenisch
Global Competence Centre
Mechatronics
HOERBIGER Ventilwerke GmbH
Vienna
Austria
markus.wenisch@hoerbiger.com

7th Conference of the EFRC
October 21th / 22th, 2010, Florence, Italy

Abstract

Machinery monitoring and protection systems are as important for reciprocating compressors as they are for rotating equipment. Because of the special requirements of reciprocating equipment, however, such systems are considerably harder to design. HOERBIGER (Vienna, Austria) as provider of “Reliable Performance of Compressor solutions” has found from the past experience of various end-users, that any such systems which are not specifically designed for reciprocating machinery perform unsatisfactorily. Accordingly, HOERBIGER as reciprocating compressor specialist has developed a monitoring and protection system which is specifically designed for reciprocating compressors. A unique vibration monitoring method has been implemented to detect failures at their earliest possible stage. The developers worked closely with customers to incorporate their needs, and took into account the wide range of applications and types of compressors in use. The resulting system is reliable, versatile and fast: it has proved its capability to safeguard reciprocating compressors, avoiding damage and the resultant loss of assets, or even injury and potential loss of life. In the TOTAL Raffinerie de Normandie (Gonfreville, France) the machinery monitoring and protection system reliably detected an arising problem and avoided extensive damages.

1 Introduction

Machinery monitoring and protection systems have been successfully used for many years to monitor and safeguard rotating equipment. Most of these systems were originally introduced decades ago and since then have constantly improved. The systems, as well as the knowledge of the users, have reached a point where protection for people, assets and the environment is provided in a very reliable and satisfactory fashion.

The machinery protection element detects hazardous conditions and automatically stops the unit in case of occurring damage. The condition monitoring element shows arising problems (defective or deteriorating components) at an early stage, where they can be corrected without any major damage to the unit itself, the associated plant, personal or the environment.

To incorporate maximum benefit and trust into such systems, reliability, meaningful information and user friendliness are very important. Unfortunately for reciprocating compressors in the past, this was not the case since no specifically designed embedded machinery monitoring and protection systems were available.

In the past, all available embedded systems were systems, or derivatives of systems, designed for rotating equipment, with the result that the specifics of a reciprocating compressor's working principle were not adequately considered. As a consequence, very often these systems, although installed, would not, in practice, be fully utilized, or even not used at all.

The new system, being specifically designed, from the outset, for the protection and monitoring of reciprocating compressors, features a unique method for monitoring vibrations in order to detect anomalies and problems at the earliest possible stage. This was proven successfully on a hydrogen make-up reciprocating compressor operated in the TOTAL refinery located in Gonfreville, France. Extensive damage to the crosshead and associated parts was successfully prevented.

2 Types of measurements

To reliably determine the condition of a reciprocating compressor and its components during operation, various types of measurements are needed. Those can be categorised into slow and dynamic types.

2.1 Level (slow) data

The slow types are typically called level or process data and are recorded without any reference to the crank angle. They can be considered to be virtually static, since they do not change within a revolution. These slow signals, usually processed as 4...20mA, are relatively simple to monitor, and this is usually done within Distributed Control Systems (DCS) or Programmable Logic Controllers (PLC). Typical examples are temperatures, levels, and stage pressures, but also included are pre-processed accelerometer/velocity measurements, i.e. RMS (root mean square) values.

These pre-processed measurements, where the transmitters have already translated the raw complex signal into representative values, must not be mixed up with dynamic measurement, that is to say, time-based vibration data, since valuable information (to diagnose the condition of a reciprocating compressors, see 3.2) is lost by this pre-processing.

2.2 Dynamic data ("phased")

The dynamic measurements vary within each revolution so these have to be measured with reference to the crank angle. They are time based with respect to the crank angle and are thus also often called "phased". This dynamic data contains the most valuable information (simplified "what happens when, and at what magnitude"), no averaging or pre-processing is applied to the raw signal – so no information is lost. For reciprocating compressors the three significant dynamic measurements are indicator pressure, rod motion and vibration.

3 Specific monitoring for recipcs

3.1 How to analyse dynamic data

The reason why specifically designed processing, analysis and diagnostics functions have to be implemented for reciprocating compressors is mainly because of the oscillating components (their motion with alternating accelerations, decelerations, and changes of direction) and all related events happening during a normal regular work cycle. These events cause impacts. Within each revolution, typical events causing impacts are valve openings and closings, crossheads moving from upper to lower slide and vice versa, etc..

Indicator pressure and rod motion analysis is exclusive to reciprocating compressors. Indicator pressure is used to monitor rod loads (maximum and reversal) as well as cylinder performance and efficiency. Rod motion is used to monitor not only rider ring wear, but also to keep a watchful eye on the oscillating motion – in other words, to determine if the mechanical integrity of the crossheads, rods and pistons is maintained.

Acceleration, that is to say vibration, is measured to determine the condition of rotating equipment as well. The knowledge of how to measure, process, analyse and interpret acceleration readings is widespread – but it is only widespread for rotating equipment. For oscillating equipment, such as our reciprocating compressors, a different approach in processing and analysing has to be done to gain satisfactory results. As mentioned previously vibration measurement can be taken, processed and analysed in several ways, but not all ways lead to success. The way to do this satisfactorily for rotating equipment is not suitable for reciprocating compressors, and vice versa – although the same principles were generally employed for both types in the past, and are even still often employed for both nowadays.

3.2 Phased acceleration monitoring

The accelerometers used to measure high-frequency vibrations are the same type (see Figure 1) for both reciprocating compressors and rotating equipment, but the processing of the raw signal afterwards should be different.



Figure 1: Accelerometer to measure high-frequency vibrations mounted on crosshead slide

Reciprocating machines are much harder to monitor because the signal changes significantly over the course of each revolution (see Figure 2).

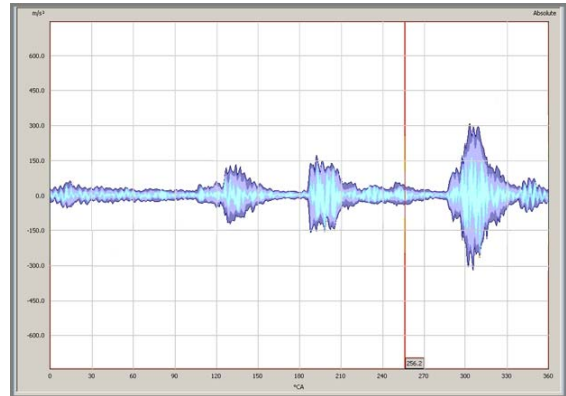


Figure 2: Time wave form of acceleration (NEW)

The mechanical impacts which occur regularly during each normal operating cycle of a reciprocating compressor produce a frequency spectrum containing many harmonics.

As a result, fault diagnosis in the frequency domain (usually by Fast Fourier Transformation, FFT) is almost impossible. Measuring the overall level, which is very common for rotating machines, is also not very suitable, because the high-frequency events (impacts) are “averaged” out. Even with significantly rising impact energies, the RMS value will not increase sufficiently to violate alarm limits. The high impacts, usually over relatively short durations (in relation to a full revolution) simply do not increase the RMS value enough.

An alternative would be simple peak-to-peak monitoring. This might be an improvement compared to RMS, but the single overall alarm level would then need to be set quite high, and as a result, changes in vibration amplitudes other than the highest regularly occurring one are unlikely to be discovered at an early stage.

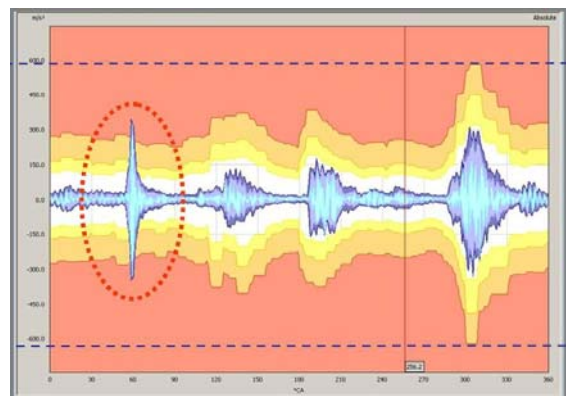


Figure 3: Conventional peak-to-peak monitoring is better than RMS monitoring, but leads to late failure detection too

Consequently it is preferable that the acceleration time-wave form itself is analysed. It is like a fingerprint of each compressor cylinder and its work cycle. The form represents all events, regular as well as abnormal ones, and has to be fully and automatically analysed in real-time to gain reliable and satisfactory results for machinery monitoring and protection.

Whenever an existing event increases, or even worse, a new event arises - this is the characteristic sign of a developing failure. Detection of this as early as possible will reduce or even completely prevent compressor damage.

3.3 Individual limits per degree crank angle

As shown previously, conventional vibration monitoring with methods traditionally employed for rotating equipment, that is to say, pre-processed vibration measurements, may not detect arising failures, or if so, at a rather late stage - the major damage may well have happened already.

Therefore a specifically designed machinery monitoring system for reciprocating compressors has to have a smart limit monitoring process for the acceleration time-wave form. Display and automatic alarming and therefore fulfilment of machinery protection function is achieved with individual limits (alarm bands, also called segments) with a resolution finer than 1 degree crank-angle ($^{\circ}\text{CA}$) over each and every revolution (see figure 4).

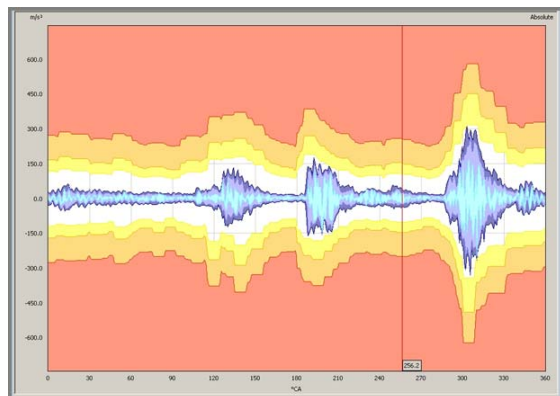


Figure 4: “Sensitive” acceleration limits with a resolution finer 1°CA for failure detection at earliest possible stage

To avoid false alarms resulting from normal changes in operating conditions, several such alarm envelopes with “sensitive” limits have to be implemented and activated, depending on the prevailing operating condition.

Thereby it is important to assign limit bands (segments) which are not too coarse. The worst examples would be one band extending over the complete revolution (which would be effectively the same as peak to peak) or a resolution greater 1°CA . Either would lead to false or seriously delayed alarming.¹

3.4 Rod motion is more than rod drop

Similar to acceleration measurements for reciprocating compressors, rod motion measurement has a long history. Already decades ago Rod Drop systems were introduced on reciprocating compressors. Their task was to determine the rider ring wear. Whether such systems work reliably or not depends to a large extent on the application and knowledge of involved technicians and users.

The heart of this measurement is the eddy current sensor (also called proximity probe), positioned below or above the piston rod and usually mounted on the main packing (see Figure 5).

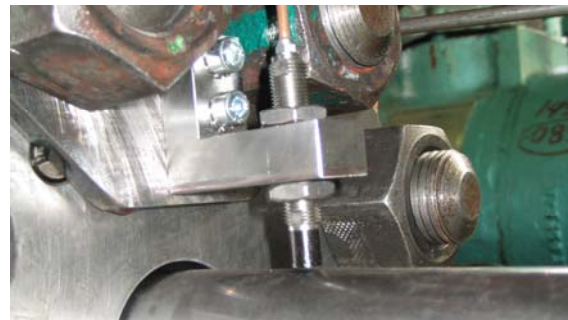


Figure 5: Eddy current sensor (proximity probe) to measure rod motion

From the sensed rod drop at this position, the drop of the piston itself, and therefore the rider ring wear, is calculated by triangulation.

The sensor itself can provide for much more if the output is processed in an advanced way – as well as now reliable rider ring wear monitoring, it can effectively serve as 24h/7 dial indicator, detecting not only mechanical characteristics of the oscillating components, e.g. crosshead shoe wear or loose connections, but also cylinder alignment problems or liner wear, in a similar way to a service technician, before starting up the compressor, mounts a dial indicator on the main packing and checks the vertical run-out of the rod over one cycle. By considering the measurement of the eddy current sensor as dynamic measurement, i.e. measurement of the signal over the complete revolution (see Figure 6), the complete motion of the rod in vertical direction can be monitored.

CONDITION MONITORING

Experiences of a new generation of machinery monitoring for recipcs, *Smail Haddadi, Markus Wenisch;*
HOERBIGER VENTILWERKE, TOTAL

The distance between sensor and rod is displayed and analysed over the complete revolution.

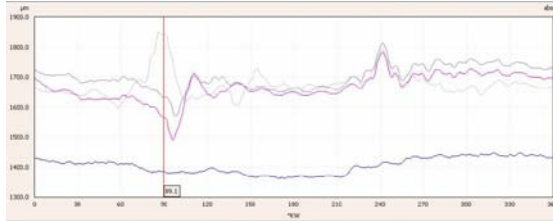


Figure 6: Rod motion and vertical run-out

Therefore the vertical run-out and all issues a dial indicator can check for only once before start-up, can be detected continuously during operation. Whenever the vertical oscillating motion gets excessive – in other words, if the mechanical integrity of crosshead, rod and piston is compromised - the compressor will be safely stopped. All these potentially hazardous failures can be detected using simple rod drop sensors, providing that the analysing technique of the sensor output is specifically designed for reciprocating compressors.

4 Prevention of major damage

At TOTAL Raffinerie de Normandie in Gonfreville/France, two Nuovo Pignone 4HF/2 reciprocating compressors are operated within a DHC plant. The compressors provide the entire hydrogen demand for the unit, and are therefore considered as very strategic plant equipment.

	1 st stage	2 nd stage
$p_{s=}$	30,0 bar(a)	72,0 bar(a)
$p_{d=}$	73,0 bar(a)	173,0 bar(a)
Capacity	2682,0 m3/h	1106,0 m3/h
Speed	370 min ⁻¹	
rated power	5850 kW	

Figure 7: Compressor Data

Both compressors were originally equipped with a condition monitoring system and were commissioned in 2006. The system comprised indicator pressure and rod position sensors, to monitor e.g.: valve efficiency, rod load, dynamic rod run-out and rider ring stand-out. Furthermore, suction valve cover temperatures, which are sensed within the actuators of the capacity control system, were integrated into the monitoring platform.



Figure 8: Compressor view K101A/B

The compressors are operated in parallel. The highest reliability of the equipment is consequently required, since a compressor failure would affect the whole DHC production. Because of this strategic importance, the existing monitoring platform was further upgraded to incorporate a protection system, which was implemented during a catalyst change in September/October 2009. The system enhancement involved the installation of acceleration transmitters on the crosshead guides and cylinder heads, and also velocity sensors on the compressor frame.

The interpretation and visualisation of the acceleration measurements is based on the phased vibration principle (see chapter 3.2), which means that the signal is processed and displayed in real time over the complete compression cycle. Furthermore, the vibration readings are triggered by, and referenced to, the rotation of the crankshaft. By monitoring the increase of existing, or the emergence of new, vibration peaks, damage to component parts can be detected at a very early stage. The following case study shows how major machinery damage was prevented by the monitoring of phased vibration and dynamic run-out data:

6th of November, 2009 / first failure indication:

The monitoring system detected an abnormal noise in compressor K101-A / cylinder 3. The corresponding vibration trend showed an initial increase (figure 9, 1) of the peak to peak signal to 170m/s^2 , starting from approx. 9 o'clock.

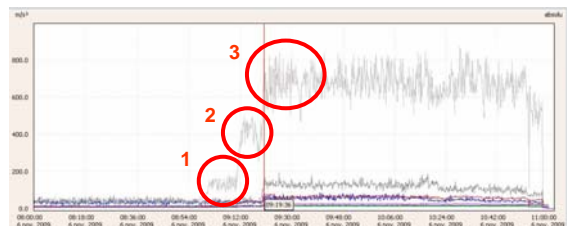


Figure 9: 3 hours vibration trend; peak to peak increase cylinder 3

CONDITION MONITORING

Experiences of a new generation of machinery monitoring for recipcs, *Smail Haddadi, Markus Wenisch;*
HOERBIGER VENTILWERKE, TOTAL

Simultaneously, the rod run-out trend increased from 100µm to 130µm-150µm (figure 10, A+B).



Figure 10: Increase of dynamic run-out cylinder 3

A more precise investigation of the historic run-out profiles showed a strong deviation of the piston rod movement. By using eddy current sensors for run-out measurement, the air gap between piston rod and sensor cap can be measured and then displayed as a function of crank angle. In most cases a change in the run-out behaviour indicates a loose connection within the piston – piston rod – crosshead assembly.

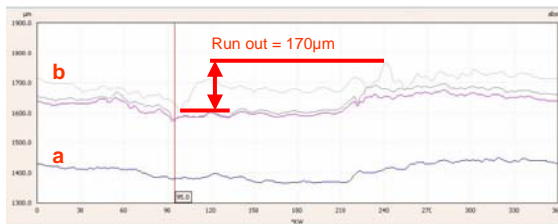


Figure 11: Run-out as function of crank-angle; 12 minutes after first failure indication

Figure 11 (a) shows the normal run-out characteristic for the compressor in good mechanical condition, while the run-out profile (b) indicates an arising problem with the mechanical integrity of the oscillating parts.

Thirty minutes after the first vibration increase (Figure 9, 3) the run-out further increased to 300µm, as shown in figure 12.



Figure 12: Run-out as function of crank-angle; 30 minutes after first failure indication

The strong vertical movement of the piston rod between 90° – 120° crank angle is the result of the rod load reversal, which caused heavy “knocking”

of the loose parts. This is also reflected in the increase of the peak to peak crosshead vibration signal to 800 m/s² (Figure 9, 3).

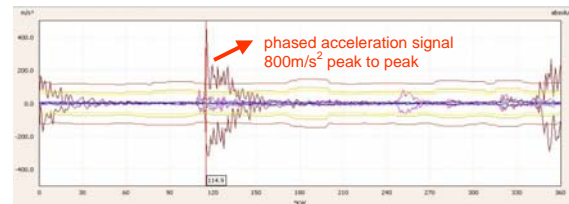


Figure 13: Phased acceleration profile over 360° crank angle

Operators were informed, and at approximately 11 o'clock the compressor was safely stopped for inspection without undue disruption to the process. Using the explicit monitoring data, maintenance activities could be prepared and focused on the oscillating parts of cylinder 3. This saved a lot of down-time compared to an unforeseen shutdown with unknown cause.

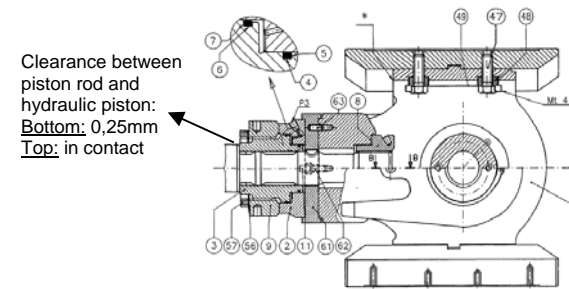


Figure 14: Drawing of crosshead – piston rod assembly

Measurements showed a misalignment between piston rod and crosshead due to the looseness of the hydraulic locking device. Parts from the hydraulic locking device had already started to break up. Also the washer (Figure 14, item nr 56) was found broken and lying in the crosshead guide of the compressor.

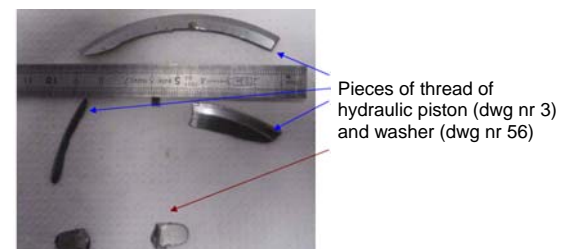
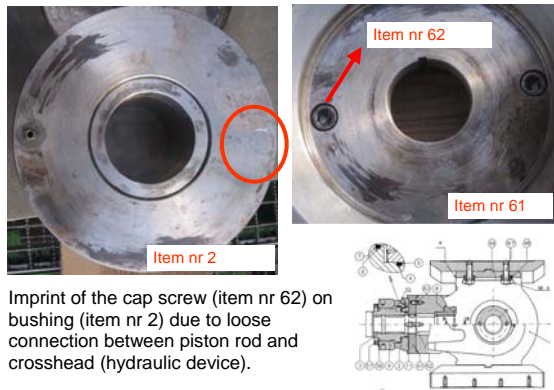


Figure 15: Debris of hydraulic tightening device

The crosshead disassembly showed imprints of the cap screws (Figure 16, item nr 2+62) used for the crosshead assembly.



Imprint of the cap screw (item nr 62) on bushing (item nr 2) due to loose connection between piston rod and crosshead (hydraulic device).

Figure 16: Wear marks on hydraulic cylinder due to loosening of tightening device

5 Conclusion

In the course of the corrective maintenance, a new piston rod and hydraulic locking device were installed. Visual inspection verified no further damages on crosshead and connecting rod. The repair could be completed within 3 days in 2 shift operation. Compared to the probable extensive mechanical breakdown of the compressor, which would have resulted from continued running, this is a comparatively short downtime and therefore the economical impact was manageable.

References

- ¹ R. Schuhmann, Ch. Prinz: Machinery protection for reciprocating compressors: experience and outlook, 6th EFRC conference, Düsseldorf, 2008



Integration of an Advanced Diagnostic Tool in an Optimization Platform

by:

Riccardo Fani
RECO Service Product Leader
GE Oil & Gas
Italy
riccardo.fani@ge.com

Gaia Rossi
Field Application Engineer
GE Energy Optimization & Control

7th Conference of the EFRC
October 21th / 22th, 2010, Florence

Abstract

The intent of this paper is to show practical examples of the achievable benefits of a model-based, real time diagnostic software designed for critical process reciprocating compressors, as part of a machinery management platform for process and equipment optimization integrated in a plant network. It provides examples of the main features of an effective on-line compressor diagnostic system that allows identification of anomalies, while the optimization tools flexibility allows leveraging stored and online data to deliver useful information for operation and maintenance needs. Such tools contribute not only to improve the reliability of reciprocating compressors in petrochemical and refining plants, but also the ability to quantify the impact of operational decisions in increasing productivity and reducing operating costs within a revised maintenance strategy that make best use the available information to make proactive business decisions.

1 Introduction

Reciprocating compressors are fundamental assets for oil and gas processes and their flexibility allows them to work in different operating conditions with high efficiency in respect with other turbomachinery. However, the related maintenance cost may be very high if they are not utilized, controlled and maintained properly. Compressor systems feeding critical refining and petrochemical processes, whose objectives are high reliability and performance, as well as short downtime, are subject to failures affecting availability and increasing maintenance costs and related downtime.

Reciprocating compressors impact significantly more on maintenance cost than centrifugal machines and in many cases the root cause of failures are not easily identified¹ (Figure 1).

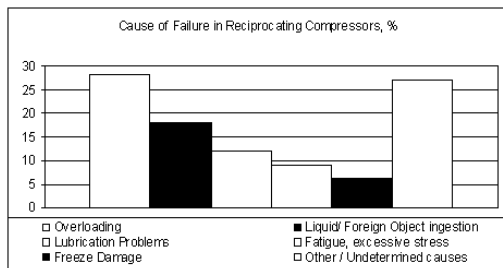


Figure 1: Cause of failure in reciprocating compressors

For instance, process gas upsets, problems with unloaders, lubrication systems, piping, or cylinder cooling systems can all have detrimental effects on the components.

While the main contributors of total maintenance cost are identified in valves, packing and rings, those are not the primary reason of other critical failures. It also appears that the root cause for a reciprocating compressors failure is often an unanswered question, bringing as consequences recurrent repeated failures with no remedy to root cause, no lessons learned, and cost for unscheduled maintenance not reduced even if it could be achievable; this is where an advanced online monitoring system can help.

Automatic online compressor diagnostic allows prediction of incipient failures that impact on performance and capacity and put at risk safety, causing extended downtime due to unscheduled shutdowns: preventive maintenance cost can be

significantly reduced, moving to Condition Based (Predictive) methodologies.

Further, the data available in an optimization tool can also be used in support of a more advanced proactive asset management methodology.

This paper describes how an advanced condition monitoring and diagnostic system combined with the information and tools available in an optimization platform can contribute to reciprocating compressor unit optimization, root cause analysis, improved failures prediction and overall operation costs.

2 Condition Based Maintenance and Plant Asset Optimization

In today's economic environment, managing costs and margins for refining and petrochemical plants has become increasingly crucial. With industry drivers being: reduction and prediction of asset life cycle cost, production planning optimization, reliability and availability improvement, these targets can only be achieved by implementing a continuous improvement process that involves all aspects of plant, with a strategic integration of technology, maintenance best practices, processes and methodologies in a coordinated, sustainable program and change in culture (Figure 2).

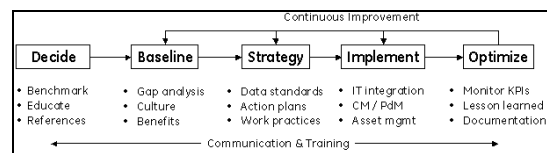


Figure 2: Example of Continuous Improvement Process Value Chain

Condition Based Maintenance (CBM) techniques impact on asset lifetime cost management by reducing maintenance costs, risks of unscheduled outages, catastrophic failures and relates costs, however may be not sufficient to optimize operation procedures and improve reliability to required levels. On the other hand, Proactive Centered Maintenance (PCM) goal is not only identifying the most appropriate maintenance methodology for each asset, but also relating to procedures, operating parameters, processes, and designs in order to limit or prevent recurring failures, and extending the mean time between asset failures. A PCM program is continually

CONDITION MONITORING

Integration of an Advanced Diagnostic Tool in an Optimization Platform, *Riccardo Fani, Gaia Rossi, GE OIL AND GAS, GE ENERGY*

being optimized with feedback from Root Cause Analysis, Preventive and Predictive Maintenance practices, aiming to proactively to keep assets in their optimal operating condition.

Relating information concerning machine condition to operation procedures, work practices, documentable information, systematically embedding lessons learned, implies a change in overall methodology, moving to a Reliability based, Proactive Maintenance strategy. This change that can cost less and still give effectiveness (availability) gains (Figure 3)

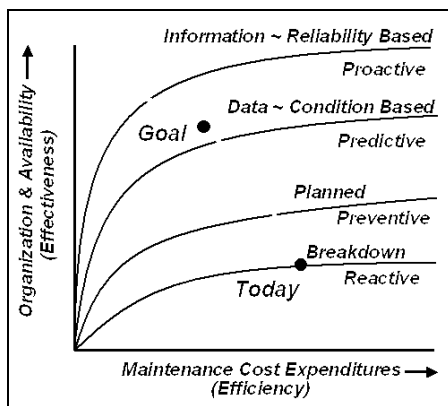


Figure 3: A revised maintenance practice

3 Proactive maintenance tools for reciprocating compressors

An effective online condition monitoring system for reciprocating compressors is based on the collection of measurements from the field: both dynamic data (e.g. rod drop, rod run-out, crosshead and cylinder vibration, cylinder pressure) and static data (e.g. process temperatures and pressures). In addition, the software provides calculated performance parameters. Therefore, a huge amount of data is available to the user, due to the quantity and type of measurements applied and the capacity of nowadays data acquisition and storage devices. However, all the stored data are often only partially utilized: the diagnostic system is used as an exception-based tool, providing notification on incipient anomalies and their severity to allow operator to plan actions and maintenance accordingly; the data stored during machine operation are rarely used unless a problem arises. Data can be leveraged by today's high capacity information management software

tools; if they are flexible enough to easily perform data manipulation and management, on-line and stored information can be used not only to help assessment of compressor condition and diagnose anomalies, but also to evaluate and improve operation over time, as will be shown in one the next examples.

3.1 Model-based diagnostic tool for reciprocating compressors

All the following examples refer to a diagnostic system installed on an API-618 single stage horizontal two- throws compressor (2HE/1) with double acting cylinders running at 470 rpm. Service gas is a hydrocarbon mixture for rubber synthesis; According to the final product request (nine different possible campaigns in order to produce different rubber grades) the gas composition changes as well as pressures and temperatures.

Operating conditions ranges are the following:

Suction pressure 8-14 bar a

Discharge pressure 19-36 bar a

Suction temperature 0-40°C

Discharge temperature 60-95 °C

Molar Weight 38-

The compressor is provided of 'stepless' valve unloaders, allowing in theory a continuo's variation of the capacity and pressure.

The compressor is provided with the field instrumentation providing the measurements for the diagnostic system based on a mathematical model of the compressor. This model-based calculation engine is embedded in a machinery management platform for process and equipment optimization, that stores, views and manages the calculated data.

The tool detects an anomaly by comparing the values measured from field with expected ones calculated by the model using the on-line measurements from the field as input data (Figure 4). The values used in the calculation are both static and dynamic data.

Several thousands associations between causes (values deviating from expected) and effects (compressor anomalies) through a failures matrix provide the diagnostic results. The matrix is dynamically implemented: a variation of number and type of online measurements deviating from the expected values produces a different calculated anomaly probability and severity.

CONDITION MONITORING

Integration of an Advanced Diagnostic Tool in an Optimization Platform, *Riccardo Fani, Gaia Rossi, GE OIL AND GAS, GE ENERGY*

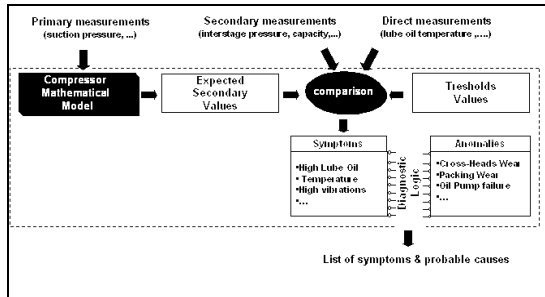


Figure 4: How the diagnostic system works

3.1.1 Example of anomaly identification by the diagnostic system

Excessive wear of the piston rider band is usually identified by rod drop measurement and is typically caused by gas contamination, failure of the cylinder lubrication system or abnormal liner roughness.

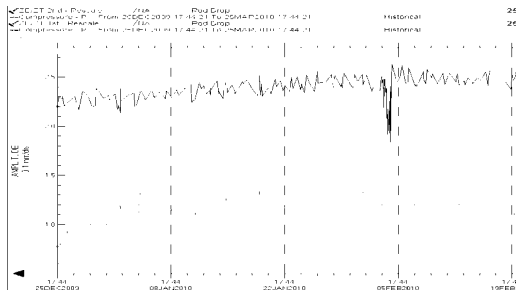


Figure 5: Rod drop 3 months trends, Cylinder 1 and 2

Rod drop trends indicate faster rider band wear in Cylinder n.2 compared to n.1 (Figure 5). After a compressor check, insufficient lubrication caused by improper behavior of lubrication system was discovered. Figure 6 shows the related system alarms: the most probable anomalies are identified and highlighted.

At the same time, the diagnostic software warned also about a piston rings issue; this was confirmed by the PV diagrams analysis (Figure 7) showing an incipient piston ring leakage (crossover of measured and theoretical pressure) in Cylinder 2. A slight increase of discharge temperature is the additional evidence of the incipient anomaly.

- Connecting Rod big End Bearings
- Main Bearings
- Cylinder N°. of Stage N°. Misalignment
- Valve Unloaders in Cylinder N°. of Stage N°.
- Loss of Efficiency in Pulsation Dampers or Orifices
- Piston Rings in Cylinder N°. of Stage N°.
- Crank Mechanism Lube Oil Filter
- Damage in the Compressor Foundations
- Gas Leakage in Cooling System
- Contamination in the Process Gas
- Main Coupling
- Improper Lubrication in Driving System Components
- Lack of Load Reversal on Crosshead Pin
- Contamination in Crank Mechanism Oil
- Piston Rider Bands in Cylinder N°. of Stage N°.
- Crosshead Shoes
- Compressor Capacity Out of Range
- Gas Flow Rate in Stage N°. Out of Range
- Cylinder N°. of Stage N°. Packing
- Measured Suction Pressure of Stage N°. Out of Range
- Measured Discharge Pressure Out of Range
- Excessive Running of Cylinder N°. of Stage N°. in Unloaded Condition
- Oil Scraper
- Gas Coolant ahead of Cylinder N°.
- Oil Cooler
- Separators or Suction Filters
- Improper Tightening of Plant Equipment
- Improper Tightening of Cylinder N°. of Stage N°.
- Improper Tightening of Driving System Components
- Improper Tightening of Frame Component
- Cylinders Lubrication System
- Packing Lubrication System
- Compressor Capacity Control System
- Carry-over of Strange Particles in Cylinder N°. of Stage N°.
- Misplacement of the Electric Motor Magnetic Center
- Measured Discharge Temperature in Cylinder N°. of Stage N°.
- Crank End Suction Valves in Cylinder N°. of Stage N°.

Figure 6: Anomalies list – color-coded alarms

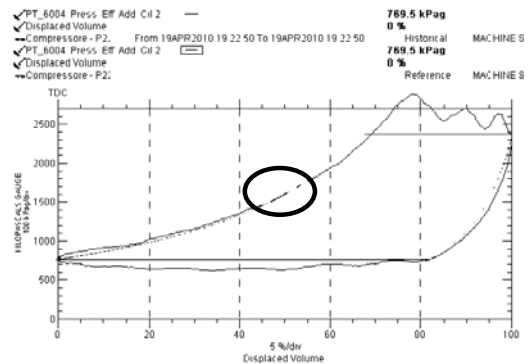


Figure 7: PV diagram showing incipient piston ring leakage (compression curve crossover)

CONDITION MONITORING

Integration of an Advanced Diagnostic Tool in an Optimization Platform, *Riccardo Fani, Gaia Rossi, GE OIL AND GAS, GE ENERGY*

While compressor vibration analysis helps in identification of anomalies as inadequate cylinder tightening, crosshead or piston assembly looseness, debris ingestion, problems at pulsation bottles or orifices, loose foundations, etc, cylinder pressure in PV diagrams describes the thermodynamic behavior of the compressor: the online model compares continuously the measured chamber pressure with the calculated theoretical cycle. Deviations indicate piston rings, valve, or pressure packing anomalies. In case of stepless unloader operation, a specific patented algorithm is able to compute the theoretical plot curve from pressure curve pattern alone, without need of input from the unloader system triggers. (Figure 8).

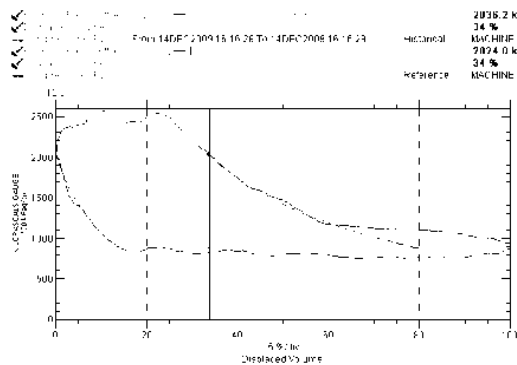


Figure 8: PV plot with overlaid measured and calculated pressure, valve stepless unloader on

4 Optimization tools - State based analysis

Reliability reports based on Mean Time Between Failure (MTBF) data may not give accurate enough interpretations if do not take into account individual machine performance.

MTBF indicates the ability of an asset not to fail under specific operating conditions. MTBF obtained from reliability calculations on operation data for groups of machines may not be helpful to assess the impact of machine operation to overall costs.

Tools as state-based analysis allow tracking the compressor operating conditions and relating them to the wear or failures that the compressor experiences. Being specific to each individual compressor, allows bad actors and their root causes of failure (as well as reliability improvements) to become more evident.

The ability to define and store data labeled with different compressor 'states' and computing the 'running hours' associated to that state allows correlation of how operating conditions are impacting on compressor health and linked to specific failures as identified by the diagnostic data. Any input parameter in the software can be used to define a compressor 'state', as for example different discharge pressures, or calculated values as capacity, or piston rod load. View of process events together with the stored data is also possible, for example Figure 9 shows how a gas composition change (imported from other online systems or manually entered) is stored and shows up in system event and alarm list and is flagged in plots.

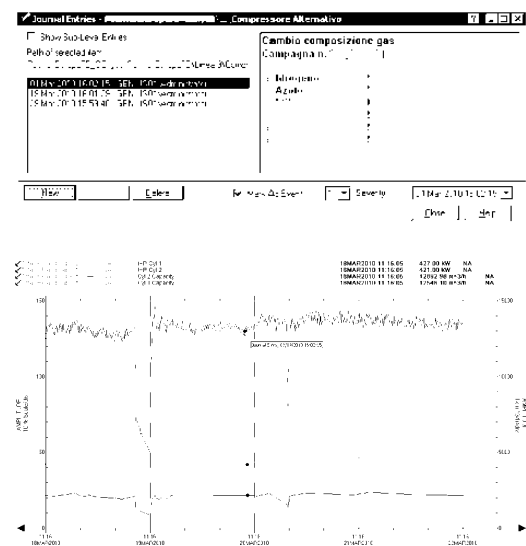


Figure 9: Gas composition changes manually entered as system event and flagged in Capacity and Indicated Power trends

The next paragraph shows an example of state based analysis applied to excess rod load events.

4.1 Example - analysis of process conditions impacting on rod load

Reliability and service life of reciprocating machines depend to a large extent on the operating of the piston rod mechanism; therefore knowing and monitoring the forces acting at the rod is essential to avoid excessive stress on machine due to anomalies or improper operation.

CONDITION MONITORING

Integration of an Advanced Diagnostic Tool in an Optimization Platform, *Riccardo Fani, Gaia Rossi, GE OIL AND GAS, GE ENERGY*

One critical failure for a reciprocating compressor is the overload, and piston rod problems are possible causes for long and unexpected shutdown. Overload conditions can be also reached due to compressor operation, usage of capacity control devices, procedures of change or adjustments in operating pressures and capacity.

While the online diagnostic system is using dynamic cylinder pressure for performance data calculation (capacity, indicated horse power, valve loss, flow balance, adiabatic discharge temperature, etc.), the protection system monitors the values of rod load and rod load reversal.

A robust and reliable compressor monitoring system must be capable of continuous rod load calculation from cylinder pressures and compressor design data, monitoring the peak rod forces (compression and tension) for each cycle. Due to the potentially immediate and extensive damage to crosshead pin and small end bearing, when rod load reversal is missing or reduced, rod load reversal must also be calculated and monitored directly by the protection system to allow reliable monitoring and alarming.

In this example, state-based analysis and hours - run statistics were used to identify and quantify overload conditions and operational problems.

The data collected from the compressor showed how variations of delivery pressure have been impacting on rod loads. As production needs require discharge pressure changes, exceeding rod load forces were occurring.

Discharge pressure peaked above protection alert set point, with rod load exceeding project values recurrently. After data evaluation, it was found that these events were linked to the manual adjustment downstream control valve to follow process requirements. When back pressure is manually controlled, faults or human errors cause the system to rely just on discharge pressure relief valve opening on time and correctly, this being a concrete risk for compressor safety.

Figure 10 shows one the recurrent events of excess pressure monitored, and counter of total running hours in rod overload condition.

Figure 11 show the related discharge temperature during the events approaching alert set point of 110 deg C (design temperature being 72 deg C).

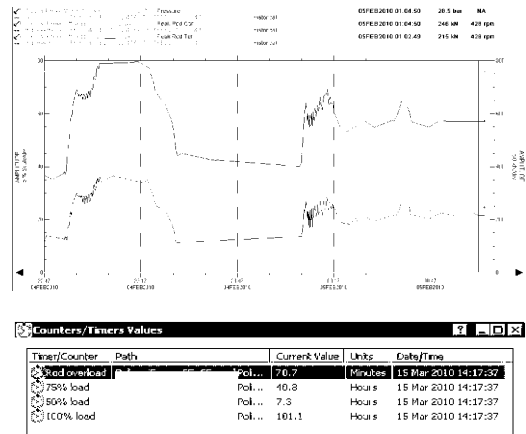


Figure 10: Discharge pressure and related peak Rod Tension and Compression exceeding alert set point for approx 30 minutes - Rod overload time counter, two months period

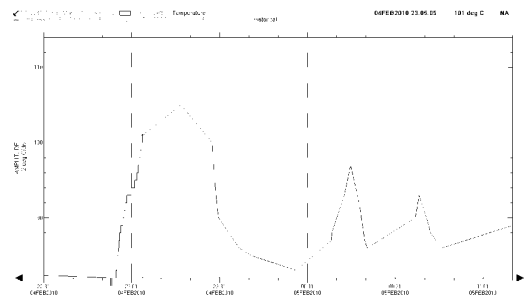


Figure 11: Discharge Temperature increase during the same event as Figure 10

Running hours of overload conditions, as well as the consecutive hours of overload can then be associated to frequency of malfunctions as predicted by the embedded diagnostic tool.

This capability is particularly beneficial for reciprocating compressors optimization, when operation changes that can impact on machine condition and failure modes need to be known and comply with Manufacturer recommendations.

CONDITION MONITORING

Integration of an Advanced Diagnostic Tool in an Optimization Platform, *Riccardo Fani, Gaia Rossi, GE OIL AND GAS, GE ENERGY*

Configuration of such calculations ('rules') can give as an output a machine status or event, or further calculated results; data can be manipulated in unlimited ways, historical data can be used to validate the rules before they are applied to online data, as well as to analyze past machinery behavior when the need is raised.

Obviously, data preprocessing techniques shall ensure that only accurate data are used for the calculations, taking into account condition variation, data input errors, etc with different methods⁶.

4.2 Example - Selection of capacity control system

Reciprocating compressor control philosophies have the target to optimize consumption; that can be calculated online by the diagnostic system. Reciprocating compressors are not always operated at optimal point from both mechanical and economical standpoint.

Performance optimization and redesign activity consist also in adapting the design to new plant operating conditions reducing unnecessary costs.

The software optimization tool allows combining compressor performance data to relevant economic data and storing calculations in the same platform, associating operating data to cost or profit. In this example, online calculated performance data are used to quantify compressor monthly energy consumption and the usage of the unloader system. The compressor has several off-peak periods during the year due to its specific type of operation and capacity reduction can be 15% and more.

Based on compressor operation, choosing either a recycle valve, clearance volume pockets or a stepless unloaders may lead to different results in terms of cost of energy and asset life costs.

For a compressor operating at variable capacity requirements, it is possible to calculate the actual power consumption and relevant costs of operating the bypass or the unloader and estimate the return on investment or the potential benefits of installing and unloader system based on capacity requirements during the year. The monetary values manually entered from the user interface.

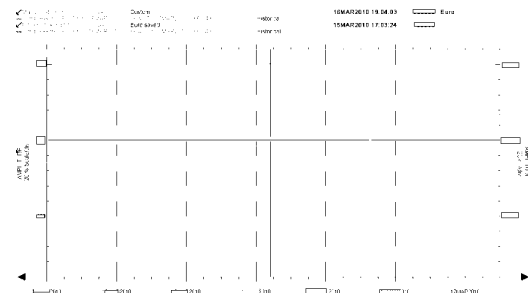


Figure 12 - Online calculation of energy expense (Euro/MWh) showing the point in the year where the cost of unloader system equals the energy savings.

Statistic information of compressor usage may be also used to evaluate compressor design, see Figure 13.

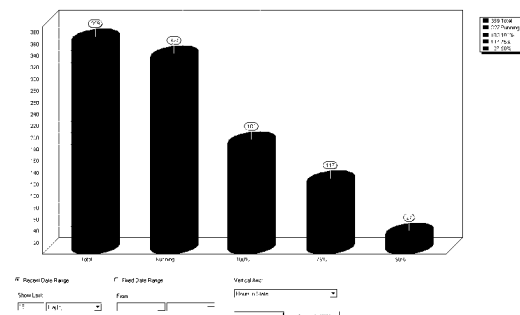


Figure 13: Compressor with step unloading, 50, 75 and 100% loads operation statistics

The compressor under study changed operation over the years: the current required capacity is only slightly reduced respect to the original design requirements and it's quite stable along the entire period examined. This could have been suggested that a de-rate would be more beneficial respect to the use of other capacity control systems allowing a load reduction as well as lower vibrations and avoiding the risk of critical failures.

5 Optimization platform profiling

An efficient diagnostic and optimization platform is characterized by a distributed client/server architecture and multiple users access at different level of the organization.

CONDITION MONITORING

Integration of an Advanced Diagnostic Tool in an Optimization Platform, *Riccardo Fani, Gaia Rossi, GE OIL AND GAS, GE ENERGY*

The definition of ‘User profiles’ is needed to selectively deliver the appropriate information to users: customized display views, different levels of data visualization and access, different rights at application usage level ensure the best usability and practicability and prevent the extensive range of capabilities and nature of information available to result in a confusing and cumbersome user interface.

User	Assigned Profile
reliability	MDS
Automation	Instrumentation
BUILTIN\Administrators	None
System1AdminGp	None

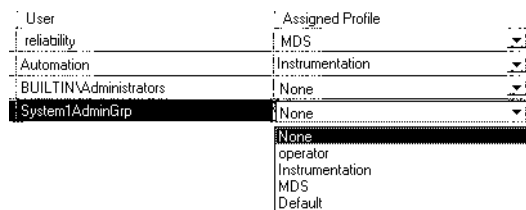


Figure 14: Profiling examples: Automation, Machinery Diagnostic, Reliability Engineers

Users can access only to the needed data for their work and avoid dealing with large amount of unneeded information: while operators receive alerts when immediate corrective actions must be taken, or for example, action is directly integrated to the Computerized Maintenance Management Systems as work order request, other information goes to different levels of the organization with different purposes.

Conclusion

Improved safety and reliability for reciprocating compressors are supported by advanced condition monitoring and optimization solutions to improve engineering and maintenance methodologies. If these technologies are properly utilized, they can also support proactive action to optimize operation by means of advanced management of the large amount of available data. The examples illustrate the benefits of getting comprehensive information from the diagnostic system as well as relating compressor performance data to operating statistics and costs. Result is that knowledge and lessons learned can be embedded in operating practices to allow optimal operation, while making it cost effective and repeatable.

References

1. Griffith, W. and Flanagan, E., “Online continuous monitoring of mechanical condition and performance for critical reciprocating compressors” Proceedings of 30th Turbomachinery Symposium.
2. Covino, L., Hanifan M., “Asset Management 101 – Part 1: Maintenance Strategy overview” – Orbit Magazine Vol.29 No.1 2009
3. Giacomelli et al. “Sistema avanzato di monitoraggio e diagnostica dedicata ai compressori alternativi”, Manutenzione T&M, Nov 2006
4. Howard, B. and Kocur, J., “Knowledge based tool development and design for reciprocating compressors”, Turbomachinery Symposium 2010
5. Schulteis, S. et al., “Reciprocating compressors condition monitoring”, Turbomachinery Symposium 2007



New crosshead lubrication design to uprate the power density of LDPE Reciprocating Compressors

Carmelo Maggi
Reciprocating Compressor
Engineering
GE Oil & Gas
Florence
Italy
carmelo.maggi@ge.com

Nicola Campo
Quality
Engineering
GE Oil & Gas
Florence
Italy
nicola.campo@ge.com

Filippo Gerbi
Technology Laboratory
Engineering
GE Oil & Gas
Florence
Italy
filippo.gerbi@ge.com

7th Conference of the EFRC
October 21th / 22th, 2010, Florence, Italy

Abstract

In recent years LDPE production plants have continuously increased in size. To satisfy this increased production demand while maintaining the overall compressor size, it was necessary to improve the power density of existing machinery. To achieve this goal, a patented design for the lubrication of LDPE compressor crossheads was optimized and validated with a scaled test rig. In addition, the precision and accuracy of the dedicated CFD design software were assessed.

1 Introduction

Hypercompressors¹ are reciprocating compressors developed to compress gas up to 3500 bar. In *Figure 1* a cross section of a GE Oil & Gas Hypercompressor is shown, indicating its main components. These compressors are used primarily for the production of LDPE (low density polyethylene), through two stages of compression obtained with a number of well referenced and proven cylinder bore diameters specified to match the capacity required by the plant.

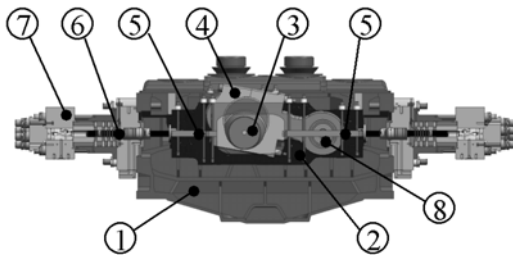


Figure 1: PK Hyper-compressor arrangement:

- 1-frame
- 2-crosshead
- 3-crankshaft
- 4-connecting rod
- 5-crosshead shoes
- 6-plunger
- 7-cylinder head
- 8-wrist pin

Figure 2 shows, the typical relationship between the number of cylinders and the maximum required plant capacity for GE Oil & Gas hypercompressors (PK Hypercompressors). The capacity currently referenced by PK Hypercompressors is 400ktpy (kilo tons per year) of polyethylene produced with an electric motor-driven twin frame with 10 cylinders in the first stage and 10 cylinders in the second stage. The proven capability of GE Oil & Gas hypercompressors can however reach 500 ktpy with a 12+12 cylinder arrangement.

Yearly plant capacity	300 ktpy	350 ktpy	400 ktpy	500 ktpy
GE O&G current (# cylinders)	14PK	18PK	20PK	
GE O&G Upgraded (# cylinders)	12PK	16PK	18PK	24PK (12+12)

Figure 2: Number of PK hypercompressor cylinders vs. plant capacity

The PK-Uprate design was launched to further increase the maximum frame load capability (Power Density concept) without compromising the GE Oil & Gas cylinder bore design philosophy² that limits the diameter to avoid compromising the compressor reliability. Moreover, the new uprate can be easily installed in units already operating in the field.

Maintaining this philosophy, the program target was set at a 20% power density increase (see *Figure 2*). This means that if the plant capacity remains the same, the new design allows the elimination of at least a couple of cylinders vs. the original design, which yields advantages in terms of cost and footprint; alternatively, an existing unit can provide an increase of 20% in plant capacity with a short return on investment.

The 20% increase in power density increases the stresses by approximately the same value. Therefore, at the structural level, each component (i.e., frame, crankshaft, connecting rod, crosshead, crosshead shoes, etc.) has been redesigned to meet the safety factor requirements³ and to contain the increase of deformation (due to increased stresses) within the required limits.

The main resources of the program, however, were focused on the development of a new lubrication concept (patented) for the lift of the crosshead shoes. To support this effort, a proprietary software tool called HyCSS (Hyper-Compressor Crosshead Shoe Simulation), was developed to optimize the geometry of the grooves of the shoes. A 1:5 scaled test rig was also developed to validate both the concept and the software.

2 Design

2.1 Description

In the PK compressor, the crosshead moves a pair of opposed plungers. The crankshaft passes through the crosshead and is connected to a connecting rod which is located inside the crosshead. The connecting rod and the crosshead are connected by the wrist pin.

The rationale of this design is to have the axes of the crankshaft, wrist pin and plungers at the same height and aligned with the sliding plane of the crosshead. This challenging alignment is one of the most competitive advantages of our design because it allows us to accommodate the effects due to thermal expansion without the need for additional components and to thereby reduce the overall dimensions. The horizontal guide system of the crosshead consists of two symmetrical lateral wings (shoes) that cover the entire crosshead length except the central section crossed by the crankshaft (see *Figure 3*).

The shoes move along the bottom and top of counter-shoes mounted in the PK frame and the crosshead sliding planes coincide with the plunger axis.

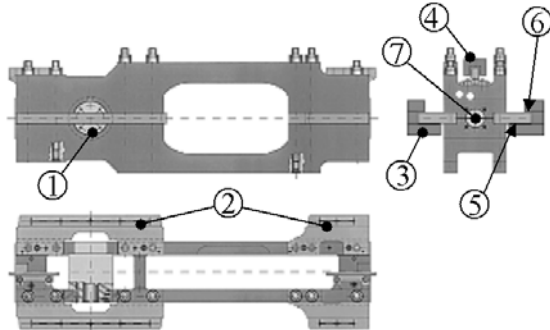


Figure 3: Crosshead arrangement:
 1 – wrist pin
 2 – lateral wings (sliding shoes or crosshead shoes)
 3 – horizontal guides (counter-shoes)
 4 – vertical guide
 5 – top shoe
 6 – bottom shoe
 7 – plunger seat

The proprietary CFD software is specialized for the analysis of the design of PK Hyper-compressor crosshead (sliding) shoes based on numerical simulation of the dynamic behaviour of the shoe. The four sliding shoes (the small-end side and the big-end side bottom and top shoes) are considered as lubricated bearings and are simulated together, taking into account their actual geometry and operating conditions.

2.2 CFD boundary conditions

The bearing analysis is based on hydrodynamic lubrication theory where the unsteady Reynolds equation for instantaneous pressure distribution in the oil film within the bearing clearance is solved numerically using an automatically generated non-uniform grid, see Figure 4.

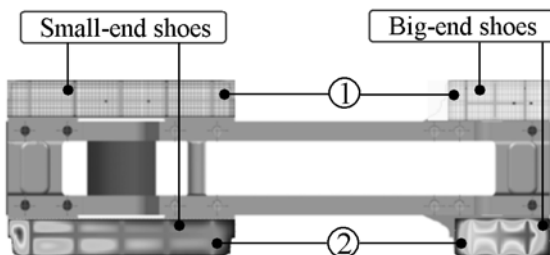


Figure 4: Crosshead arrangement:
 1 – non-uniform grids of shoes
 2 – pressure maps of shoes

In the software, the shoes are loaded by the vertical component (F_v) of the pin load acting on the connecting rod, the weight of the reciprocating masses (W) and the lift of the shoes resulting from oil films (F_1, F_2, F_3, F_4), see Figure 5.

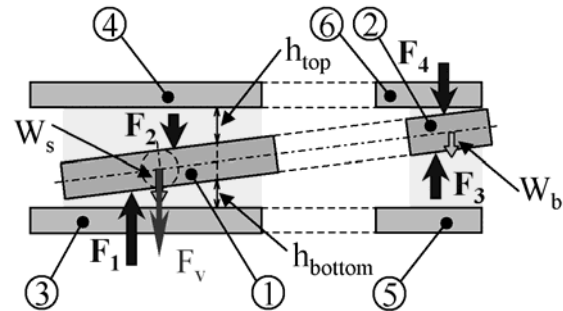


Figure 5: Loads acting on the PK crosshead shoes:
 1 – small-end sliding shoe
 2 – big-end sliding shoe
 3 – small-end bottom fixed counter- shoe
 4 – small-end top fixed counter- shoe
 5 – big-end bottom fixed counter- shoe
 6 – big-end top fixed counter- shoe

The load profile (vs. crank angle) of the axial force (F_a) is the sum of the gas forces acting on the two opposite plungers and the inertial force induced by the reciprocating movement of the crosshead assembly (with plungers). The crosshead vertical position is calculated to balance the shoes' lift and the instantaneous load imposed.

The planar bearings (or shoes) are supplied with oil through a system of holes and grooves. Oil from the header is delivered to the counter-shoes through tubes; each tube is connected to a separate hole in the counter-shoe. Special grooves on the wing surface provide oil distribution throughout the bearing.

The properties of the oil are taken into account by defining, as input data, the curve of viscosity (vs. oil temperature).

Starting from the current shoe design, the shoes' boundary conditions (oil supply pressure, arrangement of oil holes and grooves, configuration of the white metal area, etc.) were optimized, which allows a positive oil film thickness to be maintained during operation with the 20% increase in gas loads.

The difference between the original geometry and the optimized geometry of the crosshead shoes depends on the size and distribution of the grooves and on the lift surface areas.

2.3 Analytical Design of Experiment (DoE)

In order to assure a robust design after defining the uprated geometry for a specific operating condition (design point), a sensitivity analysis was performed to identify the main parameters (Vital Xs) that influence the oil film thickness and the ranges where positive oil film thicknesses can always be guaranteed to avoid any contact between the crosshead shoes and counter-shoes. The Vital Xs are:

- External wrist pin loads (gas + inertial loads)
- Total oil film clearance ($h_{bottom} + h_{top}$ of figure 5) between crosshead shoes and counter-shoes
- Oil inlet pressure
- Oil inlet temperature
- Rotational speed

Based on these Vital Xs, a custom Design of Experiment (DoE) was designed with two factors (external loads, total clearance) with two levels and three factors (input oil pressure, input oil temperature, speed of rotation) with three levels.

The resulting DoE consisted of four groups (combination of two factors that have two levels). Each group is a "full factorial face centered CCD" (combination of three factors that have three levels). The total number of points investigated in the DoE domain was 60 (15 DoE points for each group). Figure 6 shows the details of the custom DoE previously described.

X's

	Group1	Group2	Group3	Group4
Factors	Levels	Levels	Levels	Levels
Plunger Loads	MAX	MIN	MIN	MAX
Total Clearance	MAX	MAX	MIN	MIN
Full factorial face centered CCD (3 factors with 3 levels)				
P_{inlet}	Inlet oil pressure @ header			
T_{inlet}	Inlet oil temperature @ header			
ω	Rotational speed			

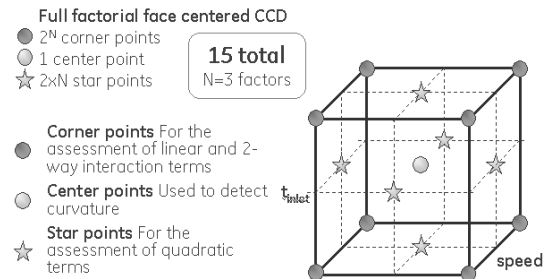


Figure 6: HyCSS sensitivity analysis (DoE: Design of Experiment) for uprated shoe geometry

The analysis performed with this software confirmed that the minimum oil film thickness (for all oil films between the shoes and the counter-shoes: upper/lower of the small-end shoes and upper/lower of the big-end shoes) was positive for the complete crankcycle at all points of the DoE domain.

Moreover, the maximum local pressure and the maximum oil heating for each oil film were also aligned with the values expected.

Figure 7 shows an example of the orbits calculated by the software for a single DoE point.

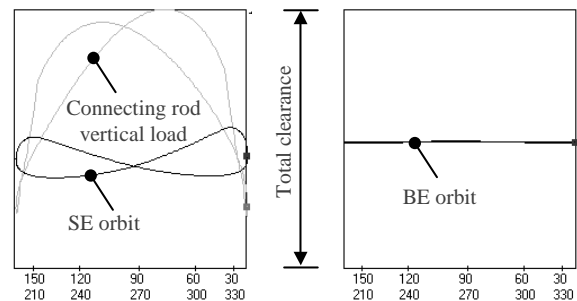


Figure 7: HyCSS Output data – Orbits of small-end shoes (SE) & big-end shoes (BE) vs. crankangle

3 Test rig for HyCSS validation

3.1 Similarity analysis

Proprietary software was used to design the optimized geometry of the shoes and a new concept (patented) for supplying lubrication oil between the shoes and counter-shoes, which provides a sustained supply of oil predominantly hydrostatically. Also, for each Vital X, the upper (USL) and the lower limits (LSL) were fixed to guarantee a constant and correct oil film thickness with gas loads increased by up to 20%.

It was necessary to validate both the new lubrication concept and the software that defines the optimal settings of all oil parameters for uprated gas loads.

The basic concept in developing the test rig was to create a design that was as close as possible to a real PK Hyper-compressor. Due to the impossibility of building a full scale (1:1) test rig to compress the process gas (ethylene) up to 3500bar, it was decided to implement a scaled test rig.

The constraints for selecting the scale were:

- Build a robust design both in terms of safety requirements and reliability of the results
- Build a test rig aligned with the development costs of the PK-Uprate program

The first task was to identify a similarity parameter to reduce the forces caused by the gas loads as well as size and impact on other characteristic variables of the problem (such as rotational speed of the crankshaft). After careful analysis of the various dimensionless parameters, the Froude number (Fr) was chosen.

The Froude number represents the ratio between inertial forces and mass forces (commonly used in naval applications). *Figure 8* shows the main differences, for our purposes, between the similarity of the Froude number and Reynolds number. The similarity of the Reynolds number does not allow scaling down the forces and increases the rotational speed by more than 6000 times.

(vs. crankshaft angle) of the gas loads, as well as volumes and masses involved, was reduced by 125 times, while the angular velocity was amplified by approximately 2.2 times (equal to the square root of 5).

3.2 PK scaled test rig

The requirements for the test rig were:

- To apply plunger load levels and profiles as per the similarity design
- To have the flexibility to change the load configuration in order to validate both the 1st and 2nd stages
- To drive the 1:5 scaled compressor within the required speed range (up to 615 rpm)
- To supply the compressor with lubrication oil flow with controlled inlet temperature and inlet pressure
- To measure the 1:5 scaled oil film thickness of the compressor shoes, at both the small-end and big-end, top and bottom side
- To measure the oil temperature and pressure at the inlet of the shoes
- To measure oil flows
- To acquire and store all measurements
- To display oil film thicknesses, pressures, plunger loads and all other acquired parameters in real time and plot them vs. the crank angle and time scale
- To have the flexibility to change the operating condition of the machine to complete the DoE in terms of speed, plunger loads, oil delivery pressure, temperature and shoe clearances

FROUDE SIMILARITY	$Fr = \frac{F_{in}}{P} = \frac{ma}{mg} = \frac{L}{gt^2} = \frac{v^2}{gL}$		
SCALE (1:λ)	SCALE FACTORS (λ=5)	FULL SCALE DIMENSIONS (1:1)	SCALED DIMENSIONS (1:5)
Force [kN]	125.0 (λ ³)	1	0.008
Rotational speed of the crankshaft ω [rpm]	0.45 (λ ^{-1/2})	1	2.236
Dynamic viscosity μ [Pa*s]	11.2 (λ ^{3/2})	1	0.089

REYNOLDS SIMILARITY	$Re = \frac{F_{in}}{F_{visc}} = \frac{\rho v_p L}{\mu} = \frac{v_p L}{\nu}$		
SCALE (1:λ)	SCALE FACTORS (λ=5)	FULL SCALE DIMENSIONS (1:1)	SCALED DIMENSIONS (1:5)
Force [kN]	1 (λ ⁰)	1	1
Rotational speed of the crankshaft ω [rpm]	0.04 (λ ⁻²)	1	6250
Dynamic viscosity μ [Pa*s]	1 (λ ⁰)	1	1

Figure 8: Froude similarity & Reynolds similarity

The Froude number, unlike the Reynolds number, allowed us to reduce the gas forces by a value equal to the cube of the scale value chosen and the linear dimensions by the scale value, and to increase the rotational speed of the crankshaft by only a factor equal to the square root of the scale chosen. Thus, having chosen a scale factor of 5, the whole profile

A first concept for the test rig was issued with the compressor coupled to an electric motor with belts and pulley. To avoid concerns associated with the gas operation and to satisfy safety and cost requirements, the cylinder assemblies and all other gas loop components (valves, pipes, heat exchanger, etc.) were replaced with a new, patented mechanical system designed to replicate the same load to the plungers of the cylinder assembly. Actually, during the rig conceptual design phase, in addition to purely mechanical means, different types of load replication system architectures were taken into account and assessed, including electromagnetic actuators, hydraulic actuators, pneumatic systems, mixed configurations. However, none of these were considered feasible or able to guarantee the needed dynamic behaviour (scaled compressor speed is 10 Hz), or they were considered more complicated to implement with respect to the purely mechanical system.

The mechanical gas load replication system consists primarily of cams, springs and rods and its principle of operation is to reproduce the gas compression and expansion with the compression and the expansion of a spring, while the gas discharge and suction phases are reproduced by sliding the springs together with the crosshead using cams. One side of the spring is linked to the plunger, which is linked to the crosshead so that the spring end always moves together with the crosshead. The other end of the spring is linked to a roller, and its position is regulated by a rotating cam.

Thus, taking as a datum the law of motion of the crosshead imposed by the crankshaft and connecting rod, one can design the cam profile needed to set the desired length of the spring to obtain the desired load on the plunger and consequently, that applied to the crosshead.

Almost constant gas loads related to the gas discharge and suction phases are replicated by keeping the spring length constant, thus letting it slide with the same law of motion as the crosshead upward and backward. The 3D model is shown in the *Figure 9*:

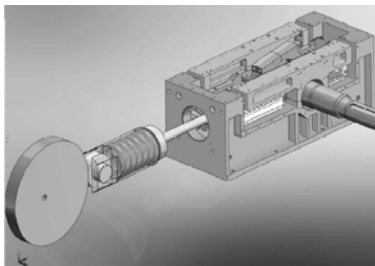


Figure 9: 3D model of mechanical load replication system

The rotation of the cams was obtained by connecting them to the electric motor through a transmission system composed of crankshafts and connecting rods. It is worth highlighting that keeping a very high grade of synchronism between the two cams and between the cams and the compressor shaft was a stringent requirement; in fact, any phase difference between the cams and crosshead would have resulted in a change in spring length with a consequent change of the load profile applied to the crosshead. Given the high accuracy required for load profiles, a very rigid transmission system had to be designed. It has been proven that the load profile accuracy requirement could not be satisfied using shafts, belts and pulleys, or chains, or gears for the connection between the main shaft and cams. Therefore, each cam shaft was linked to the main compressor shaft by two pairs of connecting rods, designed to

guarantee the right level of rigidity. Counterweights were applied to minimize vibrations.

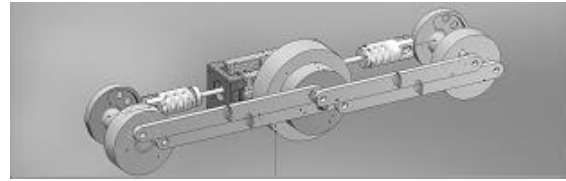


Figure 10: Conceptual design of transmission system

The design of the system was carried out by creating a complete multi-body 3D dynamic model, which took into account the geometry, the acceleration/velocity/displacement, the mass and the material stiffness of each body (crosshead, plunger, spring, roller, cams, etc.), and computing the contact pressures, contact forces, possible jumps of the roller on the cam, and also considering inertial effects. The multi-body 3D dynamic model was used to design the spring stiffness and mass, the roller and the cam profiles to give the right loads to the crosshead, avoiding excessive contact pressure or “jumps” of the roller on the cam. Several iterations were carried out for the optimization of the system for both the 1st and 2nd stage configurations, obtaining the desired load profile applied to the crosshead. The following graph shows the calculated loads to the crosshead, superimposed on the required load profile with accuracy band.

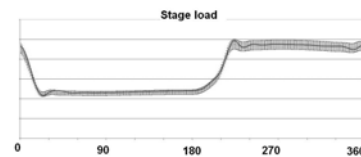


Figure 11: Calculated loads to crosshead, superimposed to required load profile with accuracy band

Since the machine to be tested was a two-throw, this was designed on both sides with a 180° phase difference. Moreover, the system was designed to be easily switched from 1st stage load to 2nd stage load configuration by only changing the two cam sets, leaving all other parts of the system, included the springs, unchanged.

During the detailed design phase of the system, every component was analyzed in terms of stress and deformation using FEM analysis.

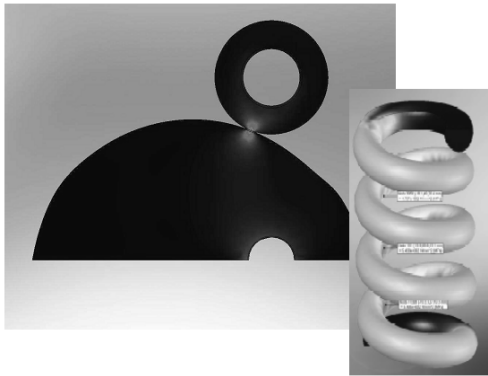


Figure 12: FEM methods were applied to design individual components of the test rig system

Besides the static design, the dynamic behaviour of the systems was assessed in terms of the natural frequencies of each component, and the torsional behaviour of the transmission system, avoiding any resonances within the operating range.

To satisfy the DoE requirement of the ability to change the applied load level by $\pm 10\%$, a nut was introduced in the design to allow adjusting the total length of the plunger, thus changing the spring pre-load.

The complete 3D model of the test rig with compressor and electric motor is shown in Figure 13.

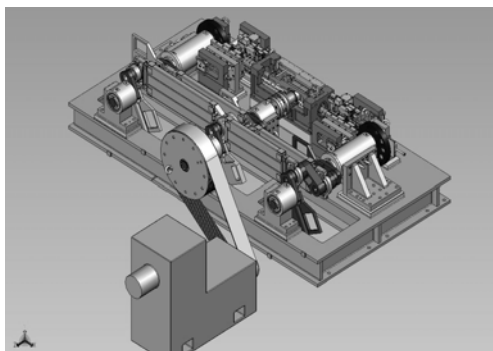


Figure 13: Complete 3D model of the test rig

It must be considered that one of the advantage of this system, besides the avoidance of the design complexity of a complete gas loop, which simplified the safety assessment and management, is the need for a smaller electric motor. In fact, compression energy is stored in the spring but is then recovered during its expansion through the cams and the shafts that are linked to the main shaft driven by the electric motor. This permitted the use of a motor which only has to compensate for the losses and satisfy the transient dynamics (i.e., accelerations and start-ups).

The following instrumentation was installed on the PK compressor prototype:

	Measurement type	nr
Design validation	shoes clearance probes (oil film thickness)	2 4
	counter-shoes inlet oil pressures	1 6
	counter-shoes inlet oil temperatures	1 6
	counter-shoes metal temperatures	2
Boundary conditions	plunger load (strain gages + telemetry)	2
	Oil skid delivery pressure	1
	Oil skid delivery temperature	1
	crankcase oil inlet pressures	3
	crankcase oil inlet temperatures	2
Oil flows	total inlet flow	1
	upper-shoes and connecting rod bearings flow	1
	main bearings flow	1
Reference	crank angle (resolver)	1
	keyphasor	1
	machine speed	1

Commercially available eddy current type sensors were used for the oil film thickness probes. For this application, the instrumentation design provided a fully integrated sensors. Probes were placed into special grooves obtained by modifying the compressor counter-shoes and, to avoid any influence of the grooves on the machine behaviour, surface continuity was restored using a resin.

After feasibility confirmation, the oil film thickness probes were installed into the compressor counter-shoes and were calibrated by the GE Oil & Gas Metrology Lab using dummy shoes of the same material as production shoes (white metal), within a few microns of accuracy. The following figure shows the bottom counter-shoe with oil film thickness probes installed.

The counter-shoe inlet oil pressures were measured with piezo-resistive probes, while the counter-shoe inlet oil temperatures were measured using type J thermocouples installed on the internal oil piping just upstream of the counter-shoes (see Figure 14).

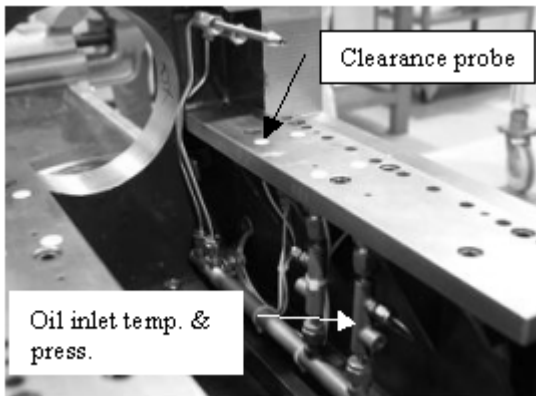


Figure 14: Bottom counter-shoe with oil film thickness probes and oil inlet pressure probes and thermocouples

In order to measure the compression load of both plungers applied to the crosshead of the compressor, a couple of full Wheatstone bridge configuration was installed. Strain gages were applied to the plunger surface and their signal was transmitted to a data acquisition system by telemetry. Both instrumented plungers, were calibrated at full-scale range and showed a force measurement accuracy within 1%. The compressor crank angle was measured by a calibrated resolver mounted directly on one crankshaft end.

The test rig was erected at the GE Oil & Gas Technology Laboratory (OGTL) facility in Florence.

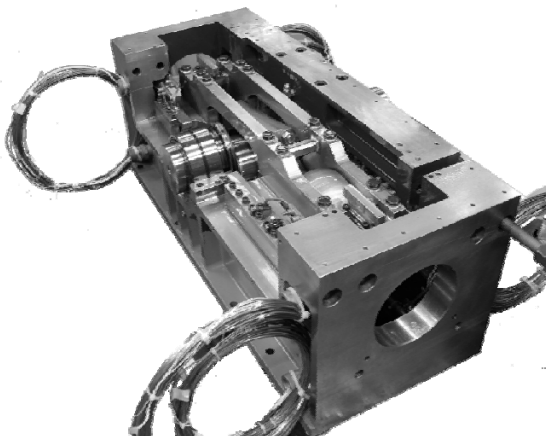


Figure 15: Fully instrumented scaled compressor



Figure 16: Complete test rig with scaled compressor

The machine was assembled and all instruments were connected to the hardware and acquired by GE OGTL proprietary software. All the data (oil film thicknesses, plunger loads, oil pressures, etc.) were plotted in real-time vs. crank angle as shown in Figure 17, thus giving the test team the ability to quickly evaluate the machine behaviour in response to operating and boundary conditions. The DoE was completed successfully, including changing speed in the desired range (503-615rpm), plunger loads $\pm 10\%$, and oil inlet pressure and temperature. The data were stored for detailed off-line analysis and comparison with CFD results.

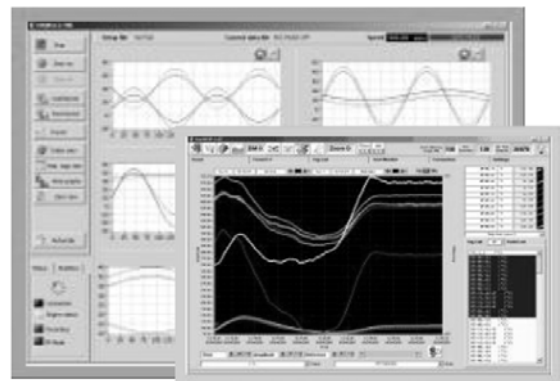


Figure 17: Screenshots of real-time measurement plots

4 Post-processing of the experimental data

For the acquisition of experimental data, a DoE with 92 points (60 points exactly replicating the analytical DoE and 32 points added to validate the experimental data acquired) was defined.

Of the 24 clearance probes installed on the counter-shoes, 16 probes were installed in the lower counter-shoes and were used for the comparison with analytical results, while the remaining 8 were installed in the upper shoes and were used to measure the total clearance of the oil films ($h_{\text{bottom}} + h_{\text{top}}$ of *Figure 5*).

Figure 18 shows the splitting of the 16 lower clearance probes into four groups, two relating to small-end shoes (small-end bottom external and small-end bottom internal) and two to big-end shoes (big-end bottom internal and big-end bottom external).

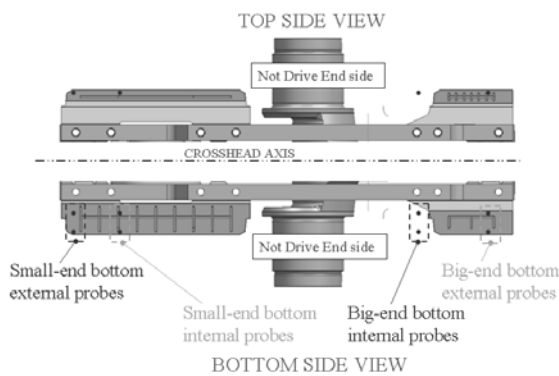


Figure 18: Clearance probe layout

4.1 Comparison between analytical & experimental data

For each group mentioned above, a single orbit (vs. crank angle) obtained from an average of the four clearance probes that compose the group was defined.

After the creation of these four averaged orbits (1 for each group) for each experimental DoE point, the main orbit parameters, h_{min} , h_{AVG} and Δ_{pp} shown in *Figure 19* were defined. Then, applying the DFSS (Design For Six Sigma) tool, for each main orbit parameter, the transfer function was built, using the 60 experimental DoE points and was validated with the additional 32 experimental DoE points.

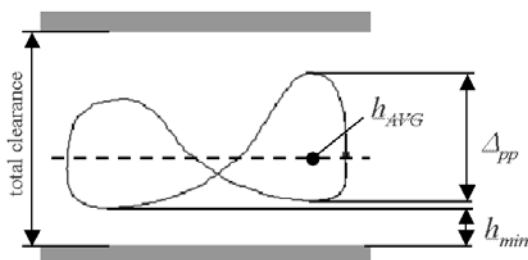


Figure 19: Main parameters of the orbit vs. stroke

With the experimental data validated, a preliminary comparison between the experimental and analytical orbits (vs. crank angle) was performed and an additional parameter, RMSE (Root Mean Square Error), was defined to quantify the mismatch.

The RMSE is defined as the square root of the sum of the quadratic differences (for each degree of the crank angle) between the values of the analytical and experimental orbits (target orbits) and was used to define the preliminary accuracy of the software through the introduction of a tolerance band of $\pm\text{RMSE}$ associated with the analytical orbit.

After the preliminary comparison, an optimization analysis was executed with the DFSS tool and the inlet oil pressure and total clearance of the software was tuned to globally reduce the RMSE of the analytical orbits and increase the software accuracy in the entire DoE domain.

Then, all 60 DoE points defined for the validation were re-executed by the software and the final orbits that were collected for the final comparison with the experimental results were obtained.

Figure 20 shows, for a small-end bottom external orbit (SEB-ext orbit) associated with a single DoE point, an example of the final comparison between the experimental and analytical data, while *Figure 21* shows the same analytical orbit with the lower standard (LSL) and upper standard limits (USL) defined by the $\pm\text{RMSE}$ (calculated for this SEB-ext orbit and for this DoE point).

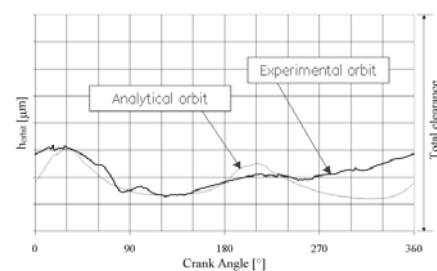


Figure 20: Final comparison between the experimental orbit and analytical orbit vs. crank angle

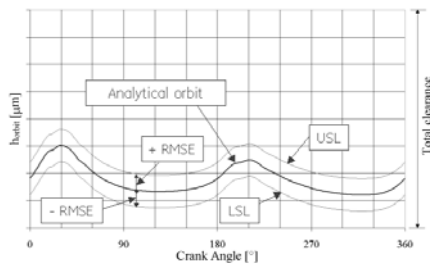


Figure 21: Final accuracy of the analytical orbit vs. crank angle

4.2 Post-processing summary

Analyzing the trends of the main parameters of the orbit, h_{AVG} , Δ_{pp} , and h_{min} , for all DoE points evaluated for the software validation, it is possible to affirm that the mismatch between the experimental and analytical data is not very close to zero for all DoE points, but, a significant reduction was obtained after tuning.

Figure 22, Figure 23 and Figure 24 show, for the loads of STAGE1, the trends (for SEB-ext clearance probes) of h_{AVG} , Δ_{pp} and h_{min} vs. inlet oil pressure, inlet oil temperature, total clearance and rotational speed (30 DoE points).

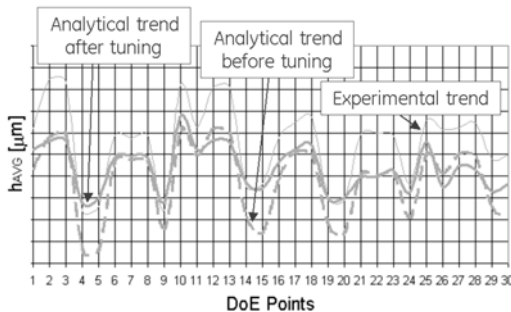


Figure 22: Final SEB-ext comparison between the h_{AVG} parameters (experimental, before tuning and after tuning) for all DoE points of STAGE1 loads

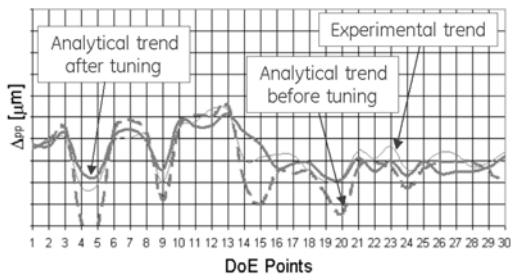


Figure 23: Final SEB-ext comparison between the Δ_{pp} parameters (experimental, before tuning and after tuning) for all DoE points of STAGE1 loads

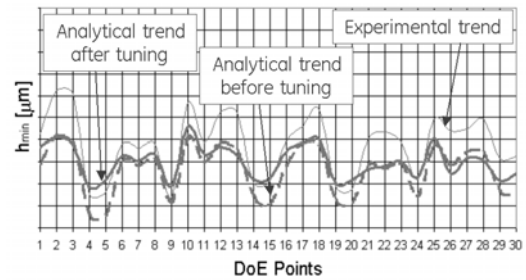


Figure 24: Final SEB-ext comparison between the h_{min} parameters (experimental, before tuning and after tuning) for all DoE points of STAGE1 loads

Finally, knowing the final RMSE of all orbits for each point in the entire DoE domain, it was possible to predict the accuracy of the software for each operating condition and to create a robust design with the optimal setting of the inlet oil pressure, inlet oil temperature and total clearance (avoiding contact between the crosshead shoes and the counter-shoes) vs. external gas loads uprated by up to 20%.

5 Conclusion

With the PK-Uprate program and the experimental results obtained from the 1:5 scale test rig, both the new concept for lubrication between the crosshead shoes and the counter-shoes, and the software, have been validated.

Thanks to the success of the program, a validated design was obtained for the geometry of the crosshead shoes for uprating by up to 20% the gas loads without penalizing the reliability of the PK hypercompressor. In addition, a robust setting of the oil parameters (inlet oil pressure and temperature) for the conditions required by customers was designed.

Summarizing the benefits of this uprate program, a reduction of a couple of cylinders on a PK twin frame configuration can be achieved with advantages in terms of cost and footprint, and without adverse impact on the overall cylinder reliability while meeting the highest plant capacity demands; moreover, in revamping an existing LDPE plant, the plant capacity could be increased by 20%.

References

- ¹ Giacomelli E., Traversari A., 2001, “Very high pressure compressors (over 100 Mpa [14.500 psi])” – Compressor Handbook, P.C. Hanlon ed, Mc-Graw-Hill, NY. Chapter7.PP.7.1-7.49
- ² Giacomelli E., Battagli P., Lumachi F., Gimignani L.,2004, “ Safety Aspects of Design of Cylinders and Hyper-Compressors for Ldpe”, PVP2004-2280,Vol.473, High Pressure Technology-Innovation and Advances in High Pressure Technology, July, San Diego, Cal. USA
- ³ Giacomelli E., Falciani F., Dini R., Giusti A. 2001, “Design and Service Engineering to Improve Reliability of Reciprocating Compressors”, NPRA 2001, Clean Fuels Challenge, Aug.28-29, Houston TX, USA, National Petrochemical & Refiners Association, CFC-01-211



Fracture Mechanics Life Assessment of Hypercompressor Lubrication Quills

Marco Manetti

Ph.D. Student

Università degli Studi

di Firenze

Florence

Italy

marco.manetti@unifi.it

Guido Volterrani

Global Service

Technical Support

Engineer

GE Oil & Gas

Florence

Italy

guido.volterrani@ge.com

Carmelo Maggi

Reciprocating

Compressor

Engineering

GE Oil & Gas

Florence

Italy

carmelo.maggi@ge.com

Nicola Campo

Quality

Engineering

GE Oil & Gas

Florence

Italy

nicola.campo@ge.com

Marco Innocenti

Materials & Processess

Engineering (MPE)

Engineering

GE Oil & Gas

Florence

Italy

marco.innocenti.labo@ge.com

**7th Conference of the EFRC
October 21th / 22th, 2010, Florence, Italy**

Abstract

Fatigue is a factor that impacts the life of all components subject to alternating loads. In fact, each component subject to fatigue (both high cycle fatigue and low cycle fatigue) can experience a failure in a very short time. In oil and gas applications, such a failure may cause large production losses. These failures are more frequent if a defect (initial flaw) nucleates in the component due to corrosion, high stress, machining imperfections, etc.. A failed lubrication quill of a hyper compressor subject to inadequate autofrettage pressure was analyzed. The study was performed in order to determine the source of failure and to prevent damage of this nature in the future by improving the component design. A laboratory analysis was performed to characterize the crack zone, to find any evidence of defects due to machining, to check the material composition and mechanical properties, and to verify the presence of oxides in the cracked area. A sensitivity analysis of the autofrettage pressure was performed to determine the correct residual stresses and to obtain a threshold defect larger than the minimum detectable defect. Fracture mechanics calculations were performed to analyze the propagation of an initial defect with different material characteristics and varying autofrettage pressures. Finally, Finite Element Analysis was used to check and validate the values of the residual stresses predicted by analytical calculation for each autofrettage pressure investigated. Based on the results of these analyses, an optimized version of this component was designed.

1 Introduction

In Low Density Polyethylene (LDPE) plants, the delivery pressure of the gas may be up to 3000-3500 bar. In order to reach these pressure values, two compressors are used: the primary compressor that increases the ethylene pressure from atmospheric to 250-300 bar and the secondary compressor, also called a hypercompressor, that achieves the final pressure level.

Because of the very high pressures and the special materials used in hypercompressors, cylinder lubrication is a key factor for compressor reliability.

A lubrication quill is a special fitting used in hypercompressor cylinders (both 1st stage and 2nd stage) to transfer oil from the external tubing to the internal cylinder ducts. Three quills per cylinder are typically used. In *Figure 1* a lubrication quill for a 2nd stage cylinder is shown circled.

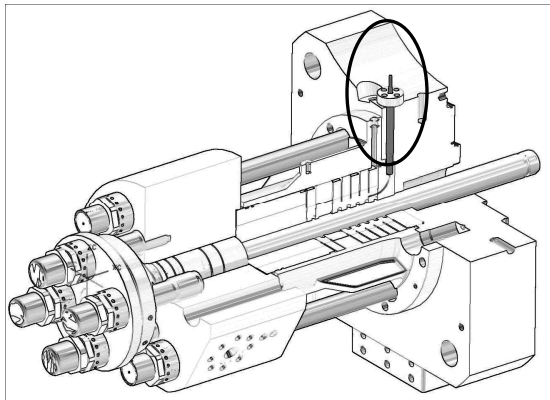


Figure 1: Hypercompressor cylinder

Due to very high pulsating pressures and consequent fatigue stresses, lubrication quills require pre-stressing autofrettage. Autofrettage is a fabrication technique in which the quill, by mean of a hydraulic pump, is subjected to very high pressure, causing internal portions of the component to yield, leading to internal compressive residual stresses in the critical areas (internal layers). The goal of autofrettage is to increase the life and capability of the final product¹.

During autofrettage, the quill is subjected to internal pressure of such a magnitude that the bore is enlarged, which causes the metal inner layers to stretch beyond their elastic limit. This means that the inner layers are stretched to a point where the steel cannot return to its original shape once the pressure within the bore has been removed.

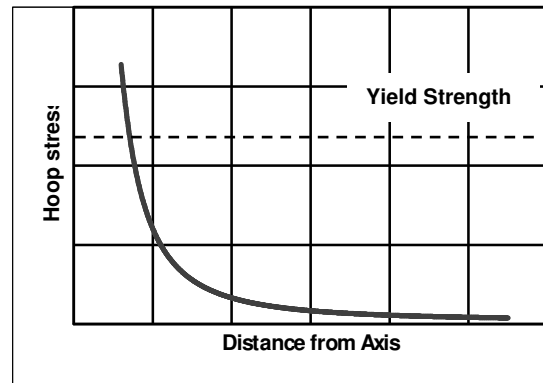


Figure 2: Elastic hoop stress vs. distance from axis in a thick wall pipe

Although the outer layers of the quill are also stressed, the internal pressure applied during the process is such that the material yield strength of these layers is not reached and therefore the outer layers are not stretched beyond the elastic limit. This happens because the stress distribution through the walls of the quill is non-uniform: its maximum value occurs at the internal diameter and decreases towards the outer layers of the tube (see *Figure 2*). Since the outer layers remain elastic, their tendency is to return to their original shape, but they are prevented from completely doing so by the now permanently stretched inner layers. The effect is that the inner layers of the metal are under compression from the outer layers as if an outer layer of metal had been shrunk on (like in the shrink fitting technique).

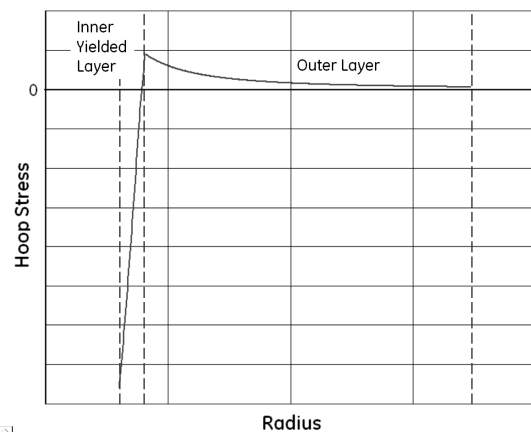


Figure 3: Residual hoop stress vs. distance from axis in a thick wall pipe.

When the autofrettage pressure is too low, the hoop stress induced in the inner layers of the metal does not reach the material yield stress or the thickness of the yielded area is smaller, resulting in a reduction of the beneficial precompression effect.

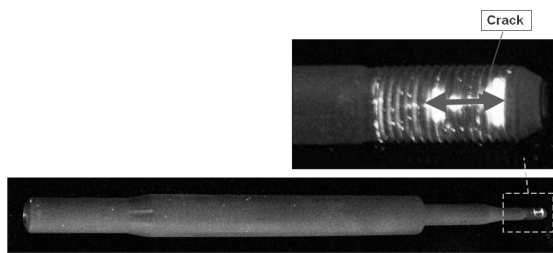


Figure 4: Failed lubrication quill

Similarly, when upgrading a material to one with higher yield strength, it is necessary to increase the autofrettage pressure, otherwise the thickness of the precompressed area will decrease and in some cases will not exist at all. Without the correct autofrettage pressure, a new material with superior mechanical properties will result in a detrimental effect on the fatigue life of the part and in a higher probability of premature failure.

The following paragraphs will show the analysis of a failed lubrication quill and the complete design check that followed this event, which led to changes in the base material specification and some of the autofrettage parameters in order to improve the fatigue strength and the sensitivity to possible machining/corrosion defects (initial flaws).

2 Laboratory analysis

An oil lubrication quill from a PK hypercompressor had been reported as damaged. The damage was associated with cracking in the threaded zone of the quill.

The crack was opened and subjected to fractographic analysis, which showed that the crack origin was located at the inner diameter. The crack propagated following a typical High Cycle Fatigue (HCF) mode.

Detailed observation revealed different fracture morphologies: the first region, closest to the crack origin, exhibited features typical of fatigue (with classical striations lines); the second region, adjacent to the first region, had features typical of rapid propagation (dimples).

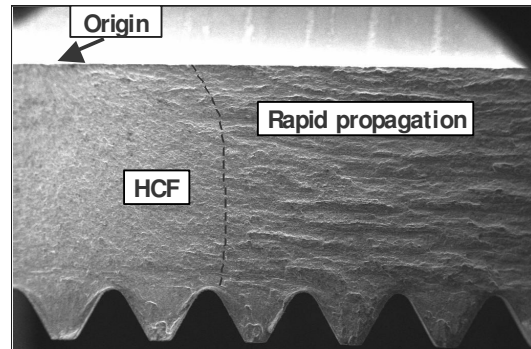


Figure 5: Fracture surface

Tensile and impact tests were performed on quill samples to verify the mechanical properties of the base material.

To verify the extension of the plasticized area induced by the autofrettage procedure, a set of Vickers microhardness checks was performed in order to draw the hardness profiles for four cross-sections taken from different locations in the quill. The assumption was that the yielded area could be identified as the work hardened zone. The findings of this investigation were in line with the expected values. An example of a measured hardness profile for a section is shown in Figure 6.

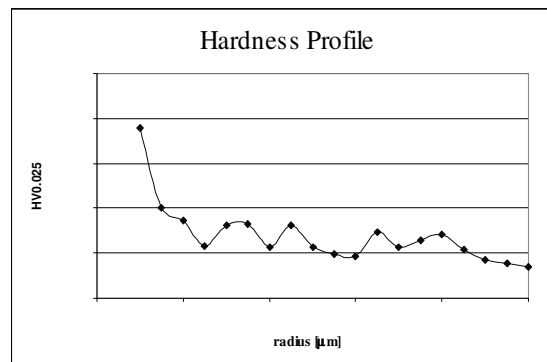


Figure 6: Hardness profile of a quill section

3 Autofrettage theoretical calculation

In order to assess and redesign the autofrettage process for actual quill dimensions and different materials, two different analytical methods were used.

3.1 ASME Section VIII Division 3

To perform a theoretical evaluation of the effects of autofrettage pressure on different sections of a lubrication quill by varying the mechanical properties of the material, thick walled cylinders were considered.

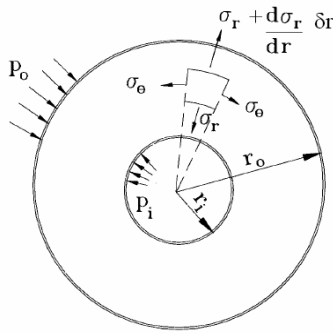


Figure 7: General case: cylinder subject to both internal and external pressure

According to the theory for thick walled cylinders, the radial (σ_r) and hoop stresses can be calculated from the following formulas, known as Lamè's equations.

$$\sigma_r = \frac{p_i r_i^2 - p_o r_o^2}{r_o^2 - r_i^2} - \frac{(p_i - p_o) r_i^2 r_o^2}{r^2 (r_o^2 - r_i^2)}$$

$$\sigma_\theta = \frac{p_i r_i^2 - p_o r_o^2}{r_o^2 - r_i^2} + \frac{(p_i - p_o) r_i^2 r_o^2}{r^2 (r_o^2 - r_i^2)}$$

Referring to the ASME Boiler and Pressure Vessel Code" Section VIII Division 3 ARTICLE KD-4², a elastoplastic model was used to evaluate the stress/strain distribution in the yielded material and the Bauschinger effect was introduced in order to correctly evaluate the maximum residual compressive stress (hence the plastic region dimension) introduced by the autofrettage.

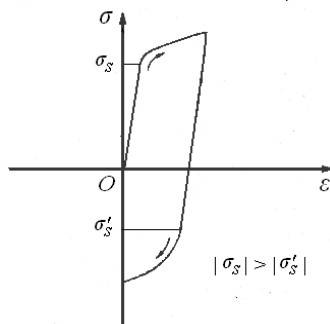


Figure 8: Bauschinger effect

The Bauschinger effect refers to a property of materials where the material stress/strain characteristics change as a result of the microscopic stress distribution of the material. While more tensile cold working increases the tensile yield strength, the local initial compressive yield strength after tensile cold working is actually reduced.

The greater the tensile cold working, the lower the compressive yield strength.

$$|\sigma'_s| \sim 0.7 \times |\sigma_s|$$

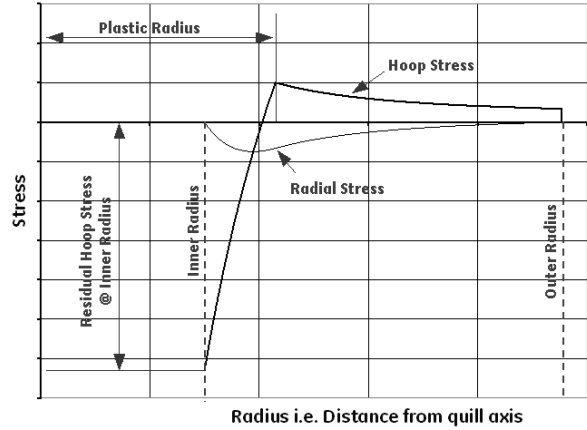


Figure 9: Main features induced by autofrettage operation

The plastic radius (i.e., the radial dimension of the yielded area) increases, increasing the autofrettage pressure value; similarly it is bigger in the quill areas where the wall thickness is smaller (the quill has an uneven thickness along its axis).

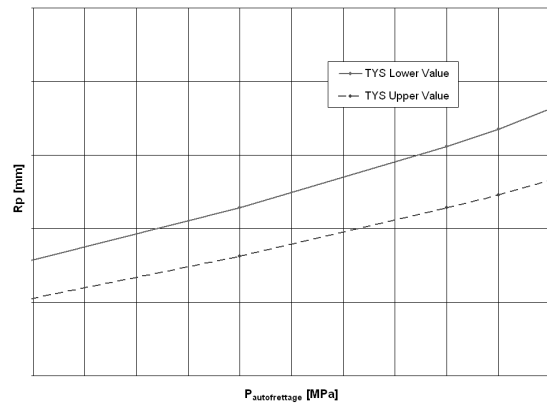


Figure 10: Plastic radius vs. autofrettage pressure

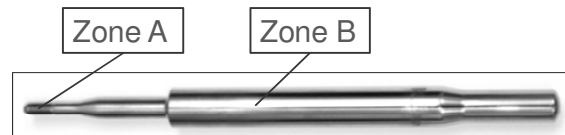


Figure 11: Quill zones investigated

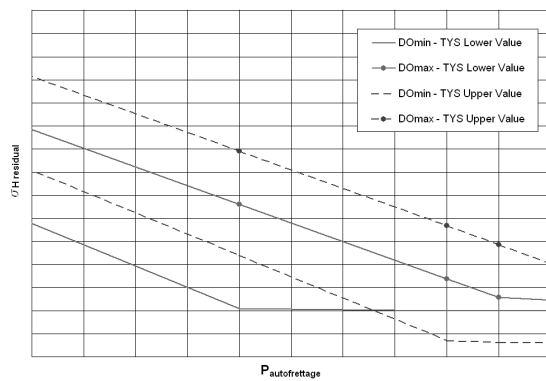


Figure 12: Residual stress on ID vs. autofrettage pressure

The residual stress on the inner layer is a function of the autofrettage pressure up to a critical value after which reverse yielding occurs and the maximum residual compressive stress reachable is directly proportional to the material yield strength.

3.2 FEM calculation

The ASME and Lamè's formulas are based on the assumptions that the solid to which the internal pressure is applied is an infinite length tube, i.e., a hollow cylinder with constant wall thickness along its axis, whose constraints are far away from the area under investigation.

Since instead, the actual quill has several different areas with different thicknesses (one of which is threaded), and the main constraints are pretty close to the investigated areas, it was decided to perform an Finite Element Method analysis to better evaluate the differences between the real quill behaviour and that predicted by the theory described in the ASME Boiler and Pressure Vessel Code" Section VIII Division 3 ARTICLE KD-4. In other words, FEM was used to validate the previous calculation.

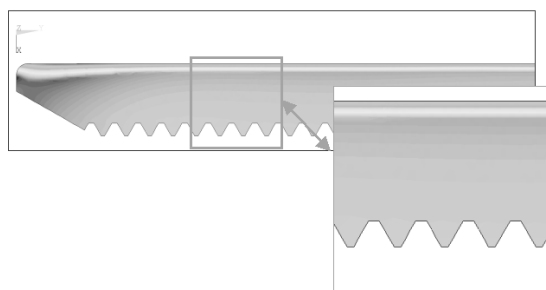


Figure 13: FEM output for the quill threaded area

In order to obtain a reliable value, FEM runs were performed considering two different autofrettage pressures for the quill, and the minimum and maximum thickness for a given TYS value. The

FEM results were compared to the results obtain with the ASME method for the same parameters.

The comparison of results (see Figure 14) showed good agreement, especially considering that the stress-strain elastoplastic models used in the two methods are slightly different; in particular, the residual stress value falls within the +/-5% tolerance, while the FEM method generally gives a slightly higher value for the plastic radius.

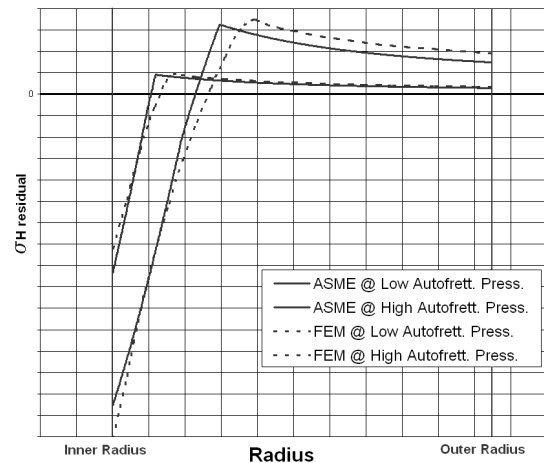


Figure 14: FEM vs. ASME comparison

4 Fracture Mechanics Calculations

4.1 Analysis Model

In order to identify parameters such as threshold defect, critical flaw, propagation of the crack, etc., the British Standards⁵ protocol for fracture mechanics calculations was used.

Threshold defect = Minimum Flaw Dimension leading to failure by HCF under a given cyclic load

Critical Flaw = Flaw dimension leading to immediate failure under a given load

This methodology is used during the design phase of structures subject to cyclic loading where it is good practice to set the threshold defect dimension bigger than the minimum detectable defect, and during RCAs to investigate the possible causes of a failure.

Because of the curvature/thickness ratio of the component in the crack area, the calculations were performed by approximating the quill as a flat plate with a superficial flaw (see Figure 15).

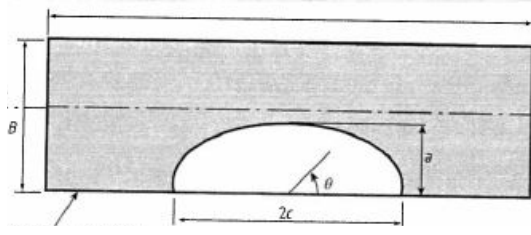


Figure 15: Flaw schematization

According to the BS protocol, the general form of the stress intensity factor range used for fatigue assessment is:

$$\Delta K_I = Y \Delta \sigma \sqrt{\pi a} \quad (1)$$

where $\Delta \sigma$ is the hoop stress variation inside the flaw due to the operating pressure loading cycle.

$\Delta \sigma$ is calculated applying some special assumptions, i.e., if the compressive hoop stresses induced by the operating conditions (autofrettage residual compressive hoop stress + tensile stress due to discharge and suction pressure) are (in module) less than the oil pressure, σ is the sum of the hoop stress due to the operating conditions (from the thick walled cylinder theory considering also the residual stresses due to autofrettage) and the oil pressure. Compressive stresses inside the flaw do not contribute to the crack growth, and therefore, zero is assumed as the minimum value for both discharge and suction stresses.

$$\begin{aligned} & \text{if} \\ & \sigma_{residual} + \sigma_{operating_pressure} < -P_{Oil} \\ & \text{then} \\ & \sigma'_{operating_pressure} = \sigma_{residual} + \sigma_{operating_pressure} \\ & \text{else} \\ & \sigma'_{operating_pressure} = \sigma_{residual} + \sigma_{operating_pressure} + P_{Oil} \end{aligned}$$

And when calculating $\Delta \sigma$ it is assumed:

$$\begin{aligned} & \text{if} \\ & \sigma'_{operating_pressure} > 0 \\ & \text{then} \\ & \sigma = \sigma'_{operating_pressure} \\ & \text{else} \\ & \sigma = 0 \end{aligned}$$

Fracture mechanics calculations according to the protocol³ were performed using in-house developed proprietary software.

The material properties used are ultimate tensile strength, yield strength, fracture toughness and Paris coefficients (Paris coefficients characterize the linear zone of the Paris curve⁴, while the threshold value ΔK_{th} is inserted separately). Since the material toughness (K_{mat}) was not available, this characteristic was estimated using the BS formula as follows:

$$K_{mat} = [(12\sqrt{C_v} - 20) \cdot (25/B)^{0.25}] + 20 \quad (2)$$

based on the Charpy value (C_v) at the operating temperature and considering the component thickness (B).

The geometric characteristics of both the component (thickness and width of the plate) and the initial flaw dimension (a and $2c$, see figure 16) are also considered in the calculation.

Finally, loads acting on the lubrication quill are introduced where principal and secondary stresses are considered separately in accordance with British Standard protocol³.

4.2 Threshold defect

A sensitivity analysis was performed to calculate the threshold defect value by varying the autofrettage pressure and TYS.

Using the equation (1) solved for the “a” dimension (flaw depth according to Figure 15) and considering the threshold value for ΔK (i.e., ΔK_{th} characteristic for each material) it is possible to calculate a_{th} (threshold defect) for different autofrettage stresses. The results are shown in the following figure.

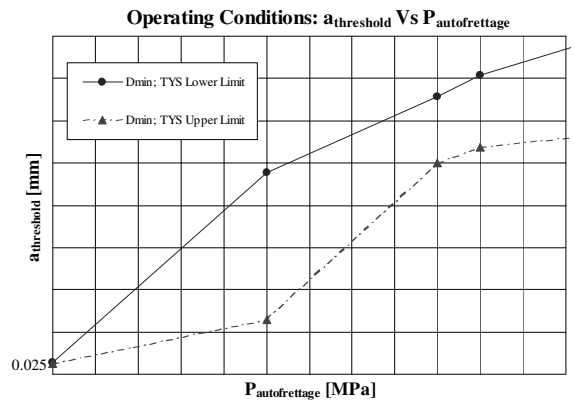


Figure 16: Threshold defect vs autofrettage pressure

Two different types of materials (min and max TYS values according to supply specification) and two different diameters (zones A and B in *Figure 11*)

were considered, varying the autofrettage pressure in five different steps. The results show that, for the minimum autofrettage pressure analyzed, the threshold defect a_{th} is very small (about 0.025 mm), i.e., smaller than the defect measured on the failed component during SEM analysis.

This calculation confirms that the defect found at the origin of the fracture, being bigger than the threshold value, could have caused the component to fail under normal operating conditions and therefore is the most likely root cause of the failure.

The main scope of the investigations was to determine the threshold defect by varying the autofrettage pressure. This was a fundamental phase of the study because a higher threshold defect means less sensitivity of the component to a potential initial defect (e.g., due to rough machining) and therefore, longer component life. *Figure 16* shows how increasing the autofrettage pressure increases the threshold defect for all the analyzed conditions.

A maximum autofrettage pressure must be specified, because although higher pressures give a larger threshold defect, they lead to a smaller critical defect during the autofrettage phase (critical defect is the flaw that causes an overpressure failure during the autofrettage phase of the component). This consideration is explained in *Figure 17*.

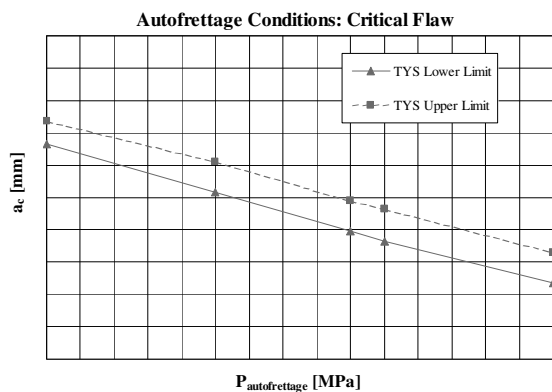


Figure 17: Critical defect during fabrication

In our specific case, an optimal autofrettage pressure range for this component was identified for specific mechanical properties of the material, by setting a minimum dimension for the threshold (see *Figure 16*).

Critical defects were calculated for both direction “a” (depth) and “2c” (length), see *Figure 15*. Direction “2c” is crucial since it represents the detectable dimension in an internal visual analysis (performed using a special boroscope).

4.2 Propagation

Laboratory analysis showed the presence of an initial flaw (larger than the threshold defect calculated in the previous paragraph) and propagation due to high cycle fatigue. Fracture mechanics analysis had to be performed in order to calculate the threshold defect as a function of the main factors that influenced the flaw propagation (i.e., material properties, autofrettage pressure, geometry, etc.) and the number of cycles to reach quill failure. The flaw propagation calculation was performed for two different materials with relevant mechanical properties (upper and lower specific limit) starting from an initial crack slightly larger than the threshold defect. The same analysis was repeated using the mechanical properties of the broken quill and the dimensions of the initial crack taken from the laboratory analysis report.

An example of the calculation performed is shown in *Figure 18*.

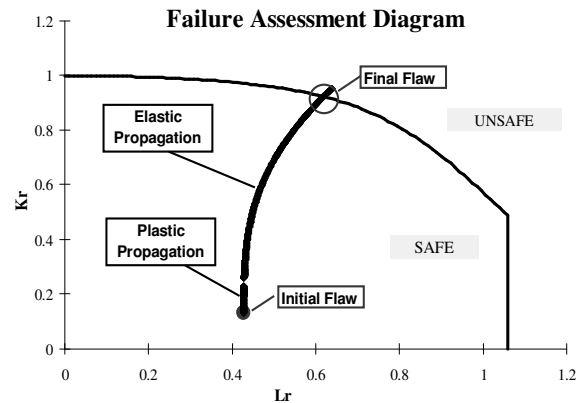


Figure 18: Typical FAD for the analysis

The graph reports the propagation of the initial crack on a K_r - L_r diagram (Failure Assessment Diagram). The two parameters are calculated in accordance with BS³ using the formulas:

$$K_r = K_I / K_{mat} \quad (3)$$

$$L_r = \sigma_{ref} / TYS \quad (4)$$

where K_I is the stress intensity factor and K_{mat} is the fracture toughness of the material; σ_{ref} is the reference stress (obtained from an appropriate reference solution).

Due to the autofrettage pressure applied, two different zones are present in the lubrication quill: the inner zone (internal diameter) is a plasticized zone (yielded material); the outer adjacent region is an elastic zone (base material did not yield). For this reason, two types of propagation modes were considered in the study: “plastic propagation” is the propagation of the crack through the plasticized region and “elastic propagation”, i.e., the progress of the crack in the material that did not yield.

By mean of these analyses it was possible to evaluate the number of cycles necessary to reach the unsafe zone of the diagram and the dimension of the final crack (i.e., the critical flaw under operating conditions). According to our calculations, for all the analyzed cases, in the presence of a flaw bigger than the threshold limit, the propagation takes a few weeks to lead to component failure.

These findings highlight the importance of increasing the threshold defect dimension by increasing the autofrettage pressure, but also taking care to keep the critical defect above a certain value (to avoid failures during the autofrettage phase of quill manufacturing).

5 Conclusion

A premature failure of a lubrication quill led to an extensive set of analyses of the damaged part and to a complete design review of the component. By deepening our calculation and inspection of this specific hypercompressor element, we were able to verify how critical its design is and how each single out of range parameter can lead to an outage in a short time.

Mechanical testing performed during the laboratory analysis showed that the material TYS was above the required limits and the material Charpy value was below the allowable value; chemical analysis showed the presence of an elevated level of sulphur (that could explain the low toughness) and phosphorus; microscopic analysis showed that the entire surface had rough machining marks that were not sufficiently removed during polishing and that the crack propagated from an initial machining defect

The autofrettage calculations were performed using the ASME Boiler and Pressure Vessel Code" Section VIII Division 3 ARTICLE KD-4" formulas for an infinite length pipe and were validated by means of Finite Element Method analysis on a real quill model. The ASME and FEM results demonstrated good agreement. The thickness of the plasticized layer calculated was in accordance with the measured dimension of the work hardened zone.

The material TYS, which exceeded the required level, led to a thin layer of plasticized material and low Residual Compressive Stress with a detrimental effect on fatigue life (ineffective autofrettage). Sensitivity charts were drawn, which show the effect of material TYS, autofrettage pressure and quill outer diameter on the plastic radius and the residual compressive stress on the inner layer.

Fracture Mechanics Calculations were performed following the British Standards³ protocol incorporating some assumptions from ASME “Section VIII Division 3 ARTICLE KD-4” in order to identify critical parameters such as the threshold defect, i.e., the minimum flaw size leading to failure under the actual operating conditions for the analyzed material; a threshold defect chart was drawn as a function of material TYS, autofrettage pressure and quill outer diameter; the critical flaw (defect size causing a sudden overpressure failure during autofrettage phase) dimension was calculated by varying the material properties and autofrettage pressure. The cycles to failure for the analyzed broken quill were calculated.

As a result of this study the following were introduced for more robust design of the lubrication quills and to minimize the possibility of future failures during operation:

- the optimal autofrettage range to maximize threshold and critical defects was identified
- additional requirements for the base material were introduced
- the manufacturing process was optimized to ensure better internal surface polishing
- examination of the internal diameter surface using a special boroscope was introduced

References

- ¹ E. Giacomelli, P. Battagli, N. Campo, F. Graziani, “Autofrettaging procedures on LDPE hyper-compressor components”, ASME Pressure Vessel and Piping Division Conference, Vancouver, July 23-27, 2006
- ² ASME Boiler and Pressure Vessel Code, Section VIII, Division 3, Article KD-4, “Alternative Rules for Construction of High Pressure Vessels”, American Society of Mechanical Engineers, Jul 1, 2007
- ³ BSI BS 7910 Document Information, “Guide to methods for assessing the acceptability of flaws in metallic structures”, British Standards Institution, Jul 27, 2005
- ⁴ P.C. Paris, F. Erdogan, “A critical analysis of crack propagation laws”, *Journal of basic engineering*, vol. 85, 1960, pp. 528-534



Cylinder Manifold Forced Response

by:

Marco Passeri
Dynamic Studies
Engineering
GE Oil & Gas
Firenze
Italy

marco.passeri@ge.com

Stefano Generosi
Design Tools
Engineering
GE Oil & Gas
Firenze
Italy

stefano.generosi@ge.com

7th Conference of the EFRC
October 21th / 22th, 2010, Florence, Italy

Abstract

The system consisting of the reciprocating compressor and associated bottles, known as the “Cylinder manifold” may potentially be the source and location of high vibration problems. Special attention must be paid to Design of the compression system to assure smooth and safe operation. The study has to include all sensitive elements (skid, frame crosshead guides, distance pieces, cylinders, bottles, connected piping and supports, etc.). However, only a model built using manufacturing drawings and validated by site measurements can provide a sufficient accurate description of the characteristics of these critical components and therefore realistic results. Knowledge of the frequencies and amplitudes of pulsation-induced forces defined by acoustical simulation, cylinder internal gas forces (cause of cylinder Stretch) and unbalanced mechanical forces and moments allow a proper forced response analysis of the cylinder manifold system. These forces are applied to the finite element model to calculate the relevant vibrations and cyclic stresses by performing a dynamic forced response of the system. When the dynamic stresses are out of the limits it is necessary to iterate between acoustical analysis and cylinder manifold system analysis to find a solution using different supports or by modifying the volume bottle design to further minimize pulsation induced forces. When the application requires a large and heavy acoustic damping system with consequently low mechanical natural frequency, or the compressor speed is significantly high, or the forces are large, the possibility to have excessive vibrations in the first design is very high. Therefore, the execution of these studies at a very early stage of the project is fundamental. Proper solution can be found only by close cooperation between the compressor manufacturer, end user, engineering contractor and vibration specialist.

1 Introduction

Reciprocating compressors have the advantage of high efficiency and flexibility of service so they are often used in chemical and petrochemical applications. On the other hand their variable flow generates pulsations and vibrations, which may produce fatigue failure of the system, loss of capacity, and increased maintenance costs. The development of the market requires processing with increased flow capacities, working pressure and fine capacity step loads. All these need increase the risk of vibrations therefore special attention must be paid to increase the safety, performance and reliability of these machines, which requires that designers make extensive use of the most advanced simulation methods to avoid vibration of the compressor itself, which represents the heart of the system. The aim of this paper is to describe a possible cost-effective compressor and dampers Design Procedure, to avoid excessive vibrations, have safe and smooth plant operation, meet contract delivery, properly estimate cost and drive the project in the right way till the bid stage.

2 Description of the Problem

As indicated in API 618 5th Edition ¹, to meet contract delivery it is necessary that all parties cooperate to schedule the design of critical component compression system. To design the compression system without any risk it is necessary a lot of info relevant to the plant system that practically are available only in a late stage of the project. Theoretically the compressor manufacturer should wait the execution of complete dynamic analysis inclusive of complete customer plant pulsation analysis prior to start the procurement of long-term delivery components such as pulsation suppression device. Customer is often in difficulty to provide necessary info and then in most of the case the project contract delivery cannot be meet unless some risks are taken. In this paper is described a way to limit these risks to final minor adjustments without impact on project schedule.

2.1 Exciting forces

Reciprocating compressors generate several dynamic exciting forces that can produce high level of vibrations, poor performance, noise, and high risk of fatigue failures. Following are then described:

2.1.1 Pressure pulsation

The most known source of forces is the pulsation-induced forces generated by the compressor pulsating gas flow, whose harmonic components

interact with plant piping and equipment, inducing resonance effects. An accurate pressure pulsation analysis ² is the means to protect plant operations by limiting their effect through proper damping-filtering system. The main purpose of this study is to minimize these forces in the compression system and relevant connected piping and equipments.

2.1.2 Gas forces due to the compression

Reciprocating compressors during the compression generate cylinder gas forces on the cylinder internals proportional to the cylinder bore and the operating pressure that are applied in the cylinder ends depending upon step loads (Figure Nr.1). Theoretically if everything is rigid (i.e. the cylinder heads and the compressor frame have no relative movements) these forces are balanced - reclosed on the compressor frame. In reality when the forces are large is almost impossible to avoid cylinder movements due to these gas loads. Typical vibration effect due to these forces, known as cylinder stretch, is the cylinder assembly lengthening and shortening. Main component of this forces occur at the compressor speed and therefore main vibration is expected at this frequency. However forces may be significant also at relatively high frequencies (i.e. up to 7 or 8 times compressor speed), therefore when the forces are sufficiently large or the mechanical natural frequency of the system is near to exciting forces frequency the vibrations of the system may be very high.

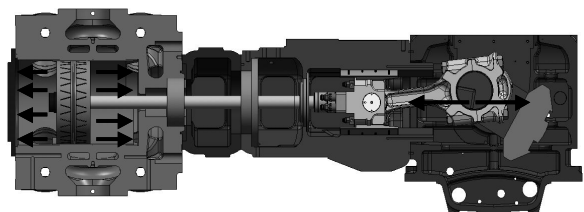


Figure 1: Gas forces

2.1.3 Loads acting on the foundations

Reciprocating compressors induced also dynamic forces on the foundations due to centrifugal forces of the rotating mass and the inertia forces of the masses having reciprocating motion. Also the torque transmitted by the motor to the compressor is a source of variable forces on the foundation. Further to these forces, in general, couples of various origins also act upon the foundation. The Design of the machine has a big influence on the nature and the values of these forces and moments (Figure Nr.2). These loads must be carefully adjusted during the compressor Design such that to be minimized.

Complete balancing is not possible for various reasons (type of crank-gear, pistons weights etc.) and therefore there are often couples acting around vertical axis (most of critical application are horizontal compressor). Once upon the compressor is balanced at the best, the verification calculations need to consider the worst cases condition. All these forces and moments must be applied to the model to design the foundation. In case of compressor mounted on skid these forces and moments are significant also for the dynamic design of the system as all variable forces described above.

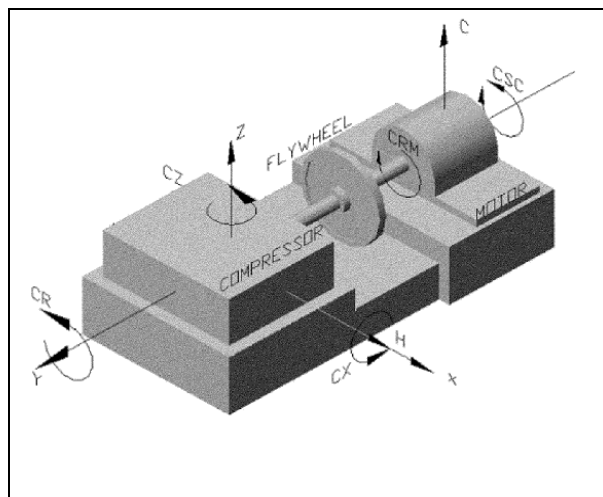


Figure 2: Loads acting on foundations

3 Bid stage Risk assessment

It is easy to understand that so many different forces applied in a complex system like a reciprocating compressors and its associated equipments and skid-foundation, is something that need to be followed with care till the first selection of the compressor type and sizing. Considering that, at the bid stage the application information is limited as the time to do the offer; the first step can only be a "risk assessments". Experience indicates that risks are linked to several application characteristics that need to be evaluated carefully. Remembering that

purpose of a proper dynamic design is to avoid mechanical resonances phenomena, compressor layout has to be selected taking into account of the following described application characteristics. Each of these vibration key players involve difficulties for the designer that need to be dully evaluated so that to put in place necessary adjustment:

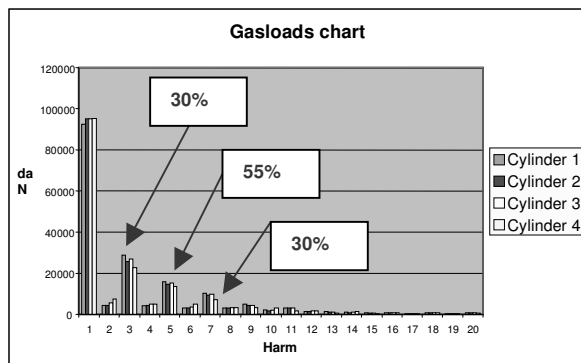
- Large cylinder size or compressor mounted suction damper weights drastically decrease mechanical natural frequency of the cylinder manifold system; possible solution may be reinforced cylinder supports and/or suction damper on dedicated foundation or supporting structure
- High operating pressure and or big cylinder bore may involve large exciting gas loads forces and pulsation induced forces; possible solution are the adjustment in the capacity control system selection and/or compressor stages ratio distribution
- Step-less capacity control, such as reflux system produce several high frequency harmonics components in respect to other system with steps such as suction valve unload or clearance pockets. These high frequencies can easily fall in the range of mechanical natural frequencies of the cylinder manifold system itself; Customer and compressor Manufacturer must discuss this issue limiting the range to the real needs
- Compressor variable speed, mean variable exciting frequencies, that may involve difficulties to detune exciting forces from cylinder manifold system mechanical natural frequencies; Customer and compressor Manufacturer must discuss this issue limiting the RPM range to the real needs
- Physical constrains and maintenance are also design constrains that often limit design choices and in some instance can oblige to complex solution. For instance, the bottle nozzles must be long enough to allow easy removal of vertical cylinder valve unloaders. This can further increase the elevation of suction damper; Customer and compressor Manufacturer must discuss these constrains and select the best compromise among the various needs
- Crank shaft phase of a multi-cylinders compressor, coupling the harmonics components, can increase the fundamental frequencies of exciting forces; when feasible alternative phase distribution should be evaluated
- High compressor speed often requires high cylinder manifold system minimum mechanical natural frequencies or anyway involve difficulties to detune exciting forces from mechanical natural frequencies; possible solution may be reinforced cylinder supports and/or suction damper on dedicated foundation or supporting structure

- Compressor Skid can be a source of compressor foundation low stiffness especially when necessary skid is high elevated; when is not feasible to reach at least a minimum natural frequency above the 2nd harmonic component detune of the system from significant exciting forces is mandatory
- Wide operating conditions may produce several resonance conditions that enlarge the amount of the exciting forces; Customer and compressor Manufacturer must discuss this issue limiting the range to the real needs

3.1 Compressor forces and damper selection

The knowledge of the running conditions allows a detailed analysis of “worst-case” cylinder gas loads harmonics distribution (Figure Nr.3). Dedicated tool create a spectrum of maximum loads and indicates for each harmonic component, which is the condition that produces the peak. In this manner the designer can easily evaluate if it is possible to adjust some parameters (e.g. capacity control system steps, compressor ratio distribution etc) to obtain a more homogenous harmonics distribution (i.e. theoretically with no peaks of harmonic components bigger than the previous ones). This activity further to adjust compressor-sizing parameters make the designer aware of the amplitude of these forces that if not properly controlled may generate severe vibrations issue.

REFLUX-STEPLESS WORST CASE



SUCTION VALVE UNLOAD WORST CASE

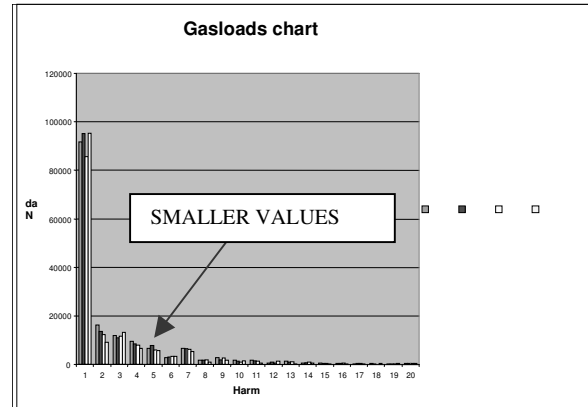


Figure 3: Cylinder Gas forces comparison

Another important step is the selection of the type (empty volume or filter) and size (volume) of the pulsation devices. A preliminary sizing dedicated program, taking data directly from compressor sizing program, calculates the volume, the diameters and length of chokes and the relevant pressure drop, optimizing the results for all operating conditions.

These basic elements are sized such that the API618¹ STD Approach 3 allowable pulsations are met with a sufficient margin (e.g., 70-80% of allowable, see also API 618 5th edition¹ section 7.9.4.2.3.4 “pre-study”) that should allow satisfactory control of the resonance conditions found during the final pulsation study.

3.2 Preliminary Layout evaluation

Starting from compression system and equipments initially selected and taking into account of above mentioned vibrations key players, evaluation of possible layout starts. Using a dedicated tool and providing application data such as compressor type, cylinder bore, operating pressure, treated gases, damper dimensions and weight etc., similar applications can be found in compressors application database. This can also give evidences of possible experienced issues and lesson learnt of similar application. This also allow Designer to understand whether the application is attempting to design is very similar to others already done or it is only comparable. If a very similar application exists the Designer have to check the relevant compressor layout and specify to Customer possible special requirements coming from these similar application such as damper on dedicated foundation or possible limitation on range based on previous experiences. In such case the bid stage can be considered closed and the work will restart when it became real.

On the contrary if a very similar application does not exist on archive it is necessary to enlarge the range of compressor data search and find anyway a comparable application. Then it is possible to go in dept on design data and results so that mechanical natural frequencies of the compressor system layout under design can be estimated (similar) interpolated (comparable) or extrapolated (prototype).

When these exercises are completed a comparison of the expected exciting harmonic frequencies components versus cylinder manifold expected mechanical natural frequencies can be made. The above activities are fundamental for the project since they allow knowing in the right moment, which is the right way to proceed in the real project to avoid vibration issues. For instance when these exercise indicate a big risk, may be better to know it at this stage, share it with customer and concur to choose proper solution. For instance concrete foundation instead of skid-base-plate or suction damper mounted on dedicate base instead of mounted on the compressor itself may be selected (Figure Nr.4). After these checks-evaluations, of necessary special solution on preliminary compressor layout the cost can be estimated. Bid stage is then completed.

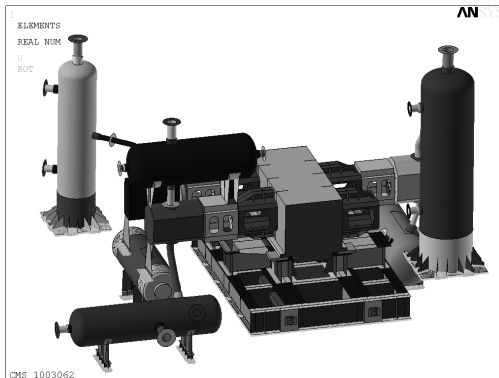


Figure 4: Example of compressor layout resulting from a big risk assessment

4 Real Project

When the project became an order the work will restart, from the results of this fast check.

The above pre-work exercise allows, when very similar applications are present in the archive, to start to derive the compressor general arrangement directly from previous positive experiences. In this case, only minor adjustments to take into account of minor difference between the applications are necessary. Then as soon the first preliminary compressor layout is available, the model necessary for the first step of dynamic response can be made.

On the contrary, when the compressor layout is only comparable or is a prototype the design must be made with special care and it is fundamental to

anticipate as soon as possible the study steps. In such cases the preliminary layout selection must be done till the beginning with a close cooperation among compressor manufacturer and vibration specialist. This in consideration that more the application is different from the previous ones more design time may be necessary to find an adequate solution. Considering that the achievement of the compressor equipments manufacturing schedule is a top priority, a possible way to limit the risk is to immediately submit the cylinder manifold system to a preliminary forced dynamic response.

4.1 Damper Design and Supports

Using the compressor data sheet, as sold, the initial basic damper data calculated during bid stage is updated. Dampers are the most efficient means to reduce pressure pulsations induced forces on the connected piping but especially the suction ones, being usually mounted directly on the machine, are often the element more sensitive to vibrations. On the basis of main parameters (e.g., diameter, length, nozzle thickness, number of supports, etc.), it is possible to estimate the 1st mechanical natural frequency of the manifold system.

This can be evaluated using a regression law program based on a historical database and adjusted taking into account of the specific dimensions.

The same program search calculated data from historical database gives also evidence of the application more similar and relevant lowest calculated cylinder manifold frequency.

The above result is then compared with the highest significant exciting harmonic of the compressor (generally the 2nd one) applying a safety margin of 20%. This preliminary design allows the evaluation of alternative compressor layouts (e.g. with one or more supports) to validate Suction dampers supports and then to submit to the study a compressor layout with high possibility to be adequate. Remembering that shaking forces are generated by the action on geometrical discontinuities the damper should have cylinder connections at the centre of the damper, when necessary internal pipes can be used.

Once the preliminary compression system drawings are available, a preliminary study can be performed with the standard program for complete acoustical analysis⁴.

The study considers the complete geometry of the damper so that to first validates the results with the endless line resulting from the initial design (residual pulsation 70-80% of allowable pulsation). In addition, replacing the piping with a resonant length is possible to estimate necessary orifice pressure drop and consider it on compressor performance calculation.

This study also evaluated the need of orifices multi-bore type, instead of the classic single hole depending upon gas flow conditions, maximum harmonic component to be dampened etc..

This simplified analysis drastically reduce the impact of problems detected during the final acoustic study and in most of the case represent the only way to meet scheduled contract delivery when necessary customer data are not available or very preliminary. Since the geometry of the damper is defined it is also possible to determinate with sufficient accuracy the amplitude and spectrum of damper shaking forces for the forced cylinder manifold study. Gas loads acting on cylinder ends are obtained from compressor design calculations. At this point the system is ready for the preliminary dynamic analysis validation.

5 System Model

All the steps and considerations done during the bid phase for the selection of the compressor, the preliminary design of dampers, the definition of a preliminary layout and the performed risk assessment, allow in a very early stage of the design the availability of sufficient and accurate data. These data are fundamental to build a very detailed model of the system capable to simulate its global dynamic behaviour.

This remembering that purpose of this analysis is to verify that the system works in safety condition in each running condition and the vibration of the system and the relevant fatigue stresses generated are always under the allowable limits. The best way to perform this task is trough a finite element model.

5.1 The FE model

The main step to build a finite element model that is able to simulate the real dynamic behaviour of a complex system like a cylinder manifold is to carry out an accurate structural evaluation of the system giving special attention to components that affect the dynamic behaviour. At the same time applying suitable simplifications is possible to achieve an appropriate balance between accuracy and rapid calculations. The performance of modern computers gives reasonable execution time even with the use of complex, accurate models. Anyway, the decision on how to develop a model for a cylinder manifold analysis that consider also the complete frame of the compressor, the dampers and part of the plant

connected to the machine has to be driven essentially by the goals to be reached.

For the compressor, the essential achievements are the correct evaluation of vibration amplitudes. In fact, the various parts of the compressor have been dimensioned in advance with all the stress analysis performed during the design of the compressor defining both the loads limits and the vibration limits to assure safety and operability. The same is not true for the dampers that are often different each time. For these equipment and their supports, it is necessary to verify not only the vibration amplitudes, but also the relevant alternate stresses. Based on the above, a good compromise to model a complex system likes the compressor, the skid (if present), the dampers and part of the plant connected is the use of shell elements. This method is very good on simulating components with small thickness compared to other geometric parameters (e.g., parts made from sheet metal) such as damper models, which are the most important components from a dynamic point of view. It is known that when applied to compressor parts it introduces a significant approximation on stresses evaluation. However considering that the study purpose for compressor parts is more interested in vibration amplitudes than in the stresses, the main objective of this part of the model is to describe at the best the mass and the stiffness distribution so that to allow a very good evaluation of mechanical natural frequencies and mode shapes. In conclusion the shell model approach, allowing at the same time an easy use of enlarged model to include all significant parts of the cylinder manifold system and maintaining the model within an acceptable level of complexity, reach the scope limiting the costs. Furthermore, this kind of elements is more flexible to changes allowing the investigation of several types of modifications without requiring complete or partial model rebuilding. For the above reasons shell element should be preferred. The development of a shell model capable to really simulate the dynamic behaviour of the system maintaining acceptable costs, require a deep standardized procedure that allow an almost automatic building of the model. This is possible starting from 3D CAD model of the compressor (Figure Nr.5), eliminating from the CAD model all the parts that are not related to the analysis (Figure Nr.6) and defining all the rules to distribute thickness and shell of each single part of the machine. Rules have also to define areas where the loads must be applied, all the constraints and mass distribution of parts not modelled (pistons, rods, bearings, bolts, etc. (Figure Nr.7).

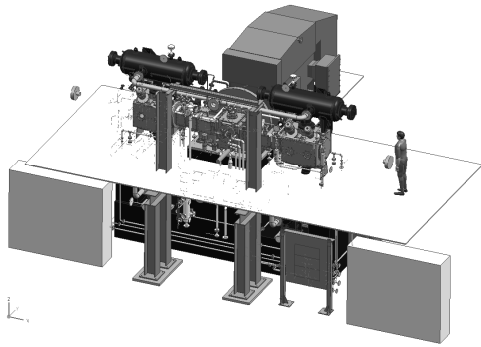


Figure 5: 3D CAD compressor model

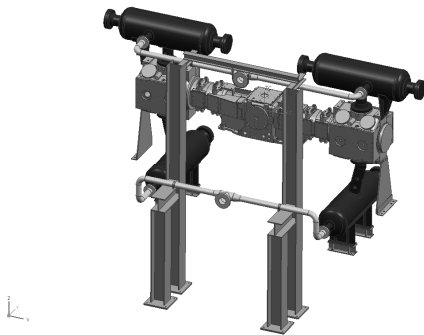


Figure 6: 3D CAD model - "cleaned"

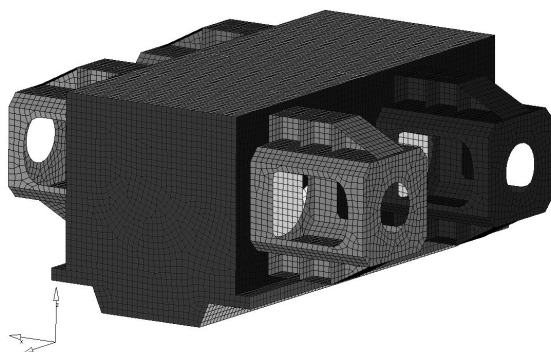


Figure 7: FE frame model

The procedure needs to be tuned by several deep analysis to define how to schematize the various part of the compressor with particular attention to the bolted junctions between cylinders, distant pieces, crosshead guides and compressor frame, that give a fundamental contribute to the global stiffness of the system. These conjunctions representing model discontinuities gives an important contributes to cylinder stretch phenomena. Proper modelling of these conjunctions producing a real deformation (i.e. experimentally verified on field) can be only made by a standardized procedure that starting from manufacturing dwgs. data such as number, diameters, length, distribution of the bolts and flange dimensions translate these junctions in equivalent springs elements (Figure Nr.8).

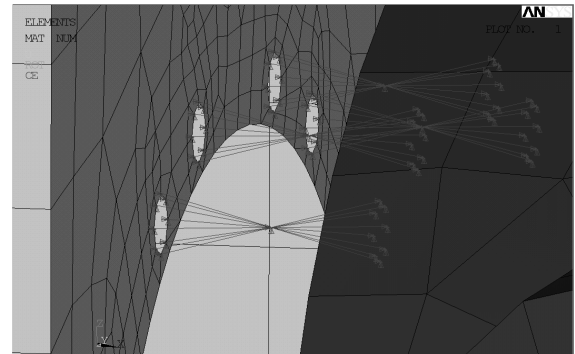
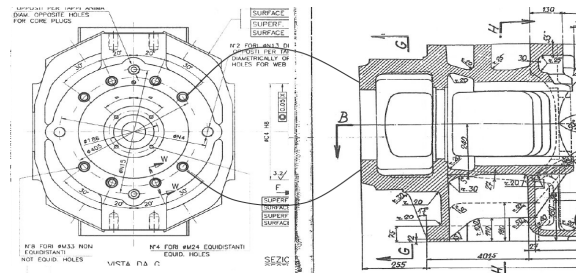


Figure 8: Junction schema

The tune of a process so complex requires a very deep knowledge of each single part of the compressor and the availability of a large amount of manufacturing and field data. This can be achieved only with synergy and cooperation between Compressor Manufacturer and vibration Specialists. All the mentioned points are the basis for the frame models database building, containing well-tuned models that can be reused every time the same compressor has to be analyzed. The only parts of the compressor model that often need to be replaced are the cylinders, but also these can be stored in a database and re-used. The other parts of the system that need to be considered in the analysis have to be added to this basic model starting every time from the drawings. Again, paying a great attention to the joining of the various parts. The models of the others equipments are easily and properly modelled by shell elements (Figure Nr.9). Remembering that constraints strongly affect the natural frequencies values the choice of the right set of constraints is a fundamental. Experience coming from field assistance and measurements play a great role, for instance indicating that restrains at the foundation should be considered only around the bolts interested section.

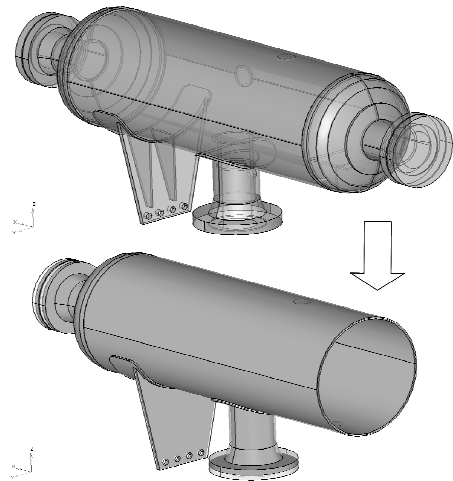


Figure 9: Damper model

Then the last effort is the introduction of the right constraints in the model (Figure Nr.10) and to apply all the exciting forces.

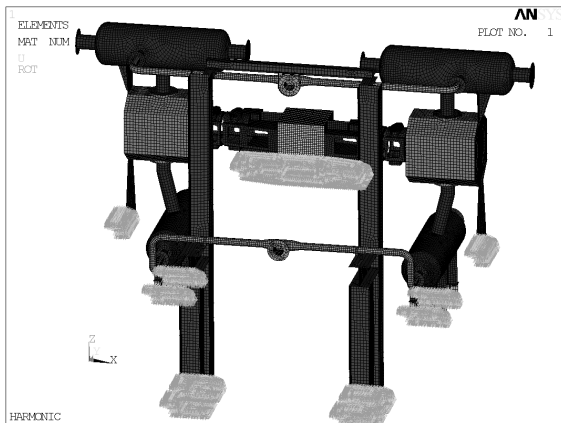


Figure 10: FE system model with constraints

Of course all the exciting forces have to be applied on the model at the right locations (Figure Nr.11).

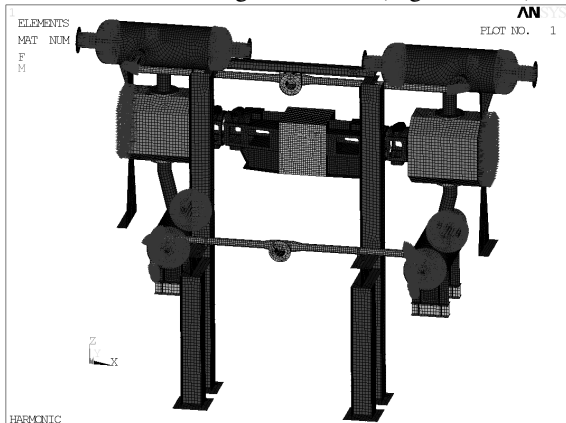


Figure 11: Forces applied on the model

6 Dynamic Analysis

6.1 Frequency analysis

This analysis consists in calculating the mechanical natural frequencies and the mode shapes of the cylinder manifold system with the initial purpose to

achieve a minimum mechanical natural frequency of the system at least 2.4 times rated speed (separation margin of 20% from 2nd harmonic component also indicated in the 5th edition of API 618¹). When this is not feasible (e.g. high compressor speed on elevated skid platform), detected mechanical natural frequencies must be anyway above the 1st harmonic component and sufficiently detuned from the 2nd harmonic (i.e. at least 20% of separation).

Evaluation of separation margin for higher harmonic components of exciting forces requires long experience on this kind of analysis. For instance, relatively low shaking force amplitude having a high frequency component, which may appear negligible, can in reality be very dangerous. In fact when exciting frequency exactly matches a mode shape of which deformation act in the same direction of the exciting forces, mechanical resonance occur and the risk that the forced response study results in excessive vibrations is very high. Therefore, special care must be taken in this step so that to apply all necessary possible modifications and stop this simple calculation, which is the base of forced response, only when all the most critical mechanical natural frequencies are sufficiently detuned from significant harmonic components of calculated exciting forces.

6.2 Forced response

The forced response³ of the described system is performed using as input data the harmonic components of all the exciting forces defined by the pulsation study, cylinder gas loads and other dynamical loads. This allows the calculation of vibration amplitudes and stresses for each mode, along with the dynamic reaction forces on the cylinder and on the discharge bottle supports.

The forced harmonic response is calculated for each possible resonance condition caused by mechanical natural frequencies and exciting force harmonic components. By the Campbell diagram correlation between mechanical natural frequencies and the exciting harmonic frequencies is possible to highlight where resonance may occur. The analysis is usually carried out for each harmonic, around (e.g. +/-10%) the nominal frequency (RPM). An important aspect in performing a forced mechanical analysis is the evaluation of the damping coefficient that is influenced by typical structural material and connection between components (joints, gasket).

Standards, piping and compressor systems typically have damping ratios from 1% - 5%, and hence amplification factors of 10 to 50. Field experiences indicated that it is conservative to only include the structural damping of the material in the standard forced response analysis. Therefore when possible damping value derived from field measurements are preferred.

The model used to evaluate the forced response of the system at the frequency is based on the uniform structural damping model³.

6.3 Analysis of results

Typical results of forced analysis are as follow:

- Cyclic stress (Figure Nr.12) to be compared with the allowable value, (API¹ cyclic stress limit 180 N/mm² (26000 psi) reduced to consider the stress concentration factors and safety factor)
- Vibration amplitude (Figure Nr.13) to be compared with allowable manufacturer for cylinder-frame-spacer block vibration levels (i.e. alarm limits with an adequate margin). For damper and piping limits such as API¹ or other based on experience and field measurements can be used

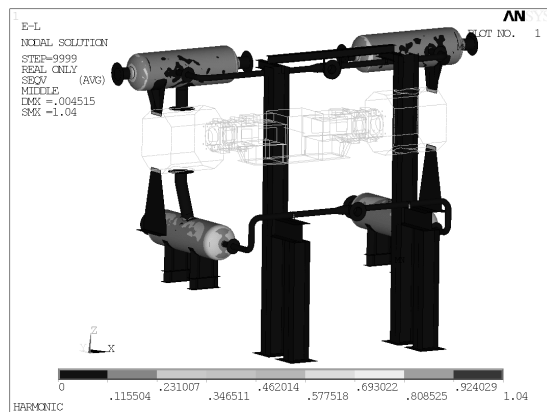


Figure 12: Cyclic stress

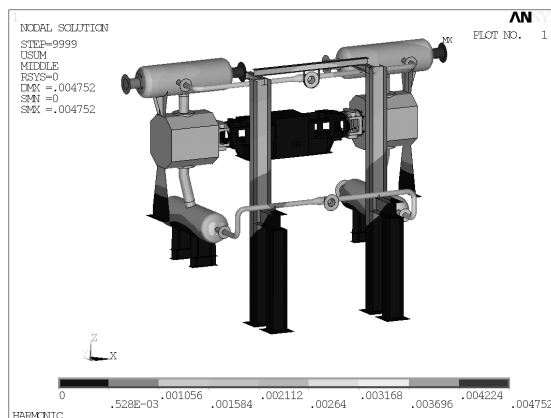


Figure 13: Vibration displacements

- Other available results may be reactions due to vibrations transmitted by the compressor system to the foundation that are very important to consider especially in case of a skid mounted (Figure Nr.14)

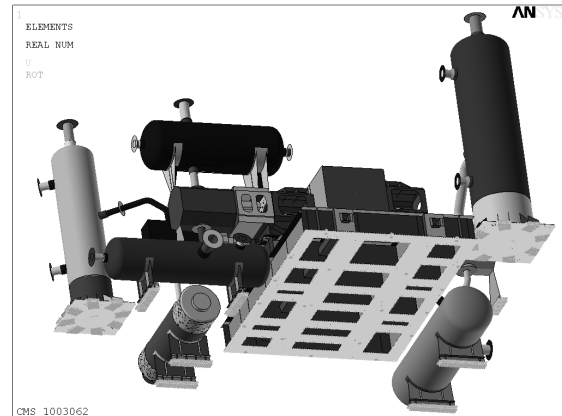


Figure 14: Compressor constrains reactions

6.4 Typical modifications

From the preliminary forced response, some modifications to the system may be required. However that this is done on an early stage of the project, then possibility to act on the system design is large. Vice versa, in case this is done when all customer plant data are available and exciting forces fully defined, the system design is generally at a stage where only minor modifications can be done. Therefore, in case of exceeding of allowable vibrations or cyclic stress it is necessary to iterate between acoustical analysis and cylinder manifold system analysis to find an acceptable solution. Typical modifications directed to modify the mechanical natural frequencies of the system (i.e. to detune them from specific exciting force frequency component) are:

- To work on the cylinder supports (Figure Nr. 15) increasing the stiffness with some reinforcements
- To add structures to increase efficiency of the suction damper supports (Figure Nr.16, 17).
- To reinforce foundation or skid (Figure Nr.18)
- To support some of suction dampers in a separate foundation (Figure Nr. 4,14)

When the above is not sufficient further possibility of exciting forces reduction are:

- To increase damper efficiency to reduce pressure pulsation effects and shaking forces
- To distribute as better as possible the gas loads in terms of amplitude and harmonic contents
- To increase mass balancing in the compressor

At this point the first step is concluded and the study re-start when all info coming from the customer is available. At the same time the compressor layout and damper manufacturing can proceed.

7 Final Acoustic & Mechanical Studies

When the entire plant system is available, the final acoustic and mechanical analysis is made considering all possible operating conditions, including speed variation, capacity control range, compressors running alone or in parallel, etc. All significant components, such as piping, cylinders, valves, orifices, dampers, coolers, separators, etc. till a proper boundary point are included in the study. Pressure pulsations and shaking forces acting on the components are then re-calculated at all significant points so that once upon reduced to acceptable levels they are used as input for the final mechanical studies. At this point, if necessary, the model is updated considering manufacturing dwg.s and inserting suitable part of connected piping (generally up to the 2nd support upstream-downstream). Using the updated model and exciting forces, the forced response is repeated and if necessary further adjustments are carried out. Generally when the described procedure has been fully applied; these final analyses only identify minor adjustments on connected piping supports and structures. Typical modifications at the compression system, with minor impact on adopted standard solution (e.g. foreseen plate on damper to connect structures), can be implemented also at late stage of the project just replacing simple separate parts (e.g. adjustable bolted damper saddle).

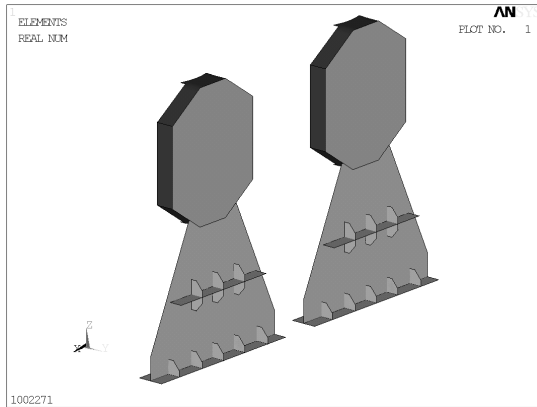


Figure 15: Cylinder supports reinforcement

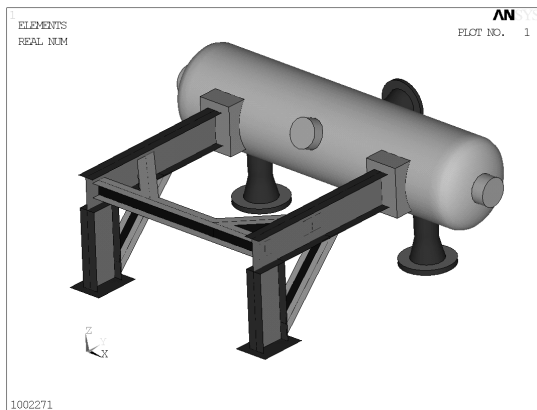


Figure 16: Adjustable-bolted Damper support

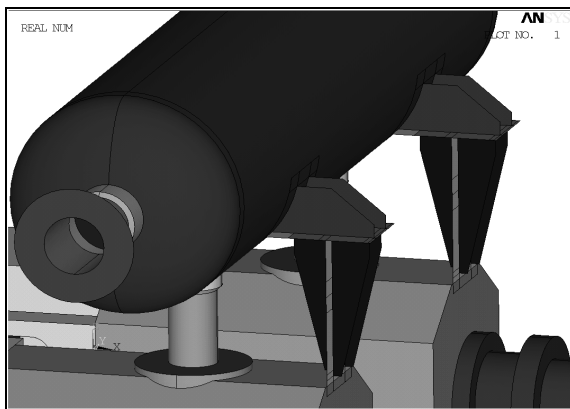


Figure 17: Adjustable-bolted Damper saddles

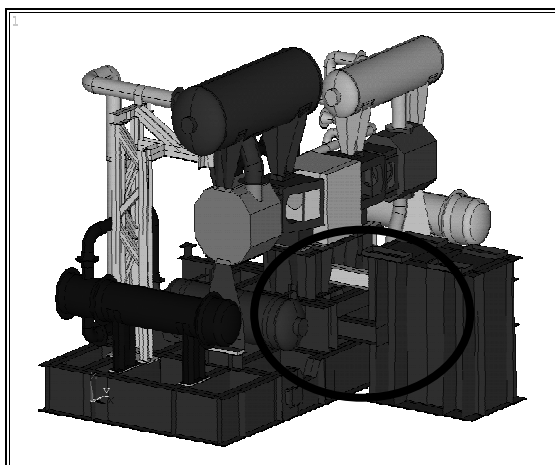


Figure 18: Connection between compressor bases

8 Conclusions

For API 618 approach 3 applications the design of the compressor manifold system is fundamental for the safety, reliability and operation of reciprocating compressors. Pulsation dampers are the most effective elements to prevent piping vibrations but at the same time they are often the element most sensible to vibrations. Specific analyses have to be performed to properly design these components from the beginning of the project in order to satisfy API Approach 3¹ requirements and to avoid major modifications that could jeopardize the contract delivery date or be discovered when the compression system is manufactured. Taking into account that, in most cases, customer plant data needed for damper fabrication validation is not available on a time frame that matches the compressor design delivery schedule, it is necessary to minimize potential risks. Manufacturer experience on “very similar” application can minimize the risk. Risk assessment represents an important step to evaluate the risk and decide the project path. However when the layout application is only comparable to other previous experience only the studies can validate the Design. For these reasons the present paper suggest to perform the cylinder manifold analysis in an early stage of the project so that to drive the necessary change till the beginning with adequate model accuracy to properly predict vibration and cyclic stress level. Then design must be dully followed during the job so that any significant change in respect to the preliminary study is evaluated. Finally the analysis has to be repeated when all info necessary from customer is available. Experience indicates that when this procedure is followed, the final studies will only require minor modifications without impact on project delivery. On the contrary, making the study only when all data are available (i.e. single study step) reduce the study cost but can exposes the project to big risks. Considering the cost and the lifetime of some application the above have to be evaluate carefully. The CAD programs now available allows the FE model to be built directly from the manufacturing drawings, thus avoiding possible translation errors and drastically reducing the cost by model database. Finally, models can be improved by validation using field measurements. All the above need a very strong synergy and cooperation between Compressor Manufacturer and vibration Specialists. Finally the project success depends from all involved disciplines that only working together can meet contract delivery and safe-smooth plant operation.

9 Acknowledgments

The authors wish to thank GE Oil & Gas for permission to publish the information reported in this paper.

References

- ¹ API 618 STD 4th and 5TH Editions, June 1995 - December 2007, "Reciprocating Compressor for Petroleum, Chemical and Gas Industry Services" American Petroleum Institute
- ² Giacomelli E., Passeri M., Giusti S., Zagli F., Generosi S., 2004, "Modeling of Pressure Pulsations for Reciprocating Compressors and Interaction with Mechanical System", Proceedings of ESDA, Engineering System Design and Analysis, 19-22 July, Manchester, UK, The American Society of Mechanical Engineers
- ³ Giacomelli E., Passeri M., Romiti M., Generosi S., 2006, "forced Response of cylinder manifold for Reciprocating Compressors applications. Proceedings of ESDA 2006: Eng System Design Analysis 4-7 July 2006
- ⁴ Giacomelli E., Passeri M., Battagli P., Euzzor M., Pressure Vessel Design For Reciprocating Compressors Applied in Refinery and Petrochemical Plants-PVP2005-71292, Proceedings of PVP conference 2005, Pressure Vessel and Piping July 17-21, 2005, Denver, Colorado, USA The American Society of Mechanical Engineers



Heavy & unusual wear of PEEK¹ piston rings in a lubricated air-cooled high-speed and high-pressure compressor

by:

HOELTL Georg

R&D Department

Leobersdorfer Maschinenfabrik GmbH & Co.KG (LMF)

Leobersdorf

Austria

georg.hoeltl@lmf.at

**7th Conference of the EFRC
October 21th / 22th, 2010, Florence**

Abstract

For reasons of the simple design & low production costs most of the biogas compressors are designed as high-speed non API machines. The trend is to go for small and local production plants which are very flexible towards the quantities of biowaste. The compressors are designed as lubricated or non-lubricated machines.

The type of tribo-interface and the lubrication are important factors for longevity. The presented report shows a piston ring failure in a 3-stage, lubricated balanced opposed compressor and the interdisciplinary investigations in the fields of thermodynamics, tribology and material science. Different types of piston rings and lubricants of different manufacturers were used and tested during operations. The unusual failure history occurred on average compression temperatures of 120°C and pressures up to 250bar.

1 Introduction

The constantly growing environmental consciousness and the need to reduce greenhouse gases lead to a growing market for biofuels. Bioethanol and biodiesel are replacements for the conventional liquid fuels. Biogas is used for gas engines, heating systems. A noticeable quantity is also feeded in pipelines. It is composed of about 95% of methan, 2% of carbon dioxide and a variety of gases which results from the fermentation of biowaste.

This special gas market is growing around metropolitan areas where a large quantity of biowaste has to be recycled. The outcome of the fermentation process is then conditioned and compressed to 200 – 300bar for an easy and economical use in different storage systems and as fuel for gas engines. The customers demand is a small and easy to service system. Those systems are in most cases high-speed non-API compliant compressors with up to 4 stages. The first LMF biogas-compressor was delivered to a Scandinavian customer. Some severe and unexpected problems occurred soon after delivery.

2 Description of the failure

Fig.1 shows the customers specification charts.

Number of stages	3	[-]
Number of axis	2	[-]
Design	hor. opp.	[-]
RPM max.	1720	[1/min]
RPM min.	900	[1/min]
Flow volume	400	[Nm ³ /h]
Suction pressure	2-4	[bar]a
max. pressure required	300	[bar]a
max. pressure effective	220	[bar]a
Cylinder cooling	air	[-]
Stage cooling	water	[-]
Biogas acc. SS 155438 ¹		

Fig.1: Specification table

Because of the high speed of the compressor and the need to regulate the mass flow, the compressor was coupled with a belt drive to the electric motor and driven by a frequency converter. No distance pieces between compressor and cylinders were used in order to produce a small and reasonably priced machine. The lubrication of the cylinders and the crankcase were therefore carried out with the same oil.

The general layout of the system is shown in fig.2.

Each compression stage includes a water cooler and a coalescing filter for the oil separation.

After 500 working hours the compressor showed an alarming vibration level and a severe power loss in

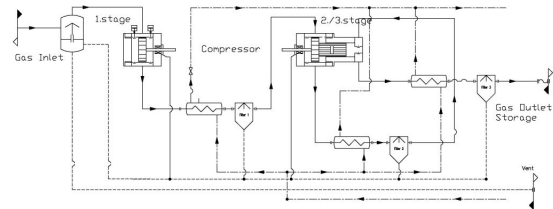


Fig. 1: Simplified general layout of the compressor



Fig. 2: Melted piston rings of the 3rd stage

the 3rd stage. The piston rings in this stage (cf. fig.3) presented a strong wear on the surface. The piston rings lost their sealing function and the oil consumption went up. After several service attempts the case was transferred to the R&D department for an in-depth failure analysis which wasn't completed until April 2010.

3 Description of the failure analysis

The following test and calculations were carried out during the failure analysis:

- Recalculation of supplier parts and re-simulation of the machine
- In-depth gas analysis
- Measurements of temperatures with the build-in temperature transmitters and verification with a thermographic camera
- Recording of the pressure in the different stages. Both build-in pressure transmitters and external pressure transmitters were used
- Measurement of the differential pressure on the coalescing filter
- Measurement of the vibration level on the compressor and pipings

- Chemical analysis of the particles from the packings and the cylinder rings and analysis of several oil samples
- Optical check of the cylinder surfaces and measurement of surface wear

4 Results

4.1 Recalculation of the compressor

Most of the parts of the compressor were recalculated during the failure analysis in order to avoid any undue influence from the original design. The in-house recalculation couldn't show any fundamental differences compared to the original one.

4.2 In-depth gas analysis

An in-depth gas analysis was carried out according ISO 6974² and showed the following results:

components	percentage [%]	error [%]
methan	96	±1,9
nitrogen	1,8	±0,1
carbon dioxide	1,8	±0,1
oxygen	0,4	±0,1
sulfur	< 10ppm	-
ammonia	< 5ppm	-

Fig. 3: Biogas composition

4.3 Measurements of the temperatures

The thermography measurements (cf. fig.5, 6, 7) were taken with a Testo 881 camera.

The stage temperatures (cf. Fig.8) were recorded with the build-in ABB TR04 EEx (PT100) temperature transmitters.

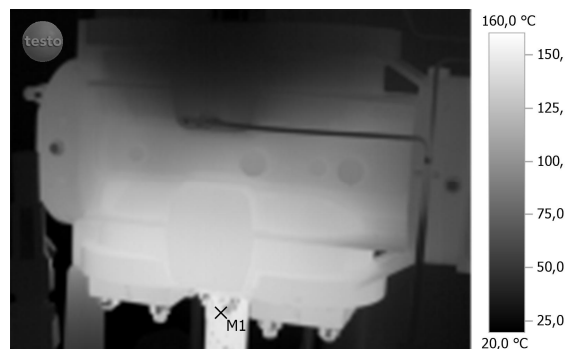


Fig. 4: Thermography of the 1st stage

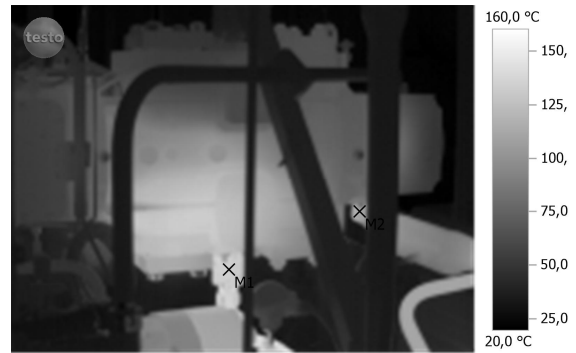


Fig. 5: Thermography of the 2nd and 3rd stage



Fig. 6: Thermography of the 3rd stage

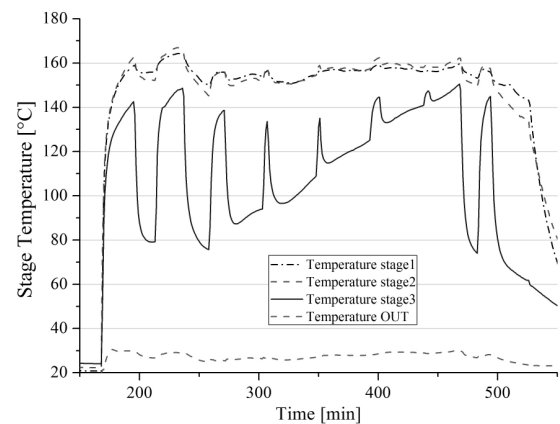


Fig. 7: Temperature of the stages recorded with the build in temperature transmitters

The temperatures are in the range of the calculated values. Stage 1 and 2 have their maximum at 165°C, the 3rd stage doesn't exceed 150°C.

4.4 Recordings of the pressures in the stages

The pressure values were measured with an ABB K51EEx pressure transmitter.

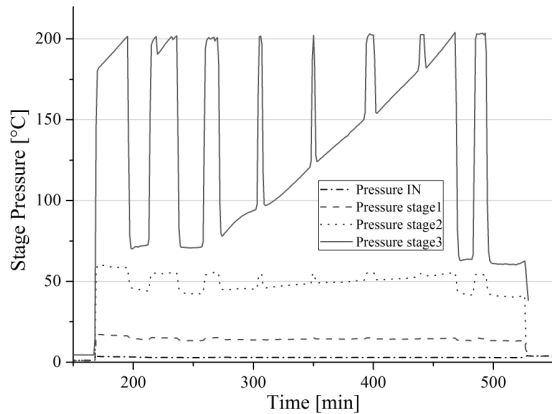


Fig. 8: Stage pressure recorded with the build in pressure transmitters

The pressure fluctuations shown in fig.9 occur during the filling of the storage system. The storages are divided into several bundles. When the first bundle is at its maximum pressure the system changes to next empty one. The peaks in fig.9 are due to the temperature compensation during the filling of the storage system. This effect occurs because of the decreasing temperature in the bundles and therefore, a decreasing pressure which has to be compensated.

4.5 Measurements of the differential pressures in the filters

1. stage	2,15 bar
2. stage	1,95 bar
3. stage	1,60 bar

Fig. 9: Differential pressure on the coalescing filters

The coalescing filters with a mesh size of 25µm are showing considerable deviations of the differential pressure compared to the design values, which should be no more than 400mbar.

4.6 Measurements of the vibration level

Some of the measurements show very high vibration values. A peek is found at the outer point of the cylinder of the 2nd and the 3rd stage. The values are RMS (Root Mean Square) values.

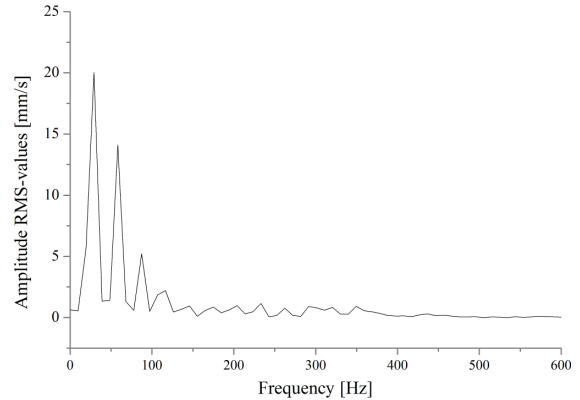


Fig. 10: DFT x-axis cylinder 2nd/3rd. stage

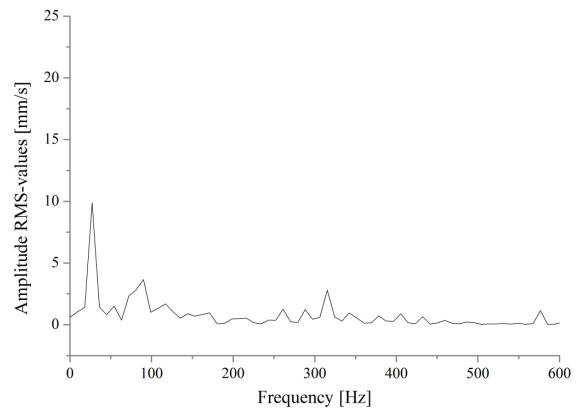


Fig. 11: DFT y-axis cylinder 2nd/3rd. stage

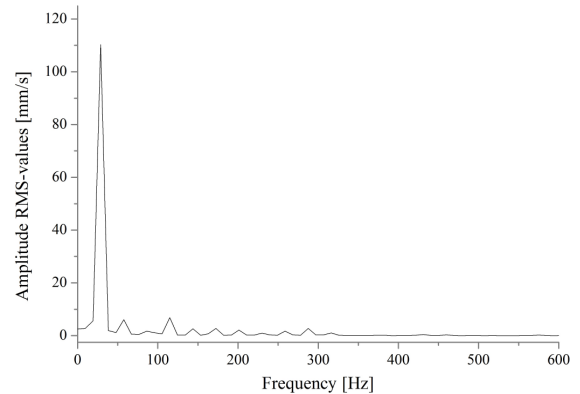


Fig. 12: DFT z-axis cylinder 2nd/3rd. stage

4.7 Chemical analysis

chem. element	classification
Cu, S	copper sulfide due to sulphide corrosion of copper materials
Fe	steel particles
C	PEEK material

Fig. 13: Materials analysis with SEM

Particles and oil samples were taken from the compression and the valves chambers. Those were analysed with an optical and a SE-microscope. The density, the acid value and the water content were measured. The oil samples were also analysed with infrared-spectroscopy.

	acid value [mg KOH/g]	water content [mg/kg]	density [g/cm ³]
ref. oil	0,27	430	0,956
used oil	0,28	550	0,955

	kin. viscosity [mm ² /s]		VI [-]
	@40°C	@100°C	
ref. oil	107,2	10,19	67,4
used oil	103,8	10,06	69,2

Fig. 14: Chemical analysis of the oil sample of the 3rd stage

4.8 Optical check

The optical check and the measurement of the cylinder surfaces didn't show any wear.

5 Discussion of the results

No noticeable deviations from the specifications were found during the gas analysis. Some traces of sulphur initiated the formation of hydrosulphide and a slight corrosion of the copper sealings. The corrosion didn't cause any severe damage to the compressor parts.

The recorded stage temperatures were proved by the thermocamera and didn't show any unexpected values except for the 1st stage. The values of the boundary layer of the piston rings, the cylinder and the piston couldn't be defined.

The pressure transmitter values didn't register any abnormality in the first place. On closer inspection the differential pressures on the coalescing filters were 10times higher than calculated. Those values were in the end responsible for the increased power consumption and higher temperatures in the 1st stage. Because of the overall low temperature level it didn't cause any major damages.

The vibrations were recorded in order to exclude damages on the compressor parts and pipings. In the x- & y-axis the values were in a normal range whereas the values for the z-axis (axis of the crankshaft) were truly alarming. Fig.13 shows a peak value at 28,7 Hz (1720rpm) which corresponds with the rotation speed of the compressor.

These vibrations weren't observed at the LMF test facility. The first suspicion was a transport damage which was observed in other cases but couldn't be proved in this one.

The chemical analysis showed no external particles in the compression chamber. All chemical elements (cf. fig.14) were identified as particles from piston rings and cylinder wear. A slight sulphide corrosion was observed on the copper sealings. A heavy abrasive wear could therefore be excluded. The oil samples from the compression chamber and the valve compartment didn't show any major deviations compared to the reference sample. The deterioration of the oil could therefore be excluded.

The optical check and the measurement of the cylinder surfaces didn't show any wear at all and no machining texture. In this case the cylinder wasn't honed, there was no sign of the typical plateau finish. This decision was made in the past because of the slower piston speeds and because of economical reasons. A strong correlation between compressor speed, oil quality and surface texture was observed.

At the same time all supplier parts were also recalculated and partly redesigned. The problem with the coalescing filters couldn't be completely solved until now. The test of 2 different designs and meshing sizes didn't solve it.

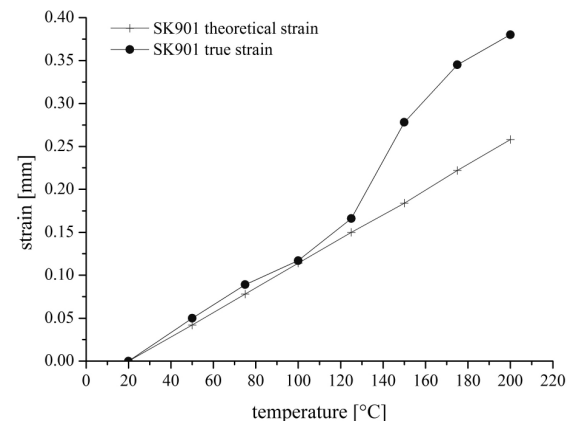


Fig. 15: Comparison of theoretical and true strain of a PEEK SK901 material

The first hint for the damages was given by the piston ring supplier. The suggestion was to redesign the grooves of the piston rings and their shape. Fig. 15 illustrates the differences between the theoretical strain, which was given by the PEEK material supplier and the true strain recorded by the ring supplier. A linear strain behaviour was observed up to 130°C. At 140°C the deviation is 10% and increases up to 55% at 200°C. Because of the strong heat expansion, the rings get stuck in the groove.

An axial movement wasn't possible anymore and the piston rings expanded in the radial direction. The increasing stress induced higher friction and lead to a collapse of the tribosystem and the melted rings.

6 Measures

The uncertainty of the real temperatures in the interface of piston, piston rings and cylinder lead to a new piston ring and piston groove design with the assumption of a higher temperature level (+15°C). The viscosity of the oil was also increased from an ISO VG100 to an ISO VG220 for the cylinder lubrication as well as for the crankcase lubrication. The oil feed rate was also adjusted. As already mentioned the filter problem is still under investigation but ameliorated with the new design. After the modification of the compressor, verifications were made every 1000h operating hours. We observed a dramatically decrease of vibrations which can be explained by the improved pressure ratios. The pistons rings didn't show any wear.

7 Conclusion

A frequent compressor damage including heavy piston ring wear and a high vibration level on a high-speed non-API compliant biogas compressor leads to an in-depth failure analysis. All parts of the compressor were recalculated or partly redesigned. In the meantime various tests were made including a thermography of the cylinders, chemical analysis and pressure and vibration measurements. In the end the test couldn't give satisfactory results. The solution was given by the piston ring supplier who made an in-depth analysis of the PEEK SK901 material and proved a strong deviation of the theoretical and the true heat strain behaviour of it. The dimensions and the shape of the piston rings and the piston grooves were improved and the oil viscosity was adapted to those conditions. Since then the piston rings didn't show any abnormal wear.

8 Forecast

For a better understanding of more complex tribosystems LMF has started a series of applied and theoretical research projects by the European Union partly funded. Further projects will be concentrated on simulation with FEM and CFD methods in order to create a strong tool for the engineering and to reduce the risks of machine failures.

9 Acknowledgements

The author would like to thank Stasskol for the kind permission to use and publish their test results.

References

-
- ¹ SS 155438, 15.09.1999, Motor fuels - Biogas as fuel for high-speed otto engines
 - ² ISO 6974, Natural gas - Determination of composition and associated uncertainty by gas chromatography



Piston rod vibrations of excessive amplitudes on a CO₂ compressor - Simulation, Measurement and Reengineering to solve the effect

by:

Gabriel Roman

Heumesser Thomas

R&D Department

Leobersdorfer Maschinenfabrik GmbH & Co.KG (LMF)

Leobersdorf

Austria

roman.gabriel@lmf.at

thomas.heumesser@lmf.at

**7th Conference of the EFRC
October 21th / 22th, 2010, Florence**

Abstract

For piston compressors, resonance behaviour caused by vibrations during operation is one of the main reasons for either a dynamic breakdown of the piston unit components, or an increase of wear of sealing and guiding rings. An important indicator for evaluating the operating conditions of that kind of compressors, are the characteristics of the piston rod deflection. Especially in the case of larger pistons with a high diameter-length-ratio and increasing pressure or high molar mass of gas being compressed (for example CO₂), amplified and, in certain circumstances, continuous by increasing deflection of the piston rod takes place. This effect cannot be verified completely with the help of a conventional dynamic simulation using continuous and idealised characteristics of the gas forces only. The missing link is to be found in the additional effects which occur within the gas during the charging and discharging process.

This paper deals with the influence of the gas impulses induced by the opening and closing action of the valves on the vibration behaviour of the piston unit. Furthermore, how this influence becomes noticeable by means of real measured characteristics of the piston rod deflection and, finally, what design features are recommended to reduce the impact of these effects.

1 Introduction

In a process gas compressor (designed according to API 618¹) for the compression of CO₂, excessive vibrations in the first stage became apparent. The compressor is a balanced-opposed, horizontally, double-acting machine with four axes, crosshead guidance and non-lubricated pistons. The excessive vibrations caused the compressor to shut down - to avoid structural damage - as soon as the piston rod deflection exceeded 1.2 mm. This meant that the maximum structural load was limited to 60 %, so that the output was far less than the contractual amount which, of course, was unacceptable to the customer who requires full load delivery.

2 Starting Basis

The compressor operates at a rotary speed of 425 rpm and has a piston stroke of 250 mm. It compresses CO₂ with a molecular weight of 44 g/mol.

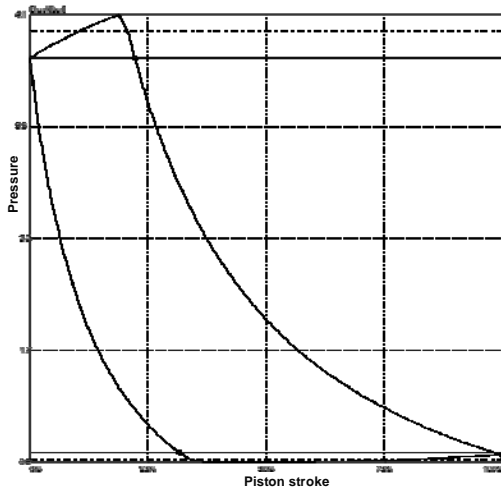


Figure 1: P-V Diagram

This study deals with a compression ratio of 3.9:1 (i.e. suction pressure of 0.97 bara to discharge pressure of 3.78 bara), at a discharge temperature of 139 °C. The initial response pressure difference is 0.05 barg for the suction valves and 0.2 barg for the discharge valves.

The double-acting piston of the first stage, moving horizontally, has a very unfavourable ratio of piston diameter to guidance length of approximately 3.1 (i.e. Ø992mm to 318mm). The three guiding rings of the piston are arranged centrally, so that they do not mask the valve slots when piston is in motion to avoid unnecessary wear. Both end faces of the piston are nearly planar, with a slight incline of 0.5°. The piston rod has a length of 2150 mm and a diameter of 80 mm.

The connection between piston rod and piston is a bolted fastening with reduced shaft with pre-loading by means of a Superbolt nut.

The gas loading and discharging of each compression chamber take place via four suction and four discharge valves. According to the regulations of the API 618, all suction valves are mounted on the circumference on the upper half-section and all discharge valves on the bottom half-section of the compression chamber. The valve slots are elongated holes of which are the tops flush with the end faces of the compression chamber. Thus the valve slots are completely masked by the piston in the dead centers.

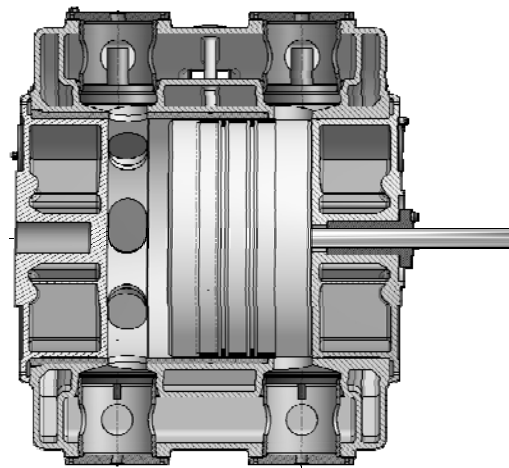


Figure 2: Cross-sectional view of the 1st Cylinder unit

The piston unit of the first stage, consisting of the piston, piston rod and crosshead, has an overall weight of approximately 680 kg.

In the prevailing operating conditions and kinematics, the following gas-, dynamic- and piston rod forces occur at the initial stage during one crankshaft revolution:

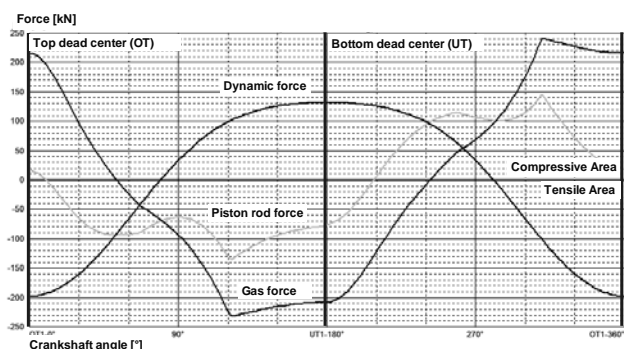


Figure 3: Gas-, dynamic- and piston rod forces

3 Operation Analysis

In order to have a basis for problem analysis, first the predominating operating conditions must be

determined. This is done by using four strain gauge measuring strips (DMS). They are arranged in pairs longitudinally opposite each other (Top-Bottom-Left-Right) at a chosen measuring point in the piston rod to measure both horizontal and vertical vibrations.

The measurements with DMS have given the following characteristics:

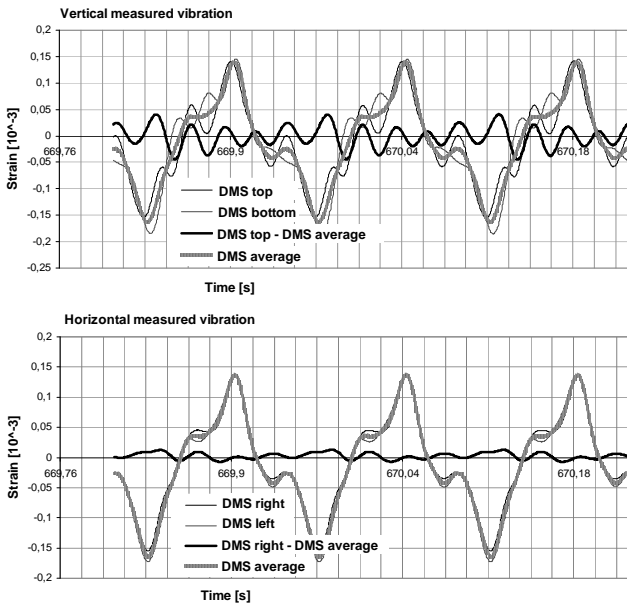


Figure 4: Characteristics of measured horizontal and vertical vibrations

The progressions of each individual DMS measurement represent total values that are obtained from the superposition of either tensile stress or compressive stress and bending stress. The amount of horizontal and vertical bending stress only therefore results from the difference between the measured total values of the respective opposite DMS:

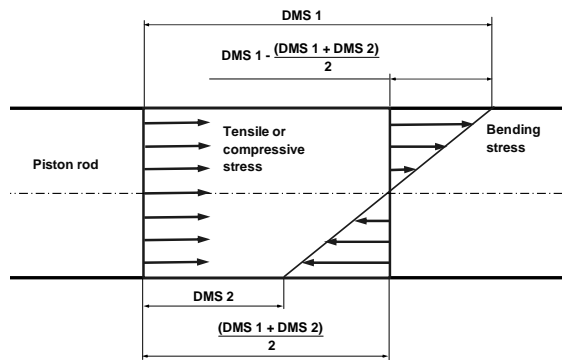


Figure 5: Superposition tensile/compressive stress and bending stress

The excitation frequency of 1st order can be calculated by means of the motor speed. At 425 rpm this is approximately 7 Hz. This means that the compressor cycles seven full turns per second, thus each revolution takes about 0.14 seconds.

The sinus oscillation resulting from the crankshaft rotation can be superposed with the measured vibration progressions being synchronised over the time and crank angle, which gives the right positions of the top (OT) and bottom (UT) dead centers.

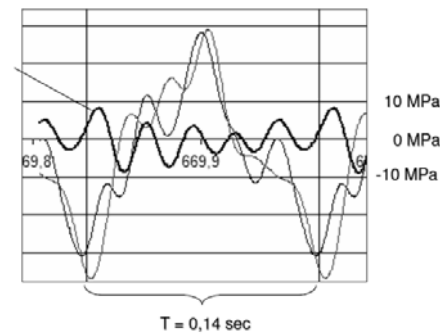


Figure 6: Synchronised measured vibration progressions over time and crank angle

Considering the measurement curves within one revolution of the crankshaft it can be seen, that the frequency of the rod vibrations is 5 times higher than the excitation frequency. The vibration frequency of the piston rod unit is therefore 35 Hz or swings in the 5th order of the excitation frequency.

4 Dynamic Model Preparation

The investigation of possible measures and their effects requires a simulation model having the same resonant behaviour as the real compressor.

A dynamic model must therefore be developed and the results are compared with the real data measured. The results can further be used as input parameters in either a structural mechanics or fatigue analysis.

The complete first stage piston unit, consisting of piston, piston rod and crosshead will be simulated. For the dynamic modelling ANSYS² is used.

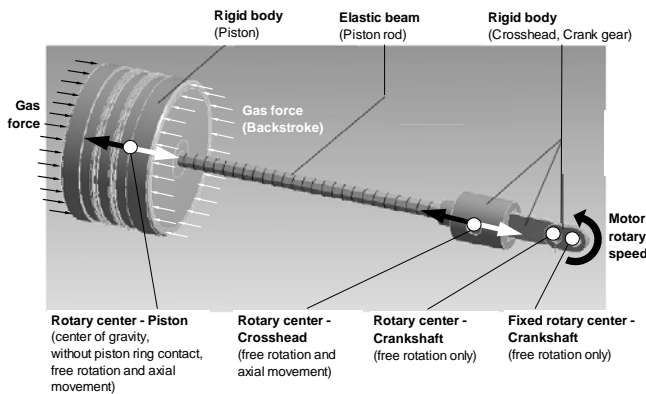


Figure 7: Dynamic simulation model

The idealized course of the gas force against both piston end faces is used for the load. The dynamic forces and also the piston rod forces are obtained automatically from the dynamic model, using the correct materials properties and existing acceleration profiles.

The guide rings of the piston are difficult to simulate due to their nonlinear behaviour and material properties hardly exist, as well. Therefore the piston ring guidance is simplified in the simulation by locating a rotary joint in the center of gravity of the piston, so that only longitudinal movement is possible.

The dynamic simulation with the assumed calculated load curves does not however give the desired result. It shows in fact that the dynamic system does not operate according to the measured vibration frequency of 35 Hz, but only 23 Hz. Moreover, the amplitude of the piston rod vibration is much lower, compared to the real values. The conclusion is therefore that there must be an additional effect, a missing link that raises the vibration frequency of the dynamic model to the expected 35 Hz.

5 Detail Analysis of Measured Data

This missing link must be found somewhere in the measured progressions of the piston rod vibration.

In order to get more significant results, the profiles of the piston rod deflection measured throughout over the period in the horizontal and vertical direction are represented in three dimensions and overlaid with the sinus oscillation of the crankshaft rotary motion.

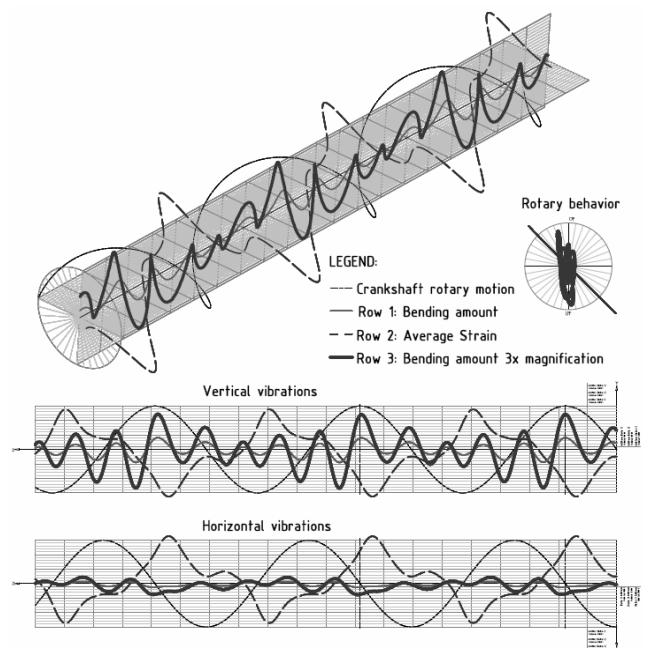


Figure 8: 3D representation of measured vibration progressions

With the help of three-dimensional representation, the problem can be considered and analyzed from different points of view. The view in axial direction could show any possible existing rotations of the piston around its longitudinal axis. However, the appearance of the progression does not refer to such behaviour. Also the horizontal component of bending vibration can be neglected. As expected, the dominant component of bending vibration is located in the vertical position of the piston rod.

For better representation the amplitude of the bending vibration in vertical direction is tripled. That points out that in particular in the area of the top dead center (OT), obviously an additional excitation takes place. Suddenly the amplitude rises rapidly in these areas. After that follows a damped oscillation behaviour with a continuously decreasing amplitude. The only possible course of this is an additional impulse.

Looking at the pv-diagram (pressure over volume) of the first stage process it appears that the impulse effect occurs between opening and closing of the discharge valves.

The first assumption on the basis of detailed analysis of measured data is based on an impulse torque around the horizontal lateral axis of the piston. This could be caused by a pressure impulse force in combination with a shift of the center of pressure.

This displacement towards the suction valves side

OPERATIONS

Piston rod vibrations of excessive amplitudes on a CO₂ compressor- Simulation, Measurement and Reengineering to solve the effect, *Gabriel Roman, Thomas Heumesser;*
LEOBERSDORFER MASCHINENFABRIK

could be based on a temporary non-uniform pressure distribution during opening of the discharge valves.

That is why the sudden opening causes a rapid increase of the outflow velocity. However, this increase does not exist uniformly in the complete compression chamber, but only in the area of the discharge valves.

Due to the large piston diameter of approximately 992 mm combined with a very small gap (clearance) of 2.5 mm (center) to 5.5 mm (circumference) between piston end faces and the end faces of the compression chamber at the dead centers, there is a velocity gradient from the suction valve side with nearly 0 m/s to the discharge valve side with the maximum velocity.

According to the Bernoulli equation the pressure behaves inversely proportional to the velocity. That is why at the moment of the non-uniform velocity distribution, there is a higher pressure at the suction valve area compared to the discharge valve area within the compression chamber. This pressure gradient leads to a shift of the center of pressure towards the higher pressure.

The pressure impulse force comes into effect on this point resulting from reducing the pressure against the piston end faces and causes a torque around the piston lateral axis in horizontal position. This impulse torque attempts to tilt the piston vertically.

6 First Model Optimization

Based on the first assumption, that in each dead center an impulse torque occurs, the dynamic simulation model is completed with an additional rectangular impulse function. According to this function the impulse torque is applied in the rotary joint of the piston each time the measured maximum amplitude is reached at the dead centers. On the basis of the measuring data the size of the torque impulse is specified at 2000 Nm.

This rotary joint in the center of gravity of the piston is furthermore furnished with an artificial rotational stiffness and damping coefficient. These factors are not known and therefore they need to be adjusted manually by means of the existing measured data.

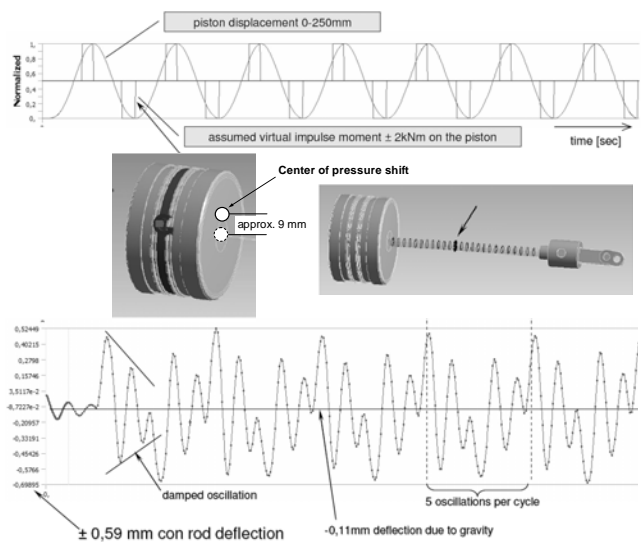


Figure 9: Rectangular impulse function and resulting vibration characteristics

The result shows that the missing link actually represents this additional impulse function. The vibration frequency of the piston unit is moved by the impulse excitation from 23 Hz to as measured 35 Hz. Thus the desired damped vibration mode is now present.

However, there are still points that are not clear.

With respect to timing, the assumed single impulse force during the discharge valves opening cannot alone be responsible for the main excitation. The opening point does not match with the time of maximum amplitude.

Even if the point in time were correct, the shift of the center of pressure would cause a torque, which tries to bend the piston rod downwards. However, the maximum amplitude at the top dead center (OT) is positive. That means that based on the DMS measuring method, on the top of the piston rod a higher tensile stress is present than at the bottom. Thus the piston rod is bent upwards exactly in the opposite direction to the simulated impulse torque.

7 Flow-Simulation by “Compressor 2D”

To answer the still outstanding questions, the performance in the compression chamber during a crankshaft revolution must also be investigated.

Based on a diploma thesis of Georg Mayer³ at the Technical University Vienna, the simulation program “Compressor 2D”⁴ was developed by DI Roland Aigner (Burkhard Compressors) cooperating with Ao. Univ. Prof. Dr. Herbert Steinrück⁵ (TU Vienna, Institute for Fluid Dynamics and Heat Transfer). This program that is specially configured for the flow-simulation in a piston compression chamber is used in determining compression characteristics, gas pressure waves and valve behaviour.

The data of the compression unit, the operating conditions, the suction and discharge geometry (valve pockets and slots, valve position and their number) and the valve operating parameters of the compressor are the initial basis for the simulation in “Compressor 2D”.

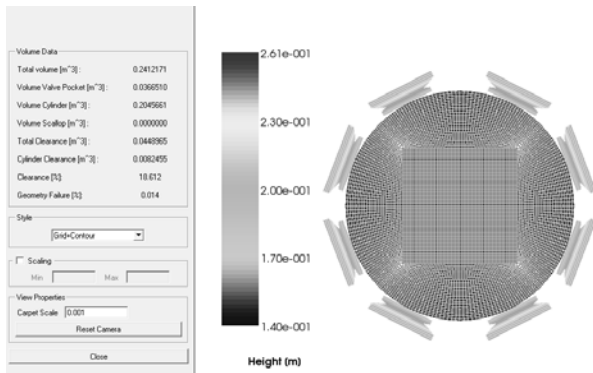


Figure 10: Simulation model in “Compressor 2D”

Among other things the simulation program provides the following progression of the pressure difference referred to the crank angle, which is relevant for the problem analysis:

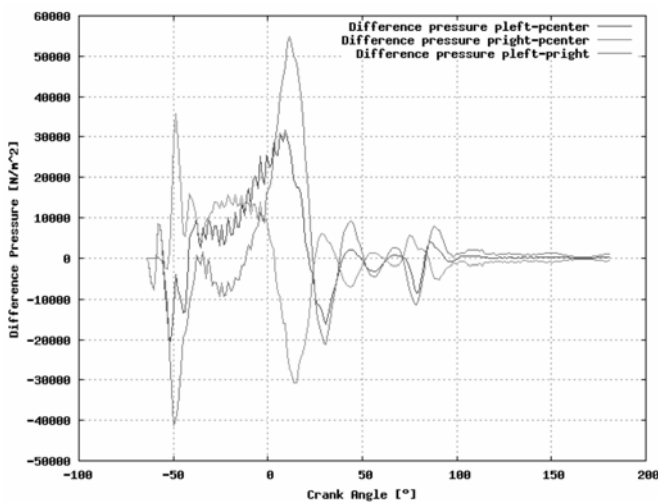


Figure 11: Progression of pressure difference Δp

Especially the characteristic of the pressure difference contains significant conclusions in consideration of the actual processes within the compression chamber. It can be seen, that it is a case of not only one, but two impulses following each other.

Therefore the pressure impulse during opening the discharge valves of the first compressor stage happens even at a crank angle of approximately 50 degrees to top dead center (OT). But directly after OT a second, stronger and contrary aligned following impulse takes place.

As a result, for the main excitation it is not only the first impulse that is responsible at the moment of discharge valves opening, but more especially the second, contrary aligned following subsequent impulse.

Consequently the pressure center is shifted downwards, producing a torque, which tries to bend the crankshaft upwards. Additionally this second impulse occurs just at the moment of the highest amplitude in the measurement curve of the vertical bending mode. If the pressure value is monitored over the crank angle, it is obvious that this second impulse occurs at the same instant the discharge valves close.

In reality, the first impulse initiates a pressure wave in the compression chamber. The sudden closing of the discharge valves piles up the wave, because of its mass inertia, and results in unbalanced pressures at the discharge and the suction valve sides. This unbalanced pressure shifts the center of pressure towards the discharge valves.

8 Second Model Optimization

Based on the pressure difference characteristic over the crank angle, which is determined by “Compressor 2D”, the first simplified assumption of the impulse function can be modified and optimized according to the real impulse excitation.

First, the determined pressure difference progression is reduced to two main impulses as a triangle function at the moment of opening and closing of the discharge valves.

For the impulse function of the dynamic model it is not the pressure difference progression, but the impulse torque progression that is necessary.

With the difference pressure the torque can be calculated directly by the following equation (Ref. 4, Page 71, (5.2)): $M = 1/8 \cdot \pi \cdot \Delta p \cdot (D/2)^3$

Thus for the dynamic model the impulse function, which is placed in the center of gravity of the piston, has the following characteristic:

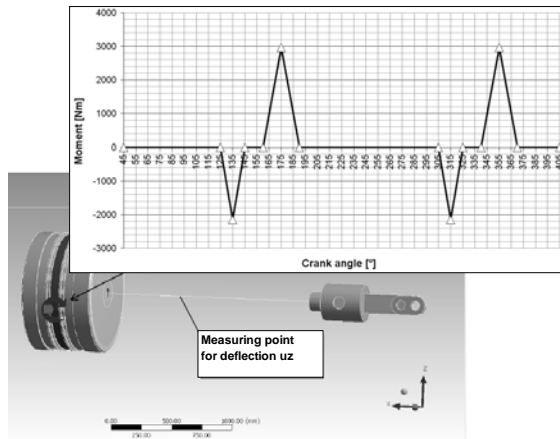


Figure 12: Double impulse triangle function

Finally the results of the dynamic simulation, using the optimized impulse torque function compared to the measured progressions, give sufficient information for the investigation of possible preventive measures.

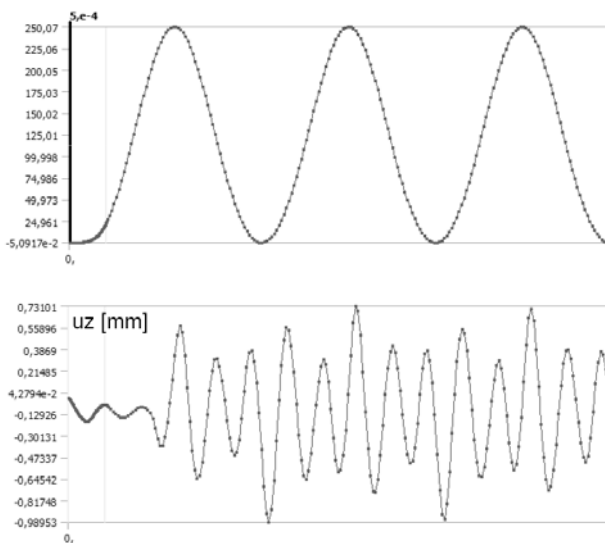


Figure 13: Resulting vibration characteristics

9 Conclusion

With the developed dynamic model combined with the flow simulation program “Compressor 2D” for the impulse identification, a powerful tool for the vibration evaluation and optimization of piston units with comparable design is now available.

9.1 Relevant Parameters

Under certain conditions, the influence of the valve function and its effect on the dynamic simulation

cannot be neglected because a shift of the vibration frequency and a reinforcement of the vibration stimulation can take place. First information gives a simplified determination of the difference of pressure process in „Compressor 2D“. Based on this information, the impulse torque that is brought to bear on the piston can be calculated directly.

In conclusion, the following important parameters can be investigated during the analysis of this vibration problem. They are considered on the assumption that all other basic conditions remain constant.

9.1.1 Piston Diameter

The larger the piston diameter the higher is the pressure difference between pressure and suction side.

9.1.2 Piston Diameter/ Guidance Length

The larger the ratio between piston diameter and piston guidance length, i.e. the more centrally the guide rings are arranged, the more effect the impulse excitation has on the vibration response of the piston unit. If the guide rings are spaced far apart as possible, this will stabilize the piston.

9.1.3 Molecular Weight

The heavier the gas, the greater is the induced impulse torque as a result of the center of pressure shift.

9.1.4 Cylinder Clearance

The smaller the gap (clearance) between piston end faces and end faces of the compression chamber in dead centers, the more unfavourable is the pressure distribution.

9.1.5 Piston Shape

A bevelling of the piston end faces increases the cylinder clearance and also the cross-section of the valve slots.

Therefore the flow rate is reduced at the moment of valve opening and the shift of the center of pressure, as well.

9.1.6 Valve Arrangement

The closer the pressure valves are arranged to the horizontal position, the smaller is the effective

distance between the suction valves and pressure valves. The smaller that effective distance, the smaller is the pressure difference.

9.1.7 Valve Position

The masking of the valve slots by the piston in motion reduces the free cross-section causing an increase in the flow rate within the valve pockets. In turn, this leads to a dependent decrease in the pressure and thus to a higher corresponding pressure difference between the suction and discharge side at the moment of discharge valve opening.

With the alignment of the valves closed as possible to the vertical position, and also with the placement of the valve slots in end face pockets of the compression chamber, out of the piston stroke area, the unmasked valve cross-section will be increased while the flow rate will be reduced accordingly.

9.1.8 Piston Mass and Mass Distribution

The greater the piston mass, the smaller is the effect of the impulse torque. Also, the mass distribution has a significant influence. The more the piston mass is concentrated outside (piston casing), the less sensitive the piston unit is. Even a pointed additional mass on the piston rod results in noticeable improvements in the vibration situation.

9.2 Problem Solving Measures

In this particular case, the following measures have been set to reduce the vibration problem. Due to the fact that the compressor being studied is already in place on site, only adaptation measures could be considered.

9.2.1 Cylinder Clearance Increasing

Due to having a sufficient delivery output surplus, it was possible to increase the gap (clearance) between each piston face surface and its appropriate compression chamber end face to 10.5 mm on each side.

Thus the impulse excitation could be reduced according to the following simulated function:

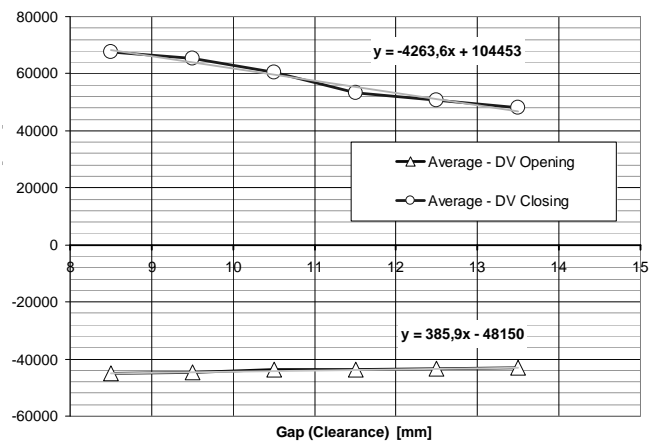


Figure 14: Pressure difference function for opening and closing of the discharge valves

9.2.2 Valve Slot Beveling

The edges of the discharge valve slots were bevelled to increase the remaining free cross-section at the dead center, where the slots are masked by the piston. That has reduced the flow rate and therefore, the effect of the impulse excitation.

9.2.3 Shutdown Limit Increasing

It was possible to determine the maximum allowed piston rod deflection based on the dynamic model combined with a structural mechanical model. According to the resulting limitation of 2.1 mm the shutdown limit was raised from 1.2 mm to 1.7 mm.

References

The author would like to thank DI Roland Aigner, Ao.Univ.Prof. DI Dr. Herbert Steinrück and Dr. Gunther Machu for their helpful assistance.

¹ API Standard 618, 5th edition, December 2007, Reciprocating Compressors for Petroleum, Chemical and Gas Industry Services

² ANSYS Inc., 2009, ANSYS Workbench V12

³ DI Georg Mayer, 2004, Simulation der Strömung in einem Kolbenverdichter, Diploma Thesis, TU Vienna

⁴ TU Vienna, Institute for Fluid Mechanics and Heat Transfer, 2003, Flow-Simulation Programm "Compressor 2D" V 0.0.3

⁵ DI Roland Aigner, Ao.Univ.Prof. DI Dr. Herbert Steinrück, 2007, Internal Flow and Valve Dynamics in a Reciprocating compressor



Challenges in use of analog of the four pole transfer matrix in the 1D time domain pulsation simulations

by:

Piotr CYKLIS, Ryszard KANTOR, Grzegorz ZELEK

**Cracow University of Technology, al. Jana Pawła II 37, 31-864 Kraków,
Poland**

pcyklis@mech.pk.edu.pl, rkantor@mech.pk.edu.pl, gzelek@10g.pl

**7th Conference of the EFRC
October 21th / 22th, 2010, Florence**

Abstract

In positive displacement compressors periodically occurring mass exchange events excite pulsations of a gas carried in the installation. Among the whole family of positive displacement compressors reciprocating machines are considered as the strongest source of pulsations.

To predict pulsation levels with a satisfactory level of accuracy special simulation tools must be deployed. Despite the fact the real installations are three dimensional structures in case of piston compressors one dimensional methods are often used. That means the real system must be modeled as a composition of properly connected pipes. The approach works fine when a wave propagating in the element is plane or in the other words its frequency is lower than the cutoff frequency – the parameter typical to the channel cross section and speed of sound in the considered gas.

The situation, however, becomes less clear in case of vessels large enough for occurrence of 3D acoustic modes or for instance sophisticated pulsation dumpers. In that case the plane wave assumption may cause justified confusions. Radical option would be then to switch to 3D simulations entirely. This paper, however, addresses to an intermediate solution – use of 1D system with a “black-box” element embedded in, defined by an analog of the four pole transfer matrix that could be determined thanks 3D simulations.

1 Introduction

Even though reciprocating compressor was not invented recently many of technical problems associated with its exploitation still remain opened. Among the most important gas pulsations are often mentioned along with efficiency, valves and capacity control related issues [2]. To understand how it can be one should take into account a trend, well visible over the industry, to build compression systems including smaller number of machines but offering the same or even higher capacity. All of that with increased rotational speeds and capacity control systems, unavoidable for part load demands, mean that modern compressors need to operate in a wider spectrum of operating conditions nowadays. Therefore a more accurate prediction of associated, unfavourable effects like i.e. eventual acoustic resonances gain on importance.

2 Remarks on modelling

Commonly, all engineering simulation tools are created and used to predict certain effects without need of checking them on real objects. That virtual process is often called modelling. Within it additionally three sub-processes can be mentioned. During the first, physical modelling, a decision must be made which factors are crucial for the expected results, which have a minor impact so that can be neglected making the model simpler. After that the physical model must be enclosed in the form of mathematical formulas. Most often it leads to a set of differential equations associated with proper boundary and initial conditions if needed. Because in the most general case mathematical model may not have an exact solution, hence proper numerical techniques must be used to find at least its approximation.

In case of the tools addressed to the pulsation issues in reciprocating compressor manifolds it is usually taken that the plane wave assumption is correct, hence the 1D approach is justified. Most often heat exchange between gas and walls is neglected as well. Taking into account low viscosity of gases in comparison to any of possible other fluids the Euler equations describing inviscid flow are rather preferred, which, under some additional assumptions, can be further reduced to the form of the wave equation. Finally to solve the problem numerically one may chose from: finite difference method, method of characteristics, transfer matrix method or any other suitable.

Several conclusions can be derived from the above paragraph. First that on each step certain discrepancies are introduced against the reality. Eventual observation of the simulated real object

usually will not be identical with the measurements

as that process is not error free as well. Therefore the weakest from the following trio: adequacy of simplifying assumptions, correctness of mathematical formulas, accuracy of solving methods determines level of trust to a simulation tool. However, as fragments of the modelling process are left in hands of the end users their experience and understanding is probably of the same order of magnitude that commitment and knowledge of the tool creators when considering level of trust to simulation results.

3 Limits and advantages of the 1D approach

Important assumption that stands behind the 1D approach is the acoustic signal propagating through the manifold can be considered as plane.

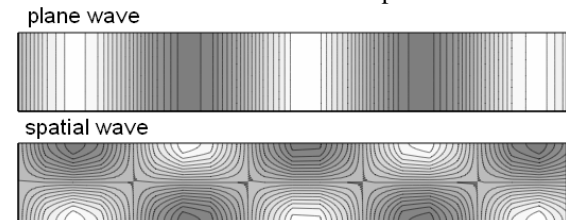


Figure 1: Plane wave vs first mode of the spatial wave travelling through the waveguide

Occurrence of the spatial modes depends on the wave frequency. When it is bellow so called cut-off frequency considered modes are not observed. For a channel with circular cross section, filled with gas the fundamental cut-off frequency will have the following form (1), where c stands for the speed of sound in the gas, D is a diameter of the pipe [4].

$$f_{cut-off} = 0.59 \frac{c}{D} \quad (1)$$

In the considered applications the plane wave assumption in most of the cases will be securely satisfied, even for higher order harmonics. Nonetheless, when think about a combination of heavy gas (low speed of sound), high-speed compressor and large enough vessel the assumption may no longer be valid.



Figure 2: Large, high-speed, reciprocating compressor [2]

In general, geometrical modelling of real installations in case of the 1D approach consists in presenting it as a properly connected composition of straight pipes. It seems to be pretty straightforward when having in mind pipelines. Things become less obvious however when consider sophisticated elements that can be met inside many of pulsation dumpers.

On the other hand the 1D approach based simulation tools in cases free from the described dilemmas may predict pulsation levels with a very good accuracy. What is more to do that they do not demand extraordinary computing resources.

4 Higher topological dimension as possible remedy for limitations of the 1D method

Computing cost as a factor becomes especially important when consider omitting the already described issues by incrementing the topological dimension of the geometrical model. In that situation, if neglect very limited number of cases that could be treated as axisymmetric (2D), the only option would be practically a direct switch to the 3D modelling. That means unfortunately a dramatic difference in terms of the computing needs when dealing with transient problems.

In general the most reasonable option when going to 3D modelling would be to use one of the already existing CFD packages. However, as they are rather universal not specially dedicated to the compressor related problems, higher pre- and post- processing efforts should be clearly expected.

Taking the issue from the other point, a fully 3D modelling of fragments where only plane wave is expected may look irrational, especially in the context of expected high computing costs. Therefore as a more reasonable option a form of hybrid approach could be pondered where 1D compressor dedicated software would be bridged with the 3D CFD tool enabling fully coupled simulations. Unfortunately as the available CFD packages are rather hermetic such plan not necessarily may appear achievable with the reasonable amount of effort. Therefore in the light of presented consideration especially promising looks to be the approach, analyzed deeper in Chapter 6.

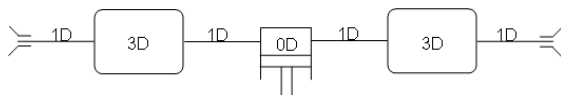


Figure 3: Hybrid approach in modelling of the compression stage

5 Shortly on the transfer matrix method

The transfer matrix method formulation as it is used to deal with pulsation problems starts from the 1D wave equation. Typically to that method parameter of flow and pressure from one port to another are transferred via special matrices according to (2). For a fragment of straight pipe of constant cross section area elements of that matrix can be given explicitly and found in [3], [5].

$$\begin{bmatrix} p_{n+1} \\ \dot{m}_{n+1} \end{bmatrix} = \begin{bmatrix} t_{11} & t_{12} \\ t_{21} & t_{22} \end{bmatrix} \cdot \begin{bmatrix} p_n \\ \dot{m}_n \end{bmatrix} \quad (2)$$

Analyzed geometry must be therefore decomposed into pipe sections. Its transfer matrix can be obtained by adequate multiplication and assembly of simple element matrices. The transfer form (2) can be rearranged into the admittance (3) or impedance (4) equivalent forms.

$$\begin{bmatrix} \dot{m}_n \\ \dot{m}_{n+1} \end{bmatrix} = \begin{bmatrix} a_{11} & a_{12} \\ a_{21} & a_{22} \end{bmatrix} \cdot \begin{bmatrix} p_n \\ p_{n+1} \end{bmatrix} \quad (3)$$

$$\begin{bmatrix} p_n \\ p_{n+1} \end{bmatrix} = \begin{bmatrix} z_{11} & z_{12} \\ z_{21} & z_{22} \end{bmatrix} \cdot \begin{bmatrix} \dot{m}_n \\ \dot{m}_{n+1} \end{bmatrix} \quad (4)$$

6 Concept of the “black-box” element

6.1 The idea

The concept of the method to which the paper addresses assumes the property of a multiport object can be determined using the 3D CFD modelling. That simulation would be done only for the considered object extracted from the whole installation. In the next step obtained properties would be introduced in the form of a “black-box” element to the model of system in the 1D pulsation tool.

The presented conception has been previously investigated [1] though, taking into account surrounding aspects like i.e. different specifics of used 1D tool, from the very beginning it was clear the implementation path must be different in our case. The plane wave pulsation solver we have available is based on Euler equations, iterated in the domain of time thanks the finite difference method. Because of that a decision was made to use the impedance rather than scattering matrix [1] when defining the “black-box” element.

The impedance matrix would be determined in series of 3D CFD transient simulations.

During the single one a base mass flow excitation would be applied to only one port while gauge pressure responses would be recorded at the each one. Repeating the operation for each port the impedance matrix could be filled. Though, in that case elements of the impedance matrix would be time dependent functions given by vectors of discrete values in time. Under certain additional conditions presented in Subchapter 6.2 knowledge of the impedance matrix would allow to reconstruct gauge pressure response for any possible incoming mass flow signals.

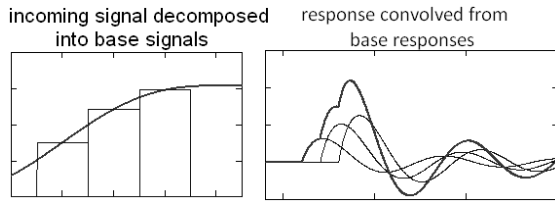


Figure 4: Prediction of the signal response

6.2 Constraints of the technique

Even if the proposed technique may seem to be a natural continuation of the consideration presented in Chapter 4 it is important to not forget that step from the fully coupled 1D/3D approach to the decoupled as sketched in Subchapter 6.1 may only be valid under some additional conditions. First of all an object that is planned to undergo such modelling treatment must be expected to respond in the linear manner as explained in Figure 5, 6 and corresponding Relationships (5), (6).

$$F(x_0) = y_0 \quad (5)$$

$$F(x_1) = F(k \cdot x_0) = k \cdot F(x_0) = k \cdot y_0 = y_1$$

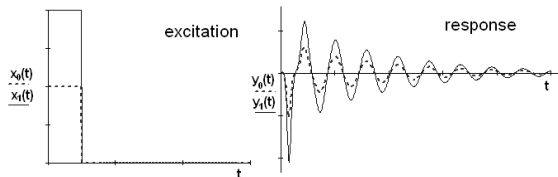


Figure 5: Multiplicative property of the linear object

$$x_1(t) = x_0(t) + x_0(t - \Delta t)$$

$$F(x_1(t)) = F(x_0(t) + x_0(t - \Delta t)) \quad (6)$$

$$F(x_1(t)) = F(x_0(t)) + F(x_0(t - \Delta t))$$

$$y_1(t) = y_0(t) + y_0(t - \Delta t)$$

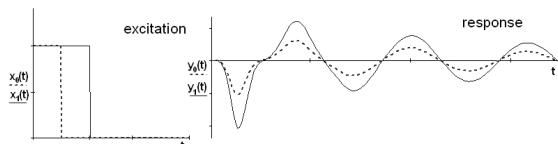


Figure 6: Additive property of the linear object

Another constraint addresses to conditions in which the impedance matrix is determined. As in general it is problematic to determine state of the mean flow inside the object not knowing the input mean flows at ports, it is assumed that its impact is negligible.

Finally, a disadvantage of the technique is that any change of gas composition or reference point of gas parameters resulting in meaningful change of speed of sound will mean necessity of redefinition of the impedance matrix. All in all its not the vessel that transfers the signals by itself but the filling medium constrained by the vessel geometry.

6.3 Description of the research

In the following subchapter an overview of a study on feasibility of the presented technique for its eventual further implementation is given. In the conducted tests we relied on self-developed, 1D Euler equation based, finite difference, time domain solver. Higher dimension CFD calculations were performed in ANSYS Fluent 12, for auxiliary purposes Mathcad 14 was used.

6.3.1 Convolution test

The first test that was carried out was intended to answer whether the linear behaviour explained in Subchapter 6.2 can be observed in results of CFD simulations. For a straight, constant diameter pipe of given length, filled with a gas, modelled in Fluent a series of transient simulations was performed. Each time on the one end the outlet condition was set. The opposite end had always applied a simple mass flow program. The excitation scenarios included constant mass flow rate lasting: 1, 2, 5, 10 fixed time steps. Afterwards mass flow rate was set to be 0. Thanks that it was possible to compare original responses for lasting longer excitations with prediction of them obtained by multiple convolving responses of lasting shorter ones. In total 5 possible comparisons were possible:

- $2 \cdot 1T_s$ vs $2T_s$,
- $5 \cdot 1T_s$ vs $5T_s$,
- $10 \cdot 1T_s$ vs $10T_s$,
- $5 \cdot 2T_s$ vs $10T_s$,
- $2 \cdot 5T_s$ vs $10T_s$.

Each time excellent numerical agreement was obtained.

6.3.2 Time-step dependence

All tests described in the Subchapter 6.3.1 was carried out with the same, fixed value of the time step. Unfortunately, it appeared that shape of resulting responses depends on the value of time step. As it was finer responses became sharper.

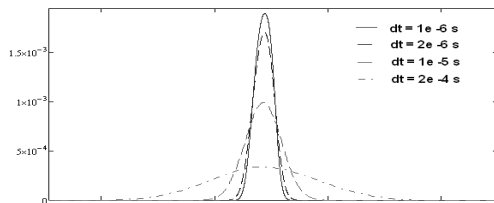


Figure 7: Time step dependent responses

It is obvious that such dependence is definitely unacceptable, especially the integration time step is a purely virtual parameter.

6.3.3 Profile of the base signal

Series of additional tests helped us to understand it is the rectangular profile of the base excitation that is mainly responsible for the problems from the previous Subchapter 6.3.2. As we recognized mainly due to the sudden value discontinuities. The situation improved a lot when the rectangular profile was exchanged with the triangular which is only discontinuous in terms of the first derivative (not value). The advantage of the triangular over the rectangular profile is that for the same width the triangular base signal enables twice as much denser interpolation of decomposed signal which in addition is piecewise linear not stepwise. What can be seen as disadvantage is the integration time step should be a magnitude of order smaller than the base signal width to reproduce well its triangular profile.

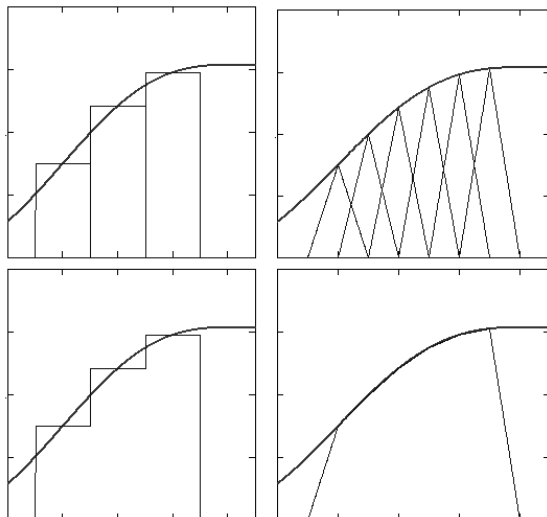


Figure 8: Rectangular and triangular base signals

6.3.4 Problem of proper boundary conditions and wave decomposition

The real object that is planned to be modelled using the “black-box” approach, responses of which are defined by the impedance matrix in reality is connected to pipelines that have non-zero but finite

impedances. Unfortunately, the outlet condition introduces impedance equal zero. Respectively, setting mass flow rate equal zero gives infinite value of the terminating impedance. To achieve the effect of proper terminating impedances in the time domain simulations performed to determine base responses of a given vessel first of all fragments of connected pipes should also be included in the model. Secondly, anechoic boundary condition (endless line) should be used instead of the outlet. In case of the active port, to which base excitation was applied, after the base profile is transmitted the boundary condition should also be switched to the anechoic. Unfortunately that type of boundary conditions is not available for immediate use in case of the transient simulations in Fluent. Possibly it could be introduced via the User Defined Functions available in that environment.

To reconstruct gauge pressure response only the incoming part of the periodic signal should be used. Hence in our case where pressure and flow variables contain all three components (mean value, periodic left going, periodic right going) it means an additional difficulty in the necessity of decomposition of the total values into the three components.

6.3.5 “Black-box” element in the benchmark test

For test purposes a case of a double acting cylinder was taken. Geometries of pulsation vessels can be found in Figures 9, 10.

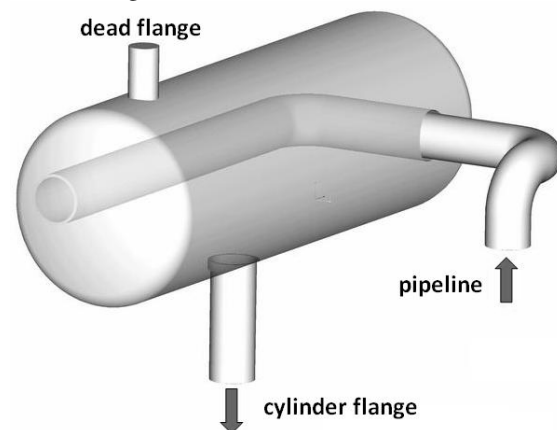


Figure 9: Suction bottle

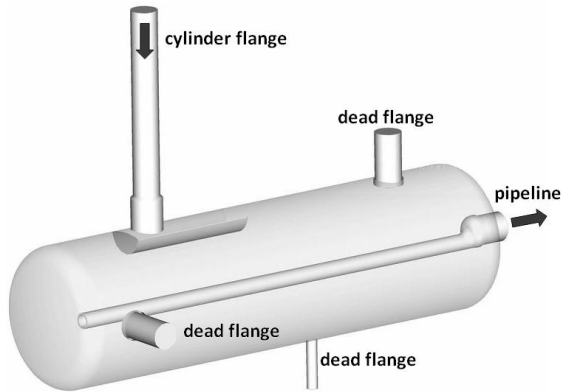


Figure 10: Discharge bottle

For the real given 3D configuration a corresponding 1D model shown in Figure 11 was built. For the sake of simplicity presence of dead flanges in the 1D model was neglected.

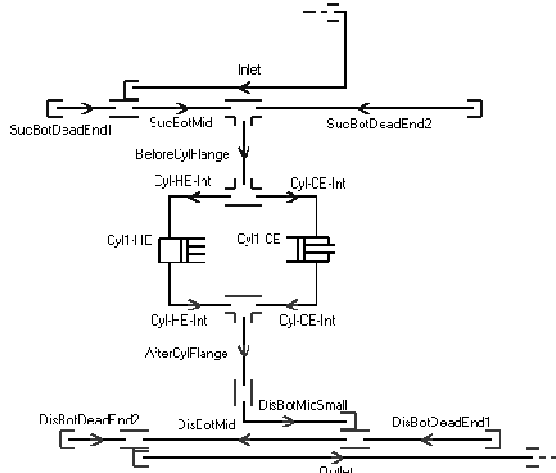


Figure 11: Simulation 1D model of the case

Figure 12 contains a comparison of pressure measurements taken at cylinder flanges and inside both compression chambers (black, background traces) against results predicted by the 1D tool (colour/lighter traces). Especially worth of emphasis is the high level of pulsations recorded at the discharge flange also very well predicted in the simulation.

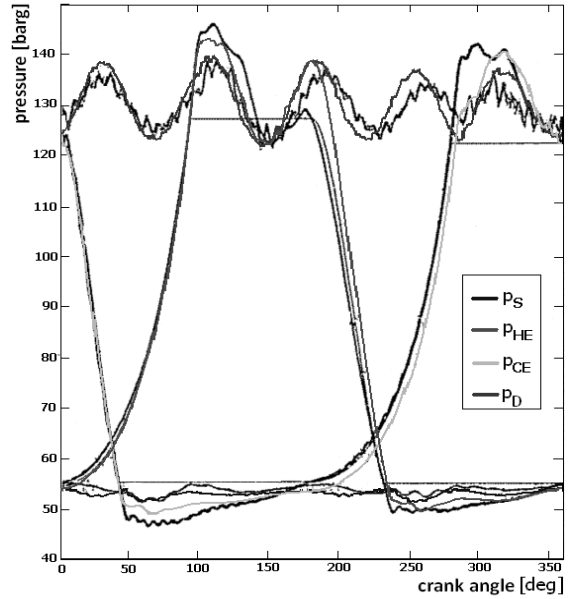


Figure 12: Measurements vs results of the 1D modelling

Next step of the study was to check how prediction of the flange pulsations will be changed when pulsation bottles are modelled as lumped volumes. Obtained results were compared with the results of the 1D simulation which from that moment is used as the reference. Figure 13 presents a compression stage model with lumped volumes representing the pulsation vessels. The comparison of the suction flange pulsations is given in Figure 14. The discharge flange situation is shown in Figure 15 respectively. Solid red lines represent the case with lumped volumes, dashed blue traces relate to the fully 1D model.

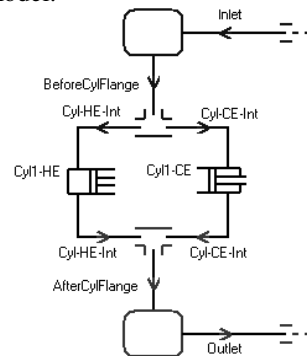


Figure 13: Simplified model of the compression stage with pulsation vessels treated as lumped volumes

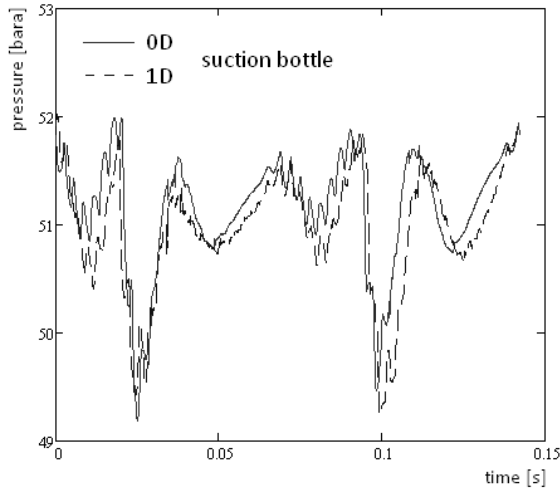


Figure 14: Different approaches in modelling suction bottles 0D vs 1D – comparison of pressure pulsations at suction flange of the cylinder

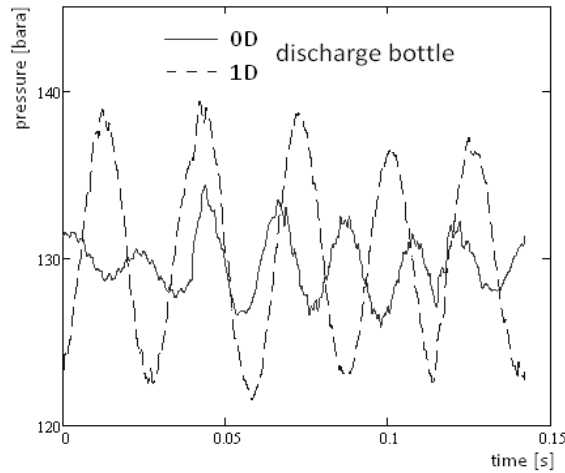


Figure 15: Different approaches in modelling discharge bottles 0D vs 1D – comparison pressure pulsations at discharge flange of the cylinder

Results of the above confrontation show minimal discrepancies in case of the suction side and meaningful differences on the discharge side. For that reason, as being more challenging the discharge bottle was selected for further evaluation of the “black-box” approach.

To ease the early stage evaluation of the new approach further simplifications were introduced to the model. The first one was to exclude suction side of the manifold. The second, to replace the mostly hidden inside the bottle original outlet pipe with the one having a constant diameter along its axis. Thanks that as the endless line condition was used at the end of that pipe the wave incoming to the bottle from the outlet side could only be zero which simplified a lot process of the response convolving. Influence of introduced modification was checked on adequate 1D model proving only its minor meaning in that particular case.

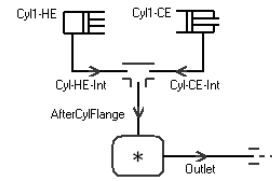


Figure 16: Model of test configuration used for final evaluation of the “black-box” approach

Prior the simulation of the model from Figure 16 was possible it was necessary to determine elements of the impedance matrix. In that case for two-port element that matrix should normally contain 4 elements and demand at least two separate simulations to fill them. However thanks the simplification of constant diameter outlet pipe only one simulation was needed. During that simulation the base mass flow rate excitation was applied to the port on the cylinder side. Gauge pressure responses were recorded both at active port (Figure 17) and at the outlet side idle port (Figure 18). Due to the difficulties with implementation of the proper boundary conditions in Fluent explained in Subchapter 6.3.4 the discharge bottle was modelled in the 1D tool.

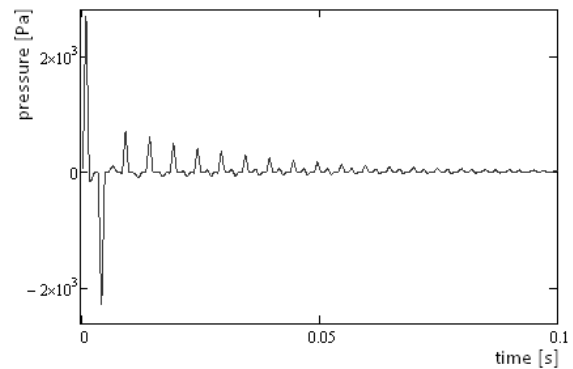


Figure 17: Gauge pressure response over time at the active port of the discharge bottle

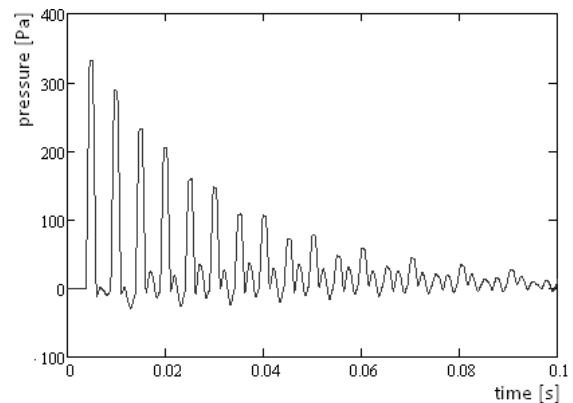


Figure 18: Gauge pressure response over time at the idle port of the discharge bottle

Process of finding solution is presented in simplified way in Figure 19. Starting from initial condition flow dependencies are iterated over time until the same periodic behaviour of flow parameters is seen in the consecutive periods. Mostly, that state is achievable and is considered to be the solution of the problem. In a way it can be compared to a problem of finding path of an uncontrolled missile moving in a given field of forces when its initial state is known. Any point on a path can be considered as initial conditions for the following part of the trajectory.

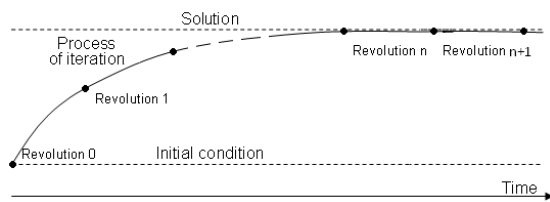


Figure 19: Running the time domain pulsation simulation – the idea

A scenario of the iteration process needs to be adjusted for use of the “black-box” element. Mainly due to the need of decomposition of mass flow records as only its periodic incoming part should be used for prediction of gauge pressure responses. Therefore the plan was introduced to run simulation with the “black-box” element working as a classic lumped volume until the convergence is achieved after that the elements would be switched to respond using its impedance matrix. The process of a sub iteration of a single revolution would consist of the following operations:

- Extraction of the periodic incoming part from the recorded at ports total mass flow rate information
- Reconstruction of the gauge pressure response
- Recall of the simulation state one revolution before and rerun of the period with the new pressure program

Unfortunately, the postulated simulation strategy in the considered benchmark case did not prove its usefulness. As shown in Figure 20 its use in consecutive subiterations led to a growth of extreme values of pressure pulsations recorded at the discharge side cylinder flange. Observed divergence resulted in destabilisation and finally in collapse of the simulation.

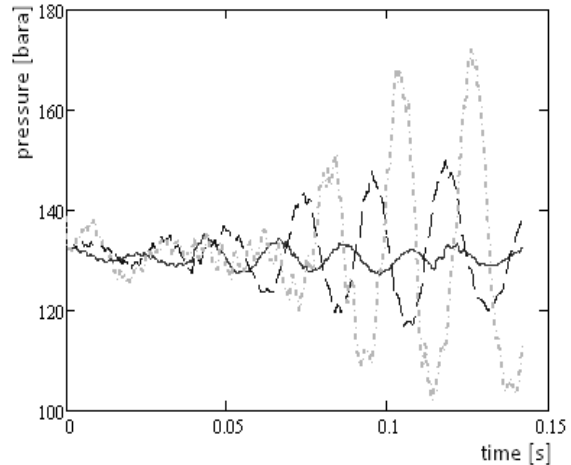


Figure 20: Divergence of pressure records at the discharge side cylinder flange collected on consecutive subiterations

7 Conclusions

The following paper contains a study on use of a new element in the 1D time domain pulsation simulations. The element would be an extended version of a lumped volume enriched additionally by the base signal response impedance matrix. The motivation for the presented research came on one hand from fundamental limits of the 1D method, namely the plane wave assumption. On the other it was driven by extensive costs of the full 3D transient simulations. The new technique at the beginning seemed to be an ideal compromise, though, as it is shown in the article its implementation is not free from difficulties and constraints. In total three critical areas of the concept has been identified. They are given in a sequence reflecting a subjective authors' impression on their importance.

- 1 As the most important issue a way of introducing the impedance matrix to the time domain simulation was found. The gauge pressure response should be composed using only the incoming part of the periodic component from the total mass flow rate inputs. In the considered benchmark case such decomposition was done after a full period was completed (thanks that mean value can be easily known) unfortunately that approach may affect stability of the process. Most likely the situation would be much better when response was composed immediately during the period. This however is problematic as it demands also an immediate decomposition of the input mass flow rates.
- 2 Initial assumptions restrict use of the method to objects in which the state of mean flow inside is negligible. In addition the object should be expected to respond linearly as explained in Subchapter 6.2.

Finally, change of filling medium or its parameters in general will mean necessity of the impedance matrix update.

- 3 Identification of the impedance matrix using time domain transient simulations occurs to be challenging, especially in terms of boundary conditions that need to be applied at ports to assure proper terminating impedances of connections. Another issues address to effect of numerical dispersion that can be observed when time step, size of mesh or profile of the base signal is chosen without care.

References

¹ Slis E., et al., 3D acoustic modelling in PULSIM for high frequency dynamics, 6th Conference of the EFRC, October 28th – 29th, 2008, Dusseldorf

² Deffenbaugh D.M., et al., Advanced reciprocating compression technology (ARCT), Final report, SwRI project No. 18.11052 DOE Award No. DE-FC26-04NT42269

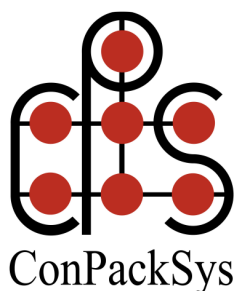
³ Cyklis P., Experimental identification of the transmittance matrix for any element of the pulsating gas manifold, *Journal of Sound and Vibration*, Volume: 244, Issue: 5, July 26, 2001, pp. 859-870

⁴ Fahy F., *Foundations of engineering acoustics*, Elsevier 2001

⁵ Axisa F. and Antunes J., *Modeling of mechanical systems: Fluid structure interaction*, Volume 3, Elsevier 2007

Acknowledgments

Authors acknowledge use of the measurement data obtained from the Hoerbiger company.



GDF SUEZ

Lessons learned from the use of a reciprocating compressor for CO₂ injection

by:

M.M.E. van Osch, C.B.P.J. van den Beemt

Flow and Structural Dynamics

TNO Science and Industry

Delft

The Netherlands

marlies.vanosch@tno.nl

M. Bezemer

ConPackSys

Dordrecht

The Netherlands

michel.bezemer@conpacksys.nl

D. D'Hoore

GDF Suez E&P

Zoetermeer

The Netherlands

daan.dhoore@gdfsuezep.nl

**7th Conference of the EFRC
October 21th / 22th, 2010, Florence**

Abstract

In response to reduce the emission of carbon dioxide (CO₂) to the atmosphere a promising solution is underground storage, for instance in depleted gas reservoirs. This topic is growing in interest and already a few pilot CO₂ sequestration sites exists, among with the Dutch platform K12-B which is operated by Gaz de France (GDF) Suez E&P. The production gas contains a high percentage of CO₂ which normally was vented to the atmosphere. Since 2004 the platform is extended by a reciprocating compressor facility developed and supplied by ConPackSys to re-inject the CO₂ into the field again, at a dept of approximately 3800 m. During the design and operation some specific challenges were being faced, like material selection, cooling, and lubrication. This paper describes the lessons learned from several years of operation of this compressor.

1 Introduction

Injection or reinjection of carbon dioxide in almost depleted oil and gas reservoirs is regarded as a most promising intermediate solution towards sustainable energy systems in the long term. CO₂ capture, transport, and storage (CCS) (Figure 1) is therefore growing in interest. During the Kyoto convention in Japan in 1997 binding commitments has been set to reduce the CO₂-emissions worldwide. These commitments have been made by 34 countries including the Netherlands. GDF Suez E&P, operator of the Dutch offshore gas field K12-B, supports the idea of (re-)injection of the CO₂ into depleted gas fields to reduce CO₂-emissions. Together with the Dutch Government, GDF Suez E&P started a project with K12-B as a demonstration site to investigate the feasibility of CO₂ injection and permanent storage in the natural gas field.

Many research programs are running worldwide to investigate CCS possibilities. Several research or demonstration sites exist or are being developed. The current progress is to make first steps to small commercial CCS applications. A final target is to have a fully operational transport network and large scale CO₂ injection.

Gas field K12-B is located in the Dutch shelf in the North Sea, some 150 km northwest of Amsterdam. Since 1987 this platform is producing natural gas, which has a relatively high content of CO₂ (13%). The CO₂ is separated from the production stream prior to the onshore gas transport. Until 2004 this CO₂ was vented into the atmosphere. Now it is injected into the field again, at a dept of approximately 3800 m. The project comprises two phases, in the first phase the CO₂ is injected into a fully depleted compartment, in the second phase the CO₂ is injected into the production field from which it originated. This field is nearly depleted and CO₂ injection could possible preserve the production.

For this application, a four stage horizontal reciprocating compressor (355 kW) was selected by ConPackSys. During the design and operation of the compressor system some specific challenges were being faced. This paper describes the lessons learned from six years of operation of this compressor facility.

First, important facts of the K12-B field are given. Subsequently section 3 discusses details of the reciprocating compressor and design issues of CO₂ compression. Then, the operational behaviour is assessed on operational experience.

The last two sections discusses the impact of CO₂ on enhanced gas recovery for the K12-B field and what is expected to change if CO₂ sequestration will be implemented at larger scale.

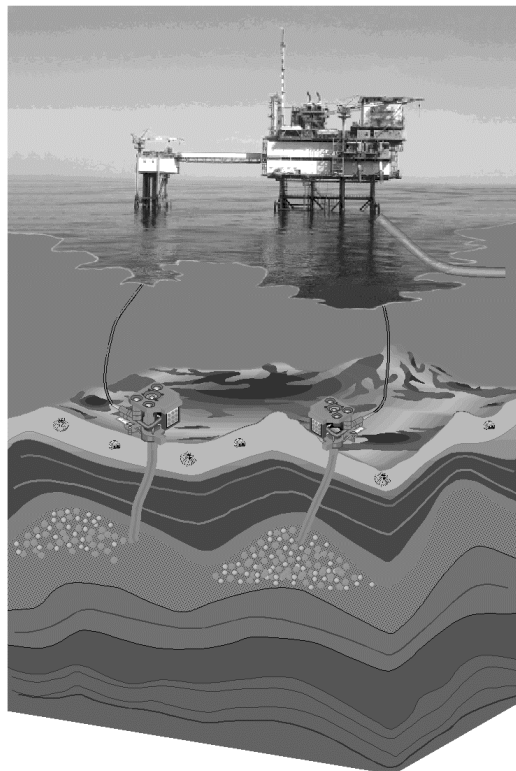


Figure 1: Schematic drawing Carbon Capture and Storage (CCS)

2 Platform K12-B

K12-B (Figure 2 and 3) is a gas production platform with a capacity of about 5.4 mio Nm³ gas/day¹. It consists of a main platform and a small drilling platform. On this drilling platform the CO₂ injection compressor is placed. The production gas then is transferred via a small pipe bridge to the main, production platform. Here the natural gas treatment takes place, consisting of a CO₂ separation column which uses an amine process to separate the CO₂ from the production gas. This process separates CO₂ with an efficiency² of 95%, leading to a production gas containing a reduced percentage CO₂ of 2%.



Figure 2: K12-B platform



Figure 3: main platform K12-B

The K12-B field consists of several compartments³ (Figure 4). The northern compartment is depleted. One well is located in this compartment and during the first phase this well is used as injector for CO₂. The pressure in the compartment is low, just about 30 Bara. In total approximately 9000 ton CO₂ is injected. In 2005 the second phase started. The CO₂ is injected into a nearly depleted reservoir compartment (compartment 3). This compartment contains three wells, two are still producing (K12-B1 and K12-B5) and the third is used now as injector (K12-B6). The pressure in this field is higher, about 50 Bara. The CO₂ injection is still continuing up to today.

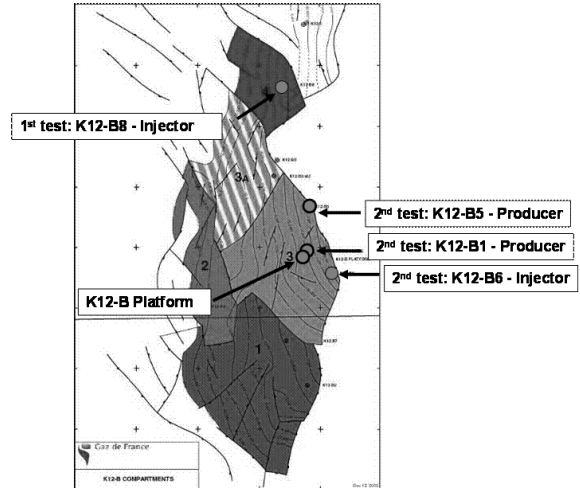


Figure 4: Structure map of K12-B reservoir

CO₂ re-injection at K12-B is subjected to several research programs, such as MONK, CATO, CASTOR and CO₂GEONET. These are mainly focused upon the behaviour of CO₂ injection⁴.

3 Compressor Design challenges

For the CO₂ injection project, the CO₂ separation installation is extended with a compressor unit. The used compressor for K12-B is a four stage horizontal reciprocating compressor; Ariel JGR/4 (see Figure 5). This compressor consists of a four crank frame with a stroke of 108 mm, and is equipped with a cylinder - and packing lubrication system. The compressor is driven by a variable speed electric drive with a maximum speed of 985 rpm, which corresponds to a maximal piston speed of 3.5 m/sec. This electric motor has a maximum shaft power of 355 kW.

On the drilling platform only a small footprint is available and due to lifting limitations of the crane the compressor should be light. The total skid dimensions are 5m x 5m x 3.5 m (length x width x height). Due to limited offshore construction time it was decided to make a complete make-up of the compressor system onshore. Therefore, no offshore welding is required and the only offshore activities were installation, assembly and wiring. This resulted to a fast start-up of five weeks from unloading. (Figure 6).

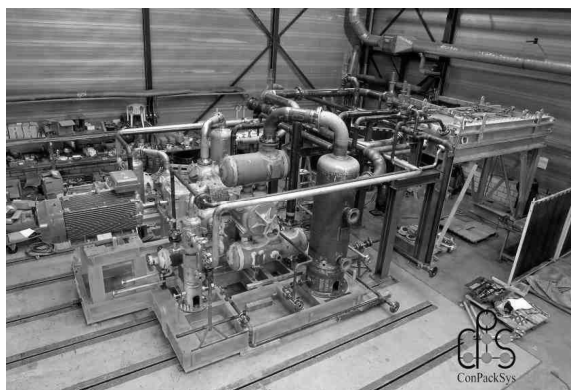


Figure 5: Ariel JGR/4 compressor



Figure 6: Compressor ready to transfer to K12-B platform

For CO₂ compression unit at K12-B the main process requirements are:

- Fluid conveyed is 100% wet CO₂
- Suction pressure is atmospheric at 40°C
- Discharge pressure ranges between 30 up to 90 Bara, temperature is 65 °C.
- The flow rate is averaged 30,000 Nm³/day CO₂ (about 55 ton CO₂ per day)

3.1 CO₂ Compression

The CO₂ properties are important for the design of the compressor. This section deals with some specific CO₂ properties which have to be taken into account.

Carbon dioxide has somewhat lower specific heat ratio ($k = c_p/c_v$) ($k = 1.28$ [-] for CO₂ at 40 °C and atmospheric pressure (inlet condition)) compared to other gasses like air ($k=1.41$) or hydrogen ($k = 1.40$), resulting in a lower temperature change on adiabatic compression. However, operating nearer to the critical point (31.1 °C, 73.9 Bar), the physical properties of CO₂ change. At higher pressures the specific heat for CO₂ increases to $k = 1.67$ [-] (at 65 °C and 53 Bar (discharge conditions)).

To retain good efficiency each discharge stage is air cooled to approximately 50 °C. The wet CO₂ contained approximately 7% water, which condensates in the intercoolers. Separators are placed after each cooler to catch the liquid water (Figure 7).

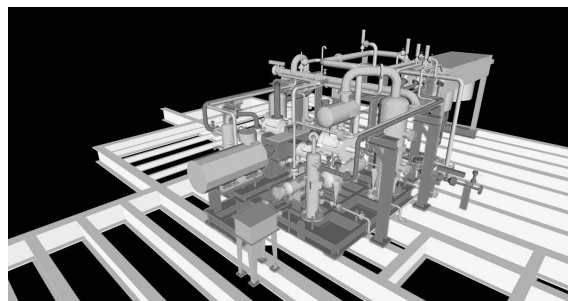


Figure 7: Design phase reciprocating compressor including separators

A property of CO₂ is that together with water the fluid becomes very corrosive. This is important when selecting the materials. ConPackSys carried out a material selection study. As a result of this duplex stainless steel is chosen as material of construction for a part of the process piping and -equipment. Another possibility is 316 alloys, which also have a good corrosion resistance. However this material can be affected by salts and is therefore less suitable. Special attention is given to the material of the valves, which also are dealing with corrosion and should resist impulse forces.

Another aspect which was considered is the poor lubrication property of CO₂, first due to the low viscosity of the gas (8.3e-6 m²/s compared to 15.7e-6 m²/s for air, at 27°C and atmospheric pressure) and second due to CO₂ gas at high pressure and temperatures have high absorption properties. The lubricant oil is dissolved. Higher levels of cylinder - and packing lubrication are therefore required than for regular gas applications.

It is known that carbon dioxide may permeate to some elastomeric materials in seals and hose connection⁵. To prevent leakage attention has been paid to types of seals.

3.2 Pulsation study

A pulsation study is performed by TNO conform the API 618. CO₂ is a heavy gas and consequently the velocity of sound is lower than for example a methane duty. At 50 Bar and a temperature of 63 °C the velocity of sound is 253 m/sec. As a result the wavelengths are generally smaller to conventional gas applications and in this small, compact pipe layout resonances can excited more easily.

The CO₂ compressor is delivered with dampers between the stages and these appeared sufficient to reduce the pulsations to a safe level.

A special layout in acoustic viewpoint is the twofold function of the scrubber as liquid separator and as acoustical damper. To reduce weight and space the inlet scrubber is used as damper for the pressure pulsations. The pressure pulsations did not influence the separation function.

3.3 Safety consideration

The compressor system is classified conform the ATEX. This classification is chosen due to its location in a flammable environment on the platform. For the compressor the Equipment group II, category 3, atmosphere G is used, for the area the category zone 2, gas group IIA, temperature class T3.

CO₂ gas in elevated concentration causes asphyxiation. However, since the CO₂ separation column is already present at the platform, no additional or new hazards are identified. The monitoring at the K12-B platform is identical to the methane line. The compressor and tie-ins are provided with regular instrumentation and controllers to measure the temperature, pressure, vibrations and flow. What's more, carbon dioxide is denser than air and the gas will sink below the high-built platform. To measure possible elevated concentrations on the platform a portable CO₂ instrumentation is present.

4 Operational experiences

The compressor is operational since 2004. It was designed for a test pilot with an estimated lifetime of half a year, however the platform is still operating today. The compressor will be reviewed according to the availability, material selection (corrosion effects) and pulsations and vibrations.

The compressor is continuously in operation. In the beginning some problems were encountered with the suction separators. The combination of water, oil and CO₂ resulted in an emulsion. This emulsion caused plugging of the separator drain lines. A solution was found in adding a chemical addition to the oil, as a result the liquid to be drained was less viscous and the separators could be easily drained. Since then the compressor is operating continuously.

During the first phase the CO₂ was being injected in a depleted gas field.

The pressure was low and the temperature of the gas was about 60 °C at the discharge side. At these conditions the CO₂ is gaseous and no abnormal behaviour was noticed. (Figure 8⁶). Possible downtime was rather on injection level than due to failure of the compressor².

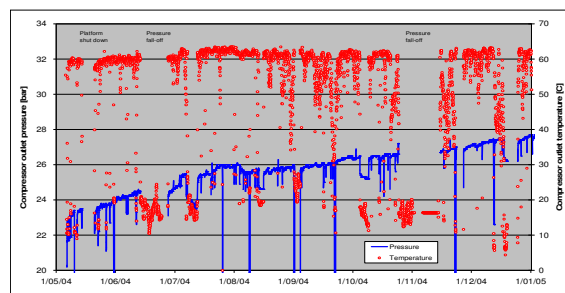


Figure 8: Operational data (pressure and temperature) compressor of first period (2004)

In the second phase the CO₂ is being injected in the almost depleted but still operational compartment. The pressure is higher at averaged 53 Bara and the temperature is averaged 65 degrees Celsius. Also in the second phase the compressor operated as expected. Except for the regular maintenance periods, no downtime due tot the compressor is recorded.

Duplex stainless steel appeared a valid choice for a part of the process gas containing piping and equipment. The vessels and piping will be checked on corrosion each 4 years and the wall thickness is measured. Up until now no problems were encountered. Also in the rest of the pipelines and equipment on the K12-B platform no extensive corrosion is found after 30 years of operation. The injection riser holds a different story. In the injection riser three times a measurement device has been put through to study corrosion effects. Some corrosion has been found but no correlation could be made between the three measurements. Also a video recorder has been put through. Some filth and rubbish has been found at the walls. Hence corrosion could become an issue, on the moment research is going on. Further corrosion measurements on the platform have not been performed.

No elevated pulsations or vibration levels are observed. Also around the scrubber manifold, which functions as well as damper, no significant deviations are observed.

5 Enhanced gas recovery

The gas field was almost depleted and CO₂ was regarded as an option to save the field by increasing the field pressure. During the first phase the field started temporarily to produce again, which was surprising. The pressure in the field increased as expected and predicted by the simulations. Presumably the CO₂ injection blow away the stone-dust which had collected around the riser and made room for the natural gas to flow.

In the second phase the enhanced gas recovery was marginal. Unlike oil recovery fields the CO₂ does not change the viscosity of the gas, gas is only recovered by bringing the compartment up to pressure. The used riser for injection was originally a production riser. It is located at the middle of the field at a relative high geometrical location. To use CO₂ as a propellant it would be more convenient to inject the CO₂ at the boundaries or corner of the compartment and at a lower geometrical dept since the CO₂ gas is denser than the methane. In principal, if you raise the pressure of the field the production increased⁷.

A negative influence occurs when the carbon dioxide mixes with the production gas. In the northern compartment (first phase) the original concentration was 13% of CO₂, after the injection the percentage raised up to 20%. In the second phase it took some time for the CO₂ to mix with the methane and to travel to the nearest production riser. The CO₂ fraction increased from 13% to 25%. GDF estimates the total enhanced production of about 1 to 2%².

Overall it is difficult to predict the enhanced gas recovery. It is unknown what will have happen if no gas was injected. Research is still going on.

6 Up-Scaling

K12-B is a demonstration site and the amount of injected CO₂ occurs on a relative small scale and in gaseous phase. For commercial applications liquefied or high dense carbon dioxide is more evident as the mass flow increases, compressibility decreases and the pressure drop reduces. For such systems the compression is provided by 5 to 10 stages compressors with final cooling. In some cases a multi-stage compressor in combination of a pump could be used for improved energy consumption.

The current challenge is to scale up CO₂ injection rates to commercial applications. For K12-B a 355 kW compressor is used. Reciprocating compressors

are flexible, have a good cost/benefit ratio and have a wide experience range, which make them suitable for demonstration sites. Reciprocating compressors can be increased up to a flow of 300 ton CO₂ per day, based upon an atmospheric suction and 50 Bara discharge, and are therefore applicable for the first, small commercial scales. For larger scales, up to 3,000 to even 25,000 ton CO₂ per day, centrifugal compressors will be applicable.

Regarding the pipeline system, transporting CO₂ in a liquid phase gives some challenges concerning pressurizing the flow (additional boosters will probably be required). Multiphase flow has to be prevented in the pipe lines. In the injection riser an unstable flow might be expected as the pressure declines and the temperature rises along the tube and multiphase flow is likely to occur.

7 Conclusion

K12-B is a Dutch gas platform in the North Sea, operated by GDF Suez E&P. Since 2004 the produced CO₂ has been re-injected into the reservoir. For this application a four stage horizontal reciprocating compressor is used.

During the design phase of the CO₂ compressor some attention is being paid to the properties of CO₂. In combination with water CO₂ very corrosive and a material selection study will be required. In our case duplex stainless steel appeared a valid choice for the part of the gas containing equipment and piping. Furthermore, oil solves easily in CO₂ at high pressures and temperatures. As a result the cylinder and packing lubrication levels need to be increased. Moreover, water, oil and CO₂ forms an emulsion which causes plugged separator drain lines. Adding an additive to the oil can solve this problem. Fourth, attention need to be paid for sealing and packaging selection as CO₂ may permeate through some elastomeric materials. Fifth, CO₂ is a heavy gas with relative short wavelengths, for compact systems this may result to resonances in the pipe layout. Finally, CO₂ is not flammable but can cause asphyxiation at elevated concentrations. At K12-B equal safety consideration are taken as methane.

After six year of operation the CO₂ reciprocating compressor at K12-B platform gives no operational problems. Even in the second phase at K12-B, where a higher discharge pressure was required, the compressor worked as expected. The main lesson learned is that reciprocating compressors can very well be used for CO₂ injection, however specific technical design issues have to be considered.

The pressure inside the field increased after starting the CO₂ injection and theoretically the production of methane is enhanced, however mixing of the injected CO₂ and the methane influence negatively the production. Research is still going on.

K12-B is a demonstration site with a relative small injection rate. The current development is to make first steps to a commercial plant. For these bigger scales the CO₂ will not be transported as a gas but a liquid form is more evident. This will give to some new challenges.

8 Acknowledgements

The authors wish to thank Bert van der Meer for his knowledge of CO₂ injection in underground storage of K12-B.

References

¹ Presentation Compressor Package, CO₂ injection: first in Netherlands, ConPackSys, <http://www.k12-b.nl>, 12 jan 2010

² Oral conversation with Daan d' Hoore, Gaz de France Suez E&P, Zoetermeer, 22 feb 2010

³ CO₂ storage and testing enhanced gas recovery in the K12-B reservoir, L.G.H. van der Meer, 23rd world gas conference, Amsterdam 2006

⁴ K12-B, CO₂ storage and enhanced gas recovery, TNO Built Environment and Geosciences, BenO uGe 057 05-2007

⁵ Fundamental process and system design issues of CO₂ vapor compression systems, Man-Hoe Kim, Jostein Pettersen, Clark W. Bullard, Progress in Energy and Combustion Science 30, 2004,

⁶ Presentation, ORC CO₂ injection Project, Injectie van CO₂ in depleted gas veld, Daan d' Hoore, 18 mei 2005

⁷ Oral conversation with Bert van der Meer, TNO BenO, 23 dec 2009



Modernization of reciprocating compressors for actual and future requirements

by:

Thomas Knebel

VNG - Verbundnetz Gas AG

Leipzig

Germany

Thomas.Knebel@vng.de

and:

Gunther Schindler - August Storm GmbH & Co. KG

Samuel Burkhalter - Burckhardt Compression AG

Andreas Raschke – VNG AG

**7th Conference of the EFRC
October 21th / 22th, 2010, Florence**

Abstract

In the following article, explanations for decisions after the longtime operation of piston compressors will be presented. The decision to continue to operate them after modernization is difficult considering the manufacturer no longer exists. Below, we will show solutions which will ensure the successful and problem-free use of the piston compressors for at least 50 years of operation. This topic is that much more interesting today, since most compressor operators have to ensure safe and trouble-free operation with a limited budget. Finally, piston compressor systems will be presented with a description of the modernization details which point out possible measures for continuing problem-free and stable compressor operation.

1 Introduction

The boxer compressors described in this paper are used for filling underground gas storage facilities. After around 20 years of operation, there is a question about whether piston compressor units with electric motor drives should continue to be used in the future. The decisions for this have been affected by the following external conditions:

- Adapting the compressor plant to the current state of the art
- Increased maintenance costs compared to comparable plants
- Modernization of the auxiliary systems because of reaching run-time limits, such as oil pumps
- Exchanging automation technology to reestablish state of the art
- Adaptation of the operating conditions of the compressor, which change over the years

The compressors were designed for compressing city gas. With the transition to the natural gas supply, there was also a change in gas composition. A continued stable and trouble-free operation to be implemented depends on whether this is done with modernization or with a new compressor system. The activities required for this are simple in the end, but there are many hard-to-solve problems of varying difficulty in the realization process. We would like to point out the work steps and the results of the implemented work and to encourage operating companies who face the same tasks to consider and follow this path with us.

2 Compressor investment / modernization

After commissioning a piston compressor investment, eliminating remaining deficiencies and starting long-term, stable operation, after 15 – 20 years of operation, before reaching the estimated utilization period limit, the question arises about how I should position myself as an operator of the compressor system for its continued use in the next few years: What measures should be taken to ensure continued use for another 15 or 20 years?

- a) Fundamental system renewal in form of reinvestment or
- b) Basic repairs with extensive modernization to current state of the art.

That being said, the following approaches result for our decisions.

In the first step, the criteria for future objectives, consisting of

technical considerations
and
business considerations

are to be formulated.

The technical options, from a complete reinvestment to possible degrees of modernization, will be worked out in detail. The business decision is then derived from the options resulting from the technical measures and the resulting costs and expenses. Here, the given utilization period limit is to be kept in mind for this consideration. These approaches are used for modernization and new investments. The engineer must take the following requirements into account:

- Low total cost
- Low operating costs
- Calculable maintenance costs
- High operational availability
- Long service life of wear parts

To make a decision for investment or modernization, the total costs of the respective variants must be compared with one another. The total costs to be assessed consist of the following.

Total costs = investment costs + operating costs (power, materials, etc.) + maintenance costs + replacement part costs + service costs.

While the investment/modernization costs are a one-time expenditure in the economic calculations, the operating costs, maintenance, procurement of wear parts, cost of drive energy, auxiliary materials (oil, control air, etc.) among other things must be paid for cyclically over the planned service life. These annually required expenses considerably influence the cost-effectiveness. A compressor system made/modernized at higher quality might have a higher budget for procuring it, but it would have lower operating costs due to less maintenance, lower wear, less energy required, etc. The business economists determine the economically optimal variant using the capital value method. An implementation plan is to be favoured if it has a positive capital value.

When deciding whether modernization or investment is the optimal solution, one also encounters issues which can't be built into the economic calculations due to lack of cost appraisals, etc..

OPERATIONS

Modernization of reciprocating compressors for actual and future requirements, *Thomas Knebel, Andreas Rasche, Samuel Burkhalter, Gunther Schindler; VNG, BURCKHARDT COMPRESSION*

These criteria include:

- Operating behaviour (large control range)
- Order processing
- Service after acceptance
- References, etc.

A rating matrix should be used for these issues, which should facilitate their inclusion in the economic evaluation. These criteria come from those criteria considered important for making the decision, which are compared with the project points of the options which can't be put into monetary terms. The positive aspects for making the decision can be treated using the corresponding rating factors.



Figure 1: Maschinenbau Halberstadt (MBH) 2 Stage 4 crank compressor installed in Kirchheilingen, year of delivery 1978

Before going into any further detail, it is to be mentioned that the piston compressor is designed as a robust, working machine and can be rated as a technical product with moderately innovative technical development. Technical advances, then, make it possible to take measures and to use these in the existing design of the piston compressor, such as the example in Figure 1.

There is no need to exchange the basic body and the individual components for continued long-term operation. The "robust" piston compressor can be brought to the state of the art purposefully with the corresponding adaptations, modernizations, etc. With improved components, such as piston rod seals, valves, bearings, etc., a modernized old compressor is almost as efficient as a new unit.

However, the required auxiliary systems for compressor operation, such as oil pumps, control/automation technology, measurement technology, etc. have meanwhile reached their utilization period limits, requiring them to be replaced. This will require adaptations to be made. As a result of further product developments, it is often not possible to replace units 1:1 when making adaptations. With this detailed consideration, a decision for new investment can usually be made relatively quickly, since partial modernizations require appropriate adaptations with limited unit

exchanges. The logistical implementation would require more effort compared to a new investment.

When making a new investment, the continued operation of the existing unit must be ensured until the replacement is completed and commissioned. This requires another place nearby which must be available and from which the required connections to the existing system must be established. Usually, compressor systems are installed in the centre of the overall system complex, which makes their replacement very complicated. If no generous shutdown times are available for this, expensive operating sequences result from this.

The following important points speak for continued operation, however:

- Perfect system knowledge from many years of operation
- Knowledge of the weak points
- Fault management is optimized
- Targeted maintenance and optimum cycles are set up and can continue to be used without limitations after modernization
- Monitoring with a simpler diagnostic system directed toward the weak points is usually sufficient.

When we started implementing our goal for long-term continued operation about 10 years ago, there were only a few partners available for this complex project. Meanwhile, companies have been increasingly faced with this challenge and have developed experience and know-how for allowing compressor systems to be modernized without complications and with a certain result. Even goals for changing the operation regime of the storage plant, and therefore also compressor operation, from "classical" shift operation, i.e. with a shift supervisor and up to two system operators, to automated operation, with the goal of eventually having unmanned operation, can be completely implemented. The following is to be given special attention and your partners should meet the following requirements:

- Carrying out recalculations, partial calculations for loads, torsional analyses, pulsation studies, vibration tests, etc.
- Design, etc. of components
- Dismantling with inventory and inspection
- Determining what replacement parts are necessary and how many
- Installation and adaptations

The contracted service company must be able to handle the required hardware changes and parts machining independently and on short notice with their own component production with an extensively equipped machine shop and tool park.

It is not recommended to assign work to subcontractors since possible time delays can become a risk along the chain with each external order. Furthermore, the service company should verify they have the required personnel with expert knowledge who can do quality work in the workshop and onsite without limitations.

3 Scope of compressor system modernization

Modernizing a compressor system involves activities on the compressor unit, including the secondary systems required for operation. The given requirements for further long-term problem-free and effective operation can only be met when the corresponding auxiliary systems are also state of the art. The table below describes the considered compressor units – boxer compressors with electric motors.

		Bernburg	Kirchheilingen
1	Quantity	4	3
2	Year of construction	1974	1978
3	Power	MW 3.0	1.8
4	Suction pressure	bar 18	12 / 36
5	Discharge pressure	bar 98	128
6	Pressure ratio	4.2	1-stage 3.6 2-stage 3.2
7	Flow rate	Nm ³ /h 104,000	25,000 15,000
8	Drive type	Electric motor 6 kV	Electric motor 6 kV

Figure 2: Summary of considered compressor units

3.1 Modernizations directly on the compressor unit

If none of the required adaptations have been made since the erection of the compressor system in the volume flow being compressed, changes in the primary and secondary pressure, assuming the compression strength and component loads have not been exceeded, the following measures are to be carried out:

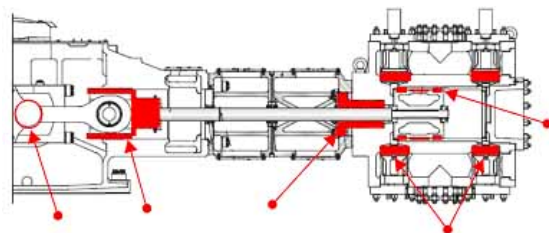


Figure 3: Areas of modernization at compressor

- Piston rod packing
- Piston rings
- Crankshaft bearings

- Crosshead
- Working valves
- Volume flow control
- Monitoring and diagnostics system

3.1.1 Piston rod seals, piston rings

The use of piston rod packings available today with the projected use period of 8000 to 12000 operating hours can sustainably reduce the cost of replacement parts. With the available sealing materials, in addition to an increased number of operating hours, the amount of leakage gas via the piston rods can also be reduced.

To determine the wear condition of the piston rod seal, a system for monitoring the leakage by measuring the volume flow at every seal (leakage gas monitoring) should be installed. The time-consuming piston rod removal can actually be reduced if condition-based maintenance is applied. Furthermore, wear of the piston rings can be reduced with coated liners and the corresponding material pairings same as for the piston rods. The service life of the piston rings can be increased.

This goes hand in hand with the option to reduce the lubrication and thus reducing the required amount of oil – the tribological wear system can then be optimally adjusted.

3.1.2 Crankshaft bearings

The manual shaving of the crankshaft bearings used at the time the compressor was manufactured is to be adapted to the state of the art by using standard bearings. With today's options for the fine drilling of crank bores by means of an onsite mobile crank bore machining, standard bearings can be used.

3.1.3 Maintenance work made easier

Work can be made easier and faster using hydraulic fastened connections and their defined tightening torques. Damage to components during installation can then be ruled out for the most part.

3.1.4 Monitoring and diagnostics system

The required scope of the diagnostic and monitoring system, from our point of view, is mainly determined by the availability of standby machines, the known fault frequency and the detailed knowledge of compressor system behaviour and the amount of maintenance work to be carried out. With regard to the equipment, we have focused on the following:

- a) Piston rod drop measurement
- b) Crosshead vibration monitoring with
- c) Valve nest temperatures of suction and discharge valves
- d) Measurement of leakage gas volumes from the respective piston rod glands.

Combining monitoring systems with alarm and shut down limits for the piston rod drop and crosshead vibration provides sufficient machine protection in our opinion. The measures to be taken for this are not expensive, are usually easy to install and are easy to handle by the operator and his local maintenance personnel. Extensive servicing should not be required for using the monitoring and diagnostic systems. In addition to the very important machine protection, measures for condition-based maintenance can also be derived from these signals. Furthermore, the monitoring system provides the conditions for safe, remotely operated and unmanned operation.

3.1.5 Oil system

The transition to economic lubrication for cylinder and crosshead lubrication, etc. can be implemented by selecting corresponding bearing and sealing materials. This way, it is possible to reduce the oil storage capacities, oil and waste oil consumption and pump power. Retrofitting to dry running can lead to a reduced service life for the piston rod seals and piston rings and was not considered for this application.

3.2 **Modernization of plant systems**

Measures to be taken on the peripheral plant system parts of the piston compressor are shown in the following figure 4.

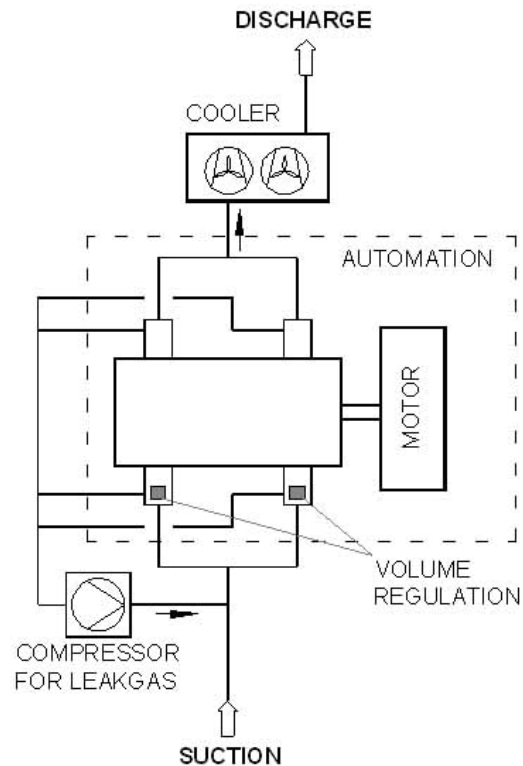


Figure 4: Areas of modernization on compressor plant

3.2.1 Automation technology

After many years of operation, it will inevitably be necessary to exchange the automation technology with modern system technology. The posed requirements will determine how much has to be realized, whereby PLC control, remote control, operating data and measurement archiving and improvements to the system safety monitoring system should be implemented.

3.2.2 Remote-controlled, unmanned operation

By implementing an automation system, unmanned operation is now possible, which is utilized after 6 p.m. on weekdays and all day on weekends and holidays.

3.2.3 Gas cooling

Gas-cooling modernizations might be necessary due to fundamental changes in the cooling process, e.g. replacing water cooling with air cooling or by changing the volume flow to be cooled by increasing the volume flow or increasing the pressure ratio with respect to the projected design parameters.

Modernizations in media cooling by using frequency-controlled fan drives, power-dependent cooling capacity, etc. can lead to considerable operating cost savings.

3.2.4 Leakage gas compression

According to the federal emissions protection law, operators are obligated to avoid environmentally harmful emissions with state of the art technology. This applies to the leakage gases which escape via the piston rod packings. We collect these leakage gases (on average 2 – 5 Nm³/h per crankshaft) in a buffer tank (approx. 5 m³). An electrically operated, oil-free small compressor feeds the accumulated leakage gases back into the suction side of the compressor.

3.2.5 Volume flow control

Although there might not have been any requirements for controlling the volume flow in earlier compressor operation, this might be necessary for further use. Mechanical/pneumatic, mechanical/hydraulic or electromechanical controls are used².

4 Realization steps and results for adapting the capacity

In the compressor system of the underground gas storage facility in Bernburg with 4 boxer compressors – with 8 cranks - the pressure in the suction line has increased from 37 - 42 bar on average to 40 - 45 bar in the past decade due to pressure rise from the connected gas pipeline. This gradual increase in the suction pressure has negatively influenced compressor operation with time.

The change in the suction pressure increased the volume flow and resulting increase of required power from the 3000 kW drive motors. This increased power input led, in turn, to an overload of the electric motor.

To solve this problem, different approaches have been considered:

4.1 Adapting the electric motor

Instead of the used 3 MW electric motor, a calculated increase of up to 3.4 MW is required. After doing some research, this increase in power is possible by using the existing electric motor, but rewinding the coils.

However, the effects on the compressor machinery must be investigated and evaluated in detail. In addition to recalculating components, such as the piston rod, the crosshead, etc., the changed loads on the bearings (crankshaft bearings, crosshead bearings, etc.), as well as the changes resulting from this in the lubricating oil supply, must be considered. With the higher bearing loads, the oil supply must be sufficient, the formation of lubrication films must be uniform, there must be sufficient heat dissipation in the bearings, etc. I.e., a multitude of detailed investigations would be required to determine the effects and the measures resulting from this to ensure stable operation.

4.2 Adapting the compressor power

During the course of the project, calculations were made concerning a reduction of the volume flow to be compressed by reducing the cylinder diameter.

After detailed results were available, the assessment of the overall situation led to the decision that the loads for the compressor components were not raised too much.

By returning the compressor to the original design volume (see Figure 2), the piping and vessel-related "problem areas" (e.g. pulsation damper, retaining the original cooler, vibration behaviour, etc.) of the compressor could be left untouched for the most part.

4.3 Decision and implementation

Due to the lower cost and technically easier solution, it was decided to change the compressor capacity by reducing the cylinder diameter. Considering the points described in chapter 2, the cost savings is 20% to 30% compared to a new investment. The savings must be estimated individually for each system due to the many aspects.

Although the machine manufacturer no longer exists, a suitable partner for carrying out the cylinder modifications could be found and assigned to the job. In particular, the cylinder with a 170 mm diameter had to be changed to a diameter of 160 mm within the scope of compressor revamp without losing a great amount of time.

Within the scope of this revision, the existing cylinder liners were drilled out and replaced with new ones having more wall thickness. During this process, the liners were given a very wear-resistant coating (60-65 HRC). The liners were shrunk into the cylinder bodies after preparation.

After completing this very efficient revision measure, the piston compressor could continue with operation without any great time losses. Commissioning and the subsequent running period have shown that the compressor works at higher efficiency and much more smoothly.

These effects have come about by returning the cylinder reduction to the range of the former design, from the compressor to the piping, pulsation dampers, etc.. In the meantime, 3 out of the 4 compressor units have had their cylinder diameters reduced.

5 Recalculating set of characteristic curves

5.1 Basics

A set of characteristic curves (or performance map) graphically represent the compressed volume and required energy with various suction and delivery conditions. For a gas storage facility, these conditions typically vary over a wide range.

For the owner of a compressor station, economic operation is a main focus. He must know the energy demand and the costs associated with it. Especially in the gas storage area, the time required to store a certain volume of gas is of interest, in order to plan the purchase of gas. The original characteristic curves, generated in 1973 in paper form (see Figure 5), no longer reflect the actual conditions due to the continuous technical improvements to the packings, sealing elements, bearings, valves, etc. and the modified operation. Due to the modernization of the compressor, the characteristics also change. In addition, the changed gas composition makes the original set of characteristic curves useless. In what used to be the usual graphical representation of the compressor performance, the flow rate as well as the power required was visually read off over the working range of the compressor. This is to be replaced by a corresponding program for the current state of the compressor.

The set of characteristic curves handed over at system delivery are no longer applicable due to the modernizations and changes in the gas composition. The excessively inaccuracy and the use of manual read-outs via the set of compression curves are no longer appropriate. Due to the longtime partnership with STORM, Deutschland, Burckhardt Compression has been assigned to create a set of characteristic curves for the two storage sites in Kircheilingen and Bernburg. The power input as well as the flow rates of the one- and two-stage Halberstadt compressors should be calculated to be +/- 3 % exact.

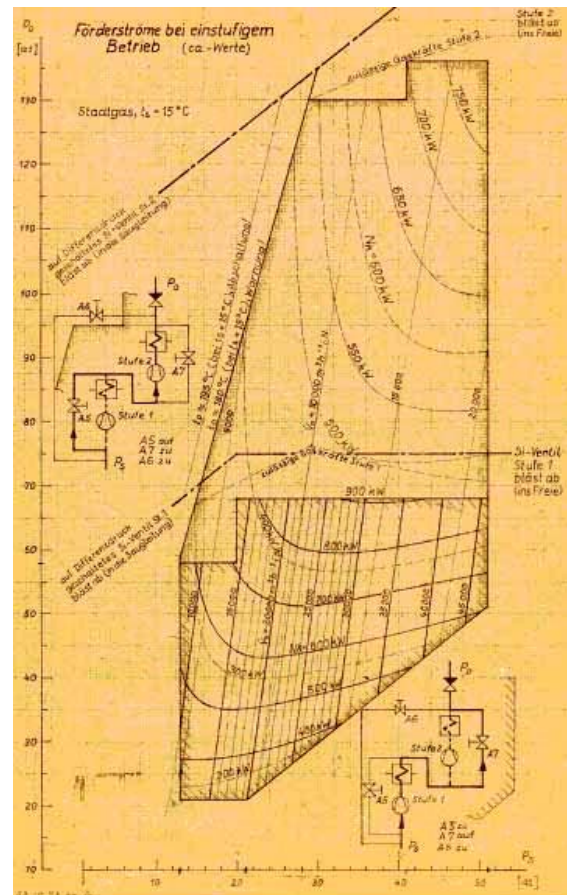


Figure 5: Original performance map dated 1973

5.3 Compressor simulation

RecipCalc™ is a calculation program developed by Burckhardt Compression for sizing and recalculation of piston compressors and their plants. There are numerous compressor components stored in a database. Any compressor can be modelled with the corresponding data. The volume flow, power input and mechanical data of the compressor are calculated for each compressor chamber and stage. The calculation is based on mass and energy conservation.

For mass balance, in addition to the mass flow in and out the compression chamber, leakages must also be considered.

For example, with a double-acting cylinder, there is a mass flow over the piston to the other compression chamber in both directions. In addition to the loss of compressed gas volume, this mass flow heats up the other compression chamber. Furthermore, there may be leakages over the packing and a leakage of the valve itself. For the energy balance, in addition to the enthalpy of the gas in and the enthalpy of the gas outflow, the mechanical workload of the compressor, including friction and losses, the heat transfer to the compression chamber surrounding the cylinder wall, cylinder head, piston and the piston rod must also be considered. The cylinder wall acts as heat reservoir. During the discharge period the wall is heated up, and during the suction period the gas is heated up, which reduces the density of the gas and therefore the mass flow of the compressor. For heat transfer, the relevant compressor design parameters include the compressor rotational speed, type of cooling and cylinder size. An advantage of solving the energy balance equation is the accurate prediction of effective discharge temperatures. Due to the importance of the energy balance, accurate gas data is required. For many applications, the gas behaviour is far from ideal. Therefore it is important to take the effects of real gas properties into account. Depending on the gas mixture and properties, different gas models must be used. Commercial tools such as PPDS from TUV NEL offer a broad range of real gas models and allow for flash calculations, which consider condensation. Other calculations can be quickly carried out with the compressor model once it has been created, such as:

- Part load operation, e.g. valve lift, clearance pockets, stage bypass, etc.
- Mechanical data, such as free forces and moments, torque diagram, piston rod and combined rod loads
- Calculation of the valve dynamics, For a detailed description, see reference ¹

5.2 Interpretation of the results

The existing measuring data is compared with the simulation results. An important indication for the precision of the model is the comparison of the deviations over the stage pressure ratio. As an example, an average cylinder clearance of 15% was used based on the existing documents of the one-stage Halberstadt compressor in Bernburg. With this, however, the calculated volume flows deviated from the measurements by up to 17%. The cylinder

clearance was measured on an existing cylinder to be 29%, so nearly twice as much as indicated in the original manufacturer documentation.

Comparing the simulation results with the system measurements indicated a strongly linearly increasing deviation over the stage pressure ratio. Calculated with the actual measured cylinder clearance, there was good correlation (see figure 6).

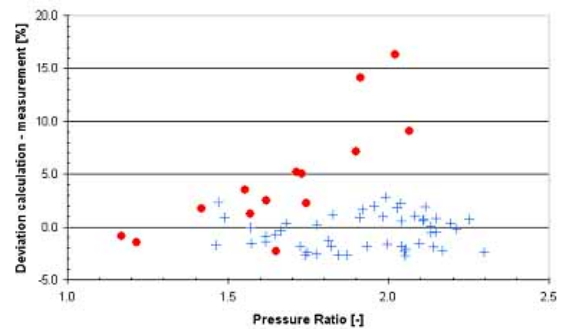


Figure 6: Deviation in % of calculated versus measured volume flow before (dots) and after (+) correction of clearance volume, plotted over pressure ratio

5.3 Creation of an interpolation program

The results from the RecipCalc™ simulation model are fed into the interpolation program for the set of characteristic curves. There, in a user-friendly input and output interface, the calculated and interpolated volume flow and energy consumption are shown for any suction and delivery state within the set of characteristic curves.

If some operation data of volume flow and energy consumption in the range of the specified set of characteristic curves is available, the results can be further improved by modifying the model according to the measurements. Afterwards the calculation program for the compressor plant in Bernburg was validated for one gas storage feed period. The achieved precision is +/-3%, both for the volume flow as well as for the power, as required.

The program, in MS Excel format, allows integration in the control system and can be used for operational evaluation, or also for checking the plausibility of measurements. Greater deviations from the expected volume outputs and power inputs are indications of defects, but cannot replace a monitoring system.

6 Examples carried out on realized compressor modernizations

In the underground gas storage facilities at the Bernburg (see also Figure 7) and Kirchheilingen sites, 7 compressor units were extensively modernized after many years of operation.

What was done specifically:

Implementation of active explosion protection

The absolutely necessary electrical equipment was left in the gas system

Change in the ventilation conditions

Earlier, compressor operation was only possible with activated technical ventilation with 3 air changes. On cold days, the heat consumption for controlling the temperature of the hall was correspondingly high. The technical ventilation was only used for air conditioning. For this, then, the following measures were required:

- The compressor hall had to be equipped according to the requirements for explosion danger zone 1
- Existing electrical equipment, which could not be retrofit to the requirements due to economic reasons (e.g. hall crane), is switched off electrically if 20% of the lower explosion limit is reached
- Adjacent rooms in the compressor hall which could contain sources of ignition are enclosed so they are gas-tight
- The gas detection system extended from 16 to 32 sensors
- Honeycomb grating is used to naturally ventilate difficult-to-access "dead zones"

Changes to auxiliary systems

- Monitoring system for cylinder lubrication pump
- Reduction of pre-lubrication times to about 5 minutes
- Monitoring of the machine hall by fire alarm system
- There are redundant systems available for ensuring the pressure and temperature
- Feedback of compression gland leaks into suction line using leakage gas compressors
- Relief of pressure side in suction side for compressor relief to reduce relief volumes
- Transition to economical lubrication
- Reduction in fresh oil supply and waste oil storage



Figure 7: Compressor station of underground gas storage facility in Bernburg

7 Summary

With the activities and solutions described here, piston compressors can be purposefully adjusted for long-term operation. By consistently maintaining the compressor itself along with state-of-the-art peripheral system technology, safe and stable compressor operation can be realized. The measures to be implemented mainly come from the production requirements on the compressor systems. Overall, the required costs for this are much less than those for a new investment.

With this, the operating companies should be encouraged to retain their familiar technical equipment for their piston compressor systems and modernize them for more efficient operation. With the implemented measures, the planned unmanned operation of the compressor plant can be run reliable and stable for much longer than the once estimated service life.

References

¹ R. Aigner, A. Allenspach / Taking everything into account, Simulation of poppet valves for reciprocating compressors / Hydrocarbon engineering, May 2010

² R. Aigner, A. Voser, A. Allenspach / Development of a stepless flow control system / 7th EFRC Conference 2010 Florence

Development of a Stepless Flow Control System

by:

R. Aigner, A. Voser, A. Allenspach

Burckhardt Compression AG

Winterthur

Switzerland

roland.aigner@burckhardtcompression.com

**7th Conference of the EFRC
October 21th / 22th, 2010, Florence**

Abstract

Capacity control systems are used to control the amount of gas delivered by a compressor and/or to ensure certain pressure levels at the intermediate stages or at the outlet of the compressor. In the present study, a new approach for a capacity control will be presented and compared to existing systems. It turns out that the new approach is superior in major aspects, such as available flow rate, amount of energy saved and reliability. The benefits are verified with simulations showing the impact of the flow control on valve dynamics and fluid dynamics and with measurements on compressors in operation.

1 Introduction

The operation of large reciprocating compressors often requires energy- and cost-efficient ways to adjust mass flow and/or to ensure certain pressure levels at the intermediate stages or at the outlet of the compressor. A wide variety of approaches are available. The most prominent are:

- Bypass: allowing the already compressed gas to expand to the suction side of a compressor stage through a dedicated gas pipe equipped with a bypass valve
- Clearance pocket: compressing gas into additional clearance pockets attached to a compression chamber
- Speed control: varying the speed of the compressor
- Suction valve lifting: keeping the suction valve open with a so-called unloader

A detailed description, advantages and drawbacks can be found in reference ¹¹ and only the latter method will be discussed further. Here, the already suctioned gas is delivered back to the suction line and this can be performed either during one or more subsequent full strokes as “intermittent flow control” or only for some portion of the compression phase as so-called “stepless reverse flow control”. According to Figure 1, which compares the efficiency of the capacity control methods described above, the intermittent flow control is more efficient than stepless flow control. On the other hand, stepless reverse flow control, as the name suggests, can adjust the mass flow and the pressure levels continuously variably.

The capacity control presented in this paper allows intermittent and stepless flow control to be combined in order to maximize efficiency and reliability. The unloader is driven by a magnetic actuator, similar to devices already presented by Kopecek, Klockow, Schmitz (2008) ² and Schiavone, Ragi (2008) ³. The simple and therefore cost-effective design and the availability of rapid design tools for the simulation and control of such mechatronic devices make this the preferred choice. In order to ensure maximum reliability, a complete simulation of the capacity control system has been used for the development of the unloader device. Furthermore, long-term test runs of prototypes have been conducted on different test compressors in operation.

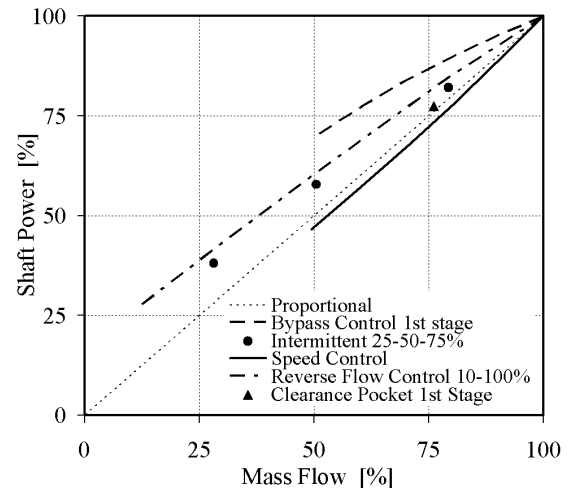


Figure 1: Power consumption of the compressor depending on the mass flow and the flow control method used

2 Description of the stepless capacity control system

2.1 Configuration of the stepless capacity control system

The main components are as follows:

- Unloader
- Magnetic actuator
- Position sensor
- Power electronics and control unit
- Master control unit and power supply

The compression chamber is separated from the suction side of the gas chamber by a conventional passive suction valve (Figure 2). The fingers of the unloader reach the sealing elements of the valve through the valve seat and can push them against the valve guard (open valve). In Figure 2, a plate valve is shown, but any kind of valve can be used (plate valve, poppet valve, ring valve). The unloader itself can be pushed down by the plunger of the magnetic actuator.

The magnetic actuator is deactivated in the initial position, and the spring holds the unloader and the armature of the magnet in the uppermost position. Therefore, the valve works without any influences.

The armature is pulled down if an electric current is running through the coil of the magnet and the plunger pushes the unloader down. The unloader, in turn, pushes against the valve plate, and therefore, the valve can be kept open, even if the pressure force of the gas flow tries to close the valve.

In order to control the motion of the unloader, a position sensor determines the state of the armature.

This signal is fed through a control unit to determine the desired electric current of the magnetic coil. In addition a master control unit coordinates the necessary control parameters and information (e.g.: crank angle) for the control units at each suction valve.

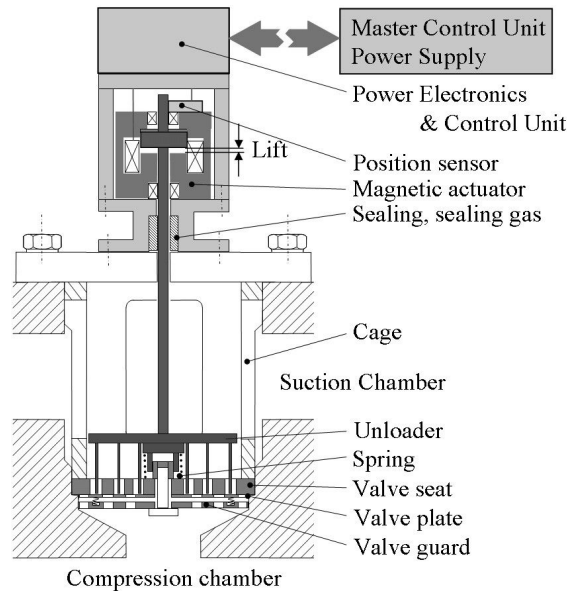


Figure 2: Main components of the stepless capacity control system

2.2 Operation of the capacity control system

2.2.1 Stepless reverse flow control

The unloader is in the initial position during the expansion phase of the compression chamber and the valve is closed (Figure 3). The resulting pressure force acting on the valve sealing element is the pressure difference between the compression chamber and the suction side multiplied by the effective force area. The valve starts to open when the resulting pressure force on the valve sealing is higher than the spring force (crank angle, CA=90°). Then the magnetic actuator is activated and the unloader moves in the direction of the valve guard. At a crank angle of approximately 145°, the unloader reaches the sealing element and presses it against the valve guard. Here the impact velocity must be smaller than 0.1 m/s (see section 2.2.4 Soft landing). In the case of uncontrolled valves, the suction valve would start to close at approximately 150° CA. The valve would be firmly closed when the piston reaches the bottom dead centre (BDC). In the case of activated stepless reverse control, the suction valve is kept open beyond the beginning of the compression phase by means of the unloader. Therefore, a part of the fluid sucked into the compression chamber is pressed back into the gas chamber of the suction side. At a certain crank

angle, the magnetic actuator is deactivated and the unloader moves towards the initial position. Due to the flow forces, the valve sealing element (e.g. valve plate) is pressed onto the unloader, causing it to close. The flow forces can be much higher than the spring forces, especially with heavy gases, high suction pressures and high-speed compressors. The unloader is used to control the motion of the sealing element. In this example, the sealing element is put gently on the valve seat at a crank angle of 290°. Again, the impact speed must be small to achieve soft landing. The time of closing the suction valve determines the quantity of the fluid remaining in the compression chamber, and thus the mass flow of the gas delivered. Finally, the unloader returns to its initial position.

Figure 5 shows the thermodynamic cycle in the pressure-volume diagram. Line 4 corresponds to the reverse flow control. The area enclosed by this line represents the thermodynamic work of the process. The difference in the areas of the full-load cycle (line 5) and the reverse flow control cycle is equal to the amount of saved energy.

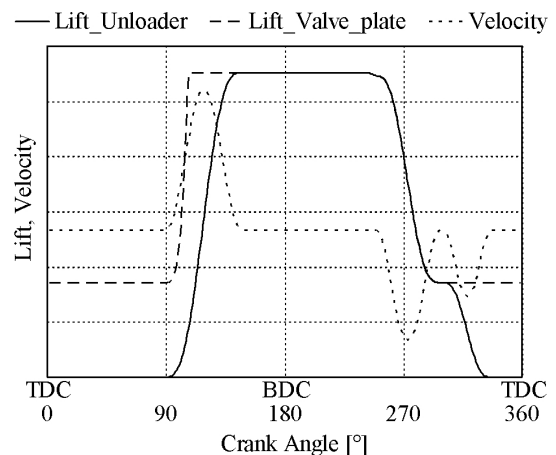


Figure 3: Reverse flow control: motion of the unloader and valve plate during one compression cycle

2.2.2 Intermittent capacity control

In the case of intermittent flow control, the suction valve is kept open for a whole cycle (Figure 4). All the gas sucked into the compression chamber is pressed back to the suction side during the compression phase. This compression chamber then delivers no gas in this cycle. In order to deliver approximately 50% of the mass, the suction valve is kept open every other cycle.

Almost any mass flow and/or intermediate pressure can be set by choosing the number of working and idle cycles.

Due to the pressure losses of the gas flowing in and out of the compression chamber, a small amount of energy is spent. The corresponding thermodynamic work can be found in Figure 5 (area enclosed by line 3).

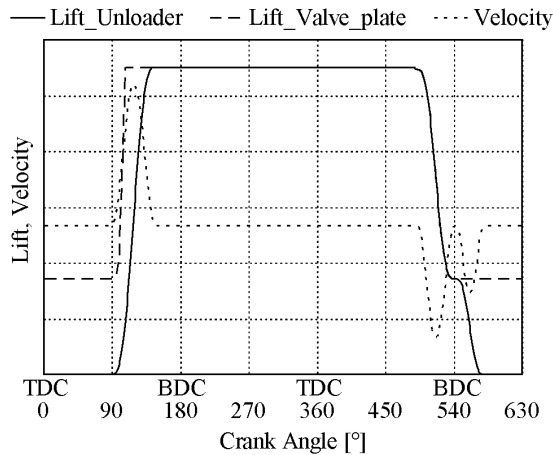


Figure 4: Intermittent capacity control: motion of the unloader and valve plate during one compression cycle

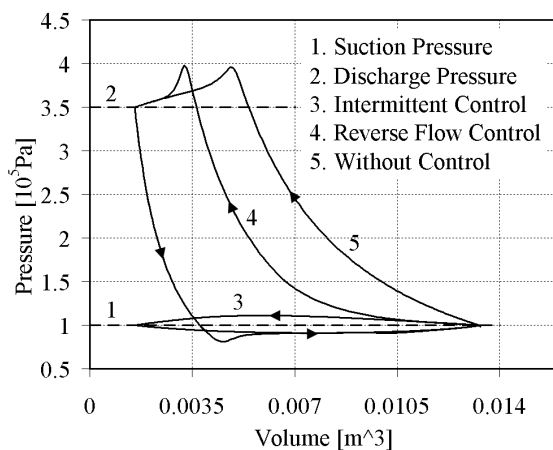


Figure 5: Pressure-volume diagram: different capacity controls

2.2.3 Combined capacity control: Intermittent control and reverse flow control

Combining the intermittent control and stepless reverse flow control also combines their advantages and their disadvantages vanish.

The main advantage of reverse flow control is that a continuously variable mass flow can be set. However, small capacities cause difficulties. Calculations and experiences have shown that the discharge valves have shorter life times for this load. There are two reasons: firstly, the discharge valve does not work at the designed operating point, which can lead to late closings of the valve,

unpredictable movements and loads of the sealing element. Secondly, the closing impact velocities of the valve sealing element can increase (Figures 6 and 7).

Intermittent capacity control is slightly more efficient (Figure 1). Furthermore, the durability of the control components increases since not every cycle is controlled. The drawback is that the mass flow can only be adjusted gradually.

A combined capacity control functions as follows:

- **High mass flows:** Basically, stepless reverse flow control is used. But in this case, the magnetic actuator is not activated every cycle, so that the suction valve can operate one or two cycles without influences. The advantage is that the durability of the components increases and the capacity control itself uses less energy.
- **Medium mass flows:** The reverse flow control is activated in every cycle.
- **Low mass flows:** Basically the intermittent capacity control is used and the suction valve is kept open for one or two cycles. Moreover, the retreating of the unloader can be delayed (reverse flow control) and stepless adjustment of the compressor capacity is possible.

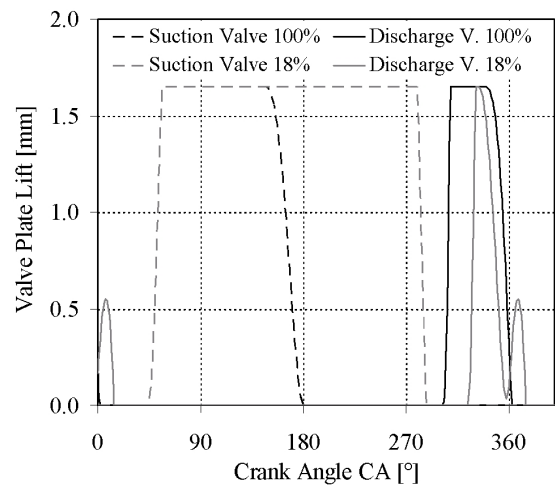


Figure 6: Valve plate lift: 100% mass flow when the capacity control is switched off. 18% mass flow when the reverse flow control is used

	Mass Flow	
	100 %	18%
Rel. Impact Velocity*, Opening CE [%]	60	40
Rel. Impact Velocity*, Closing CE [%]	40	100
Closing Angle, CE [°CA]	365	375
Rel. Impact Velocity*, Opening HE [%]	73.3	60
Rel. Impact Velocity*, Closing HE [%]	70	90
Closing Angle, HE [°CA]	363	376

Figure 7: Influence of the reverse flow control on the discharge valve. *Impact velocity related to allowed impact velocity

2.2.4 Soft landing

The term “soft landing” refers to a motion where the impact velocities of a moving part (the valve sealing element or the unloader) are below 0.1 m/s. Here, the limit of 0.1 m/s has been chosen because noise and wear are considered to be low. In other words, soft landing guarantees high durability. In addition, in cases where low noise levels are required, the capacity control does not add much noise (Figure 8).

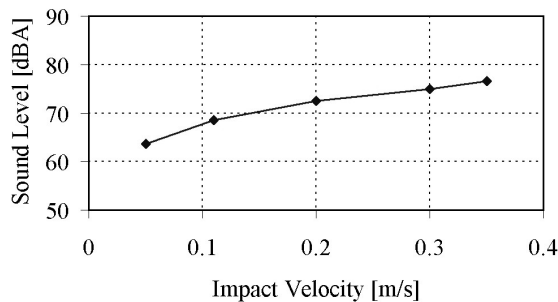


Figure 8: Measurement of the sound level (distance to capacity control: 0.5 m) depending on the impact velocity without compressor noises

High impact velocities lead to wear within short time periods (Figure 9). The impact of the unloader on the valve sealing element is especially critical. The selected contact materials also play an important role.

2.3 Components of the capacity control

2.3.1 Magnetic actuator

A wide range of actuators are available to operate the unloader. Not only magnetic actuators but also hydraulic actuators provide the necessary main features.

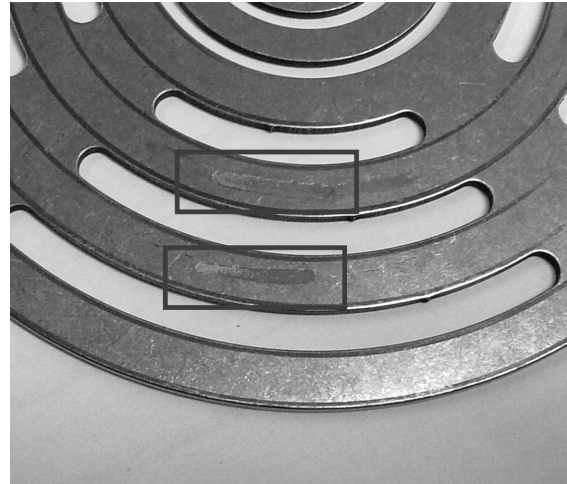


Figure 9: Wear of the valve sealing element caused by the unloader after 200 hours of operation with high impact velocities

The advantage of the hydraulic actuator is its compact design. However, the drawbacks outweigh the advantages of this solution. Firstly, the hydraulic system has high acquisition and maintenance costs. Secondly, it is prone to oil leakage. On the other hand, the advantage of the electromagnetic actuator is that rapid design changes of the motion control are possible and rapid design tools for simulation and control are available. However, soft landing requires advanced control approaches. Everything considered, a magnetic actuator was chosen.

The development of an electromagnetic actuator is based on the most-used concept of electromagnetic controlled valves in the automotive industry^{4,5,6}. In Figure 10 / Magnet, A the basic principle of such an actuator is shown. Two springs force the armature of the magnet to be in a middle position. A small retaining magnet is placed at each side of the armature. A typical cycle proceeds as follows: The armature is held in an end position by the retaining magnet. When the magnet is switched off, the springs accelerate the armature towards the opposite end position. The armature runs through the central position at maximum speed and is then slowed down because of the springs. Finally, when the armature reaches the opposite end position, the second retaining magnet is switched on and the armature is captured and held. When using this system in reciprocating compressors, three problems occur:

- When using reverse flow control, the actuator should slow down the movement of the valve sealing element and should put the sealing element gently onto the valve seat. Since this actuator cannot stop the armature between the two end positions, the sealing element of the valve has a high impact velocity when the valve closes

- As the valve closes, the flow force can be much higher than the friction and the spring forces. Hence the armature is accelerated beyond the middle position, resulting in high armature impact velocities. Soft landing is not possible since the system is not capable of decelerating the movement
- If the armature does not reach the opposite end position due to increased friction or a malfunctioning motion control system, the armature ends up in the middle position and leaves the valve half open, which may cause problems. Furthermore, the initialization of the magnet (moving the armature back to an end position again) will take some time

In order to overcome the problems stated above, the two magnets have been reduced to one stronger magnet, which is capable of applying enough force on the armature over the whole lift (Figure 10, Magnet B). In addition, only one spring is necessary to provide the returning force.

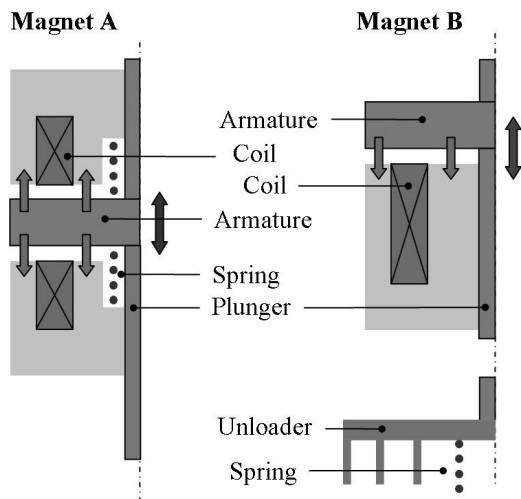


Figure 10: Different armature configurations: Magnet A consists of two magnetic actuators. The springs hold the armature in centered position. Magnet B consists of one magnet only and the returning force is derived from the spring mounted on the unloader

Two different solenoid configurations have been considered (Figure 10, Magnet B and Figure 11, Magnet C). Only one working air gap is in the magnetic circuit of Magnet C. This leads to increased forces at high lifts and slightly decreased forces at low lifts compared to Magnet B. The drawback of design C is the higher load of the bearings due to the transverse forces in case of imperfect symmetry. In comparison, Magnet B has two working air gaps, which lead to small transverse forces. However the magnet has to be bigger to achieve the same force at high lifts.

Taking everything into consideration, Magnet C was chosen.

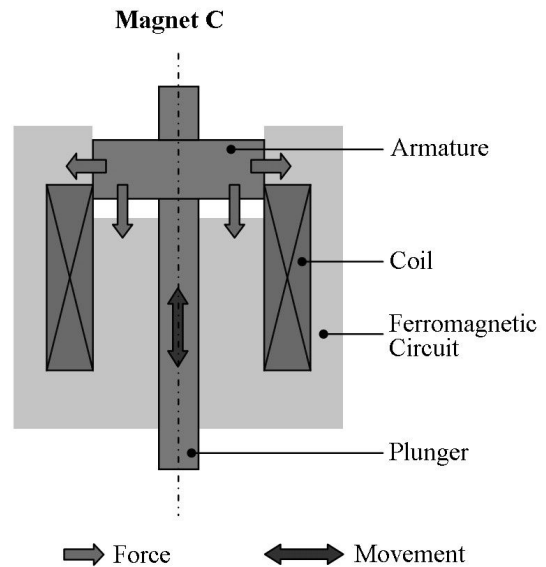


Figure 11: Final solenoid configuration: Magnet C has one working air gap in the magnetic circuit

2.3.2 Unloader

There are two main technical requirements for the unloader (Figure 12). Firstly, the unloader must have low weight in order to reduce the cycle time of the capacity control and, in this context, the required force of the actuator. Secondly, a low drag coefficient reduces the required force of the actuator, guarantees unaffected operation of the valve during idle times, and keeps the pressure losses, and therefore the energy losses, low.



Figure 12: Unloader for the Burckhardt poppet valve™

2.3.3 Position sensor

The motion control quality strongly depends on the performance of the position sensor of the magnetic actuator. High standards must be demanded regarding linearity, resolution, frequency response and temperature stability, to name but a few. An eddy current sensor or an incremental magnetic position system fulfils these requirements.

2.3.4 Power electronics and control unit

The power electronics and control unit determine and deliver the required amount of electric current for the magnet coil based on the actual position.

In order to achieve soft landing (see section 2.2.4) the armature of the magnet must follow a given position trajectory, and must therefore be provided with the corresponding electric current. However, if the electric current or the position of the armature is changed (both effects alter the inductivity of the magnet), eddy currents prevent the immediate change of the magnetic force. In other words, the build-up of magnetic force is delayed in comparison to the current running through the coils. Therefore, experiments have shown that a simple PID-controller (proportional – integral - derivative controller) in closed-loop control achieves only poor results. The armature cannot follow the desired trajectory and the impact velocities are high.

Performance improvements of the trajectory following can be obtained with an additional feedforward loop (Figure 13). With this, the behaviour of the system can be altered in advance, depending on the reference signal r . Robustness against disturbances is warranted by the feedback controller, which compensates the error e , the difference between reference position r and the actual position y . The total input u to the plant is the sum of the feed-forward signal u_F and the feedback signal u_C , representing the necessary electric current. This signal is sent to a chopper that delivers the current to the coils of the magnet ⁷.

2.3.5 Power supply and master control unit

The power supply and master control unit can be located far away from the compressor (e.g.: outside the explosive area). It supplies the necessary control parameters and information (e.g. crank angle) for the control units at each suction valve. For diagnosis and monitoring purposes, the control units send their status, error and monitoring signals to the master control.

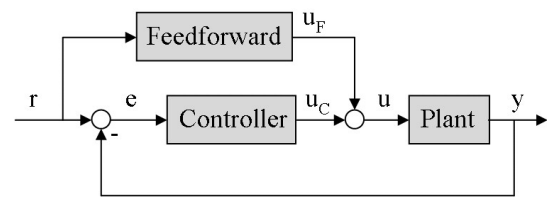


Figure 13: Motion control: r =reference signal (position), e =error, u_F =output of feedforward controller, u_C =output of feedback controller, u =total plant input (current), y =output (motion)

3 Simulation

3.1 Dynamic model

A dynamic model of the capacity control takes the following subsystems into account:

- Compression chamber and piping (fluid dynamics, thermodynamics)
- Valve dynamics
- Dynamics of unloader, spring and magnetic actuator
- Controller unit and chopper (electrodynamics)

The modelling of the compression chamber, piping and valve is well-known and a detailed description can be found in the references ^{8,9,10}. Moreover the modelling of the unloader and spring dynamics, electronics for the controller unit and chopper are straightforward and will not be discussed further.

Three different approaches are used to capture the behaviour of the magnetic actuator ^{1,7}.

Firstly, the governing equations of the magnetic field are solved by means of finite element methods (FE methods). Comparison of simulation and measurement results shows that differences in static magnetic forces are very small. Hence, this approach is used to optimise the static specifications of the magnet (size of magnet, magnetic flux density of the ferromagnetic circuit (Figure 14) and number of windings).

Secondly, an analytical function is used where the static magnetic force depends on the armature lift and electric current. This equation is extended with terms describing the dynamic build-up of the magnetic force. Even eddy currents can be taken into account. Since the structure of the dynamic model is known, model-based feedback and feed-forward controllers can be designed and optimised.

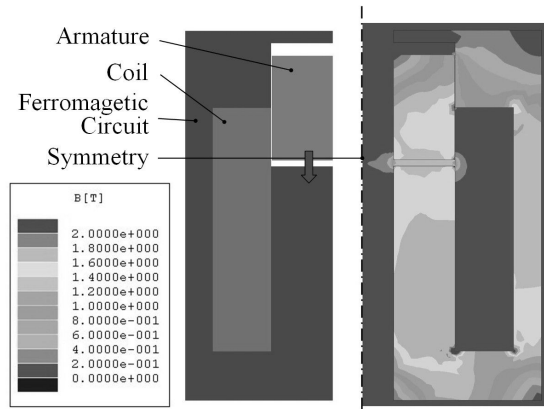


Figure 14: Magnetostatic FE-simulation 2D: magnetic flux density B of the magnet

Thirdly, a lumped magnetic network is used. Here the ferromagnetic circuit and the working air gap are replaced by magnetic reluctances. Again, eddy currents can be taken into account. Short calculation times are the advantage of this method compared to FE methods. However, differences between calculated and measured forces can be remarkable but sufficiently small for simulating the complete system of the capacity control.

The results of the complete simulation of the unloader lift, velocity and coil current show that soft landing should be possible (Figure 15). Observing the electric current trajectory gives better insight into the magnetic actuator. High electric currents are needed in order to set the unloader in motion. During the motion towards the valve guard, the current is reduced (90° CA). Since the unloader lift decreases, the necessary current is very low for holding the unloader in the end position. In this case, the pressure forces on the valve sealing element are rather high compared to the spring forces. Therefore, a high amount of electric current is needed to achieve softlanding during the backward motion.

3.2 Thermal simulations

The electric current running through the coil produces heat (up to approximately 200 W). CFD (computational fluid dynamics) simulations have shown that natural convection is not sufficient to keep the temperatures of the capacity control system below a critical temperature. Not only must the coil and surface temperatures be limited, but the power electronics and control unit also cannot endure high temperatures.

Forced convection has a much higher heat transfer coefficient. Figure 16 shows a simplified model of the capacity control, including a pressure vessel where air is forced through cooling channels. In this case, the maximum temperature of the coil does not

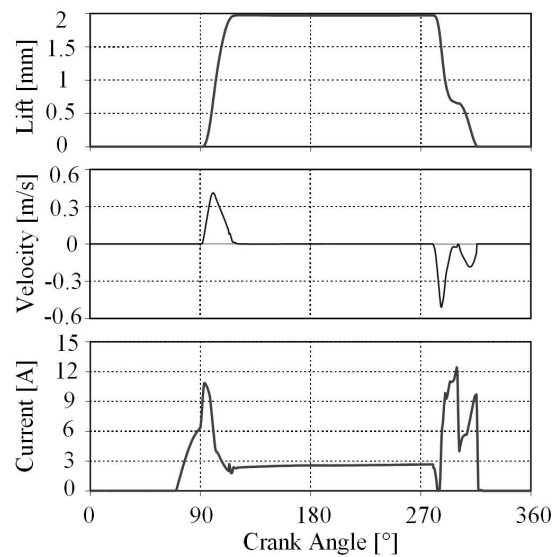


Figure 15: Simulation results: lift and velocity of the unloader and current through the coil

exceed 53°C when the ambient temperature is assumed to be 30°C.

Forced convection has a much higher heat transfer coefficient. Figure 16 shows a simplified model of the capacity control, including a pressure vessel where air is forced through cooling channels. In this case, the maximum temperature of the coil does not exceed 53°C when the ambient temperature is assumed to be 30°C.

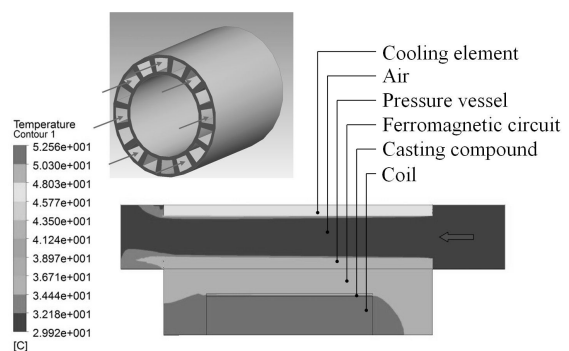


Figure 16: CFD simulation: cooling system of the capacity control, forced convection

4 Measurements

Long-term test runs have been conducted on two different test compressors in operation to test the functionality of the prototypes and verify the simulation results. The first test was conducted on a single-stage, double-acting compressor, where air is compressed from 1 to 4 bar. Here, the design of the capacity control and the motion control was optimised.

It turned out that using a slightly different approach motion for the unloader improves the impact velocity considerably. Instead of moving the unloader towards the valve guard all at once, the unloader comes to a brief halt before reaching the final end position next to the valve guard (Figure 17). In this case, the unloader devices were fitted to plate valves with a lift of 1.35 mm. Therefore, the lift of the magnetic actuator was limited to 1.55 mm. The opening impact velocity is kept below 0.1 m/s (0.45 m/s) and hence soft landing is achieved. The closing impact velocity is slightly higher (0.75 m/s, Figure 18).

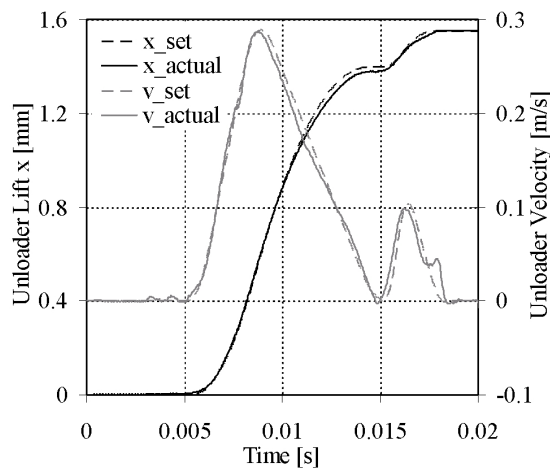


Figure 17: Measurement of the unloader lift and velocity during the motion towards the valve guard

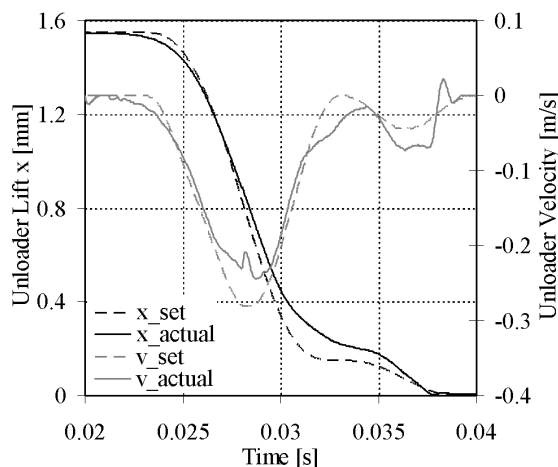


Figure 18: Measurement of the unloader lift and velocity during the motion away from the valve guard

In order to test the impact of the capacity control on a multi-stage compressor, a two-stage compressor was fitted with a set of prototypes (Figure 19). Moreover, a long-term test run (500 hours) was conducted and every component was analysed afterwards. Not only the mechanical parts, but also the used control were verified to function reliably.



Figure 19: Capacity control mounted on a two stage test compressor

5 Summary and outlook

The development of a capacity control system was presented in detail. Not only the basic principles of such a device, but also the main design problems were discussed.

The investigation showed that an electromagnetic system actuating unloaders has many advantages. Furthermore, the best way of operating the unloaders (regarding reliability, durability and efficiency) is choosing between intermittent and reverse flow control, depending on the desired mass flow. The advantages of both operation methods are used and the drawbacks vanish.

An advanced control unit is used to control the motion of the unloader in order to achieve soft landing. Soft landing, in turn, guarantees the reliable and durable operation of the capacity control.

The basic principles of the simulation of such a system were discussed and important simulation results highlighted. It turned out that forced convection has to be used in order to limit the operating temperature range of the magnetic actuator and the power electronics.

The prototypes were tested and optimised on two different compressors. The simulation results were verified and the functionality of the mechanical parts and the motion control were proven.

In the near future, field tests must be conducted and approval for operation in explosive areas must be obtained.

6 Acknowledgements

The authors want to thank P. de Lapersonne and M. Lehmann for many fruitful discussions.

References

- ¹ Kallenbach, E., Eick, R., Quendt P., Ströhla, T., Feindt, K., Kallenbach, M. (2008): Elektromagnete. Vieweg Teubner
- ² Kopecek, H., Klockow, H., Schmitz M. (2008): Development and Test of an Electrical Valve Actuator for Reverse Flow Capacity Control of Reciprocating Compressors. 6th EFRC-Conference, 98-104
- ³ Schiavone, M., Raggi, A. (2008): Electromechanical Actuator for Reciprocating Compressor Stepless Control. 6th EFRC-Conference, 180-187
- ⁴ Hoffmann W., Peterson, K., Stefanopoulou, A. G. (2003): Iterative learning control for soft landing of electromechanical valve actuator in camless engines. IEEE trans on control system technology, 11(2), 174–184
- ⁵ Peterson, K., Stefanopoulou, A. G. (2004): Extremum seeking control for soft landing of an electromechanical valve actuator. Automatica, vol. 40, no. 6, pp. 1063–1069
- ⁶ Tsai, J., Koch, Ch. R., Saif, M. (2008): Cycle Adaptive Feedforward Approach Control of an Electromagnetic Valve Actuator. Proceedings of the 47th IEEE Conference on Decision and Control, 5698-5703
- ⁷ Keilig, R. (2007): Entwurf von schnellschaltenden (hochdynamischen) neutralen Elektromagnetsystemen. Dissertation TU Ilmenau
- ⁸ Costagliola, M. (1950): The Theory for Spring Loaded Valves for Reciprocating Compressors. J. Appl. Mech, 415-420
- ⁹ Aigner, R. Meyer, G., Steinrück H. (2005): Valve Dynamics and Internal Waves in a Reciprocating Compressor. 4th EFRC-Conference, 169-178
- ¹⁰ Aigner, R. (2007): Internal Flow and Valve Dynamics in a Reciprocating Compressor. Dissertation TU Vienna
- ¹¹ Workshop documentation of the 5th EFRC-Conference (2007): Capacity Control

Noise Reduction at a Hydrogen Compressor Plant

by:

Andreas Allenspach

Samuel Burkhalter

Burckhardt Compression AG

Winterthur

Switzerland

andreas.allenspach@burckhardtcompression.com

samuel.burkhalter@burckhardtcompression.com

**7th Conference of the EFRC
October 21th / 22th, 2010, Florence**

Abstract

Loud noise was reported at the commissioning of a hydrogen compressor in a refinery. Despite the low compressor rotation speed of 495 rpm, the reported frequency of the noise was over 1000 Hz.

A measurement campaign at the compressor plant showed, that the noise was generated around some of the installed orifices. Some orifice modifications showed a huge improvement in the noise produced, some not. Therefore, the noise generation around orifices was investigated in detail. In this paper, the measurement campaign, the following root cause analyses and the results, as well as a few methods to avoid the problem will be presented.

1 Introduction

Loud noise was reported at the start up of a hydrogen compressor, which was built according the API 618 guideline. The compressor rotation speed is 495 rpm. Hydrogen is compressed from 19 to 167 bars in three stages for feeding a hydrocracker in a refinery. The motor power for the 4-crank compressor is 3.4 MW. Despite the recommendation of API 618⁹, no pulsation study was carried out for the piping system of this compressor.

This paper describes the subsequent measurement campaign and the investigation to solve the noise problem.

2 Measurement campaign

2.1 Measurement methods

2.1.1 Simple method

The sound pressure measurement from the client indicated a noise level of 90 to 101 dBA, taken near the compressor. However, with the compressor located indoors next to other compressors, including a turbo compressor, the source could not be clearly identified. A field service engineer roughly estimated, without any measurement tools, that the orifice flange after the 3rd stage discharge pulsation damper was the source. This orifice was replaced with a multi-bore restriction orifice (MBRO). After starting up again, the noise was still present.

2.1.2. Portable vibration monitoring tool

Subsequently, a thorough measurement campaign was carried out. Vibration spectra were taken at different locations along the process piping (Figure 1). A standard hand-held vibration monitoring device with a pick-up frequency of 1 to 5000 Hz delivered satisfactory results. With increasing amplitude towards the noise source, the area around the 1st stage suction and discharge pulsation dampers were chosen for the permanent measurement installation.

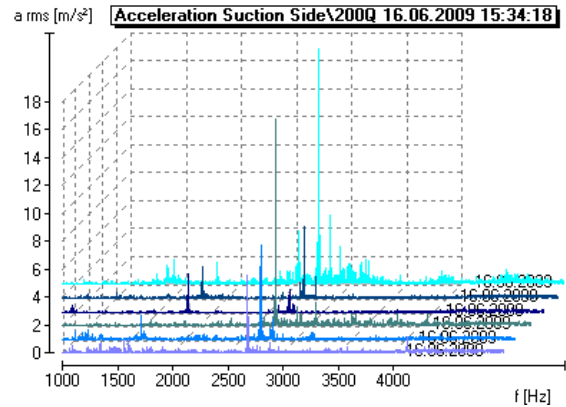


Figure 1: Spectra obtained with hand-held vibration diagnostic tool from measurements taken along 1st stage process piping

2.1.2. Installation of accelerometers

A total of seven accelerometers were installed at the damper inlet and outlet flanges using measurement equipment and the services from the Machinery Dynamics and Acoustics department⁸ of Sulzer Innotec. Between these flanges, orifices were installed for pulsation dampening. The goal of the measurement was to evaluate the source of the noise.

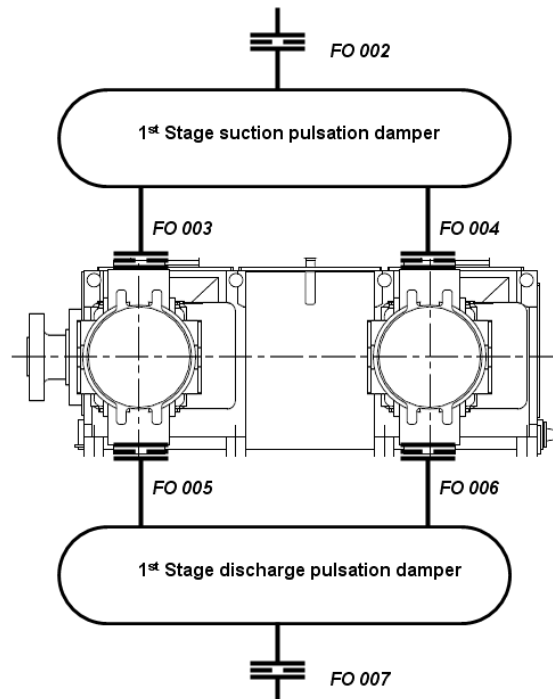


Figure 2: Overview of first compression stage pulsation dampers and orifice flanges

In addition, a microphone was placed next to the 1st stage of the compressor, in order to compare the noise frequency to the measured vibration frequency, so that the location of the noise could be identified.

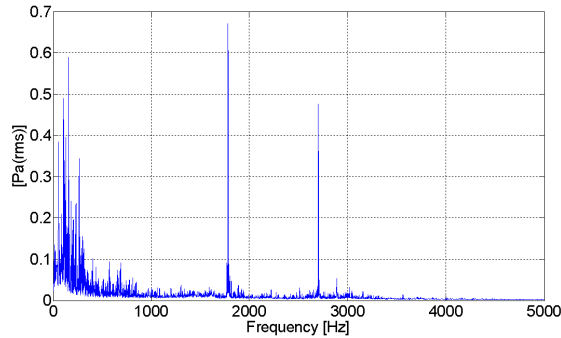


Figure 3: Noise spectra from microphone showing two peaks, one at 1780 Hz and the other one at 2700 Hz

The measured data was recorded simultaneously on an eight-channel recorder. This way, the two dominant frequencies of the noise could be attributed to their emitting source.

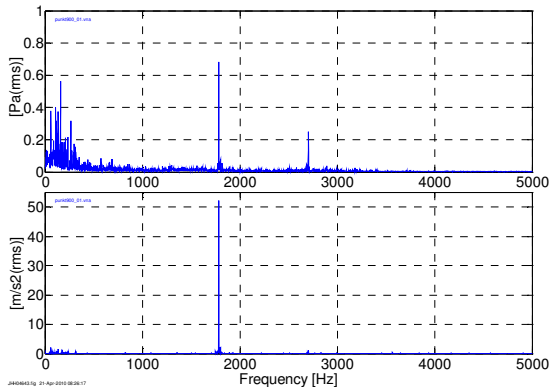


Figure 4: Spectra from microphone compared to acceleration measurement at orifice flange FO 007

By comparing the noise and the vibration measurement, the frequency at 2700 Hz could be allocated to the damper flange before the first stage suction damper FO 002. The noise at 1780 Hz could be allocated to the damper flange FO 007 after the first stage discharge damper (Figure 2).

The suction pressure, bypass mass flow and compressor capacity were varied in order to evaluate the sensitivity of the noise to changing process conditions. The noise disappeared if the capacity was reduced to 75% or below by suction valve unloaders, but there was no change from modifying the suction pressure or the compression ratio (what results in modified discharge temperatures).

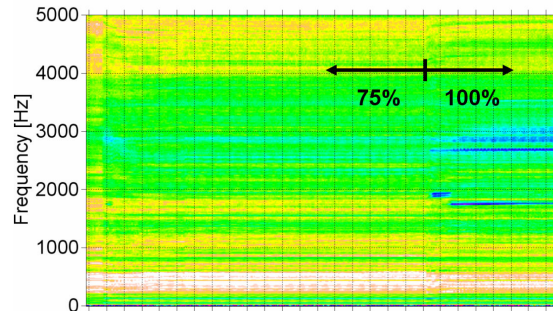


Figure 5: Measured noise frequency with varying process parameters plotted over time

2.2 Onsite adjustments

2.2.1 Multi-bore restriction orifice (MBRO)

After the first estimation without measurement tools, the third stage discharge orifice was reported as generating the noise. This orifice was replaced by a MBRO the next time the compressor was shut down. An MBRO is known to dampen high-frequency pulsations more effectively (see references ⁵ and ⁶). Only client personnel were present for the re-start, who reported the noise still was present. However, at the later site visit for the measurement campaign, with the same field service engineer present, his impression was that the noise had clearly changed. The vibration measurements at this orifice flange also indicated no dominant high frequency. The special features of MBROs will not be discussed in this paper.

2.2.2 Enlarged circular orifice

After the measurement campaign, the customer asked for a quick adjustment. With the limited time (plant was in full production) and limited material (no spare blank orifice plates), the proposed modification was to increase the inner diameter of the orifice and to change the shape of the orifice edge. Since compressor operation was smooth regarding pulsations and vibrations, reducing the pulsation dampening with a larger inner orifice diameter was acceptable.

TAG No	Pipe diameter [mm]	Orifice diameter ID [mm]	Orifice thickness C [mm]
FO 002	193.4	89 / 95	10
FO 007	193.4	64 / 70	10

Figure 6: Orifice dimensions

The original dimensions of the two noise-generating orifices can be seen in Figure 6. In the “Orifice diameter” column, the first value is the diameter before modification and the second value is the diameter after modification. The geometry can be seen in the sketch below (Figure 7).

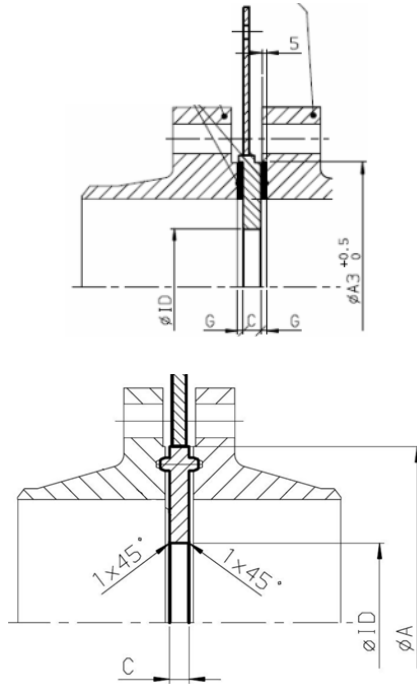


Figure 7: Orifice geometry FO 002 (upper) and FO 007 (lower) before modification

The new, enlarged inner diameter was so that any influence would be measurable. The inner orifice diameter for FO 002 was increased to 95 mm, and for FO 007 to 70 mm (Figure 6). In addition to the enlarged inner diameter, the chamfer angle was changed to 30°.

After the modification of the first stage orifices, the compressor was re-started to repeat the noise measurement and verify the influence of the hardware change.

The high-frequency noise peaks disappeared. There were only two smaller peaks around 3000 Hz (Figure 8).

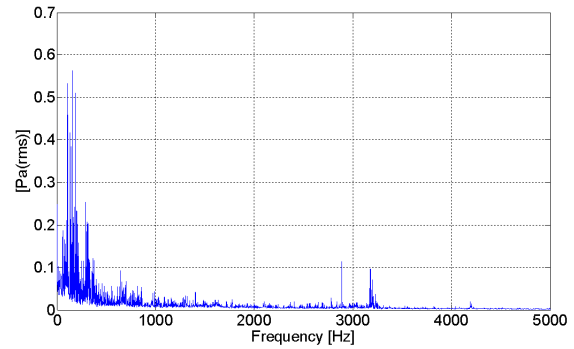


Figure 8: Noise spectra from microphone after modification of the orifices

The modifications eliminated the two noise sources, but did not solve the problem in general. Knowing that enlarging the diameter of the orifice as well as the multi-bore solution would eliminate the noise helped to find the root cause of the problem.

3 Root cause analyses

3.1 Fault tree analyses

All measurement data was analyzed, and subsequently, all possible sources for the load noise were investigated (Figure 9).

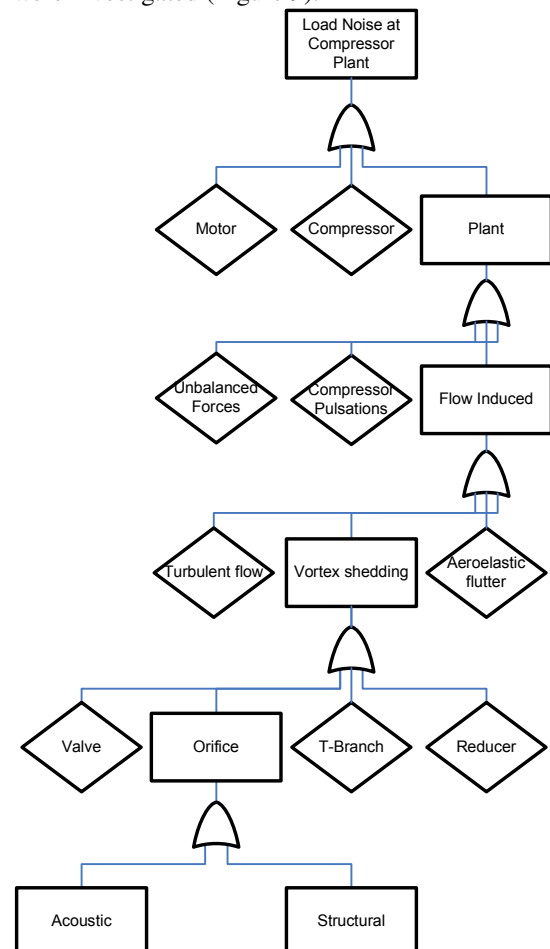


Figure 9: Simplified fault tree for noise problem

Already, initial measurements indicated that the noise was coming from the plant-side equipment. The only thing which went against normal procedure in designing the plant-side equipment was that there was no pulsation study performed for this project. Therefore, the orifice diameters were sized according to the internal Burckhardt Compression standard without pulsation study. To avoid any vibration issues due to compressor pulsation, these orifices were designed with a rather small inner diameter, which resulted in better damping of the resonant pressure pulsations, but also in a somewhat higher pressure drop at the orifices, and therefore a higher power consumption of the entire compressor. Just as an aside, the pulsation study would have been amortized in one or two years, assuming a realistic power reduction of one percent due to the lower pressure drop generated by orifices. With the high measured frequency of up to 3000 Hz, the pulsations from the compressor could not be the source of the problem anyway. Pulsations at this frequency are damped quickly after the source. Therefore, standard pulsation studies only consider pulsations up to the 32nd order of the compressor speed (264 Hz in this case). With step less reverse-flow capacity control, higher frequencies are possible⁷, but there are only valve unloaders at this plant, and no step less reverse-flow regulation. Nevertheless, the rather small inner orifice diameter remained.

The highest unbalanced forces are normally of the first or second order of the compressor rotation speed (8.25 or 16.5 Hz). Much higher frequencies don't have to be considered. Therefore, the source of the high frequency noise is assumed to be in the area of flow-induced pulsations or vibrations. It is typical for flow-induced phenomena to occur the higher the flow velocity is, as shown in Figure 5. To understand the connection to an orifice, the problem of flow-induced pulsations or vibrations was further investigated.

3.2 Flow-induced pulsation

One source of flow-induced pulsations is vortex shedding, which is caused when a fluid flows past a blunt object. Typical points where vortex shedding occurs in the piping system are T-branches, reducers, valves, tube bundles in heat exchangers or orifices.

For the frequency at which vortex shedding takes place, the dimensionless Strouhal number is an important value.

The dimensionless Strouhal number St is given by

$$St = \frac{f \cdot L}{U}, \quad (1)$$

Where f is the frequency of vortex shedding, L is the characteristic length and U is the velocity of the fluid. The Strouhal number depends on the geometry of the body as well as on the Reynolds number.

According to references ¹ and ², a sharp-edged single-bore orifice has the maximum potential to generate noise at a Strouhal number between 0.2 and 0.35, with the orifice thickness t as the characteristic length and the flow velocity inside the orifice U_o . Therefore, the vortex shedding frequency of a sharp-edged single-bore orifice can be calculated as follows:

$$f_{vs} = \frac{St \cdot U_o}{t}, \quad (2)$$

with a given Strouhal number between 0.2 and 0.35. For orifices with different geometries, like multi-bore orifices, different Strouhal numbers must be considered, so different frequencies will also result.

The calculation of a few dimensionless numbers for the two noisy orifices is shown in Figure 10.

TAG No	Noise frequency Hz	Strouhal Number	Reynolds Number in pipe	Mach Number in orifice
FO 002	2700	0.30	428'589	0.068
FO 007	1780	0.19	193'689	0.072

Figure 10: Calculation of Strouhal, Reynolds and Mach number for the two noisy orifices

The Reynolds number is calculated with the pipe diameter D_p , the fluid velocity inside the pipe U_p and the kinematic viscosity ν of the gas.

$$Re = \frac{U_p \cdot D_p}{\nu}. \quad (3)$$

The calculated Strouhal numbers are just at or within the limits described in reference¹. Considering that the Reynolds numbers are at the upper limit with respect to the reference.

The good agreement with the literature allows one to say that vortex shedding is part of the solution. However, all the other orifices also have a vortex shedding frequency in the range of 400-4000 Hz, but no noise or vibrations were detected there. Therefore, the surrounding piping was investigated with regard to resonance.

3.3 Acoustical resonance

For acoustical resonance, the wavelength must be calculated. With λ as the wavelength, c as the speed of sound in the medium and f the exciting frequency (e.g. from vortex shedding), the wavelength is calculated as follows:

$$\lambda = \frac{c}{f}. \quad (4)$$

Resonance occurs if a pipe length between a closed end (e.g. closed valve) and an open end (e.g. damper volume) equals a quarter of the wavelength, or if a pipe length between two closed or open ends, respectively a pipe diameter, matches the half of the wavelength. As well resonances of higher orders (a multiple of the wavelength matches the corresponding length) or resonances due to a volume and pipe system (Helmholtz resonance) is possible.

TAG No	Noise frequency Hz	Wavelength / 2 [mm]	Wavelength / 4 [mm]
FO 002	2700	244	122
FO 007	1780	427	213

Figure 11: Wavelength at noise frequency

No agreement in the calculated wavelength (Figure 11) and the pipe length around the orifice flange could be found. In addition, a variation in the operating pressure and the pressure ratio did not lead to different noise frequencies during measurement. But a variation of the pressure ratio leads to different discharge temperatures. The different temperatures result in a different speed of sound. If there is acoustical resonance, different frequencies should be excited with different speeds of sound (Equation 4). Therefore, acoustical resonance can be ruled out.

For this case, the relevant pipe lengths surrounding the orifices are longer. If the relevant wavelength due to vortex shedding is calculated, the following formula results:

$$\lambda = \frac{c \cdot t}{St \cdot U_o}. \quad (5)$$

For common plant layouts (as in this case), a thicker orifice is more likely to get locked into acoustical resonance because the wavelength increases and the exciting frequency decreases (Equation 2). Pipe lengths (e.g. damper length, length to safety valves) in the area of 1 to a few meters are common in process piping for API 618 compressors. Lower frequencies are less damped for acoustical sound propagation, and therefore the probability of

hearing an audible noise is higher. In other words, the vortex shedding frequency is preferred to be higher than the acoustical resonance frequencies with L as the shortest characteristic pipe length. Therefore, the orifice should be as thin as possible regarding acoustical resonances.

$$\frac{St \cdot U_o}{t} = f_{vs} > f = \frac{2 \cdot c}{L}. \quad (6)$$

Reference³ reaches a similar result based on measurements. Thicker orifices tend to generate more noise due to vortex shedding, combined with acoustical resonances. But contrary to this case, the orifices in reference³ are comparably thick, and all structural natural frequencies of the orifice plates in reference³ are significantly greater than 10'000 Hz.

In any case, acoustical resonance can be avoided by calculating the vortex shedding frequency of the orifice and comparing this with the surrounding pipe length.

3.4 Structural resonance

The vibration measurement indicated heavy vibration directly at the orifice plate. Therefore, a modal analysis of the orifice plate was performed. The different design of the orifice-supporting outer ring (Figure 7) has a relevant influence on the first natural frequency. Figure 12 shows the first natural frequency of the orifice plate FO 002.

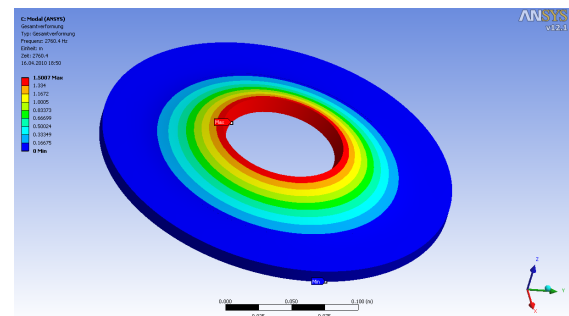


Figure 12: First natural frequency of orifice FO 002 at 2760 Hz (calculated). Support modeled including gasket

The calculated natural frequencies for both orifices agree with the vortex shedding frequencies. The root cause has been found.

Due to the fact that every plate has higher-order frequencies (like in the acoustical system, but much less damped), the vortex shedding frequency should be below the first natural frequency f_0 of the single-bore orifice plate.

$$f_0 > f_{vs}. \quad (7)$$

According to reference⁴, the first natural frequency of an orifice plate is proportional to its thickness

$$f_0 \approx t \quad (8)$$

Regarding structural resonance, the thicker the cylindrical single-bore orifice, the better. The ratio of the first natural frequency to the vortex shedding frequency changes quadratically with the plate thickness. A quick improvement is made by adjusting the plate thickness, keeping in mind that the modification can be negative with regard to acoustical resonance.

$$\frac{f_0}{f_{vs}} \approx t^2. \quad (9)$$

A remaining question is why the structural resonance problem of the orifice plate occurred at this plant. One reason is that for the same pressure drop, the ratio of the orifice diameter to pipe diameter decreases for a gas with lower density (like with hydrogen). In addition, no pulsation study was performed for this plant. Therefore, the ratio is further decreased. According to reference⁴, the ratio of the orifice diameter to the pipe diameter has a significant influence on the first natural frequency of a fixed clamped orifice (Figure 13).

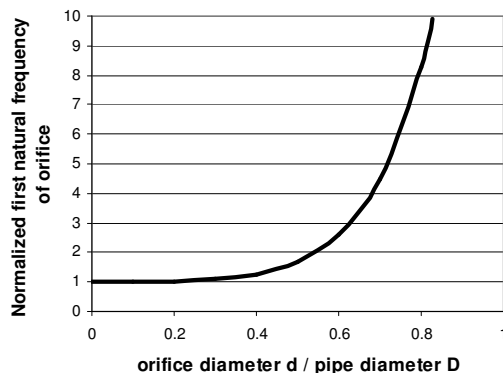


Figure 13: Natural frequency of a fixed clamped orifice plate depending on the ratio of the inner orifice diameter d to the pipe diameter D , according to reference⁴

Another point is that, due to the high speed of sound in hydrogen, higher velocities in the pipe are allowed. The small orifice bore leads once more to higher velocities in the orifice. This increases the vortex shedding frequency and the kinetic energy in the flow. Finally, the thickness of the orifice plate is to the same as in most other plants.

4 Conclusion

The thickness of a sharp-edged, single-bore cylindrical orifice must be carefully selected.

The orifice must be thin enough so that the vortex shedding frequency is sufficiently high, such that no acoustic resonance develops near the orifice, but must still be thick enough so that the orifice plate natural frequency does not equal the vortex shedding frequency. By avoiding matching frequencies, the problem is solved.

With a multi-bore orifice or an orifice with beveled edge, different Strouhal numbers must be considered because of the modified geometry, thus resulting in a different vortex shedding frequency. One advantage of these configurations is that the kinetic energy (due to the orifice) in the turbulent flow can be reduced, thus reducing the potential for loud noise. But the principle problem of any acoustical or structural resonance remains.

The remaining question is what energy is required for a resonant system with an acoustical or structural natural frequency to create an audible noise, including acoustical or structural damping.

References

- ¹ P.Testud et al. / The whistling potentiality of an orifice in a confined flow using an energetic criterion / Journal of Sound and Vibration 325 2009 page 769-780
- ² P.Testud et al. / Experimental Validation of a Whistling Criterion for Orifices in Air Pipe Flow / 2006
- ³ Karthik Balachandrian / The aero acoustics of an orifice in a circular duct / PhD Thesis, Department of Aerospace Engineering, Indian Institute of Technology, Madras Chennai India October 2003
- ⁴ A.Leissa / Vibration of Plates / Acoustical Society of America 1993 originally issued by NASA 1973
- ⁵ M.C.A.M.Peters / Evaluation of low frequency pulsation damping devices / TNO TPD Delft 2nd EFRC Conference The Hague 2001
- ⁶ M.C.A.M.Peters / Evaluation of low frequency pulsation damping devices / TNO TPD Delft TNO report DMP-RPT-040244 2004
- ⁷ Harry Korst. Willem Bocus / Noise Reduction at a NAM-compressor Station / TNO TPD Delft, NAM-EPE-T-PC 4th EFRC Conference Antwerp 2005
- ⁸ S. Huijbers / Whistling noise measurement piston compressor / Technical report, Sulzer Innotec 2009
- ⁹ API Standard 618 / Fifth edition page 54 / December 2007

Straight or Twisted ? - ‘Laser Talks’

by

Mr Stefan Damberg

Project Engineer – Laser Technology

Stefan.Damberg@NEAC.de

and

Mr Harry Lankenau

Head of Engineering and Technical Support

Harry.Lankenau@NEAC.de

NEAC Compressor Service GmbH & Co. KG

Uebach-Palenberg, Germany

7th Conference of the EFRC

October 21th / 22th, 2010, Florence

Abstract

Good alignment of rotating machinery axes – such as multi bearing shaft lines, multi stage cylinders and cylinders to crosshead guides – have ever since been an important engineering and construction subject. The alignment accuracy contributes to proper and reliable running of the machine. Particularly reciprocating compressors may reach a lifetime of 50 and more years and they are naturally subject to “wear and tear” with the potential consequence that alignment accuracy deteriorates with time. Since process requirements are likely to change during its lifetime it may need to be trimmed to match the new requirements and consequently undergo significant modifications. In this case it is essential and economic to check the alignment before and after carrying out the work. Last not least foundations tend to deteriorate with time which may cause twisting of the crankcase. If the alignment is – for whatever reason – in doubt or a thorough check is required for reasons outlined above the laser technique has proven to be a quick, practical and easy-to-apply tool. Lasers do the “Laser Talk” if this tool is utilized by experienced engineers who handle it on a day-to-day basis. This paper will outline examples for the typical application of state-of-the-art laser equipment in conjunction with field repair activities.

1 Introduction

After many hours of operation for every machine - particularly if integrated in an important section of a chemical plant, refinery or in natural gas storage application with large amount of money being involved – there is a time when a comprehensive overhaul is due.

It is not unusual that some unexpected abnormal wear is found in the run of such a major revision. For example a worn out or even damaged bearing may be found or the wear pattern of rider bands is excessive and much different from that seen during previous maintenance work.

In such cases the “revision” turns into “repair” and naturally the question is raised: “Why did that happen?” The question is, of course, also asking for an answer and in order to be able to give that answer adequate investigations need to be defined.

Apart from the aspect of high loads during operation being the cause for the damage it is also the geometry and shape of the frame and its throws which may be in doubt. Is the frame still in perfect level and the main bearing way well aligned? – Has the quality of the foundation deteriorated and the frame is not as tight to the ground as it should be ? – Did the soil underneath the foundation allow for overall sagging ? - Any high loads from the piping and vessels – such as stress from thermal elongation – which had pushed the throws aside and thus twisted the frame?

To achieve clarification with regard to main bearing way alignment, perpendicularity of throws vs. main bearing way, planarity of frames and foundations the Laser Technology is exactly the tool to be utilized.

If the machine is “straight or twisted” – the Laser “talks”.

2 Foundation Repair with Compressor Frame Removal - Example for Laser Application

Piston compressor foundations and their frames typically suffer long term deterioration from:

- Unbalanced mass loads
- Oil penetration into the concrete (picture no. 1)



Picture no. 1: Oil penetrated Foundation Block

- Unfavourable ambient conditions (e.g. ice formation, corrosion, aggressive product)
- Cracked off concrete or grouting and loose or broken foundation bolts (picture no.2)



Picture no. 2: Cracked off Grouting and bad Bolting

Frame twisting on a poor foundation and rocking movement may cause deformation, misalignment and consequently increase material stress; potentially reaching or even exceeding yield limits.



Picture no. 3: Major Damage of Foundation

OPERATIONS

Straight or Twisted ? – ‘Laser Talks’, *Stefan Damberg, Harry Lanckenau; NEAC COMPRESSOR SERVICE*

If a condition has been reached as shown on pictures no. 1 through 3 it is time to consider a sound foundation repair - and most likely also the machine itself may want some service activities.

Laser technology renders the desired assistance as outlined in the example below.

After removal of the complete compressor and its accessories the oil contaminated top of the foundation was chipped off (picture no. 4).



Picture no. 4: Oil contaminated Foundation Top chipped off

Picture no. 5 shows the foundation after reconditioning with the application of epoxy resin and frame support blocks already installed.

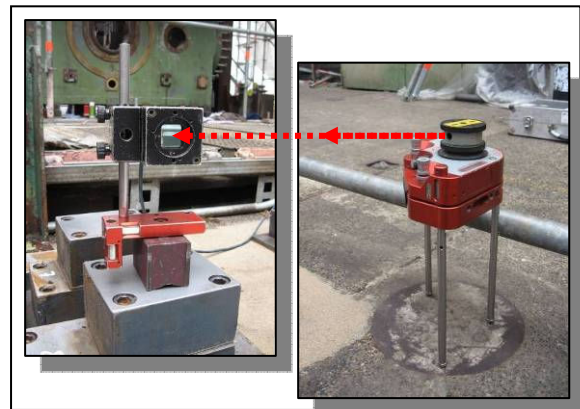


Picture no. 5: Reconditioned Foundation

Prior to the installation of the compressor frame the planarity of the support block top surface was checked with laser equipment to ensure that the compressor crankcase will be in perfect level when put back in place - here shown for a second foundation that was also reconditioned (picture no. 6, 7a and 7b).



Picture no. 6: Laser Planarity Check



Picture no. 7a and 7b: Laser Planarity Check

Once the planarity of the supporting blocks had been verified it was time for the compressor to return to its place.

Picture no. 8 illustrates how the crankcase is “flying in“ and service technicians are watching that the anchor bolts are properly sliding into their foundation sleeves which are going to hold the frame tight on the new supporting blocks and the new foundation underneath.



Picture no. 8: Frame “flying in”

After the frame came back on its base the laser was applied again to check if the main bearing way is “straight” – which means well aligned (picture no. 9).



Picture no. 9: Bearing Way Alignment Check

Finally a planarity measurement was conducted – again with the laser equipment – to see if all check points on the frame top are in the same plane to make sure that the frame is not twisted (picture no. 10).



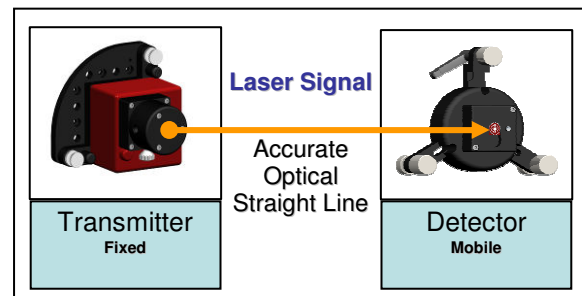
Picture no. 10: Frame Top Planarity Measurement

Through following chapters the various measurements and their application are outlined in more detail.

3 The Way the Laser works

The basic principle of the laser is very simple (picture no. 11). The transmitter (left) sends out a perfectly straight and none diffusive light beam towards the detector (right). This optical line acts as a reference line.

For every point along this laser beam its form and position can clearly be measured and defined.



Picture no. 11: Laser Principle

The signals being sent out from the transmitter and taken up by the detector (picture no. 12) are forwarded via cable to the display unit for data collection and evaluation.



Picture no. 12: Display Unit

4 Various Alignment Technologies

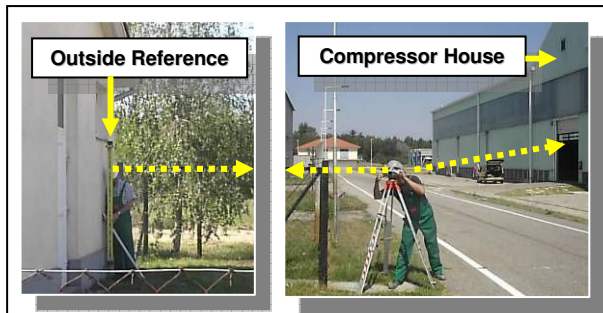
4.1 Levelling and 3D-Laser Foundation Planarity Verification

For the compressor unit shown in picture no. 13 a comprehensive foundation check was to be conducted to verify the exact position, level and geometrical shape of the compressor base.



Picture no. 13: Compressor Unit subject to Foundation Check

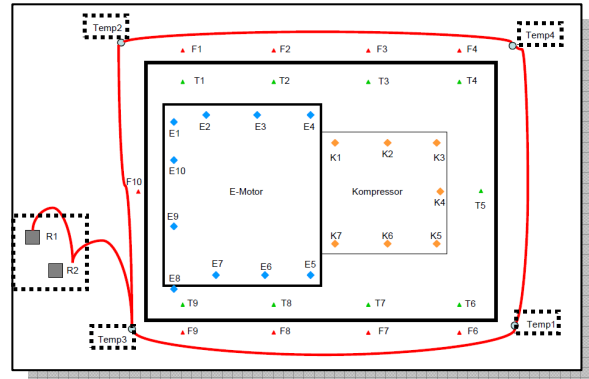
Since none of the points on the concrete block itself inside the compressor house could be used – because those were to be checked - it became necessary to “transfer” reliable outside reference points into the compressor house (picture no. 14) to create temporary reference points there which were then used for the foundation survey.



Picture no. 14: Reference Points “R1” and “R2” transferred into Compressor House to specify Points “Temp 1 - 4”

This “reference point transfer” was a standard level procedure. With the laser a “Loop Closing Accuracy” of 0.01 mm could be achieved.

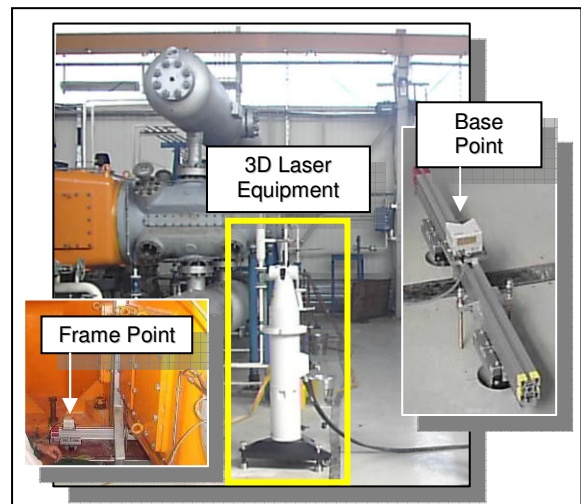
Picture no. 15 depicts the foundation with its various reference points “R1” and “R2” outside and “Temp 1 - 4” inside the compressor house.



Picture no. 15: Foundation Check Points

Based on the temporary reference points the actual foundation form and position check could be started. That measurement was performed with a 3D laser tool.

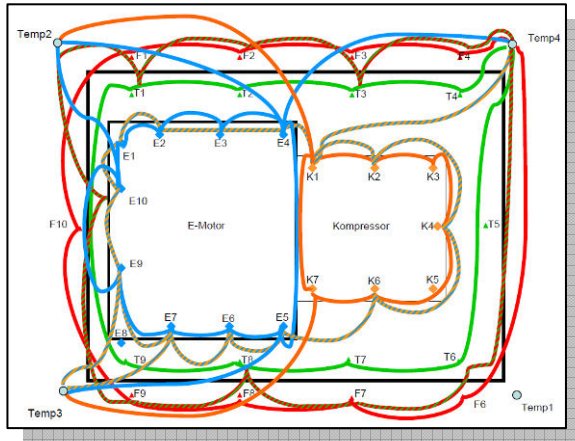
Numerous frame and base points were defined (picture no. 16) and the laser beam moved around, up and down, to collect a vast amount of foundation geometry data.



Picture no. 16: 3D-Laser with Check Points

Picture no. 17 shows the foundation again – this time with the foundation check points inside the compressor house.

For this inside laser check a “Loop Closing Accuracy” of 0.02 mm was achieved.

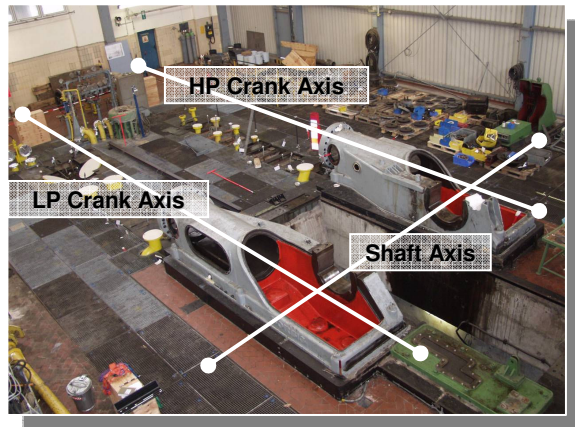


Picture no. 17: Foundation Check Points

The result was that the frame was indeed neither straight nor perfectly flat.

4.2 Traditional Wiring vs. Laser Alignment

The two new frames on the picture no. 18 below had to be set-up and perfectly aligned to each other because they form a kind of twin-frame configuration as part of one combined compressor unit.



Picture no. 18: Twin-Frame Alignment

There are basically two methods of alignment measurement:

1. Traditional Wiring
2. Laser Technology

In this particular case both methods were applied to see if they confirm each other and to have a double check option.

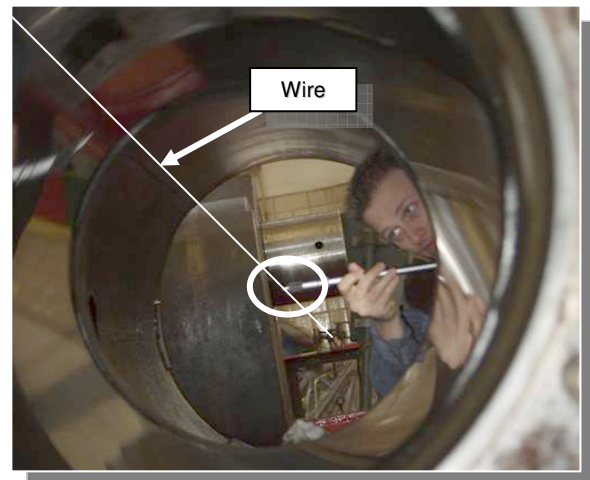
The traditional wiring – which is a procedure that was typically used before the laser was available – is widely forgotten, hardly considered these days and utilized only by few maintenance specialists who still have the experience “how to do it”.

The wiring works with a steel wire which is stretched through the centre of e. g. a cylinder bore (picture no. 19).



Picture no. 19: Alignment through Steel Wire

The space between the wire and the cylinder or liner wall is measured with a micrometer (picture no. 20). To prevent any radial force being applied to the wire – which would result in a wrong measurement – a small voltage is supplied to the arrangement which generates a tone in the head phones worn by the person performing the measurement. Thus every slight contact with the wire - without any force pushing the wire aside – is announced and then the reading can be documented.



Picture no. 20: Radial Alignment Check

There is no need to stress that this procedure is time consuming.



Picture no. 21: Laser Application

In parallel to the traditional wiring a laser alignment, planarity and perpendicularity check was performed (picture no. 21).

Results of “Traditional Wiring” vs. “Laser Measurement for Verification”:

- Wiring versus Laser Measurement confirmed each other
- Laser results verified Wiring within $\pm 0.025\text{mm}$ accuracy
- Typically it is observed that Laser Measurements are faster (2 days vs. 10 days)

4.3 The NEAC Equipment (2D-Laser)

Everything in life is a compromise. The more sophisticated the laser equipment is the more volume and weight has to be hauled. That aspect becomes particularly important if measurements have to be conducted at locations far away from the headquarter.

According to the motto “We do not try to look fancy ... we hand-carry what we need” NEAC took the decision to purchase a 2D Laser Equipment which covers the majority of typically required measurements in the NEAC field and can easily be hand-carried to nearly every place in the world (picture no. 22).



Picture no. 22: NEAC 2D Laser Equipment

Numerous measurements have been conducted over the past years and the equipment has proven to render exactly the required results which provide a much better insight into true frame and throw form and position characteristics.

5 Application of Laser Technology for geometrical Checks - Examples

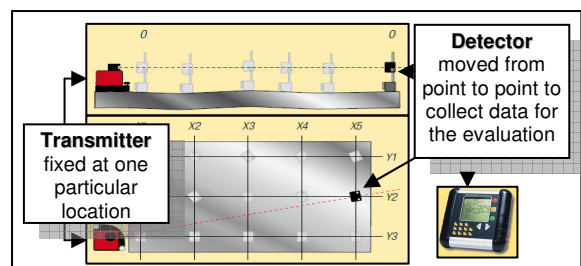
5.1 Foundation Planarity Check

It is a common procedure to check the foundation top with a straight edge and a water level gauge to see if the supporting structure - which will carry e. g. a compressor crankcase - is properly levelled.

The larger the foundation is and the more often the straight edge needs to be moved the longer the measurement takes and the less accurate it becomes.

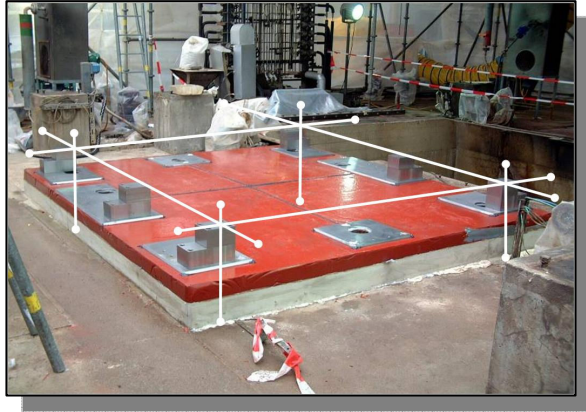
The laser is the faster and more accurate tool - and distance is no issue for its optical beam (up to 40m).

Picture no. 23 depicts the comparably easy procedure of such a planarity check. The transmitter is set-up and adjusted at a suitable point. The laser beam is then sent out in various directions always towards the detector which is moved around and placed on the check points - one by one - to collect the level data for evaluation through the display unit.



Picture no. 23: Principle of Planarity Measurement

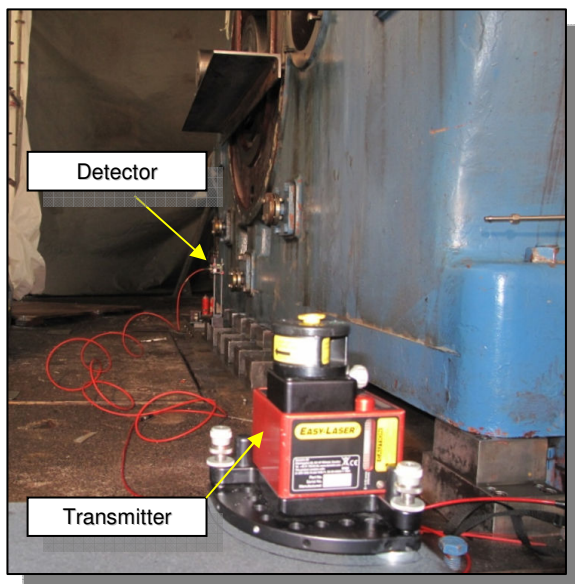
As already outlined in the example of chapter no. 2 the supporting steel blocks shown in picture no. 24 (being placed on a renewed foundation) are going to carry a large compressor frame which is sensitive to twisting and potential rocking.



Picture no. 24: Planarity Check – Principle for a new Foundation

Therefore the planarity check is of the essence for a proper set-up - and the laser did it.

Below is an example for a planarity measurement of the supporting structure of a compressor base during revision activities while the compressor frame is still in place (picture no. 25).



Picture no. 25: Field Planarity Check

5.2 Crankcase Planarity Check

In the everyday practice the water level gauge is the standard tool utilized for crankcase level verification. Crosshead guide, cylinder (liner) bore and main bearing journals are the typical places which are indeed true reference locations.

If the compressor is completely assembled these points are no longer accessible. Other machined surfaces are used instead which, however, need not be true faces, because they have no accurate geometrical relevance to the frame internals.

Furthermore, none of these locations are able to show if the frame is in plane and none-twisted condition.

Having recognized the importance of the planarity and none twisted condition as basic requirement for trouble free operation particularly for large frame sizes, NEUMAN & ESSER (NEA) decided to add machined surfaces on the frame top which run true versus the main bearing way. These can and shall be used for crankcase laser levelling checks later in the field. These surfaces are protected to remain unharmed for future verifications.

Picture no. 26 shows a typical NEA frame size 500 (4 throws) in the NEUMAN & ESSER workshop with encircled machined true face on top.



Picture no. 26: Frame Top True Faces

Picture no. 27 depicts how these surfaces are utilized for a planarity measurement of the frame by using the 2D laser equipment.



Picture no. 27: Utilization of Frame Top True Faces for Planarity Check

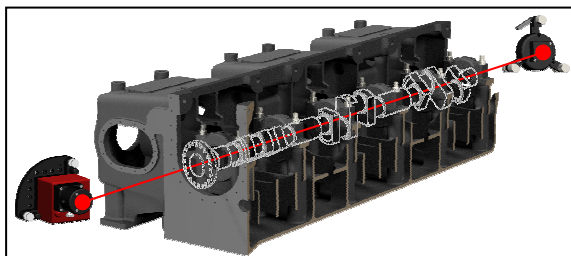
From one fixed transmitter position the laser beam is sent out towards the detector which is moved from surface to surface.

Note: The laser equipment does not allow the check if the frame is parallel vs. horizontal ground level. Therefore the water level gauge is still required to verify the latter.

5.3 Main Bearing Way Alignment

One of the most important locations for alignment checks is the main bearing way. Once the crankshaft is installed the web deflection gives an indication if it is running true – but then it is too late for reconditioning of the bearing blocks, should their alignment be in doubt.

Picture no. 28 is a sketch of the main bearing way alignment before the crankshaft shall be installed.



Picture no. 28: Main Bearing Way Alignment

The procedure is comparable with those being described before. The transmitter has to be fitted to one of the end bearing blocks or at the nearest head frame cover close by.

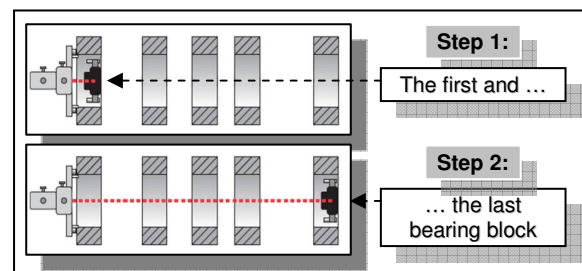
Picture no. 29 is an example for the transmitter fixation at the first compressor main bearing block.



Picture no. 29: Transmitter Fixation at Bearing Block

This fixation is of the essence for the accuracy of the measurement. It must by no means be shifted as long as laser check is ongoing.

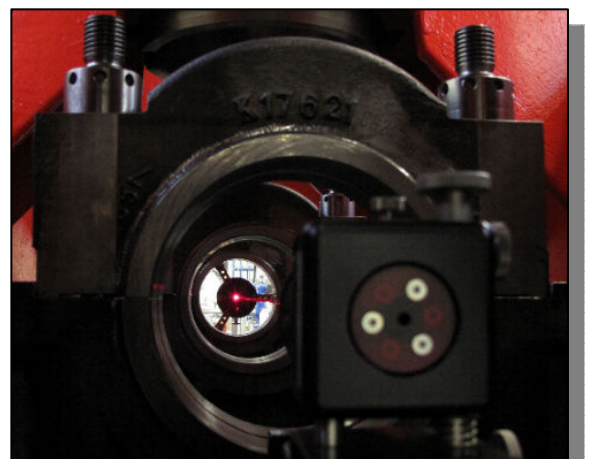
Then the detector is placed at the opposite end of the frame at the last bearing block (picture no. 30).



Picture no. 30: Determination of the Laser Reference Line through the End Bearing Blocks

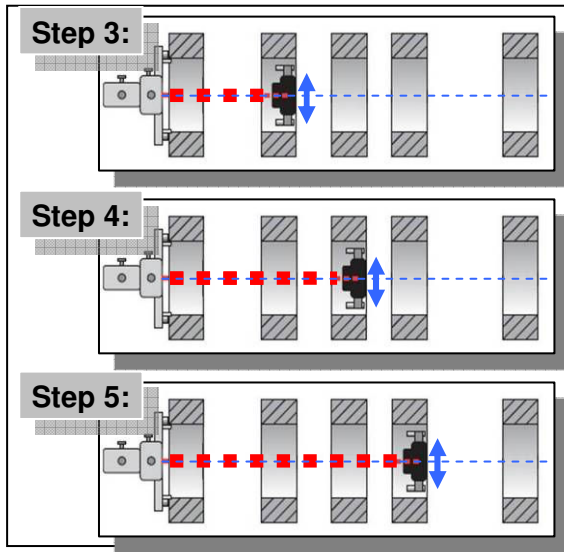
Thus the reference line for the other bearings in-between is defined.

Picture no. 31 perfectly illustrates a practical application in the field.



Picture no. 31: Laser Beam through Main Bearings

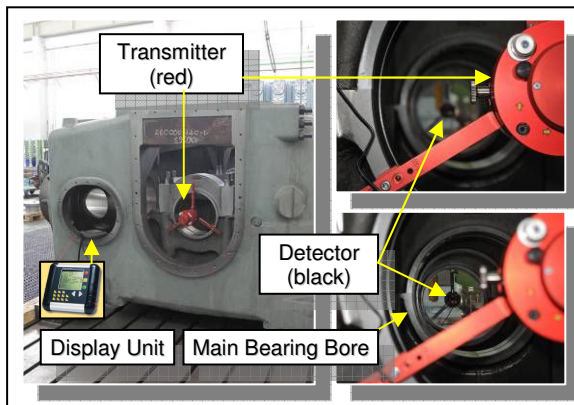
In successive steps (picture no. 32) each bearing block - with or without bearing shell - is checked.



Picture no. 32: Main Bearing Alignment Check

For each bearing block the off-set (if any) from the centre line is identified through the detector moved from bearing block to bearing block.

Such laser measurements are not only conducted in the field but also in the workshop to verify proper machining quality (picture no. 33).



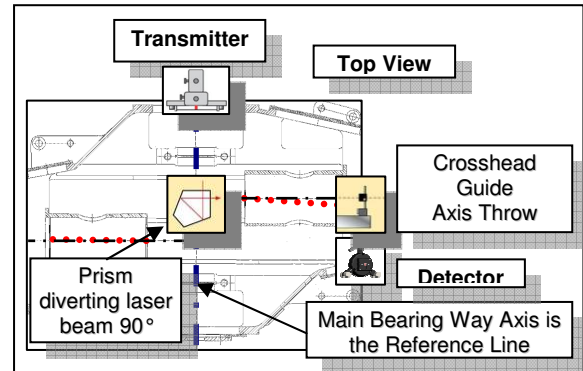
Picture no. 33: Main Bearing Alignment Check in the Workshop

5.4 Perpendicularity of Main Bearing Way versus Crosshead Guide

When the compressor frame planarity and main bearing way alignment have been confirmed it is still not yet clear if the throws are in proper orientation versus the crankcase. The perpendicularity may be disturbed e. g. through abnormal forces from the piping and/or the attached vessel arrangement – typically through thermal elongation and consequential stress being forwarded towards the compressor. Design calculations usually check such forces and the piping lay-out together with the support structure is adjusted to keep

thermal loads below admissible limits. But supports may come loose or corrosion converts a piping “guide” into a “fixed point”. That can have dramatic effects on the integrity of the machine.

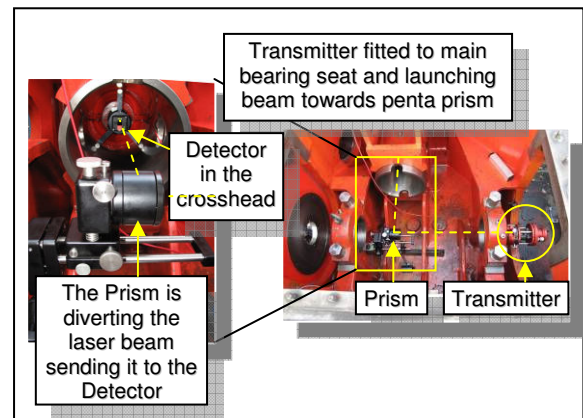
The perpendicularity measurement is depicted in picture no. 34 below.



Picture no. 34: Perpendicularity Measurement

After the reference line through the main bearing way has been defined a penta prism is used to divert the laser beam exactly 90° into the relevant throw. Then the crosshead guide orientation is verified in reference to the main bearing way.

Picture no. 35 allows a glance into a compressor crankcase where all tools are installed for the perpendicularity measurement of the crosshead guide vs. the main bearing way.



Picture no. 35: Perpendicularity Measurement inside Frame and Throw

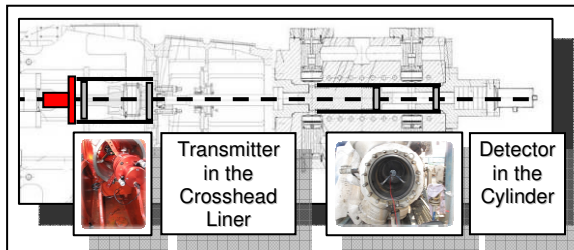
The transmitter – fixed on the right hand side - was previously used for the bearing block alignment check. The prism diverts the laser beam into the crosshead where the detector is located in the guide.

5.5 Cylinder Bore to Crosshead Guide Concentricity

Last not least the crosshead guide may not be in perfect line with the cylinder (liner) bore. Wear and/or inaccurate secondary machining of mating surfaces are potential sources for an alignment off-set between these two parts.

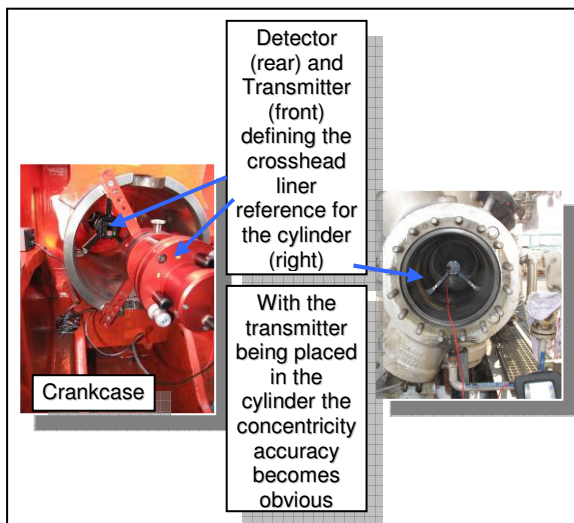
The procedure is very similar to that of the main bearing way alignment. The transmitter is fitted to the crosshead guide end. The detector is set at the head end of the cylinder bore and all check points along this axis are checked if located on that reference line or how much they are off (picture 36).

The evaluation of all collected data outline the true axis – if straight or buckled.



Picture no. 36: *Concentricity Measurement of the Crosshead Guide (left) vs. Cylinder Bore (right)*

Picture no. 37 is again a field example showing the typical location of the transmitter fixation and detector location inside the cylinder.



Picture no. 37: *Concentricity Measurement of the Crosshead Guide vs. Cylinder Bore in the Field*

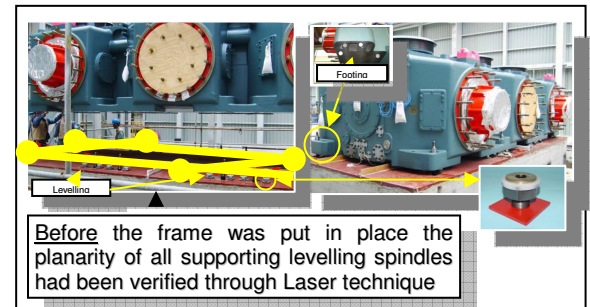
6 Typical Compressor Set-up for new large 6-Crank Machines

Large frames are strong to withstand the process loads along the piston rod axes. But they are sensitive to twisting and sagging. Therefore this 6-crank frame size 500 compressor (picture no. 38) was carefully checked for flatness of the crankcase through application of laser technique.



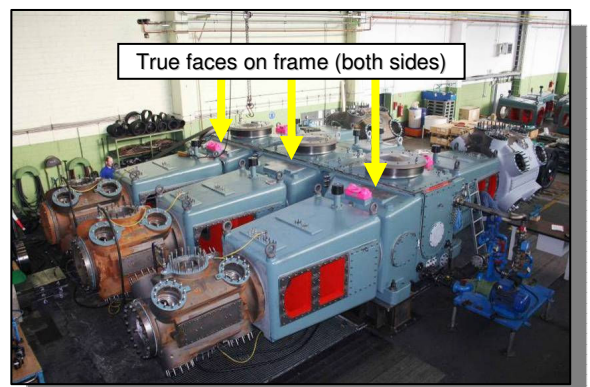
Picture no. 38: *6-Crank NEA Frame Size 500 Compressor*

Before the frame was put in place the planarity of all supporting levelling spindle top spots had been verified through laser planarity measurement to confirm and improve the water level gauge check which had earlier been done in the run of the spindle setting on the foundation (picture no. 39).



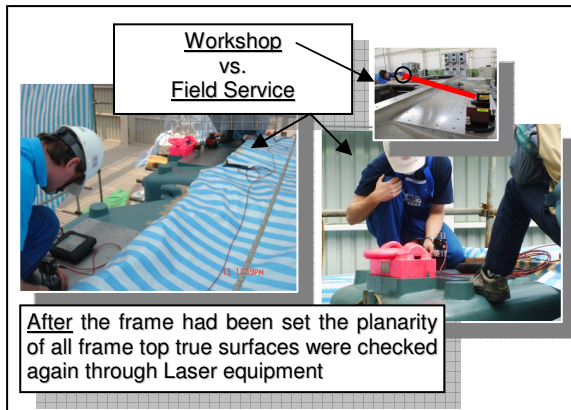
Picture no. 39: *Frame Size 500 Set-Up – Short before touch down (left) and after being set (right)*

Picture no. 40 shows the same compressor in the NEUMAN & ESSER workshop being prepared for mechanical test run. The true faces on the frame top are clearly visible from this top view.



Picture no. 40: *Machined Surfaces on the Frame*

After the frame had been set at site the planarity of all frame top true surfaces were checked again with the laser equipment (picture no. 41).



Picture no. 41: Laser Frame Top Planarity Check

Afterwards there was no doubt: The frame was perfectly set-up and levelled.

7 Conclusion

The significance of proper machine alignment has been recognized ever since. Long before the laser was invented or became available for every day application it was the steel wire which served as straight reference line – usually (but not exclusively) for concentricity checks; typically the alignment of long multi-stage cylinder arrangements. These days the knowledge of wiring is in the process of complete disappearing.

The water level gauge has been and still is the most commonly used equipment to verify good levelling; but its ability to identify poor form and position of e. g. a crankcase is very limited.

The laser has taken over and is widely utilized. Field experience - as shown in the few examples above - has proven how useful and necessary the laser alignment, planarity, perpendicularity and concentricity measurements are and how much the

results can tell about the geometrical shape of the investigated piece of machinery.

Even though the laser principle is easy, however, the application requires sound knowledge, experience and every day practice.

When the NEAC Laser Team is out at the machine and handle the equipment, they “listen” carefully when the laser “talks” to them.

Reliability Check for a 70 Year old Compressor

by

Ms Qing Yang

Rotating Equipment - Reciprocating Compressors

Qing.Yang@BASF.com

BASF SE

Ludwigshafen, Germany

and

Mr Harry Lankenau

Head of Engineering and Technical Support

Harry.Lankenau@NEAC.de

NEAC Compressor Service GmbH & Co. KG

Uebach-Palenberg, Germany

**7th Conference of the EFRC
October 21th / 22th, 2010, Florence**

Abstract

BASF in Ludwigshafen is operating a number of reciprocating compressors which were built in the 30s of last century. These so called 'Einheitsverdichter'-which could be translated as 'Standard Compressor'-were built in Germany by different manufacturers such as Demag, Borsig, Halberg, Schwartzkopf and others. The design was standardized so that most parts of these machines were interchangeable, no matter who built them.

Their typical field of operation is hydrogen processing up to some 320 bar or carbon monoxide and carbon dioxide service. BASF has accumulated a wide knowledge how to maintain and treat these 'old fellows'. Despite their age they still render good service and have proven to be economical compared to the investment of an optional new machine. Process requirements have changed over the decades and some of the old compressors were modified, such as number of stages being reduced, cylinder size adjusted or pressures changed to match the new process requirements. Over the past years NEUMAN & ESSER and NEAC Compressor Service had conducted a number of engineering studies for aged compressors to simulate the thermodynamic behaviour and check their mechanical properties.

This presentation will show the path through such a study with the obstacles that had to be overcome including the conducted pv-diagnostics to obtain a well matching thermodynamic simulation model – and the lessons that were learned for future projects of this kind.

1 Introduction

BASF SE is the world-wide largest chemical company with the headquarters in Ludwigshafen / Rhine.

Picture no. 1 - the BASF headquarters in Ludwigshafen, consists of over 2,000 buildings and spreads over 10 km², being the largest interdependent chemistry area of the world belonging to a single company. A wide network of pipeline enables efficient supplying of the plants with raw materials and energy. In the production group intermediate materials for the followers are manufactured just in time.



Picture no. 1: BASF SE in Ludwigshafen

BASF in Ludwigshafen is operating various reciprocating compressors which were built in the late 30s of last century.

Their typical field of operation is hydrogen or carbon monoxide and carbon dioxide processing up to a pressure of approximately 320 bar.

BASF has accumulated a wide knowledge how to maintain and treat these “old fellows”. In grateful manner and despite their age they still render good service in various applications. With more than 70 years of age they have proven to be as reliable as in the old days when they were much younger and they are, therefore, still economical compared to the investment of an optional new machine.

Process requirements have changed over the decades and some of the old machines were modified, such as number of stages being reduced, cylinder size adjusted or pressures changed to match the new process requirements.

Safety aspects force BASF to ensure that the old units are safely operated as per today's requirements, particularly under conditions off the original design parameters.

Over the past years NEUMAN & ESSER and NEAC Compressor Service had conducted engineering studies for aged compressor units of various kinds to simulate their thermodynamic behaviour and check the rod loads to verify that they are still man enough for the actual duty.

This paper will show the path through the engineering work for one particular old compressor with the obstacles that had to be overcome and how BASF and NEAC cooperated to obtain a well matching thermodynamic simulation model – and the lessons that were learned for future engineering studies of this kind.

2 Today's Application at BASF

The steam cracker and the synthesis gas plant - picture no. 2 - are at the beginning of the value chain. All CO/H₂-alloys are described as synthesis gas, regardless of the processes in which they occur.

The produced synthesis gases are hydrogen and oxo gas. Oxo gas is a mixture of carbon monoxide and hydrogen. Approximately 90 plants at the location Ludwigshafen are customers of these products. The synthesis gas plant is thereby a very important supplier for technical gases in BASF SE.

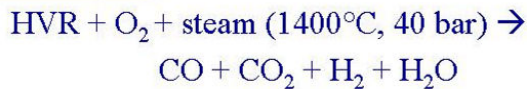


Picture no. 2: Synthesis gases plant

Ludwigshafen operates a partial oxidation of vacuum residuum from refineries, which supply CO/H₂ proportion about 1:1. In the generators of the synthesis gas plant high-viscosity vacuum residuum is converted with pure oxygen at 1400 °C and 40 bar - picture no. 3. A synthesis gas results with CO/H₂ proportion about 1:1. This gas is called oxo gas. Furthermore, the synthesis gas plant has two very low-temperature resolutions, in which the hydrogen is separated from the CO-hydrogen results at 25 bar, the CO pressure-less.

OPERATIONS

Reliability Check for a 70 Year Old Compressor, *Qing Yang, Harry Lankenau; BASF, NEAC COMPRESSOR SERVICE*



Picture no. 3: Generation of synthesis gas

Picture no. 3 depicts the gas generation. Hydrogen is compressed up to 40 bar and 325 bar, and is then delivered into the inter-plant pipeline. The main application of hydrogen in the BASF is for the chemical processes of hydrogenation. This is also the basis for different raw material for application in paint, varnish and coatings, plastics, pharma products etc..

3 The “Einheitsverdichter”-History

The hydrogen is compressed after the reactor from 25 bar up to 325 bar with reciprocating compressors. After them the hydrogen is supplied into the network to the different production plants. Picture no. 4 depicts one of the large machine halls where these machines have been doing their duty ever since.



Picture no. 4: BASF Machine Hall

Their tasks are compression of hydrogen, carbon monoxide and carbon dioxide up to 325 bar. The compressors have been continuously in use for over 70 years. This can only be achieved by regular and appropriate maintenance and deep knowledge of the physics and mechanics. BASF has a comprehensive wealth of experience which both maintenance and the engineering expertise for such compressors.

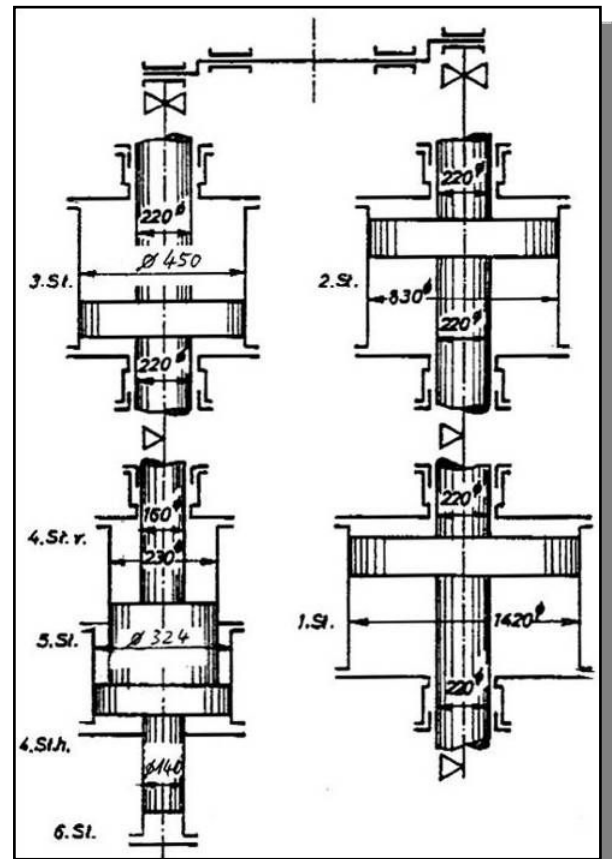
Picture no. 5 - which is showing one of those units - makes it obvious at first glance that these machines have been well maintained over the decades.



Picture no. 5: Typical “Einheitsverdichter”

Picture no. 6 depicts the original cylinder and stage lay-out of the two throws on either side of the electric motor being set in the centre of the compressor unit.

The advantage of the standard design with its interchangeability of parts - which was followed by the various manufacturers - is still utilized today if spares are needed and can be taken from a machine elsewhere which is no longer in service.



Picture no. 6: Original Compressor Lay-out

4 Modifications done to the U7-Unit

Due to changing demands for the process and plants different versions of the former "Einheitsverdichter" exist. The machines were partly converted in accordance with changed needs. Following the new requirements also the U7 unit had to be adjusted to fit into the process. Stages 1 to 3 were no longer needed and therefore two major modifications were done (picture no. 7).

1. The low pressure throw on the right hand side was completely replaced by a 2nd high pressure throw.
2. The original 3rd stage piston was simply removed from the cylinders in both throws.

From the original 6-stage low and high pressure arrangement only a high pressure 3-stage twin crank compressor was left.

It should be noted that the original 4th stage cylinder diameter had increased over the years due to re-machining of the cylinder bore.

From the 3rd stage only the cylinder is still in place and the space left. The piston does no longer exist.

The 4th stage is the new/actual 1st stage. This stage comprises two volumes in each of both throws:

1. A small one with cylinder diameter of 232mm and crank end rod diameter of 160 mm.
2. A large one with cylinder diameter of 324mm and head end rod diameter of 140 mm.

All 4th stage cylinders are equipped with stepless suction valve reverse flow capacity control devices.

The 5th stage is the new/actual 2nd stage with cylinder diameter of 324 mm and a crank end rod diameter of 232 mm.

The 6th stage is the new/actual 3rd stage with cylinder diameter of 140 mm.

Both axes of this machine are structurally the same - but not 100% identical. The arrangement shown in picture no. 7 which outlines today's configuration refers to the engineering work.

5 Reason for Engineering Study

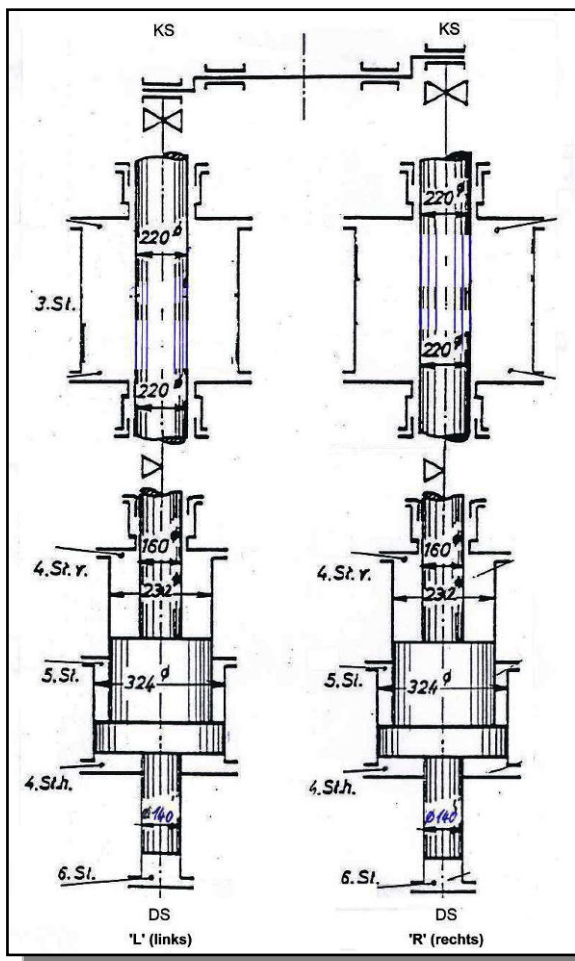
Safety is today more and more frequently regarded. An international widely held method for the recognition of potential problems of the safety and the functionality of technical systems are HAZOP studies (HAZard and OPERability).

For the completion of such a HAZOP study an investigation of the compressor regarding its mechanical load capability had to be conducted. It was necessary to carry out an engineering study in order to determine the true forces inside the machine in comparison with the original design limits.

6 Scope of Investigation

The scope of the investigations for the engineering study to be conducted by NEAC Compressor Service had been defined by BASF as follows:

1. Determination of the frame and rod load for the original design parameters.
2. Determination of the frame and rod load for actual conditions. Various full load process readings as well as the results from BASF cylinder pressure measurements should be used for comparison purposes.



Picture no. 7: Actual Cylinder / Stage Arrangement

For better understanding a few details shall be explained here.

3. Determination of the min. possible flow which can be achieved through the suction valve reverse flow capacity control devices in respect of the max. admissible frame and rod load.
4. Min. possible flow if 4th (↔1st) and 5th (↔2nd) stage would be equipped with so called “Hoerbiger Hydrocom” suction valve capacity control devices and a recycle line around the 6th (↔3rd) stage under consideration of the max. admissible frame and rod load.

Compressor unit U6 - which is also an “Einheitsverdichter” of similar kind - had earlier been investigated through NEUMAN & ESSER concerning its capabilities under modified process conditions. Frame and rod load limits had been derived from - and compared with - the results from this previous analysis.

7 1st Simulation vs. Reality: Conflicts

After the first thermodynamic computer simulation model had been created actual process data - which had been submitted by BASF - were used as input data to check if the results from the model match the real conditions in terms of interstage pressure, stage discharge temperature, flow capacity and power consumption.

Apart from numerous input parameters the volumetric efficiency η_v of each cylinder always is of the essence for a realistic performance check.

The suction pressure p_s and discharge pressure p_D is usually known. The isentropic coefficient χ is a gas constant. Compressibility Z_S and Z_D for the suction and discharge condition can be calculated from the gas characteristics. With the clearance volume ϵ (as a fraction of cylinder displacement) the volumetric efficiency can easily be calculated as follows:

$$\eta_v = 1 - \epsilon * \left[\frac{Z_S}{Z_D} \left(\frac{p_D}{p_S} \right)^{\frac{1}{\chi}} - 1 \right]$$

The determination of the volumetric efficiency becomes, however, difficult if documents do not show the clearance volume or if cylinders have been modified and original values are no longer true. The latter was the case here.

Some time in the past BASF had undertaken a cylinder pressure measurement survey (pv-diagnosis) to verify the thermodynamic condition of the machine.

The original plan was to read the volumetric efficiency from the pv-charts created from these measurements and determine the true clearance volume for further simulations with the formula below:

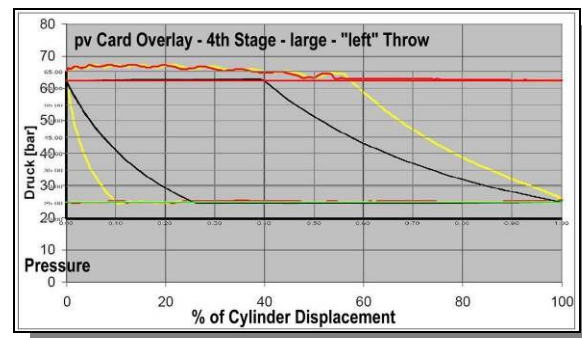
$$\epsilon = \frac{1 - \eta_v}{\left[\frac{Z_S}{Z_D} \left(\frac{p_D}{p_S} \right)^{\frac{1}{\chi}} - 1 \right]}$$

As smart as this idea appeared to be as great was the disappointment that thermodynamic model and true machine condition could by no means be correlated.

Picture no. 8 is a typical example of the off-set between simulation (black line) and the pv-charts from the measurements (yellow line) even though true process data were used for the simulation.

Note: The green and red lines are depicting the process line side pressures before and after the 4th stage.

An interesting occurrence was the fact that the discharge line pressure (depicted here in red) during the discharge phase was showing nearly the same shape as the cylinder pressure. Usually a difference can be seen between cylinder and line pressure due to the valve pressure losses. Here the valve pressure drop is almost “0” and some kind of other restriction seems to push up the discharge line pressure simultaneously with the cylinder pressure.



Picture no. 8: 4th stage large “left” throw - pv-card

Even with several variations of the input data it was impossible to match this overlay of measurement vs. the simulation. The results for the other stages and throws were not much better.

A close look at the details revealed a total of seven major conflicts explaining why theory vs. reality deviated so much:

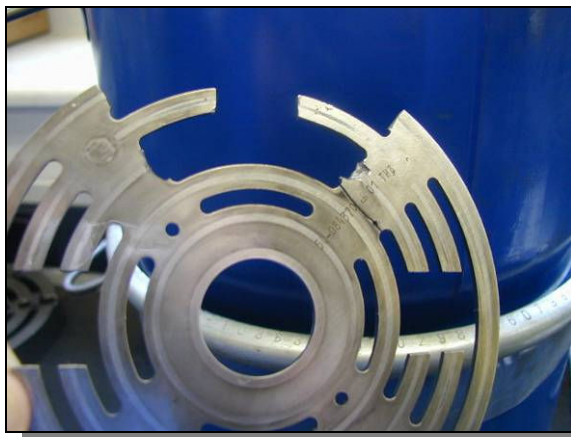
OPERATIONS

Reliability Check for a 70 Year Old Compressor, *Qing Yang, Harry Lankenau; BASF, NEAC COMPRESSOR SERVICE*

1. Clearance volumes - calculated with above shown formula - were far off reality.
2. Process data which should be used for the comparison 'simulation \Leftrightarrow true running' were taken for a part load condition with suction valve unloading. This is not a useful condition for a simulation check which shall be utilized for performance predictions.
3. The flow values from the process control devices did not match the values derived from the measured pv-cards.
4. Discharge pressures in both 5th stages were abnormally high (picture no. 11 and 12).
5. The interstage pressures before and after the 5th stage in both ends "left" and "right" – which should be identical in all aspects – were significantly different in level (picture no. 11 and 12).
6. Power consumption readings did neither match the values derived from the pv-charts nor the results from the thermodynamic simulation.
7. The 5th and 6th stages were suffering from frequent valve failures (picture no. 9 and 10).



Picture no. 9: Holes in valve plate 5th stage



Picture no. 10: Broken valve plate 6th stage

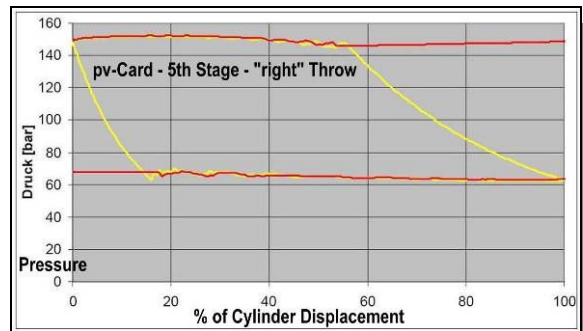
Picture no. 11 and 12 below are showing the pv-charts of both 5th stages; "left" and "right" throw.

Particularly the left throw (picture no. 11) is showing the high cylinder pressure during the discharge phase with a peak value of nearly 160 bar.



Picture no. 11: 5th stage "left" throw - pv-chart

In the right throw the cylinder pressure during the discharge phase (picture no. 12) is also elevated but reaches only some 150 bar; some 10 bar below the theoretically identical left throw shown above.



Picture no. 12: 5th stage "right" throw - pv-chart

Suction pressure 5th stage is also deviating between left and right throw; not excessively but also too much for two "identical" cylinders.

The conclusion which had to be drawn from these findings was:

Particularly the 5th stage had an "issue" - and that needed to be clearly identified before any successful engineering progress could be achieved.

BASF took the decision to repeat the pv-diagnostics (dynamic cylinder pressure measurement) at a time after the U7 compressor had gone through a thorough full size revision and with a valve performance without any doubt. The same applied to the piston rings. Only in new best condition it can be ruled out that ring slippage is misleading the conclusions drawn from pv-card readings.

8 2nd Simulation vs. Reality: Results

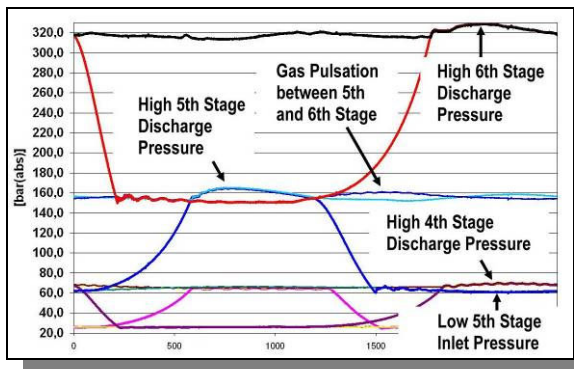
When the results from the 2nd pv-diagnostics had been submitted to NEAC to continue the engineering work it became obvious that readings - this time - were much better and a lot more reliable.

The measurements, however, again revealed a number of abnormalities in both axes which the previous diagnosis had already indicated:

1. 4th stage discharge pressure inside cylinder is untypically high for a hydrogen compressor
2. Cylinder suction inlet pressure 5th stage is abnormally low
3. 5th stage discharge pressure inside cylinder is also untypically high for this application. As already mentioned above it is even higher for the “left” than for the “right” side
4. There is a certain distinct gas dynamic pressure pulsation visible between 5th and 6th stage; it appears to be a kind of acoustic resonance
5. 6th stage discharge pressure inside cylinder - only in the “left” throw - is comparably high

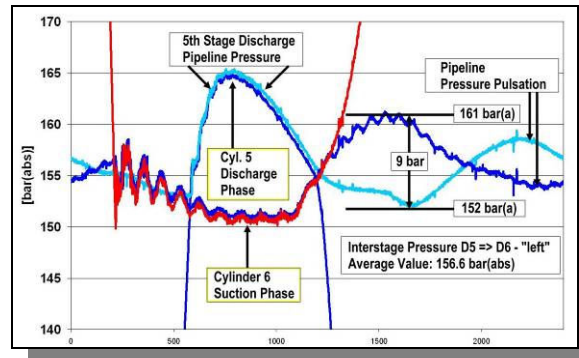
Picture no. 13 shows the pressure-over-time signal for all three “left” stages for one crank shaft revolution.

Arrows with short comments highlight the particular findings in this axis.



Picture no. 13: pt-chart all “left” stages

Picture no. 14 is a zoom of the 5th to 6th interstage condition. The small blue line is the 5th stage cylinder pressure with quite a high peak. At the same time the red 6th stage cylinder pressure is showing a low peak and a little dynamic during the suction phase right after valve opening. Last not least the bold blue and light blue line side pressure signals reveal a clear pressure pulsation with opposite phase between outlet 5th stage and inlet 6th stage. It very much looks like an acoustic resonance being excited from the cylinders of both stages.



Picture no. 14: pt-chart 5th-6th “left” stages

The first indication from the previous measurement that both throws are not behaving in identical manner was confirmed. Consequently this machine – although being one unit - had to be treated as two separate compressors. Therefore it was “split” in two simulation models: a “left hand” and a “right hand” unit.

The following differences between both needed to be addressed and modelled accordingly:

1. Clearance volumes (dead volume) in the two 6th stages are different.
2. The interstage pressure between 5th and 6th stage is not the same.
3. Cylinder discharge phase pressure peaks in 5th and 6th stage are higher in the left throw.

Any kind of common reciprocating computer simulation model would hardly be in a position to take all the above into consideration.

Detailed model tuning was required here to obtain true results.

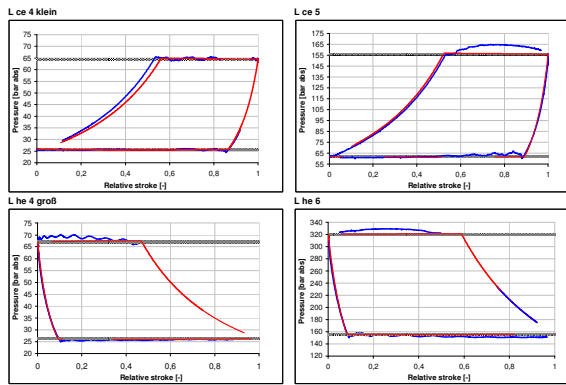
It must be considered that all the odds found from the pv-diagnosis measurement do have an impact on the compressor load which had to be reliably assessed to determine the limits of the same.

The thermodynamic engineering for each of the two individual throws was performed in the 4 steps outlined in the “Scope of Investigation”.

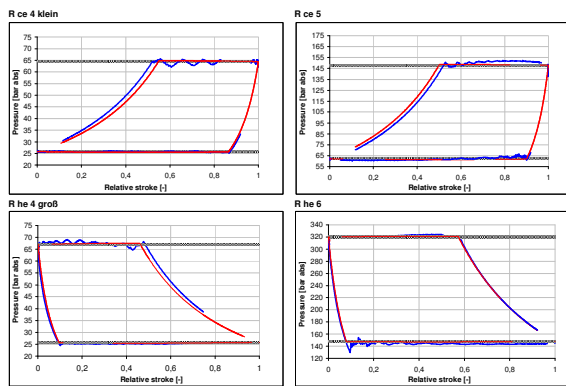
For the first step - “determination of the frame and rod load for the original design parameters” - a pv-card simulation was conducted for each individual stage and cylinder of the two - not - identical axes (picture no. 15 and 16).

OPERATIONS

Reliability Check for a 70 Year Old Compressor, *Qing Yang, Harry Lanckenau; BASF, NEAC COMPRESSOR SERVICE*



Picture no. 15: pv-card simulation - "left" throw



Picture no. 16: pv-card simulation - "right" throw

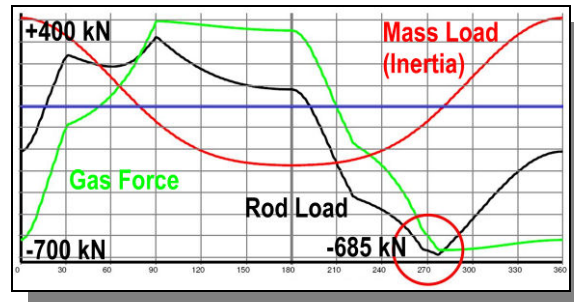
These pv-cards were then compared with the latest measurements and tuned such to match, thus showing the applicable volumetric cylinder efficiencies.

It also became obvious that most cylinder ends - apart from the high discharge pressure observed - did not perfectly follow the isentropic compression.

A close look also revealed that both 4th stages and also the left 5th stage suction valves seemed to be closing late. The suction valve lifting devices were suspicious of not being properly adjusted or not performing well.

After the compressor model was done the rod load was calculated and checked if within given limits.

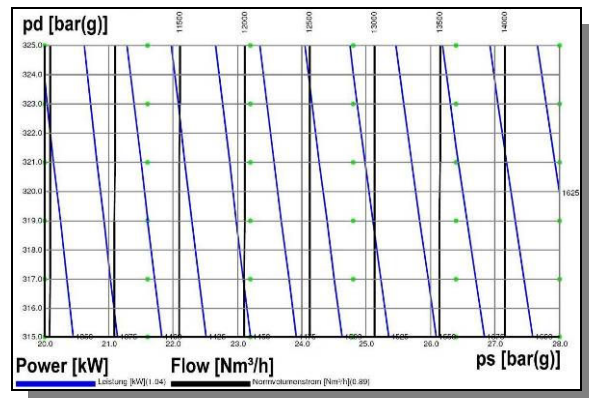
Picture no. 17 shows the various loads as example here for the "left" axis. Green is the gas force; red the pure (inertia) mass load and black the combined overlay of both. With 685 kN the combined rod load is far below the limit of 860 kN.



Picture no. 17: Various rod loads - "left" throw

Finally the conditions for various suction/discharge pressures and temperatures; 100% capacity and suction valve unloading conditions were investigated.

These results were outlined in so called PanHandle diagrams (picture no. 18): Flow capacity (black lines) and power consumption (blue lines) are shown as a function of suction pressure (x-axis) and discharge pressure (y-axis).



Picture no. 18: PanHandle Chart

More detailed figures were also put in tables with a yellow and red pattern as an alert signal where limits - either temperature and/or load - are exceeded (picture no. 19).

Load [%] / Control		50% RSR - St. 4 Head End (4 gr)					
ps 4th Stage	[bar(g)]	20	25	28	20	25	28
ts 4th Stage	[°C]	0	0	0	40	40	40
Stage - Disch. Pr.							
pd 4	[bar(g)]	34,8	42,9	47,8	31,2	38,5	42,9
pd 5	[bar(g)]	93,8	110,6	120,7	85,9	101,4	110,4
pd 6	[bar(g)]	325	325	325	325	325	325
Stage - Disch-Temp.							
td 4	[°C]	56	55	55	88	87	87
td 5	[°C]	126	120	118	129	123	120
td 6	[°C]	165	140	127	176	153	140
Flow	[Nm³/h]	6890	8534	9517	6166	7638	8519
Shaft Power	[kW]	928	1040	1101	858	964	1020
max. Gas Force	[kN]	581	598	607	568	582	590
max. Rod Load	[kN]	463	478	488	465	487	496
max. PRV Gas Load	[kN]	920	882	859	932	896	876
max. PRV Rod Load	[kN]	666	659	652	678	673	668

Picture no. 19: Table with detailed results

The diagrams and table above may be a little small to read the values but the details are of minor significance here because more important is the way the study went rather than the results.

In the end a comprehensive overview of the various load and thermodynamic conditions could be presented which served as assessment for future potential modified process and flow control conditions.

It was also surprising to realise, how sensitive such a machine reacts in terms of rod load if inlet conditions vary only slightly.

Apart from the initial scope of the engineering study it also pin-pointed at items which may need a little particular attention, such as the performance of the valves as well as the design and sizing of the equipment between the stages with their significant impact on the actual compressor load.

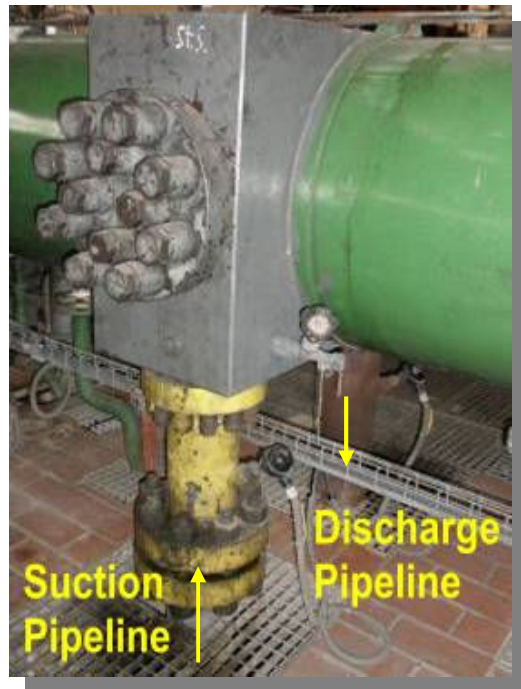
9 Plant Arrangement Details

Up to here all aspects concentrated exclusively on the compressor. Having realised that both geometrically identical throws do not behave accordingly the question had to be addressed why these deviations occur.

As mentioned before the unusual pressure rise inside the cylinder during the discharge phase is not related to a compressor valve pressure drop. This is evident because the relevant line pressure – taken from the cylinder gas passage after the valves – is showing the same increase.

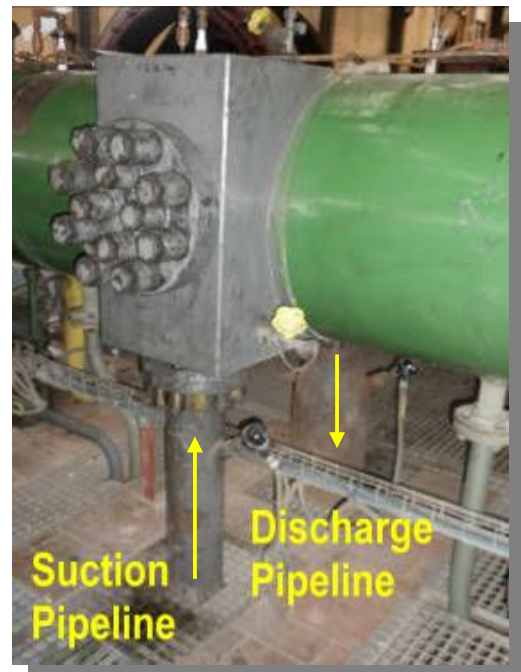
It appears as if the flow of the gas being pumped into the discharge pipeline system is somehow restricted, thus building up a pressure peak.

A closer view on the P&ID as well as the check of the plant configuration at site made this phenomenon obvious (picture no. 20 and 21).



Picture no. 20: 5th stage “left” side

Picture no. 20 shows the 5th stage “left” cylinder with the suction and discharge pipeline. The discharge pipeline has a diameter of 120 mm. It is reduced from 120 mm to 45 mm and then split into two cooler entrances.



Picture no. 21: 5th stage “right” side

Picture no. 21 shows the 5th stage “right” cylinder with the suction and discharge pipeline. This discharge pipeline has a diameter of 267 mm. It is split and reduced from 267 mm to two small pipelines with a diameter of 45 mm each which form the inlet of the cooler tubes.

Both pipe configurations are creating bottlenecks and consequently some kind of pressure drop – or “gas flow jam”.

Due to the different layout their impact on the thermodynamic and gas dynamic behaviour of the 5th stage is much different between the “left” and “right” throw, which nobody had been aware off ever before this study was conducted.

10 Conclusion

For the analysis of the performance of reciprocating compressors including thermodynamic modelling, it is not sufficient to only type process data and the machine geometry into a sophisticated computer programme.

Influence of the piping and accessories as well as the true behaviour (occasionally far from perfect) of wearing parts with particular attention to the compressor valve performance may result in a machine characteristic being completely different from what would be expected and what is typically found in the books.

For full understanding of such a complex machine it is vital to submerge in the details of the complete unit and look into its “heart”.

If the companies with their personnel have a sound knowledge of the machinery and if they can also provide for the capabilities of compressor diagnosis in conjunction with powerful simulation tools, the machine can be understood and its limits clearly recognized.

The close cooperation between the BASF SE Rotating Equipment department and NEAC resulted in a much better understanding of this aged compressor unit and lead to the comprehensive knowledge of the complete process in which this machine is integrated. and last, but not least the HAZOP-requirements were met.

Comparison of Field Vibration Data with “EFRC Guidelines for Vibrations in Reciprocating Compressor Systems”

R. Schuhmann

**Rotating Equipment - Diagnostik & Monitoring
BASF**

**Ludwigshafen, Germany
roland.schuhmann@basf.com**

A. Eijk

**Flow and Structural Department
TNO Science and Industry
Delft, The Netherlands
andre.eijk@tno.nl**

**7th Conference of the EFRC
October 21th / 22th, 2010, Florence**

Abstract

The R&D group of the EFRC has developed recently a guideline for vibrations in reciprocating compressor systems. This guideline includes many years of experience and knowledge of engineers who are working in the field of rotating machinery. The worldwide acceptance of such a guideline will increase when it is proven that the values from this guideline are realistic.

Many reciprocating compressors are installed at the chemical plant of BASF in Ludwigshafen in Germany, ranging from low to high power consumption compressors, fixed and variable speed compressors from different manufacturers and from very old to very new. For that reason BASF had the opportunity to measure the vibration levels for all of these compressors under various operation conditions which can be compared with the levels of the EFRC Guidelines. From the measured vibration data it can be concluded that all measured levels fits extremely well within the different levels of the EFRC Guidelines. This paper will give a summary of the project and the measured vibration data.

1 Introduction

The reciprocating compressor's flexibility to handle large capacity ranges, independent of density, makes it a vital component in today's energy markets. One of the disadvantages of a reciprocating compressor is that it generates pulsations and vibrations, which, without limitation and proper attention during design, manufacturing, installation and operation, can lead to fatigue failures, inefficiency, capacity limitations and unsafe situations.

The integrity of compressor systems is being judged by measuring vibration levels, and comparing those levels with limit levels from standards. Several international standards (ISO and VDI) have been developed during the past decade with vibration levels for reciprocating machinery. Besides several international standards, there is a wide variety of internal guidelines, which have been developed and are being used by compressor manufacturers, engineering offices and operators. Most of these internal guidelines have been derived from international standards.

Because there is an interaction between the different elements in a compressor installation, the compressor and pipe system should be treated as one integrated system, as indicated in figure 1.

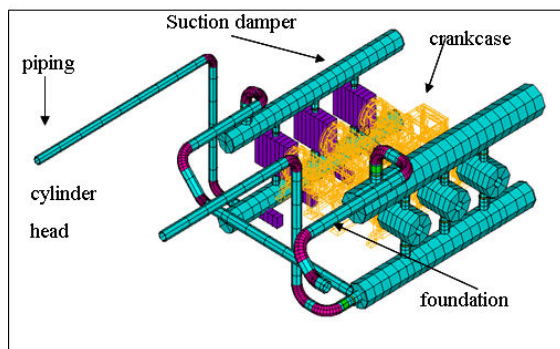


Figure 1: Different parts of a reciprocating compressor system

However, most of the international standards do not make a good distinction between vibration levels for different parts of the compressor e.g. foundation, crankcase, cylinder, pulsation damper and pipe system.

For that reason EFRC Guidelines for vibrations in reciprocating compressor systems have been developed recently in an R&D project of the

EFRC^{1,2}. These guidelines can be downloaded free of charge from the EFRC website (www.recip.org).

The levels from these guidelines should be used during a field survey to judge the safety, reliability and efficiency for the long term. It should be emphasized that the guideline is not intended for condition monitoring. The vibration levels from the EFRC Guidelines were accepted by a group of international representatives from OEM's and operators during an international workshop.

To investigate how the values of the vibration from field vibration data fit into the EFRC Guidelines, BASF in Ludwigshafen has carried out extensive field vibration measurements on all type of reciprocating compressors from low to high power consumption compressors, fixed and variable speed compressors from different manufacturers and from very old to very new. This paper will summarize the EFRC Guidelines and will give the results of the detailed vibration measurements with a comparison with the vibration levels from the EFRC Guidelines.

2 Summary of the EFRC Guidelines

2.1 Measuring procedure

The measurement procedure is as follows:

- a. Preferably use acceleration transducers and detect overall velocity levels in mm/s RMS
- b. If frequencies below 10 Hz are expected/observed, it is recommended to measure the overall vibration displacement in mm RMS (it is common practice to measure displacement in micrometers $1 \mu\text{m} = 10^{-6}$ meters)
- c. If frequencies above 200 Hz are expected/observed, it is recommended to measure the overall RMS vibration acceleration in m/s^2 RMS
- d. All levels must be within the guide levels for acceptable overall vibrations as summarised in chapter 2.4.

2.2 Key to zones

The following typical evaluation zones are defined in the same way as defined in ISO 10816 to permit a qualitative assessment of the vibration on a given compressor and to provide guidelines on possible actions. Numerical values assigned to the zone boundaries are primarily intended to serve as guide values and are not intended to serve as a final acceptance criterion.

The guide values for acceptable vibrations are intended to ensure that gross deficiencies or unrealistic requirements are avoided.

In certain cases, there may be specific features associated with a particular compressor system which would require different boundary values (lower or higher) to be used. In such cases, it is normally necessary to explain the reasons for this and, in particular, to confirm that the compressor system will not be endangered by operating with higher vibration levels. Interim values for the zone boundaries for reciprocating compressor systems are defined as follows and have been summarised in table1 as follows:

- A: The vibration of newly commissioned compressors would normally fall within this zone
- B: Compressors with vibration within this zone are normally considered acceptable for long-term operation
- C: Compressors with vibration within this zone are normally considered unsatisfactory for long-term continuous operation. Generally, the compressor may be operated for a limited period in this condition until a suitable opportunity arises for remedial action
- D: Vibration values within this zone are normally considered to be of sufficient severity to cause damage to the compressor

Table 1: Definition of key zones:

Zone	Level	Description	Notes
A	< A/B boundary	Good	1
B	>A/B – B/C	Acceptable	2
C	>B/C – C/D	Marginal	3
D	>C/D boundary	Unacceptable	4

Notes

1. Test-bed, as-designed, on-installation
2. Acceptable for in-field operation
3. Analysis and possible correction. Clarify between OEM and operator that the compressor is suitable for long term safe operation
4. Urgent correction or shutdown

2.3 Measuring locations

The vibration measurements must be carried out minimum on the following locations which are shown in figure 2 and figure 3:

- Foundation: at all compressor foundation bolt locations

- Compressor frame: on each corner point and on each connection of the crosshead guide for a compressor with more than 2 cylinders, all at the top of the frame
- Compressor cylinder: at the rigid part of each cylinder cover flange
- Suction and discharge pulsation dampers: at the inlet/outlet flange and at the heads (for vertical dampers only the head on the top)
- Piping: at all critical parts in the system including small bore piping, to be determined in agreement with operator

The measurements must be taken in 3 perpendicular directions.

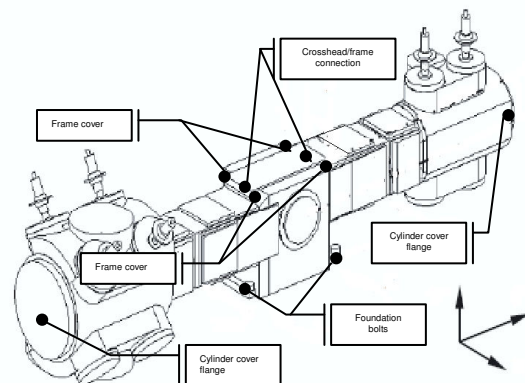


Figure 2: Measurement locations for a horizontal compressor

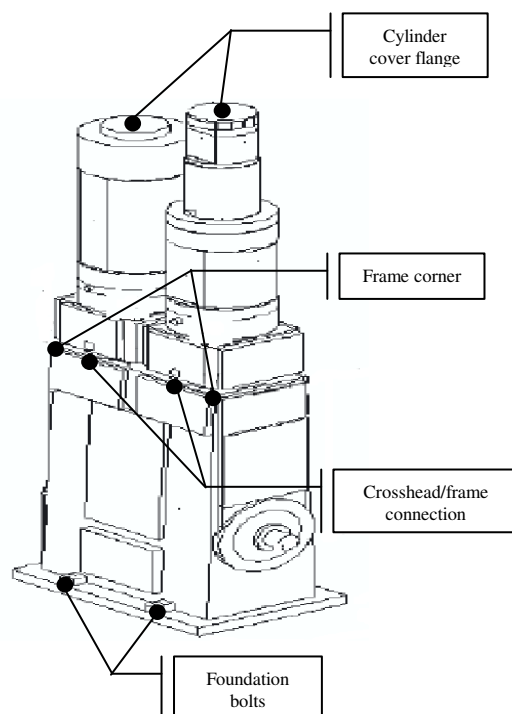


Figure 3: Measurement locations for a vertical compressor

2.4 Acceptable vibration levels

The guide values for acceptable vibration displacement, vibration velocities and vibration accelerations levels for a horizontal and vertical compressor system are summarised in table 2 through 4 and in figure 4 through figure 6 for different parts of a horizontal compressor. The values for a vertical compressor only differ for the cylinders: the values of the lateral and rod direction of the vertical compressor are respectively the values of the rod and lateral direction of the horizontal compressor.

Table 2: Summary of vibration displacement levels for different parts and key zones

Part	Horizontal compressors [mm RMS]		
	Key zones		
	A/B	B/C	C/D
Foundation	0.032	0.048	0.072
Frame (top)	0.084	0.127	0.191
Cylinder (lateral)	0.139	0.255	0.302
Cylinder (rod)	0.170	0.207	0.382
Dampers	0.202	0.302	0.454
Piping	0.202	0.302	0.454

Table 3: Summary of vibration velocity levels for different parts and key zones

Part	Horizontal compressors [mm/s RMS]		
	Key zones		
	A/B	B/C	C/D
Foundation	2.0	3.0	4.5
Frame (top)	5.3	8.0	12.0
Cylinder (lateral)	8.7	13.0	19.5
Cylinder (rod)	10.7	16.0	24.0
Dampers	12.7	19.0	28.5
Piping	12.7	19.0	28.5

Table 4: Summary of vibration accelerations levels for different parts and key zones

Part	Horizontal compressors [m/s ² RMS]		
	Key zones		
	A/B	B/C	C/D
Foundation	2.5	3.8	5.7
Frame (top)	6.7	10.1	15.1
Cylinder (lateral)	10.9	16.3	24.5
Cylinder (rod)	13.5	20.1	30.2
Dampers	16.0	23.9	35.8
Piping	16.0	23.9	35.8

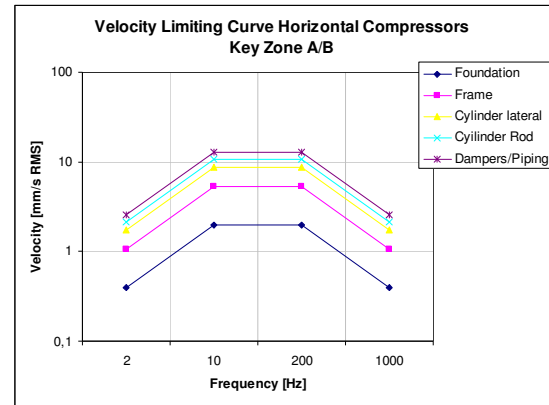


Figure 4: Vibration velocity limiting curve in for a horizontal compressor for key zone A/B

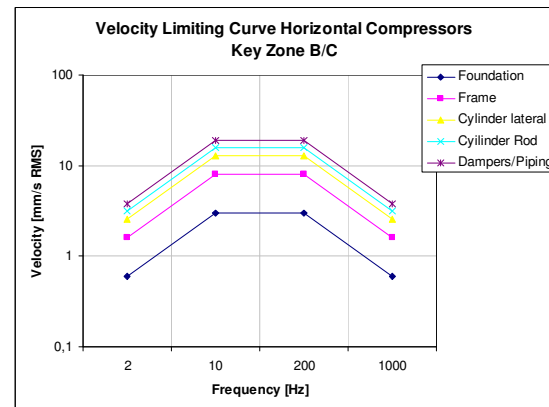


Figure 5: Vibration velocity limiting curve for a horizontal compressor for key zone B/C

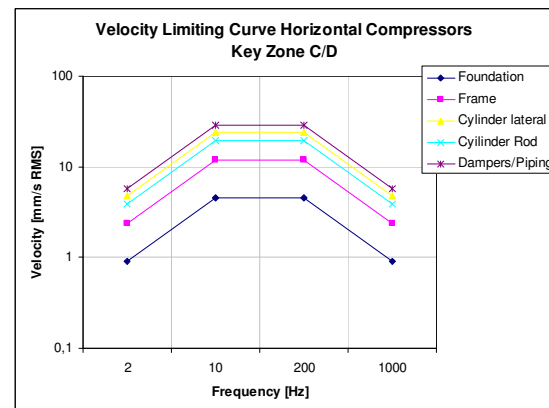


Figure 6: Vibration velocity limiting curve for a horizontal compressor for key zone C/D

3 Field vibration measurements³

3.1 Introduction

BASF SE operates a lot of compressors in their chemical plants around the world. Especially at the largest plant site in Ludwigshafen more than 200 different reciprocating compressors are installed and operated.

The power range is from a few kW up to 4 MW and includes all types (horizontal/vertical/ lubricated and dry running) of compressors. They compress very different gases from atmospheric up to 2500 bars. Many of the compressors are quite old – some of them are built in 1938 – but also new installations were installed last years.

As a member of the EFRC expert group which has discussed the values of the EFRC guidelines, it was recognised that the experts of different companies have very different experiences. For that reasons the idea came up to carry out field measurements to investigate how the EFRC guideline values fit to the compressors as installed at BASF SE.

The measurements were carried out in 2009 on more than 20 different compressors and will be continued to get a more extensive and representative database.

3.2 Measurement system and setup

At the beginning of the discussion with the EFRC expert group, there was a discussion about different measurement systems and on different calculations of the rms value. There are measurement systems on the market which determine the so called “true rms” directly out of the filtered time signal. Other systems carry out an FFT analyses first and after that it calculates the rms value out of the spectrum. Besides that different transducers (velocity/ accelerometers) can be used which can also have an influence on the measured levels, e.g. integration of the vibration acceleration level to achieve vibration velocities can also have an influence on the results. Different values will be retrieved, especially if the frequency spectrum contains many harmonics, see figure 7 for an example. BASF has the possibility to measure in both ways the different vibration levels with different measurement systems. This means that the results of different systems can be used and compared by checking the overall levels when measuring the levels e.g. at a reciprocating compressor system.

With measurement system “A” it is possible to choose whether the rms calculation should be done with the filtered time signal or with the frequency spectrum. Measurement system “B” always calculates the rms value out of the filtered time signal. Besides that different types of velocity and accelerometer transducers have been used to check the influence of the integration.

The results of the vibration data with different systems and vibration transducers are shown in table 5.

			System A		System B	
Velocity sensor	time	v	1,01 mm/s	Velocity sensor	v	1,16 mm/s
		s	143 µm		s	142 µm
	FFT	v	0,985 mm/s			a
		s	142 µm		v	
accelerometer	time	a	0,134 g	accelerometer	a	135 µm
		v	1,19 mm/s			
		s	121 µm			
	FFT	a	0,119 g		v	1,18 mm/s
		v	1,18 mm/s			
		s	110 µm			

Table 5: Results of different rms calculations

From table 5 the following conclusions can be made:

Comparing the results of the velocity and displacement levels for the different calculation methods (time and frequency spectrum) of system A it can be concluded that there are no large differences of the values which means that the influence of the calculation method can be neglected. There are larger differences for the acceleration signals which can be explained by the fact that high frequency components are reduced by the averaging process during the FFT calculation.

The table also shows that the differences are the highest for the acceleration levels. The reason for that is that small differences in mounting of the accelerometer can lead to significant changes of the natural frequencies of the mounted accelerometer. Figure 8 shows this influence which is described in the standard ISO 5348⁴. Accurate mounting of an accelerometer is therefore very important.

Looking at the displacement levels it is obvious that the values measured with velocity sensors differ from these measured with accelerometers.

It can be stated that each calculation (integration or double integration) will have a negative influence on the result. It can be concluded therefore that measuring vibration velocity and vibration displacement should be done therefore preferably with velocity sensors. However, the EFRC Guidelines recommends measuring the vibration and displacement levels with accelerometers.

The reason for this is that it is more common practice today to use accelerometers because they are cheaper and also suitable for other diagnostic measurements like measuring the vibrations of roller bearing for condition monitoring purposes.

The final conclusion out of this investigation is that there will always be differences between the results when measuring the vibration levels with different systems. However, the results of the measurements as carried out by BASF show that a deviation of about approximately 20% is possible.

However, these differences are acceptable for this kind of overall vibration measurements.

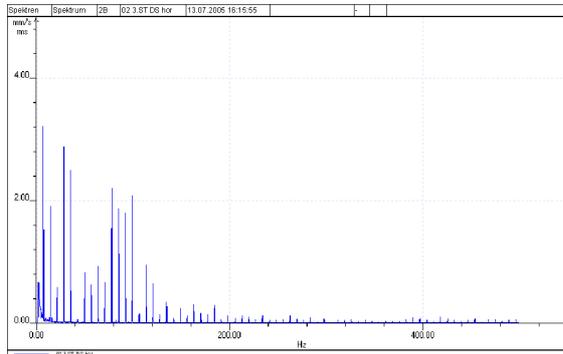


Figure 7: Frequency spectrum of a vibration measurement on a reciprocating compressor

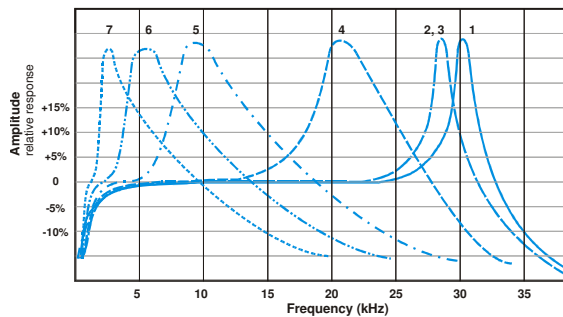


Figure 8: Influence of mounting the accelerometer

3.3 Measurement results

All measurements were carried out with the compressors running at normal conditions. The compressors are all in long term operation and did not have excessive wear or failures up to now. The vibration levels of these compressors can be regarded therefore as good reference values for this project. It is expected therefore that the measured values should be within zone A or B (light and dark green) of the EFRC guidelines. The different colours in the figures are representing the different zones as follows:

- dark green: zone A
- light green: zone B
- yellow: zone C
- red: zone D.

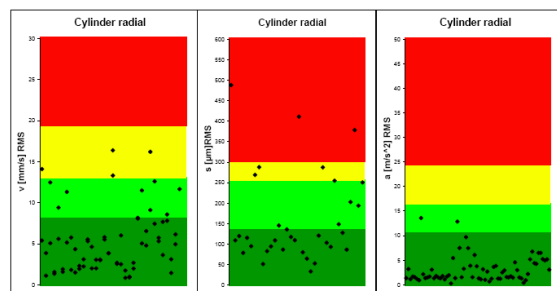


Figure 9: Cylinder radial vibration for horizontal compressors

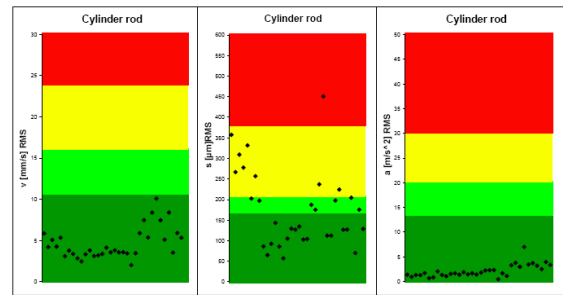


Figure 10: Cylinder rod direction vibration for horizontal compressors

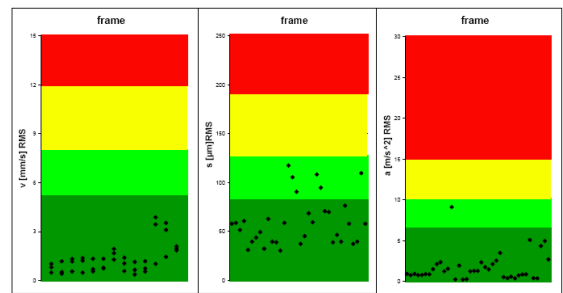


Figure 11: Frame vibration for horizontal compressors

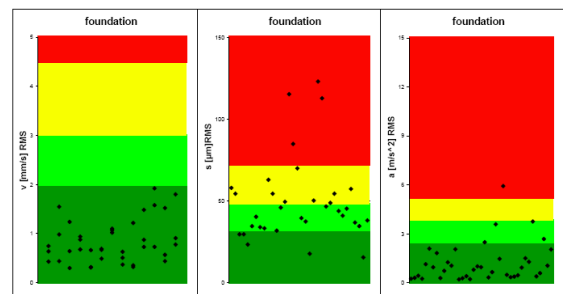


Figure 12: Foundation vibration for horizontal compressors

3.3.1 Horizontal compressors

Figures 9 to 12 show the results compared with the limits of different zones for horizontal compressors and the results are as follows:

Vibration velocity levels

From the charts it can be concluded that the measured levels fit well within zone A and B of the EFRC guidelines, except for the cylinder radial vibrations. The reason of the vibration velocities that fall within zone C is probably caused by the fact that some rather old compressors with very long multistage rods are included.

Vibration displacement levels

From the figures it can be concluded that most of the measured values fall within zone C and D of the EFRC guidelines.

The compressors are running without any problems and means that the values of the EFRC guidelines are too low. It is also quite remarkable that the EFRC values of the foundation are much too low.

It was shown that the vibration velocity level is quite good which means that the cross-over frequency should be decreased

To match the measured levels with the levels of zone A and B, the cross-over frequency has to be decreased approximately a factor of 2.5 for all parts. Due to the fact that foundation problems have not occurred up to now, a higher value of the vibration level (e.g. approximately a factor of 1.25) together with a lower cross-over frequency (e.g. 5 Hz) could be applied for this part.

Vibration acceleration levels

From the charts it can be concluded that the measured levels fit well within zone A and B of the EFRC guidelines. In fact the EFRC levels could be decreased approximately a factor of 1.5. It was shown that the vibration velocity is quite good which means that the cross-over frequency could be decreased to approximately 150 Hz.

3.3.2 Vertical compressors

Figures 13 to 16 show the results compared with the limits of different zones for vertical compressors and the results are as follows:

Vibration velocity levels

From the charts it can be concluded that the measured levels fit well within zone A and B of the EFRC guidelines, except for the foundation which falls within zone C and D. It is expected that the vibration levels for foundations in the vertical direction are higher than the levels of horizontal compressors. Due to the fact that foundation problems have not occurred up to now for the displacement and velocity, a higher value of the vibration level (approximately a factor of 1.5) could be applied.

Vibration displacement levels

The same conclusions as drawn for the horizontal compressors apply to the vertical compressor, especially for the foundation. If an increase in vibration displacement together with a lower cross-over frequency (e.g. 5 Hz) is chosen the measured levels will fall are within zone A and B.

Vibration acceleration levels

The same conclusions as for the horizontal compressors apply for the vertical compressors.

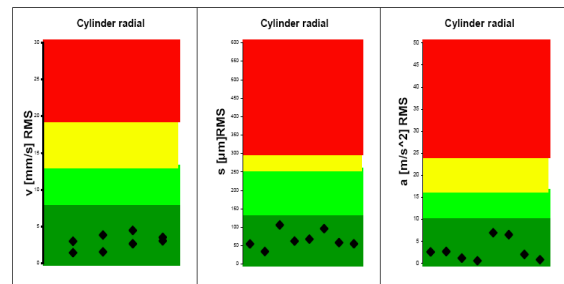


Figure 13: Cylinder radial vibrations for vertical compressors

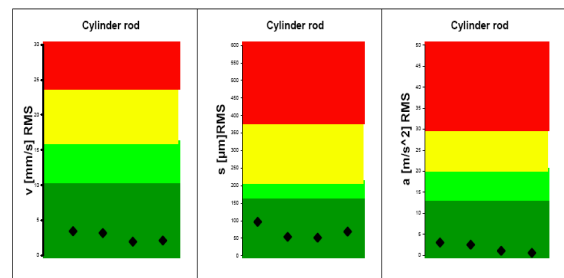


Figure 14: Cylinder rod direction vibrations for Vertical compressors

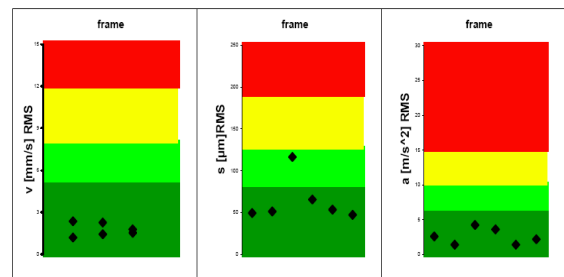


Figure 15: Frame vibration for vertical compressors

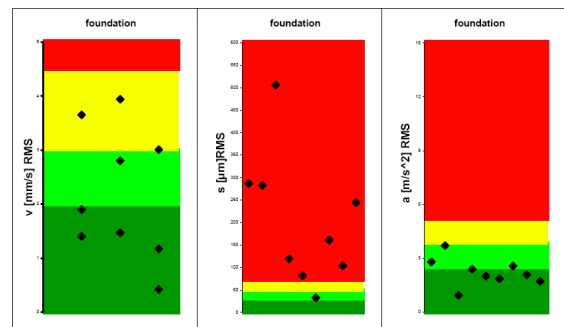


Figure 16: Foundation vibration for vertical compressors

3.4 Vibration dependencies

The intention of the EFRC guidelines was to make it as easy as possible for the user. For that reason it was decided not to make a distinction between different types of compressors, e.g. single versus double distance piece, low versus high power, low versus high speed etc.. The final decision was to make only a difference between vertical and horizontal compressors.

Due to the fact that the vibration measurements have been carried out on different type of compressors, the question was now if it was possible to find correlations between the measured data and different type of compressor configurations. With other words: was the assumption correct that it was not necessary to make a distinction between vibration levels of different compressor configurations (except for the difference between horizontal and vertical compressors). If it appeared from the measurements that there is indeed a big difference between the levels of different compressor configurations, the question is if the EFRC guidelines should be adjusted accordingly. With the results of the measurements the relation has been investigated for different parameters of the compressor configurations for both the horizontal and vertical compressors. The data for the vertical compressors are limited and for that reason the conclusions will only be made for the horizontal compressors. Figure 17 through 21 show the results of the different correlations for the cylinder radial vibration displacement, vibration velocity and vibration acceleration measurements. The correlations have been investigated for the speed and power of the compressor. To get an idea of the influence of the length of the distance piece, the values are also correlated for the length between the crosshead guide and the cylinder cover plate of the cylinder. Two other factors were also correlated: the first is the factor k which is the product of power and speed and the second is the power per throw instead of the total power of the compressor. The blue line is the linear interpolated correlation for horizontal compressors and the purple line is for vertical compressors.

From figure 17 it can be concluded that the values of the vibration displacement and vibration velocity do not depend on the speed of the compressor. The acceleration values increase with an increase of the compressor speed, which is quite reasonable because the vibration acceleration levels are more sensitive for higher frequencies.

From figure 18 it can be concluded that the values of the vibration displacement and vibration velocity do not depend much on the power of the compressor. The vibration velocity levels and vibration acceleration levels decrease for higher powers with respectively a factor of 1.5 and 2.5 for a power ratio of 8.

From figure 19 it can be concluded that the vibration displacement values increase with length (approximately a factor of 1.3 for a power ratio of 8). This is reasonable and is expected due to the fact that a system is more flexible with longer distance pieces.

The vibration velocity levels do not depend much on the length (approximately a factor of 1.1 for power ratio of 5). Further on it is interesting to note that the vibration acceleration values decrease with longer distance pieces (approximately a factor 2 for a power ratio of 5).

From figure 20 it can be concluded that the vibration displacement levels decrease approximately a factor of 1.4 for a ratio of k of 4.25. Further on it can be concluded that the vibration velocity and acceleration levels do not change much with a higher value of k (product of power and speed). One could think about introducing the k factor in the next edition of the EFRC guidelines and this should be discussed for that reason.

From figure 21 it can be concluded that the vibration displacement level decrease approximately a factor of 1.3 for a power/throw ratio of 8. The vibration velocity level does not vary as a function of power/throw and the vibration acceleration level increase approximately a factor of 2 for a power/throw ratio of 8.

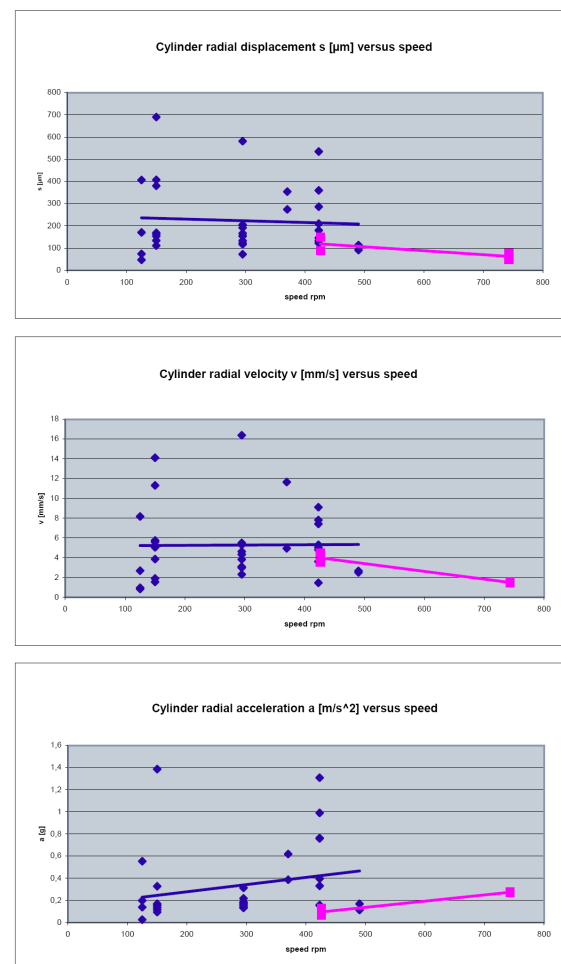


Figure 17: Cylinder radial vibration versus speed

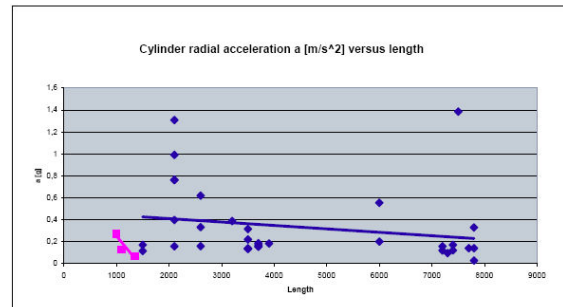
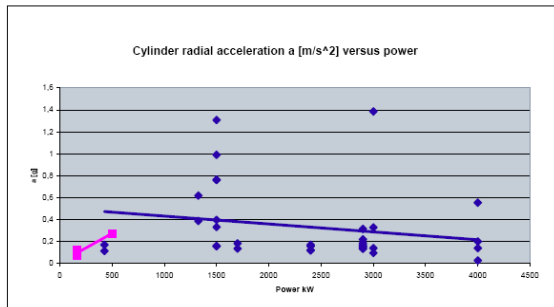
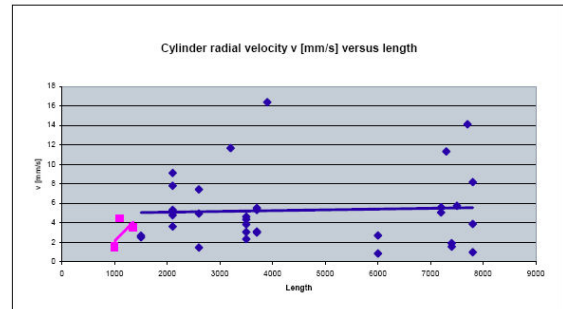
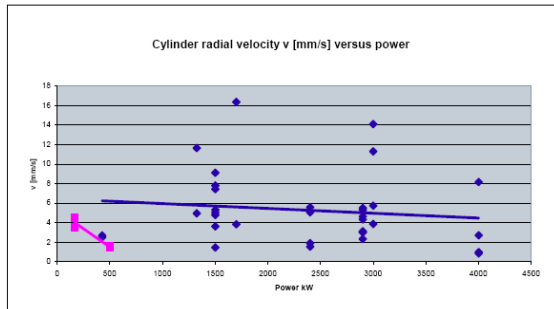
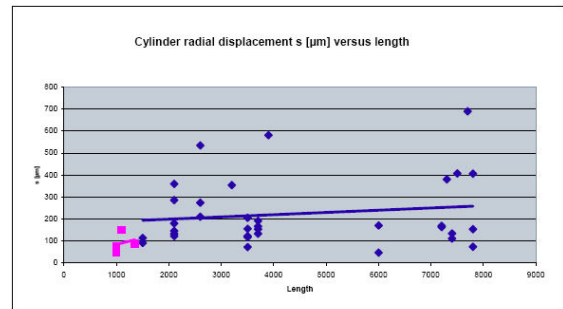
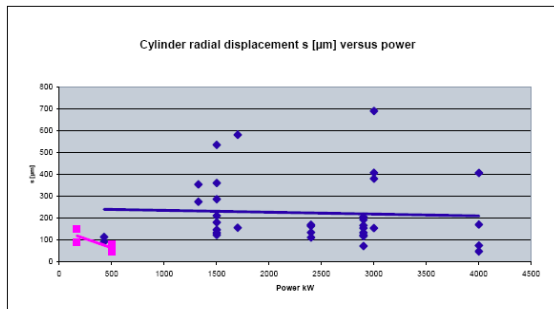


Figure 18: Cylinder radial vibrations versus power

Figure 19: Cylinder radial vibrations versus length

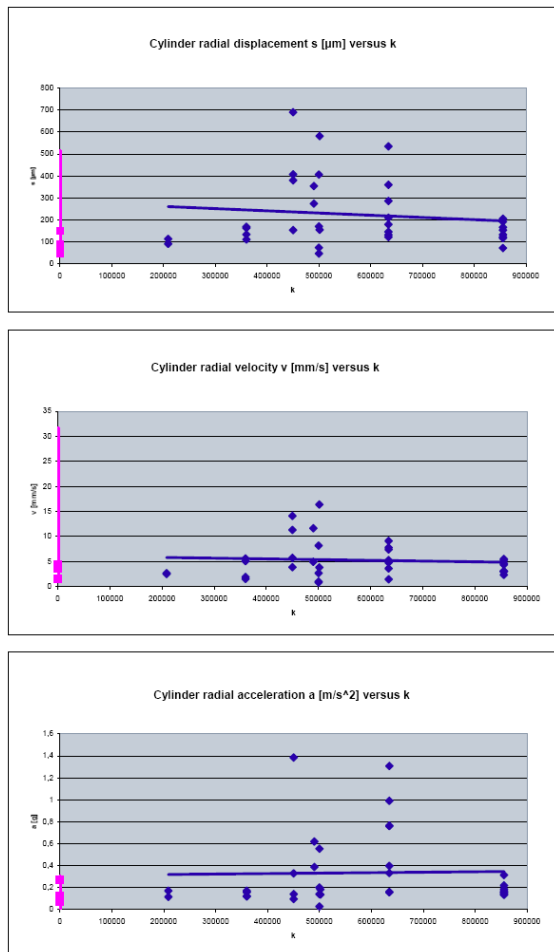


Figure 20: Cylinder radial vibrations versus k (product of power and speed)

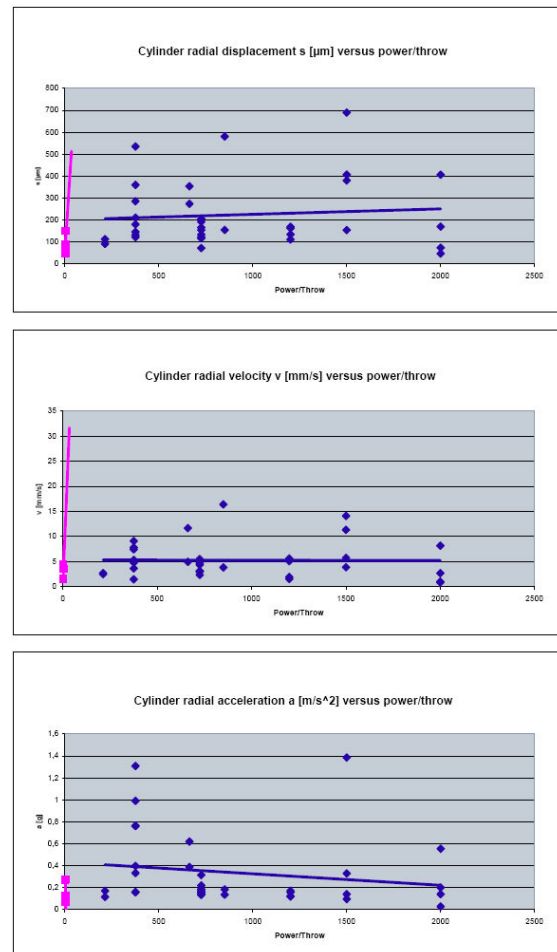


Figure 21: Cylinder radial vibrations versus power/throw

4 Conclusions

Permissible vibration levels for reciprocating compressors are described in the ISO standard 10816-6⁵. This standard gives limits for different classes of compressors. The problem for the practical use of this standard is that the classes of the compressors are not defined and no distinction is made between different parts of the compressor system: foundation, crankcase, cylinder, dampers and piping. For that reason EFRC Guidelines for vibrations in reciprocating compressor systems have been developed in an R&D project of the EFRC.

The EFRC guidelines are developed with a group of experts from the OEM's and end users with many years of experience and give clear definitions and limits and is easy to use in the field.

To prove if the EFRC guidelines match reality, extensive vibration measurements were carried out on many different configurations of reciprocating compressors which are installed at the BASF SE plant site in Ludwigshafen, Germany.

These measurements show that most of the values match zone A/B, which makes the values reasonable because the compressors are operating already for a long term without any vibration problems. It seems that the vibration displacement values for the foundation as given in the EFRC guidelines are a bit to low. Due to the fact that there are no foundation problems the levels for foundations could be increased together with a lower cross-over frequency. A second step was to find possible correlations between the vibration levels and different parameters such as power, speed and length of distance piece. It can be concluded that the vibration velocity and vibration acceleration level is independent for the product of power and speed of the compressor.

Due to the fact that the investigation is only limited to the installed compressors at the BASF side, the statistical bases is still quite low. For that reason more data is necessary to get better results and the authors invite everybody to add their results to the database. In this way it will be possible to adjust the values of the 1st edition of the EFRC guidelines even better to reality which may result in a second release. This will make the acceptance by the end users all over the world easier and it will be easier to determine if a reciprocating compressor system can run safe and reliable for the long term without any vibration problems.

5 Acknowledgements

The authors would like to thank BASF for sponsoring the vibration measurement project and for the permission for publishing the results of the field vibration data.

References

- ¹ Eijk, A, "EFRC Guidelines for vibrations EFRC Guidelines for Vibrations in Reciprocating Compressor Systems", 6th Conference of the EFRC October 28-29th, 2008, Düsseldorf, Germany
- ² Eijk, A, EFRC report "EFRC Guidelines for Vibrations in reciprocating compressor systems", October 2009
- ³ R. Schuhmann, Internal BASF report: "Field vibration data on different reciprocating compressor systems", 2010
- ⁴ ISO 5348: Mechanical vibration and shock-Mechanical mounting of accelerometers. Second edition 1998-05-15

⁵ ISO 10816-6: Mechanical vibration-Evaluation of machine vibration by measurements on non-rotating parts- Part 6: Reciprocating machines with power ratings above 100 kW. First edition 1995-12-15.



Operating experience of CC Valves installed in Refinery plant

by:

F. Manfrone, A. Raggi
Dott.Ing.Mario COZZANI S.r.l.
Arcola (SP)
Italy
info@cozzani.com

7th Conference of the EFRC
October 21th / 22th, 2010, Florence

Abstract

Energy saving aspects and reliability become more and more significant and innovations are continuously ongoing for improvements, then high quality valves are required both for new units and for already operating ones.

Valve designing is carried out today with advanced mathematical models, aiming to an optimization of the mechanical behaviour and a minimum energy consumption. The results include plate displacement, pressure drop, compression cycle. The research has allowed to develop some special profiles of the rings after a careful evaluation of the models applied. The possibility of reducing the pressure drop and improving the drag coefficient has evidenced efficiency savings.

This paper shows the theoretical and experimental results carried out on CC Valves, characterized by concave profiled ring. Two reciprocating compressors, installed in a refinery plant with H₂ and HC duty gas mixtures, have been equipped with this type of valves and the operation has been investigated during the time. In this lecture CFD and FEM analysis, measurements made on site and inspections about the state of the valves after three year will be shown.

1 Introduction

Energy saving and reliability are two of the aspects that over the years have assumed always growing importance in the field of reciprocating compressors.

The achievement of these targets pass through the development of automatic valves installed on the cylinders of the compressor. For this reason, Dott. Ing. Mario Cozzani S.r.l. always invested considerable resources in research and development of its own products. The high efficiency valves, called “CC valves”, represent one of the achievements of these investments. CC valves are characterized by an innovative type of concave shutter profile capable of combining the high fluid dynamic efficiency of the profiled shutters without renouncing the good sealing performances obtainable only with flat surfaces and at the same time assuring the easy maintainability of the classic flat rings or plates valves. This aspect is considered as very important as it is connected with overhauling equipments and costs.

The article shows some of the activities carried out for the development of the CC valves and presents the results obtained, both in terms of performance and reliability, by such valves installed on hydrogen ancillary units of the RHU catalytic hydro conversion plant at the refinery in Taranto.

2 CC Valves

In 2001 Dott. Ing. Mario Cozzani s.r.l. realized and patented a new high efficiency valve called with the mark CC valve (Figure 1) which was introduced in the same year during the 2nd EFRC Conference in Den Haag.

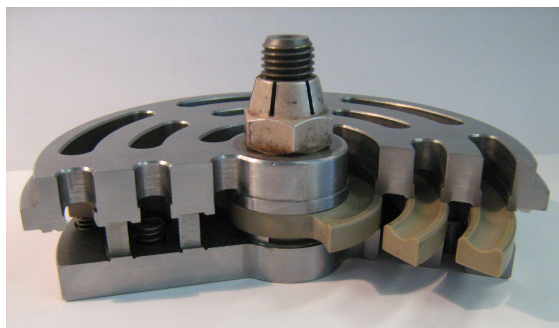


Figure 1: CC Valve section

This kind of valve uses a fluid dynamic phenomenon known in literature as “Coanda effect”, largely utilized in aeronautical field, which allows to drive a turbulent flow by a pilot pressure.

This effect is obtained inside the valve by using a concave profiled shutter which creates a pressure

bag in the central zone (Figure 2) and can drive the flow through the guard channels, as highlighted by the CFD analysis.

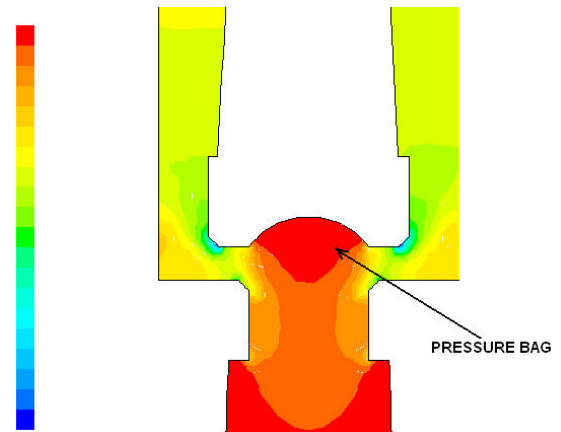


Figure 2: Fluid pressure in concave shutter

This produces a distribution of velocity, as shown in Figure 3, where the higher gas velocity is located in the minimum passage section close to the sealing surfaces.

This represents a double advantage in comparison with the use of “flat shutter”, where the highest values are reached inside the guard channel.

First of all, the high velocities like in figure 3 helps the cleaning of the sealing surfaces keeping them free of impurities that can be carried away by the gas. This avoids undesired leakages that can cause losses in efficiency.

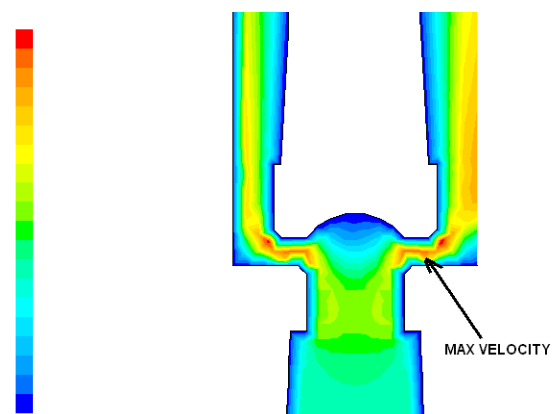


Figure 3: Fluid velocity with concave shutter

In addition, this kind of flow distribution presents smaller deviations and low turbulences which lead to an increase of the fluid dynamic efficiency compared with the standard flat shutters.

Such increase varies according to the lift in a range between 15% and 23% (*Figure 4*).

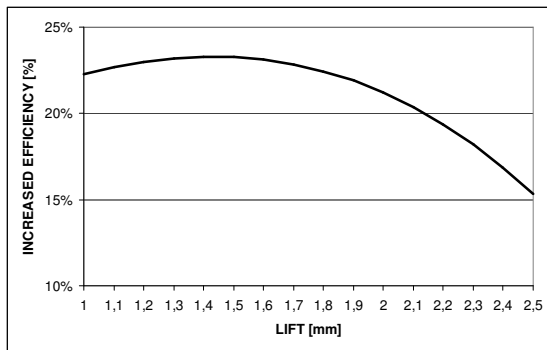


Figure 4: CC fluid dynamic efficiency increasing

The low pressure drops and consequently the high valve efficiency of CC solution in comparison with standard flat valves have been confirmed by the measures done through the test bench using different capacity and pressure values (*Figure 5*). The experimental test results obtained in University laboratories show a capacity improvement, at a constant pressure drop, of 20% for CC valves compared to flat ones.

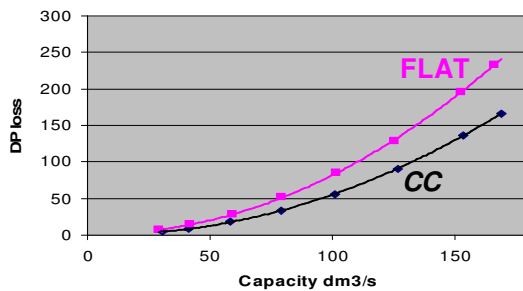


Figure 5: Pressure loss vs capacity (experimental tests)

3 FEM Analysis

During the last years the analysis by means of software using finite element method have assumed an always growing part in the field of mechanical design. Such software allows to solve the systems of partial differential equations (PDEs) in approximate way and offers an efficient support in decreasing designing time and reducing the doubts referred to complex geometries.

For CC rings the FEA techniques have represented a great support in analyzing the shutter deformations when exposed to high thermal stress and in evaluating their resistance in comparison with standard shutters.

Considering the valve operating temperature conditions, the thermoplastic shutters show much higher thermal expansions in comparison to steel

valve bodies. For such effect convex or chamfered shutters, show greater sealing difficulties if compared to the flat ones or, more precisely, the sealing of these shaped shutters implies a torsion of the shutters. On the contrary, the sealing behavior of the CC profile differs from all other previously mentioned profiles, as its shape combines a flat part dedicated to the sealing with a concave one for the efficiency. Through FEM analysis, done by imposing a temperature gradient of 200°C, it has been possible to observe (*figure 6*) the different expansions between seat and CC shutters that are implicit to the materials, but don't affect the sealing.

Another essential aspect of CC profile is referred to the valve overhauling operations. In fact, flat sealing surfaces don't require the use of special equipments for refurbishing and checking, with cost saving related to the use of standard overhauling equipments. We can assert that the CC valve is the only valve with shaped profile and flat sealing.

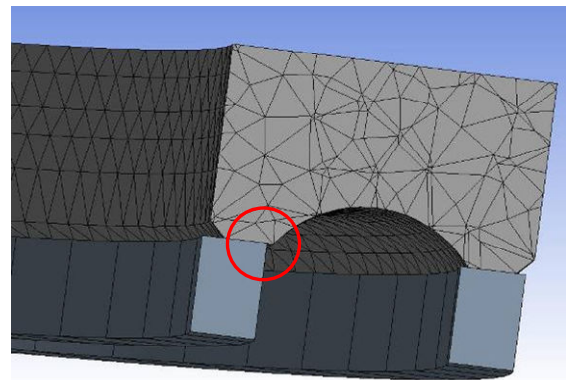


Figure 6: Displacements due to temperature

In order to evaluate the strength of CC shutters, FEA simulations have been done to perform comparisons with standard shutter types. These verifications carried out for different shutter sizes and same boundary conditions have showed very similar stress distribution (normalized according to the applied loads). *Figure 7* and *Figure 8* show the results of simulations where same colors represent same stress ranges.

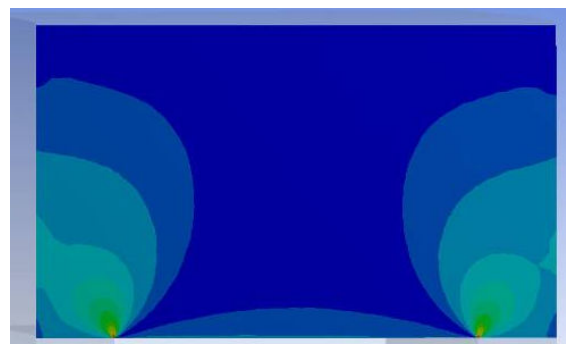


Figure 7: Flat ring FEM Analysis

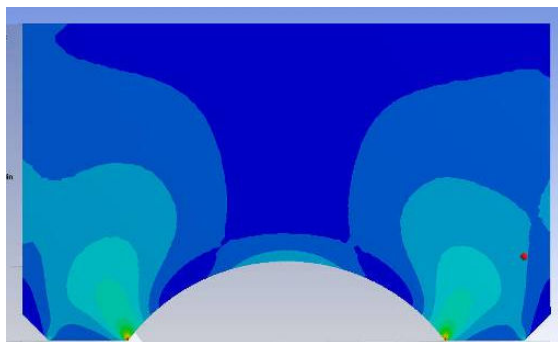


Figure 8: CC ring FEM analysis

In both cases the maximum stresses have been detected close to the seat flow channels. It has been proved that CC shutter maximum stresses don't exceed 10% more than flat ones.

4 Compressor Tests

4.1 ENI Plant in Taranto

Taranto Refinery is located in the industrial area that overlooks the bay with same name. It came into operation at the end of the Sixties and over the years it has been subject to a continuous improvement process of its facilities in relation to the requirements of the oil industry market. With a balanced refining capacity of 110 kbb/d and a conversion index of 64,6%, this refinery can process a wide range of crude and of other feedstock. It mainly produces fuels for automotive use and residential heating purposes for the Southern Italian markets.



Figure 9: Taranto Refinery

Besides the primary distillation plants and the relevant facilities, including two units for the desulphurization of middle distillates, the refinery contains a two-stage thermal conversion plant

(visbreaking/thermal cracking) and an RHU conversion plant (Residue Hydroconversion Unit) for the hydrogen conversion of high sulphur content residues into valuable products and catalytic cracking feedstocks.

4.2 Reciprocating compressors

On the ancillary hydrogen plant used in the RHU there are two identical compressors, one usually operating and the other available in case of need (backup or plant requirements).



Figure 10: Compressor on ENI plant

Each compressor is equipped with two cylinders and handles the gas from approximately 4 bar to 35 bar. The cylinders are non lubricated and compress a gas mixture composed by hydrogen (55%), hydrocarbon and H₂S with molecular weight varying from 18 to 24 kg/kmole depending on the composition of the treated gas.

Each compressor runs at 590 rpm by a 50 Hz three-phase electric induction motor with a 740 kW rated power.

The valves used in these compressors, started up at the beginning of the Nineties, have been produced by Dott. Ing. Mario Cozzani s.r.l.

In 2004, on customer request, a project for the improvement of the valves was carried out, in order to increase the performances from an efficiency point of view. The only restriction imposed on the designing phase was the perfect interchangeability between the new and the old valves (*Figure 11*).

RINGS, VALVES & PACKINGS

Operating experience of CC Valves installed in Refinery plant, *Andrea Raggi, Fabio Manfrone;*
 DOT. ING. MARIO COZZANI



Figure 11: Flat ring valve (on the left) and CC valve (on the right)

4.3 Dynamic Simulations

In the automatic valves for reciprocating compressors the shutter movement is due to the force generated by the difference between the pressure inside the cylinder and the pressure on the inlet/outlet side of the suction/discharge valve and by the duly dimensioned springs.

In order to predict the real behavior of the shutters which during their operating life are subject to shocks, wear and high specific stresses, Cozzani has developed its own simulation software by using Matlab/Simulink.

By knowing the characteristics of the reciprocating compressor (bore, stroke, angular velocity, etc.), those relevant to the operating conditions (gas, pressures, temperatures, molecular weight, etc) and the characteristics of the valves (lift, sections, springness etc.) the software is capable of determining the pressures trends inside the cylinders and in the suction and in the discharge volumes, of simulating the valve shutter movements, providing a series of indications useful to the designer like impact velocity, flow rate, valve pressure and power losses.

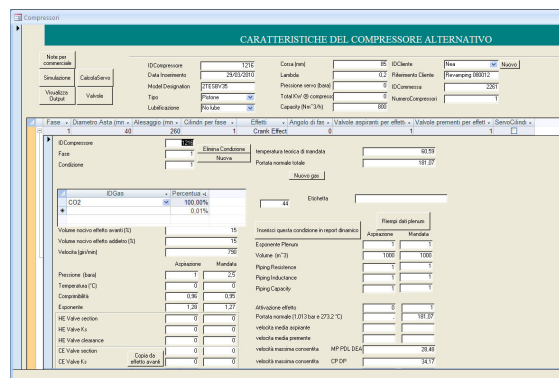


Figure 12: Input data for Dynamic Simulation

The analysis of these graphs, supported by numeric values, allows to choose the best compromise between loss of pressure and reliability of the valves. In fact a low pressure loss effects a high

fluttering of the shutters, which reduces the lifetime of the springs with consequent possible problems also to the shutters.

With reference to the compressor described in paragraph 4.2, simulations have been carried out in order to compare the dynamic valve behavior of the standard flat ring valves previously installed and the CC ones, used from 2004.

The results of these simulations are set forth below:

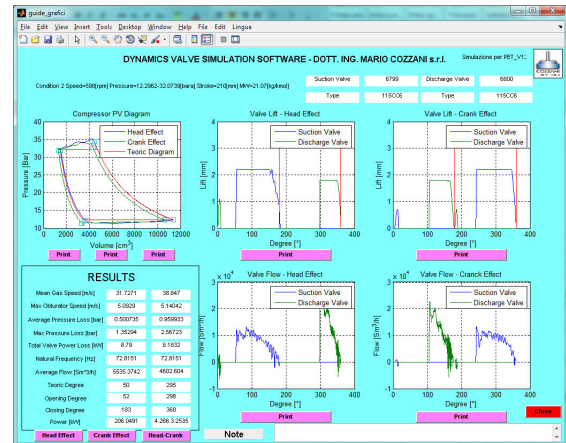


Figure 13: Main results of Dynamic Simulation (CC valves case)

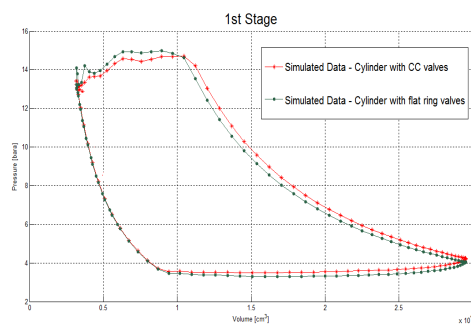


Figure 14: 1st stage PV cycle (comparison between standard ring valves and CC valves)

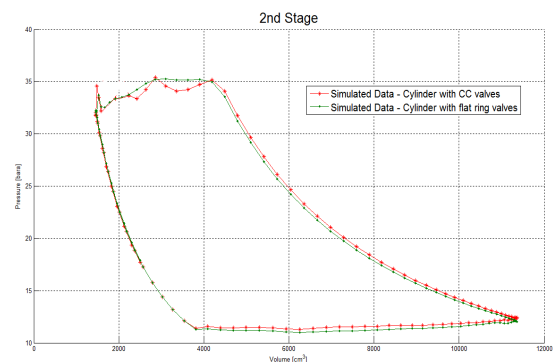


Figure 15: 2nd stage PV cycle (comparison between standard ring valves and CC valves)

The analysis of the cylinder pressure behaviour allows to evaluate that in the case of CC valves the pressure drop on the valves is lower (*Figure 16*).

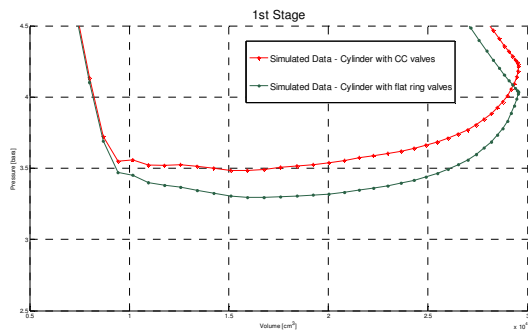


Figure 16: 1st stage suction pressure

Consequently also the power loss at the valves is lower, in fact in case of CC valves it is approximately 22% less than for flat ring valves, which means a simulated indicated power saving of about 2.5% (*Figure 17*).

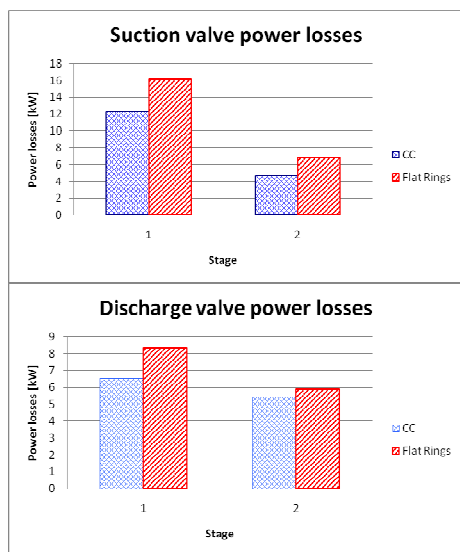


Figure 17: Power losses with standard and CC valves

4.4 Measures on the compressor

One of the two reciprocating compressors of the plant has been equipped with instrumentation suitable for saving the indicated cycles.

The instrumentation consists of a set of pressure sensors with different ranges, related to the maximum value of the size to be measured, used to determine the pressure inside the cylinders and in the upstream/downstream volumes of the suction/discharge valve, and a position sensor to acquire the TDC.

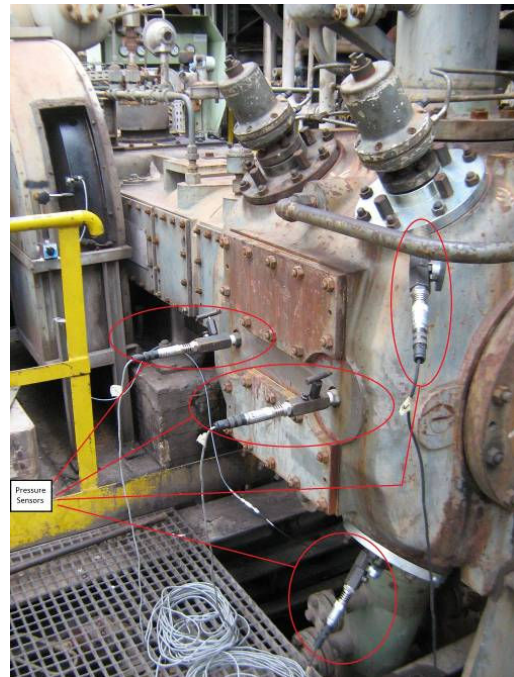


Figure 18: Pressure sensors installed on the compressor

The complete sensor set has been connected to an acquisition board and the several signals have been processed by a dedicated software.

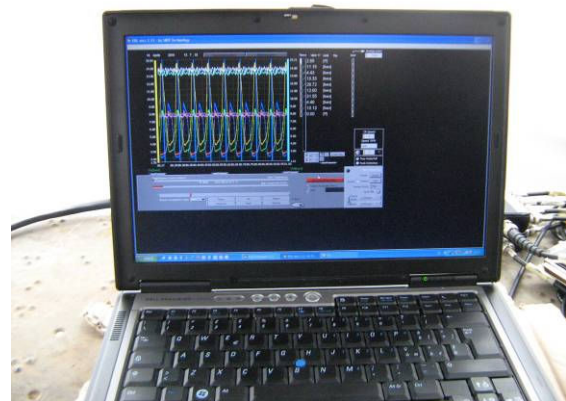


Figure 19: Data acquisition and processing

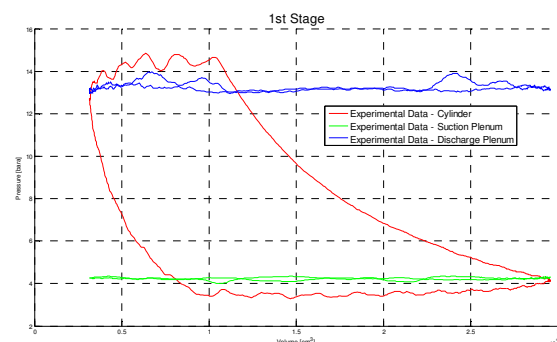


Figure 20: 1st stage experimental measures

4.5 Comparison between experimental tests and dynamic simulations

In order to validate the dynamic analysis, the experimental indicated cycles have been compared to the theoretical ones.

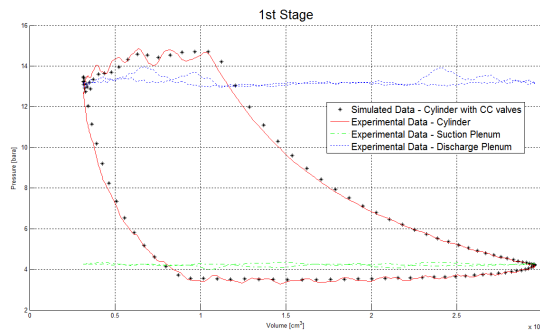


Figure 21: Comparison between 1st stage experimental tests and simulations

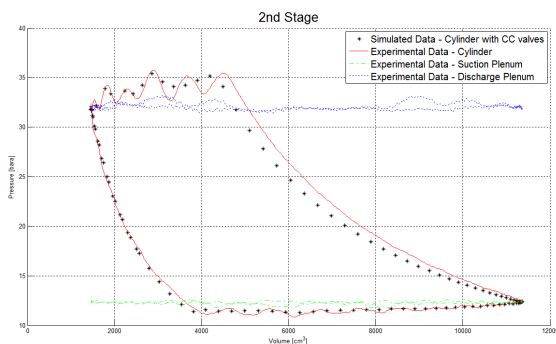


Figure 22: Comparison between 2nd stage experimental tests and simulations

The comparison of the indicated cycles highlighted a good correspondence between the measured pressures and the simulated ones. Then also the energy saving evaluated by simulations is confirmed by the experimental tests.

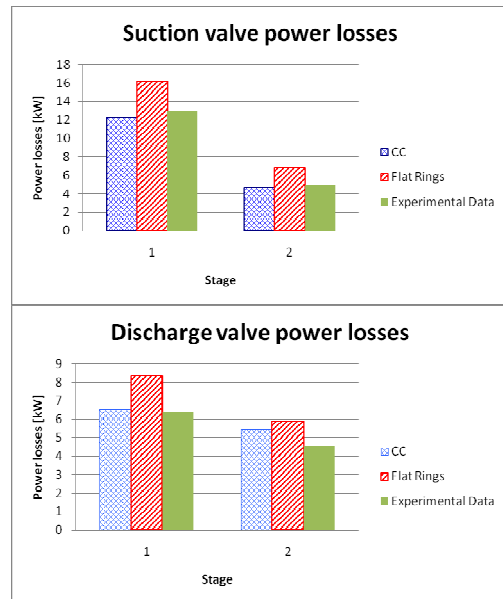


Figure 23: Valve power losses comparison

4.6 Inspection on the valves

The inspections carried out over the years on several CC valve sets installed in petrochemical plants, delivered to Cozzani S.r.l. for standard overhauls, have confirmed what was expected in terms of life and wear resistance.



Figure 24: Valve from the Taranto Refinery

In particular the valves installed on the compressors of the ENI Taranto plant, where the campaign of experimental tests was carried out, have achieved 3 years operating.



Figure 25: Internal parts of a CC valve

Although the valves were installed on compressors operating with a particularly dirty and corrosive gas, the inspections have confirmed excellent behavior of CC type, as proved by the conditions of valve bodies, springs (Figure 25) and concave rings (Figure 26).



Figure 26: Concave rings for CC valves

5 Conclusions

The CFD analysis and the workbench tests done on CC valves types highlighted a theoretical fluid dynamic efficiency approximately 20% higher than the standard flat type. The FEM analysis established that the decreasing of the section due to the adoption of a concave profile doesn't affect the shutter structural resistance. In addition the flat sealing surfaces adopted in the CC shutters, in comparison with the convex one, limit the thermal expansion effects on the sealing and make the overhauling easier.

Two compressors running on Taranto Refinery have been analyzed through valve dynamic simulations in order to define PV cycles and the power consumption due to the valves.

In this way it was possible to estimate a decreasing of the overall valve power losses equal to 22% obtained by replacing the standard flat ring valves with CC ones, which corresponds to a 2.5% energy saving of the indicated power.

The experimental tests done at the ENI Taranto Refinery, based on the acquisition of pressures inside the cylinders and on the valve cages, allowed to verify the real power losses. The energy saving evaluated through the dynamic simulations has been confirmed by the experimental tests done on the compressor.

The inspections done on CC valves delivered by several plants for overhauling showed a very good reliability reaching three year operating smoothly.

References

- 1 – API Standard 618 “Reciprocating Compressors for Petroleum, Chemical and Gas Industry Services”, 4th Edition, June 1995
- 2 – Matlab User’s Guide
- 3 – A. Bianchi, M. Schiavone, "New profile for Thermoplastic Shutter of Compressor Valves ", 2nd EFRC-Conference 2001 Den Haag.
- 4 – J. H. Ferziger, “Computational Method for Fluid Dynamics” Springer 2002
- 5 – Z. Xiaobua, Z. Chonghui, M. Schiavone, M. Pucci, E. Giacomelli, “Operation and Maintenance of valves for reciprocating compressors in H2 service Daqing Luboil Plant” A.I.M.A.N. 2009
- 6- Tritton, D.J., “Physical Fluid Dynamics - The Coanda Effect (sect.22.7)”, Van Nostrand Reinhold, 1977
- 7- Giorgio Uggeri, “Servocomandi Pneumatici” Hoepli 1968



Supplementary challenges for UGS applications of reciprocating compressors in combination with centrifugal machinery

by:

Dipl.-Ing. Joachim Wermeling
RWE Gasspeicher GmbH
Dortmund
Germany
Joachim.Wermeling@RWE.com

Dipl.-Ing. Burkhard Lenth
RWE Rheinland Westfalen Netz
AG
Essen
Germany
Burkhard.Lenth@RWE.com

7th Conference of the EFRC
October 21th / 22th, 2010, Florence, Italy

Abstract

In view of a growing gas market and gas demand, RWE has made the decision to develop UGS in Epe and Staßfurt to ensure the continuity of future supplies. This paper describes the current situation in relation to the development of both compressor facilities, as well as caverns, in detail. The specific combination of reciprocating and centrifugal compressors is outlined. Both compressor variants are being installed at each facility. The chosen compressor setup reflecting what is confidently expected to be the optimal solution for RWE. Combining the reciprocating and the centrifugal compressor creates the possibility for RWE to meet the flexible demand in the gas market.

1 Introduction

The gas industry has to be in a position to match the supply of natural gas to the demand. Storage facilities are indispensable. Traditionally, gas was stored during the summer period and the entire volume was withdrawn in the winter period due to the seasonal variation in demand. But times are changing, also for gas storage facilities. Single-cycle operations are being replaced by multi-cycle operations, mainly driven by commercial factors arising from market liberalization. As a consequence, we need high reliability and availability of compressor stations.

The RWE group has 16 gas storage facilities with about 50 compressor units. In Germany RWE Rheinland Westfalen Netz AG (RWN) operates 5 gas storage facilities with 12 compressor units.

Due to these new challenges RWE is pursuing the strategy to combine the advantages of reciprocating compressors and centrifugal machinery optimally. The technical and economic interdependence and its pros and cons will be discussed.

2 RWE RWN – short overview:

- RWE RWN AG is the company with responsibility for the distribution grid and investment holdings in the RWE Group in Germany
- RWE RWN AG operates electricity, gas and water grids. Its portfolio also includes five gas storage facilities
- In all, RWE RWN AG serves an electricity network of some 185,000 km in length and a gas network of 30,000 km
- Employees (in 2010): 7,300
- RWE Gas Storage Company is a wholly-owned subsidiary of RWE RWN AG
- RWE Gas Storage Company runs and markets a variety of different storage types in Germany (cavern and aquifer reservoirs as well as LNG storage facilities)
- Its five sites in North Rhine-Westphalia, Lower Saxony and Saxony-Anhalt have storage capacities of some 1,1 billion m³ of natural gas
- RWE decided to install the combination of reciprocating and centrifugal compressors at its cavern storage facilities in Epe and Staßfurt

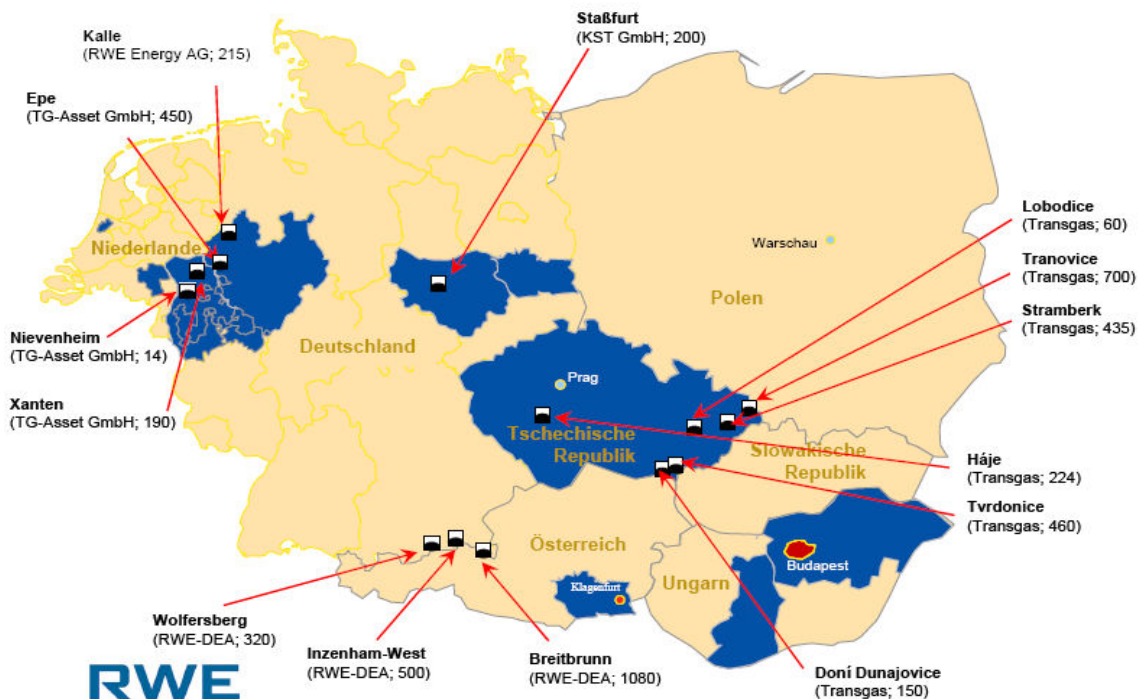


Figure 1: Location of the natural gas storages of RWE

3 General Description of UGS facilities

An underground storage system consists of an above ground facility and the underground storage itself. Gas is transported from the gas source to the storage facility via a pipeline. Gas is fed from the pipeline and flows through an entry filter of the gauging station into the compressor station. In this station gas is compressed from pipeline pressure to the maximum cavern pressure, and then cooled

down before it flows in through an oil separator. Afterwards it is transported to the caverns via a manifold. During withdrawal natural gas flows via the water separator to the pressure reduction and flow control valves. Here the pressure is reduced to the pipeline level. Due to the Joule Thomson law, decompression has a rapid cooling effect. In order not to fall below the dew point the gas is therefore pre-heated. Finally the gas is dehydrated and flows into the pipeline. The necessary process equipment for storage operating-mode is shown in figure 2.

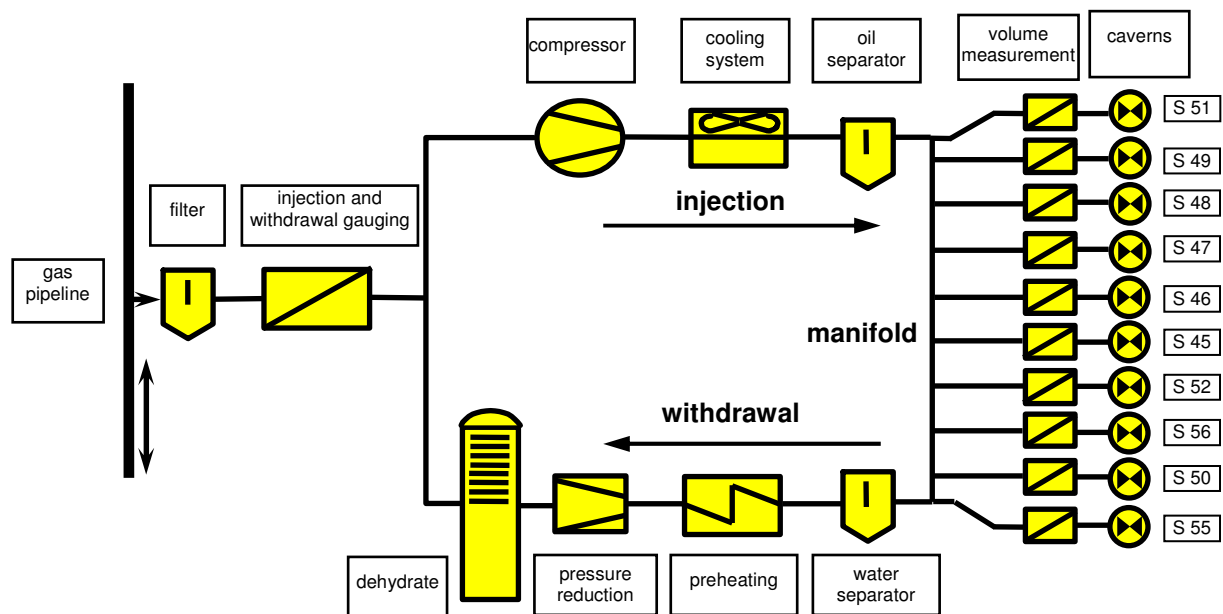


Figure 2: Schema of storage operating-mode

4 Description of the UGS in Epe

- Epe is located at the German-Dutch border near Gronau
- With 3 billion m³ storage capacity, Epe is Europe's largest cavern storage field
- RWE Gasspeicher GmbH owns a storage capacity of 500 million m³ in Epe which is operated by remote control from headquarter in Dortmund (Germany)

- 10,000 m³/h – 75,000 m³/h
- 3 synchronous electrical motors with frequency converter

withdrawal

- 5 discharge lines with 1,080,000 m³/h
- preheating of natural gas with ca. 35 MW
- 5 absorber
- 1 vortex tube separator with 140,000 m³/h

Summing up technical data of UGS Epe: caverns

- number = 10
- geometrical volume = 3 mcm
- working gas volume = 500 mcm
- total volume = 630 mcm

injection

- 6 gauging stations
- 3 two-stage reciprocating compressors
- 28 – 211 bar

manufacturer:	BORSIG	BORSIG
type:	BX 45-80/63/4S2	BX 45-80/63/4S2
name:	V1+V2	V3
year of manufacture:	1988	1990
no. of cylinders:	4	4
stages:	2	2
capacity:	20,000 / 80,000 Nm ³ /h	20,000 / 100,000 Nm ³ /h
control system:	suction valve unloading	suction valve unloading

power:	3,700 kW	3,700 kW
rotation speed:	200 / 370 rpm	180 / 370 rpm
piston stroke:	270 mm	270 mm
diameter of the piston rod:	130 mm	130 mm
cylinder bore 1 st -stage:	365 mm	365 mm
cylinder bore 2 nd -stage:	265 mm	265 mm

Figure 3: technical data of installed reciprocating compressor

4.1 Enlargement of the injection capacity at UGS in Epe by an additional centrifugal compressor

manufacturer:	MAN Turbo
name:	EPE-VD4
year of manufacture:	2010
stages:	2
power:	990 / 7,300 kW
rotation speed:	7,810 / 13,010 rpm
low pressure level	
capacity:	46,100 / 124,800 Nm ³ /h
suction pressure:	28 / 70 bar
discharge pressure:	46 / 139,5 bar
high pressure level	
capacity:	24,000 / 124,500 Nm ³ /h
suction pressure:	28 / 137,4 bar
discharge pressure:	46 / 225 bar

Figure 4: Technical data of additional centrifugal compressor

manufacturer:	Siemens
type:	1TZ1240-8BU02-Z
power:	8,458 kW
voltage :	4,160 V
rotation speed:	1,750 rpm
standard:	IEC 60034
configuration:	IM 1001
protection class:	IP 55
explosion protection class:	II2GEEpII T3
thermal class:	F

Figure 5: Technical data of the electric motor

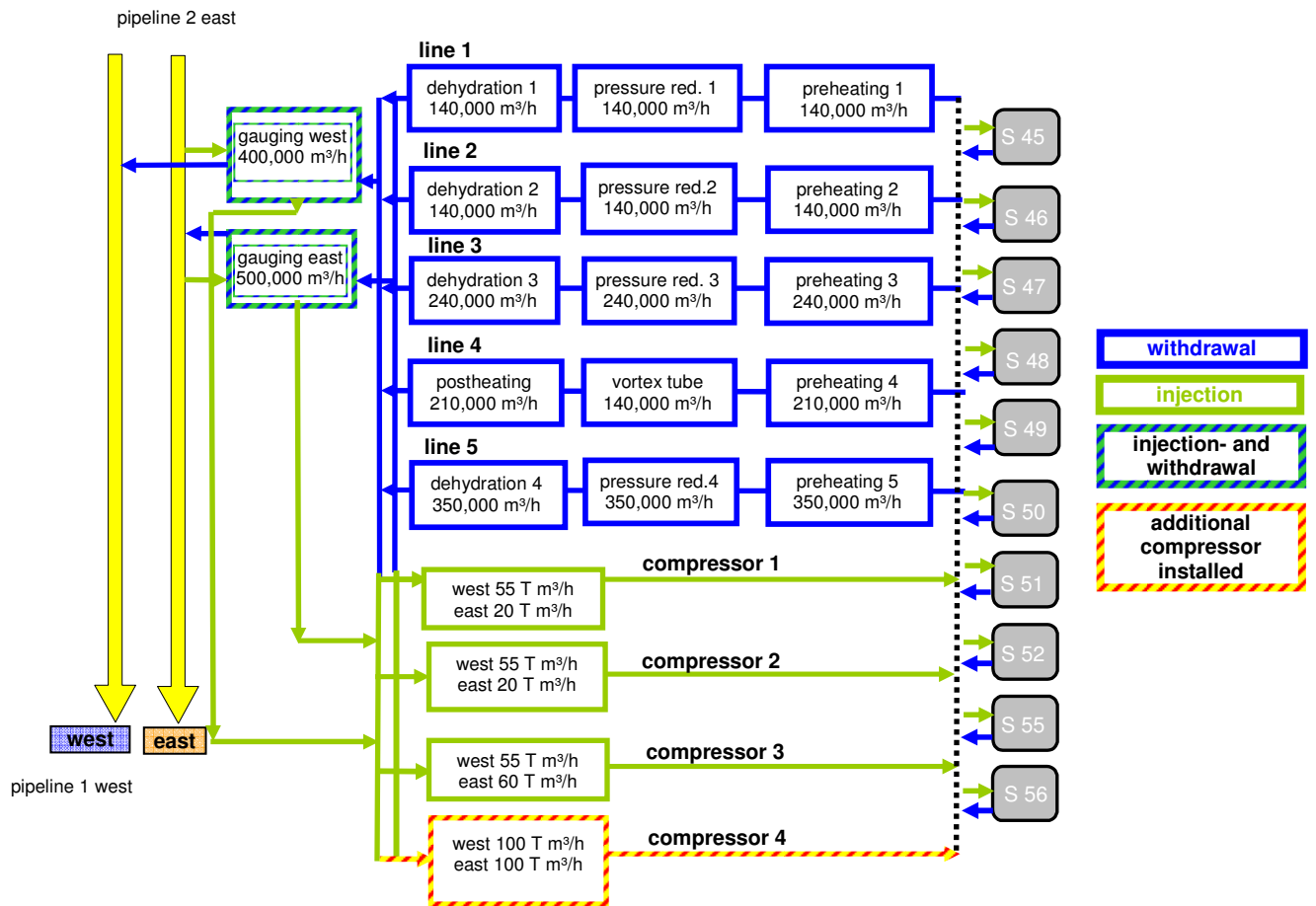


Figure 6: Flow chart of Epe after installation of an additional compressor

- 2 withdrawal lines with 285,000 m³/h

5 Description of UGS in Staßfurt

- Staßfurt is located 40 kilometer south of Magdeburg in the eastern part of Germany
- Staßfurt has a 4 million m³ geometrical storage capacity
- Natural gas is compressed from 25 bar to 186 bar
- The compressors are able to operate in parallel or in series to raise the flow rate

Summing up technical data of UGS Staßfurt: caverns

- number = 5
- geometrical volume = 4 mcm
- working gas volume = 279 mcm
- total volume = 340 mcm

injection

- 2 gauging stations
- 2 two-stage reciprocating compressors
- 24 – 160 bar
- 10,000 m³/h – 75,000 m³/h

withdrawal

manufacturer:	BORSIG	Neuman & Esser
type:	BX 40-40/4S2	2 SVL 500
name:	V1	V2
no. of cylinders:	4	4
stages:	2	2
capacity:	25,000 Nm³/h	75,000 Nm³/h
driver:	asynchronous AC motor (10,5kV, 50Hz)	synchronous AC motor (10,5kV, 50Hz)
power:	1,800 kW	3,800 kW
suction pressure:	25 / 50 bar	25 / 69 bar
discharge pressure:	186 bar	186 bar

Figure 7: Technical data of installed reciprocating compressors

5.1 1st project stage: Installation of one reciprocating and an additional turbo compressor at UGS Staßfurt

The technical data for the centrifugal compressor is not being published for the time being, because the order has not been placed yet. The project for the enlargement of the storage facility at Staßfurt is divided into three stages. In the first stage three caverns will be added, which requires one additional reciprocating and one centrifugal compressor. The data for the additional reciprocating compressor is shown in figure 8. After completion of two more caverns, we will probably need another centrifugal compressor. Raising the capacity of the geometrical storage volume to a level of 600 million m³ will require two more caverns at the last stage.

manufacturer:	Neuman & Esser
type:	2 SVL 500
name:	V3
no. of cylinders:	4
stages:	2
capacity:	75,000 Nm ³ /h
controller system:	suction valve unloading
power:	4,981 kW
revolution speed:	598 rpm
suction pressure	21 / 61 bar
discharge pressure	167 bar

Figure 8: Technical data of additional reciprocating compressor

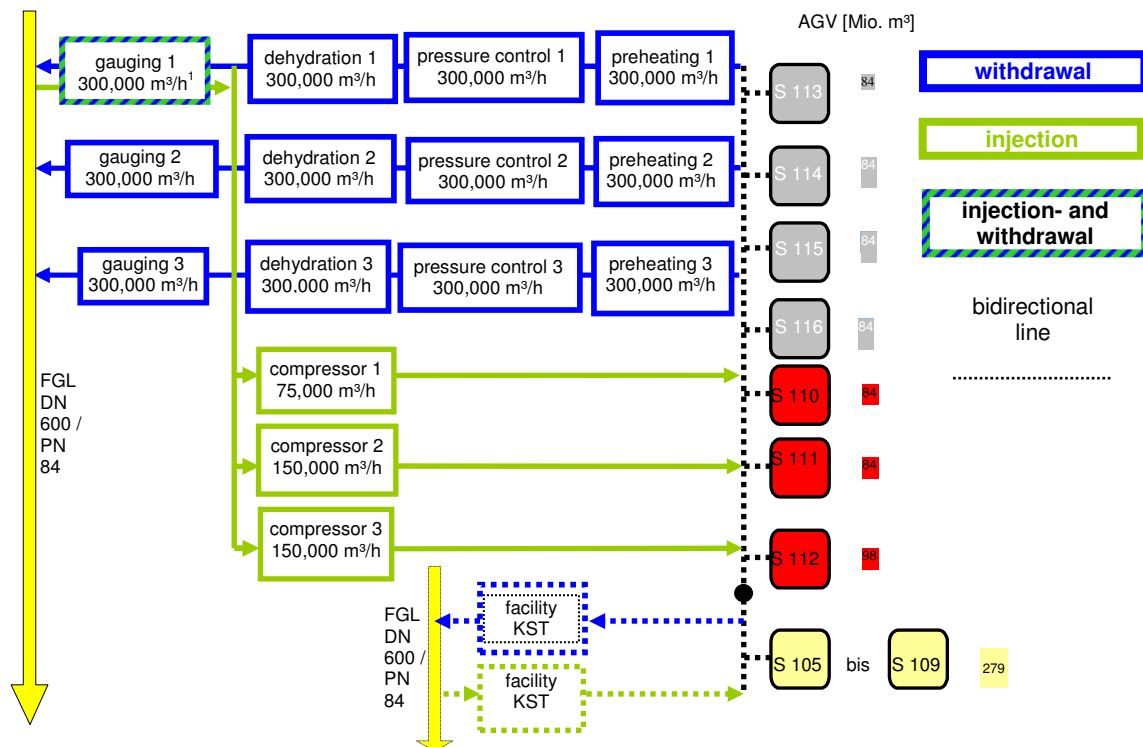


Figure 9: Flow chart of Staßfurt after installation of three additional compressors

6 Comparison of reciprocating versus centrifugal compressors

To determine the optimal compressor set-up for a defined operating range there are several advantages and disadvantages which have to be ranked. A distinction is drawn between technical and economic aspects of the different kinds of compressors and is taken into account. In this case,

the reciprocating and the turbo compressor are compared. First of all, RWE had to make the

general decision about which kind of compressor was to be employed. To get a representative economic result both compressor types were analysed with the dynamic investment calculation “Net Present Value” (NPV) method.

As a result, the reciprocating compressor emerged as the most economic version for reasons of lower investment costs (CAPEX), lower energy consumption and higher efficiency (OPEX).

The turbo compressor has a limited working range with limited pressure ratio to work efficiently, but within its pressure range the working capacity is much higher in comparison to the working capacity of the reciprocating compressor. Disadvantages of the reciprocating compressor are the gas pulsation, the more frequent maintenance intervals and the much higher need for spare parts. The use of turbo compressor results in operating without gas pulsation, torsional vibrations and no need of pulsation bottles (as needed for reciprocating compressor plants). To store gas the reciprocating compressor is the best solution, but to store in high capacities of gas up to 150,000 m³/h it makes sense to combine both kind of compressors and employ a centrifugal compressor. For a short overview the main advantages and disadvantages of both compressor variants are summarized in the following sheet.

	reciprocating compressor	turbo compressor
availability	low	high
flexibility regarding to pressure drops and flow rate changes	high	low
flow rate control	suction valve unloader, rotation speed control	rotation speed control, limited by pump limit and stonewall
capacity control	wide control range	narrow control range
pulsation	yes	no
running characteristics	torsional vibration	smooth
request on foundation	high	marginal
efficiency	high	low
costs for maintenance and repair	high	low
costs for spare and wear parts	high	low

Figure 10: Pros and cons of both versions

7 Combination of reciprocating and centrifugal compressors as the best solution

To enlarge the two storage facilities Epe and Staßfurt, RWE decided to respond to the need for flexible storage solutions and the growing economic challenges. To find out which compressor units should be employed, RWE carried out a series of studies focused on economic and technical aspects. As a result of these studies the combination of reciprocating and centrifugal compressors was identified as the ideal solution.

On the one hand reciprocating compressors are mainly employed at high pressure levels with a wide capacity control range. In view of this, the reciprocating compressor is applied in the first filling of the caverns, during residual filling of the caverns and during periods of time with a demand for small and medium gas capacity. On the other hand the centrifugal compressors are applied at a medium pressure levels, in times of high demand and to store in high capacities.

Following these two projects and given that the combination of reciprocating and centrifugal compressors has now been established as the appropriate solution in the gas storage market, RWE has the possibility to inject more natural gas with flexible flow rates into the caverns and the possibility to offer flexible short term contracts to the customers. The use of the dual compressor set-up and higher capacity storage facilities form the basis for offering flexible storage periods.

8 Summary

During the operating life of an underground gas storage facility, engineering operations and management continually examine ways to optimize the plant equipment to achieve the highest return on investment. In view of the usage of different compressors in combination RWE is extremely well-placed to meet customer needs and has an excellent strategic position in the European gas market.



Next generation valve technology for high speed compressors

by:

B. Spiegl, M. Testori, G. Machu
HOERBIGER KT Holding

Vienna

Austria

bernhard.spiegl@hoerbiger.com

7th Conference of the EFRC
October 21th / 22th, 2010, Florence

Abstract

The trend towards high compressor speed is continuing in almost all compressor market segments. In the last 20 years significant research was undertaken to achieve sufficient valve lifetime in these demanding applications. New polymer materials and spring technologies, together with better valve simulation helped to make the plate type compressor valve (HOERBIGER CT valve) the work horse in the natural gas industry with acceptable reliability in the high speed segment. Nevertheless, there existed room for improvement in applications with compressor speeds higher than 1200 rpm especially with additional issues like over lubrication, dirt and frequent liquid slugs.

A newly developed valve family, (CPs valves), applies a unique design concept which simultaneously applies significant improvement in reliability, efficiency and robustness, as recent field testing has proved. The use of innovative materials and processing technology allow the design concept of a “profiled valve plate” thereby combining the advantages of ring valves and plate valves. The high opening impact speeds inherent with demanding applications are handled by a new springing and damping concept. More than 1000 CPs valves are running successfully in former “troublemaker” applications globally with impressive results in reliability and energy saving. In addition, the high efficiency of the valve concept allows the change of design guidelines for compressor cylinders and opens the door for new innovative compressor concepts.

1 Introduction

Natural gas is becoming more and more important to satisfy the increasing energy consumption of the world. The demand for gas gathering, gas transport and gas storage compression equipment is increasing rapidly.

Most existing gas fields suffer from decreasing gas pressure, thereby further increasing the need for efficient gas compression to boost the gas pressure to the needed pressure levels of the pipelines.

In order to keep investment cost down, gas field and pipeline operators press for increased compressor speed. If increased compressor speed is not matched with appropriate valve technology the end user could be faced with reduced compressor efficiency and reliability. Standard plate valve technologies had reached their physical limits.

High speed compressors in natural gas are still seen as critical with regard to valve lifetime, reliability, and sufficient lifetime is only achieved by sacrificing valve efficiency.

At the 5th EFRC conference in 2007 in Prague [1] a new valve concept with high number of narrow individual valve rings with synchronized valve opening motion was presented. This valve is running successfully in critical applications and shows that the applied ideas work out.

The progress in material science, material processing and precision machining opens the door for even more advanced technical solutions which will be outlined in this paper.

Modern valve development is a combination of the latest knowledge in valve design, valve motion simulation, sealing material technology and valve spring technology. In addition, during development, the known critical load situations in the specific applications need to be taken into account. In the case of North American natural gas compression, with its high speed compressors and the increasing gas production in so called “unconventional” gas fields, over lubrication and frequent liquid slugs need to be taken into account during the design phase.

Thereby new valve concepts should be discussed in respect to their ability to handle:

- Valve opening impact
- Over lubrication and liquids
- Valve closing impact
- Differential pressure resistance
- Valve efficiency

In the reciprocating compressor business a compressor speed higher than 1200 is seen as a high

speed compressor. In this paper special emphasis is given to the valve diameter range from 50 to 100 mm – majority of high speed compressors range in this valve diameter size.

2 Limitation of existing valve designs

Typical valves used in the high speed market are narrowly spaced plate valves (HOERBIGER R-Type valves, CT valves and similar designs). Beside some new installations almost no ring valves found their way in this application.

Lately, field returns from demanding applications indicated that the predominant failure mode is impact initiated valve plate breakage from high impact loads during opening or closing. In most cases the failure goes hand in hand with a failure of the spring element – either coil springs or spring plates – or was initiated by a failed spring element.

Figure 1 shows pictures of typical failure modes that can be found with standard technology in high speed compression. Valve plate breakage from high opening impact speed is in most cases, a combination of high compressor speed and oil sticktion on the seat (see Fig. 3). Oil sticktion itself is a function of oil quantity, viscosity and seat geometry [1]. Very often the oil sticktion situation becomes critical after improper seat repair when the seat land geometry is changed.

Another reason for opening impact failures is liquids going through the compressor. The mechanism of liquids passing compressor valves cannot be modelled entirely. Significantly higher impact speeds need to be assumed [1]. High quantities of liquids could also lead to seat and guard breakage and damages on the compressor.

The component of the valve suffering most under continuous high opening impact speeds are the spring elements of the valve. In case of spring plates we have to differentiate between three failure modes (see Fig. 1):

- Fatigue breakage caused by bending stresses (supported by surface defects)
- Overstressing in critical areas due to plate flattening during guard impact
- Impact fatigue of moving parts of spring plate by hitting the steel guard

The first two failure modes can be solved by suitable engineering. The third mode is a design inherent problem of valves with spring plates. Continuous steel to steel impact with speeds higher than 4 m/s will lead to local material fatigue.

In case of coil springs, the effect of high opening impact speeds is different. A properly designed coil spring, using the latest principles of spring design and spring wire technology, can handle impact speeds up to 3-4 m/s without overstressing or coil contact (speeds measured from field installations). With higher impact velocities coil contact occurs – leading to wire thinning and wire breakage (see Fig. 2). Multiple higher impact speeds lead to plastic deformation in the spring wire and length reduction [1]. The loss of spring load will influence valve closing behaviour significantly.



Figure 1: Typical failure modes of standard valve plates in high speed compressors

Failure from high valve closing impact speed is another typical failure mode to be found in high speed compressor valves. High closing impact speeds originate typically from improper springing, spring failures or the combination of step pressure rise rates in conjunction with over lubrication. Beside the general material impact resistance, the seat geometry can also lead to preliminary failures. Improperly serviced seat land with sharp edges can initiate cracks in non-metallic valve plates leading to plate breakages starting at the seat lands.

In general the spring plates have a competitive advantage over coil springs in regard to preventing high closing impact speeds.

The non linear springing characteristic of spring plates helps to

separate the sealing element from the guard, even before the gas flow changes direction and builds up a high differential leading to high acceleration.

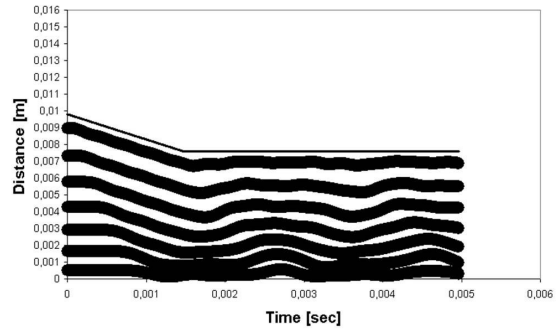


Figure 2: Motion of individual coils over time of a spring during opening event of a valve. Coil contact due to improper design



Figure 3: p-t traces at two different times laid onto each other reveal a sharp pressure rise (grey curve) at the discharge valve opening hinting at oil sticktion [1]

3 New valve concept (CPs)

The new valve concept is based on a fundamental investigation of the field failures, latest simulation know how, and research on the technical possibilities of advanced “designed to application” non-metallic’s.

The starting point was the development work done for HOERBIGER CM [1] valve introduced in 2007. Fundamental research led to a new understanding of valve ring motion, oil sticktion and valve efficiency. At that time the conclusion was that a high performance ring valve with a high number of rings can only work reliably if the ring motion is synchronized (see Fig. 4).

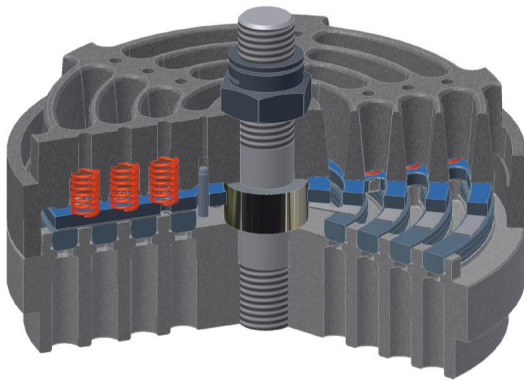


Figure 4: CM valve with synchronizing plate published at 5th EFRC Conference in 2007[1]

The logical extension of a concept of multiple rings with motion synchronization, is to combine the individual rings and synchronizing plate to one moving part.

A narrowly spaced valve plate, with profiled seat lands, is an old dream of every valve engineer looking at the flow deflection in a plate type valve. The main problem why this concept was never applied, is the leakage and wear situation resulting from the thermal behavior of standard non metallic materials.

High precision machining equipment is needed to achieve a good sealing solution. In difference to ring valves, sealing is more difficult due to the connecting webs hindering the ring segments to tilt. In addition, a material is needed with a thermal expansion of steel to keep the tight tolerances.

In the last years considerable progress was made in the area of fiber reinforced non metallic materials [3]. A proprietary material (HOERBIGER HP) was designed specifically for valve applications, initiating a new class of “designed” materials for valve applications, the 3X materials. With the help of tailored materials it is possible to adjust the thermal expansion to certain levels.

The combination of high precision machining and non-metallic’s, having the thermal expansion of steel allowed finally the breakthrough of making a profiled valve plate possible. First test installations with profiled valve plates were done in 2005 in PET compressors with high success [4]. At that time, the high cost material with differential pressure limitations did not allow the application in high pressure installations.

In order to make this technology applicable for high speed market the cost and differential pressure resistance needed to be improved by a new material and production technique.

With this new valve concept not only the efficiency aspect is addressed. Even more emphasis is given on the reliability with respect to the typical failure modes addressed in section 2 above.



Figure 5: New valve concept for high speed compressors CPs. The green cushion plate is fixed on the guard side and does not move

On first glance, the introduction of profiled valve plates and seat lands originates purely from a flow and valve efficiency standpoint – but there is much more behind this choice. The concept will be discussed in respect to the typical load situation occurring in high speed compressors:

3.1 Handling high opening impact speeds

As mentioned above critical opening impact speeds are supported by: high compressor speed, over lubrication, liquids and seat geometry. The allowable levels are defined by the impact resistance of the sealing and springing element.

Springing element:

In the new concept an advanced technology of spring plates is applied: Surface and heat treatment are optimized to provide (in theory) infinite lifetime independent of impact speed. This was achieved by running full 3D FEM calculations of the spring plate (including curvature). As a result, even if the plate is compressed completely no excessive stresses violating the fatigue limit occur.

Furthermore, the use of the cushion plate prevents a steel to steel contact of the moving parts of the spring plate with the guard, thereby eliminating another prominent failure mode of existing valve designs.

Valve plate material:

The valve plate is produced in a new and innovative way using a high impact resistant tailored material (see Fig. 8). All applied measures lead to a much higher impact resistance than PEEK materials.

Seat geometry and oil sticktion:

Profiled seat lands exhibit lower oil sticktion than standard seat lands due to the line contact vs. area contact situation. In case of profiled valve plates another effect is helpful in separating the valve plate from the seat: on the micro scale a profiled valve plate never fits perfectly to the seat. A pressure differential of ~1 to 3 bar is needed to achieve a good sealing. This slight initial “preload” helps to separate the plate from the seat in the initial phase of valve opening and significantly reduces oil sticktion and delayed opening.

Resistance to liquids:

The mechanical strength of the valve plate was optimized to provide superior robustness against extra loads like liquid slugs. This fact in combination with the optimized spring plate (which by its unique design simply cannot be overstressed) leads to a very reliable solution especially in harsh environments.

Efficiency and opening impact:

Another major development goal was to significantly improve the valve efficiency to be able to cope with future requirements. The effective flow area of the CPs valve is typically 30 to 60% larger than standard plate type valves (see Fig. 4, 7).

The effect of valve efficiency on opening impact speed was neglected for a long time. Since advanced simulation models are available, taking the instationary flow in the cylinder into account, it can be seen that the pressure reduction in the initial phase of the valve opening event plays an important role in the calculation of the opening impact speed. Better valve efficiency leads to reduced impact speeds [2].

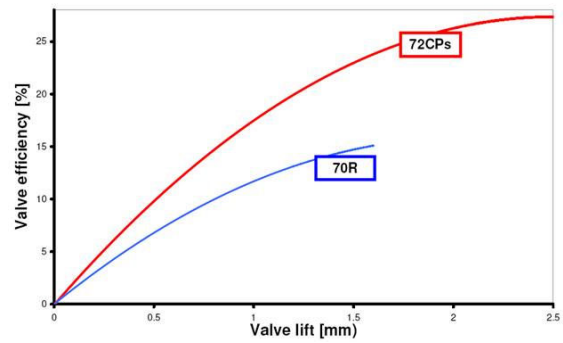


Figure 6: Effective flow area of new valve (CPs) compared to typical plate valve (R-type)

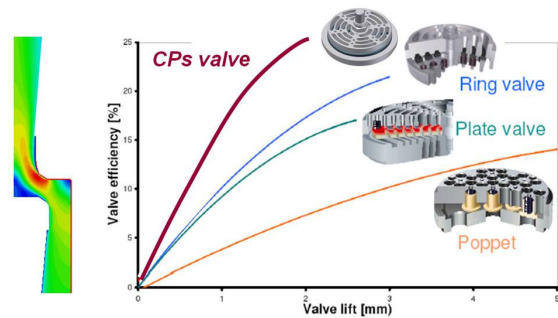


Figure 7: Left: Optimized flow between contoured seat lands and profiled valve plate, Right: Normalized valve efficiency of different valve concepts depending on valve lift. The CPs valve demonstrates the efficiency of a profiled valve plate

3.2 Handling high closing impact speeds

The main design element to reduce high closing impact is the spring plate design. To withstand high impact speeds is a question of seat geometry and valve plate material.

Springing element:

The nonlinear springing characteristic of the spring plate starts the valve closing event before the flow direction changes. This reduces the probability of late valve closure even under high lube rates.

Seat geometry:

The contoured seat land and profiled valve plates not only provide outstanding flow performance, they also have a significant effect on the tolerance to high closing impact speeds. The absence of sharp seat lands (typically leading to local crack initiation) allow up to 2 time higher closing speeds compared to plate type valves.

Valve plate material:

Beside the seat geometry and springing concept the unique, “designed to application” properties of the sealing element material itself provide significantly better reliability against high closing impact speed. Figure 8 shows the runtime of the used new material (HTCX) against standard PEEK GF30 in our valve lifetime tester. The tailored material achieves up to 5 time higher lifetime.

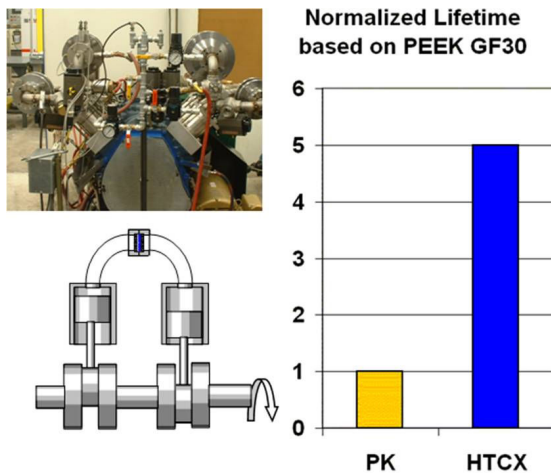


Figure 8: Lifetime tester for accelerated life time testing of valve plate materials. Lifetime comparison between standard PEEK GF30 (HOERBIGER PK) and newly developed material grade HOERBIGER HTCX [3]

3.2 Valve efficiency and differential pressure resistance

Figure 7, 9 and 10 demonstrate the outstanding levels of efficiency achievable with narrowly spaced profiled valve plates. Compared to the first type series (CP) the efficiency level at low lift was further increased with the latest valve version for the small sizes (CPs, “s” stands for small diameters).

In a lift range of 2 mm the valve reaches its maximum flow area, a normalized efficiency of 25% is reached. This means actually, that 25% of the available valve pocket area is used as effective flow area! If highest efficiency is not needed, the lift can be significantly reduced while still retaining a similar flow area as a plate valve (see Figure 6), hence further increasing the lifetime.

Figure 9 shows the p-t measurement of a PET compressor before and after the installation of the new valves. The valve losses went down by 50% in average over all compression stages.

In Figure 10 a p-V diagram simulation of a typical high speed compressor in gas gathering with standard valve equipment (90CT) is shown. In order to achieve sufficient lifetime the valve lift of standard valves needs to be reduced to 1.2 mm. The new valve concept allows the utilization of the full lift potential leading to significantly reduced valve losses (>60%) with increased robustness and reliability.

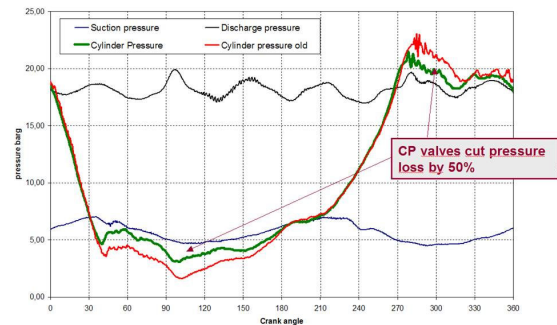


Figure 9: p-t trace of PET compressor, red curve with original plate valves, green with new profiled valve plate valve

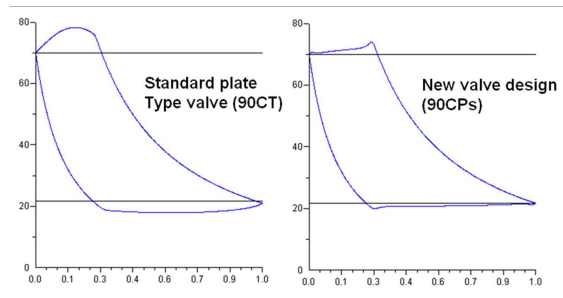


Figure 10: p-V diagram simulation for high speed compressor in gas gathering comparison between standard plate valve and new valve concept (CPs)

High differential pressure resistance is achieved by innovative molding, post heat treatment and finishing processes. The control over the fiber orientation during the injection molding process provides a perfect fiber structure and fatigue strength in critical areas. In addition, a high amount of 3D- fiber reinforcement increases the shear strength of the polymeric material and thereby leads to high differential pressure resistance. Figure 11 shows a CPs valve running with more than 250 bar differential pressure.

4 Field experience

4.1 Selection of field test

The new valve concept has been installed in the field for three years. In the selection of the field installations emphasis was given on critical applications where insufficient valve lifetime or high energy consumption was reported.

Some of the installations in the field were done together with the OEM, others were installed by the end user himself.

In more than 40 different and demanding installations over 1000 valves are running successfully. The applications cover natural gas (gathering and storage), nitrogen, air reinjection, high pressure ethylene (see Fig. 11), CNG, CO₂+H₂S,... In some of the installations the lifetime of the standard valve in use before was lower than 10 days.

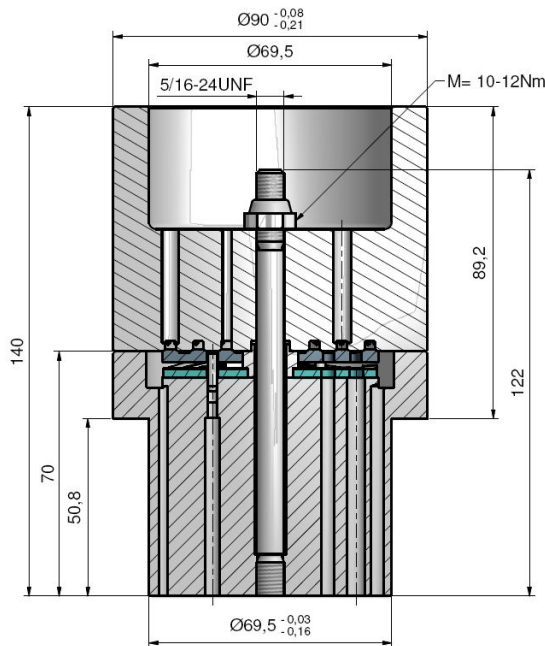


Figure 11: High pressure CPs valve for ethylene. Running since 2009

4.2 Valve inspection during field test

Almost all of the installed valves are working in critical installations. Beside a small problem with the first prototype, valves in one installation all of the valves are working successfully – making it difficult to inspect the running valves because the user is so satisfied he wants to keep them going.

Figure 12 shows pictures of a valve inspection after 5000 hours of operation in a demanding gas gathering installation in Canada. All the parts are in perfect condition. No indications of wear on seat, guards and valve plates. The high amount of lubrication can be seen on the valve parts. High oil sticktion can be assumed. Valves were reinstalled after inspection and will stay in operation until 16000 hours are reached.



Figure 12: Valve inspection of a 90CPs valve after 5000 hours of operation in demanding gas gathering installation in Canada

5 Summary and Outlook

The trend towards higher compressor speeds is still ongoing. Higher compressor speed means better equipment utilization, higher throughput, lower footprint, flexible installation and altogether lower investment cost.

Natural gas is becoming more and more important in safeguarding the energy hunger of the world.

The increasing production of gas from so called unconventional gas resources, further boost the demand for more compression equipment in the gas fields. Especially the latest boom in shale gas and coal bed methane causes increased market need for small size high speed compressors.

In many cases operators are not satisfied with the valve reliability and efficiency of today's standard valve equipment. In order get better reliability, which is especially important in remote locations, the valve efficiency is often sacrificed by valve lift reduction leading to high energy consumption.

It is not only the high compressor speed causing challenges for the valve designer. It is the combination of high speed and the typical way of operation with over lubrication and the extra loads inherent with the application itself - like frequent liquid slugs. A new valve concept needs to be judged in respect to it handles the complex load spectrum. A new valve design was presented based on the latest know how in valve design and material science. The main feature is a narrow spaced profiled valve plate, providing outstanding flow performance and allowing significantly higher impact speeds. The critical valve springing situation is solved by using a new designed spring plate technology in combination with a non metallic cushion plate which damps the impact on the valve guard. The profiled valve plate is produced in a unique process in order to ensure highest impact resistance and a thermal expansion of steel. The used material was tailored for the application and provides multiple impact resistance compared to today standard valve materials.

The valve is running successfully in field test since three years. In the selection of field tests emphasis was given on critical and demanding applications where standard valve reach their physical limits. In all cases the valve lifetime problems could be solved. The inspection of the running valves revealed no indications of wear on seat, guards or sealing elements.

The fundamental research in materials, flow, oil sticktion and latest spring technology has transferred into a very innovative new product (HOERBIGER CPs valve). The new product will significantly increase the reliability levels of high speed compressors in all markets. The concept provides further potential for the next step in compressor speed without compromising the overall compressor efficiency.

Due to the impressive performance of the valve concept we are encouraged to extend the underlying design principles to large diameters and concentric valves. In addition, the high efficiency of the valve

concept allows the change of design guidelines for compressor cylinders and opens the door for new innovative compressor concepts.

References

- [1] B. Spiegl, G. Machu, P. Steinrueck: The role of improved valve technology in the utilization of natural gas resources, *5th EFRC Conference (Prague, 2007)*
- [2] G. Machu: Pulsationen im Verdichtungsraum – eine potentielle Schadensursache?, *Industriepumpen + Kompressoren 2 (2005)*, pp. 70 - 73
- [3] B. Spiegl, T. Kriechbaum, P. Steinrueck: Material Design for Valve Applications, *6th EFRC Conference (Duesseldorf, 2008)*
- [4] B. Spiegl, G. Machu, P. Steinrueck: New Technologies for Efficiency Improvements in PET Air Compressors, *6th EFRC Conference (Duesseldorf, 2008)*



The BCD packing ring – a new high performance design

by:

Dr. Tino Lindner-Silwester, Christian Hold

Research & Development

HOERBIGER Ventilwerke GmbH & Co KG

Vienna

Austria

tino.lindner-silwester@hoerbiger.com

**7th Conference of the EFRC
October 21th / 22th, 2010, Florence**

Abstract

As a result of a series of research activities with respect to the fundamental working principles of rings and packings, the authors have developed a new high performance packing ring design, the BCD packing ring. The BCD ring is characterized by both a high sealing efficiency and a low wear rate. In the development of this ring design, clarifying the thermophysical processes in a pressure packing, gaining an understanding of the wear pattern of a packing ring, and elucidating the factors governing the sealing efficiency of a packing ring have played key roles and have enabled the design of this largely improved, rather unconventional design. Tests on the in-house test compressor and numerous field tests have consistently proven the high potential of the new BCD packing ring.

1 Introduction

The piston rod sealing system is one of the key factors when it comes to the reliable and efficient operation of a reciprocating compressor. This is especially true of compressors running in non-lubricated mode where great demands are made on the pressure packing. In absence of any lubricating oil much more frictional heat is released in the surfaces of contact between the packing rings and the piston rod. Depending on the resulting operating temperature of the packing, unfavourable tribological conditions may occur. As a consequence, the wear rate of the rings, already considerably higher than in lubricated operation, can reach values where an economic operation of the compressor is no longer achievable.

The requirement to be met by a packing ring design is to provide a high sealing efficiency under a variety of operating conditions over sufficiently long periods of time. In order to create a new ring design that provides significant advantages over currently available ones, a thorough analysis of the root causes of the application limits of today's solutions is required. In the present case, this analysis has been based upon several fundamental investigations into all fields identified to be related to the performance of packing rings as well as on comprehensive field experience.

2 Fundamental investigations

Packing rings are “self-energizing seals” which means that their seal effect arises from the differential gas pressure to be sealed. This differential pressure forces the side face and the counterface of the ring against the housing and the rod, respectively. An important quantity is the contact force $F^{(unbalanced)}$ per unit length in circumferential direction with which the ring gets pressed against the rod. This force is proportional to the differential pressure (the garter spring loading is usually negligible) and is determined by the gas pressure distribution in the counter face and the relationship between the pressure $p_{outer}=p_1$ acting on the outer diameter and the mean pressure p_{inner} on the inner diameter required for mechanical equilibrium (cf. Fig. 1). The latter relationship is a characteristic of the ring design, Fig. 1 shows a configuration for which $p_{inner}=p_{outer}$.

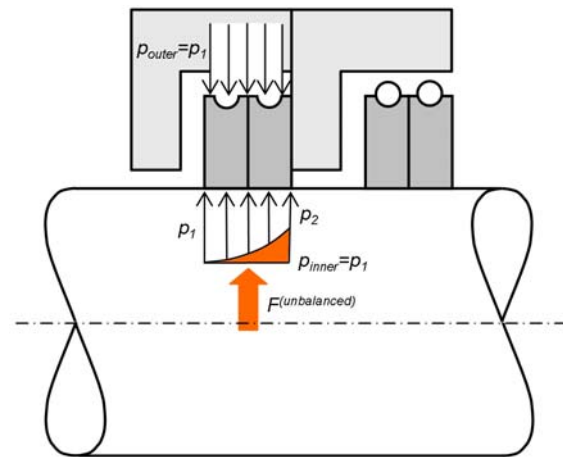


Fig.1: Self-energizing seal effect: pressure differential p_1-p_2 across ring pair gives rise to contact force $F^{(unbalanced)}$ between rod and ring pair.

An adequate sealing efficiency, i.e. a sufficiently low blow-by leakage across the ring, requires a certain minimum contact force $F^{(unbalanced)}$. Hence, packing rings are inevitably subject to some wear, and both a low wear rate and the ability of a packing ring to maintain a high sealing efficiency even when wearing away are of great importance for a pressure packing to operate reliably and efficiently. Especially in non-lubricated applications, the wear rate may become so high that the lifetime of the packing goes down to unacceptably low values. Such excessive wear rates may, on the one hand, be a direct consequence of poor tribological conditions. On the other hand, the frictional heat generated in the surfaces of contact between the packing rings and the piston rod may, depending on the amount of heat released and the efficiency with which it is removed, give rise to high counterface temperature levels. With the characteristic of many packing ring materials to show a pronounced increase in the wear rate with temperature it becomes of importance to stay below certain temperature limits during operation of the packing rings. Since both the rate at which a packing ring wears away as well as the amount of frictional heat released are proportional to the contact force $F^{(unbalanced)}$, knowledge of the counterface gas pressure distribution is of great importance for the design of a new ring to find an optimum balance between sealing efficiency and lifetime.

2.1 Counterface gas pressure

The formation of a gas pressure distribution in the ring's counterface is related to the (microscopic) roughness asperities of the surfaces in contact.

Contact spots are interspersed with gaps through which gas can leak under the action of a pressure-gradient.

On the (macroscopic) length scale of the packing ring, the gas pressure distribution is governed by the thin-film limit of the compressible Navier-Stokes equations¹.

Fig. 2 shows the counterface gas pressure distribution of a radial/tangential cut ring pair. The gas pressure is broken down from the higher value p_1 , acting upstream the radial cut ring, to the lower value p_2 , acting downstream the tangential cut ring. Isobars show how the gas pressure distribution is affected by the wear compensation gaps.

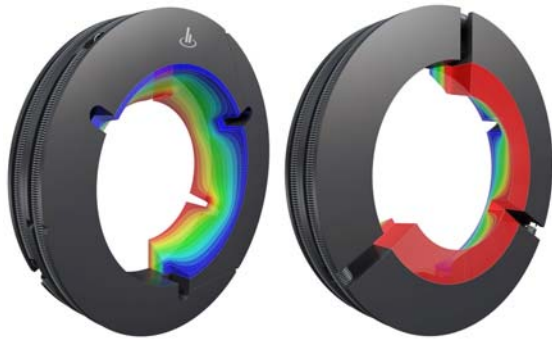


Figure 2: Gas pressure distribution in counterface of radial/tangential cut ring pair.

2.2 Ring wear pattern

2.2.1 Introductory remarks

It is well-known that packing rings and cylinder rings usually wear away in a non-uniform way along their circumference (Fig. 3). The significance



Fig. 3: Non-uniform wear pattern of a cylinder ring pair

of understanding how such a wear pattern evolves stems from the close relation between wear and sealing efficiency. It is found empirically that the rate at which non-lubricated polymer rings wear away is proportional to the load applied (to be precise: to the contact pressure p_c arising from the

applied load) as well as to the relative speed v between the sliding contact partners.

Test rig results show that this relationship is to a good approximation a linear one

$$\frac{dw}{dt} = K p_c v \quad (1)$$

as long as the load and the temperature stay within reasonable limits. Herein, w denotes the wear and K [m^2/N] is called the wear factor. Note that the wear-factor is not a true property of the material but depends on many additional factors (gas environment, counterface material and finish, ...).

To predict how a packing ring wears away under a certain “ p_v ” load it is necessary to take the counterface gas pressure distribution as well as elastic effects into account. For the subsequent analysis, a rod of diameter $d=2R$ in contact with a radially cut ring segment (segment angle α) of constant radial height h are considered (Fig. 4). Emphasis is laid upon variations of the wear in circumferential direction φ rather than axial direction. Hence, all pressures (contact pressure, gas pressure) are averages along the axial direction in the subsequent analysis.

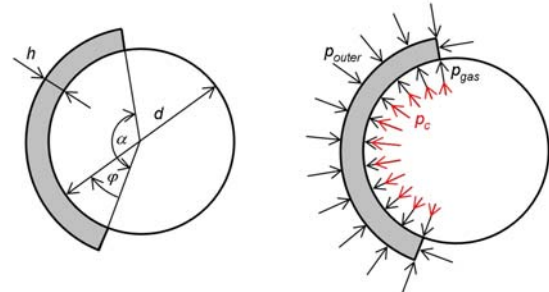


Figure 4: Left: geometrical parameters characterizing ring segment. Right: stresses acting on ring segment

In the initial and undeformed state the counterface of the ring segment shall have a constant curvature equal to that of the rod. It is evident that the inner pressure p_{inner} , where $p_{inner}=p_{gas}+p_c$, is equal to the pressure loading p_{outer} acting on the outer segment diameter in this initial state (Fig. 4). If the ring segment were part of a radial cut ring in a radial/tangential ring pair configuration, the (axially averaged) counterface gas pressure p_{gas} would vary along the circumference according to Fig. 2, being lowest where the wear compensation gaps of the tangential cut ring are located. Such gas pressure variations cause corresponding variations in p_c and the wear rate. With the ring wearing away in a non-uniform manner, the counterface curvature will no longer stay uniform and the segment will no longer conform to the rod in the undeformed state.

Due to the bending stiffness of the segment, p_{inner} will then no longer be constant nor equal to p_{outer} which will lead to further changes in how the contact pressure p_c varies along the counterface. The whole evolution of this ongoing process leads to the final wear pattern.

2.2.2 Mathematical model

In order to express the described evolution of the wear pattern in mathematical form, a relationship between the ring loading, the radial ring displacement u required for maintaining contact between the rod and the ring when material is worn away, and the contact pressure p_c has to be established. For the sake of simplicity, a ring segment of constant cross-sectional area is considered in what follows. In addition, the ring wear w is assumed to be so small compared to the radial ring height h that, to a first approximation, both the cross sectional area A and the cross-sectional moment of inertia J do neither vary appreciably with time (as a result of the wear) nor in peripheral direction (as a result of the non-uniformness of the wear). Furthermore, the rod diameter d is assumed to be large compared with the radial ring height h . Under these assumptions, the well-known relations for the deformation of a slightly-curved beam can be used². For a configuration as sketched in Fig. 4, the following relationship between radial ring displacement u (positive when pointing radially outward) and pressure loading can be derived

$$\frac{\partial^4 u}{\partial \varphi^4} + 2 \frac{\partial^2 u}{\partial \varphi^2} + u = \frac{R^4 B}{EJ} (p_{inner} - p_{outer}) \quad (2)$$

where φ , E , and B denote, respectively, the peripheral angle, the elastic ring modulus, and the axial ring thickness. Thermal expansion effects can be easily incorporated into the analysis by adding the term

$$R\alpha(\Delta T - R\theta)$$

to the right-hand side of (2) where α , ΔT , and θ denote the coefficient of thermal expansion, the difference between the actual and a reference temperature, and the temperature moment

$$\frac{1}{J} \int_A T z \, dA$$

of the ring, respectively. By inserting (1) into (2), making use of the contact condition $w = -u$, and noting that $p_{inner} = p_{gas} + p_c$ one arrives at the partial differential equation

$$\frac{\partial^4 u}{\partial \varphi^4} + 2 \frac{\partial^2 u}{\partial \varphi^2} + u = \frac{R^4 B}{EJ} \left(-\frac{1}{Kv} \frac{\partial u}{\partial t} + p_{gas} - p_{outer} \right) \quad (3)$$

that describes how the wear pattern $w = -u(\varphi, t)$ evolves with time. Herein, v is the mean rod speed. Noting that the bending moment and the shear force vanish at both free ends of the ring segment gives the boundary conditions

$$\varphi = 0, \alpha : \frac{\partial^2 u}{\partial \varphi^2} + u = -\frac{p_{outer} R}{E}, \quad \frac{\partial^3 u}{\partial \varphi^3} + \frac{\partial u}{\partial \varphi} = 0 \quad (4)$$

In Fig. 5, a numerical solution of equation (3) subject to the boundary conditions (4) is compared with a measured wear pattern. As can be seen, there is very good agreement which shows that the principal mechanisms governing the wear pattern formation are correctly modelled. For more complicated configurations, e.g. configurations where the cross sectional area noticeably changes in peripheral direction, this whole procedure requires the successive use of FEM methods.

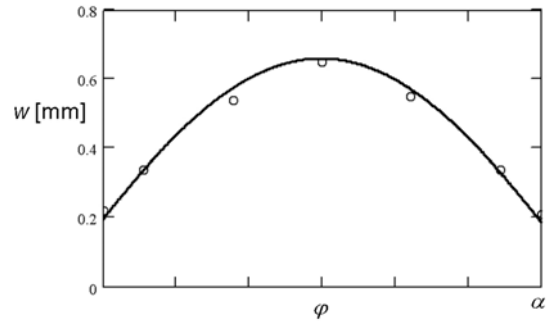


Fig. 5: Comparison of calculated variation of wear w along circumference (solid line) with measured one (circles)

2.3 Rod temperature distribution

The key ingredients for determining how much frictional heat is released during operation of the pressure packing are the counterface gas pressure distribution and the coefficient of sliding friction. However, since the crucial piece of information governing the packing performance is the temperature level the rod heats up to, it is important to know not only how much heat gets released but also how efficiently this heat is transferred away.

The latter involves, amongst others, such processes as heat conduction along the rod, convective heat transfer to the gas surrounding the rod, transfer of heat through the packing rings etc. A detailed description of a model that takes all these effects into account can be found elsewhere¹.

2.4 Further experimental investigations

2.4.1 Frictional force measurements

A test rig (Fig. 6) has been constructed for frictional force measurements of packing as well as cylinder rings.



Fig. 6: Test rig for performing measurements of the frictional forces acting in the counterfaces of packing and cylinder rings

This test rig has been designed such that it can be converted from a configuration where a piston rod oscillates against a stationary packing case to a configuration where a liner reciprocates with the piston stationary. Fig. 7 illustrates that very good agreement has been found between measured and calculated values of the frictional force.

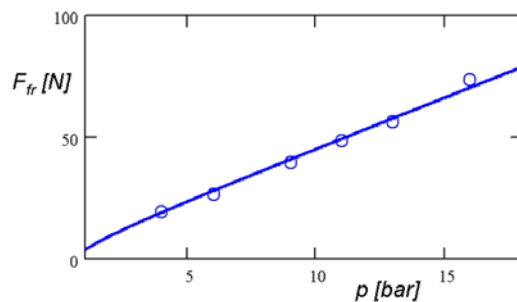


Fig. 7: Dependence of frictional force F_{fr} on gas pressure p to be sealed against ambient pressure (circles measurements, solid line calculation)

2.4.2 Static leakage tester

To achieve a high ring sealing efficiency, attention has to be paid to all cuts and gaps through which gas can leak. It is crucial to maintain a high level of sealing efficiency when the ring wears away.

Whereas the effect of the wear on the ring leakage can only be determined on a real-world compressor

in operation, valuable insights can nonetheless be gained by taking leakage measurements on simpler configurations. Such tests have been performed on an easy-to-handle static leakage tester (Fig. 8). This tester resembles a packing consisting of only one container with the rod 1 stationary. Air is fed with a certain pressure level p into the container and the leakage through all gaps formed by the ring 2, the rod 1, and the container is measured.

As already mentioned, it is crucial to find a balance between high sealing efficiency and low ring wear. Whereas the former typically involves high contact pressures, the latter requires low contact pressures between the ring and the rod. The significance of the study of what is happening in the counterface arises from these two opposing requirements.

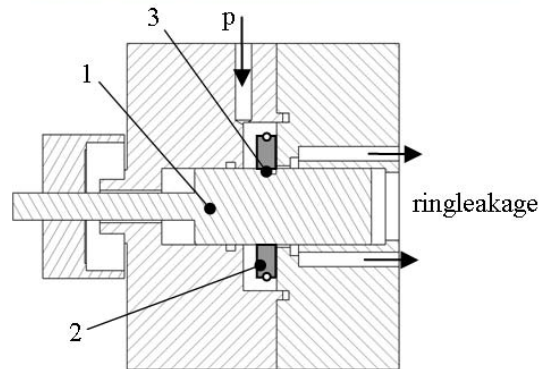


Fig. 8: Photograph (upper part) and sketch (lower part) of static leakage tester

A small capacitive distance sensor 3, carefully embedded into the surface of the rod, allows for such a study in an experimental manner. The underlying measuring principle is based upon the fact that real surfaces always have a certain roughness so that only the asperities touch each other when two surfaces come into contact. The deformation of these contact asperities is due to the applied load which gives rise to a relationship between the load and the mean surface separation.

Keeping the applied load fixed and having the gaps the contact spots are interspersed with filled with gas, the mean surface separation will increase with increasing gas pressure and decrease when the gas pressure is lowered. Hence, local small-scale length measurements as performed by the capacitive distance sensor provide insight into the contact pressure distribution.

2.4.3 In-house test compressor

Piston and packing rings can be tested on a two-stage in-house test compressor under very challenging conditions (final pressure level up to 400bar, speed up to 1500rpm, stroke 88.9mm, no lubrication). This test compressor is fully instrumented (measurement of cylinder and packing cup pressures, packing leakage, rod temperature distribution, humidity of gas, capacity of compressor, rod runout, ...) which provides a detailed insight into the processes going on in the pressure packing during operation.¹ By performing benchmark tests, the potential of new rings and packings solutions can quickly be assessed.

3 New BCD packing ring design

3.1 Description

All the findings stemming from the fundamental investigations have been incorporated into the design of the new, patented BCD (balanced cap design) packing ring. The BCD ring is comprised of four segments (Fig. 9). On the high-pressure-facing side of the ring (left-hand side of Fig. 9), four radial gaps are formed by these segments that make the ring single-acting. On the low-pressure-facing side of the ring, two wear-compensating gaps are formed between the two main segments 1. These gaps are sealed by the cap segments 2 in axial and radial direction.

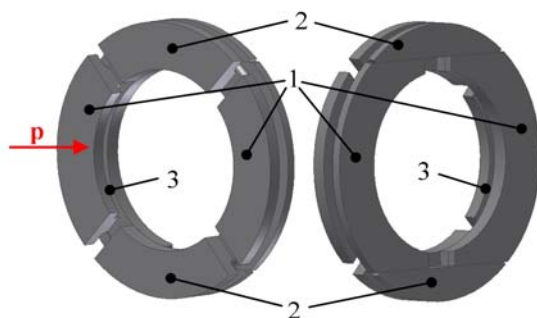


Fig. 9: BCD packing ring

Thus, the ring is gastight without the necessity of having an additional ring in front to cover any gaps.

Chamfers on the circumferential ends of the segments 1 ensure a high sealing efficiency of the cap segments 2 by avoiding any undesirable pressure build-up in the wear-compensating gaps. The style of this ring provokes a controlled wear pattern where the two main sealing segments 1 wear away in a symmetric manner. In contrast to radial/tangential cut ring pairs where asymmetric wear may cause the tangential cuts to lose contact with each other, a high sealing efficiency is maintained in the cuts of the BCD (Fig. 10). Pressure-balancing grooves 3 in the segments 1 reduce the wear rate as well as the frictional heat generation without impairing the high sealing efficiency.

Summing up, the BCD is characterized by the following features:

- Maintenance of high sealing efficiency over lifetime
- High lifetime due to low wear rate and optimum utilization of ring material
- Low generation of frictional heat due to pressure-balancing and small axial ring width
- Robust one-ring design that consumes less space and therefore, allows for shorter packing cases



Fig. 10: Back views of virgin BCD ring (left-hand), worn BCD ring (middle), and worn tangential cut ring

3.2 Test results

Before being released into the market, each HOERBIGER product has to prove its potential in a well-defined minimum number of field tests.

3.2.1 In-house test compressor

During the very first test runs on the in-house test compressor, the high potential of the BCD packing ring design became apparent. The in-depth view into what is going on in the packing during operation, enabled by the instrumentation of the in-house test compressor, did not only reveal that BCD rings run significantly cooler than radial/tangential rings but also that their operation is more stable, at least as far as temporal variations of the packing leakage rate are concerned.

Fig. 11 shows that the leakage rate of the packing, when equipped with BCD rings, did barely vary with time. In contrast, the leakage of radial/tangential rings showed considerable variations, being sometimes as low as the leakage of BCD rings, sometimes almost ten times higher. The continuous recording of all data during each test showed that these increases of the leakage rate coincided with changes in the cup pressure distribution, i.e. changes in how the total differential pressure is broken down by the individual rings in the packing. Such behaviour was not observed for the BCD.

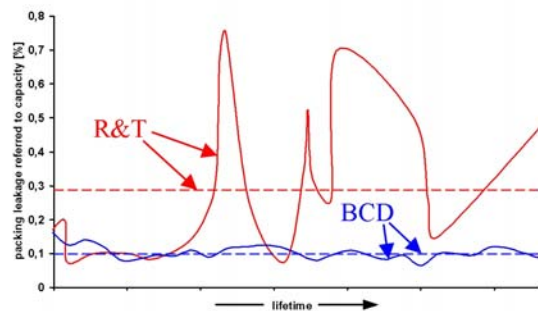


Fig. 11: Comparison of packing leakage rates (BCD vs. radial/tangential ring pair) measured on in-house test compressor. Dotted lines represent mean values of temporal leakage rate variations (solid lines)

3.2.2 CHP service

Gas turbines operated at cogeneration plants (combined heat power, CHP) have to be fed with natural gas at pressures up to 50bar. In cases where those plants are only served by low-pressure gas mains, the natural gas is often pressurized by reciprocating compressors. These compressors have to cope with frequent load changes and stops. In order to prevent damages to the gas turbines, the compressed gas has to be clean and oil-free. Therefore, many reciprocating compressors in gas turbine services operate in non-lubricated mode to avoid expensive removal of oil from the compressed gas. With no oil to lubricate while frequently running off-load to accommodate load changes, natural gas compression for CHP is a challenging duty for rings and packings, characterized by high operating temperatures and high ring wear rates.

According to the Operations Coordinator of the port of Liverpool E.ON UK CHP plant, there were problems with the compressors from day one when this CHP plant started up in 2004. One of the problems was excessive packing leakage with run times of the packing rings as low as 300 hours.

Gas was wasted and could be smelled everywhere which worried the neighbours of the plant. All of the packing problems were finally solved in May 2008 by equipping the packings of the two compressors with BCD rings. Since then, the BCD rings have been running (runtime at the end of December 2009: compressor one 5500 hours, compressor two 1600 hours) with no problems and no measurable leakage so far.

More CHP gas turbine boosters have been equipped with BCD rings in the meantime with the consistent result of substantially improving both the lifetime and the sealing efficiency.

3.2.3 PET service

High pressure air compressors for PET bottle blowing fall into another class of non-lubricated machines where required performance levels are often not reached. The high pressure stages are characterized by high temperatures which, together with the highly oxidising gas atmosphere, can lead to excessive ring wear rates. BCD rings were also installed on a typical representative of this class of machines (4th stage, mean rod speed 4.0m/s, $p_s=14\text{bar}$, $p_d=42\text{bar}$). Off-load operation over extended periods of time gives rise to very high packing temperatures on this compressor. As a result, the desired service interval of one year could not be maintained in the past due to packing problems. With the BCD, no leakage could be heard by the operator of the compressor any more. Inspection of the rings during the scheduled compressor service in March 2010 showed that they were still in a relatively good condition after overall operating hours of 5600 hours.

3.2.4 Process gas

The BCD is also running in a number of process gas applications. Customer feedback is very positive so far.

4 Conclusions

Operators of reciprocating compressors demand better performance from the piston rod sealing system, the main room for improvement being seen in the areas of lifetime, reliability, and emissions. A sound analysis of the thermomechanical processes governing the packing ring operation has paved the way for the development of the new BCD packing ring. Several field tests have repeatedly and consistently shown that the BCD ring design enables a boost in performance, reliability, and efficiency, offering lower wear and therefore higher lifetime as well as lower leakage rates.

References

¹ Lindner-Silwester, T.: “Advances in fundamental understanding of the dynamic sealing action in packing systems”. 5th EFRC conference (2007), 75-82

² Parkus, H.: “Mechanik der festen Körper”. Springer Verlag (1966)



Educating reciprocating compressor engineers at the EFRC

by:

Dr-Ing. Siegmund V. Cierniak
RWE Rheinland Westfalen Netz AG
Essen
Germany
Siegmund.Cierniak@RWE.com

Chairman of the EFRC Educating Committee

7th Conference of the EFRC
October 21th / 22th, 2010, Florence

1 Why educate reciprocating compressor engineers?

The design, selection, operation and maintenance of reciprocating compressors makes the education and training of different types of engineers a must. Due to these facts all compressor manufacturers, packagers and end users have a need for highly qualified, educated and skilled engineers. Our branch need now and in the future, well educated and highly motivated graduates from the best universities and colleges.

The EUROPEAN FORUM for RECIPROCATING COMPRESSORS - EFRC is creating co-operation between the members of EFRC, other compressor makers, packagers, subsuppliers users and the well known universities, colleges, institutes and their students.

2 Some examples of these co-operative efforts:

- common supported thesises
- presentations – made by people from companies at the universities
- excursions to workshops and facilities in our branch
- practical work of students in firms
- information about jobs for graduates
- sponsoring of first class results of student's (thesis', etc.)
- realisation of workshops as platform for recent students and graduates
- publication of studies, theses, research work

3 What EFRC members are already doing:

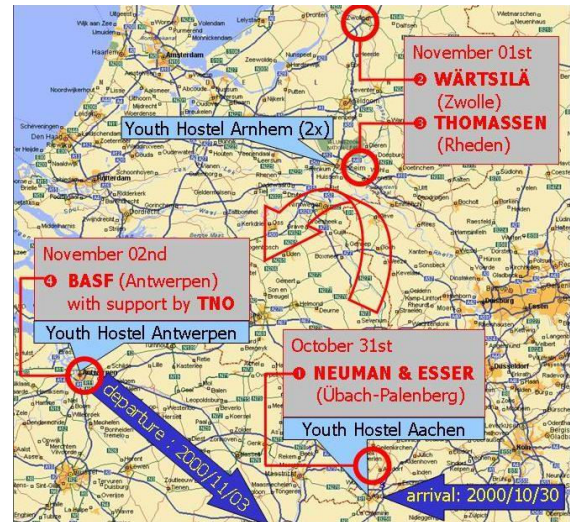
- participating in EFRC promotion committee
- hosting of excursions
- organizing of internships
- sponsoring of events
- subsidizing highly qualified students and graduates

4 Advantages for EFRC members:

- access to qualified engineers
- influence on the education of students
- part time jobs of students

5 Important results of the EFRC activity „Educating reciprocating compressor engineers”

5.1 Autumn 2000: EFRC Workshop “The Netherlands and Belgium”



Picture 1: Students' excursion 2000

Tour on the facilities of -

- NEUMAN & ESSER GmbH, Übach-Palenberg / Germany
- WÄRTSILÄ Nederland B.V., Zwolle / The Netherlands
- THOMASSEN Intern. B.V., Rheden / The Netherlands
- BASF AG, Antwerp / Belgium
- TNO Inst. of Applied Physics, Delft / The Netherlands



Picture 2: BASF AG, Antwerp/Belgium

5.2 Spring 2002: EFRC Workshop “Northern Germany”

- Natural Gas Underground Storage Kraak (near Schwerin / Germany)
“HEINGAS Hamburger Gaswerke GmbH” / compressors “ARIEL / HGC”
- Natural Gas Underground Storage Hamburg-Reitbrook
“HEINGAS Hamburger Gaswerke GmbH” / compressors “ARIEL / HGC”



Picture 3: Workshop participants at the Natural Gas Underground Storage Kraak Germany

Workshop’s tasks

A computerized simulation program „Reciprocating Compressors in Natural Gas Underground Storages“ > “Selection and sizing”



Picture 4: Tour on the facilities of the Tarnow site Poland

5.3 Spring 2004: EFRC Workshop “Poland”

Beginning of June 2004 the EFRC organized an event which was once again very successful.



Picture 5: Students in front of the lab of the Wroclaw University/Poland

App. 30 students from Austria, Czechia, Germany, Poland and the Netherlands travelled to Poland and visited the universities of Wroclaw and Krakow and its laboratories and also the compressor plants at the natural gas pipeline station of Tarnow and at the natural gas gathering station of Zanok. The participants had a very interesting training course reg. reciprocating compressor technology.



Picture 6: The group of students in front of the Krakow University/Poland

Workshop’s tasks

Diagnostics of leaking valves in reciprocating compressors.

5.4 Spring 2006: EFRC Workshop “Switzerland and Italy”

One of the statutory tasks of EFRC is to educate young people to the design operation and management of reciprocating compressors.

In June 2006 EFRC the 4th workshop for students in reciprocating compressors sciences happened. We had a trip to some famous plants.

- Burckhardt Compression AG, Winterthur / Switzerland
- Polymeri Europa S.p.A., Ferrara / Italy
- General Electrics Oil and Gas Nuovo Pignone S.p.A., Firenze / Italy



Picture 7: Tour on the facilities of Burckhardt Compression AG Winterthur/Switzerland



Picture 8: Training of the students in the premises of General Electrics Oil and Gas Nuovo Pignone S.p.A. , Florence / Italy



Picture 9: The group of students in the premises of General Electrics Oil and Gas Nuovo Pignone S.p.A. in Florence/Italy

5.5 Spring 2008: EFRC Workshop “Vienna / Austria”

In May 2008 EFRC arranged the 5th Students’ workshop, this time in Vienna / Austria.



Picture 10: The group of students in the premises of Leobersdorfer Maschinenfabrik AG Leobersdorf/Austria

The group of students guided by Dr. Siegmund Cierniak / RWE and Andre Eijk / TNO visited the following companies:

- LMF Leobersdorfer Maschinenfabrik AG Leobersdorf / Austria
- Hoerbiger Ventilwerke GmbH & Co KG Vienna / Austria
- BOREALIS Polyolefine GmbH Schwechat / Austria
- OMV Raffinerie AG Schwechat / Austria



Picture 11: The OMV-refinery in Schwechat/Austria

At the end of the workshop the 25 students from seven different nations (Germany, Switzerland, India, Austria, Poland, England, The Netherlands) were assigned with a theoretical task to develop in the following four weeks with the understanding that the three best homeworks would be compensated with a prize.



Picture 12: The group of students, listening to a presentation in the premises of HOERBIGER Ventilwerke, Vienna / Austria

5.6 Spring 2010: EFRC Workshop “United Kingdom”

During the time between May 25 and May 28, 2010 a group of approximately 25 students came over to England and participated in the 6th EFRC Students’ workshop.

Due to the fact that all former workshops had been so successful everything went according the well experienced procedures:

- Tour of facilities
- Presentations
- Tasks (home work)



Picture 13: The route of EFRC’s Students’ Workshop 2010 in the United Kingdom



Picture 14: Down-town Chester – the home of COOK-Compression



Picture 15: Students at LNG-facilities in Isle of Grain



Picture 16: Isle of Grain (LNG – Terminal)

Students from Poland, Turkey, Austria, Germany, Greece, Holland and England participated in the workshop and visited the LNG-plant Isle of Grain (Burckhardt-compressors), Dresser-Rand, COOK Compression and the Shell-refinery in Stanlow.

The goal for the attending students was – as all the times - to present a report (home work) to a committee of EFRC members and getting an award and once again very attractive prizes for the three best students.

- | | |
|-----------------------|---|
| 1 st prize | A free of charge compressor training course at Ariel's in Mount Vernon /Ohio/USA
+
a free of charge participating at 2010's EFRC conference in Florence / Italy |
| 2 nd prize | 500,00 € cash
+
a free of charge participating at 2010's EFRC conference in Florence / Italy |
| 3 rd prize | a free of charge participating at 2010's EFRC conference in Florence / Italy |

Evaluations of the individual works were made by EFRC members from RWTH Rheinisch Westfälische Technische Hochschule, Aachen / Germany and RWE, Essen / Germany.

6 Next EFRC Workshop 2012

- Spring 2012 in France or Spain
- Details will be published in Fall 2011

7 Prize winners 2010

1st prize

Markus Schwab



e-mail:

markus.schwab@rwth-aachen.de

RWTH Aachen

Aachen
GERMANY

2nd prize

Patrick Tetenborg



e-mail:

patrick.tetenborg@gmx.de

Berufsakademie Emsland

Lingen
GERMANY

3rd prize

Christiane Hammer



e-mail:

christiane.hammer@tu-dresden.de

Technische Universität Dresden

Dresden
GERMANY



Design Challenges for Reciprocating Compressors in Specialty Gas Services

by:

Kelly Eberle and Michael Cyca

Engineering Design

Beta Machinery Analysis

Calgary, AB

Canada

keberle@betamachinery.com mcyca@betamachinery.com

**7th Conference of the EFRC
October 21th / 22th, 2010, Florence**

Abstract

Many software tools are used to simulate compressor performance and pressure pulsations in piping systems. Designers of reciprocating equipment rely on these tools to accurately simulate gas properties and pressure pulsations for specialty gases. Two case studies on reciprocating compressors, involving ethane and ethylene, outline the root causes and consequences of inaccurate performance and pulsation predictions. Both systems experienced many problems after commissioning. Field analysis and subsequent simulation found inaccuracies in compressor performance modeling.

This paper outlines a number of design tips and “lessons learned” that will be helpful to engineers involved in all reciprocating compressor applications.

1 Introduction

Computer models are used to simulate many different aspects of the operation of reciprocating compressors. Typical applications of computer models include simulating the compressor performance, torsional and lateral responses, deflection and stress in the skid beams due to lifting, dynamic response of the compressor cylinders, bottles, piping and thermal expansion of the piping. Modeling of the compressor systems requires representing the physical properties of the compressor, vessels, piping and gas. The physical properties of the compressor, vessels, and piping are well defined. The physical properties of the gas are determined by testing and thermodynamic theory. Many different mathematical models exist for calculating gas properties. Each of these models has various strengths and weaknesses in terms of the accuracy with which they represent the gas physical properties. Mathematical models have been developed, which are well known and have been proven to accurately simulate common gases such as natural gas in pipeline applications. Compressors operating in a refinery or manufacturing facility are often used in applications where the gases are unique and simulation of the physical properties is not well understood. These specialty gases require proper selection of the model techniques to ensure that the results from the simulations result in a safe and reliable design.

Case studies will be presented to show the impact of incorrect modeling of gas properties. In the first case study, compressor performance simulation of an ethane service by many programs produce erroneous results. The second case study shows how inaccurate simulation of pressure pulsations leads to excessive vibrations on the compressor. Before discussing these case studies in detail, some background on compressor performance modeling, calculating gas properties and pressure pulsation analysis in these applications is necessary.

2 Background

2.1 Compressor Performance Simulation and Equations of State

Simulating or modeling the performance of a reciprocating compressor involves calculating the expected flow, power consumption, discharge temperature, etc., based on the compressor geometry and operating information.

The operating information typically includes inlet pressure, discharge pressure, inlet temperature, and gas composition.

The gas composition and operating data is used to calculate thermodynamic properties of the gas; these properties are then used in the performance calculation. For example the adiabatic discharge temperature for the gas that is being compressed, T_D , can be calculated from the following equation.

$$T_D = T_S \cdot R^{\left(\frac{k-1}{k}\right)}$$

where

T_S = suction temperature (absolute)

R = compression ratio (absolute discharge pressure divided by absolute suction pressure)

k = ratio of specific heats

The ratio of specific heats is a physical, or thermodynamic characteristic, of the gas. There is no theoretical means of calculating characteristics such as the ratio of specific heats for gases. Typically, experimentation is done to determine these properties at a few temperatures and pressures and then models or equations of state (EoS) are derived. These equations of state can then be used to calculate the thermodynamic properties of gases for a range of pressures and temperatures. Many EoS have been developed, such as Van der Waals, Redlich-Kwong, Peng Robinson, Berthelot and Dieterici to name a few. All EoS have pressure and temperature ranges and gas mixtures where they are more accurate than others, so care must be taken to properly select the appropriate equation for the particular application.

Another factor that is important in the calculation of the gas properties is determining where the particular operating point is relative to the "critical point." The critical point, also called a critical state, specifies the conditions (temperature and pressure) at which a phase boundary ceases to exist. It is extremely difficult to obtain the fluid properties at, or around, the critical point experimentally, or from EoS models. The other region where an EoS is inaccurate is at very high pressure, both above and below critical temperature, unless careful modifications to the EoS are made, as will be demonstrated later in a case study.

The image shown in Figure 1 is a representative pressure-temperature phase diagram for water. The calculation of the gas properties is relatively simple for a gas when the process remains within the gaseous phase and below the critical temperature and pressure.

In some cases the gas process transitions from one area of the phase diagram to another requiring a more robust model of the gas properties.

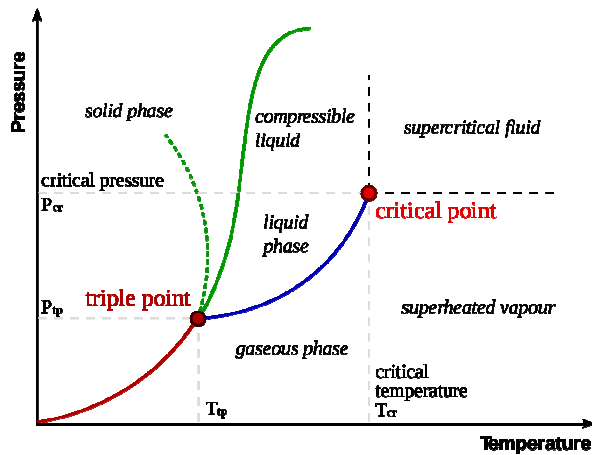


Figure 1: Typical Phase Diagram

The discharge temperature was cited earlier as one output from the compressor performance simulation that is dependent on accurate calculation of the gas properties. Other compressor performance results, such as, volumetric efficiency, flow, and power are dependent upon gas properties, such as, the compressibility, ratio of specific heats, polytropic exponent, viscosity, and specific gravity. Accurate calculation of these gas properties is key to accurate calculation of the compressor performance.

2.2 Pressure Pulsation Simulation

2.2.1 Gas Properties

The previous section described the importance of accurately simulating the gas properties when calculating compressor performance. Similarly, simulating pressure pulsations generated by reciprocating compressors involves many of the same aspects of simulating gas properties. One key parameter in the understanding of pressure pulsations in a reciprocating compressor system is the acoustic velocity, or speed of sound in the gas. The acoustic velocity, c , can be calculated using the following equation.

$$c = 30.87 \left(\frac{k \cdot T \cdot Z}{SG} \right)^{1/2} \quad (\text{SI units})$$

$$c = 41.42 \left(\frac{k \cdot T \cdot Z}{SG} \right)^{1/2} \quad (\text{Imperial units})$$

where

k = ratio of specific heats

T = absolute temperature (°K, or °R)

Z = compressibility

SG = specific gravity

The acoustic velocity in the gas is one of the most fundamental and critical characteristics calculated for a pulsation analysis. Other acoustical characteristics are also dependent on the gas properties. Accurate calculation of gas properties is key for an accurate pulsation analysis.

2.2.2 Pulsation Model

The mathematical model of the flow dynamics is as important as the calculation of the gas properties. There are different computer programs available for simulating pressure pulsations in reciprocating compressor installations. The programs fall into two basic groups. The first group is the first generation of programs that are based upon acoustic plane wave theory. These programs were developed in the 1970s and 80s to replace analog computers. These programs include many simplifying assumptions which allow for the acoustic equations to be solved in the frequency domain. Thus, they are called Frequency Domain, or FD, programs. The second generation of pressure pulsation simulation programs started to be developed during the 1990s. These programs used a more sophisticated model of the fluid dynamics and were able to consider nonlinearities and time varying boundary conditions at the compressor cylinder valves. These programs simulate the fluid dynamics in the time domain and are commonly referred to as TD programs. TD pulsation analysis programs are much more sophisticated than the older FD based programs, yielding more accurate results. Also, the TD programs are able to calculate characteristics like dynamic pressure drop, which cannot be accurately determined by FD based programs. The main drawback to TD programs is the longer solution times. Faster computer hardware and more advanced solvers are required.

The methodology used by the pulsation analysis program to analyze the reciprocating compressor system is also key to a successful design. Shaking forces are generated by pressure pulsations coupled with the piping geometry. These forces must be minimized to ensure vibrations are acceptable. API 618 5th Edition^[1] includes guidelines for shaking forces from pressure pulsations on piping and pulsation bottles. However, there are other pulsation shaking forces that must be evaluated that are not yet included in API 618.

One such force that Beta Machinery Analysis (Beta) has identified during many years of design and field experience is the shaking force acting between the pulsation bottle and the compressor cylinder, referred to as the cylinder shaking force. Figure 2 is a general arrangement drawing for a typical horizontal reciprocating compressor package showing this force.

This shaking force is the result of the different pressure pulsation amplitudes and phases in the gas passage and pulsation bottle and has been shown to cause excessive vertical vibration on horizontal compressors^[2] and, in some extreme cases, has caused failure of head end cylinder supports. This shaking force can also result in high vibration in vertical compressors, as shown in Case Study 2.

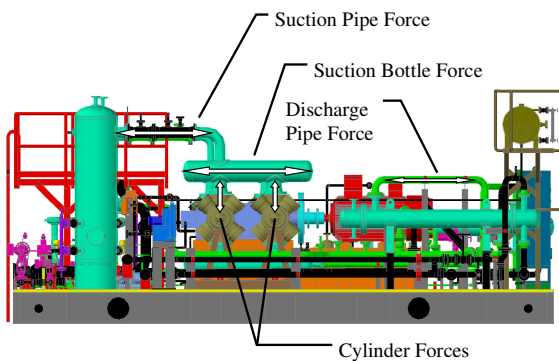


Figure 2: Some Shaking Forces in a Reciprocating Compressor Package

The following case studies show the effect of gas properties on the simulation of compressor performance and pulsation analysis.

3 Case Study 1

3.1 Background

This case study includes a 6 throw, two stage horizontal compressor in ethane service. A plan and elevation view of the compressor package is shown in Figure 3. The compressor is driven by a 3900 kW (5200 HP) induction motor with a fixed full load speed of 885 rpm. Nominal suction and discharge pressures are 21.5 barg to 84 barg (413 to 1215 psig). The compressor package is relatively simple with scrubbers on the first and second stage suction. An interstage cooler is not required in this application as is typical for compressors in this type of application. The discharge temperatures are well within the allowable range of safe operation. The gas in this service is 96% ethane, with the remainder of the gas being methane, propane, and iso-Butane, resulting in a specific gravity of 1.04.

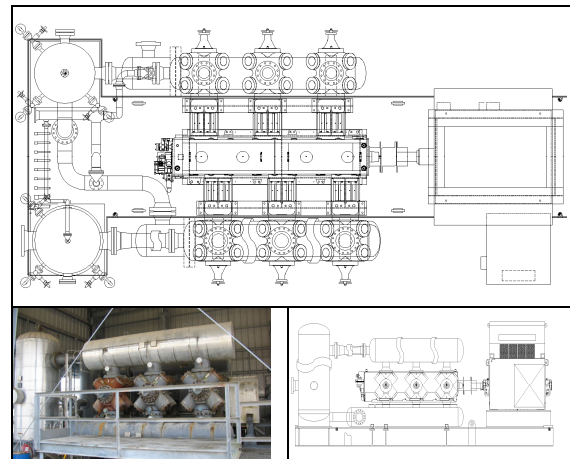


Figure 3: Compressor Plan and Elevation Views

Once the unit was in operation, the owner had noted that the compressor was not performing as expected. There was a noticeable difference in the flow and power requirement.

3.2 Investigation

The review of the performance calculations showed a significant difference between the calculated and measured temperature of the first stage discharge. A cursory review of the original performance calculations showed the expected first and second stage discharge temperatures were 26°C (79°F) and 54°C (129°F) compared to the observed temperatures of 51°C (124°F) and 88°C (191°F), a difference of 10% based on the absolute temperature. The temperatures are measured at the cylinder nozzles and, hence, include the valve heating effects. A difference of 10% between a compressor performance model and observation is generally acceptable; however, in this case the error continues to be compounded as temperature is used in other calculations of compressor performance and gas properties and by the fact that there was no cooler. Further investigation showed other performance factors, such as, flow and power were significantly different, much higher than 10%, when the original performance calculations were compared to the observations.

Before the pulsation model could be investigated, the inaccuracies in the compressor performance model needed to be resolved. Additional performance calculations were done using a variety of OEM programs, commercial programs, and Beta's own compressor performance program. The different performance programs showed a wide variation in result. None of the OEM or commercial programs tested were able to accurately calculate the compressor performance.

Several of the programs were not able to calculate the compressor performance for the two stage operation as the proper gas properties could not be calculated and the program was not able to achieve a mass balance for the first and second stage (the programs crashed or aborted due to errors). Beta’s compressor performance program calculated the first and second stage discharge temperatures to be 49°C (121°F) and 86°C (188°F), less than 1% of absolute from measured.

Figure 4 shows the different discharge temperatures that were calculated by the various performance programs. The discharge temperature is one of the fundamental characteristics of the compressor performance, which must be calculated accurately as it is used in many other calculations. Errors in the discharge temperature calculation will be compounded in later calculations resulting in greater errors.

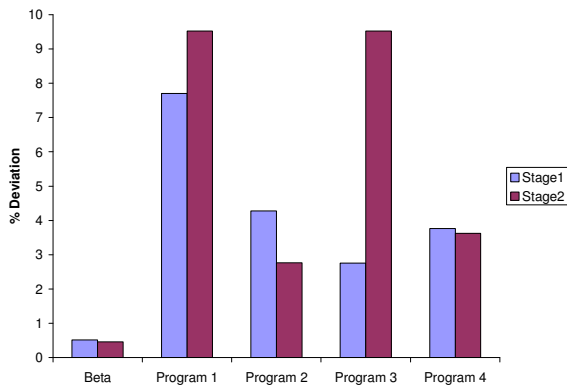


Figure 4: Percent Deviation in Calculated Discharge Temperature from Measured

The main reason for the variation in the discharge temperature calculated in this case is that the first stage discharge conditions were significantly above the critical pressure and temperature of the ethane phase diagram. Figure 5 shows a Mollier diagram for ethane with the first and second stage operating points shown. Additional corrections are required for ethane in this region to accurately calculate the gas properties used in the compressor performance.

Compressor valve loss calculations would also be inaccurate because of errors in thermodynamic property variations. This error would lead to inaccurate overall performance predictions for the compressor system. Careful consideration of the EoS and how it predicts pressure-volume-temperature relationships needs to be considered. As previously stated, inaccurate prediction of these relations would be carried over to all thermodynamic properties.

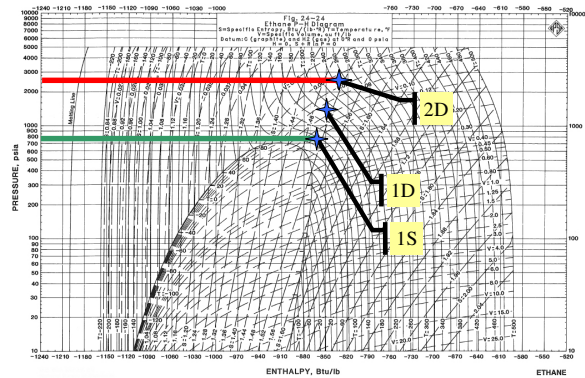


Figure 5: Mollier Chart^[3] Showing Two Stage Compression

3.3 Problem Resolution

A pulsation analysis of the compressor package was done with the initial, and incorrect, compressor performance. The original study resulted in pulsation bottles with baffles and choke tubes to create filters that controlled pulsations to very low levels. This design resulted in bottles being over conservative. Beta conducted a pulsation analysis with the more accurate compressor performance model. Results indicated the pulsation control was very conservative. A solution with lower pressure drop and HP losses could have been developed if the original pulsation study had been done with a more accurate compressor performance model.

4 Case Study 2

4.1 Background

This case study has a 4 throw, single stage vertical compressor in ethylene service, as shown in Figure 6. The compressor is driven by a 1250 kW (1650 HP) motor at 420 rpm. The nominal suction and discharge pressures are 23 barg (330 psig) and 63 barg (915 psig).

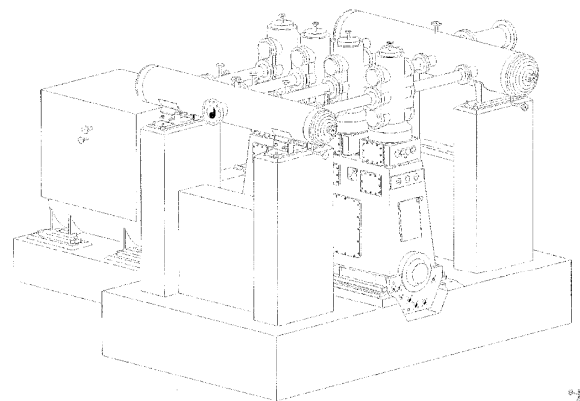


Figure 6: Isometric View of the Compressor Installation

At commissioning the compressor had several vibration problems on the piping and vessels. Many support modifications were implemented, which helped reduce vibrations. The compressor cylinder vibrations remained high and were increasing over time, such that the compressor was becoming unsafe to operate. Beta was contacted to determine causes and solutions.

4.2 Investigation

The evaluation began first with a review of the measurements and work previously conducted. A pulsation and mechanical analysis of the compressor installation had been conducted by another consultant prior to construction. Beta conducted site testing on the compressor to measure pressure pulsations, vibrations, and mechanical natural frequency measurements. Figure 7 shows an isometric of the piping system with test point locations.

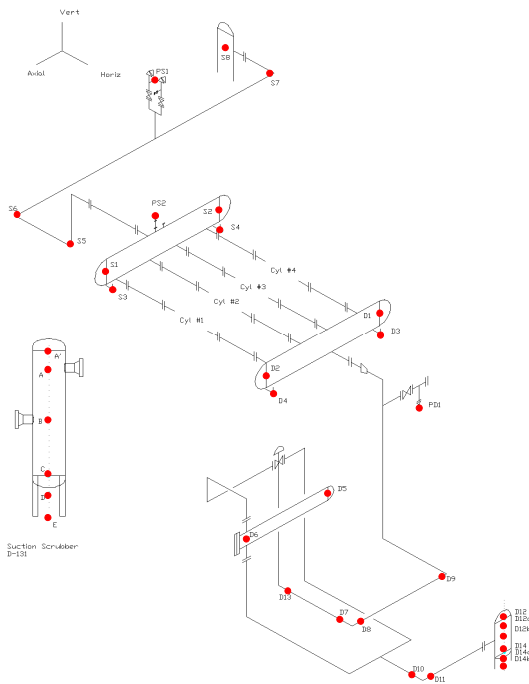


Figure 7: Test Point Locations

Vibration measurements showed the frequency of the highest vibration was at the 4th order of compressor speed, approximately 28 Hz. The direction of the highest vibration in the suction and discharge system was in the horizontal direction, that is, the direction perpendicular to the crankshaft axis. Figure 8 shows a sample of the vibrations measured on one of the compressor cylinders and the discharge piping. The cylinder and piping vibration is more than twice guideline levels.

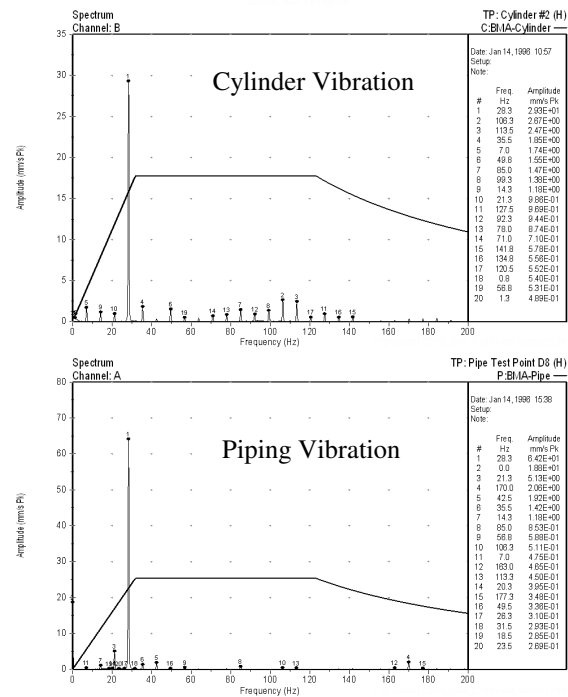


Figure 8: Sample Vibration Data

Pressure pulsations were measured at locations in the suction and discharge system. The pulsations were also highest at the 4th order of compressor speed. Pressure pulsations were more than twice API 618 guidelines at several locations. The results from the original pulsation analysis showed that pressure pulsations should be at or below API 618 guidelines. Note that the original pulsation study used FD pulsation software. This large discrepancy between measured and calculated pulsations raised concerns with the accuracy of the original pulsation analysis. To resolve this puzzle, a pulsation analysis was conducted using Beta's Time Domain software to assess the suction and discharge systems. Figures 9 and 10 show plots of the pulsation models.

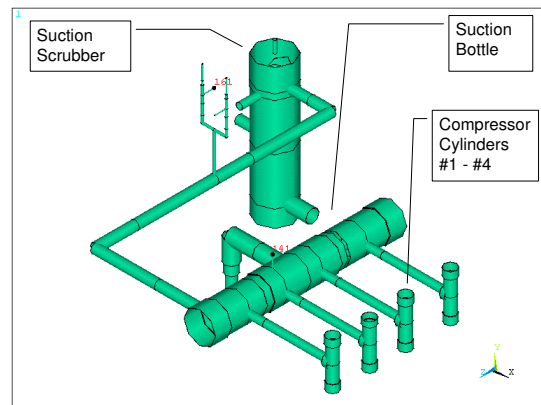


Figure 9: Suction System Pulsation Model

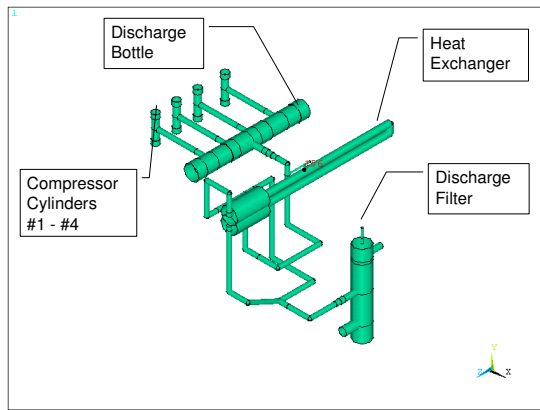


Figure 10: Discharge System Pulsation Model

Pressure pulsations calculated by the TD simulation were compared to measured pulsations as well as the pulsations calculated in the original pulsation model. These are shown in Figure 11. The pressure pulsations from the TD simulation agree with the measurements of the actual system. Note that the pressure pulsations from the TD model are calculated for a speed range of $\pm 10\%$ of the compressor speed range. The actual compressor run speed is fixed at 420 rpm, so there is only one pulsation value at each order of compressor run speed in the field data.

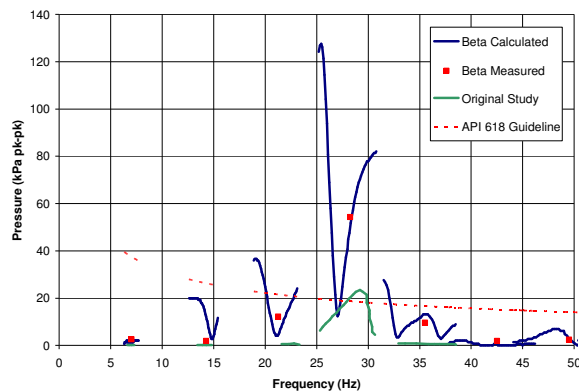


Figure 11: Calculated and Measured Pressure Pulsations

The pressure pulsations calculated by the original pulsation model are shown to be significantly less than the measured pulsations. The difference in the pulsations levels is, in part, due to the original study using a FD pulsation model. Beta also has a FD pulsation model and the simulation was rerun with it. The comparison between Beta's FD and TD models showed only a small difference in pulsation results. The remainder of error in the original pulsation study model is from the calculation of the gas properties. As shown later, the calculation of the acoustical velocity is key to accurately calculating pulsation in this case.

The suction and discharge pulsation models were then evaluated in more detail, since the measurements showed the TD model more accurately represented the gas properties and pulsation characteristics generated by the compressor. The shaking forces from pressure pulsations were generally found to be at low levels for the suction system in the piping upstream of the suction pulsation dampener (bottle) and downstream of the discharge pulsation dampener. A high shaking force was calculated between the compressor cylinders and the discharge bottle at the 4th order of compressor run speed. This force is the result of an acoustical resonance between the bottle and cylinder, as shown in Figure 12. A $\frac{1}{4}$ wave acoustical resonance sets up between the cylinder and bottle with high pulsations at the compressor cylinders and low pulsations at the bottle. The relatively long spool piece between the cylinder and bottle, and the properties of the gas at the discharge operating conditions, results in this resonance and, in addition, a high horizontal force acting on the compressor cylinders and bottle, as illustrated in Figure 13. Note that this shaking force was not even calculated as part of the original pulsation study.

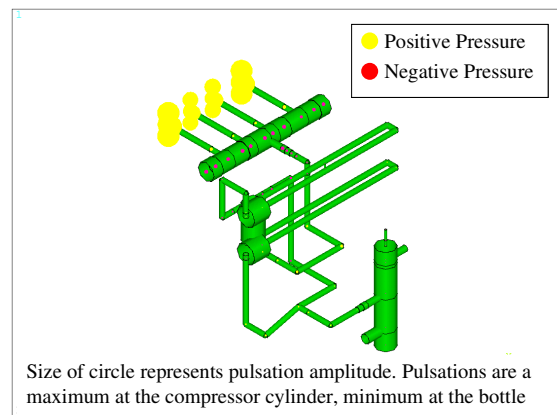


Figure 12: Pulsation Operating Deflected Shape Plot showing resonance between cylinder and bottle

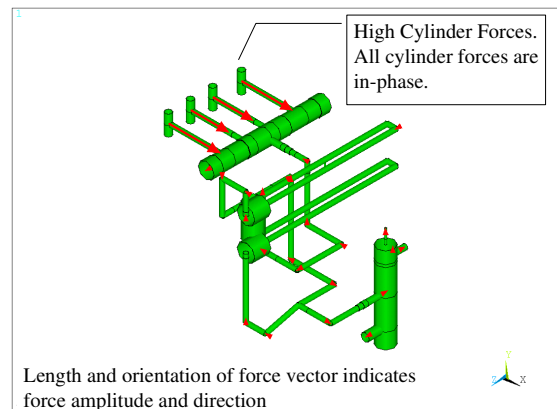


Figure 13: Discharge system forces at 4th order of compressor speed

Figure 14 shows spectrum plots of the discharge system cylinder horizontal forces. The forces acting on cylinders #2 and #3 are slightly lower than #1 and #4 because of the configuration of the internals in the pulsation bottle. In the 1990s, Beta developed a field tested and proven cylinder nozzle force guideline. The amplitude of the cylinder forces at the 4th order of compressor speed are approximately twice Beta’s cylinder nozzle force guideline. Note that API 618 does not recognize or include a guideline for this force.

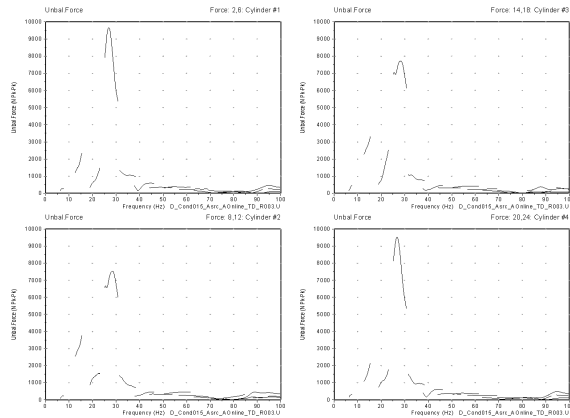


Figure 14: Discharge Cylinder Forces

The cylinder forces are high when each force is considered individually. Since the cylinders are connected to a common bottle and support structure, the vector sum of all the forces needs to be considered. This compressor is a 4 throw unit with 90 degree phasing between the throws. This crank phasing results in the cylinder forces being perfectly in-phase at the 4th order of compressor speed. The vector sum of the cylinder forces is shown in Figure 15, a force magnitude of more than 30 kN peak-peak (6750 lb_f p-p). This combined cylinder force is clearly the cause of the compressor cylinder vibration.

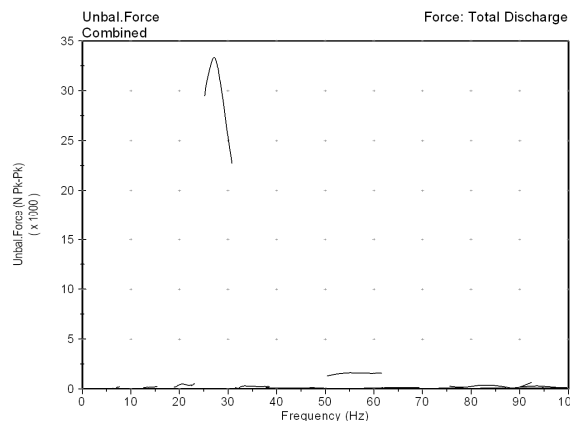


Figure 15: Combined Discharge Cylinder Force

The suction system cylinder force was also evaluated to determine its effect on the cylinder

vibration. The suction cylinder force was found to be much lower than the discharge cylinder force. The different gas properties on the suction cylinder and the different pulsation energy do not result in high suction cylinder forces.

The discharge pulsation model showed that a ¼ wave acoustical resonance between the compressor cylinder and pulsation bottle is the source of the high shaking forces. The calculation of the acoustical resonant frequencies is dependent upon an understanding of the acoustic velocity. As noted in section 2.2.1, the acoustic velocity is dependent upon accurate calculation of the gas properties. The pulsation modeling done in this case study showed that the gas properties were accurately simulated as the measured pulsations agreed with the simulations. The original pulsation model did not accurately calculate the gas properties and the pulsations resulting from the ¼ wave resonance.

4.3 Problem Resolution

The cause of the compressor cylinder vibration is obviously the cylinder shaking force from pressure pulsations. Beta’s TD pulsation model results agreed with the measured compressor system.

With consideration of the gas properties, a computer model can be used during the design stage. Modifications were evaluated with the pulsation model to determine a solution to minimize the cylinder force generate by pressure pulsations. The primary cause of the cylinder force is an acoustical resonance between the compressor cylinder and bottle. One method of changing this acoustical resonance is to install a Helmholtz resonator in the pipe spool. The Helmholtz resonator, named after Hermann von Helmholtz, was first described in the 1850s. A Helmholtz resonator is device with an acoustical resonance that can be tuned to a specific frequency. The resonance frequency can be tuned by changing the volume and/or restriction of the resonator. An example of how a Helmholtz resonator works is an uncorked wine bottle. When air is blown across the opening, a sound is heard at one frequency. The frequency of the sound can be altered by varying the amount of liquid in the bottle. Helmholtz resonators have been used by pulsation designers for many decades to control pressure pulsations in compressor systems. The main benefit of a Helmholtz resonator is that it introduces no (or very small) pressure drop. The downside of resonators is that they are effective over a narrow frequency range and they introduce additional resonances (pass bands) into the system. This compressor installation is an ideal application for a Helmholtz resonator since there is only one acoustic resonance to be eliminated and the compressor has a fixed speed.

Figure 16 is a drawing of the proposed resonator design. The resonator includes a 660 mm (26") section of 6" pipe with a 2" choke tube that is 356mm (14") long to achieve the necessary Helmholtz frequency.

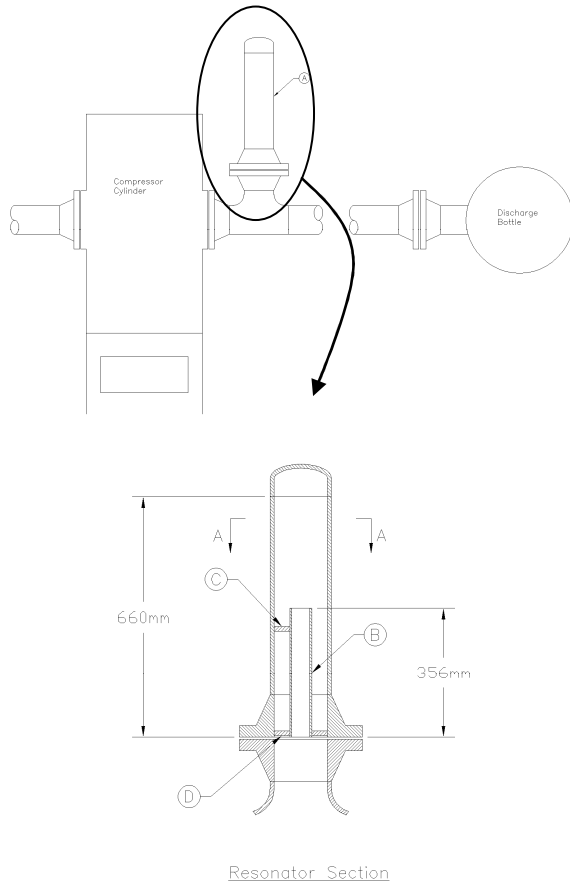


Figure 16: Resonator Design

Figure 17 shows the combined suction and discharge cylinder force for all cylinders for the original system design as well as with the Helmholtz resonator installed. The resonator is calculated to reduce the compressor cylinder force to 20% - 40% of the current levels. A similar reduction in vibrations is expected. New spool pieces were fabricated to connect the cylinders with the bottle, which now include the Helmholtz resonators. The spools were installed during an unscheduled shut-down due to work in another part of the facility.

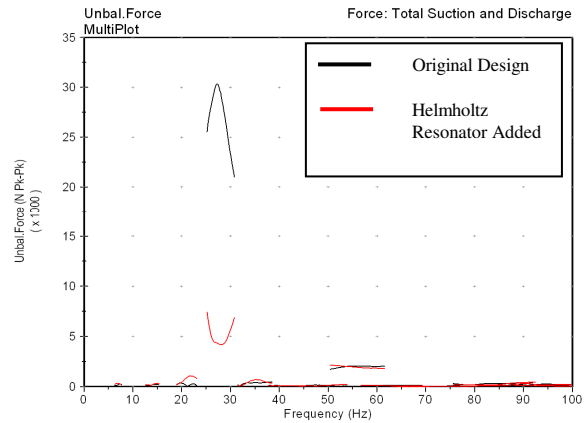


Figure 17: Combined Cylinder Force for Original and Modified Design

Figure 18 shows the overall cylinder vibrations recorded by the vibration transmitters installed on the compressor cylinders before and after the resonators were installed. The resonators were very effective in reducing the cylinder vibrations to acceptable levels.

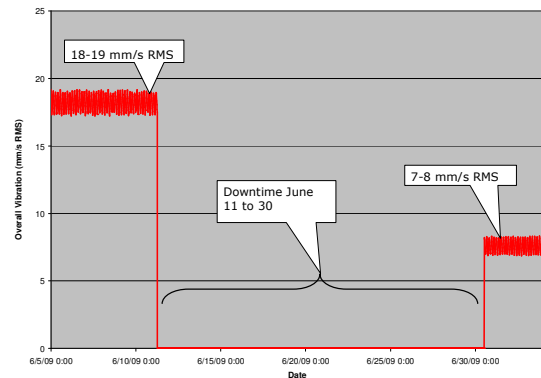


Figure 18: Overall Compressor Cylinder Horizontal Vibration

5 Conclusion

This paper demonstrates that a thorough understanding of specialty gas properties is key to accurately simulating the performance of reciprocating compressors. OEM and commercial performance programs may have difficulty accurately simulating the compressor performance in some applications.

The case studies illustrate the strength of pulsation analysis software that include consideration of specialty gas properties and a non-linear Time Domain model of the fluid dynamics. Accurately calculating gas properties is crucial to determining the acoustic velocity and acoustical resonances in the piping and vessels. Frequency Domain pulsation software has severe limitations producing less

accurate model results, which may compromise the safety of the reciprocating compressor installation.

The design criteria specified in API 618 are the minimum standard for pulsation studies. Other criteria, such as the pulsation generated shaking force between the compressor cylinder and pulsation bottle, must also be considered.

Conducting compressor performance simulations and pulsation studies for specialty gases requires sophisticated, field proven, engineering software.

6 Acknowledgements

Contributions from Brian Howes, Chief Engineer, and Hemanth Satish, Project Analyst, of Beta Machinery Analysis, were significant to the development and implementation of these concepts into Beta's design and field services.

References

- 1 American Petroleum Institute, "Reciprocating Compressors for Petroleum, Chemical, and Gas Industry Services, API Standard 618" 5th Edition, December 2007
 - 2 B. Howes, Vertical Forces Cause Vibration in a Reciprocating Compressor, Pipeline and Compressor Research Council – Gas Machinery Conference, 1997
 - 3 Gas Processor Suppliers Association, "Engineering Data Book Volume II", Gas Processor Association, 1987
-

Automatic Early Failure Detection and Shutdown of a Critical Compressor due to a Crosshead Fracture

by:

Tobias Ahlert

Customer Support Department

PROGNOST Systems GmbH

Rheine

Germany

tobias.ahlert@prognost.com

**7th Conference of the EFRC
October 21th / 22th, 2010, Florence, Italy**

Abstract

A PROGNOST customer in Germany operates four 4-cylinder reciprocating compressors at a natural gas production facility in Northern Germany. This case study describes the detection of a critical damage in the crosshead with a subsequent safety shutdown to avoid consequential damage. Different parameters such as crosshead slide vibration and piston rod position are monitored for the detection of the failure and shutdown of the compressor.

This paper describes the development of the failure and its detection, as well as the root cause of the failure in the demanding H₂S environment.

1 Introduction

Over the last few years it has become more and more apparent that operators of piston compressors use specific monitoring systems particular for their reciprocating machines that implement an automatic machine shutdown function to prevent catastrophic machine failures.

The current trend is moving away from simply placing a velocity vibration sensor on the frame of critical machines. In fact it is much more effective to have safety shutdown criteria on the basis of measured acceleration values directly at the crosshead slide and to measure the dynamic piston rod motion continuously. Specifically this kind of safety monitoring is possible, since modern and fast data acquisition systems are available.

Furthermore, the method of automatic data interpretation plays an essential role. It is simply not enough to develop such an analysis to calculate an average value over a specific period and compare it with the appropriate alarm limits. With piston compressors it is important to recognize and analyze the individual events over one revolution. This however carries the responsibility to manage more system limit values. In doing so, the experience on which actual limit-values one adjusts with this modern monitoring system plays a very large and important role.

Usually these limit values are based on actual measured values. This is because each piston compressor has specific vibration responses and signatures according to its design and operating conditions. It is challenging to commission a machine with correct limit values without specific knowledge of the machinery vibration response or what we refer to as baseline data.

This paper describes that with only the default factory safety limits installed, a machine failure has been detected and an automatic shutdown successfully occurred. With this successful automatic shutdown, further damage was prevented.

2 Monitoring system equipment

A PROGNOST customer in Germany operates four 4-cylinder reciprocating compressors in natural gas service within a H2S environment.

Since December 2006 all machines are equipped with a PROGNOST©-NT Monitoring System. The system works with acceleration sensors on the crosshead slide (CHS) and on the cylinder.

In addition proximity probes are mounted on the packing flange to measure displacement of the piston rod motion. Figure 1 show the arrangement, which is mounted on all cylinders.

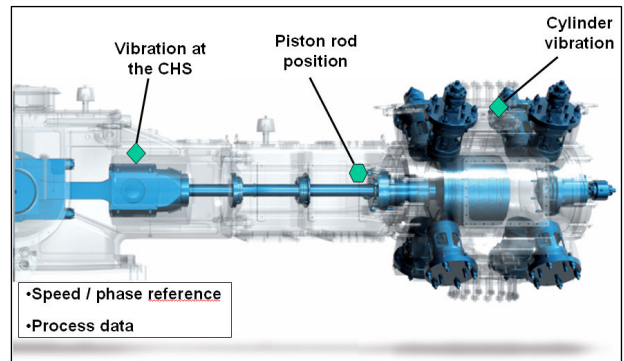


Figure 1: Sensor positions

The monitoring system itself is configured with the following software modules:

- Safety
- Early Failure
- Wear
- Process Data Analysis

to give the operator a high grade on performance.

Sensor data	CHS / Cylinder	Measuring range Low pass filter Samples	±5000 m/s ² 10 kHz 16384
	Piston rod position	Measuring range Samples Position	2250 µm 8192 above
Software Modules	-Safety analysis (CHS, piston rod position) -Early failure detection (CHS, Cyl. and piston rod pos.) -Wear monitoring (piston rod position) -Process data analyses		

Table 1: Specific monitoring system data

3 Machine data

In January 17th 2010 the PROGNOST customer support specialist received a hotline call. This call was made by the customer to ask for verification of data based on a current automatic machine shutdown by the PROGNOST monitoring system. One of the 4-throw reciprocating machines was tripped on “CHS vibration RMS 36 Segment / cylinder 2”, but the operator could not see anything from the outside of the machine. Note: This call was based on the customer’s service agreement procedure.

The discussed machine has the following technical data:

Machine type:	4-throw, double acting
Service:	Natural gas transportation
Stages:	1
Piston stroke:	175 mm
Cylinder bore:	245 mm
Rotation speed:	380 ... 740 rpm
Power:	1700 kW
Model year:	2005
Volume regulation:	Stepless speed & valve unloader (25-50-75-100%)
Suction pressure:	30 bar
Discharge pressure:	80 bar
Suction temperature:	15 °C
Discharge temp.:	150 °C

4 Safety limit configuration

The proven strategy for vibration analysis is the so called segmented vibration analysis based on 36 segments. Each 10° crank angle (CA) represents one segment per revolution on which the RMS vibration value is calculated. For each segment there is an individual limit which can be set independently from each other to avoid false alarms given by higher values caused for example by, high discharge valve impacts or higher vibrations levels at the rod load reversal points. As well the system checks the peak-to-peak value of the piston rod position signal based on 8 segments per revolution (Table 2). In addition the system counts the quantity of segments during a specific number of rotations and in which and how many segments a limit is violated.

other which are displayed in Figure 3.

The advantage to doing the settings independently is because of the different vibration behavior within one revolution. The piston rod position safety limit adjustment is similar.

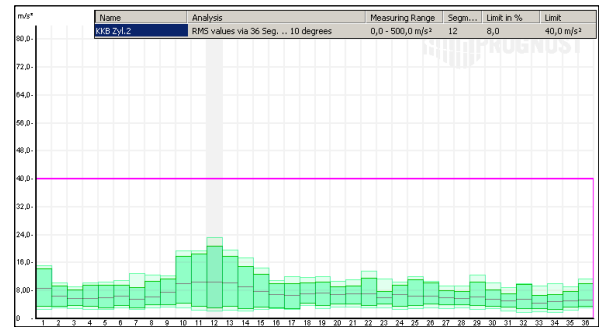


Figure 2: Equal safety limits with the measured values – CHS vibration cylinder 2

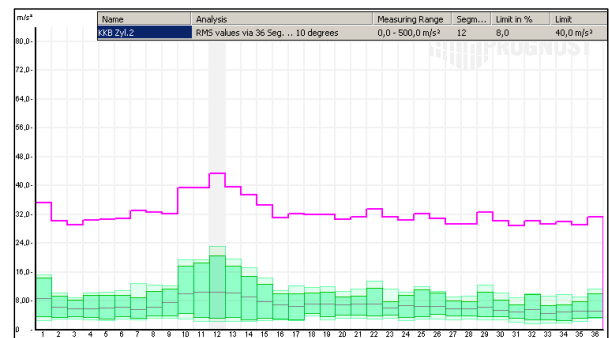


Figure 3: Independent safety limits with the measured values – CHS vibration cylinder 2

Safety Settings, Valid Speed [250,0 - 900,0 1/min]	
V11 Copyright© PROGNOST Systems GmbH 1990-2010	
Name	Type of Analysis
Kolbenstangenlage 1	Peak-Peak over 8 Seg. ... 45 degrees
Kolbenstangenlage 2	Peak-Peak over 8 Seg. ... 45 degrees
Kolbenstangenlage 3	Peak-Peak over 8 Seg. ... 45 degrees
Kolbenstangenlage 4	Peak-Peak over 8 Seg. ... 45 degrees
Kreuzkopfbahn Zylinder 1	RMS values via 36 Seg. ... 10 degrees
Kreuzkopfbahn Zylinder 2	RMS values via 36 Seg. ... 10 degrees
Kreuzkopfbahn Zylinder 3	RMS values via 36 Seg. ... 10 degrees
Kreuzkopfbahn Zylinder 4	RMS values via 36 Seg. ... 10 degrees

Table 2: List of safety relevant analysis

Figure 2 shows the safety limit adjustment of the crosshead vibration sensor from crank 2 with the actual measured values. In this case the limit is equal over all segments with a value of 40 m/s² instead of set the limits independently from each

CONDITION MONITORING

Automatic Early Failure Detection and Shutdown of a Critical Compressor due to a Crosshead Fracture,
Tobias Ahlert; *PROGNOST SYSTEMS*

5 Data analysis

On this January at 12:59 the monitoring system detected a catastrophic crosshead failure and it triggered an automatic shutdown of the machine. The first early warnings were registered around 12:38.

Around 21 hours prior to the shutdown, PROGNOT was delivering first messages of the early failure recognition. This is shown in the following extract of the system log book (Figure 4).

Type	Date	Measuring Point	Message
Information	17.01.2010 12:59:13		Maschine steht
IMPORTANT	17.01.2010 12:59:06	KKB Zyl.2	Status HzA: Safety-Grenze in mindestens 6 Segmenten überschritten
IMPORTANT	17.01.2010 12:59:04	KKB Zyl.2	Status VzA: Safety-Grenze in den folgenden Segmenten überschritten: 7
Event	17.01.2010 12:58:59	KKB Zyl.2	9 RMS values 5 RMS values
Event	17.01.2010 12:56:00	KKB Zyl.2	8 Absolute m6 RMS value:9 RMS value:5 Absolute m6 Absolute m9 Absolute m8 RMS
Information	17.01.2010 12:55:00		Neues Zustands-Muster Nr. 1022 eingetragen
IMPORTANT	17.01.2010 12:54:09	KKB Zyl.2	Status VzA: Safety-Grenze in den folgenden Segmenten überschritten: 10
Event	17.01.2010 12:52:59	RD Zyl.2	2 Peak-Peak 2 Peak-Peak
Event	17.01.2010 12:50:59	KKB Zyl.2	6 Absolute maximum:8 Absolute maximum 6 RMS values 6 Absolute m
IMPORTANT	17.01.2010 12:49:19	KKB Zyl.2	Status VzA: Safety-Grenze in den folgenden Segmenten überschritten: 5
IMPORTANT	17.01.2010 12:49:12	KKB Zyl.2	Status VzA: Safety-Grenze in den folgenden Segmenten überschritten: 7
IMPORTANT	17.01.2010 12:48:40	KKB Zyl.2	Status VzA: Safety-Grenze in den folgenden Segmenten überschritten: 7
IMPORTANT	17.01.2010 12:48:14	KKB Zyl.2	Status VzA: Safety-Grenze in den folgenden Segmenten überschritten: 7
IMPORTANT	17.01.2010 12:48:10	KKB Zyl.2	Status VzA: Safety-Grenze in den folgenden Segmenten überschritten: 7
IMPORTANT	17.01.2010 12:48:06	KKB Zyl.2	Status VzA: Safety-Grenze in den folgenden Segmenten überschritten: 5
IMPORTANT	17.01.2010 12:48:05	KKB Zyl.2	Status VzA: Safety-Grenze in den folgenden Segmenten überschritten: 10
Event	17.01.2010 12:48:00	RD Zyl.2	2 Peak-Peak 2 Peak-Peak
IMPORTANT	17.01.2010 12:46:09	KKB Zyl.2	Status VzA: Safety-Grenze in mindestens 3 Segmenten überschritten
Event	17.01.2010 12:45:59	KKB Zyl.2	8 Absolute maximum 9 Absolute maximum
IMPORTANT	17.01.2010 12:45:32	KKB Zyl.2	Status VzA für die Safety-Grenzen aufgehoben
IMPORTANT	17.01.2010 12:45:22	KKB Zyl.2	Status VzA: Safety-Grenze in mindestens 3 Segmenten überschritten
IMPORTANT	17.01.2010 12:45:19	KKB Zyl.2	Status VzA für die Safety-Grenzen aufgehoben
IMPORTANT	17.01.2010 12:44:51	KKB Zyl.2	Status VzA: Safety-Grenze in mindestens 3 Segmenten überschritten
IMPORTANT	17.01.2010 12:44:47	KKB Zyl.2	Status VzA für die Safety-Grenzen aufgehoben
IMPORTANT	17.01.2010 12:44:36	KKB Zyl.2	Status VzA: Safety-Grenze in mindestens 3 Segmenten überschritten
IMPORTANT	17.01.2010 12:44:33	KKB Zyl.2	Status VzA für die Safety-Grenzen aufgehoben
IMPORTANT	17.01.2010 12:44:17	KKB Zyl.2	Status VzA: Safety-Grenze in mindestens 3 Segmenten überschritten
IMPORTANT	17.01.2010 12:44:16	KKB Zyl.2	Status VzA: Safety-Grenze in den folgenden Segmenten überschritten: 6
Event	17.01.2010 12:43:00	RD Zyl.2	2 Peak-Peak
IMPORTANT	17.01.2010 12:41:13	KKB Zyl.2	Status VzA: Safety-Grenze in den folgenden Segmenten überschritten: 8
Event	17.01.2010 12:37:59	RD Zyl.2	Peak to Peak Spp Peak to Peak Spp
IMPORTANT	17.01.2010 12:37:55	KKB Zyl.2	Status VzA: Safety-Grenze in den folgenden Segmenten überschritten: 9
Event	17.01.2010 12:32:00	RD Zyl.2	Peak to Peak Spp
Event	17.01.2010 09:17:59	RD Zyl.2	Peak to Peak Spp Peak to Peak Spp
Event	17.01.2010 07:32:00	RD Zyl.2	Peak to Peak Spp Peak to Peak Spp
Event	17.01.2010 06:54:00	RD Zyl.2	Peak to Peak Spp
Event	17.01.2010 06:52:59	RD Zyl.2	Peak to Peak Spp
Event	17.01.2010 06:47:00	RD Zyl.2	Peak to Peak Spp Peak to Peak Spp
Event	17.01.2010 06:40:59	RD Zyl.2	Peak to Peak Spp Peak to Peak Spp
Event	17.01.2010 06:38:00	RD Zyl.2	Peak to Peak Spp Peak to Peak Spp
Event	17.01.2010 06:08:00	RD Zyl.2	Peak to Peak Spp Peak to Peak Spp Peak to Peak Spp
Event	17.01.2010 05:41:00	RD Zyl.2	Peak to Peak Spp Peak to Peak Spp Peak to Peak Spp
Event	17.01.2010 05:37:59	RD Zyl.2	Peak to Peak Spp Peak to Peak Spp Peak to Peak Spp
Event	17.01.2010 05:07:00	RD Zyl.2	Peak to Peak Spp Peak to Peak Spp
Event	16.01.2010 17:20:00	RD Zyl.2	Peak to Peak Spp Peak to Peak Spp
Event	16.01.2010 16:13:55	RD Zyl.2	Peak to Peak Spp
Event	16.01.2010 16:12:55	RD Zyl.2	Peak to Peak Spp
Information	15.01.2010 11:16:57		Gutzustandswerte für Betriebszustand 'Saugdruck > 30 bar(2)' geladen

Figure 4: Log book

CONDITION MONITORING

Automatic Early Failure Detection and Shutdown of a Critical Compressor due to a Crosshead Fracture,
Tobias Ahlert; *PROGNOST SYSTEMS*

The following diagram (Figure 5) represents the RMS value of the segment 8 (70 - 80° CA). The safety limit for this segment (40 m/s²) was exceeded at 12:38 the first time. The shutdown took place 11 minutes later. Because the production personnel at site were not able to detect a failure they started the machine a second time. This resulted in tripping the machine based on the same condition again!

Figure 6 shows the measured crosshead RMS vibration of all 36 segments and the piston rod position peak-to-peak of all 8 segments in one colored 3D trend view for a period of 2 months. It is visible to see how the vibration rose slowly, and then progressed to measure clearly high values. It is to be assumed thus the damage did not occur abruptly.

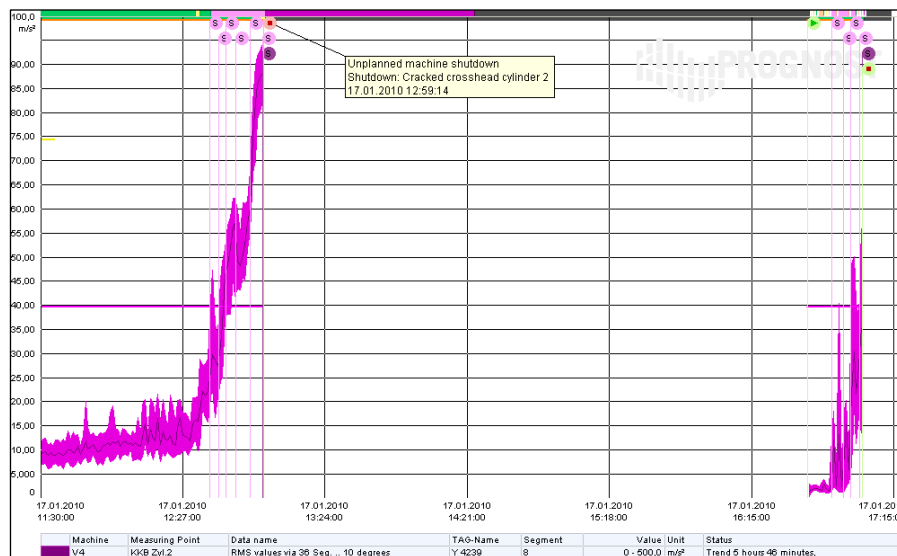


Figure 5: Trend of the crosshead RMS vibration (segment 8 only)

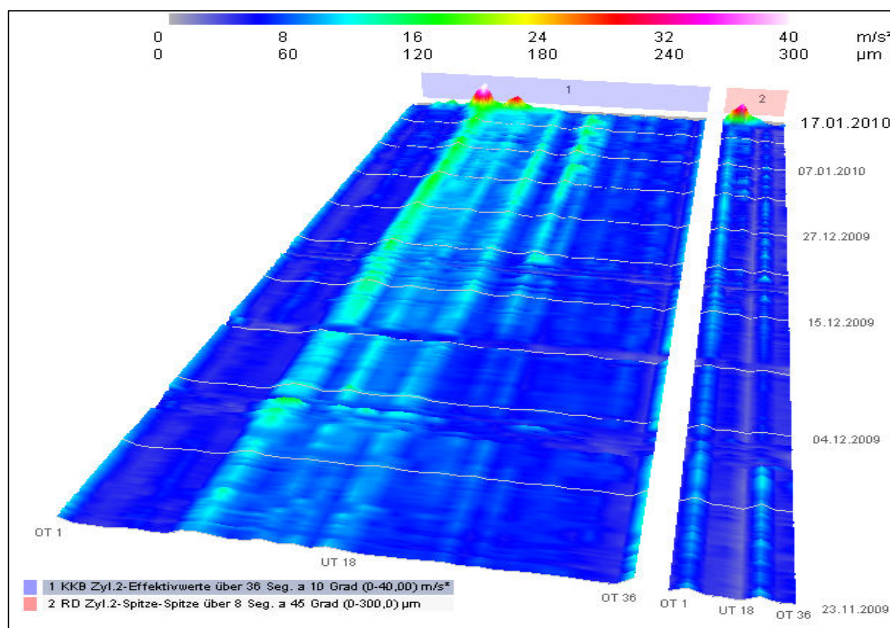


Figure 6: 2-month 3D trend of the crosshead RMS vibration and piston rod position peak-to-peak

CONDITION MONITORING

Automatic Early Failure Detection and Shutdown of a Critical Compressor due to a Crosshead Fracture,
Tobias Ahlert; PROGNOST SYSTEMS

Finally, the rise of the vibration occurred in only 6 of the 36 total segments which would increase the total vibration of the full revolutions approximately 6%. Since the protection system was able to be focused on the right period of segments, the measured RMS value was high enough for a clear detection.

The following diagram (Figure 7) shows the safety relevant signals of cylinder 2 over one revolution. The purple signals are at the moment of shutdown, the red signals are 3 hours before and the blue one represents a known good condition. For a better representation the signals (purple, red, and blue) are shown with an offset. This high speed data was stored in the PROGNOST® systems rings buffer. The increased vibration is clearly visible between 40° and 100° CA.

Within this time period a machine normally experiences the moment of rod load reversal. Exact determination of the force points of reversal can take place only by indicated pressure signals, which are not installed here. The piston rod position signal shows likewise an increased movement, which lies however below the safety limit of 600 µm. The data evaluations are showing no indication for liquid impacts or foreign particles in the compression chamber. Such an event becomes manifested as increased vibrations and strong piston rod movements are found approximately around the dead centers. In fact the crank angle position of the increased vibrations and the relatively small deflection of the piston rod position pointed to a problem with the crosshead and/or the crosshead connections. The analyst, who takes the hotline call as this time, stated that the machine condition was very critical.

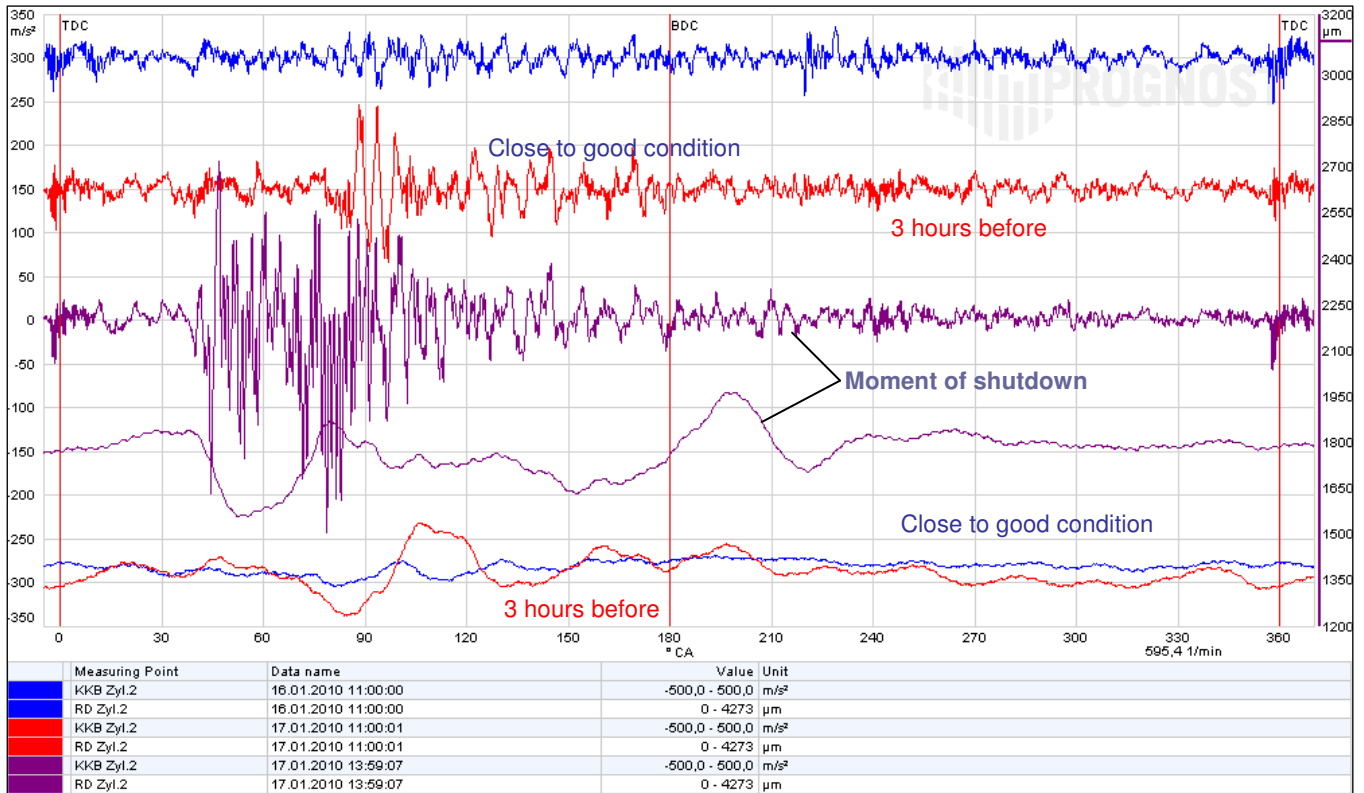


Figure 7: Online ring buffer data of the crosshead vibration and piston rod position

CONDITION MONITORING

Automatic Early Failure Detection and Shutdown of a Critical Compressor due to a Crosshead Fracture,
Tobias Ahlert; PROGNOT SYSTEMS

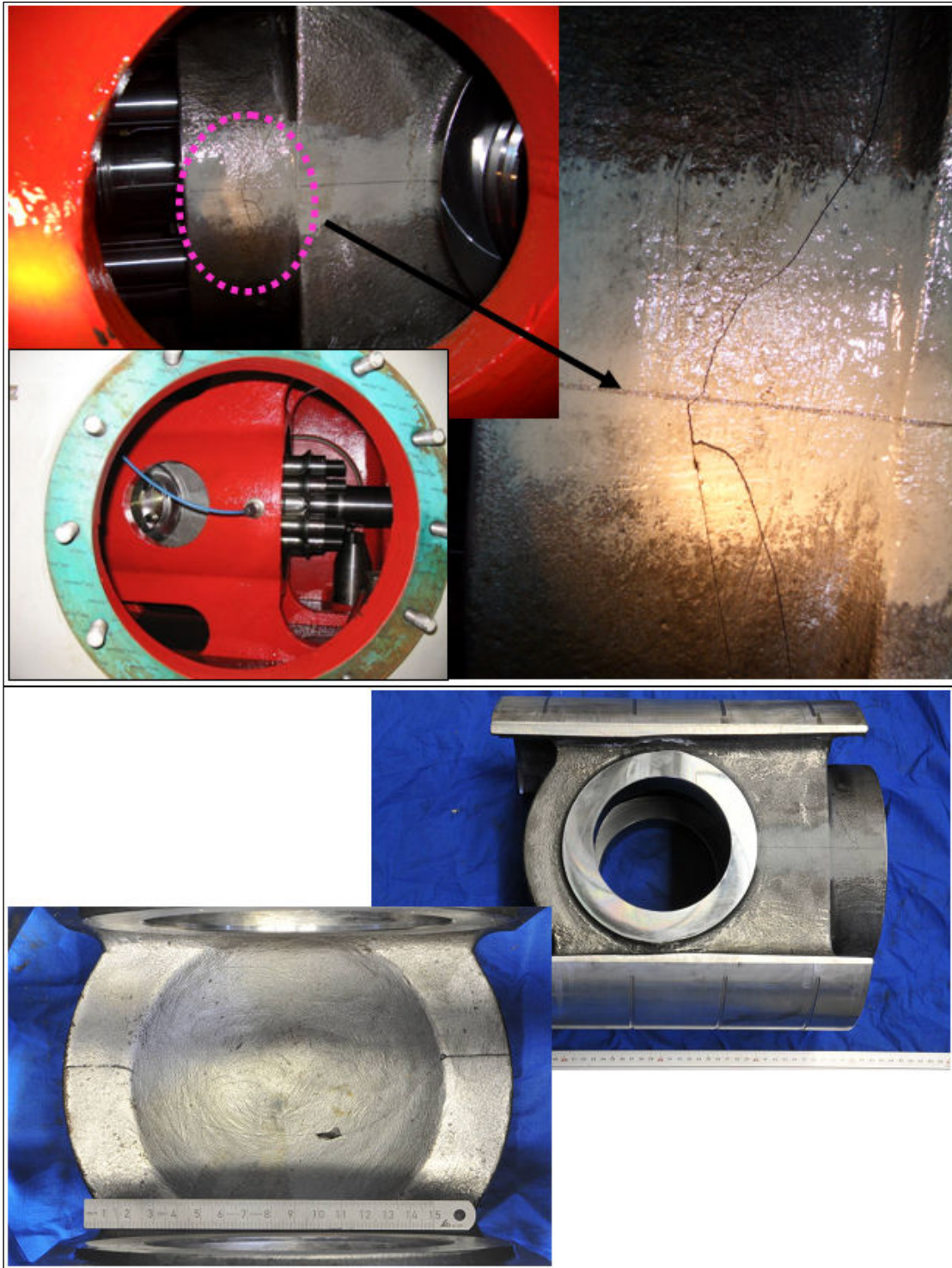


Figure 8: Pictures of the failed crosshead

6 Conclusion

The above mentioned case study illustrates on the basis of an automatic shutdown at that crucial moment with no human interaction how important it is to protect a machine with a modern monitoring technology to detect failures at an early stage to enable the maintenance team right in time.

Furthermore, it is important to have the opportunity to set individual limits, locate the importance sensors and use the right analysis. If you did this homework you will prevent catastrophic failure right in time, where no consequential damages were caused.

ITW Polymer Technologies

Best Practices in Compressor Mounting

by:

James A. Kuly

Chief Engineer

ITW Polymer Technologies

Montgomeryville, Pennsylvania

U.S.A.

jkuly@itwpolytech.com

**7th Conference of the EFRC
October 21th / 22th, 2010, Florence**

Abstract

Large reciprocating compressors are found in many industries including gas, oil and petrochemical production, transmission and storage. Operationally they generate very large gas and inertia forces. Their mounting systems must manage and transmit weight loads, vertical and horizontal gas and inertia loads, vertical anchor bolt forces, and the forces of thermal growth. The effectiveness and integrity of their installation is therefore crucial. This paper addresses the best practices related to installation techniques, component design, and materials used in the mounting of large reciprocating compressors including:

- Equipment Preparation
- Foundation & Mat
- Anchor Bolts & Sleeves
- Grouting & Chocking

1 Introduction

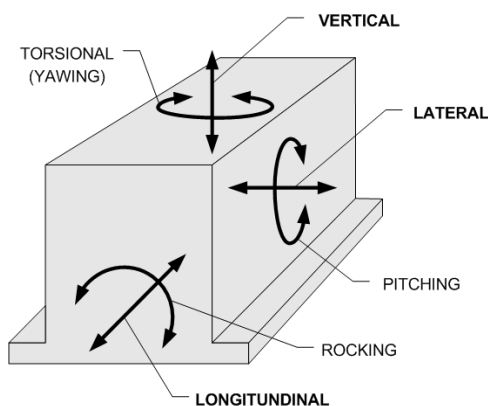
Large reciprocating compressors are found in a number of industries including gas, oil and petrochemical production, transmission and storage. Operationally they generate very large gas and inertia forces. Their mounting systems must manage and transmit weight loads, vertical and horizontal gas and inertia loads, vertical anchor bolt forces, and the forces of thermal growth. The effectiveness of the mounting system and integrity of its installation are therefore crucial.

The purpose of the mounting system on a reciprocating gas compressor is simple. The mounting system must do three things:

- 1 **Position and support the compressor, its driver and related equipment.** Hold the compressor and driver in perfect alignment while accommodating all of the loads applied to it including horizontal gas and inertia loads, weight loads, anchor bolt loads and loads due to thermal growth and frame distortion
- 2 **Effectively transmit the vibration produced by dynamic forces down through the foundation** while reducing or eliminating the harmful effects of those vibrations
- 3 **Accomplish items #1 and #2 above for 30 years or more**

While the purpose of a compressor's mounting system is simple, its construction is not. Reliable, long-term reciprocating compressor operation depends on the quality of the design and construction of the compressor mounting system and the integrity its foundation. Degradation of the foundation or loss of the mounting system's integrity can cause excessive frame vibration and misalignment, and eventually crankshaft failure.

The primary problem making compressor mounting systems difficult to design and install is vibration. A compressor can vibrate in six different ways or modes – three in translation (vertical, lateral, longitudinal) and three in rotation (pitching/yawing, torsional, rocking).



All these modes of vibration have their own natural frequencies where resonance can occur. In addition, one mode of vibration can be either “coupled” or connected to other modes and drive them. Finally, vibrations can be transmitted in series or in parallel from one component to the next. A well designed and constructed foundation will not only accommodate all of the loads applied to it including horizontal gas and inertia loads, weight loads, anchor bolt loads and loads due to thermal growth and frame distortion, but it will act to reduce then effectively pass those vibrations down to the soil below.

The complexity of analyzing and mitigating the negative affects of vibrations in a compressor installation is difficult and complex. The only way to properly analyze and design a good foundation is with the aid of such tools as Finite Element Analysis (FEA) and foundation design programs. In addition to these tools, there are also many practical design and installation “rules of thumb” that should be used. Unfortunately, many of these are only learned through years of experience. They are the small things that are often left off of the installation drawings and specifications but have a big impact on the longevity of a foundation.

This paper will focus on those “rules of thumb” practices or techniques used in compressor installation design and installation that directly influence the quality of construction and integrity of the foundation and how both of these directly affect vibration attenuation. It will not address the interaction of the foundation and the soil.

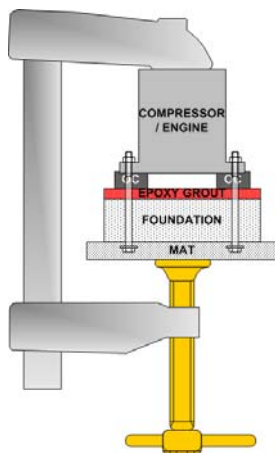
2 Best Practices Related to Mitigating Vibration

To achieve a strong, high-quality yet cost-effective installation it is important to recognize two very important elements in the design of the mounting system:

- **The compressor and its foundation must form a tightly integrated structure.** Vibration energy travels in the form of waves down and out through the foundation where the soil can absorb it. Breaks, cracks or separations in the integrated compressor / foundation structure will prevent the vibration waves from traveling downward.

- **A compressor installation must be treated as a series of interacting structures that move and vibrate.** Vibration energy actually deforms the structure as it passes through the structure. This is because the steel, grout and concrete are all flexible. Preventing foundation degradation and cracking means making sure that all mounting components work together and none act to harm the other components or mounting system. For example, the design and installation of the anchor bolts should not cause the concrete to crack.

The one best word to describe what it means to "form a tight integrated structure" is **Monolithic**. A monolithic structure is one that is cast as a massive, seamless, uniform, and rigid piece. The design objective behind a compressor installation is therefore to create a monolithic structure that clamps the series of interacting pieces together (the compressor and its driver to a well designed concrete foundation) with enough size and mass to separate the dynamic response frequencies from the excitation frequencies. This means that the mat, concrete foundation, grout and machinery must become one.



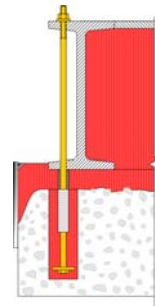
The following describes the best construction practices that help reduce the impact of vibration in the structure.

2.1. Best Practices Related To the Construction of the Foundation

The foundation has the biggest influence on mitigating vibration in a reciprocating compressor. The following are best practices related to the construction of the foundation that have to do with reducing the impact of vibration.

2.1.1. Install the compressor and driver on a concrete block foundation. Concrete absorbs vibration more easily than a steel frame or skid because its internal molecular structure absorbs vibration energy.

2.1.2. If the compressor has to be mounted on a skid, two best practices are to run the anchor bolts to the top of the skid and to fill the void spaces inside the skid with epoxy grout. These practices act to stiffen the steel.



2.1.2. Design the installation as a rigid structure whose dynamic response will depend only on the dynamic load, the mass of the foundation and on soil characteristics. Make the weight of the foundation 4 to 8 times the weight of the compressor. The width of the foundation should be at least 1.5 times its height.

2.1.3. Keep the center of gravity of the block and mat within 15 to 20 cm (6 to 8 inches) of the vertical centreline of the compressor's crankshaft.

2.1.4. Minimize the elevation difference between the machine's dynamic forces and the center of gravity of the machine-foundation system.

2.1.5. Mechanically isolate the foundation block from any surrounding structures.

2.2. Best Practices Related to Epoxy Grout & Chocks

The following are best practices associated with epoxy grout and chocks.

2.2.1. A non-shrink grout is required between the top of concrete foundation and the bottom of the compressor and its driver so precise alignments can be achieved. The use of epoxy grout and epoxy chocks are, by themselves, considered a "Best Practice" over the use of cementitious grout because of their...

- Higher physical properties
- Superior bond strength to concrete and steel
- Resistance to cracking
- Imperviousness to attack by oil and chemicals

2.2.2. The best practice is to cover the foundation with a full bed of grout then to mount the compressor and driver on individual chocks. The full bed of epoxy grout not only helps to support the machinery it seals and protects the concrete foundation. Because individual chocks are separated by a gap, air can easily flow under and around compressors and drivers. Chocks also allow the recess in the foundation for the pan to be built shallower to reduce the weakness in this area of the block that was prone to cracking.

2.2.3. Individual chocks can be either the poured-in-place type or the pre-manufactured adjustable type chocks. Both are good practice. The adjustable chocks must be installed on a sole plate while the poured-in-place type chocks can be placed either directly on top of the grout or on sole plates.

2.2.4. Poured-in-place chocks can be made from either 3-component epoxy grout or 2-component epoxy chocking compounds. The best practice regarding which product to use is based on size of the chock. With any single chock over 610 mm (24 inches) in length or 75 mm (3 inches) in depth it is best to use an epoxy grout rather than a chocking compound.

2.3. Best Practices Related to Anchor Bolts

Anchor bolts clamp foundation and equipment layers together. Their purpose is to prevent movement of the equipment or separations between the layers. Separations act as a barrier preventing vibrations from passing completely through the foundation to the soil.

2.3.1. To reduce vertical vibration and lessen its impact, a best practice is to maximize anchor bolt tension. This may seem like an obvious statement but anchor bolt tension is often arbitrarily limited. For example, API 686 suggests an anchor bolt stress of only 30,000 psi (207 MPa). If this value is used, the anchor bolt will be tightened to only 23% of its Yield Strength. I believe that to be fully effective an anchor bolt should be tightened to 60% to 70% of its yield strength.

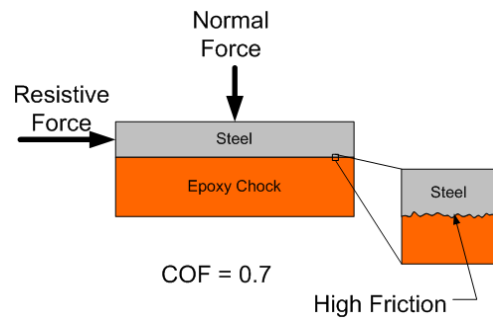
2.3.2. The static loading on the epoxy chocks or grout should be under 6.9 MPa (1,000 psi) to minimize creep. Static loading is made up of a combination of deadweight loading and the loading caused by the tensile stress on the anchor bolts. This should be a sufficient to firmly anchor the compressor and its driver. It also provides a 14 to 16 X Safety Factor to manage any dynamic loads before the compressive strength of the grout is reached.

2.3.3. Terminate the anchor bolts half way into the mat. This combined with heavy rebar connecting the mat to the foundation will help hold the layers together.

2.3.4. Increase the portion of the anchor bolt that is being stretched. The anchor bolts are essentially springs that stretch and apply a clamping load. To create an effective clamping force, an anchor bolt must stretch over about 50% of its length.

2.3.5. To mitigate horizontal vibration, increase the Coefficient of Friction (COF) of the layers. It is

the Coefficient of Friction created by the anchor bolts that prevent sideways or lateral vibrations and movement. Anchor bolts create the Normal Force that, in conjunction with a high COF creates a very high Resistive Force that absorbs the shaking force and prevents movement. A high COF is caused by the intimate fit of epoxy to steel because it fills every little scratch, sandblast divot and machining mark on the bottom of a compressor / driver. *Resistive Force* is found by multiplying *Normal*



Force pushing down by the Coefficient of Friction.

2.4. Best Practices Related to Frame, Rail, Sole Plate and Foundation Preparation

Cleanliness of the compressor frame, engine rails, sole plates or concrete foundation has always been a best practice. There can be no oil in the concrete and all paint, oil, grease dirt, etc. must be removed from the frame, sole plates and rail. Cleanliness is the best way to prevent the various surfaces from de-bonding and from sliding due to a low COF. The following are some additional best practices for component preparation that will help mitigate vibration.

2.4.1. Sand blast and clean metal frame, sole plates or rail to SP 6. Do not prime them. Just remove anything on the surface and give the surface a light texture. This will increase the COF.

2.4.2. If a primer is required on steel to prevent it from rusting prior to installation, that primer must be a straight epoxy primer (NO ZINC) and it must be applied no more than 2 to 3 mills thick.

2.4.3. Chip off the surface of the concrete foundation removing all laitance and expose 50% chipped and broken aggregate. This will provide a structurally solid surface to transfer vertical and horizontal loads down through the grout and into the concrete.

3 Best Practices to Prevent Foundation Degradation

In addition to applying Best Practices to mitigate vertical and horizontal vibration, it is also important to do everything possible to prevent cracks in the foundation and the penetration of oil and chemicals that can degrade the concrete and allow vibrations to increase. This section contains the best practices related to the construction of the foundation and the installation of the machinery related to preventing foundation degradation.

3.1. Best Practices Related To Foundation Design & Installation

3.1.1. Concrete specification - The quality of concrete used in the foundation is extremely important for ensuring a long successful life of the foundation. Best practice calls for a minimum grade of M25 or M30 concrete. This is concrete with a compressive strength of 25 to 30 N/mm² (3,625 to 4,350 psi) and a tensile strength of 3.2 to 3.6 N/mm² (464 to 522 psi). Use crushed stone in the concrete that has angular faces. The bond of angular faced stone to the cement paste is better than round stone.

3.1.2. Tensile strength - A best practice is to increase tensile strength of concrete to at least 1,000 psi using steel fibers. Steel fibers reinforce the concrete in 3 directions. Steel fibers have a high modulus of elasticity and high tensile strength to withstand excess strain and prevent cracking. Because the modulus of elasticity of the fiber is higher than the matrix (concrete or mortar binder), it can help carry the load by increasing the tensile strength of the material.

3.1.3. Concrete curing - Do not allow any grout to be installed until the concrete is fully cured. Improperly cured concrete can have its design strength reduced by as much as 50%. Good curing practice means keeping the concrete damp enough and at a uniform temperature long enough so it can reach its desired compressive and tensile strengths. The key factors in curing are 1) shrinkage complete, 2) full tensile strength and 3) water content reduced.

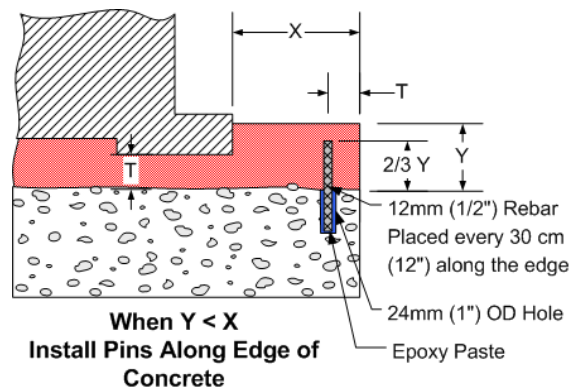
3.1.4. Concrete placement and consolidation - Best practice is to limit the time delay between layers of concrete to no more than 25 to 30 minutes. However, breaks in concrete placement of as little as 15 minutes can result in a cold joint separation between layers. Also, do not add water to the concrete mix at the site as it will reduce the compressive strength, the modulus of elasticity, and tensile strength of the concrete

3.1.5. Foundation design – Best practice is to

remove all sharp corners, points, internal or “re-entrant” corners in the foundation to reduce built-in stress. In other words, anything that can act as a stress riser inside the concrete must be softened or removed. Instead, round sharp corners and points. Install a large radius on any internal angles in the foundation. Apply a large radius to everything that penetrates concrete. Also, anchor bolt holes should be round and not square and grout pockets recessed into the concrete foundation should be avoided. Install troughs around the unit to take away oil.

3.1.6. Vertical connections - There should be no vertical connections between different materials in a foundation. For example, there should be not be a vertical connection between concrete and grout. Connections should be horizontal only. Also, do not install keys or lips as they cannot restrain thermal growth forces.

3.1.7. Edge-lifting – Edge-lifting is a common problem on many installations. It is a de-bonding of the concrete just below the epoxy – concrete bond line. It can occur when large there are wide open areas where epoxy grout covers the foundation but does not support any equipment. There are three methods of preventing edge-lifting: 1) Round the outer edge of the concrete foundation, 2) Pin the edge of the foundation using 12 mm (1/2”) rebar set into a 24 mm (1”) hole every 30 cm (12”) along the edge of the foundation. 3) Install mechanical anchors in the surface of the concrete. These are rebar staples or wickets that improve the bond of the grout to the concrete.



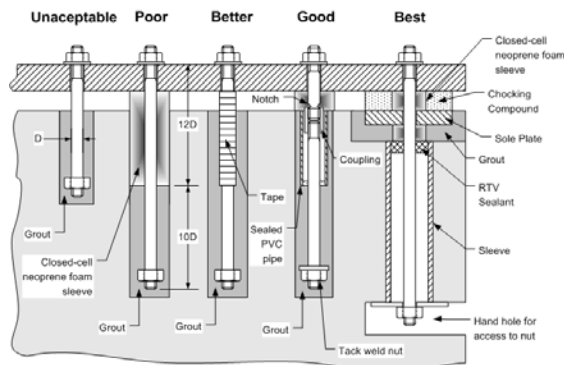
3.1.8. Rebar specification – Best practice is #6 (3/4”) rebar on 6” centers. Second best is #8 (1”) rebar on 8” centers due to the increased difficulty in placing the concrete. Dense placement in the upper 1/3rd of the foundation block and lighter density in the lower 2/3rds of the foundation. Look for and eliminate stress risers that could potentially be created in the concrete which could be caused by the ends of rebar. Also, eliminate possible stress points in the concrete by installing rebar so it crosses at all internal corners of foundation.

3.2. Best Practices related to anchor bolts, nuts and washers

The number one reason for foundation failure is cracking, and the number one cause of cracking is improperly designed and installed anchor bolts. Anchor bolts cannot be eliminated so the quality of their installation must be increased and their negative affects must be mitigated.

3.2.1. Anchor Bolt Grade & Materials – For reciprocating compressor mounting the anchor bolts must be made from 4140 ASTM A193 B7 material. Nuts should be 2H.

3.2.2. Anchor Bolt Types – There are many different anchor bolt designs. The primary difference is the design of their termination or bottom end. Free-standing bolts are a best practice because they can easily be moved and positioned without putting a strain on the bolt or concrete. They have advantages over embedded bolts because the holding force is governed by the bolt's tensile strength rather than the concrete's tensile strength. If bolts are to be cast into the foundation do not cast them into the foundation until the compressor is set in place.



3.2.3. Anchor Bolt Terminations – If free-standing bolts are not used, then any other long bolt can be used, but as a best practice its terminations must be round. This not only means that the plate at the bottom of the anchor bolt should be round, but the plate itself must have round edges. The diameter of the plate should be 3 to 4 times bolt diameter so that the tensile forces on the concrete are pushed further out from the bolt. Also, the thickness of the plate should be 1.5 x bolt diameter.

3.2.4. Free-stretch - No matter the style or type of anchor bolt, the bolt itself must be prevented from touching epoxy grout over the upper half of its length. This allows the bolt to free-stretch. To accomplish this, the upper half to the bolt must be wrapped with tape or covered with pipe insulation foam. Wrapping a bolt also provides the bolt with a large thread clearance which allows the nut to rock slightly on the bolt thread reducing the

bending stress that will be imposed on the bolt thread.

3.2.5. Tension monitoring - It is also a best practice to install anchor bolts with a built-in tension monitoring device.

3.2.6. Anchor bolt length - It is best practice to make anchor bolts as long as possible and to terminate the anchor bolts half way into the mat. Longer bolts reduce loss in tension resulting from creep and reduce stress in concrete at their termination point. In addition, long bolts separate the stress area from the source of oil. At a minimum the anchor bolts should be 1.2 m (48") in length.

3.2.7. Spherical washers – The use of spherical washers is a best practice. Spherical washers allow the tension on the bolt to be spread uniformly around the anchor bolt rather than on just one side. This is very important because nut face angularity of 1 to 2 degrees can have a significant effect of the fatigue life of a bolt.

3.2.8. Nuts – Anchor bolt nuts should be ASTM A-194 high strength nuts. They must be lubricated so the torque is not wasted in friction between the threads or between the nut and washer. Super nuts are a very good practice but can be expensive.

3.2.9. Bolt torque & tension – The nuts on all anchor bolts should be hand-tool tight while the grout is being installed. After the grout has hardened the bolts should be tensioned per the equipment manufacturer's instructions. For a tight foundation and mounting system, the preload on the anchor bolts should be as high as possible, but not higher than 70% of tensile strength of bolt.

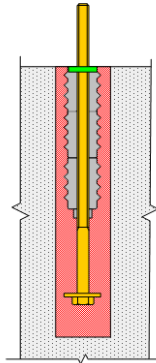
3.2.10. Bolt tensioning – The only accurate way to tighten an anchor bolt is to stretch it. Twisting or torquing a bolt can be very inaccurate because torque is often wasted on friction between the threads of the nut and bolt and between the bottom face of the nut and the washer. Therefore the use of a hydraulic bolt tensioner is a best practice. It is also a best practice to re-tighten anchor bolts after compressor and driver have come up to temperature.

3.3. Best Practice Related To Anchor Bolt Holes / Sleeves / Covering / Sealing

Anchor bolt sleeves or covers are a best practice. They cover a length of bolt so it can stretch sufficiently when tensioned. If properly sealed top and bottom, they also protect the bolt from chemical attack, rust and corrosion.

Many people mistakenly believe that the purpose of a bolt sleeve is to allow the compressor installer to easily bend the anchor bolt for alignment purposes during compressor installation. This is not true. Pushing an embedded anchor bolt puts a strain on it as well as the surrounding concrete that could lead to cracking. For this reason it is a best practice NOT to embed any anchor bolts until the compressor is set in place and aligned.

3.3.1. Corrugated anchor bolt sleeves are a best practice because they have an ability to give under compression rather than to drive themselves up into the grout or down into the concrete. In any event, anchor bolt sleeves should be cut off even with the top of the concrete. If they are allowed to stick partway up into the grout, they will eventually crack the grout.



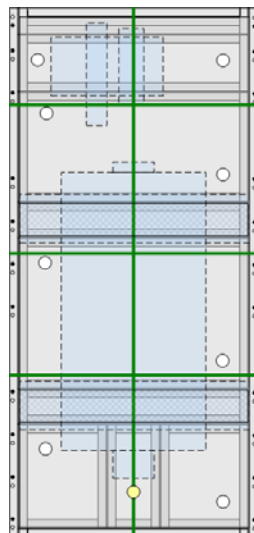
3.3.2. Not too close to the edge - It is good practice to keep bolts and pockets as far as possible away from the sides of the foundation – 30 cm (12” minimum)

3.3.3. Well sealed – the top and bottom of the sleeves should be well sealed to prevent them from filling up with oil or water.

3.3.4. Wrap bolt threads - The bolt threads sticking up above sleeve must be covered using foam backed tape or foam pipe insulation. This prevents grout or chocking compound from going up into the bolt hole on the compressor and preventing the bolt from moving or stretching.

3.4. Best Practices Related To Expansion Joints

The use of expansion joints is a best practice. Expansion joints serve 2 purposes – 1) they prevent the concrete and epoxy grout from coming apart due to the difference in thermal expansion and contraction rates and 2) they guide flow of grout into areas of limited size. Using expansion joints will ensure that the epoxy grout flows everywhere it is needed and that it will stay in place once there.



3.4.1. Proper layout - Proper spacing and

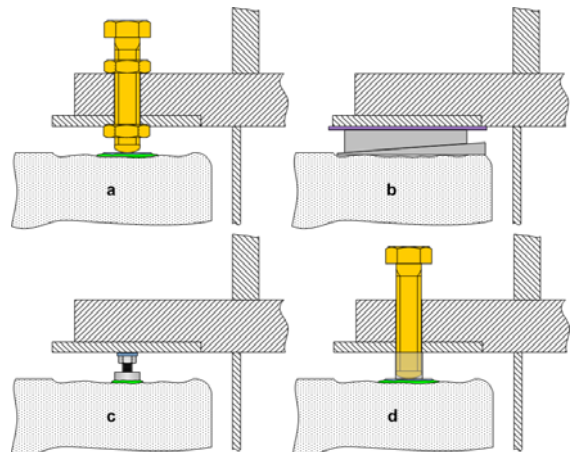
configuration of expansion joints is usually based on the grout used and the extremes of weather and the thermal cycling expected. The larger the expected difference in seasonal temperatures the closer the expansion joints should be but is typically either 1.2 m (4 ft) square or 1.8 m (6 ft) square.

3.4.2. Well sealed - Expansion joints must be well sealed at the bottom so they cannot allow any liquids to pass down next to them.

3.5. Best Practices Related To Alignment Tools

Some sort of jacking device must be used to position the compressor and driver. There are many different types of jacking devices and all (except nuts on anchor bolts under the mounting plate) are acceptable **IF** they are removed completely from the grout. Jacks, wedges, shims, and blocks of any shape or size must never be left inside the grout. Cracks are guaranteed if they are.

3.5.1. Jacking screws - The best practice here is to use jacking screws (d) and back out the screw completely after the grout has cured. This can be done if the threads of the jacking screws are coated with non-melt grease. Jacking devices that are isolated and grouted around must have a second pour to fill in the space where the jacking screw was located. This is costly and unnecessary. The best practice is to use jacking screws with non-melt grease on their threads. This is more cost effective as it allows the entire area to be grouted at one time.



3.5.2. Round landing plate - Another best practice is to have the jacking screw touch down on a relatively thin, round, landing plate with rounded edges. This provides a stable place for the jacking screws to rest that will not add any stress risers to the grout.

Bond the round landing plates to the surface of the concrete with a fast setting epoxy paste.

3.6. Best Practices Related To Epoxy Grout & Chocks

Only epoxy grout and epoxy chocking compound are discussed in this section as their use is considered a “Best Practice” over cementitious grouts. It is important to first differentiate between an epoxy “Grout” and an epoxy “Chock” or “Chocking Compound.” Epoxy grouts are mixtures of resin, hardener, and aggregate. Because of the aggregate, grouts have the consistency of lumpy oatmeal. However, the aggregate also allows the grout to be poured in large, thick sections because it absorbs the exothermic heat created by the resin and hardener. Epoxy chocking compounds have no aggregate. As a result they get much hotter and must be poured in small blocks typically around individual anchor bolts. Chocking compounds have a smooth and creamy consistency.

3.6.1. Eliminate stress risers in grout and chocks. Stress risers are created when re-entrant angles are cast into the grout, equipment mounting feet or sole plates with sharp corners instead or well rounded corners are installed in the grout. Also, screw threads, welding slag, sharp edges, and points of any kind increase the stress in both grout and chocks which can lead to cracking.

3.6.2. Manage temperatures of the grout and chock to eliminate over heating. Over heating can cause high thermal stresses that can lead to cracking. High temperatures also cause an over expansion of the epoxy followed by an over contraction that can lead to soft foot problems.

3.6.3. Manage depth of pour – The larger the mass of epoxy chock or grout, the more exothermic heat it generates and that too can lead to a larger than expected expansion then contraction in the epoxy. For this reason the depth of pour is important. For most epoxy grouts the maximum depth should be no more than 30 cm (12”). The depth of most epoxy chocking compounds should be about 5 cm (2”).

3.6.4. Grout / Chock level - Most installation drawings show the level of grout or chock at the same level as the bottom of the mount. This is not correct and should not be done. The grout/chock level should always be 12mm to 24 mm (1/2 to 1”) above the bottom of the mount. This puts a head pressure on the epoxy surrounding the mount which in turn puts an upward force on the epoxy under the mount. This upward force ensures that any contraction in the epoxy has little or no effect on the alignment.

3.6.5. Chock Overpour – The overpour is not just the place where the chocking compound is poured in place. The overpour also plays a vital role in the curing of the chocking compound. It is the place where the chocking compound can expand up into and contract down from so the epoxy in it must remain cool and liquid. This is done using metal dams placed no more than 19 mm (3/4 inch) away from the mounting foot. The overpour should be along the long side of the mounting foot. It can also be on the opposite long side but it should never extend around the entire mounting foot.

3.6.6. Foam strip - Install a foam strip around the mounting foot or sole plate to take up a small amount of shaking movement without causing the chock or grout to crack.

3.7. Best Practices Related To Coating and Sealing the Foundation

After the compressor and driver have been grouted and/or chocked in place and the forms removed, prepare the exposed concrete surfaces under and around the installation by following these best practices.

3.7.1. Concrete preparation - The surface of the foundation must be firm, free of any laitance or efflorescence, clean, free of any adverse moisture conditions, have an appropriate surface profile, and be fully cured before coating. Newly poured concrete must age at least 30 days at temperatures over 70°F before coating. Form release agents, sealers, curing compounds, salts, hardeners and other foreign matter will interfere with adhesion and must be removed. Shot-blasting, mechanical scarification, suitable chemical means, or sandblasting should be employed to prepare substrate. The surface profile of the concrete should be CSP-3 to CSP-5 meeting ICRI (International Concrete Repair Institute) standard guideline #03732 for coating concrete, producing a profile equal to 60-grit sandpaper or coarser. Moisture vapor transmission should be 1.4 kg (3 pounds) or less per 93 square meter (1,000 square feet) over a 24 hour time period, as confirmed through a calcium chloride test, as per ASTM E-1907. All surface irregularities, cracks, expansion joints and control joints should be properly addressed prior to application.

3.7.2. Concrete coating – Mix and apply an epoxy primer and a 2-part, 100% solids, epoxy top coat over the concrete areas not covered by epoxy chocks or grout. This will protect the surrounding areas from oil penetration.

3.7.3. Seal mounting feet - After the grout or chock cures, seal around the mounting foot or sole plate with a sealant that will prevent oil from penetrating underneath and causing the COF to decline.

3.7.4. Seal Expansion joints – Remove 12 mm (1/2") of the top and end of the expansion joints. Pour liquid expansion joint sealant into this space to prevent oil from penetrating underneath.

The depth of the sealant should be only half as wide as the expansion joint.

3.7.5. Drip pans - Install drip pans under the equipment with drain piping and troughs around the unit to take away oil.

4 Acknowledgements

The author would like to acknowledge the invaluable verbal contributions by the following experts to the content of this paper:

- Mr Tom Hoekstra, EMHA Technisch Bureau B.V., Ridderkerk, Holland, verk.emha@emhabv.com
- Mr Mark Huggins, Engineered Industrial Products, Aylesbury, Bucks, U.K., info@eiproducts.co.uk
- Mr Lothar Idler, Marine-Und-Industrie-Montage GmbH, Hamburg, Germany, idler@mim-hamburg.de
- Mr Bernard Mirabaud, Polyresine, Boissy L'Aillierie, France, bmirabaud@polyresine.fr
- Mr Piero Arduino, Wartsila Italia S.P.A., Genova, Italy, piero.arduino@wartsila.com
- Mr Ramon Zubiaga Garteiz Jr., Sintemar, Vizcaya, Spain, rgz.sintemar.com

5 Conclusion

The only sure way to actively manage vibrations in a compressor and foundation system is by understanding the entire system as whole using FEA and working to effectively control all aspects of the installation at the design stage. However, all this work can be for nothing if the simple yet crucial best practices for installing the compressor and driver are not followed. The above paper was not intended to be a complete list of Best Practices. Installation "Best Practices" should be accumulated, confirmed and applied by every company involved in reciprocating compressor foundation design and installation.

References

1. Prakash, S. and V.K. Puri, "Foundations for Vibrating Machines", *Journal of Structural Engineering*, April – May 2006
2. ACI 351.3R-04 "Foundations for Dynamic Equipment", Reported by ACI Committee 351, James P. Lee, Chair and Yelena S. Gold, Secretary
3. "Shear Strength of Steel Fiber Reinforced Concrete Beams Without Stirrups", Yoon-Keun Kwak, Marc O. Eberhard, Woo-Suk Kim and Jumbum Kim, *ACI Structural Journal*, Technical Paper Title No. 99-S55 http://faculty.washington.edu/eberhard/publications/kwak-eberhard_aci-journal_jul02.pdf
4. Smalley, A.J., P.J. Pantermuehl, R.M. Lewis and E.A. Johnson, "Design of Reciprocating Compressor Mounting Systems and Foundations for Integrity and Reliability", 1996 PRCR Gas Machinery Conference, 1996
5. Mandke, Javant S. and Anthony J. Smalley, "Parameter Studies for Enhanced Integrity of Reciprocating Compressor Foundation Blocks", Pipeline and Compressor research Council Technology Assessment, September 1994.
6. Bhatia, K.G., "Foundations for Industrial Machines", D-CAD Publishers, 2008
7. Smalley, A.J. and P.J. Pantermuehl, "Foundation Guidelines", Gas Machinery Research Council Report No. TR-97-2, January 1997
8. Smalley, A.J., "Crankshaft Protection: Guidelines for Operators of Slow Speed Integral Engine/Compressors", Gas Machinery Research Council Report No. TR-97-1, January 1997
9. "Recommended Practices for Machinery Installation and Installation Design", American Petroleum Institute, Practice 686, April, 1996.
10. Harrison, Don, "The Grouting Handbook", Gulf Publishing Co. Houston, TX, 2000